U.S. Department
of Commerce

Volume 98
Number 2
April 2000

# Fishery Bulletin

**U.S. Department of Commerce**

William M. Daley
Secretary

**National Oceanic and Atmospheric Administration**

D. James Baker
Under Secretary for Oceans and Atmosphere

**National Marine Fisheries Service**

Penelope D. Dalton
Assistant Administrator for Fisheries

# Fishery Bulletin

**Scientific Editor**
**Dr. John V. Merriner**

**Editorial Assistant**
**Sarah Shoffler**

Southeast Fisheries Science Center
National Marine Fisheries Service, NOAA
101 Pivers Island Road
Beaufort, NC 28516

**Managing Editor**
**Sharyn Matriotti**

National Marine Fisheries Service
Scientific Publications Office
7600 Sand Point Way NE, BIN C15700
Seattle, Washington 98115-0070

**Editorial Committee**

**Dr. Andrew E. Dizon** National Marine Fisheries Service
**Dr. Harlyn O. Halvorson** University of Massachusetts, Boston
**Dr. Ronald W. Hardy** University of Idaho, Hagerman
**Dr. Richard D. Methot** National Marine Fisheries Service
**Dr. Theodore W. Pietsch** University of Washington, Seattle
**Dr. Joseph E. Powers** National Marine Fisheries Service
**Dr. Harald Rosenthal** Universität Kiel, Germany
**Dr. Fredric M. Serchuk** National Marine Fisheries Service

***Fishery Bulletin* web site: fishbull.noaa.gov**

The *Fishery Bulletin* (ISSN 0090-0656) is published quarterly by the Scientific Publications Office, National Marine Fisheries Service, NOAA, 7600 Sand Point Way NE, BIN C15700, Seattle, WA 98115-0070. Periodicals postage is paid at Seattle, WA, and at additional mailing offices. POSTMASTER: Send address changes for subscriptions to Fishery Bulletin, Superintendent of Documents, Attn.: Chief, Mail List Branch, Mail Stop SSOM, Washington, DC 20402-9373.

Although the contents of this publication have not been copyrighted and may be reprinted entirely, reference to source is appreciated.

The Secretary of Commerce has determined that the publication of this periodical is necessary according to law for the transaction of public business of this Department. Use of funds for printing of this periodical has been approved by the Director of the Office of Management and Budget.

**For sale** by the Superintendent of Documents, U.S. Government Printing Office, Washington, DC 20402. Subscription price per year: $50.00 domestic and $62.50 foreign. Cost per single issue: $19.00 domestic and $23.76 foreign. **See back for order form.**

The *Fishery Bulletin* carries original research reports and technical notes on investigations in fishery science, engineering, and economics. It began as the Bulletin of the United States Fish Commission in 1881; it became the Bulletin of the Bureau of Fisheries in 1904 and the *Fishery Bulletin* of the Fish and Wildlife Service in 1941. Separates were issued as documents through volume 46; the last document was No. 1103. Beginning with volume 47 in 1931 and continuing through volume 62 in 1963, each separate appeared as a numbered bulletin. A new system began in 1963 with volume 63 in which papers are bound together in a single issue of the bulletin. Beginning with volume 70, number 1, January 1972, the *Fishery Bulletin* became a periodical, issued quarterly. In this form, it is available by subscription from the Superintendent of Documents, U.S. Government Printing Office, Washington, DC 20402. It is also available free in limited numbers to libraries, research institutions, State and Federal agencies, and in exchange for other scientific publications.

U.S. Department
of Commerce
Seattle, Washington

Volume 98
Number 2
April 2000

# Fishery Bulletin

## Contents

*Articles*

227–235 **Acha, Eduardo M., and Gustavo J. Macchi**
Spawning of Brazilian menhaden, *Brevoortia aurea*, in the Río de la Plata estuary off Argentina and Uruguay

236–249 **Brewster-Geisz, Karyl K., and Thomas J. Miller**
Management of the sandbar shark, *Carcharhinus plumbeus*: implications of a stage-based model

250–263 **Keon Alonso, Mariano, Enrique A. Crespo, Susana N. Pedraza, Néstor A. García, and Mariano A. Coscarella**
Food habits of the South American sea lion, *Otaria flavescens*, off Patagonia, Argentina

264–282 **Lo, Nancy C. H, John R. Hunter, and James H. Churnside**
Modeling statistical performance of an airborne lidar survey system for anchovy

283–289 **Macchi, Gustavo J., and Eduardo M. Acha**
Spawning frequency and batch fecundity of Brazilian menhaden, *Brevoortia aurea*, in the Río de la Plata estuary off Argentina and Uruguay

290–298 **Manickchand-Heileman, Sherry C., and Dawn A. T. Phillip**
Age and growth of the yellowedge grouper, *Epinephelus flavolimbatus*, and the yellowmouth grouper, *Mycteroperca interstitialis*, off Trinidad and Tobago

299–318 **Mollet, Henry F., Geremy Cliff, Harold L. Pratt Jr., and John D. Stevens**
Reproductive biology of the female shortfin mako, *Isurus oxyrinchus* Rafinesque, 1810, with comments on the embryonic development of lamnoids

319–335 **Mortensen, Donald, Alex Wertheimer, Sidney Taylor, and Joyce Landingham**
The relation between early marine growth of pink salmon, *Oncorhynchus gorbuscha*, and marine temperature, secondary production, and survival to adulthood

The conclusions and opinions expressed in *Fishery Bulletin* are solely those of the authors and do not represent the official position of the National Marine Fisheries Service (NOAA) or any other agency or institution.

The National Marine Fisheries Service (NMFS) does not approve, recommend, or endorse any proprietary product or proprietary material mentioned in this publication. No reference shall be made to NMFS, or to this publication furnished by NMFS, in any advertising or sales promotion which would indicate or imply that NMFS approves, recommends, or endorses any proprietary product or proprietary material mentioned herein, or which has as its purpose an intent to cause directly or indirectly the advertised product to be used or purchased because of this NMFS publication.

336–344 **Orbacz, Elizabeth A., and Patrick M. Gaffney**
Genetic structure of tautog (*Tautoga onitis*) populations assayed by RFLP and DGGE analysis of mitochondrial and nuclear genes

345–352 **Rivera, Glauco A., and Richard S. Appeldoorn**
Age and growth of dolphinfish, *Coryphaena hippurus,* off Puerto Rico

353–363 **Rocha-Olivares, Axayácatl, H. Geoffrey Moser, and Jason Stannard**
Molecular identification and description of pelagic young of the rockfishes *Sebastes constellatus* and *Sebastes ensifer*

364–374 **Schaefer, Kurt M., and Charles W. Oliver**
Shape, volume, and resonance frequency of the swimbladder of yellowfin tuna, *Thunnus albacares*

375–388 **Sévigny, Jean-Marie, Patrice Gagné, Yves de Lafontaine, and Julian Dodson**
Identification and distribution of larvae of redfish (*Sebastes fasciatus and S. mentella*: Scorpaenidae) in the Gulf of St. Lawrence

389–399 **Stevens, Bardley G., Ivan Vining, Susie Byersdorfer, and William Donaldson**
Ghost fishing by Tanner crab (*Chionoecetes bairdi*) pots off Kodiak, Alaska: pot density and catch per trap as determined from sidescan sonar and pot recovery data

400–409 **Stokesbury, Kevin D. E., Jay Kirsch, Evelyn D. Brown, Gary L. Thomas, and Brenda L. Norcross**
Spatial distributions of Pacific herring, *Clupea pallasi,* and walleye pollock, *Theragra chalcogramma,* in Prince William Sound, Alaska

410–420 **Vølstad, Jon H., Alexei F. Sharov, Glenn Davis, and Brenda Davis**
A method for estimating dredge catching efficiency for blue crabs, *Callinectes sapidus,* in Chesapeake Bay

*Notes*

421–426 **Ahrenholz, Dean W., Deborah D. Squires, James A. Rice, Stephen W. Nixon, and Gary R. Fitzhugh**
Periodicity of increment formation in otoliths of overwintering postlarval and prejuvenile Atlantic menhaden, *Brevoortia tyrannus*

427–438 **Powell, Allyn B., David G. Lindquist, and Jonathan A. Hare**
Larval and pelagic juvenile fishes collected with three types of gear in Gulf Stream and shelf waters in Onslow Bay, North Carolina, and comments on ichthyoplankton distribution and hydrography

439 *Subscription form*

# Spawning of Brazilian menhaden, *Brevoortia aurea*, in the Río de la Plata estuary off Argentina and Uruguay*

**Eduardo M. Acha**
Dto. Ciencias Marinas
Universidad Nacional de Mar del Plata
Funes 3350
(7600) Mar del Plata, Argentina
Present address: Instituto Nacional de Investigación y Desarrollo Pesquero (INIDEP)
Paseo V. Ocampo N° 1
(7600) Mar del Plata, Argentina
E-mail address: macha@inidep.edu.ar

**Gustavo J. Macchi**
Consejo Nacional de Investigaciones Científicas y Técnicas (CONICET)
Rivadavia 1917
(1033) Buenos Aires, Argentina

**Abstract.**–Brazilian menhaden, *Brevoortia aurea*, is the only species of the genus *Brevoortia* in South American Atlantic waters and is abundant in the Río de la Plata estuary. We found that *B. aurea* in this area spawns almost exclusively in this estuary. We studied the temporal and spatial reproductive pattern of this menhaden and related the pattern to the major hydrographic features of the region. We based evidence of spawning activity on the presence of females with hydrated oocytes and on the occurrence of menhaden eggs in plankton samples. Our results show that *B. aurea* spawn during virtually every month of the year, but that they spawn mainly from September (late winter) to January (early summer). In the Río de la Plata estuary, spawned eggs occur in a thermohaline range of 13–23°C and 10–25 psu, mainly in stratified waters. *Brevoortia aurea* spawn very near the bottom salinity front, probably in a convergent flow between the riverine and estuarine waters that helps to retain eggs. In contrast to menhaden of the northern hemisphere (*B. tyrannus* and *B. patronus*), which spawn offshore and which drift during early life history stages, *Brevoortia aurea* in the Río de la Plata estuary are spawned and held in estuarine waters near spawning sites. The latter reproductive pattern is also shared by *Micropogonias furnieri* (whitemouth croaker), the most abundant fish species in the area.

Manuscript accepted 29 November 1999.
Fish. Bull. 98:227–235 (2000).

The Río de la Plata drains the second largest basin of South America. It flows into the Atlantic Ocean with an average discharge of 22,000 $m^3/s$, generating a large estuary of about 35,000 $km^2$ and 5–15 m in depth, located at 36°S, 56°W (Framiñan and Brown, 1996). Brazilian menhaden, *Brevoortia aurea*, is abundant in this estuary (Cousseau, 1985; Boschi, 1988); it also inhabits coastal and estuarine environments from 13°S (Brazil) to 40°S (Argentina). Historically, two species of menhaden were thought to inhabit Brazilian–Argentine waters (de Ciechomski, 1968; Weiss et al., 1976; Weiss and Krugg, 1977; Whitehead, 1985; Lasta and de Ciechomski, 1988); however, Cousseau and Díaz de Astarloa (1993) concluded that *B. aurea* is the only species that inhabits South American Atlantic waters.

Little is known about the reproductive biology of *B. aurea*. De Ciechomski (1968) described eggs and early larval stages of *B. aurea* and reported a period of 86–88 hours from the time of spawning to hatching at 13–14°C. Spawning has been detected in the Río de la Plata estuary (Lasta and de Ciechomski, 1988). Although their planktonic eggs also have been found in inshore waters along the Uruguayan and Argentine coasts (de Ciechomski, 1968; Hubold and Ehrlich, 1981; Cassia and Booman, 1985; Sánchez and de Ciechomski, 1995), Samborombón Bay (a shallow area inside the estuary) seems to be the locus of intensive spawning, where *B. aurea* eggs are exposed to low salinities (5–15 psu) (Lasta and de Ciechomski, 1988). Estuarine spawning by species producing pelagic eggs is uncommon (Dando, 1984; Haedrich, 1992; Potter et al., 1993); however no attempts have been made to describe the basic spawning habitat requirements of *B. aurea*. Furthermore, in the Río de la Plata, *Micropogonias furnieri*, the species with the largest biomass, releases pelagic eggs in the inner zone of the estuary (Macchi et al., 1996; Acha et al., 1999).

The life cycles of Northern Hemisphere menhaden, mainly *Brevoortia tyrannus* and *Brevoortia pat-*

* Contribution 1130 of the Instituto Nacional de Investigación y Desarrollo Pesquero (INIDEP), (7600) Mar del Plata, Argentina.

*ronus* (the Atlantic and gulf menhaden, respectively) are well understood. Both species are typical representatives of estuarine dependent species that spawn in the marine environment (Lawler et al., 1988; Day et al., 1989) in contrast to the Brazilian menhaden, which spawns in an estuarine environment.

Since 1983 the coastal resources of the Argentine–Uruguayan Common Fishing Zone have been monitored by a number of cruises, and results pertaining to menhaden form the basis for this paper. Our objectives were to describe the timing and spatial occurrence of spawning in relation to the major hydrographic features of the region in order to gain insight into the spawning habitat requirements of the Brazilian menhaden. Whenever possible, comparative analyses with other species of the estuary and menhaden of the Northern Hemisphere were performed.

## Materials and methods

Samples from 47 cruises from 1983 through 1998 were analyzed in our study. Twenty-two of these cruises were on research vessels of the National Institute for Fisheries Research and Development (INIDEP), covering the Río de la Plata estuary and adjacent coastal waters, throughout which stations were randomly distributed. Twenty-five cruises took place in Samborombón Bay, on small fishing boats using a systematic sampling design. Monthly distribution of the sampling effort is shown in the insert of Figure 1. During 1983 and 1987, nineteen cruises in Samborombón Bay were performed every 30–45 days during the entire year. The remaining six cruises in this bay correspond only to spring months (October, November, and December). Cruises were made with several objectives, hence covering different periods, but sampling effort was higher in spring (October–November) when cruises for stock assessment were performed. The high number of plankton samples in May was due mainly to one cruise, designed to study physical variables and plankton in the estuary. Cruises on the small boats and on the research vessels were not simultaneous. All data were employed as a composite representing mean conditions.

Plankton was collected at 980 sampling stations by oblique tows of 60-cm bongo nets, 20-cm bongo nets, or a Nackthai sampler (a modified Gulf V high-speed plankton net, see Nellen and Hempel, 1969). All nets were equipped with flowmeters. The volume filtered in each tow ranged from 10 to 400 $m^3$. Sampling depth was estimated from measurements taken with an angle indicator (inclinometer) and a wheelout meter. All samples were preserved in 5% buffered formalin. Plankton samples were sorted and analyzed in the laboratory. *Brevoortia aurea* eggs were identified following the description of de Ciechomski (1968).

Estimates of egg density from the different samplers were not intercalibrated. They were arranged into four broad density classes (<10, 10 to 99, 100 to 999, ≥1000 eggs/$m^3$), and marked on a map to delineate the geographic location of the spawning area. Monthly distribution of the average number of eggs per tow (catch per unit of effort, CPUE) and the percentage of positive stations for menhaden eggs were plotted to identify the spawning season. Stations with no catch were included in the CPUE estimates.

Data from the November 1995 cruise were useful for gaining insight into the vertical distribution of menhaden eggs. During that cruise, plankton was sampled at five stations in a small area near Montevideo, where schools of spawning *B. aurea* were previously detected. In each of those stations, two tows were conducted with the Nackthai net, one to sample the surface and the other to sample the bottom layers as defined by a strong halocline. The depth of the halocline was previously measured with a conductivity-temperature-depth (CTD) profiler.

On all cruises, menhaden were collected with bottom trawls, and the presence of females with hydrated oocytes (macroscopic examination) was considered evidence of imminent spawning. The percentage of females with hydrated oocytes for each tow was also indicated on the map to identify the location of the spawning area. In addition, the mean monthly percentage of females with hydrated oocytes was used to determine the spawning season.

Temperature and salinity information was taken from the oceanographic database created by Guerrero et al. (1997a), which included all the CTD stations sampled during the cruises that we performed. Bottom salinity and temperature data for spring–summer were used because they could be matched to the vertical distribution of the eggs and the main reproductive period. Salinity is expressed as psu (practical salinity units; Anonymous, 1981). Horizontal and vertical salinity contour lines were made to compare the spawning area with the salinity field. Egg density was plotted into a temperature-salinity diagram to show the environmental ranges of the spawning habitat of the Brazilian menhaden.

## Results

### Eggs in the plankton

Brazilian menhaden eggs were detected virtually all year round (Fig. 1). The highest CPUE occurred from

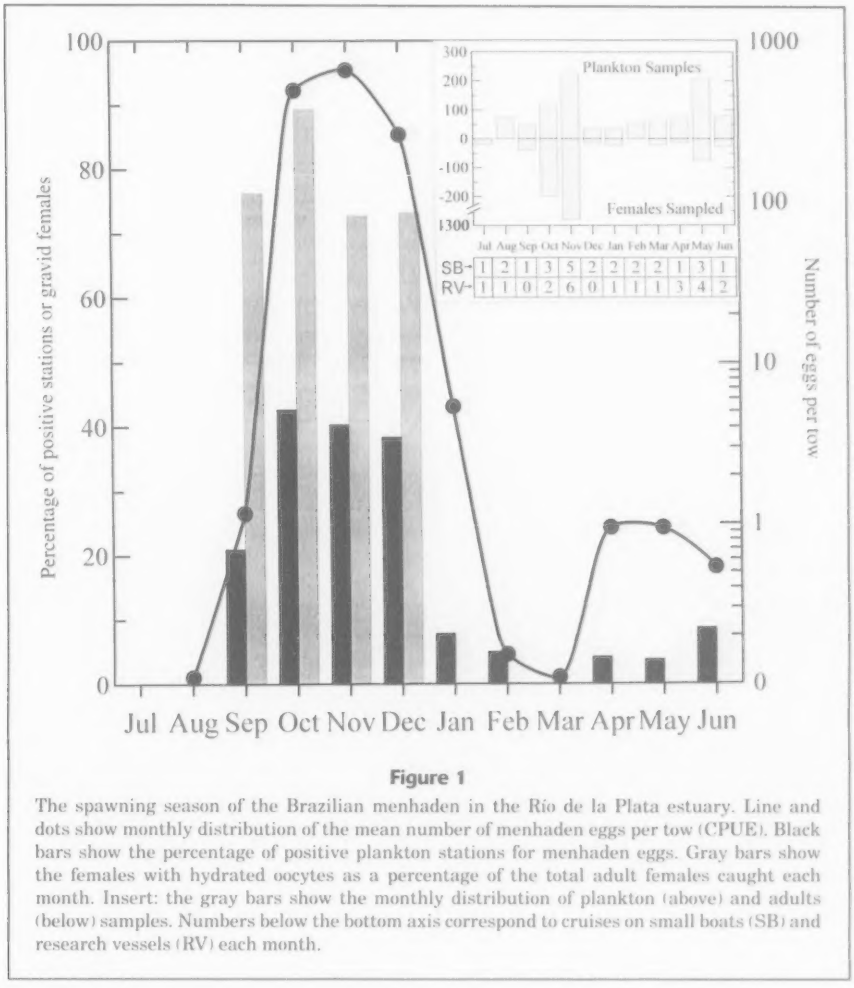
Percentage of positive stations or gravid females
Number of eggs per tow
Jul Aug Sep Oct Nov Dec Jan Feb Mar Apr May Jun
Plankton Samples
Females Sampled
SB→ 1 2 1 3 5 2 2 2 2 1 3 1
RV→ 1 1 0 2 6 0 1 1 1 3 4 2

**Figure 1**

The spawning season of the Brazilian menhaden in the Río de la Plata estuary. Line and dots show monthly distribution of the mean number of menhaden eggs per tow (CPUE). Black bars show the percentage of positive plankton stations for menhaden eggs. Gray bars show the females with hydrated oocytes as a percentage of the total adult females caught each month. Insert: the gray bars show the monthly distribution of plankton (above) and adults (below) samples. Numbers below the bottom axis correspond to cruises on small boats (SB) and research vessels (RV) each month.

September through January and diminished during late summer, followed by a secondary peak during the fall (April–June). The percentage of positive stations for menhaden eggs had a similar pattern to that of the CPUE. There was no plankton sampling in July.

Menhaden eggs were identified in 220 samples that represented 22.5% of all samples analyzed. The eggs were found mainly in estuarine waters (Fig. 2A), especially at depths <10 m. Highest densities of eggs were found in Samborombón Bay and west of Montevideo in the innermost part of the estuary, where salinity values ranged between 10 and 20 psu. Medium egg densities were found along the Uruguayan coast between Montevideo and Atlántida (55°45'W) and in the middle area of the river between Montevideo and Punta Piedras. Lowest densities (<10 eggs/$m^3$) were present in the rest of the estuary and adjacent coastal waters.

The study area (5 stations) of the vertical distribution of *B. aurea* eggs is shown by an arrow in Figure 2A. Total depth in this area was 6.5–7.5 m and halocline depth was 4.8–6.5 m. Menhaden eggs were present in the water layer below the halocline but were extremely scarce in the upper layer. In the bottom layer, egg density ranged from 50–2100 eggs/$m^3$. Eggs were found within a thermohaline range of 9.7–27.3 psu and 18.5–20.2°C. The upper layer was less saline (0.7–10.8 psu) and warmer (19.7–21.7°C). Strong haloclines up to 21.5 psu/m were observed. Figure 3 shows the vertical distribution of salinity and *B. aurea* eggs along a transect in the estuary. This transect includes four of the five plankton stations sampled above and below the halocline. Menhaden eggs were detected in the region where the salt wedge intersects the bottom (the bottom salinity front). In this area of stratified

waters, depth of bottom layer (measured from the halocline to the bottom) was less than 3 m, and menhaden eggs were located below the halocline.

Menhaden eggs occurred in a wide environmental range (Fig. 4). Densities of >100 eggs/m$^3$ were found in a salinity range of 10 to 25 psu; minor densities were located in waters with salinities reaching 33 psu (continental shelf waters). The low salinity boundary for egg distribution seems more abrupt than the high salinity boundary; very few eggs were detected below 10 psu. Most eggs produced over the prolonged spawning season were found at temperatures between 13 and 23°C.

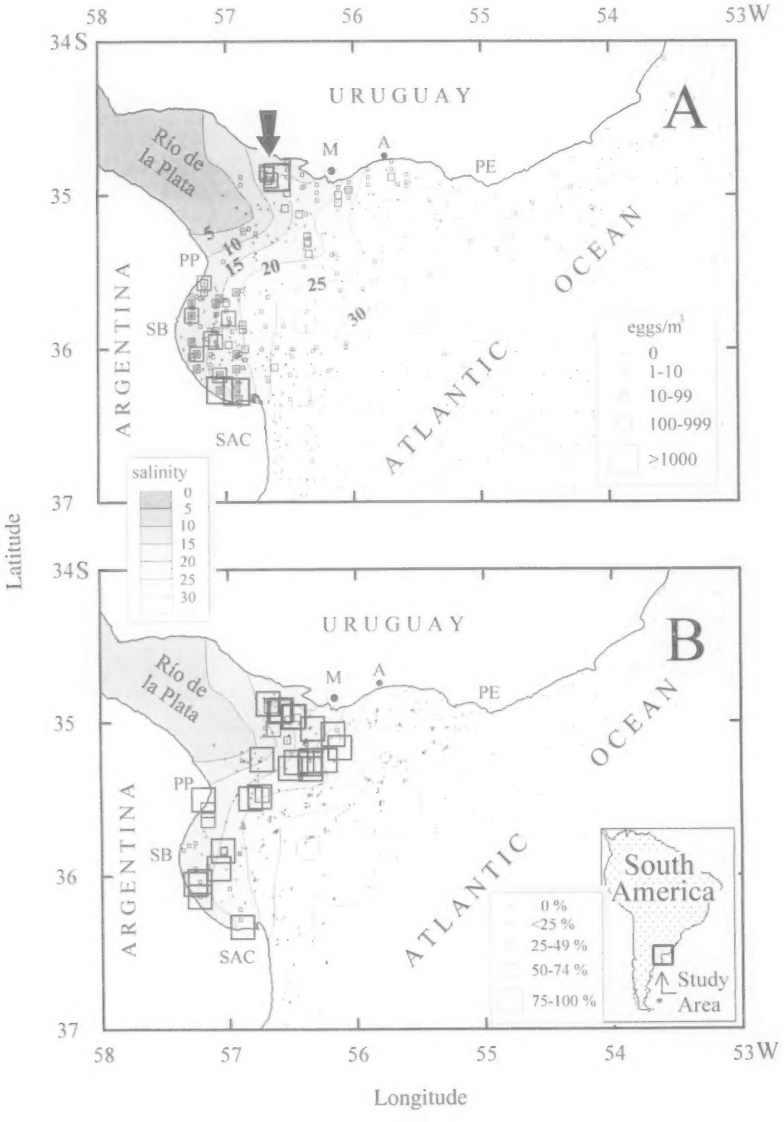


**Figure 2**

Location of the spawning area of the Brazilian menhaden. **(A)** The size of the symbols is proportional to the egg density from the plankton samples; the arrow shows the study site for examining the vertical distribution of eggs (see the text). **(B)** The size of the symbols is proportional to the percentage of females with hydrated oocytes. In both maps, the isohalines (expressed as psu) represent the bottom salinity field for spring-summer. PE = Punta del Este; A = Atlántida; M = Montevideo; PP = Punta Piedras; SB = Samborombón Bay; SAC = San Antonio Cape.

### Gravid females

A total of 375 sampling stations were analyzed, in which 1084 gravid females were identified. All the gravid females were caught from September through December. In these months, the total percentage of females with hydrated oocytes ranged from 72.8% to 89.4% (Fig. 1).

Gravid females were detected across the river between Montevideo and Punta Piedras, and in Samborombón Bay (Fig. 2B). In that region, percentages of gravid females in each tow were >50%. The highest percentages of females with hydrated oocytes appeared to be associated with the highest horizontal salinity gradient (the salinity front). No females with hydrated oocytes were detected in continental shelf waters.

## Discussion

The distribution of eggs and gravid females reveals that *B. aurea* spawn in the estuary (Fig. 2). Gravid females were found in a more restricted area than that where eggs were found, thus providing a more accurate picture of the spawning spatial pattern, because currents may move eggs to more distant areas. An echo sounder showed Brazilian menhaden below the halocline on all cruises, including the occasions when spawning individuals were collected. The halocline was detected by

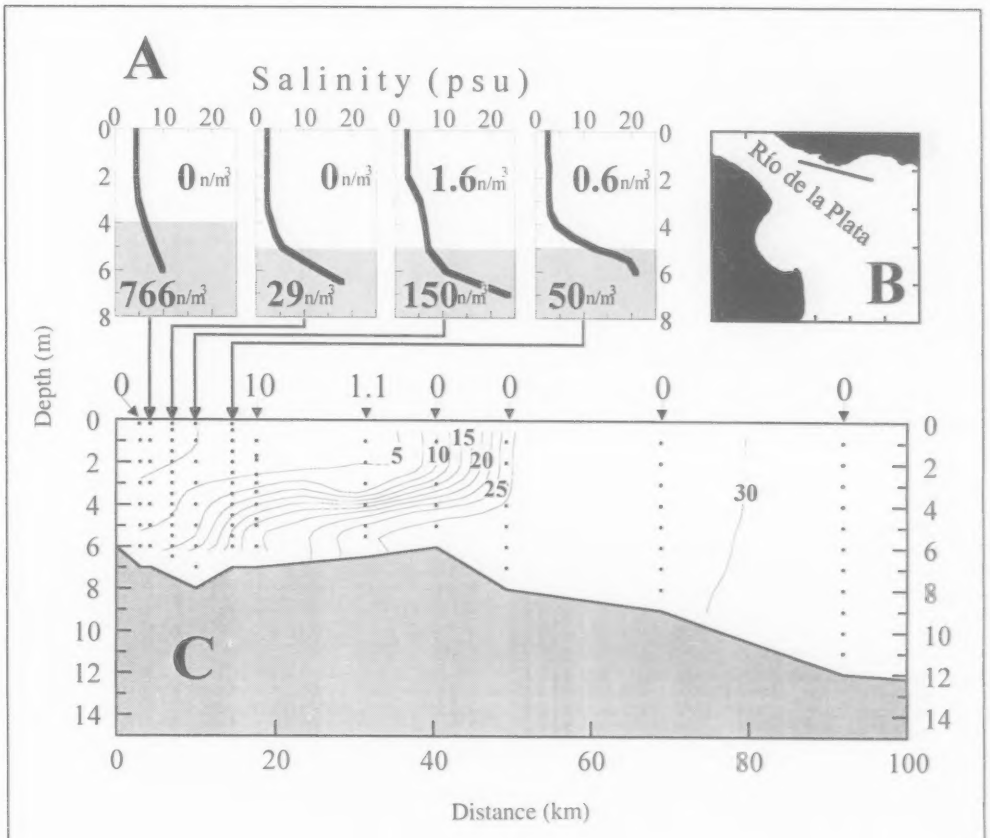


**Figure 3**

Vertical distribution of Brazilian menhaden eggs. (**A**) Vertical distribution of eggs at the head of the salt wedge, where the upper and bottom layers were sampled separately. Numbers in the white areas show eggs/$m^3$ above the halocline, numbers in the gray areas show egg concentrations below the halocline. Black lines show salinity profiles. (**B**) Location of the transect in the estuary. (**C**) Salinity section in the estuary. Isohalines are each 2.5 psu; vertical dots indicate CTD observations. Numbers above the top axis show eggs/$m^3$ in oblique plankton tows from bottom to surface.

the echo sounder as a scattering layer, owing to the concentration of zooplankton (Madirolas et al., 1997). Brazilian menhaden appears to spawn close to the bottom, at the salinity front. The mean position of this front is strongly related to bottom topography (Guerrero et al., 1997a), having a relatively fixed location. This spawning area extends into the stratified waters of the estuary between Montevideo and Punta Piedras, and along Samborombón Bay. However, because waters of the inner zone of the bay are vertically homogeneous, or weakly stratified (Guerrero et al., 1997a), some high egg concentrations occur in nonstratified waters.

Menhaden eggs occurred in a wide range of salinities and temperatures. Because the bottom front is a zone of major salinity changes, the eggs are exposed to a wide range of salinity values, and because the reproductive season extends over a long period, eggs are exposed further to a wide thermal range (Fig. 4). Low egg densities at low temperatures and high salinities represent samples taken in continental shelf waters, which were cooler than the estuarine waters during the warm season (Guerrero et al., 1997a, 1997b).

Presence of Brazilian menhaden eggs in the plankton year-round (Fig. 1) is strong evidence that they have a protracted reproductive season. Major spawning activity, based on incidence of eggs and hydrated ovaries (gravid females), occurs from September to January. Other reports of menhaden eggs, based on

partial temporal or spatial coverage, or both, fall within the temporal limits that we detected (de Ciechomski, 1968; Hubold and Ehrlich, 1981; Cassia and Booman, 1985; Lasta and de Ciechomski, 1988).

*Brevoortia aurea* eggs remain in the bottom layer of the water column, near where the halocline intersects the bottom (Fig. 3). At this frontal interface, a convergent flow near the bottom (Largier, 1993) would serve to retain eggs near the confluence of river and marine waters, minimizing their drift. Thus, specific gravity of the eggs seems to be an important feature of the reproductive strategy of *B. aurea*, allowing the eggs to stay in the saltier (and denser) bottom waters. Typically, bottom waters move landward in salt-wedge estuaries (Kjerfve, 1989; Mann and Lazier, 1991). Lower egg concentrations in the rest of the estuary probably indicate some dispersion of eggs or reduced spawning in these areas.

Disruptive events such as storms, which destroy the halocline (Guerrero et al., 1997a), intermittently occur in this region. These meteorological events are characterized by strong winds over 13 m/s from the southeast (Balay, 1961). The events have a characteristic duration of 1–3 (occasionally 5) days, occur throughout the year, and are usually the strongest from May to October (Anonymous, 1995). During these events, the estuarine circulation is modified, thus altering the egg retention properties of the system as well. The protracted reproductive season and multiple spawning of *B. aurea* (Macchi and Acha, 2000) may help to ensure that enough eggs survive in this unpredictable environment.

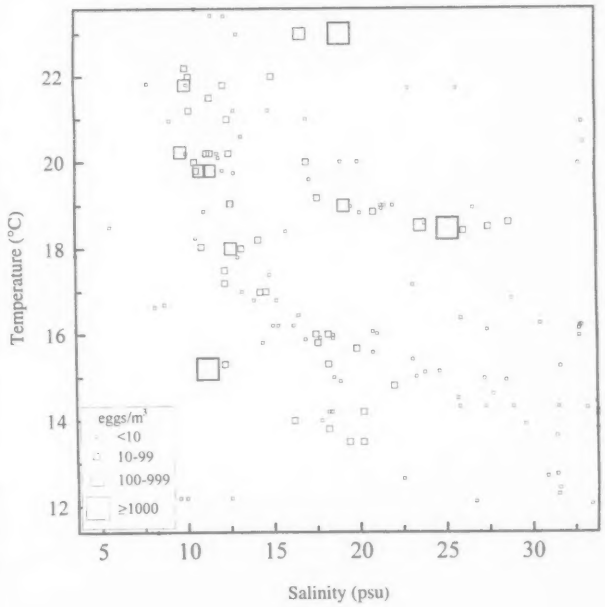


**Figure 4**

Thermohaline range of Brazilian menhaden eggs determined from plankton samples taken from the Río de la Plata estuary and adjacent coastal waters. The size of the symbols is proportional to egg density.

The four menhaden species in the Northern Hemisphere are the small-scaled menhaden *B. smithi* and *B. gunteri* and the large-scaled menhaden *B. tyrannus* and *B. patronus* (Ahrenholz, 1991). There is little information on the biology of *B. smithi* and *B. gunteri*. Conversely, *B. tyrannus* and *B. patronus* have been intensively studied, and the information on their life histories has been broadly reviewed (Ahrenholz, 1991; Powell, 1994). Both species have protracted reproductive seasons and a main spawning period in winter (Nelson et al., 1977; Shaw et al., 1985; Powell, 1994). Spawning of these menhaden takes place in marine waters. Larvae swim and drift with tides and currents toward estuaries where metamorphosis from larvae to juveniles takes place. In the case of *B. tyrannus*, larvae must be transported from the intensive spawning area south of Cape Hatteras, up to 100 km to estuarine nursery areas (Warlen, 1992; Powell, 1994). *Brevoortia patronus* seems to spawn relatively close to estuarine nursery areas (Shaw et al., 1985).

*Brevoortia aurea*, *B. tyrannus,* and *B. patronus* all have protracted spawning periods. The southern species is a spring–summer spawner; the northern ones spawn during cooler months. In the case of *B. tyrannus,* however, adults search for temperatures ≥17°C to spawn, and as larvae are transported nearer the coast, they enter cooler water (Warlen, 1992). Notwithstanding, the reproductive thermal range of the northern species (12.9–21.2°C for *B. patronus*, and ≥17°C for *B. tyrannus* (Warlen, 1988; 1992) lies close to that of *B. aurea*. The proposed advantage of winter spawning refers to maximum onshore transport during that season, providing a mechanism for transporting larvae of both species into the vicinity of estuaries (Nelson et al., 1977; Warlen, 1988).

The main differences between *B. aurea* and those northern menhaden seem to be the population biomass and the spawning habitat. *Brevoortia tyrannus* and *B. patronus* exhibit large population sizes and are a significant component of United States fishery landings (Vaughan, 1991; Powell, 1994). Although there is no biomass assessment for *B. aurea*, it has

little importance as a fishery species (Argentine landings in 1997 were 893 t (Anonymous, 1998). Life history characteristics of *Brevoortia aurea* are probably more similar to those of *B. smithi* and *B. gunteri*, which tend to be more nearshore and estuarine-oriented species, form loose aggregations in coastal waters, and have protracted spawning periods during fall–winter months (Ahrenholz, 1991). Not enough information, however, on their reproductive biology exists to make further comparisons.

Drift of early life history stages is a major feature in the life cycle of *B. patronus*, and especially of *B. tyrannus*. On the contrary, egg retention seems to be a main property of the life cycle of the Brazilian menhaden in the Río de la Plata estuary. However, in southern Brazil, *B. aurea* does not seem to be an estuarine spawner (reported as *B. pectinata*, Weiss et al., 1976; Weiss and Krug, 1977; Weiss, 1981; Sinque and Muelbert, 1997). The greatest number of eggs occurred in nearshore waters, in a saline range of 33.04–35.50 psu. Several eggs were also found in the access channel to Lagoa dos Patos (a large coastal lagoon in southern Brazil, 32°S) during high salinity events, although its larvae and juveniles were distributed throughout the estuary in low salinity conditions (Weiss et al., 1976; Weiss, 1981; Sinque and Muelbert, 1997). The spawning area of *M. furnieri*, the most abundant fish species in the Río de la Plata, partially overlaps that of *B. aurea*, and the eggs of *M. furnieri* are retained in the estuary below the halocline (Acha et al., 1999). Like *B. aurea*, *M. furnieri* is an estuarine spawner in the Río de la Plata (Macchi et al., 1996) but seems to be a saltwater spawner in southern Brazil (Sinque and Muelbert, 1997). Both species have the potential for estuarine reproduction, but the eventual spawning site depends on the dynamic properties of the environment.

Major reviews of the role of estuaries for fishes state that spawning of pelagic eggs within estuaries is an unusual episode (e.g. Day et al., 1981; Day et al.,1989; Haedrich, 1992). Owing to the net seaward movement of estuarine waters, export of early life-history stages from the estuaries seems to be a major problem for estuarine spawners (Boehlert and Mundy, 1988).

In the Río de la Plata estuary, at least two fish species (*B. aurea* and *M. furnieri*) spawn pelagic eggs, taking advantage of the retention properties at the head of the salt wedge. These retention properties are not a feature unique to the Río de la Plata because estuaries with salt wedges are well known features (e.g. Mann and Lazier, 1991; Officer, 1992); however spawning of pelagic eggs at those locations is an uncommon event. Retention of eggs and larvae in the convergence zone may not be complete and the net nontidal flows (residual currents) may drive them seaward. Given the large size of the Río de la Plata estuary, distance from the spawning area to the offshore limit of the salt wedge may reach 250 km (Guerrero et al., 1997a, 1997b). Therefore, larvae probably have enough time to develop to the stage where they become able to control their vertical position in the water column. The migratory behavior of larvae is manifested mostly in the vertical rather than horizontal plane (Norcross and Shaw, 1984). Thus, larval menhaden could take advantage of the two-layered circulation pattern and through vertical migrations compensate for the horizontal transport. This movement would be an important adaptation to maintain population (as the reproductive unit) coherency (Boucher, 1988; Sinclair and Iles, 1989).

## Literature cited

**Acha, E. M., H. W. Mianzan, C. A. Lasta, and R. A. Guerrero.**
**1999.** Estuarine spawning of the whitemouth croaker *Micropogonias furnieri* in the Río de la Plata, Argentina. Mar. Freshwater Res. 50(1):57–65.

**Anonymous.**
**1981.** Background papers and supporting data on the Practical Salinity Scale 1978. Tec. Pap. Mar. Sci. 37, UNESCO, Paris, 144 p.
**1995.** Derrotero Argentino. Parte 1 Río de la Plata, 10th ed. Servicio de Hidrografía Naval, Armada Argentina, Buenos Aires, 273 p.
**1998.** Capturas marítimas totales 1997. Ministerio de Economía y Obras y Servicios Públicos. Secretaría de Agricultura, Ganadería, Pesca y Alimentación. Subsecretaría de Pesca. Dirección Nacional de Pesca Acuicultura, Buenos Aires, 45 p.

**Ahrenholz, D. W.**
**1991.** Population biology and life history of the North American menhadens, *Brevoortia* spp. Mar. Fish. Rev. 53(4): 3–19.

**Balay, M. A.**
**1961.** El Río de la Plata entre la atmósfera y el mar. Servicio de Hidrografía Naval, Argentina, Público H-621, 153 p.

**Boehlert, G. W., and B. C. Mundy.**
**1988.** Roles of behavioral and physical factors in larval and juveniles fish recruitment to estuarine nursery areas. Am. Fish. Soc. Sym. 3:51–67.

**Boschi, E. E.**
**1988.** El ecosistema estuarial del Río de la Plata. An. Inst. Cienc. del Mar y Limnol., Univ. Nal. Autón. México 15(2): 159–182.

**Boucher, J.**
**1988.** Space-time aspects in the dynamics of planktonic stages. *In* Toward a theory of biological-physical interactions in the world ocean: proceedings of the NATO advanced workshop, Casteria Verduzan, France, 15 June 1987 (B. J. Rothschild, ed.), p. 203–214. Kluwer Academic Press, Dordrecht.

**Cassia, M. C., and C. I. Booman.**
**1985.** Distribución del ictioplancton en el Mar Argentino en los años 1981–1982. Physis 43(105):91–111.

**Cousseau, M. B.**
**1985.** Los peces del Río de la Plata y su Frente Marítimo. *In* Fish community ecology in estuaries and coastal lagoons: towards an ecosystem integration (A.Yáñez-Arancibia, ed.), p. 515–534. DR(R) UNAM Press, México.

**Cousseau, M. B., and J. M. Díaz de Astarloa.**
**1993.** El género *Brevoortia* en la costa Atlántica Sudamericana. Frente Maritimo 14:49–57.

**Dando, P. R.**
**1984.** Reproduction in estuarine fish. *In* Fish reproduction: strategies and tactics (G. W. Potts and R. J. Wootton, eds.) p. 155–170. Academic Press, London.

**Day, J. H., S. J. M. Blaber, and J. H. Wallace.**
**1981.** Estuarine fishes. *In* Estuarine ecology with particular reference to southern Africa (J. H. Day, ed.), p.197–221. A.A. Balkema, Rotterdam.

**Day Jr., J. W., C. A. S. Hall, W. M. Kemp, A. Yáñez-Arancibia, and L. A. Deegan.**
**1989.** Nekton, the free-swimming consumers. *In* Estuarin ecology (Day et al., eds.), p. 377–437. John Wiley and Sons, New York, NY.

**de Ciechomski, J. D.**
**1968.** Huevos y larvas de tres especies de peces marinos, *Anchoa marinii*, *Brevoortia aurea* y *Prionotus nudigula* de la zona de Mar del Plata. Bol. Inst. Biol. Mar. 17, 28 p.

**Framiñan, M. B., and O. B. Brown.**
**1996.** Study of the Río de la Plata turbidity front. Part I: spatial and temporal distribution. Cont. Shelf Res. 16(10):1259–1282.

**Guerrero, R. A., E. M. Acha, M. B. Framiñan, and C. A. Lasta.**
**1997a.** Physical oceanography of the Río de la Plata Estuary, Argentina. Cont. Shelf Res. 17(7):727–742.

**Guerrero, R. A., C. A. Lasta, E. M. Acha, H. W. Mianzan, and M. B. Framiñan.**
**1997b.** Atlas hidrográfico del Río de la Plata. Comisión Administradora del Río de la Plata-Instituto Nacional de Investigación y Desarrollo Pesquero, Buenos Aires-Montevideo, 109 p.

**Haedrich, R. L.**
**1992.** Estuarine fishes. *In* Ecosystems of the world, vol. 26, Estuaries and enclosed seas (B. H. Ketchum, ed.), p. 185–207. Elsevier, Amsterdam.

**Hubold, G., and M. D. Ehrlich.**
**1981.** Distribution of eggs and larvae of five clupeoid fish species in the Southwest Atlantic between 25°S and 40°S. Meeresforschung 29:17–29.

**Kjerfve, B.**
**1989.** Estuarine geomorphology and physical oceanography. *In* Estuarine ecology (J. W. Day, C. A. S. Hall, W. M. Kemp, and A. Yáñez-Arancibia, eds.), p.47–78. John Wiley & Sons, New York, NY.

**Largier, J. L.**
**1993.** Estuarine fronts: How important are they? Estuaries 16(1):1–11.

**Lasta, C. A., and J. D. de Ciechomski.**
**1988.** Primeros resultados de los estudios sobre la distribución de huevos y larvas de peces en Bahía Samborombón en relación a temperatura y salinidad. Publ. Com. Téc. Mix. Fr. Mar. 4:133–141.

**Lawler, J. P., M. P. Weinstein, W. Y. Chen, and T. L. Englert.**
**1988.** Modelling of physical and behavioral mechanisms influencing recruitment of spot and Atlantic croaker to the Cape Fear estuary. Am. Fish. Soc. Sym. 3:115–131.

**Macchi, G. J., and E. M. Acha.**
**2000**. Spawning frequency and batch fecundity of Brazilian menhaden, *Brevoortia aurea*, in the Río de la Plata estuary off Argentina and Uruguay. Fish. Bull. 98:283–289.

**Macchi, G. J., E. M. Acha, and C. A. Lasta.**
**1996.** Desove y fecundidad de la corvina rubia (*Micropogonias furnieri*, Desmarest, 1826) en el estuario del Río de la Plata, Argentina. Bol. Inst. Español Oceanogr. 12:99–113.

**Madirolas, A., E. M. Acha, R. A. Guerrero, and C. A. Lasta.**
**1997.** Sources of scattering near an estuarine frontal system. Sci. Mar. 61(4):431–438.

**Mann, K. H., and J. R. N. Lazier.**
**1991.** Dynamics of marine ecosystems: biological-physical interactions in the oceans. Blackwell Science Publications, Boston, MA, 466 p.

**Nellen, W., and G. Hempel.**
**1969.** Versuche zur Fängigkeit des "Hai" und des modifizierten Gulf-V-Plankton-Samplers "Nackthai." Ber. Deuts. Wiss. Komm. Meeres. 20:141–154.

**Nelson, W. R., M. C. Ingham, and W. E. Schaaf.**
**1977.** Larval transport and year-class strength of Atlantic menhaden, *Brevoortia tyrannus*. Fish. Bull. 75(1):23–41.

**Norcross, B. L., and R. F. Shaw.**
**1984.** Oceanic and estuarine transport of fish eggs and larvae: a review. Trans. Am. Fish. Soc. 113:153–165.

**Officer, C. B.**
**1992.** Physics of estuarine circulation. *In* Ecosystems of the world, vol. 26, Estuaries and enclosed seas (B. H. Ketchum, ed.), p. 15–41. Elsevier, Amsterdam.

**Potter, I. C., G. A. Hyndes, and F. M. Baronie.**
**1993.** The fish fauna of a seasonally closed Australian estuary. Is the prevalence of estuarine-spawning species high? Mar. Biol. 116:19–30.

**Powell, A. B.**
**1994.** Life history traits of two allopatric clupeids, Atlantic menhaden and gulf menhaden, and the effects of harvesting on these traits. N. Am. J. Fish. Manage. 14:53–64.

**Sánchez, R. P., and J. D. de Ciechomski.**
**1995.** Spawning and nursery grounds of pelagic fish species in the sea-shelf off Argentina and adjacent areas. Sci. Mar. 59(3-4):455–478.

**Shaw, R. F., J. H. Cowan Jr, and T. L. Tillman.**
**1985.** Distribution and density of *Brevoortia patronus* (gulf menhaden) eggs and larvae in the continental shelf waters of western Louisiana. Bull. Mar. Sci. 36(1):96–103.

**Sinclair, M., and T. D. Iles.**
**1989.** Population regulation and speciation in the oceans. J. Cons. Int. Explor. Mer 45:165–175.

**Sinque, C., and J. H. Muelbert.**
**1997.** Environment and biota of the Patos Lagoon Estuary: ichthyoplankton. *In* Subtropical convergence environments: the coast and sea in the Southwestern Atlantic (Seeliger et al., eds.), p. 51–56. Springer-Verlag, Heidelberg.

**Vaughan, D. S.**
**1991.** Menhaden: the resource, the industry, and a management history. Preface. Mar. Fish. Rev. 53(4):1–2.

**Warlen, S. M.**
**1988.** Age and growth of larval gulf menhaden, *Brevoortia patronus*, in the northern Gulf of Mexico. Fish. Bull. 86(1):77–90.
**1992.** Age, growth and size distribution of larval Atlantic menhaden off North Carolina. Trans. Am. Fish. Soc. 121: 588–598.

**Weiss, G.**
**1981.** Ictioplancton del estuario de Lagoa dos Patos, Brasil. Ph.D. diss., Univ. Nacional de La Plata, Facultad de Ciencias Naturales y Museo, La Plata, Argentina, 164 p.

**Weiss, G., and L. C. Krug.**
**1977.** Características do desenvolvimento e metamorfose de *Lycengraulis olidus* (Engraulidae) e *Brevoortia pectinata* (Clupeidae) no estuário da Lagoa dos Patos, Brasil. Atlântica 2(1):83–117.

**Weiss, G., J. A. Souza, and A. Santos.**
**1976.** Contribuição ao conhecimento do ictioplancton marinho da plataforma sul do Brasil. Atlântica 1(1/2):7–78.

**Whitehead, P. J. P.**
**1985.** Clupeoid fishes of the world: an annotated and illustrated catalogue of the herrings, sardines, pilchards, sprats, anchovies and wolf-herrings. Part I: Chirocentridae, Clupeidae and Pristigasteridae. FAO Fisheries Synopsis 125, vol. 7, 303 p.

# Management of the sandbar shark, *Carcharhinus plumbeus*: implications of a stage-based model*

**Karyl K. Brewster-Geisz**
Highly Migratory Species Management Division
National Marine Fisheries Service
1315 East West Highway
Silver Spring, Maryland 20910
E-mail address: Karyl.Brewster-Geisz@noaa.gov

**Thomas J. Miller**
Chesapeake Biological Laboratory
University of Maryland Center for Environmental Sciences
P. O. Box 38
Solomons, Maryland 20688-0038

**Abstract.**–Sandbar sharks (*Carcharhinus plumbeus*) support an important commercial fishery. They are managed as a component of a multispecies group, termed large coastal sharks, by the National Marine Fisheries Service (NMFS) under the Fishery Management Plan (FMP) for Atlantic sharks. Currently, large coastal sharks, generally, and sandbar sharks, specifically, are considered overfished. Several management options, including nursery ground closures and size limits, are being considered to conserve the fishery. We explored the implications of management options for large coastal sharks within the framework of a stage-based model. Based on biological criteria, the life cycle of the sandbar shark was represented as five stages: neonate, juvenile, subadult, pregnant adults, and resting adults. The model followed only females. From a fishing mortality rate ($F$) of 0.20, estimated in the 1996 stock evaluation workshop (SEW), the model projects a population decline to 13% of its current abundance within 20 years. The population is not stabilized until $F$ is reduced to 0.07. In one run of the model, we assumed that $F$ on neonates and pregnant adults was zero in order to assess the impact of a "perfect" nursery ground closure. Under this scenario, the population continued to decline unless $F$ on the remaining stages was reduced to 0.097. Even with the closure of nursery grounds or the introduction of size limits to protect neonates and juveniles, $F$ has to be reduced substantially. The model is highly sensitive to the dynamics of juveniles and subadults, which implies that management should protect these immature sharks to rebuild the stock.

Manuscript accepted 26 November 1999.
Fish. Bull. 98:236–249 (2000).

The sandbar shark (*Carcharhinus plumbeus*) is a species of primary importance in the Atlantic and Gulf of Mexico shark fishery (NMFS, 1993; NMFS[1]; Branstetter and Burgess[2]). It is managed as a part of the large coastal shark group defined under the Atlantic shark Fishery Management Plan (FMP; NMFS, 1993). Since the mid 1980s, the demand for shark has increased (NMFS, 1993). The fishery peaked in 1989 with landings of approximately 4600 metric tons (t) dressed weight (dw; NMFS[3]). Catch per unit of effort of large coastal sharks declined rapidly during the 1970s and 1980s. To prevent overfishing, the FMP imposed an annual quota of 2570 t dw from 1994 to 1996 for the large coastal fishery, required mandatory reporting of landings, and prohibited the removal of fins (NMFS, 1993). At the 1996 stock evaluation workshop (SEW), scientists found no evidence of improvements in the large coastal stocks and recommended reducing fishing mortality by 50% (NMFS, 1996). In response, the National Marine Fisheries Service (NMFS) reduced the annual quota in 1997 by 50% to 1285 t dw and reported to Congress that large coastal sharks were overfished (NMFS, 1997). The most recent data indicate that fishing mortality rates have not declined as much as expected and may still be too high to stabilize the sandbar shark stock (NMFS[4]). A size limit equivalent to approximately 12–13 years of age (140 cm fork length) was recommended.

The NMFS is mandated, through the Magnuson-Stevens Fishery Conservation and Management Act, to

* Contribution 3264 of the University of Maryland Center for Environmental Sciences Series, Chesapeake Biological Laboratory, University of Maryland, Solomons, MD 20688-0038.

[1] 1996. Report of the shark evaluation workshop. Southeast Fisheries Science Center, Natl. Mar. Fish. Serv., NOAA, Miami, FL, 80 p.

[2] Branstetter, S., and G. Burgess. 1997. Continuation of an observer program to characterize and compare regional efforts in the directed commercial shark fishery in the eastern Gulf of Mexico and South Atlantic. Gulf and South Atlantic Fisheries Development Foundation, Inc., Tampa, FL. University of Florida, Gainesville, FL., 83 p.

[3] 1997. Shark evaluation annual report. Southeast Fisheries Science Center, Natl. Mar. Fish. Serv., NOAA, , Miami, FL, 12 p.

[4] 1998. Report of the shark evaluation workshop. Southeast Fisheries Science Center, Natl. Mar. Fish. Serv., NOAA, Panama City, FL.

rebuild the large coastal stocks to the optimum yield level. In October 1998, the NMFS released a draft FMP for Atlantic tunas, swordfish, and sharks. The measures in this FMP were designed to halt overfishing and to rebuild these stocks. Management options under consideration for large coastal sharks included restrictions on effort, size limits, and area closures that were focused on nursery grounds.

Many traditional approaches that could be used to compare management options, such as surplus production models or age- and size-structured approaches, rely on catch or effort data, or both. However, because logbook reporting in the shark fishery was not mandatory until 1993, fishery-dependent time series have been insufficiently long to permit reliable application of these approaches. Yet a comparison of the efficacy of the potential management options is still required. The paucity of fishery-dependent data suggests that demographic approaches, such as life-table or stage-based analyses, may be the appropriate tools to explore the potential response of shark populations to management actions.

Life-table analysis is a common age-structured demographic approach with a long history in population dynamics (Kingsland, 1985). It is a matrix projection approach that estimates the contribution of each age class to future generations. Sminkey and Musick (1996) applied a life-table approach to sandbar sharks. From the intrinsic rate of natural increase, $r$, predicted by the model, they concluded that the population could not sustain the observed rates of fishing mortality. Heppell et al. (1999) developed matrix-based life tables for leopard (*Triakis semifasciata*) and angel (*Squatina californica*) sharks. Heppell et al. calculated the elasticity or proportional sensitivity of the population growth rate to changes in survival and fecundity and concluded that the two species differ in the degree to which each can compensate for changes in exploitation. Simpfendorfer (1999) developed a life table for the dusky shark (*Carcharhinus obscurus*). He concluded that in the absence of exploitation, dusky shark populations in southwestern Australia would increase at 4.3% annually. Analysis also indicated that current patterns of exploitation were sustainable. However, there are problems in application of life-table analysis to long-lived marine species. The intrinsic rate of natural increase predicted is dependent on the products of survival and fecundity for all ages and the estimated generation time. Thus, life tables require estimates of the schedules of mortality (survival) and fecundity over the entire age range (Gotelli, 1995). Consequently, in a long-lived species such as the sandbar shark, small errors in parameter estimates can become magnified.

Stage-based modeling is a matrix-based demographic approach that considers aggregate stages (defined in terms of size or life history stages) that represent functional biological units (Gotelli, 1995). It too has a long history in the field of ecological population dynamics (Kingsland, 1985). A stage-based model can be formed by collapsing a life table into discrete stages. Thus, unlike the life-table analysis that requires estimates for every year the organism lives, the stage-based model requires only estimates for each stage. Therefore, the realism of a many-staged model can be balanced with the precision of a simpler model when parameter estimation error is of concern. As with life tables, stage-based projection models can easily be solved analytically to permit formal sensitivity analysis (Caswell, 1989). Anderson (1990), and Hoenig and Gruber (1990) have suggested that stage-based models may provide a more realistic view of the dynamics of some populations.

The population dynamics of several marine species, including sandbar sharks (Cortés, 1999), sea turtles (Crouse et al., 1987; Crowder et al., 1994), blue crabs (Miller and Houde[5]), sardines (Lo et al., 1995), and anchovies (Pertierra et al., 1997) have been explored by using stage-based models. Cortés (1999) developed a stochastic stage-based model for sandbar sharks in the western North Atlantic. He used the model to explore the implications of three different harvest strategies on population viability when fecundity varies. He concluded that in the absence of exploitation, the sandbar shark population should increase slowly by about 1.3% annually. Additionally, Cortés concluded that all three patterns of exploitation would cause declines in population abundance. Cortés' model and results indicate the utility of stage-based models in exploring potential management alternatives for sandbar sharks.

Here, we develop a deterministic stage-based model for sandbar shark populations. The model includes the two-year reproductive cycle of fertile and resting periods known to occur in sandbar sharks, but which were not included in Cortés's (1999) original description. We chose to use a deterministic framework to permit a formal elasticity (proportional sensitivity) analysis of the basic model. Stages to which the population dynamics are most sensitive can be interpreted either as being stages at which management action is likely to have the most impact or as stages at which parameter estimates have to be most precise because of impacts of potential environmental stochasticity. We use the model to examine the expected change in population growth resulting from

[5] Miller, T. J., and E. D. Houde. 1998. Blue crab targeting. U.S. EPA Chesapeake Bay Program Report, Annapolis, MD, 167 p.

two particular management options, nursery ground closures and size limits. We exercised the general model framework to address four fundamental questions. What is the intrinsic rate of increase of sandbar shark populations under current patterns of exploitation? What is the sustainable level of fishing mortality ($F_{CRITICAL}$)? What is the effect of eliminating fishing mortality on early stages, either through nursery ground closures or through the introduction of size limits? For each question, we provide the results, predictions, and interpretation of sensitivity analyses to indicate the reliability of our conclusions.

## Materials and methods

### Life history of sandbar sharks

The first step in developing a stage-based model is to review the life history of a species to identify appropriate stages. Results of tagging and age and growth studies (Springer, 1960; Casey et al., 1985; Casey and Natanson, 1992; Sminkey and Musick, 1995, 1996) indicate that sandbar sharks are a long-lived species with low fecundity. These studies also indicate that females, males, and juveniles segregate by water depth and distance from shore. However, estimates of key vital rates are inconsistent. The generally accepted estimate of mortality and fecundity schedules indicates that sandbar sharks mature between 12 and 15 years of age and live to around 30 years of age (Casey et al., 1985; Sminkey and Musick, 1996). Another estimate suggests that sandbar sharks may not mature until age 29 and may live past 50 (Casey and Natanson, 1992). In our model we used an age at maturity of 15 years. From the biological function and the migration pathways determined by these studies, we identified five stages in the life history of the sandbar shark: neonates, juveniles, subadults, pregnant adults, and resting adults (Fig. 1).

Neonates are young-of-the-year sharks. Sandbar shark neonates are born fully developed at a fork length (FL) between 43 and 52 cm (Castro, 1983; Branstetter and Burgess[1]). They remain in this stage for one year before becoming juveniles. Juveniles are the first stage to show a seasonal pattern of movement. In the winter, juveniles migrate to warmer waters, often to the edge of the Gulf Stream off North Carolina. In the summer, juveniles return to their nursery grounds. They continue this seasonal migration until they are between 6 and 10 years old (Casey et al., 1985; Branstetter and Burgess[1]). In contrast, subadults, while still not yet mature, follow the adult migration pattern. This migration pattern consists of swimming along the Atlantic coast of the United States as far north as New England

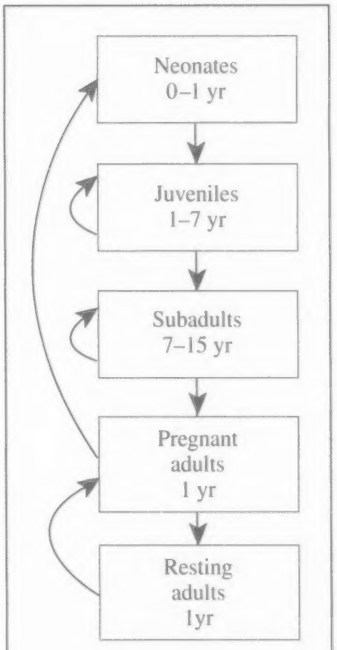


**Figure 1**
Diagram of the five-stage model. Arrows indicate individuals surviving and growing to the next stage or surviving and remaining in the same stage.

in the summer and traveling south to warmer waters in the winter (Castro, 1983). In this model, individuals remain in the subadults stage for 8 years, at which point they may be 15 years of age, and then join the reproductive population.

Fifty percent of female sandbar sharks are mature at about 150 cm FL (Springer, 1960; Casey et al., 1985; Sminkey and Musick, 1996) or 12 to 15 years of age depending on the von Bertalanffy model. Female sandbar sharks give birth at an average of 8 or 9 pups once every other year (Springer, 1960; Sminkey and Musick, 1996). Larger sharks do not appear to give birth to a greater number of pups (Sminkey and Musick, 1996). Gestation lasts between 9 and 12 months (Castro, 1983). Pregnant females pup in shallow bays and estuaries along the east coast of North America, including Chesapeake Bay (Sminkey and Musick, 1996), Delaware Bay (Pratt and Merson[6]) and the waters off the coast of South Caro-

[6] Pratt Jr., H. L., and R. R. Merson. 1996. Report of the 1996 apex predators investigation: sandbar shark nursery grounds project. Apex predators investigation. Northeast Fisheries Science Center, Natl. Mar., Fish. Serv., NOAA, Narragansett, RI.

lina (Castro, 1993). In the model, females alternate between pregnant and resting adult stages, spending one year in each. Thus, the stage durations used in the model were the following: 1 year for neonates; 6 years for juveniles; 8 years for subadults; 1 year for pregnant females; and 1 year for resting females.

### Model development

The approach we present below is based on the general framework presented by Caswell (1989). Details on the general background of the approach can be found in Caswell (1989). In all equations, matrices and vectors are shown in boldface type, parameters in italic type.

The model is a postbreeding census, follows only females, and uses a yearly time step. The total number of sharks in the population at time $t$ can be expressed in vector form as $\mathbf{N}_t$. Each element of $\mathbf{N}_t$ represents the number of sharks in the appropriate stage at time $t$. There are three possible transitions for each individual in each stage: the probability of surviving and growing to the next stage, $G_i$; the probability of surviving yet remaining in the same stage, $P_i$; or the probability of dying, $1–G_i–P_i$. The individual transition probabilities $G_i$ and $P_i$ may range between 0 and 1. The sum of $G_i$ and $P_i$ is further constrained such that when a stage is not subject to mortality, $G_i + P_i = 1$. One other parameter, stage-specific fecundity, is required to estimate the number of young females produced per breeding female per year.

The vital rates governing the dynamics of the shark population can be expressed mathematically in a $5 \times 5$ transition matrix, $\mathbf{A}$. The fundamental equation to estimate the stage-structure in the population at any time $t$ is given by

$$\mathbf{N}_t = \mathbf{A}^t - \mathbf{N}_0, \tag{1}$$

where $\mathbf{N}_t$ = a vector of the number of individuals in each stage at time $t$; and
$\mathbf{A}$ = the transition matrix $\mathbf{A}$ for sandbar sharks given by

$$\begin{bmatrix} 0 & 0 & 0 & G_4 \times f_4 & 0 \\ G_1 & P_2 & 0 & 0 & 0 \\ 0 & G_2 & P_3 & 0 & 0 \\ 0 & 0 & G_3 & 0 & G_5 \\ 0 & 0 & 0 & G_4 & 0 \end{bmatrix}. \tag{2}$$

For large values of $t$, $\mathbf{AN}_t = \lambda\mathbf{N}_t = \mathbf{N}_{t+1}$, where the scalar $\lambda$ is the finite rate of population increase. Further, $\ln\lambda = r$, the intrinsic rate of increase.

The columns of the matrix represent the fates of individuals in each stage. For example, surviving neonates can grow only to the juvenile stage ($G_1$) whereas surviving juveniles can either remain a juvenile ($P_2$) or survive and grow into a subadult ($G_2$). Surviving pregnant adults can give birth and become resting adults ($G_4$). Surviving resting adults ($G_5$) can grow only into a pregnant female. The rows represent the origins of individuals in each stage. Neonates arise from pregnant adults who survive ($G_4 \times f_4$) whereas juveniles arise from neonates surviving and growing into juveniles ($G_1$) or from juveniles surviving and remaining juveniles ($P_2$). Pregnant adults can arise from subadults surviving and growing into a pregnant female ($G_3$) or from resting adults surviving and becoming pregnant adults ($G_5$). Resting adults can arise only from pregnant adults that survive ($G_4$).

The transition probabilities, $P_i$ and $G_i$, can be calculated from estimates of the probability that during a single time step an individual of stage $i$ survives, $\sigma_i$, and an individual of stage $i$ grows, $\gamma_i$. In this way $G_i$, the probability of surviving and growing to the next stage is given by

$$G_i = \sigma_i\gamma_i. \tag{3}$$

Consequently $P_i$, the probability of surviving, but not growing to the next stage is given by

$$P_i = \sigma_i(1 - \gamma_i). \tag{4}$$

The probability of survival, $\sigma_i$, over a single time step can be expressed as

$$\sigma_i = e^{-Z_i}. \tag{5}$$

Following traditional fisheries models, total mortality ($Z_i$) is calculated by using the equation $Z_i = F_i + M_i$, where $F_i$ is the rate of fishing mortality and $M_i$ is the rate of natural mortality at stage $i$.

Estimates of $\gamma_i$ can be obtained in several different ways. Caswell (1989) recommended assuming constant stage duration for all individuals in the stage when only a relatively crude estimate of survival over broad age ranges is available. For this approach, individuals entering the stage have an equal probability of survival as individuals nearing the end of the stage. Employing this assumption yields an estimate of $\gamma_i$ as

$$\gamma_i = \frac{(\sigma_i/\lambda_{init})^T - (\sigma_i/\lambda_{init})^{T-1}}{(\sigma_i/\lambda_{init})^T - 1} \tag{6}$$

where $T$ = the expected stage duration of a single stage; and

$\lambda$ = the finite rate of population increase given by the dominant eigenvector of A ($\ln\lambda=r$, the intrinsic rate of increase).

We began with an initial value of $\lambda_{init} = 1$. We then iterated $\lambda$ until the value of $\lambda$ given by an eigenanalysis of the matrix **A** (see below), equaled the value of $\lambda_{init}$ used in Equation 6. Together, Equations 1–6 described above allow estimates of $G_i$ and $P_i$ within **A** to be defined.

Fecundity must also be defined. The fecundity term, $f_i$, is simply the expected number of female offspring produced by a female in stage $i$. For sandbar sharks only one stage is reproductively active and thus the only fecundity term in the matrix **A** is $f_4 = 4.5$. This estimate is based on an equal sex ratio, 9 pups per brood, and one brood per year. However, as the model is a postbreeding census, the fecundity has to be discounted by the probability that a pregnant female will survive the gestation year to pup. Thus the realized fecundity term used in the model is $G_4 \times f_4$. All parameters within the matrix **A** are now defined.

One feature of stage-based projection models that motivated their use was that they allowed us to solve **A** analytically in order to calculate important demographic features and find the sensitivity of the model to parameter estimates. The two demographic features that can be calculated from **A** are the stable stage distribution and the reproductive value of each stage. Once the stable stage distribution has been reached, the relative proportion of individuals in each stage remains constant over time. The reproductive value is the relative number of offspring that are yet to be born by individuals in a given age (Gotelli, 1995). This value depends on individuals surviving to maturity and reproducing. Thus, the youngest stages should have the lowest reproductive values because individuals in those stages must survive and reach maturity before they can reproduce. Both features can be calculated from an eigenanalysis of **A**. For any $\{n\times n\}$ matrix one may define up to $n$ scalar values ($\lambda_{1..n}$) and $n$-associated right and left vectors such that

$$\mathbf{Aw} = \lambda\mathbf{w} \tag{7}$$

$$\mathbf{vA}^{\mathrm{T}} = \lambda\mathbf{v} \tag{8}$$

where $\mathbf{A}^{\mathrm{T}}$ = the transpose of **A**;
$\lambda$ = the eigenvalue; and
**w** and **v** = the right and left eigenvectors of **A**.

The sandbar shark transition matrix has five possible eigenvalues and eigenvectors. However, our interpretation is simplified for the sandbar shark transition matrix, **A**, because it is non-negative, irreducible, and primitive. Thus, we are guaranteed that there is a single, dominant eigenvalue, $\lambda_1$, that is real, positive, and strictly greater than all other possible $\lambda$s. This dominant eigenvalue, $\lambda_1$ will eventually describe the population rate of increase and $\ln \lambda_1 = r$, the intrinsic rate of increase of the population. Moreover, the right and left eigenvectors associated with $\lambda_1$ will be strictly positive. The population structure will eventually become proportional to a single stable stage distribution, given by $\mathbf{w_1}$. Finally, there will be a single vector, $\mathbf{v_1}$, associated with $\lambda_1$, that expresses the relative contributions of each stage to the future population—a vector of reproductive values. Reproductive values are standardized so that the reproductive value of an individual in the first stage is one.

We were interested in calculating the change in $\lambda$ following a change in vital rates expressing a transition from stage $i$ to any other stage (including remaining in $i$) that may have been caused by management activities. This change reflects the sensitivity of $\lambda$ to the transition probability. If entries in the transition matrix **A** are represented as $a_{i,j}$, it can be shown that

$$\frac{\partial\lambda}{\partial a_{ij}} = \frac{v_i w_i}{\langle w,v\rangle}. \tag{9}$$

where <**w**,**v**> = the scalar product of the two vectors.

Simply stated, the sensitivity of the population growth rate to changes in any vital rate is the product of the reproductive value of stage $i$ and the proportional level of stage $j$ in the stable stage distribution.

Because transition probabilities are censored parameters, varying only between 0 and 1, and fecundity is noncensored, it is more helpful to report the elasticity of $\lambda$. This is defined as the proportional change in $\lambda$ for proportional changes in $a_{i,j}$. Elasiticities are calculated as

$$e_{ij} = \frac{a_{ij}}{\lambda}\frac{\partial\lambda}{\partial a_{ij}}. \tag{10}$$

Importantly, elasticities are additive, such that the sum of elasticities for each stage defines the proportional contribution of $a_{ij}$ to overall population growth, $\lambda$, as

$$\sum_i\sum_j e_{ij} = 1.$$

Elasticities depend on a stable stage distribution and should be compared qualitatively.

### Transition probability estimation for management options

**Current conditions** Fishing mortality ($F$) and especially natural mortality ($M$) are difficult to estimate. Owing to the uncertainty in estimates and in order to simplify the model, we used an estimate of $M = 0.1$ for all stages and all projections (NMFS[1]; Sminkey and Musick, 1996). We projected the population forward using $F = 0.20$ for juveniles and older stages, as estimated in the 1996 shark evaluation workshop (SEW) for sandbar sharks only (NMFS[3]). For neonates a lower value of $F = 0.10$ was used because small sharks may be, but are not as likely to be, caught on the same gear as older sharks (Branstetter and Burgess[1]). Using these values of $F$ and $M$ and $f_4$=4.5, we iterated Equation 6 to estimate all $P_i$ and $G_i$ values. We initialized the population with 1000 neonates. Then we estimated the initial number in subsequent stages using the 90% survival schedule for sandbar sharks given in Sminkey and Musick (1996). These calculations yielded an initial population of 9640 sharks ($N_0$).

**Estimate of $F_{CRITICAL}$** We defined $F_{CRITICAL}$ as the limiting level of fishing mortality that is sustainable, i.e. the $F$ for which $r = 0$ or $\lambda = 1$, where $r = \ln\lambda$. We systematically reduced $F$ on all stages to define the relationship between $F$ and $r$. For our estimations, $F_1$ remained 0.10 as long as $F_{2,3,4,5}$ was ≥0.10. For any $F_{2,3,4,5} < 0.10$, $F_1 = F_{2,3,4,5}$. Thus, the fishing mortality of neonates was never greater than the fishing mortality on other stages.

**Protecting neonates and pregnant adults: an extreme example** We used the model to determine how efficient protecting different stages would be in promoting recovery of sandbar shark stocks. We asked the question: If neonates and pregnant adults are removed from the commercial fishery, how much will $F$ on other stages need to be reduced to arrive at a sustainable population level? To address this question, we modified the model to remove all mortality on neonates ($F_1$=0, $M_1$=0) and to protect all pregnant adults from fishing pressure ($F_4$=0). In reality, we could not completely protect neonates from mortality (i.e. $M_1$>0) and we could not fully protect pregnant adults from commercial fishing. Thus the scenario represents an idealized nursery closure scheme. Fishing mortality on juveniles, subadults, and resting adults remained at 0.20. The fecundity for pregnant adults was left at 4.5.

**Nursery closures and size limits** We also ran the model using more realistic scenarios. In this case $F$ on neonates and juveniles was 0, and $F$ on the older stages was 0.20. Natural mortality for all stages remained at 0.10. This scenario is a fairly realistic size limit or nursery ground closure because sandbar sharks segregate by size. This scenario is similar to, but not as strict as, the 1998 SEW's recommended size limit.

Size limits protecting only one stage are another management option available. This method can be used to reduce the fishing mortality on any range of sizes. In this paper, two scenarios of this type are presented: 1) a size limit which reduces the $F$ on juveniles to 0; and 2) a size limit which reduces the $F$ on subadults to 0. Fishing mortality was equal to 0.20 in all other stages except neonates, where $F$=0.10. Implementing such management actions would be difficult because the gear (longlines) cannot realistically avoid catching only the restricted stage, but the results would be indicative of the potential of these mechanisms to improve stocks.

Using the relationships (Eqs. 1–10) and vital rate estimates defined above, we now proceed with an analysis of the population dynamics of sandbar sharks. For each scenario, we calculate the stable stage distribution, the proportional reproductive value for each stage, and the elasticity of $\lambda$ to changes in each matrix parameter, and compare the population growth rate and potential population reduction after 20 years for each scenario.

## Results

### Current conditions

When $F = 0.20$ for all stages except neonates, the population decreases (Table 1). The model predicts the intrinsic rate of natural increase, $r$, of the population as $r = -0.124$. The population is 13% of the initial abundance when projected 20 years forward. Population growth rate, stable stage distribution, and reproductive values are not affected by choice of the actual numbers used for initial abundance. The stable stage distribution is reached after 21 years in this scenario.

The largest proportion of the population (>0.56) are juveniles (Table 2). The smallest proportions (0.04, 0.03) are pregnant and resting adults, respectively. Adults have much larger reproductive values than prereproductive stages (Table 3).

The pattern of model proportional sensitivity is shown in Figure 2. The elasticity of $\lambda$ to a small change in fecundity was expressed only in the preg-

**Table 1**

The reduction in population abundance after 20 years of each scenario.

| Scenario | Fishing and natural mortality rates used | Intrinsic rate of increase, $r$ | Reduction (%) in population abundance after 20 years[1] |
|---|---|---|---|
| Current conditions | $F_1$=0.10; $F_{2-5}$=0.20 $M$=0.10 | –0.124 | 87 |
| Protecting neonates and pregnant adults | $F_{1,4}$=0; $F_{2,3,5}$=0.20 $M_1$=0; $M_{2-5}$=0.10 | –0.079 | 62 |
| Protecting neonates and juveniles | $F_{1,2}$=0; $F_{3-5}$=0.20 $M$=0.10 | –0.058 | 51 |
| Protecting juveniles only | $F_1$=0.10; $F_2$=0 $F_{3-5}$=0.20; $M$=0.10 | –0.069 | 62 |
| Protecting subadults only | $F_1$=0.10; $F_3$=0 $F_{2,4,5}$= 0.20; $M$=0.10 | –0.048 | 50 |

[1] This percent reduction in population abundance is based on numbers generated in the model. Population abundance can also be calculated by using the equation

$$1 - e^{rt},$$

where $r$ = the intrinsic rate of increase; and
$t$ = the number of years.

Use of this equation results in a greater reduction in the population abundance.

**Table 2**

The stable stage distributions for each stage of the model and each scenario. The values of all stages under a scenario should sum to one.

| Model stage | Current conditions, unstablized | Current conditions, stablized | Protecting neonates and pregnant adults | Protecting neonates and juveniles | Protecting juveniles | Protecting subadults |
|---|---|---|---|---|---|---|
| Neonate | 0.15 | 0.16 | 0.15 | 0.10 | 0.12 | 0.19 |
| Juvenile | 0.56 | 0.54 | 0.60 | 0.54 | 0.51 | 0.51 |
| Subadults | 0.22 | 0.22 | 0.18 | 0.31 | 0.31 | 0.21 |
| Pregnant adults | 0.04 | 0.04 | 0.03 | 0.03 | 0.03 | 0.05 |
| Resting adults | 0.03 | 0.04 | 0.03 | 0.02 | 0.03 | 0.04 |

nant adult stage (because this is the only stage that is reproductively active). The highest elasticities were for the transition from neonate to juvenile and juvenile to subadult stages (Fig. 2). The elasticities for sharks remaining in the stage were equal for neonate, juvenile, subadult, and pregnant female stages. As discussed, the individual elasticities can be summed to estimate the overall contribution of each stage to $\lambda$. It is clear from Figure 2 that the peak elasticity occurs in the subadult stage. Estimates of elasticity suggest that the model is 2.3 times more sensitive to changes in this stage than in pregnant adults.

## Estimate of $F_{CRITICAL}$

The relation between $F$ and $r$ is linear (Fig. 3). $F_{CRITICAL}$ = 0.071 when $M$ = 0.10. Therefore, the population is sustainable if $F$ = 0.071. The value of $F_{CRITICAL}$ will vary with the value of $M$ that is chosen. Our analyses showed that total mortality ($Z$) must be less than 0.17 for all stages if the population is to increase (Fig. 4). The population will increase at a rate $r$ = 0.05 if $Z$ = 0.122, and the population will decrease at a rate $r$ = –0.05 if $Z$ = 0.222.

At $F_{CRITICAL}$, the population abundance stabilizes and the population reaches a stable stage distribu-

**Table 3**

The proportional standardized reproductive values of each stage under each scenario. Neonates will always equal one.

| Model stage | Current conditions, unstablized | Current conditions, stablized | Protecting neonates and pregnant adults | Protecting neonates and juveniles | Protecting juveniles | Protecting subadults |
|---|---|---|---|---|---|---|
| Neonate | 1.00 | 1.00 | 1.00 | 1.00 | 1.00 | 1.00 |
| Juvenile | 1.08 | 1.19 | 0.92 | 1.04 | 1.26 | 1.29 |
| Subadults | 3.10 | 3.32 | 3.48 | 1.34 | 1.52 | 5.83 |
| Pregnant adults | 12.72 | 13.06 | 20.44 | 9.23 | 9.65 | 8.84 |
| Resting adults | 10.67 | 11.00 | 16.38 | 7.25 | 7.66 | 6.87 |

tion (Table 2). In this scenario, the proportion of neonates, pregnant adults, and resting adults in the population has increased compared with the proportion of stages in previous scenarios. The pattern in reproductive values remains largely unchanged (Table 3). As with the baseline scenario, the elasticities show the model to be the most sensitive to changes at the juvenile and subadult stages.

In summary, these model runs suggest that to stabilize and increase the sandbar shark population, $F$ needs to be reduced below 0.07 ($Z \leq 0.17$). An $F$ of this magnitude requires more than the full 50% quota reduction to be implemented.

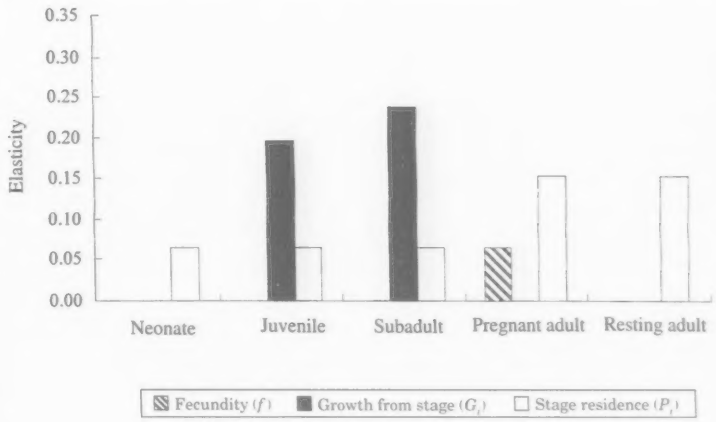


**Figure 2**

The proportional sensitivities (elasticity) of each stage to fecundity, growth, and stage residence under current fishing conditions ($F$=0.20).

### Protecting neonates and pregnant adults: an extreme example

Results show that, even after protection of neonates and pregnant females, at current levels of $F$ the population still decreases rapidly ($r$=–0.079). The population, projected 20 years forward, is only 38% of the initial abundance (Table 1). This percentage compares with reductions to 13% of initial abundance and $r$=–0.124 in the base run, where $F_{2,3,4,5} = 0.2$. In order to have a stable population ($r$=0) under this scenario, we needed to decrease $F$ to 0.097. Without protecting neonates and pregnant females, $F$ must be reduced to 0.07. Thus, protecting neonates and pregnant females provides a 37% increase in the $F$ required to maintain a sustainable population (Table 4). However, it must be emphasized that although this option does provide some protection, implementation would still require a 52% reduction in $F$ over those levels currently estimated to be operating in the fishery. This reduction is in contrast to the 64% reduction in $F$ required to reach sustainable rates of exploitation in the absence of this protection.

Juveniles had the highest proportion of individuals in the stable stage distribution (Table 2). Pregnant females and resting adults have the highest reproductive values (Table 3). Similar to the previous scenario, projections show the highest overall sensitivity to transitions involving the abundance of subadults (Fig. 5). However, in contrast with earlier simulations, projections show additional substantial sensitivity to transitions into the resting adult stage (Fig. 5).

### Nursery ground closures and size limits

Results of this scenario show that the protection of neonates and juveniles from all fishing mortality slowed the decline ($r$=–0.058) but could not stabilize the population. When projected forward 20 years, the population abundance is 49% of the initial abundance (Table 1). In order to stabilize this model, $F$ had to be reduced on subadults and adults to 0.109. Thus, this closure provides a 54% increase in the $F$ required to maintain a sustainable population over that required in the absence of nursery closures and a 12% increase in $F$ over the extreme option modeled above (Table 4). Protecting neonates and juveniles through nursery ground closures or size limits would require a 46% reduction in $F$ over those levels currently estimated to be operating in the fishery.

Juveniles have the highest proportion of individuals in the stable stage distribution (Table 2). Pregnant adults and resting adults have the highest reproductive values (Table 3). Again, the model shows the highest sensitivities to the juvenile and subadults stages (Fig. 6).

Protecting either juveniles or subadults alone still leads to a declining population. When $F_2$=0, after 20 years the population is 38% that of the initial population (Table 1). When $F_3$=0, the population at 20 years is 50% that of the initial population (Table 1). Further runs indicated that the population is stabilized if $F_{3,4,5}$ = 0.101 (when $F_2$=0) or if $F_{2,4,5}$ = 0.120 (when $F_3$=0). Quota reductions of 50% and 40%, respectively, are required to achieve these critical levels of $F$. In both cases the stable stage distribution is achieved within 24 years. The stable stage distribution proportions and reproductive values of each stage are listed in Tables 2 and 3. Figure 7 shows the sensitivity of the model to fecundity, growth, and stage residence when $F_2$ = 0. These sensitivities were approximately the same when $F_3$ = 0. As in the other models, juveniles and subadults have the highest sensitivity.

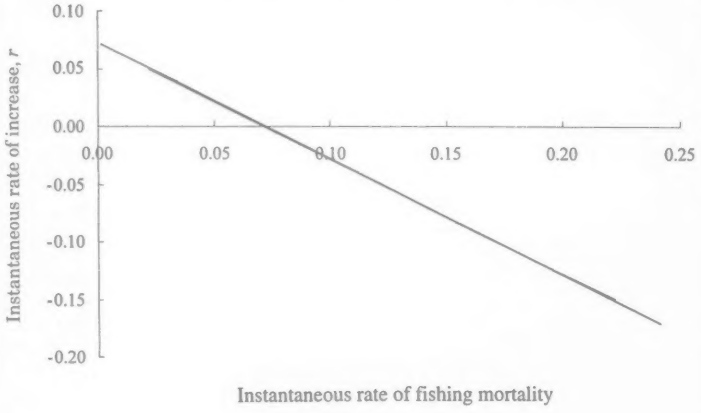


**Figure 3**

The relation between the intrinsic rate of increase ($r$) and fishing mortality ($F$). $F_{critical}$ is reached at 0.071. If $F$ is less than $F_{critical}$, the population will increase. If $F$ is greater than $F_{critical}$, the population will decrease.

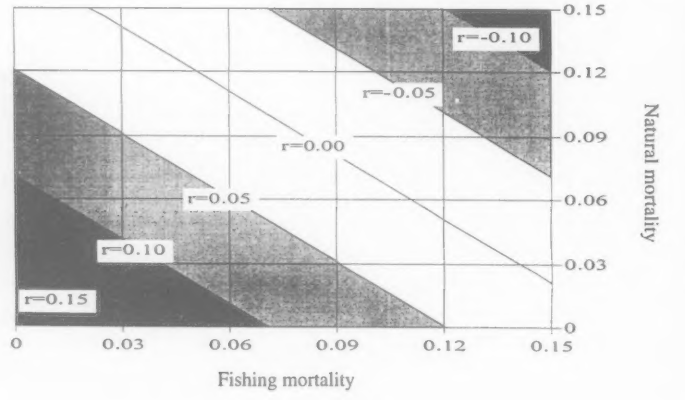


**Figure 4**

Isoclines showing the intrinsic rate of increase ($r$) at different rates of fishing ($F$) and natural mortality ($M$). The population will increase if $r$ is greater than zero. The population will decrease if $r$ is less than zero.

## Discussion

The model projects that the sandbar shark population is unlikely to increase unless $F$ is reduced below $F_{CRITICAL}$. The value calculated here is less than the $F_{CRITICAL}$ value of 0.10 that Sminkey and Musick (1996) predicted by using a life table. Both Sminkey and Musick's (1996) and Cortés's (1999) results and those presented here indicate that current estimates of $F$ are

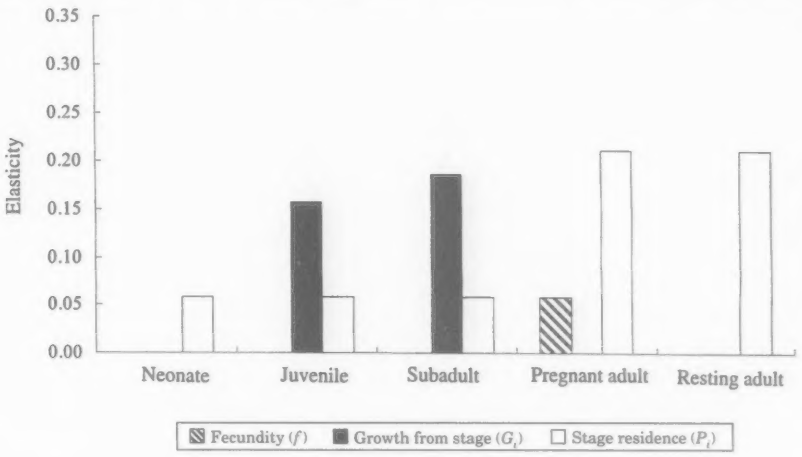


**Figure 5**

The proportional sensitivities (elasticity) of each stage to fecundity, growth, and stage residence if neonates and pregnant adults are protected ($F_{1,4}$=0; $F_{2,3,5}$=0.20).

**Table 4**

The percent reduction in fishing mortality needed to stabilize the population if $F_{Current}$ = 0.20. $F_{Critical}$ is the fishing mortality level at which the population abundance is stable. $F_{Current}$ is the fishing mortality level estimated in the 1996 stock assessment.

| Scenario | Fishing and natural mortality rates used | $F_{Critical}$ | % reduction needed |
|---|---|---|---|
| Current conditions | $F_1$=0.10; $F_{2-5}$= 0.20<br>$M$=0.10 | 0.071 | 64 |
| Protecting neonates and pregnant adults | $F_{1,4}$=0; $F_{2,3,5}$=0.20<br>$M_1$= 0; $M_{2-5}$=0.10 | 0.097 | 52 |
| Protecting neonates and juveniles | $F_{1,2}$=0; $F_{3-5}$=0.20<br>$M$=0.10 | 0.109 | 46 |
| Protecting juveniles only | $F_1$=0.10; $F_2$=0<br>$F_{3-5}$=0.20; $M$=0.10 | 0.101 | 50 |
| Protecting subadults only | $F_1$=0.10; $F_3$=0<br>$F_{2,4,5}$=0.20; $M$=0.10 | 0.120 | 40 |

too high to maintain the population and must be reduced. At the 1996 SEW, it was determined that reducing $F$ levels by 50% was likely to increase the chances of recovering the large coastal stock (NMFS[1]). In response to this, NMFS reduced the quota in 1997 for Atlantic large coastal sharks by 50% in order to reduce $F$ by 50%. Assuming that the estimate of $F$ from the SEW is accurate, that a 50% quota reduction is equivalent to a 50% decrease in $F$, and that the reduction in $F$ is equally distributed across age classes, we believe our results indicate that a 50% quota reduction may not stabilize the stock. Our model predicts that without alternative management strategies, the population will not begin to recover unless $F$ on sandbar sharks is reduced to below 0.07, requiring a reduction in current estimates of $F$ of greater than 50%.

Nursery ground closures and size limits are possible management strategies. These strategies would protect neonates, pregnant adults who are in the

nursery grounds to pup, and any juveniles who may have returned for the summer. One of the scenarios we ran is extreme in that every neonate survives ($Z$=0) and pregnant adults are not fished for the entire time they are pregnant. But in this scenario, juveniles are not protected. If $F$ is not reduced on juveniles, subadults, and resting adults, the model shows that the population will decrease until $F$ is reduced to 0.097. This is higher than the $F = 0.07$ which would be needed to stabilize the population without any protection for neonates, and would almost be met by the 50% reduction in quota as suggested by the 1996 SEW. However, these scenarios assume complete protection of protected stages from either fishing or natural mortality. Thus, they probably over-estimate the effectiveness of the potential management action. Overall, these models indicate that nursery ground closures or size limits that protect only neonates and juveniles, or neonates and pregnant adults, are not likely to be the ultimate solution. Additional measures will need to be taken to protect the sandbar shark.

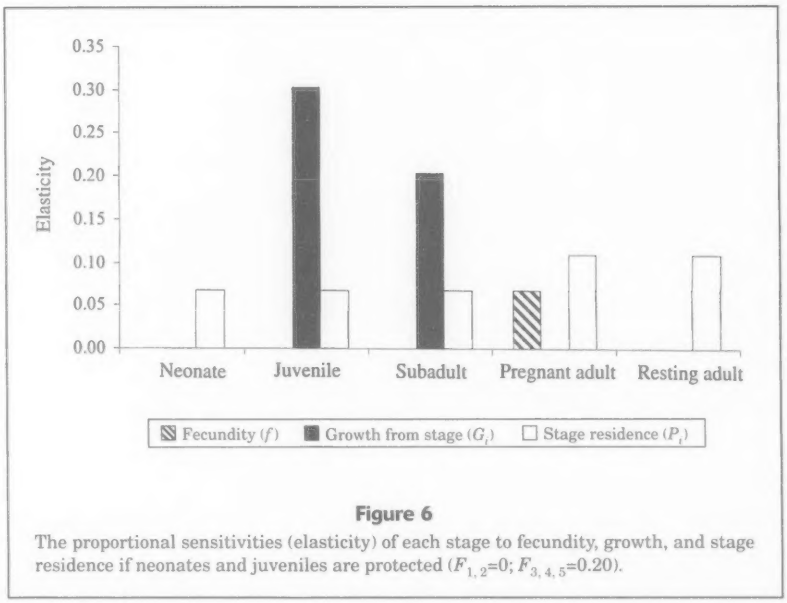


**Figure 6**

The proportional sensitivities (elasticity) of each stage to fecundity, growth, and stage residence if neonates and juveniles are protected ($F_{1,2}$=0; $F_{3,4,5}$=0.20).

Subsequent runs of the model showed that size limits that protect juvenile and subadult stages will not act to rebuild the population alone, despite the fact that the model indicates these stages are the most sensitive to survival. In these cases, $F$ needs to be reduced to 0.10 or 0.12, respectively. If the current $F$ estimate of 0.20 is correct and if a 50% reduction in quota reduces $F$ by 50%, size limits to protect either stage and a reduction in quota of between 40% and 50% may be sufficient to stabilize the population.

All scenarios indicate that the sandbar shark stock will most likely be rebuilt through a combination of management strategies. With nursery closures or size limits that protect only one stage, the stock will decline if fishing mortality remains the same as that currently estimated. Because the model's estimates of population growth are sensitive to survival at the juvenile and subadult stages, because these stages have the highest proportion of the population in the stable stage distribution, and because subadults have relatively high reproductive values, ideally any management strategies selected should be those that conserve these stages.

Most of the model projections indicate that the total sensitivities of juveniles and subadults are the greatest. The sensitivity of population growth to events during these stages suggests two things: management needs to focus on protecting juveniles and subadults, and scientists need to collect accurate estimates of $F$ and $M$ for juveniles and subadults. Possible conservation efforts could include minimum sizes to protect immature sandbar sharks or time-area closures to protect both juveniles and subadults during their migrations. If our model is correct, it is important to take measures to protect these stages soon, not only because the model shows that the population abundance decreases quickly at current estimates of $F$, but also because there is evidence of strong year classes of immature sandbar sharks entering the fishery (Branstetter and Burgess[1]). In 1994, Sminkey suggested that the 1987, 1989, and 1992 year classes in Chesapeake Bay were exceptionally strong. It will be easier for the fishery to recover if we have strong year classes on which to build.

This is not the first time the use of a stage-based model has concluded that conservation efforts should target juveniles and subadults of a long-lived species more than newborns. Rates of population growth in many marine species are effected more by changes in survival of juvenile and subadult stages than by changes in survival of other stages, or by changes in fecundity (Heppell et al., 1999). For example, Crouse et al. (1987) and Crowder et al. (1994) concluded that population growth rate was most sensitive to the survival of large juvenile loggerhead sea turtles.

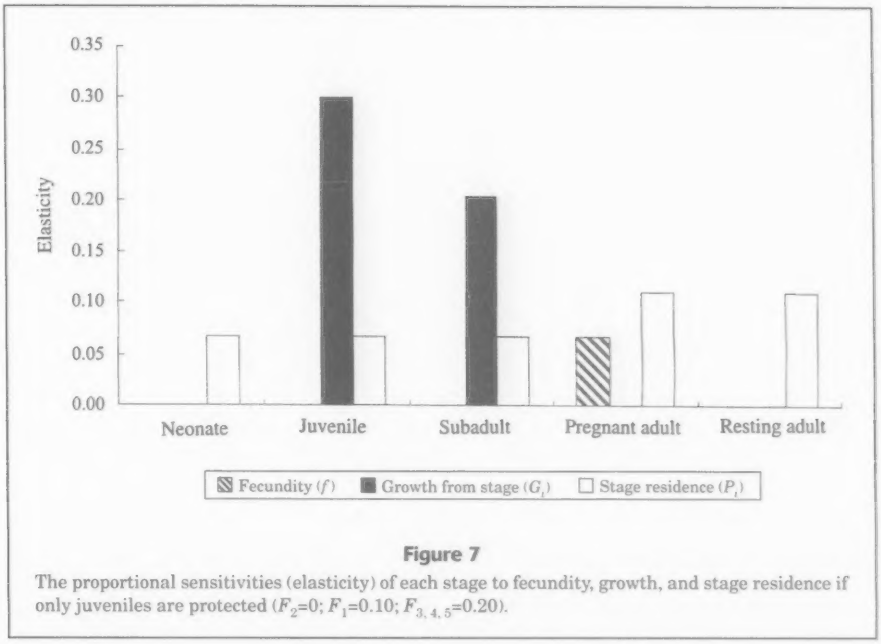


**Figure 7**

The proportional sensitivities (elasticity) of each stage to fecundity, growth, and stage residence if only juveniles are protected ($F_2$=0; $F_1$=0.10; $F_{3,4,5}$=0.20).

They suggested that the use of turtle excluder devices would protect juvenile sea turtles and aid in conservation and recovery of this species. Additionally, Heppell et al. (1996) indicated that population enhancement by means of hatchery production of sea turtles would likely not be successful. In contrast, marine mammals show a different pattern of sensitivity. For these taxa, population growth appears most sensitive to events occurring during the adult stages (Heppell et al., 1999). Studies indicate that marine fish may also show a different pattern of sensitivity, where there is increased sensitivity to events in the early life history (Heppell et al. 1999; Quinlan and Crowder, 1999).

Three features of our approach require one to use caution in interpreting our conclusions. First, there are problems in using stage-based models, or demographic models of all types, with highly migratory animals such as sharks. For instance, most demographic models assume that the population is closed. In the case of the sandbar shark this assumption may not hold true. Tagging studies show that a small percentage of sandbar sharks tagged in U.S. waters are caught in Mexican waters. Because it is currently unknown if there are nursery grounds in Mexican waters, this migration to Mexico may represent an additional source of loss to the population that may not be replaced. The model does not consider this loss. If a significant number of sandbar sharks are found to migrate to Mexican waters, current estimates of $F$ may be underestimates. If this is the case, even greater reductions in $F$ may be necessary to help the stock recover.

Second, we have presented a deterministic model of sandbar shark population dynamics. Thus, we have ignored uncertainty of and plasticity in vital rates such as growth and fecundity. Tuljapurkar (1997) and Nations and Boyce (1997) have discussed the potential biases that may result from basing harvest strategies on results from a deterministic model, particularly when juvenile survival is closely tied to environmental conditions. In addition to potential biases in the results, a deterministic model yields only a point estimate of population growth rate. Cortés (1999) included a stochastic term for fecundity in his model for sandbar sharks. Subsequently, he used Monte Carlo simulations to generate distributions of predicted population growth rates when fecundity varies stochastically. His results indicate that predicted population growth rates may vary by 2–3% when fecundity is allowed to vary. The impact of stochasticity in survival and growth on the predicted population growth rates is unknown. However, given the sensitivity of the model to transition involving growth and survival for juvenile and subadult animals, its impact may be substantial.

Finally, unlike many traditional fishery models, our demographic model does not take into account density dependence or compensation. However, given the longevity and age to maturity of sandbar sharks, and sharks in general, compensation may not be as signif-

icant or as observable as that for teleost fish. Sminkey and Musick (1995) have suggested three mechanisms of compensation in sharks: decreases in natural mortality of younger sharks as the abundance of predatory larger sharks is reduced; compensatory increases in fecundity when food is more available or when uterine mortality is reduced; and an increase in growth rate and thus a decrease in natural mortality and possibly earlier maturity when food is abundant. In Chesapeake Bay, they found evidence of a slight increase in growth rate of juvenile sharks after the population had been depleted but were not able to ascertain if the age of maturity had also been reduced. Late age at maturity due to relatively slow growth rates reduces the probability that small increases in growth or increased neonate survival through density-dependent mechanisms will compensate for fishing mortality (Heppell et al., 1999).

In summary, the results when $F = 0.20$ for older stages indicate that sandbar shark stocks are currently being fished above their ability to replace themselves (i.e. $r$ is negative for the best estimate of $F$). Thus, management action (e.g. time area closures, reduced quota, minimum size) is needed to reduce $F$ to the level where $r$ is zero or positive. Because the model is highly sensitive to juvenile and subadult survival, management actions that reduce the mortality rates of these stages would likely be more effective than nursery closures that protect only neonates and pregnant females.

Although our study suggests that the protection of juvenile and subadult sandbar sharks may aid in recovery of sandbar sharks, our method may not work as well on other shark species, because life history traits differ. Sandbar sharks are often confused with other shark species such as the dusky shark; therefore, whichever management strategy is chosen, it should work for all large coastal shark species. These problems, combined with a paucity of data on pupping grounds, age at maturity, and other traits, make selection of a conservation method difficult. The model in our study should be viewed as a starting point for looking at the effect of the different options available and for comparing these options among the shark species involved.

## Acknowledgments

We thank Selina Heppell, Pamela Mace, Michael Fogarty, John Musick, Thomas Sminkey, Ed Houde, and Steve Branstetter for comments on an earlier draft of this manuscript. Support for this work comes from the Chesapeake Bay Program USEPA (grant CB-993080-02), the Hudson River Foundation (grant 008/98A), and the University of Maryland Center for Environmental Sciences.

## Literature cited

**Anderson, E. D.**
**1990.** Fishery models as applied to elasmobranch fisheries. *In* Elasmobranchs as living resources: advances in the biology, ecology, systematic, and the status of the fisheries (H. L. Pratt, S. H. Gruber, T. Taniuchi, eds.), p. 473–484. U.S. Dep. Commer., NOAA Technical Report NMFS 90.

**Casey, J. G., and L. J. Natanson.**
**1992.** Revised estimates of age and growth of the sandbar shark (*Carcharhinus plumbeus*) from the western North Atlantic. C. J. Fish. Aquat. Sci.49:1474–1477.

**Casey, J. G., H. L. Pratt Jr., and C. E. Stillwell.**
**1985.** Age and growth of the sandbar shark (*Carcharhinus plumbeus*) from the western North Atlantic. Can. J. Fish. Aquat. Sci. 42:963–975.

**Castro, J.**
**1983.** The sharks of North American waters. Texas A&M Univ. Press, College Station, TX, 180 p.
**1993.** The shark nursery of Bulls Bay, South Carolina, with a review of the shark nurseries of the southeastern coast of the United States. Environ. Biol. Fish. 38:37–48.

**Caswell, H.**
**1989.** Matrix population models. Sinauer Associates, Inc., Sunderland, MA, 328 p.

**Cortés, E.**
**1999.** A stochastic stage-based population model of the sandbar shark in the western North Atlantic. Am. Fish. Soc. Symp. 23:115–136.

**Crouse, D. T., L. B. Crowder, and H. Caswell.**
**1987.** A stage-based population model for loggerhead sea turtles and implications for conservation. Ecology 68:1412–1423.

**Crowder, L. B., D. T. Crouse, S. S. Heppell, and T. H. Martin.**
**1994.** Predicting the impact of turtle excluder devices on loggerhead sea turtle populations. Ecol. Appl. 4:437–445.

**Gotelli, N. J.**
**1995.** A primer of ecology. Sinauer Associates, Sunderland, MA, 206 p.

**Heppell, S. L., L. B. Crowder, and D. T. Crouse.**
**1996.** Models to evaluate headstarting as a management tool for long-lived turtles. Ecol. Appl. 6:556–565.

**Heppell, S., L. B. Crowder, T. R. Menzel.**
**1999.** Life table analysis of long-lived marine species, with implications for conservation and management. Am. Fish. Soc. Symp. 23:137–148.

**Hoenig, J. M., and S. H. Gruber.**
**1990.** Life history patterns in the elasmobranchs: implications for fisheries management. *In* Elasmobranchs as living resources: advances in the biology, ecology, systematic, and the status of the fisheries (H. L. Pratt, S. H. Gruber, T. Taniuchi, eds.), p. 1–16. U.S. Dep. Commer., NOAA, Tech. Report NMFS 90.

**Kingsland, S. E.**
**1985.** Modeling nature: episodes in the history of population ecology. Chicago Univ. Press, Chicago, IL, 267 p.

**Lo, N. C. H., P. E. Smith, and J. L. Butler.**
**1995.** Population growth of northern anchovy and Pacific sardine using stage-specific matrix models. Mar. Ecol. Prog. Ser. 127:15–26.

**NMFS (National Marine Fisheries Service).**
**1993.** Fishery management plan for sharks of the Atlantic ocean. Office of Sustainable Fisheries. U.S. Dep. Commer., National Oceanic and Atmospheric Administration (NOAA), NMFS, Silver Spring, MD, 173 p.
**1997.** Report to Congress: status of fisheries of the United States. U.S. Dep. Commer., NOAA, Silver Spring, MD, 75 p.

**Nations, C. S., and M. S. Boyce.**
**1997.** Stochastic demography for conservation biology. *In* Structured models in marine, terrestrial and freshwater systems (S. Tuljapurkar and H. Caswell, eds.), p. 450–469. Chapman and Hall. New York, NY, 643 p.

**Pertierra, J. P., J. Lleonart, and N. C. H. Lo.**
**1997.** Application of a stage-specific matrix model and length-cohort based analysis to assess the anchovy fishery in Catalan coastal waters (NW Mediterranean Sea). Fish. Res. 30:127–137.

**Quinlan, J. A., and L. B. Crowder.**
**In press.** Searching for sensitivity in the life history of Atlantic menhaden: inferences from a matrix model. Fish. Oceanog.

**Simpfendorfer, C. A.**
**1999.** Demographic analysis of the dusky shark fishery in southwestern Australia. Am. Fish. Soc. Symp. 23:149–160.

**Sminkey, T. R., and J. A. Musick.**
**1995.** Age and growth of the sandbar shark, *Carcharhinus plumbeus*, before and after population depletion. Copeia 4:871–883.
**1996.** Demographic analysis of the sandbar shark, *Carcharhinus plumbeus*, in the western North Atlantic. Fish. Bull. 94:341–347.

**Springer, S.**
**1960.** Natural history of the sandbar shark, *Eulamia milberti*. U.S. Fish Wildl. Serv. Fish. Bull. 61:1–38

**Tuljapurkar, S.**
**1997.** Stochastic matrix models. *In* Structured models in marine, terrestrial and freshwater systems (S. Tuljapurkar and H. Caswell, eds.), p. 59–87. Chapman and Hall. New York, NY, 643 p.

# Food habits of the South American sea lion, *Otaria flavescens*, off Patagonia, Argentina

**Mariano Koen Alonso**

**Enrique A. Crespo**

**Susana N. Pedraza**

Centro Nacional Patagónico (CONICET)
and Universidad Nacional de la Patagonia
Boulevard Brown 3600
(9120) Puerto Madryn, Chubut, Argentina
E-mail address: koen@cenpat.edu.ar

**Néstor A. García**

Centro Nacional Patagónico (CONICET)
Boulevard Brown 3600
(9120) Puerto Madryn, Chubut, Argentina

**Mariano A. Coscarella**

Centro Nacional Patagónico (CONICET)
and Universidad Nacional de la Patagonia
Boulevard Brown 3600
(9120) Puerto Madryn, Chubut, Argentina

**Abstract.**—Food habits of the South American sea lion (*Otaria flavescens*) off Patagonia were studied by means of stomach content analysis. The samples were collected during 1982–1987 and 1990–1998 in northern and central Patagonia. The samples ($n$=59) came from individuals found dead on beaches and from animals recovered in incidental catches of the fishery. Forty-one prey species (including fishes, cephalopods, crustaceans, gastropods, polychetes, sponges, and tunicates) were identified; most important were Argentine hake (*Merluccius hubbsi*), red octopus (*Enteroctopus megalocyathus*), Argentine shortfin squid (*Illex argentinus*), "raneya" (*Raneya brasiliensis*), Patagonian squid (*Loligo gahi*), and Argentine anchovy (*Engraulis anchoita*). Differences in diet were found between sexes but not between geographical area of sampling, period of sampling, or source of samples. Females fed mostly on benthic species, whereas males fed mostly on demersal-pelagic species. The difference in diet between sexes was associated with different feeding grounds or different home ranges and could be produced by different constraints in the feeding behavior of each sex. These different constraints and restrictions could lead females to feed in more coastal and shallower waters than those waters where males feed. Some of the important prey were commercial species (Argentine hake, Argentine shortfin squid, Patagonian squid) consumed at both commercial and noncommercial sizes by sea lions. The presence of gastroliths was independent of the presence of stomach parasites; however, gastrolith weight was positively correlated with individual sea lion's length, indicating that gastroliths could be involved in buoyancy control. In summary, these stomach content analyses indicate that South American sea lions feed primarily on demersal and benthic species and, in general terms, use resources according to their environmental availability.

Manuscript accepted 9 August 1999.
Fish. Bull. 98:250–263 (2000).

The South American sea lion (*Otaria flavescens*) is one of the most common and abundant marine mammal species in the southwestern Atlantic and is distributed along the coasts of South America from Peru to southern Brazil in both the Pacific and Atlantic Oceans (Vaz Ferreira, 1982; Crespo[1]). Most investigations on South American sea lions have been focused on social behavior, breeding biology, and population dynamics (Vaz Ferreira, 1982; Campagna and Le Boeuf, 1988; Cappozzo et al., 1991; Crespo and Pedraza, 1991; Crespo[1]). Recent research has provided new data on the interactions between South American sea lions and fisheries (Crespo et al., 1994, 1997), on population size and trends (Reyes et al., 1999; Dans et al.[2]), and on diving behavior of lactating females (Werner and Campagna, 1995).

South American sea lions are considered opportunistic and broad-spectrum feeders, feeding on fish, squid, crustaceans, and occasionally on sea birds (Vaz Ferreira, 1982; George-Nascimento et al., 1985; Crespo et al., 1997). In Chilean waters, their most important prey are the Patagonian grenadier (*Macruronus magellanicus*) and the kingclip (*Genypterus* spp.); no relationship has been found between predator and prey sizes (George-Nascimento et al., 1985). For Patagonian waters, only preliminary information has been published about feeding (Crespo et al., 1997). Several studies (Hamilton, 1934; Vaz Fer-

[1] Crespo, E. A. 1988. Dinámica poblacional del lobo marino del sur *Otaria flavescens* (Shaw, 1800) en el norte del litoral patagónico. Doctoral thesis, Facultad de Cs. Exáctas y Naturales, Universidad Nacional de Buenos Aires, Buenos Aires, Argentina, 298 p.

[2] Dans, S., E. A. Crespo, S. Pedraza, R. González, and N. García. 1996. Estructura y tendencia de los apostaderos de lobos marinos de un pelo (*Otaria flavescens*) en el norte de Patagonia. Informes Técnicos del Plan de Manejo Integrado de la Zona Costera Patagónica. Fundación Patagonia Natural (Puerto Madryn, Argentina) 13:1–21.

**Table 1**

Number of South American sea lion stomachs analyzed in our study by period of time, geographical area, sex, and source of sampling. The number of empty stomachs is given in parentheses.

| | | Males | | Females | |
|---|---|---|---|---|---|
| Period | Area | Dead on shore | Caught incidentally | Dead on shore | Caught incidentally |
| 1982–87 | Northern Patagonia | 6 (1) | | 3 (1) | |
| | Central Patagonia | | | 1 (0) | |
| 1990–98 | Northern Patagonia | 13 (4) | | 20 (4) | |
| | Central Patagonia | 1 (1) | 8 (0) | 4(0) | 3(0) |

reira, 1982; George-Nascimento et al., 1985) have reported the presence of gastroliths in this species, and others (Taylor, 1993) have suggested functions for them (food processing, buoyancy control, elimination of internal parasites, and alleviation of hunger).

The marine ecosystem in Patagonia supports one of the most intense fisheries in the world, with approximately one million tons of catch per year during the 1990s (Anonymous, 1996). South American sea lions are reported to be caught incidentally in the trawl fisheries for Argentine hake (*Merluccius hubbsi*) and Argentine red shrimp (*Pleoticus muelleri*) (Crespo et al., 1994, 1997). Some of the target and bycatch species of these and other fisheries, such as the Argentine shortfin squid (*Illex argentinus*) fishery, are consumed by South American sea lions (Crespo et al., 1997). The development of the fisheries may have been one factor that slowed the recovery of the South American sea lion population after harvesting of this marine mammal species ended in the mid 1960s (Crespo and Pedraza, 1991).

The objectives of this research were to describe the diet of South American sea lions off Patagonia, to evaluate some hypotheses on the function of gastroliths, and to explore the possibility of trophic competition with commercial fisheries.

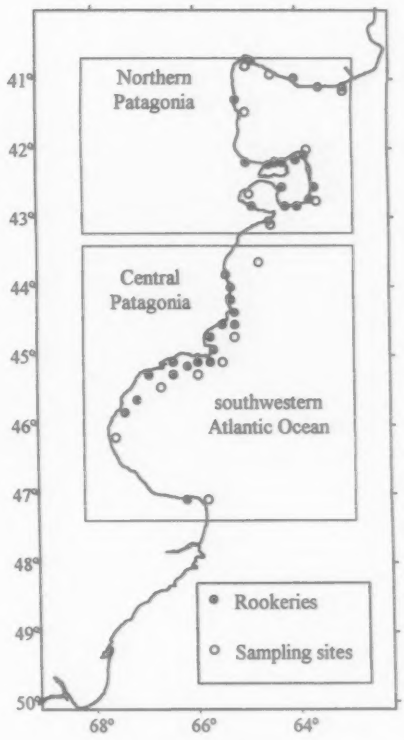


**Figure 1**

Study area, showing the two geographical areas considered in this work: northern and central Patagonia. The filled circles indicate the location of rookeries of South American sea lion and the empty circles indicate sampling sites.

## Materials and methods

### Sample studied

The total sample was composed of 59 stomachs from 28 males and 31 females, obtained in the periods 1982–1987 and 1990–1998 (Table 1). Most of the 1982–1987 sample ($n$=10) was collected in the northern area of Patagonia (Fig. 1). These animals were found dead on shore. The 1990–1998 sample ($n$=49) was collected in the northern and central Patagonian areas (Fig. 1). During this period, the animals were obtained from two sources: shores where animals were found dead (14 males and 24 females) and fisheries where animals were caught incidentally (8 males and 3 females) (Table 1). Samples were clumped

into geographical areas based on the spatial distribution of rookeries (Fig.1) and the reported animal movements between rookeries in northern Patagonia (Crespo and Pedraza, 1991; Crespo[1]; Dans et al.[2]). Sex and standard length (SL, cm) were recorded when possible. Males ranged from 114 to 243 cm SL, whereas females ranged between 102 to 196 cm SL (Fig. 2).

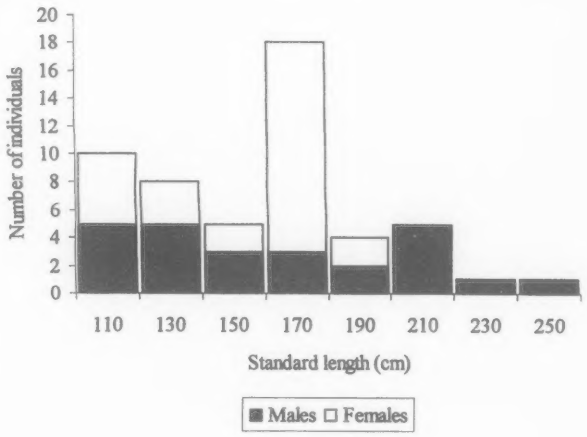


**Figure 2**

Length-frequency distribution of the total sample of South American sea lions analyzed in this work. Three males and four females were not included in this figure because their standard lengths could not be obtained.

### Stomach content analysis

Stomach contents were preserved in 70% alcohol or frozen at –20°C. Hard pieces were recovered by using sieves of different mesh sizes (from 0.5 to 10 mm) flushed with water and by using decantation trays. Fish otoliths and bones, cephalopod beaks, crustacean exoskeletons and other hard remains were used to quantify and identify the prey species. Identification was made by using local species reference collections at the Marine Mammal Laboratory, Centro Nacional Patagónico, CONICET, and available catalogues (Clarke, 1986; Menni et al., 1984; Roper et al., 1984; Boschi et al., 1992; Gosztonyi and Kuba[3]). Complete and undigested elements (complete prey, otoliths and beaks) were measured with digital calipers. When digested and broken hard pieces were found in a stomach, the measurements for these elements were assigned from a random sample of undigested and whole parts of the same species obtained within the same stomach (Koen Alonso et al., 1998).

Size (total length ([TL]) of fish and dorsal mantle length ([DML]) of squid, cm) and wet weight (W, g) of prey were estimated from hard pieces by using allometric regressions (Clarke, 1986; George-Nascimento et al., 1985; Koen Alonso et al., 1998) (Table 2). In those cases where regressions were not available, regressions of related species were employed (Table 2). When related species regressions did not exist, weight was assigned by direct comparison with measured and weighed individuals of similar size for the same species or by weighing the fragments found in the stomach. The presence of stomach stones and parasites was recorded and all the gastroliths were weighed in each stomach.

### Data analysis

The relative importance of prey species was evaluated by means of the index of relative importance (IRI) (Pinkas et al., 1971). The IRI was calculated for each prey species as

$$IRI = (\%N + \%W)\%FO,$$

Where $\%FO$ = the percent frequency of occurrence;
$\%N$ = the percentage by number; and
$\%W$ = the percentage by regression-estimated wet weight.

This IRI is a modified version of the index where the original term of percentage by volume was replaced by the $\%W$ term (Koen Alonso et al., 1998). In order to make easier the interpretation of the IRI, this index was expressed on a percent basis ($\%IRI$) (Cortés, 1997). Graphical representation of the diet was also employed to present some results (Cortés, 1997).

Two overlap indices, the general overlap index (GO) and the specific overlap index (SO) (Petraitis, 1979; Ludwig and Reynolds, 1988), were used to examine dietary differences. These indices were selected because they are based on the same theoretical framework, have associated statistical tests (Petraitis, 1979), and the GO presents a small bias even when the sample size is small (Smith and Zaret, 1982).

[3] Gosztonyi, A., and L. Kuba. 1996. Atlas de huesos craneales y de la cintura escapular de peces costeros patagónicos. Informes Técnicos del Plan de Manejo Integrado de la Zona Costera Patagónica. Fundación Patagonia Natural (Puerto Madryn, Argentina) 4:1–29.

**Table 2**

Regressions used to estimate size and wet weight of prey of the South American sea lion off Patagonia, with their sample size ($n$), coefficient of determination ($r^2$), and source. Total length (TL) and dorsal mantle length (DML) are given in centimeters, otolith length (OL), lower rostral length (LRL), and lower hood length (LHL) are given in milimeters, and wet weight (W) is in grams.

| Prey species | Regressions | $n$ | $r^2$ | Source |
|---|---|---|---|---|
| Teleosts | | | | |
| *Engraulis anchoita* | $TL=2.36817+3.56OL$ | 79 | 0.70 | Koen Alonso et al., 1998 |
| | $W=0.0025TL^{3.353}$ | 81 | 0.93 | Koen Alonso et al., 1998 |
| *Seriolella punctata* | $TL=-0.1533+4.1987OL$ | 45 | 0.8956 | present study |
| | $W=0.0182TL^{2.8635}$ | 22 | 0.8782 | present study |
| *Stromateus brasiliensis* | $TL=3.042OL^{1.159}$ | 51 | 0.98 | Koen Alonso et al., 1998 |
| | $W=0.0006418TL^{3.917}$ | 63 | 0.98 | Koen Alonso et al., 1998 |
| *Nemadactylus bergi* | $TL=-3.8317+5.6735OL$ | 56 | 0.9079 | present study |
| | $W=0.0144TL^{2.9301}$ | 23 | 0.9824 | present study |
| *Merluccius hubbsi* | $TL=1.823OL^{1.072}$ if $OL<15$ | 447 | 0.93 | Koen Alonso et al., 1998 |
| | $TL=1.984OL^{1.05}$ if $OL\geq15$ | 693 | 0.91 | Koen Alonso et al., 1998 |
| | $W=0.00476TL^{3.061}$ if $OL<15$ | 469 | 0.92 | Koen Alonso et al., 1998 |
| | $W=0.00972TL^{2.886}$ if $OL\geq15$ | 742 | 0.96 | Koen Alonso et al., 1998 |
| *Acanthistius brasilianus* | $TL=10.4444+1.8673OL$ | 23 | 0.7816 | present study |
| | $W=0.0082TL^{3.1713}$ | 11 | 0.9654 | present study |
| *Pseudopercis semifasciata*[1] | $TL=-12.9242+4.6425OL$ | 27 | 0.9789 | present study |
| | $W=0.005TL^{3.2066}$ | 13 | 0.9807 | present study |
| *Genypterus blacodes* | $TL=-18.3696+5.6394OL$ | 45 | 0.7890 | present study |
| | $W=0.0016TL^{3.2251}$ | 24 | 0.9783 | present study |
| *Raneya brasiliensis* | $TL=-0.7671+3.1968OL$ | 52 | 0.6819 | present study |
| | $W=0.0022TL^{3.2685}$ | 26 | 0.9349 | present study |
| *Patagonotothen* spp.[2] | $TL=-3.33204+4.21936OL$ | 121 | 0.7175 | present study |
| | $W=0.0013TL^{3.668}$ | 75 | 0.9729 | present study |
| *Triathalassothia argentina* | $TL=0.8116+2.775OL$ | 4 | 0.4278 | present study |
| | $W=0.1987TL^{2.1123}$ | 4 | 0.6161 | present study |
| *Paralichthys isosceles* | $TL=-0.9035+4.6962OL$ | 17 | 0.9436 | present study |
| | $W=0.0013TL^{3.6036}$ | 8 | 0.9975 | present study |
| Agnathans | | | | |
| *Mixine* sp. | $W=0.003TL^{2.81089}$ | 7 | 0.9314 | present study |
| Cephalopods | | | | |
| *Illex argentinus* | $DML=-3.178+5.617LHL$ | 27 | 0.93 | Koen Alonso et al., 1998 |
| | $DML=0.08257+6.009LRL$ | 63 | 0.87 | Koen Alonso et al., 1998 |
| | $W=0.00982DML^{3.238}$ | 66 | 0.98 | Koen Alonso et al., 1998 |
| *Loligo gahi*[3] | $DML=-0.712+4.622LHL$ | 98 | 0.76 | Koen Alonso et al., 1998 |
| | $W=0.026DML^{2.753}$ | 102 | 0.93 | Koen Alonso et al., 1998 |
| *Octopus vulgaris*[4] | $W=e^{1.82+3.03\mathrm{Ln}(LHL)}$ | 108 | — | Clarke, 1986 |
| *Eledone* sp. | $W=e^{1.68+2.85\mathrm{Ln}(LHL)}$ | 214 | — | Clarke, 1986 |

[1] These regressions were also used for *Pinguipes brasilianus*.
[2] These regressions were used for *Patagonotothen cornucola*.
[3] These regressions were also used for *Loligo sanpaulensis*.
[4] This regression was used for *Enteroctopus megalocyathus* and *Octopus tehuelchus*.

The GO evaluates the probability of obtaining the utilization curve of each group from the common utilization curve of all groups (Petraitis, 1979). This index has a minimum value which depends on the sample size and the number of prey species considered. To compare the index obtained from different samples, it was adjusted to vary between 0 and 1 ($GO_a$) (Ludwig and Reynolds, 1988). The null

hypothesis of a complete overlap (GO=1) can be statistically tested by using the *V*-statistic (Ludwig and Reynolds, 1988).

The SO is a pairwise nonsymmetric index which evaluates the probability of obtaining the utilization curve of one group from the utilization curve of the other (Petraitis, 1979; Ludwig and Reynolds, 1988). The probability of obtaining the utilization curve of the group $i$ from the utilization curve of group $k$ is denoted by $SO_{ik}$. The null hypothesis of a complete overlap ($SO_{ik}$=1) can be tested with the *U*-statistic (Ludwig and Reynolds, 1988).

The comparisons made were 1) geographical area of sampling (between northern Patagonia and central Patagonia), 2) period of sampling (between 1982–1987 and 1990–1998), 3) source of sampling (between dead animals on shore and entangled animals in the fishery), and 4) sex (between males and females). Because entangled individuals were mostly males and were obtained only during the 1990–1998 period (Table 1), comparisons were made between entangled and nonentangled males in the period 1990–1998.

The data employed for this analysis were those data on the occurrences of prey species that presented an %IRI greater than 2% in the pooled sample. Inherent in the use of occurrences of prey species is the assumption that each prey species in a stomach was consumed independently. For this reason, the correlations between the prey species used in our analyses were evaluated with the Spearman rank correlation coefficient ($r_s$) (Siegel and Castellan, 1995). The use of occurrences of prey species as data also increases the sample size for these comparisons because the stomach of one sea lion usually contained more than one prey species.

Differences in prey sizes consumed were tested by using the nonparametric two-sample Mann-Whitney *U* test in those cases where differences were detected (Siegel and Castellan, 1995).

The relationship between mean length of prey in each stomach and predator SL was evaluated using the $r_s$ (Siegel and Castellan, 1995). This analysis was performed by using the pooled sample and analyzed by sex of predator.

### The function of gastroliths

The role of gastroliths in eliminating stomach parasites and the potential function of gastroliths in buoyancy control were investigated. The independence between the presence of gastroliths and the presence of parasites in the stomachs was tested with Fisher's exact test. The relationship between SL and total weight of gastroliths found in the stomach (GW) was evaluated with the Spearman rank correlation coefficient ($r_s$) (Siegel and Castellan, 1995). This relationship was analyzed by considering each sex and the pooled sample.

## Results

### Prey species

Forty-eight of 59 stomachs analyzed contained food remains (Table 1). Aproximately 37 prey species were identified, mostly fishes and cephalopods (Table 3). Additionally, the stomach of one female found dead on the beach contained two sponge species, tube polychetes, nudibranchs and hagfish (*Mixine* sp.). Because this specimen was considered sick and anomalous, it was excluded from the analysis.

The collection analyzed was composed of 1449 individual prey, and the total estimated weight was 209.9 kg.

Males consumed a broader trophic spectrum of 32 prey species (Table 3), dominated by Argentine hake, followed by Patagonian squid, *Loligo gahi*, Argentine shortfin squid, "raneya," *Raneya brasiliensis,* and red octopus, *Enteroctopus megalocyathus*. Only the Argentine hake had a %IRI greater than 10%. The total number of prey found in male sea lions stomachs was 738 and the total estimated biomass was 91.4 kg. The five most important prey represented 74.0% by number and 74.6% by weight.

Twenty-nine species were found in female sea lion stomachs. The important prey were red octopus, Argentine shortfin squid, Argentine hake, "raneya," and Argentine anchovy (*Engraulis anchoita*) (Table 3). Only the first three species had %IRIs greater than 10%. The total number of prey found in the female stomachs was 711 and the estimated weight of this collection was 118.5 kg. The five most important prey represented 75.5% by number and 91.3% by weight.

### Homogeneity of the sample

Six species (Argentine hake, red octopus, Argentine shortfin squid, Patagonian squid, "raneya," and Argentine anchovy) had an %IRI greater than 2% in the pooled sample (Fig. 3). All pairwise correlations for these prey species were nonsignificant ($P$>0.05). Data on the occurrences of these species were used in the overlap analysis.

Considering the GO, no differences in diet were found between geographical areas and between periods of sampling (Table 4). However, the SO indicates differences in diet between the periods 1990–1998 and

**Table 3**

Number (*n*), percent frequency of occurrence (*%FO*), percent number (*%N*), percent estimated wet weight (*%W*), and percent index of relative importance (*%IRI*) of prey of the South American sea lion off Patagonia. The ecological group for each species is shown in parentheses (P=pelagic, B=benthic, DP=demersal pelagic, DB=demersal benthic, NA=not assigned). Ecological groups were assigned following Angelescu (1982), Menni (1983), Menni et al. (1984), Angelescu and Prenski (1987), and Boschi et al. (1992).

| | Females | | | | | Males | | | | |
|---|---|---|---|---|---|---|---|---|---|---|
| Prey | *n* | *%N* | *%W* | *%FO* | *%IRI* | *n* | *%N* | *%W* | *%FO* | *%IRI* |
| Teleosts | | | | | | | | | | |
| *Merluccius hubbsi* (DP) | 101 | 14.2 | 9.0 | 34.6 | 11.9 | 286 | 38.8 | 52.4 | 72.7 | 68.6 |
| *Raneya brasiliensis* (DB) | 151 | 21.2 | 3.0 | 19.2 | 6.9 | 67 | 9.1 | 2.8 | 40.9 | 5.0 |
| *Engraulis anchoita* (P) | 123 | 17.3 | 2.0 | 15.4 | 4.4 | 33 | 4.5 | 0.8 | 27.3 | 1.5 |
| *Patagonotothen cornucola* (DB) | 34 | 4.8 | 0.3 | 7.7 | 0.6 | 40 | 5.4 | 0.4 | 22.7 | 1.4 |
| *Paralichthys isosceles* (B) | 18 | 2.5 | 0.7 | 7.7 | 0.4 | 8 | 1.1 | 2.6 | 18.2 | 0.7 |
| *Triathalassothia argentina* (B) | 13 | 1.8 | 0.4 | 15.4 | 0.5 | 5 | 0.7 | 0.2 | 9.1 | 0.1 |
| *Genypterus blacodes* (DB) | 12 | 1.7 | 0.7 | 3.8 | 0.1 | 3 | 0.4 | 3.4 | 9.1 | 0.4 |
| *Pseudopercis semifasciata* (DB) | 3 | 0.4 | 0.9 | 3.8 | 0.1 | 3 | 0.4 | 11.4 | 9.1 | 1.1 |
| *Stromateus brasiliensis* (DP) | 5 | 0.7 | 0.7 | 3.8 | 0.1 | 5 | 0.7 | 1.4 | 9.1 | 0.2 |
| *Acanthistius brasilianus* (DB) | 1 | 0.1 | 0.4 | 3.8 | <0.1 | 2 | 0.3 | 1.4 | 9.1 | 0.2 |
| *Seriolella punctata* (DP) | — | — | — | — | — | 9 | 1.2 | 0.5 | 4.5 | 0.1 |
| *Iluocoetes fimbriatus* (DB) | — | — | — | — | — | 7 | 0.9 | 0.2 | 4.5 | 0.1 |
| *Percophis brasiliensis* (DB) | 1 | 0.1 | 0.8 | 3.8 | 0.1 | 1 | 0.1 | 0.6 | 4.5 | <0.1 |
| *Pinguipes brasilianus* (DB) | 2 | 0.3 | <0.1 | 3.8 | <0.1 | 1 | 0.1 | 0.1 | 4.5 | <0.1 |
| Unidentified fish (NA) | 1 | 0.1 | <0.1 | 3.8 | <0.1 | 1 | 0.1 | 0.1 | 4.5 | <0.1 |
| *Nemadactylus bergi* (DB) | — | — | — | — | — | 3 | 0.4 | 0.2 | 4.5 | <0.1 |
| *Prionotus punctatus* (B) | — | — | — | — | — | 1 | 0.1 | 0.1 | 4.5 | <0.1 |
| *Trachurus picturatus* (P) | 1 | 0.1 | 0.1 | 3.8 | <0.1 | — | — | — | — | — |
| Elasmobranchs (DB) | 6 | 0.8 | 3.0 | 7.7 | 0.4 | 1 | 0.1 | 0.5 | 4.5 | <0.1 |
| Agnathans | | | | | | | | | | |
| *Mixine* sp. (B) | — | — | — | — | — | 18 | 2.4 | 0.7 | 13.6 | 0.4 |
| Cephalopods | | | | | | | | | | |
| *Enteroctopus megalocyathus* (B) | 54 | 7.6 | 61.7 | 53.8 | 55.0 | 21 | 2.8 | 9.3 | 27.3 | 3.4 |
| *Illex argentinus* (DP) | 108 | 15.2 | 15.7 | 38.5 | 17.5 | 27 | 3.7 | 8.2 | 54.5 | 6.7 |
| *Loligo gahi* (DP) | 18 | 2.5 | 0.2 | 26.9 | 1.1 | 145 | 19.6 | 1.9 | 40.9 | 9.1 |
| *Octopus tehuelchus* (B) | 6 | 0.8 | 0.1 | 11.5 | 0.2 | 9 | 1.2 | 0.4 | 22.7 | 0.4 |
| *Eledone* sp. (B) | 6 | 0.8 | 0.1 | 7.7 | 0.1 | 18 | 2.4 | 0.3 | 13.6 | 0.4 |
| *Loligo sanpaulensis* (DP) | 3 | 0.4 | <0.1 | 7.7 | 0.1 | 1 | 0.1 | <0.1 | 4.5 | <0.1 |
| *Semirossia tenera* (DB) | 2 | 0.3 | <0.1 | 3.8 | <0.1 | 3 | 0.4 | <0.1 | 4.5 | <0.1 |
| Crustaceans | | | | | | | | | | |
| Crabs (B) | 9 | 1.3 | <0.1 | 15.4 | 0.3 | 4 | 0.5 | <0.1 | 13.6 | 0.1 |
| *Pleoticus muelleri* (DB) | 3 | 0.4 | <0.1 | 3.8 | <0.1 | 6 | 0.8 | 0.1 | 9.1 | 0.1 |
| Amphipods (P) | 12 | 1.7 | <0.1 | 3.8 | 0.1 | — | — | — | — | — |
| *Munida subrugosa* (B) | 2 | 0.3 | <0.1 | 3.8 | <0.1 | 1 | 0.1 | <0.1 | 4.5 | <0.1 |
| *Munida gregaria* (B) | — | — | — | — | — | 2 | 0.3 | <0.1 | 9.1 | <0.1 |
| *Serolis* sp. (B) | — | — | — | — | — | 2 | 0.3 | <0.1 | 9.1 | <0.1 |
| *Peisos petrunkevitchi* (DB) | — | — | — | — | — | 5 | 0.7 | <0.1 | 4.5 | <0.1 |
| *Heterosquilla platensis* (B) | 1 | 0.1 | <0.1 | 3.8 | <0.1 | — | — | — | — | — |
| Polychetes | | | | | | | | | | |
| *Eunice argentinensis* (B) | 8 | 1.1 | <0.1 | 3.8 | 0.1 | — | — | — | — | — |
| Tunicates | | | | | | | | | | |
| *Pedicle tunicate* (B) | 7 | 1.0 | <0.1 | 7.7 | 0.1 | — | — | — | — | — |

1982–1987 (Table 4). The Argentine anchovy was not found in the small sample for the period 1982–1987, and was the least important of the six prey species selected for the overlap analysis. When the analysis was performed excluding this prey species, no differences were found between periods in either of the

two overlap indices (Table 4). No differences were also found between entangled and nonentangled males in the period 1990–1998 (Table 4).

When the difference in feeding between sexes was analyzed, no differences were found with the GO, but the SO indicated significant differences in diet (Table 4). Taking into account that the GO analyzes the differences between the utilization curves of the groups with reference to a common utilization curve, whereas the SO analyzes one utilization curve with respect to the other one, our data suggest that there are some differences in the diet between sexes.

### Prey size

No differences were found in the sizes of Argentine hake ($U$=13,785.5; $n_{males}$=286; $n_{females}$=101; $P$=0.496), Argentine shortfin squid ($U$=1,331.5; $n_{males}$=27; $n_{females}$=108; $P$=0.486), and Argentine anchovy ($U$=1,627; $n_{males}$=33; $n_{females}$=123; $P$=0.080) consumed by the two sexes. Seventy-four percent of the Argentine hake eaten by sea lions were less than 30 cm TL. Argentine shortfin squid consumed by sea lions had a DML greater than 15 cm, whereas Argentine anchovy consumed by sea lions were mostly between 12 and 17 cm of TL (Fig. 4). Red octopus consumed by males weighed significantly less than those consumed by females ($U$=194.5; $n_{males}$=21; $n_{females}$=54; $P$<0.0001). Patagonian squids consumed by males were larger than those consumed by females ($U$=880; $n_{males}$=145; $n_{females}$=18; $P$=0.024), but the range of DMLs of squid consumed by females was greater than that of squid eaten by males. Larger "raneya" was consumed by male sea lions than "raneya" eaten by female sea lions ($U$=2,681; $n_{males}$=67; $n_{females}$=151; $P$<0.0001) (Fig. 5).

No relationships were found between mean length of prey and predator SL with the pooled sample ($r_s$=0.007; $n$=37; $P$=0.964), with males only ($r_s$=0.004; $n$=19; $P$=0.985) or with females only ($r_s$=0.118; $n$=18; $P$=0.641).

### Gastroliths

Of the stomachs analyzed, 60.4% had gastroliths and 87.9% had parasites. The parasites found in the stomachs were mostly nematodes. The presence of parasites and gastroliths was independent (Fisher exact test; $P$=0.999). A positive correlation was found between the SL of South American sea lions and GW ($r_s$=0.572; $n$=45; $P$<0.0001) (Fig. 6).

Gastroliths were found in 56.7% of females sea lions and 90.0% of females had parasites. The presence of gastroliths and parasites was independent (Fisher exact test; $P$=0.5645). A positive correlation was found between SL and GW ($r_s$=0.66; $n$=23; $P$=0.0006).

Gastroliths were found in 85.7% of the male sea lion stomachs, and 64.3% of males had parasites. The independence between the presence of gastroliths and parasites could not be rejected (Fisher exact test; $P$=1), and a positive correlation was found between SL and GW ($r_s$=0.599; $n$=22; $P$=0.0032).

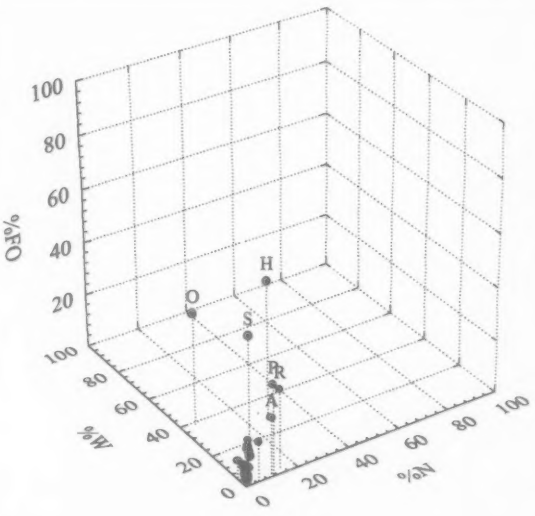


**Figure 3**

The diet of South American sea lions. The axes are %FO = percent frequency of occurrence, %N = percentage by number, and %W = percentage by regression-estimated wet weight. Only the labeled species had an %IRI>2%, and they were H = Argentine hake, O = red octopus, S = Argentine shortfin squid, P = Patagonian squid, R = "Raneya," and A = Argentine anchovy.

## Discussion

The samples analyzed was collected over a broad range of time and space and were derived from two sampling sources. For that reason several subsamples were tested for homogeneity before a sample could be considered to be representative of the diet of South American sea lions. Those subsamples were tested by means of the GO and SO indices because they have associated statistical tests. The GO has only a small bias related to the difference in sample sizes even when the total sample size is relatively small (Smith and Zaret, 1982), and both overlap measures do not change if the resources are divided

**Table 4**

Diet overlap analyses between the major sources of variation in the sample studied. GO = general overlap index; $GO_a$ = adjusted general overlap index; $V$ = the statistic to test the null hypothesis that GO = 1; df = degrees of freedom; $P$ = probability of the statistic; $SO_{ik}$ = specific overlap of group $i$ onto group $k$; $U$ = statistic to test the null hypothesis that $SO_{ik} = 1$. The number of prey occurrences in each category are indicated in parentheses.

| | General overlap index | | | | |
|---|---|---|---|---|---|
| Source of variation | GO | $GO_a$ | $V$ | df | $P$ |
| Period of time | 0.987 | 0.953 | 2.870 | 5 | 0.720 |
| Period of time[1] | 0.997 | 0.990 | 0.585 | 4 | 0.965 |
| Geographic area | 0.986 | 0.971 | 2.989 | 5 | 0.702 |
| Source of sampling | 0.983 | 0.966 | 1.715 | 5 | 0.887 |
| Sex | 0.970 | 0.940 | 6.514 | 5 | 0.259 |

| | Specific overlap index | | | | | |
|---|---|---|---|---|---|---|
| Source of variation | $i$ | $k$ | $SO_{ik}$ | $U$ | df | $P$ |
| Period of time | 1982–1987 (11) | 1990–1998 (96) | 0.869 | 3.078 | 5 | 0.688 |
| | 1990–1998 (96) | 1982–1987 (11) | 0.197 | 311.532 | 5 | <0.001 |
| | 1982–1987[1] (11) | 1990–1998[1] (86) | 0.971 | 0.658 | 4 | 0.956 |
| | 1990–1998[1] (86) | 1982–1987[1] (11) | 0.969 | 5.367 | 4 | 0.252 |
| Geographic area | central Patagonia (38) | northern Patagonia (69) | 0.942 | 4.545 | 5 | 0.474 |
| | northern Patagonia (69) | central Patagonia (38) | 0.937 | 8.951 | 5 | 0.111 |
| Source of sampling | nonentangled males (29) | entangled males (22) | 0.932 | 4.066 | 5 | 0.540 |
| | entangled males (22) | nonentangled males (29) | 0.933 | 3.037 | 5 | 0.694 |
| Sex | females (49) | males (58) | 0.870 | 13.606 | 5 | 0.018 |
| | males (58) | females (49) | 0.894 | 13.029 | 5 | 0.023 |

[1] Analysis performed excluding the Argentine anchovy.

into classes below the organism's level of discrimination (Petraitis, 1979). However, one cannot evaluate the interaction between sources of variation with these analyses. For this reason, as in any statistical test, the lack of a difference for a particular source of variation does not indicate the absence of a difference, it means only that there is not enough information to affirm that this source of variation is significant.

The marine communities for both areas in this study comprise the same species and are considered to be relatively homogeneous along the entire geographical areas range covered by the study area (Fig. 1) (Menni, 1983; Menni and López, 1984; Angelescu and Prenski, 1987). In addition, the trend of sea lion stocks in northern and central Patagonia has followed a pattern of decline and recovery during recent decades. The northern Patagonia stock declined to one fifth of its original population size between 1930 and the mid-1960s as a consequence of intense harvesting. Then it remained stable between 1972 and 1990, when it began to recover (Crespo and Pedraza, 1991). The central Patagonia stock had not been harvested but declined in a similar proportion during the mid-century and has shown evidence of population increase in recent years—a fact that suggests a strong connection and interchange of individuals between these regions (Reyes et al., 1999). In addition, preliminary results based on electrophoresis analysis of blood enzymes and proteins codified by 10 loci have indicated that nine of these loci are monomorphic, suggesting that South American sea lions from both areas have had a strong gene flux between them and possibly constitute an unique biological population (Crespo[4]).

Regarding the two sampling periods, the differences in the diet detected with the SO are surely associated with the absence of Argentine anchovy in the 1982–1987 samples. The SO indicated that the utilization curve of food resources of the period 1990–1998 could not be drawn from the utilization

[4] Crespo, E. A. 1998. Laboratorio de Mamíferos Marinos, Centro Nacional Patagónico (CONICET), Boulevard Brown 3600, (9120) Puerto Madryn, Chubut, Argentina. Personal commun.

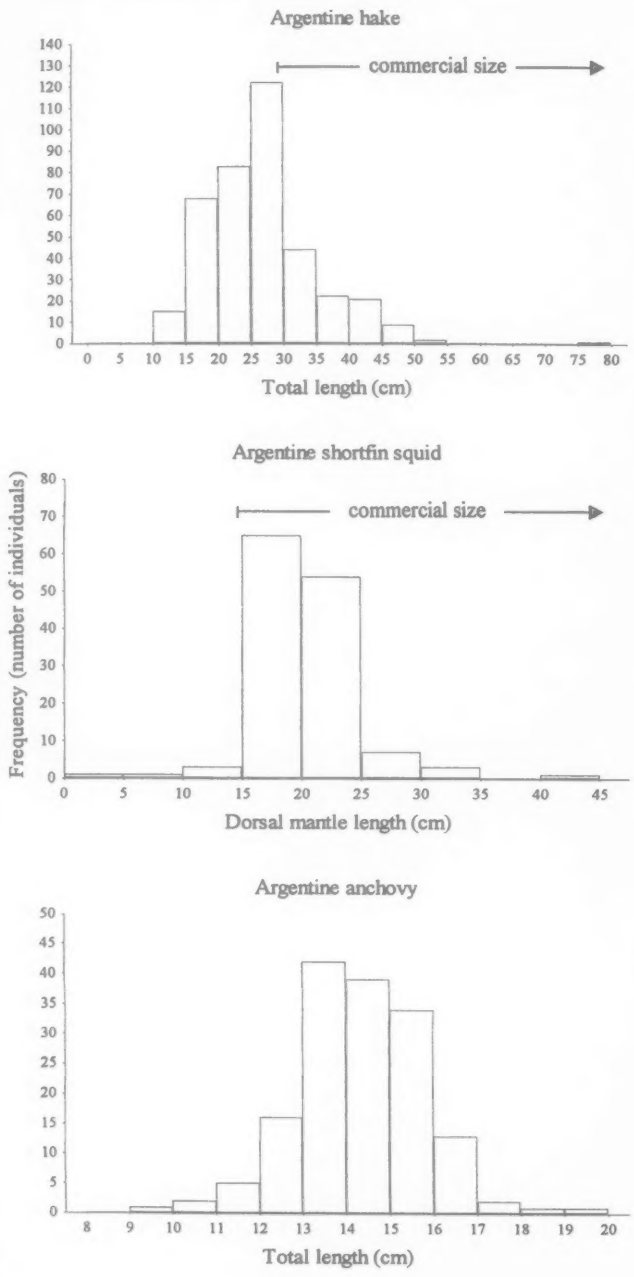


**Figure 4**

Regression-estimated size-frequency distribution of Argentine hake (*Merluccius hubbsi*), Argentine shortfin squid (*Illex argentinus*), and Argentine anchovy (*Engraulis anchoita*) consumed by South American sea lions off Patagonia collected in our study. The arrows indicate commercial sizes for Argentine hake and Argentine shortfin squid. All the sizes for Argentine anchovy are commercial.

curve in the period 1982–1987. Nevertheless, when the Argentine anchovy is excluded from the analysis, no differences were found between the two periods in either at the two overlap indices. Probably, the absence of Argentine anchovy in the period 1982–1987 is related to the small size of the sample collected and to the fact that Argentine anchovy was the least important prey species among the six prey species selected for the overlap analysis (Fig. 3) because the available information indicates that the abundance of Argentine anchovy was high and roughly constant during the entire study period (Ciechomski and Sánchez, 1988; Pájaro et al.[5]).

No differences in diet were detected when shore and entangled individuals were analyzed, even though several sources of bias could be operating at the same time. The diet information obtained from individuals found dead onshore could be biased, depending on the degree of digestion of the stomach contents. In our study, the use of several (and complementary) hard remains, such as otoliths and bones, allowed us to reduce this source of bias. Even when a small otolith was totally digested, the fish bones (mostly skull bones) permitted us to identify and quantify these prey. Thus, estimating prey size by regressions avoided underestimating the importance of small or highly digested prey. In some cases, when we used the regression of a related species, the results were likely partially biased. Samples from entangled sea lions probably did not hold any of these biases because all the stomach contents were presumably composed of fresh materials. The source of bias in this case would have been due to individuals that fed inside the net. Nevertheless, a comparison

[5] Pájaro, M., R. Sánchez and G. Macchi. 1997. Evaluación de la biomasa de adultos desovantes de la población norteña de anchoíta (*Engraulis anchoita*) en el período 1993–1996. Abstracts of the XII Simposio Científico-Tecnológico de la Comisión Técnica Mixta del Frente Marítimo, Montevideo, Uruguay, November 12–14, 1997, 4 p.

of dead, beached males with entangled males did not show any significant difference.

The only difference in diet found between subsamples was that shown by sexes. In this case differences in behavior and feeding habits could reflect differences in diet. Even if each sample source may have had different potential biases and the overlap analysis between them did not detect differences, we consider our sample to be, even with its limitations, a reasonable approximation of the diet of South American sea lions in Patagonia.

The diversity of prey species (Table 3) found in the diet of the South American sea lion indicates that it is a broad-spectrum predator. Some of these prey species (Argentine hake, Argentine shortfin squid, and Argentine anchovy) are abundant key species in the Patagonian continental shelf ecosystem and have commercial value (Angelescu, 1982; Angelescu and Prenski, 1987; Brunetti, 1990; Bezzi et al., 1994).

Argentine hake and Argentine shortfin squid are the two major target species of the Argentine fleet (Anonymous, 1996), and Patagonian squid is also exploited in the Falkland (Malvinas) Islands (Hatfield, 1996). Sea lions ate these prey species at both commercial and noncommercial sizes (Fig. 4).

The fishery catches Argentine hake with length modes between 35 and 40 cm TL (Cañete et al., 1986), and the minimum commercial size of this species is 30 cm TL. Mostly noncommercial sizes of Argentine hake (less than 30 cm TL) were consumed by South American sea lions (Fig. 4). Estimates of stock number by age by using virtual population analysis indicated that the most abundant Argentine hakes are those of age-1 and age-2 year classes (approximately 30 cm or less in TL), which represent around 56% in number of the estimated hake stock (Bezzi et al., 1994). These data indicate that sea lions are feeding on this species according to prey-size distribution and availability in the environment. Hakes smaller than 10 cm

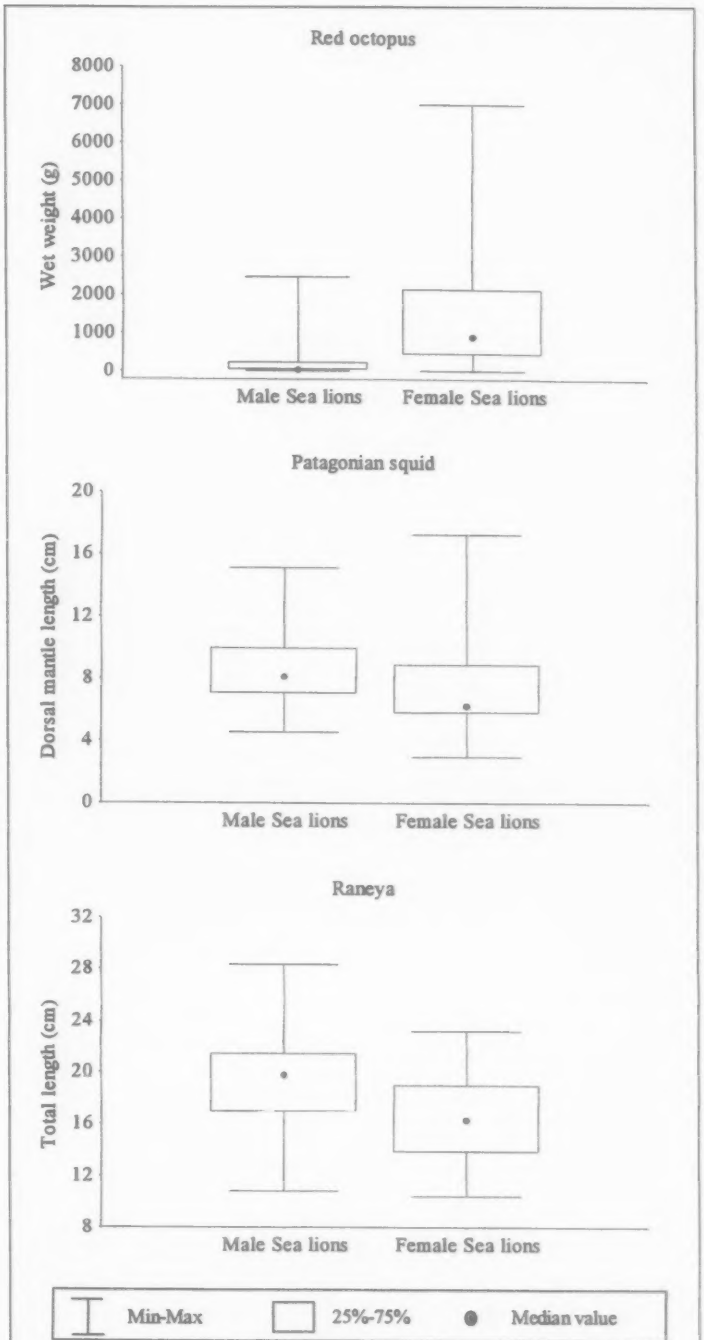


**Figure 5**

Box plots of regression-estimated size of red octopus (*Enteroctopus megalocyathus*), Patagonian squid (*Loligo gahi*), and "raneya" (*Raneya brasiliensis*) consumed by male and female South American sea lions collected in our study.

TL are not caught by either sea lions or the fishery because of the pelagic behavior of fish in this size range (Angelescu and Prenski, 1987).

The commercial squid species found in the diet of sea lions (Argentine shortfin and Patagonian squid) form schools of restricted size range (Brunetti and Ivanovic, 1992; Hatfield, 1996). Therefore, it is difficult to determine if the consumed sizes represent the environmental availability of these prey species. The commercial size of shortfin squid is approximately 15 cm DML, and this species was consumed by sea lions at commercial sizes (Fig. 4). Patagonian squid was consumed mostly at noncommercial sizes (less than 10 cm DML) because that most of the squid catches in the Falkland fishery were between 10 and 15 cm DML (Hatfield, 1996).

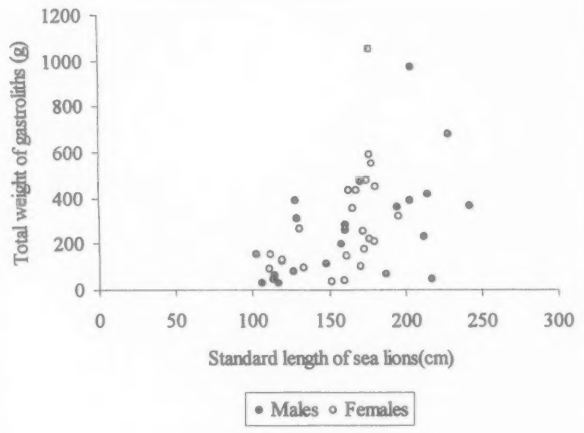


**Figure 6**

Scatterplot of total weight of gastroliths versus standard length for South American sea lions, by sexes.

These results indicate some overlap between the South American sea lion diet and fishery catches but not enough to conclude that competition exists with the fishery. The population of South American sea lions in northern Patagonia has been increasing during recent years at a rate of increase greater than 3% (Crespo and Pedraza, 1991; Dans et al.[2]). There is no indication that fishery catches affect the availability of food for sea lions at the present time. More detailed estimates of food consumption by South American sea lions are needed. Also, estimates of the catch and bycatch of the fishery are needed to evaluate conclusively the existence of ecological competition.

Differences in the diet between sexes are probably associated with different utilization of common and frequent food resources, suggesting some kind of differential feeding behavior between the sexes. The South American sea lion is a dimorphic and polygamous species. Therefore each sex must have different ecological constraints. Adult female feeding trips last for about three days during reproductive (Cappozzo et al., 1991) and nonreproductive (Reyes and Crespo[6]) seasons. Nursing pups may limit the distance that females can travel to feeding ground. Males are not restricted by nursing pups and their feeding trips seem to be less constant (Reyes and Crespo[6]). There is also some evidence obtained from sightings from fishing vessels that males move farther offshore than do females which remain closer to the coast (Crespo et al., 1997). Thus, differences in the diet could be associated with different feeding grounds or different home ranges between the sexes.

The prey of female South American sea lions were more evenly distributed within ecological groups than the prey of males (Fig. 7). The prey of females were mostly benthic and demersal-pelagic species. The mean dive depth recorded by lactating females in Patagonia was 60.9 m, and 69% of the dives were flat-bottomed and U-shaped (Werner and Campagna, 1995)—data that agree with the bottom and coastal feeding behavior suggested by the stomach contents. On the other hand, the most important prey of males were demersal-pelagic species (Fig. 7).

The Patagonian squid spawns in shallow waters, and the new generation migrates offshore to feed, grow, and mature (Hatfield, 1996). This migration pattern implies that small Patagonian squid must be more abundant in shallow, coastal waters than in deeper, offshore areas, but their size range in the coastal area must be broader than that in offshore areas because mature (and large) squids return to shallow waters to spawn. The consumption of larger Patagonian squid by male sea lions and the broader range size of Patagonian squid eaten by female sea lions agree with the hypothesis that females feed in more coastal and shallower waters than do males.

The red octopus lives mostly in caves on rocky bottoms (Ré, 1998) and is the most important prey species of female South American sea lions. Red octopus reach maturity around 120 mm DML and 850 g of total weight (Ré, 1998); male sea lions consumed

[6] Reyes, L. M., and E. A. Crespo. 1993. Variaciones diarias y lunares y viajes de alimentación en el lobo marino del sur *Otaria flavescens* en el norte de Patagonia. Abstracts of the Jornadas Nacionales de Ciencias del Mar "93," 19–25 September 1993, Puerto Madryn, Argentina, 156 p.

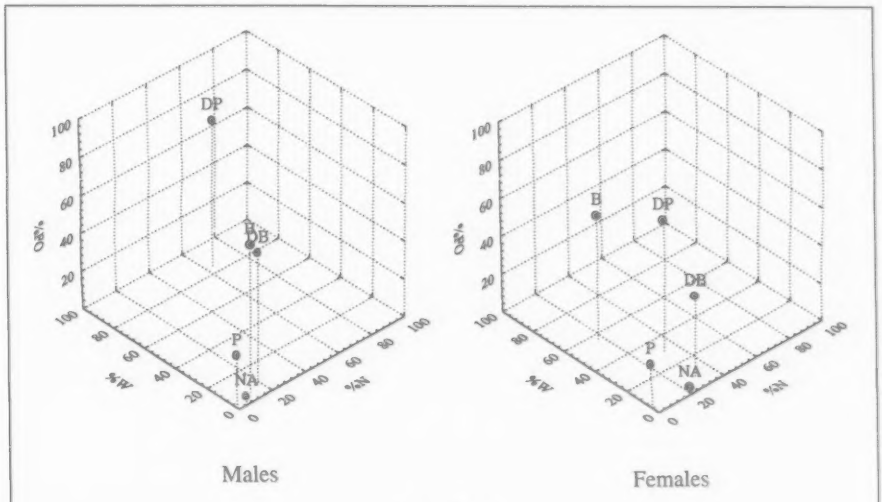


**Figure 7**

Ecological groups in the diet of male and female South American sea lions in our study. %FO = percent frequency of occurrence, %N = percentage by number, and %W = percentage by regression estimated wet weight. P = pelagic, B = benthic, DP = demersal pelagic, DB = demersal benthic, NA = not assigned.

mostly immature individuals whereas female sea lions consumed mature ones. If females search for prey on rocky bottoms, they will catch the mature and larger red octopus. Instead, if male South American sea lions feed mostly in the water column near the bottom, they could catch the younger red octopus when they are actively moving on the bottom. Younger octopus could be more vagrant than adults, and in some species, posthatching octopuses do exhibit pelagic behavior (Boletzky, 1977). The difference in the size of red octopus that South American sea lion consumed could be associated with this characteristic in prey biology, thus supporting the hyphothesis of different feeding behavior between the sexes.

In regard to gastrolith function, the hypothesis of buoyancy control has been postulated with the evidence of the presence of gastroliths in several living and extinct tetrapods that swim using their limbs in the form of an underwater fly (Taylor, 1993). Taylor (1993), in an extensive comparative study, demonstrated that there is no correlation between the presence of gastroliths and diet, but he found a correlation between gastroliths and underwater flying. Another explanation for the ingestion of stones is that gastroliths "grind up" parasitic worms that usually infest seals (Riedman, 1990). The role of stomach stones seems to be better explained as "buoyancy control" than as "elimination of stomach parasites" because of the independence between the presence of parasites and gastroliths, and the significant correlations between predator size and gastrolith weight. Gastroliths found in the South American sea lions could be considered "ballasts" that allow the sea lions to regulate their buoyancy. Moreover, the gastroliths can also be quickly swallowed and vomited, allowing sea lions to change buoyancy according to their needs (Harrison and Kooyman, 1968).

In summary, these stomach content analyses indicate that South American sea lions feed primarily on demersal and benthic species and, in general terms, use resources according to their environmental availability. Males and females appear to have different constraints in their feeding behavior and these restrictions could lead females to feed in more coastal and shallower waters than those where males feed. These potential differences in feeding grounds or home ranges, or both, could explain the observed differences in diet between the sexes.

## Acknowledgments

The authors wish to thank Pablo Mariotti, Bárbara Berón Vera, Nancy Mora, Pablo Nepomnaschy and Laura Reyes for their help with the stomach contents analysis; Silvana L. Dans, Pablo Yorio and Guillermo Harris for their critical reading and useful comments on earlier versions of the manuscript; and all of the

fishermen and wildlife wardens for their help aboard ship and in the field. Three anonymous reviewers (especially no. 817) and Sarah Shoffler made important and useful comments that enhanced the analysis of results and the expression of the ideas. As always, Sharyn Matriotti gave us important help with this article. Institutional support was provided by Centro Nacional Patagónico (CONICET), Universidad Nacional de la Patagonia, Fundación Patagonia Natural, Prefectura Naval Argentina, and the government of Chubut Province. The fishing companies Harengus S.A. and Alpesca S.A. collaborated with the authors in the retrieval of entangled sea lions and gave their permission for work onboard their fishing vessels. This work was carried out with the financial support of the National Geographic Society (Grant 5548/95 to E.A. Crespo and A.C.M. Schiavini), the Whale and Dolphin Conservation Society, the Patagonian Coastal Zone Management Plan (GEF/UNEP FPN/WCS) and the Programa de Cooperación Científica con Iberoamérica (1996–1998).

## Literature cited

**Angelescu, V.**
**1982.** Ecología trófica de la anchoíta del Mar Argentino (Engraulidae, *Engraulis anchoita*). Parte II. Alimentación, comportamiento y relaciones tróficas en el ecosistema. INIDEP (Instituto Nacional de Investigación y Desarrollo Pesquero), Contribution 409, 83 p.

**Angelescu, V., and L. B. Prenski.**
**1987.** Ecología trófica de la merluza común del Mar Argentino (Merlucciidae, *Merluccius hubbsi*). Parte 2. Dinámica de la alimentación analizada sobre la base de las condiciones ambientales, la estructura y las evaluaciones de los efectivos en su área de distribución. INIDEP, Contribution 561, 205 p.

**Anonymous.**
**1996.** Captura 95. Redes 88:24–40.

**Bezzi, S., G. Cañete, M. Pérez, M. Renzi, and H. Lassen.**
**1994.** Report of the INIDEP working group on assessment of hake (*Merluccius hubbsi*) north of 48°S (Southwest Atlantic Ocean). INIDEP Doc. Cient. 3:5–28.

**Boletzky, S. V.**
**1977.** Post-hatching behavior and mode of life in cephalopods. Symp. Zool. Soc. Lond. 38:557–567

**Boschi, E. E., C. E. Fischbach, and M. I. Iorio.**
**1992.** Catálogo ilustrado de los crustáceos estomatópodos y decápodos marinos de Argentina. Frente Marítimo 10 (sec. A):7–94.

**Brunetti, N. E.**
**1990.** Evolución de la pesquería de *Illex argentinus* (Castellanos, 1960). Inf. Técn. Inv. Pesq. 155, 19 p.

**Brunetti, N. E., and M. L. Ivanovic.**
**1992.** Distribution and abundance of early life stages of squid (*Illex argentinus*) in the south-west Atlantic. ICES J. Mar. Sci. 49:175–183.

**Campagna, C., and B. J. Le Boeuf.**
**1988.** Reproductive behavior of Southern sea lions. Behaviour 104:233–261.

**Cañete, G. R., R. G. Perrotta, and J. A. Pérez Comas.**
**1986.** Aspectos comparativos entre muestreos de desembarque y muestreos en alta mar de la especie merluza (*Merluccius hubbsi*), considerando el descarte efectuado por la flota marplatense en el período julio 1979–Setiembre 1980. Publ. Com. Téc. Mix. Fr. Mar. 1:447–453.

**Cappozzo, H. L., C. Campagna, and J. Monserrat.**
**1991.** Sexual dimorphism in newborn Southern sea lions. Mar. Mamm. Sci. 7(4):385–394.

**Clarke, M. R.**
**1986.** A handbook for the identification of cephalopods beaks. Clarendon Press, Oxford, 273 p.

**Cortés, E.**
**1997.** A critical review of methods of studying fish feeding based on analysis of stomach contents: application to elasmobranch fishes. Can. J. Fish. Aquat. Sci. 54:726–738.

**Crespo, E. A., J. F. Corcuera, and A. López Cazorla.**
**1994.** Interactions between marine mammals and fisheries in some coastal fishing areas of Argentina. *In* Gillnets and cetaceans (W. F. Perrin, G. P. Donovan, and J. Barlow, eds.), p. 269–281. Rep. Int. Whal. Comm. (special issue 15).

**Crespo, E. A., and S. N. Pedraza.**
**1991.** Estado actual y tendencia de la población de lobos marinos de un pelo (*Otaria flavescens*) en el litoral norpatagónico. Ecología Austral 1:87–95.

**Crespo, E. A., S. N. Pedraza, S. L. Dans, M. Koen Alonso, L. M. Reyes, N. A. García, M. Coscarella, and A. C. M. Schiavini.**
**1997.** Direct and indirect effects on the high seas fisheries on the marine mammal populations in the northern and central patagonian coast. J. Northwest Atl. Fish. Sci., 22:189–207.

**de Ciechomski, J. D., and R. P. Sanchez.**
**1988.** Análisis comparativo de las estimaciones de biomasa de la anchoíta (*Engraulis anchoita*) en el Atlántico Sudoccidental en diferentes años y con distintas metodologías. Publ. Com. Téc. Mix. Fr. Mar. 4:117–132.

**George-Nascimento, M. F., R. A. Bustamante, and R. C. Oyarzun.**
**1985.** Feeding ecology of the Southern sea lion *Otaria flavescens* Shaw, 1800: food contents and food electivity. Mar. Biol. Prog. Ser. 21:135–143.

**Hamilton, J. E.**
**1934.** The Southern sea lion *Otaria byronia* (de Blainville). Discovery Rep. 8:269–318.

**Harrison, R. J., and G. L. Kooyman.**
**1968.** General physiology of the Pinnipedia. *In* The behavior and physiology of pinnipeds (R. J. Harrison, R. C. Hubbard, R. S. Peterson, C. E. Rice, and R. J. Schusterman, eds.), p 221–296. Appleton-Century-Crofts, New York, NY.

**Hatfield, E. M. C.**
**1996.** Towards resolving multiple recruitment into loliginid fisheries: *Loligo gahi* in the Falkland Islands fishery. ICES J. Mar. Sci. 53:565–575.

**Koen Alonso, M., E. A. Crespo, N. A. García, S. N. Pedraza, and M. Coscarella.**
**1998.** Diet of dusky dolphins, *Lagenorhynchus obscurus*, in waters off Patagonia, Argentina. Fish. Bull. 96:366–374.

**Ludwig, J. A., and J. F. Reynolds.**
**1988.** Statistical ecology. John Wiley and Sons, New York, NY, 337 p.

**Menni, R. C.**
**1983.** Los peces en el medio marino. Estudio Sigma S.R.L., Buenos Aires, Argentina, 169 p.

**Menni, R., and H. L. López.**
**1984.** Distributional patterns of Argentine marine fishes. Physis 42 (issue 103, sec. A):71–85.

**Menni, R. C., R. A. Ringuelet, and R. A. Aramburu.**
**1984.** Peces marinos de la Argentina y Uruguay. Editorial Hemisferio Sur S.A., Buenos Aires, Argentina, 359 p.

**Petraitis, P. S.**
**1979.** Likehood measures of niche breadth and overlap. Ecology 60(4):703–710.

**Pinkas, L., M. S. Oliphant, and I. L. K. Iverson.**
**1971.** Food habits of albacore, bluefin tuna and bonito in California waters. U.S. Dep. Fish. Game, Fish Bull. 152:1–105.

**Ré, M. E.**
**1998.** Pulpos octopódidos (Cephalopoda, Octopodidae). *In* El mar argentino y sus recursos pesqueros (E. Boschi, ed.), tomo 2: Los moluscos de interés pesquero. Cultivos y estrategias reproductivas de bivalvos y equinoideos, p 99–114. Instituto Nacional de Investigación y Desarrollo Pesquero, Secretaría de Agricultura, Ganadería, Pesca y Alimentación, Mar del Plata, 231 p.

**Reyes, L. M., E. A. Crespo, and V. Szapkievich.**
**1999.** Distribution and population size of the southern sea lion (*Otaria flavescens*) in central and southern Chubut, Patagonia, Argentina. Mar. Mamm. Sci. 15(2):478–493.

**Riedman, M.**
**1990.** The pinnipeds: seals, sea lions and walruses. Univ. California Press, Berkeley, CA, 439 p.

**Roper, C. F. E., M. J. Sweeney, and C. E.Nauen.**
**1984.** FAO species catalogue: an annotated and illustrated catalogue of species of interest to fisheries, vol. 3: Cephalopods of the world. FAO Fish. Synop. 125, 277 p.

**Siegel, S., and N. J. Castellan.**
**1995.** Estadística no paramétrica aplicada a las ciencias de la conducta, 4th Spanish edition. Editorial Trillas S.A., Mexico D.F., Mexico, 437 p.

**Smith, E. P., and T. M. Zaret.**
**1982.** Bias in estimating niche overlap. Ecology 63(5): 1248–1253.

**Taylor, M. A.**
**1993.** Stomachs stones for feeding or buoyancy? The occurrence and function of gastroliths in marine tetrapods. Philos. Trans. R. Soc. Lond. (B Biol. Sci.) 341:163–175.

**Vaz Ferreira, R.**
**1982.** *Otaria flavescens* (Shaw), South American sea lion. *In* Mammals of the world, FAO Fish. Series 5(IV), p 447–495. FAO, Rome.

**Werner, R. and C. Campagna.**
**1995.** Diving behavior of lactating southern sea lions (*Otaria flavescens*) in Patagonia. Can. J. Zool. 73:1975–1982.

# Modeling statistical performance of an airborne lidar survey system for anchovy

**Nancy C. H. Lo**

**John R. Hunter**

Southwest Fisheries Science Center
National Marine Fisheries Service, NOAA
P.O. Box 271, La Jolla, California 92038
E-mail address (for N.C.H. Lo): Nancy.Lo@noaa.gov

**James H. Churnside**

Ocean Remote Sensing Division
Environmental Technology Laboratory
325 Broadway, Boulder, Colorado 80303

**Abstract.**—The objective of our study was to model the performance of an airborne lidar survey system for northern anchovy in terms of survey accuracy and precision. Our analyses indicated that swath width would have little or no effect on the probability that at least one fish school would be encountered. In typical coastal waters off California (attenuation coefficient=0.1/m), about half of the schools were detected by the lidar during the day and about 64% during the night. A greater proportion of schools were detected during the night because anchovy have a shallow vertical distribution, whereas in the day, schools may extend down to 155 m; schools below about 40 m depth were not detectable to the laser. Although schools tended to be more diffuse during the night than during the day, even the very diffuse schools of anchovy (0.5 fish/$m^3$) were detectable at night throughout the upper 20 m of the water column with a lidar. With a substantial increase in instrument and survey costs, it would be possible to increase the equivalent laser-pulsed power by a factor of 10 over that of the "off-the-shelf system," as used in our model. Such a change would increase the maximum detection depth of the lidar system by about 10 m but would have a negligible effect on the probability of detecting schools during the day owing to the skewed vertical distribution of anchovy schools. More effective approaches for improving the accuracy and precision of potential lidar surveys for fisheries would be to improve school detection algorithms and to develop a lidar survey model based on line transect theory to obtain an unbiased estimate of abundance. To produce an accurate reconstruction of the average vertical distribution of schools for a particular season and region, a synthesis of acoustic and lidar surveys of school distribution is required.

Manuscript accepted 18 November 1999.
Fish. Bull. 98:264–282 (2000).

Airborne lidar surveys are an attractive alternative to the methods presently used in fishery-independent surveys of epipelagic fishes (Hunter and Churnside[1]). They would cost much less per survey mile than ship-based methods (acoustic-trawl, ichthyoplankton), and the survey would extend to greater depths than present aerial methods. A lidar, (li[ght] d[etecting] and r[anging]) system, in its most basic form, produces short pulses of laser light that pass through the water surface and reflect off fish and particles in the water; a receiver measures the returning reflected pulse; the strength of the returning pulse separates fish targets from small particles, and the elapsed time from start to return of pulses indicates the range (depth below the surface) of the target. The application of lidar technology to fishery surveys is still in its infancy. Fish schools have been detected with a variety of lidar systems (Churnside and Hunter, 1996), but schools have never been systematically studied with lidar, nor has existing lidar technology been adapted to fish-survey needs; formal fish surveys have never been conducted.

A lidar survey system for fishery-independent monitoring of epipelagic fish stocks is being developed jointly by two laboratories of the National Oceanic Atmospheric Administration (NOAA): Environmental Technical Laboratory, Boulder, CO; and Southwest Fisheries Science Center, La Jolla, CA. The approach is to combine evaluations of prototype instruments at sea with modeling of survey performance to develop an optimal lidar survey system. The goal is to develop a system that will deliver the greatest statistical precision for the lowest survey cost, while minimizing potential biases. In our study, we modeled a lidar survey with the objective of evaluating how instruments would affect survey precision or accuracy. Two classes of instrument design were considered, those affecting fish schools in the horizontal plane (swath width) and those affecting the detection of fish schools in the vertical plane (depth-specific detection). We also analyzed a trade-off between swath width and penetration depth, which is analogous to changing from a visual-based aerial survey (wide swath, shallow penetration) to a lidar-based

[1] Hunter, J. R., and J. H. Churnside, eds. 1995. Airborne fishery assessment technology—a NOAA workshop report. SWFSC Admin. Rep. LJ-95-02, 33 p. Southwest Fish. Sci. Ctr., NMFS, NOAA, P.O. Box 271, La Jolla, CA 92038.

aerial survey (narrow swath, deeper penetration). We discuss each.

Precision of an airborne lidar survey will depend upon the number of transects flown and the probability of encountering schools along them. The width of the transect lines (swath width), may affect the probability of encountering schools and therefore could be one of the few factors affecting precision that involve instrument design. Swath width could be increased in a variety of ways (flying higher, scanning or optically expanding the laser beam), but such changes are accompanied by disadvantages (loss in penetration depth, reduced resolution, increased instrument cost and weight). In our study, we modeled how the width of the swath (width of transect line) cut by the survey instrument affects the probability of encountering fish schools, and therefore the precision of the survey estimate, assuming fish are uniformly distributed in the water column.

The accuracy of a biomass survey depends on the extent to which the entire stock is vulnerable to the counting technique and on the variability in size of the uncounted fraction (Gunderson, 1993). The key issue for accuracy of a lidar survey is the vulnerability of a stock to being counted in the vertical plane. Depth-specific detection by a lidar depends upon laser power, sensitivity of the detection system, the rate of exponential decay of the laser pulse with water depth, the way the fish-detection function of the instrument changes with signal attenuation, fish size and reflectivity, school packing density, and, of course, the vertical distribution of the fish. Using a set of models and taking into account many of these variables, we evaluated the effect of instrument and survey design on the accuracy of an aerial lidar survey for measuring fish abundance. We considered how variations in laser power, school size, diel changes in vertical distribution of schools and school packing density (number of fish per $m^3$) would affect the accuracy of the survey. We also used these models to estimate the maximum depth at which schools might be detected by a single lidar pulse. For our study, we chose to use anchovy because more data exist on anchovy schools than most other species. Lo et al.[2] have, however, recently applied the same models to sardine and herring schools.

## Materials and methods

We used various models to evaluate the potential effects of instruments on survey design. To evaluate how swath width may affect survey accuracy, simulation runs were used for a school-group encounter model. To evaluate the relation between laser power and maximum detection depth for fish schools, we computed the probability of detecting schools as a function of the signal-to-noise-ratio and estimated laser power and the laser attenuation coefficient. School parameters, size, distribution and density, and survey area (46,204 $km^2$=333 km (180 nmi) × 138.75 km (75 nmi)) were taken from acoustic surveys of northern anchovy in the Southern California Bight (Mais, 1974; Fiedler, 1978; Smith, 1981; MacCall[3]). For daytime profiles, vertical distributions of schools were based on northern anchovy off California (Holliday and Larsen, 1979); for nighttime profiles we used the distribution of early stage anchovy eggs (Pommeranz and Moser, 1987) and acoustic data for anchoveta off Peru (Castillo Valderrama, 1995). Signal-to-noise ratio was based on information on packing density of schools provided by Aoki and Inagaki (1988) and Graves (1977).

Many pelagic fish schools form distinct aggregations or school groups (Cram and Hampton, 1976; Fiedler, 1978). The area of an anchovy school (expressed by school diameter in our study) is highly variable, as are the size and number of schools within a school group. Because of this complexity, simulations were used to compute the probability of encountering anchovy schools in a survey area (Fiedler, 1978).

In the simulation, school groups were randomly assigned in the survey area. The sizes of the anchovy schools within a group were generated from the frequency distribution of the diameters of northern anchovy schools in the Southern California Bight (Fiedler, 1978; Smith, 1981; Table 1). The number of anchovy schools within an anchovy school group was generated from the area occupied by the group and the density of schools. Both the diameters of school groups and the density of schools within a school group were assumed to follow the lognormal distributions measured for anchovy in the Southern California Bight (Fiedler, 1978; Smith, 1981) (Fig. 1). Simulations were used to compute the encounter probability ($p_Y$) for various swath widths ($y$).

The locations of school groups were randomly allocated in north–south (n–s) and east–west (e–w) directions. When school groups overlapped (intersected) in the north–south directions, they were combined as a "single" school group for computing the encoun-

[2] Lo, N. C. H., J. R. Hunter, and J. H. Churnside. 1999. Modeling properties of airborne lidar surveys for epipelagic fish. Admin. Rep. LJ-99-01. Southwest Fish. Sci. Ctr. NMFS, NOAA. P.O. Box 271, La Jolla, CA 92037.

[3] MacCall, A. 1975. Anchovy population survey simulation: a report of CalCOFI Anchovy Workshop Group on methods of estimating anchovy abundance, July 21–22, 1975, Contribution 4, 9 p. Marine Life Research Group, Scripps Institution of Oceanography, 9500 Gilman Drive, La Jolla, CA 92037-0227.

**Table 1**

The frequency distribution of school sizes of anchovy in the Los Angeles Bight based on sonar mapping conducted by the California Department of Fish and Game (Mais, 1974; Smith,1981).

| School diameter (m) | Frequency | Sample proportions |
|---|---|---|
| 10 | 9906 | 0.4338 |
| 30 | 9002 | 0.3942 |
| 50 | 1822 | 0.0798 |
| 70 | 706 | 0.0309 |
| 90 | 824 | 0.0361 |
| 110 | 178 | 0.0078 |
| 130 | 217 | 0.0095 |
| 150 | 50 | 0.0022 |
| 170 | 40 | 0.0018 |
| 190 | 51 | 0.0022 |
| 210 | 19 | 0.0008 |
| 230 | 7 | 0.0003 |
| 250 | 3 | 0.0001 |
| 270 | 1 | <0.0001 |
| 290 | 2 | 0.0001 |
| 310 | 1 | <0.0001 |
| 330 | 3 | 0.0001 |
| 350 | 0 | 0 |
| 370 | 0 | 0 |
| 390 | 2 | 0.0001 |

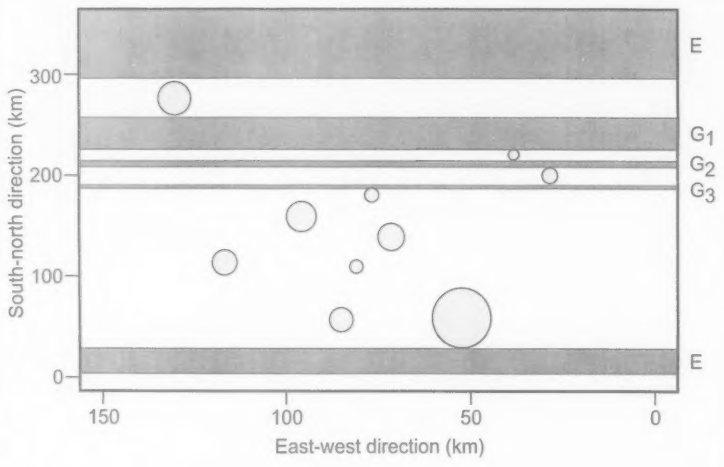


**Figure 1**

A spatial distribution of school groups from one simulation run. Circles indicate areas covered by school groups for a population of 80,000 schools. This graph was generated from lognormal distributions with mean = 3.91 and variance = 0.51 for school density (number of schools/nmi$^2$) and from lognormal distribution with mean = 2.319 and variance = 0.676 for diameter (nmi) of school group (nmi was later converted to km). G1, G2, G3, and E are the gaps used to compute the encounter probability (Eq. 1).

ter probability. Only the north–south direction was relevant because the transect was run from east to west. Similarly, schools were randomly allocated within a school group and when schools overlapped in the north–south direction, they were combined as a "single" school for computing purposes. This process continued until all schools were separated in the north–south direction and termed "disjoint" schools. The distance (gaps) between disjoint schools in the north–south direction were summed for each school group and later summed for all fish groups. The sum of n–s gaps within school groups was termed "total gap within." Similarly, a "total gap between" (disjoint school groups) was also computed. Both "total gap within" and "total gap between" were used to compute the encounter probability ($p_y$) (the probability that at least one fish school is detected):

$$p_y = 1 - (\textit{total gap within} + \textit{total gap between})/L$$

or

$$p_y = 1 - \frac{\sum_{i}^{n}\sum_{j}^{J_i-1}(g_{ij}-y) + \sum_{i}^{n-1}(G_i - y) + E}{L}, \quad (1)$$

where $y$ = the swath width in meter;

$g_I$ = the gap length between $j^{th}$ and $j$+1$^{th}$ disjoint school within a school group and the quantity of $g_{ij} - y$ is set to zero if $g_{ij}$ is less than $y$;

$G_I$ = the gap length between $i^{th}$ and $i$+1$^{th}$ disjoint school groups and $G_i - y$ is set to zero if $G_i$ is less than $y$;

$E$ = the distance between the north and south end of the survey area and their nearest anchovy schools;

$N$ = number of school groups disjoint in the north–south direction; and

$L$ = 333 km (180 nautical miles [nmi]) which is about the length of the coastline along the Southern California Bight.

Smith (1981) reported that the diameter (nmi) of a school group followed a lognormal distribution and had a logarithmic mean of 2.319 and a logarithmic variance

of 0.676, and that the density of fish schools/nmi$^2$ in a school group had a logarithmic mean of 3.91 and a logarithmic variance of 0.51 based on data from MacCall.[3] The number of schools within a school group is the product of the area of the school group and the density of schools within. Thus, the mean number of schools was 10,274[4] in a school group (Table 2). The diameter of anchovy schools was generated from the frequency distribution of the diameters of anchovy fish schools in the Southern California Bight (Table 1).

On average, there were 150,000 anchovy schools in the Southern California Bight in the 1970s (Mais, 1974). In recent years, the population has decreased to one fifth of that level (Jacobson et al., 1994). In the simulation, we constructed populations comprising 80,000, 32,000, and 16,000 schools with an average biomass of 12 metric tons (t). At each population level of anchovy, we simulated school groups for nine combinations of three school diameters and three school densities, each with a multiplier of 0.5, 1, and 1.5 applied to both mean and standard deviation of ln(*school diameters*) and of ln(*density of schools*) respectively (Table 2). For example, for a population of 32,000 schools, a multiplier of 0.5 applied to both mean and standard deviation of ln(*diameter*) (an area of 9.45 nmi$^2$ or 32.34 km$^2$) for a school group,[5] and a multiplier of 1.5 applied to the mean and standard deviation of ln(density) (625 schools /nmi$^2$ or 182 schools/km$^2$),[6] would yield an average number of 5914 schools per school group and an average of six school groups (32,000/5914) (Table 2). This population was denoted as 32,000 (0.5,1.5). The encounter probabilities for seven swath widths (1, 10, 50, 200, 500, 900, and 1600 m for a total of 63 ($3 \times 3 \times 7$) sets of scenarios) were simulated (in computation, numeral 1 was used to represent diameters less than or equal to 1 m). For each of the three populations, 500 iterations were run for each of 63 sets. The mean of the encounter probabilities from 500 runs was used to estimate the mean encounter probability.

For multiple swaths ($n$), the probability ($p_{y,n}$) that at least one of the swaths intercepts schools is computed as

$$p_{y,n} = 1 - (1 - p_y)^n, \tag{2}$$

where $p_y$ is computed from Equation 1.

[4] The mean diameter is 14.25 nmi = exp(2.319+0.676/2) and the mean density of fish schools is 64.39 schools/nmi$^2$ = exp(3.91+ 0.51/2), the mean number of fish schools in a school group = $(14.25/2)^2$ 64.39 =10,274.

[5] $[\exp(2.319 \times 0.5 + 0.676 \times 0.5 \times 0.5/2)/2]^2 \times 3.1416 = 9.45$ nmi$^2$.

[6] $\exp(3.91 \times 1.5 + 0.51 \times 1.5 \times 1.5/2) = 625.62$ schools/nmi$^2$.

**Table 2**

The average number of school groups for three population sizes and the average number of schools per school group for combinations of different multipliers for the school densities and the school diameters (see text).

| Multipliers for diameter of school groups | Multipliers for school density 0.5 | 1.0 | 1.5 |
|---|---|---|---|
| Average number of school groups for three population sizes: | | | |
| Population: 16000 schools | | | |
| 0.5 | 224.79 | 26.28 | 2.71 |
| 1.0 | 13.32 | 1.56 | 0.16 |
| 1.5 | 0.56 | 0.07 | 0.01 |
| Population: 32000 schools | | | |
| 0.5 | 449.58 | 52.56 | 5.41 |
| 1.0 | 26.64 | 3.11 | 0.32 |
| 1.5 | 1.13 | 0.13 | 0.01 |
| Population: 80000 schools | | | |
| 0.5 | 1123.94 | 131.41 | 13.53 |
| 1.0 | 66.59 | 7.79 | 0.80 |
| 1.5 | 2.81 | 0.33 | 0.03 |
| Average number of schools per school group | | | |
| 0.5 | 71.18 | 608.77 | 5914.65 |
| 1.0 | 1201.33 | 10274.66 | 99826.39 |
| 1.5 | 28429.65 | 243150.98 | 2362398.24 |

## Estimating the number of swaths needed in a survey

Typically, the optimal sample size for a survey is computed by minimizing the variance of the estimate subject to a fixed cost. Because this information was not available, we defined a desirable sample size in terms of the minimum number of transect lines or swaths needed to guarantee at least one positive sighting at an acceptable probability. Therefore, from $p_y$ in Equation 1, one can compute the number of swaths ($n$) needed for a desired value of $p_{y,n}$ by using

$$n = \frac{\ln(1 - p_{y,n})}{\ln(1 - p_y)}. \tag{3}$$

## Probability of detecting fish by depth with signal-to-noise ratios (SNR)

The signal level of a lidar system decays exponentially with depth. The decaying signal of a single pulse can be expressed by the equation

$$S(z) = S_0 \frac{\beta_w(z) + \beta_f(z)}{\beta_0} \exp(-2\alpha z), \tag{4}$$

where $z$ = depth in meters;
$S_0$ = the signal level at the surface;
$\beta_w$ = the clear-water backscatter coefficient;
$\beta_f$ = the backscatter coefficient of a school of fish;
$\beta_0$ = the backscatter coefficient at the surface; and
$\alpha$ = the lidar attenuation coefficient.

The backscatter coefficients, $\beta$, have units of 1/m and represent the fraction of the energy that would be scattered upward by a 1-m layer of either clear water or fish. By clear water we mean natural sea water with its attendant load of yellow substance, plankton, silt, etc., but without fish. The lidar attenuation coefficient is related to the absorption and scattering coefficients of the water, in a way that is not completely understood, but depends on the field of view of the lidar. In an operational system, this parameter can be obtained directly from the lidar data. A very narrowly collimated system (defined as one where the field of view is much smaller than the average scattering angle in the water and much smaller than the ratio of the beam attenuation coefficient to the lidar height) will have an attenuation that is very close to the sum of the absorption and scattering. A wide field of view collects multiple scattered photons, and the attenuation is closer to the absorption coefficient.

The noise in a lidar system can come from several different processes. One of these is likely to predominate in any particular set of circumstances. One source is thermal noise in the receiver. This is an additive noise that is independent of the signal level. It is Gaussian with a zero mean. Another source of noise is the shot noise from the sum of the signal current, background-light-generated current, and detector dark current. This is a Poisson process that depends on the total detector current. However, except for very low illumination levels, the Poisson distribution is nearly Gaussian, and we made this approximation. Also, we noted that if the signal from the fish school is very large, the detection probability is nearly unity, and accurate modeling of the noise distribution is not critical. If the fish signal is small, the shot-noise variance will be very nearly the same whether fish are present or not. This is the situation that must be treated accurately, and so we assumed that shot noise could be approximated by an additive signal-independent Gaussian process for the purposes of our study. The final noise source is caused by variations of the optical properties of the water with depth. Variations that are slow in comparison with the depth resolution of the lidar can be estimated and eliminated. However, more rapid fluctuations would be indistinguishable from noise. In the absence of a better model for these fluctuations, we also assumed that they were Gaussian. Thus, an additive signal-independent Gaussian noise was considered, and the source of this noise was not considered further. The final results would not be very different if the dominant noise was not Gaussian. Non-Gaussian noise would change the numerical values of the detection and false-alarm integrals. Because of the strong exponential decrease in signal level with depth, small changes in these values would correspond to small changes in detection depth. A similar effect was caused by our choice of threshold level, which also changed the detection and false-alarm integrals. We show that the results are not very sensitive to our choice of threshold level for the same reason. It is possible that the variations in optical properties produce a highly non-Gaussian noise that will have a significant effect, but we have no evidence for this.

The probability density function (pdf) of the instantaneous signal ($s$) for a single pulse at some depth can therefore be approximated by a normal pdf with mean = $S$ and variance = $\sigma^2$. For illustration, we assumed that $\sigma$ was not depth dependent, although $s$ clearly was.

Detection was accomplished by setting a threshold signal level above which we asserted that fish were present. The detection probability is the probability that the instantaneous signal is above this threshold when fish are present (i.e. when $\beta_f > 0$). Thus,

$$p(detection) = P(s > T) = 1 - \Phi\left(\frac{T - S_f}{\sigma}\right),$$

where $T$ = the threshold level;
$S$ = a normal random variable with mean= $S_f$ and variance = $\sigma^2$;
$S_f$ = the signal level with fish present; and
$\Phi(u)$ = $P(U<u)$ is normal distribution function of $U$ with mean = 0 and variance = 1.

Specifying that fish are present whenever the received signal exceeds some threshold value entails some probability of a "false alarm." This probability can be calculated from

$$P(false\ alarm) = P(s > T) = 1 - \Phi\left(\frac{T - S_w}{\sigma}\right),$$

where $S_w$ = the signal from clear water.

To reduce the number of free parameters, we normalized everything by the noise level. Thus, we defined a signal-to-noise ratio, $SNR = (S_f - S_w)/\sigma$

and a threshold-to-noise ratio, $TNR = (T - S_w)/\sigma$. Then $P(detection) = 1 - \Phi(TNR - SNR)$ for signals following normal distribution with mean SNR and variance 1 when fish are present, and $P(false\ alarm) = 1 - \Phi(TNR)$ for signals following normal distribution with mean = 0 and variance = 1 when no fish are present.

The maximum detection depth, $z_{max}$, was defined as the depth at which the detection probability is 0.5, i.e. the $SNR_z$ is equal to the $TNR$ because of the sharp drop in detection probability from 1 to 0 with depth (Fig. 2).

$$TNR = SNR_z = SNR_0 e^{(-2\alpha z)}. \quad (5)$$

We could rearrange the terms in Equation 5 and calculate that

$$z_{max} \approx -\frac{1}{2\alpha} \ln\left(\frac{TNR}{SNR_0}\right). \quad (6)$$

We investigated the degree that maximum detection depth for schools is affected by the setting of the false-alarm rate by calculating $z_{max}$ as a function of the false-alarm probabilities and determining the value of $TNR$ to be used in Equation 6. The detection probability ($P(detection)$) can be approximated by unity for depths above this $z_{max}$ and by zero for depths below it (Fig. 2). That is

$$P(detection) = 1 \text{ for } SNRz > TNR \text{ or } z < z_{max}$$
$$= 0 \text{ otherwise.}$$

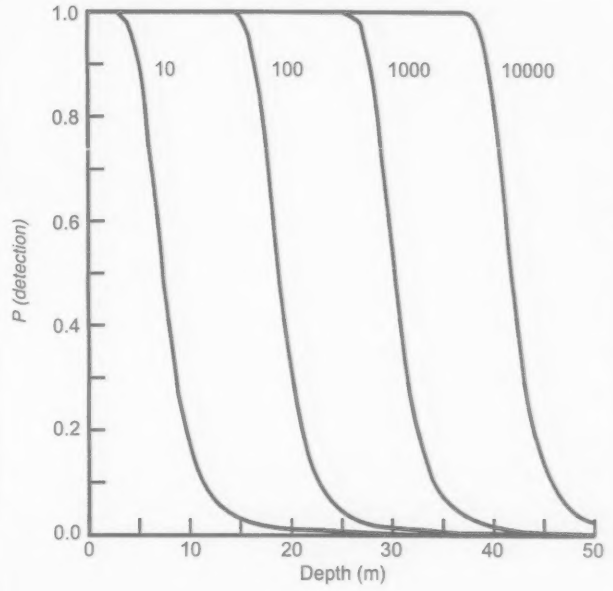


**Figure 2**

Detection probability as a function of depth for a lidar system with a false-alarm probability of 0.01 operating in water with an attenuation coefficient of 0.1/m. Curves are labeled by the value of the signal-to-noise-ratio ($SNR_0$) at the surface.

## Laser power and penetration depth

To get an idea of the ranges of depths that might be available to the lidar for a reasonable cost, we calculated the maximum penetration depth ($z_{max}$) with a lidar model that was developed to perform engineering trade-offs quickly and easily. Input parameters and lidar components can be changed easily by the user, and the computer program automatically calculates all of the affected quantities. Plots can be quickly generated within the program to allow the results to be immediately viewed. The lidar system was assumed to be similar to that currently used by NOAA (Churnside et al., 1997). Actual parameters are presented in Table 3.

Only laser power effects were considered. Clearly, other factors were also important. These included receiver telescope diameter, detector sensitivity, background light conditions, fish species, density, etc. However, a full investigation of the effects of all pertinent parameters was beyond the scope of our study. The effects of some of these parameters, however, could be estimated. Doubling the receiver telescope area, detector sensitivity, or fish density, for example, is equivalent to doubling the laser power, and we could have considered an equivalent laser energy that included differences in these parameters. Because of the assumptions used in our calculations, our calculations should be taken as representative and are not necessarily precise.

Because of the interference with the surface, it was difficult to actually calculate $SNR_0$. Instead, we noted that

$$SNR_0 = SNR_z \exp(2\alpha z), \quad (7)$$

where $z$ = any arbitrary depth; and
$SNR_z$ = the signal-to-noise ratio at that depth.

The calculations were done with a fish school deep enough so that surface effects (e.g. specular reflections of the tail of the laser pulse) did not contribute to the received signal from the school. Equation 7 does not hold for fish within about 1 m of the surface,

but the errors are negligible for the depth distributions of fish used in our study.

The signal and noise levels can be defined at any one of a number of points in the receiver, including optical power on the detector, current out of the detector, the voltage generated by that current through a standard 50-Ω resistance, the output of the log-amplifier, or the integer value that this produces when digitized. We consistently used the voltage across 50 Ω, which is the input voltage to the log-amplifier. For an infinitesimally short laser pulse, this signal varies in time as the pulse propagates through the water. We could relate this time to the depth at which the light was scattered back to the receiver because we knew the speed at which light travels through water. Therefore, we could write the signal as a function of depth as for a nadir-pointing:

$$S'(z) = \frac{P(z)\pi d^2 R\beta(\pi)}{4(z+nh)^2}\exp(-2\alpha z), \quad (8)$$

**Table 3**

Baseline model parameters for computing laser power and penetration depth.

| Parameter | Value |
|---|---|
| Transmitter | |
| Wavelength | 532 nmi |
| Pulse length | 15 nsec |
| Pulse energy | 1 mJ–1 kJ |
| Pulse repetition rate | 10 Hz |
| Height above surface | 100 m |
| Beam divergence | 25 mrad |
| Receiver | |
| Aperture diameter | 20 cm |
| Field of view | 25 mrad |
| Optical bandwidth | 10 nm |
| Electronic bandwidth | 100 MHZ |
| Sample rate | 1 GHz |
| Receiver noise | 140 microvolts |
| Detector type | R5800 photomultiplier tube @ 1200 V |
| Polarization | Unpolarized |
| Environment | |
| Aircraft height | 100 m |
| Water type | IB, III |
| Background light | 1/4 moon |
| Background light fluctuations | 2 percent |
| Fish school | |
| Fish type | anchovy |
| Length | 10 cm |
| Reflectivity | |
| Packing density | 0.5/ $m^3$ |
| School thickness | 10 m |

where $S'$ = the received signal per unit depth at depth $z$;
$P$ = the laser power;
$R$ = the responsivity of the detector and load in V/W;
$\beta(\pi)$ = the backscatter coefficient of the water plus any fish present at that depth;
$h$ = the height of the aircraft above the surface;
$n$ = the index of refraction of water (1.33); and
$\alpha$ = the lidar attenuation coefficient.

To get the actual signal voltage, we had to integrate Equation 8 over the finite duration of the laser pulse. To get the short pulses desired, it was necessary to use Q-switching. With this technique, the laser resonator is blocked electro-optically while the energy is stored in the lasing medium. The cavity is then quickly opened. Lasing begins rapidly, and the output power quickly builds to a high value. As the energy in the lasing medium is depleted, the output power decreases back to zero. This technique produces a characteristic pulse shape that can be approximated by

$$P(t) = \frac{Et}{\tau^2}\exp\left(-\frac{t}{\tau}\right), \quad (9)$$

where $E$ = the total pulse energy; and
$\tau$ = 0.408 times the full width of the pulse at one half of its maximum value.

We converted this time to distance through the speed of light, and integrated Equation 8 over depth.

Two water types were used. These were Jerlov (1968) types IB and III. These specify only the diffuse attenuation coefficient $K_D$. To obtain an estimate of lidar attenuation we needed to have an estimate of the volume scattering function $\beta(\vartheta)$, where $\vartheta$ is the scattering angle. We used the general functional form of Petzhold (Petzhold, 1972; Mobley, 1995) with the exact values scaled by the value of the scattering coefficient inferred from the different values for $K_D$. We first noted that

$$K_D = a + 2\pi b\int_{\frac{\pi}{2}}^{\pi}\frac{\beta(\theta)}{b}\sin(\theta)d\theta, \quad (10)$$

where $a$ = the absorption coefficient of sea water;
$b$ = the scattering coefficient; and
$\beta(\vartheta)/b$ = the normalized scattering function of Petzhold.

From this expression, we obtained the scattering coefficient and the backscatter coefficient for each of the Jerlov water types. The beam attenuation coefficient is given by

$$C = a + b. \quad (11)$$

The lidar attenuation coefficient lies somewhere between the diffuse attenuation coefficient and the beam attenuation coefficient in such a way that it depends on the beam divergence of the lidar and on the spot size of the laser at the surface. The details of this dependence are not completely understood, and therefore we made what we hoped were reasonable estimates. Following Feigels and Kopilevich (1994), we estimated the divergence angle effect for a beam of negligible size by assuming that photons scattered at angles greater than the lidar divergence angle $\Phi/2$ are lost. We then applied a correction to this value for the finite size of the spot at the surface based on a curve fitted to the results of Gordon (1982). The final result was an estimate for the lidar attenuation coefficient given by

$$\alpha = K_D + 2\pi b \exp(-0.8c\phi h) \int_{\frac{\phi}{2}}^{\frac{\pi}{2}} \frac{\beta(\theta)}{b} \sin(\theta) d\theta, \quad (12)$$

where $h$ = the height of the lidar above the surface.

The results were fairly sensitive to this parameter; a factor of 2 in $\alpha$ is equivalent to a factor of 2 in depth penetration. The values used in our study were consistent with observations in the Southern California Bight, and are representative of what can be expected. However, more work is needed before accurate predictions of detection probability can be made for a specific water mass based on measurements of the optical properties. Direct measurements of $\alpha$ can provide better detection predictions and can also be used to refine this relationship.

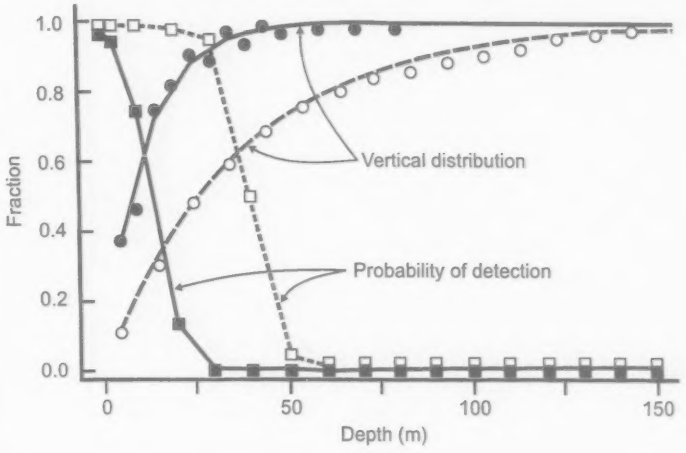


**Figure 3**

Vertical distribution and probability of detection (Eq. 16) by lidar of anchovy during day (open symbols) and night (solid symbols). The mean depth of anchovy schools was 38.98 m during the day and 11.64 m during the night (Eq. 13).

### Vertical distribution and packing density of fish schools

The vertical distributions of schools below the surface, their packing density, and fish size are critical biological properties affecting detection of schools with a lidar. Two vertical distributions of anchovy fish schools were used in our analyses. One represented an average distribution of anchovy schools during the day and the other, average distribution of anchovy schools during the night (Fig. 3). The daytime vertical distribution fitted the average of the cumulative proportion of fish schools during the May 1997 and September 1997 surveys of Holliday and Larson (1979), who used the acoustic reflection from the bottom as a better way to probe the upper 10–20 m than that afforded by conventional acoustic methods. The nighttime vertical distribution curve fitted the cumulative proportions of newly spawned anchovy eggs from two California sites (Pommeranz and Moser, 1987) and anchovy schools from three anchoveta acoustic surveys in Peru (Castillo Valderrama, 1995). The depth of early-stage anchovy eggs may indicate school depth because anchovy spawn during the night. Vertical distributions during the daytime and nighttime were fitted to an exponential distribution function:

$$F(z) = p(Z < z) = 1 - \exp(-z/\lambda), \quad (13)$$

where $F(z)$ = the proportion of fish schools in the upper $z$ meter depth; and
$\lambda$ = the mean depth of the fish schools.

Direct measurements of school packing density (numbers of fish/m$^3$) for anchovy were taken from the literature (Table 4). Graves (1977) deployed a

**Table 4**

Estimated mean, standard deviation (SD) of packing density($x$; fish/m$^3$) of anchovy and herring, and the log-transformed data ($y$=ln($x$)) during day and night. Coefficient of variation (CV)= SD/mean.

| | | Packing density($x$) | | | $y$=ln($x$) | | | |
|---|---|---|---|---|---|---|---|---|
| Species | Night or day | mean | SD | CV | mean | SD[1] | Fish length (cm) | Reference |
| Anchovy | night | 53 | 0.257<br>$n$=5 | 0.48 | -0.74 | (0.52)<br>1.11 | 10 | Aoki and Inagaki, 1988 |
| Anchovy | day | 114.8 | 99<br>$n$=10 | 0.86 | 4.505 | (0.67)<br>1.11 | 10 | Graves, 1977 |
| Herring | day | 2.57 | 3.99<br>$n$=20 | 1.55 | 0.0725 | 1.344 | 3 | Misund, 1993 |

[1] 1.11=sqrt(ln(1.55$^2$ + 1)), where 1.55 is the CV for 34-cm herring (Eq. 14). Values in parentheses were computed from original data sets.

"dropped" camera by day and Aoki and Inagaki (1988) used a tethered camera by night and obtained the packing density of anchovy with an average length of 10 cm.

The standard deviations (SD) of packing density of anchovy computed from data collected by Aoki and Inagaki (1988) and Graves (1977) measured only the variation among schools and would underestimate the overall variation of packing density. For this reason, we used the coefficient of variation of packing density of herring (1.55) (Misund, 1993; Lo et al.[2]), a more realistic measurement of the variation of packing density, together with the mean packing density of anchovy to estimate the mean ($\mu_y$) and variance ($\sigma_y^2$) of log-transformed data: $y = \ln(x)$, where $x$ is the packing density for 10-cm anchovy:

$$\hat{\sigma}_y^2 = \ln\left[cv^2(x)+1\right], \tag{14}$$

$$\begin{aligned}\hat{\mu}_y &= \ln(\bar{x}) - \hat{\sigma}_y^2/2 \\ &= \ln(\bar{x}) - \ln\left(cv^2(x)+1\right)/2,\end{aligned} \tag{15}$$

where $cv(x)$ was that of herring (=1.55). Equations 14 and 15 were derived from the following two relations:

$$\mu_x = \exp(\mu_y + \sigma_y^2/2) \text{ and}$$
$$\sigma_x^2 = \exp(2\mu_y + \sigma_y^2)\left[\exp(\sigma_y^2) - 1\right].$$

### Depth-specific probability of detection ($p_a$(z)) based on packing density

As mentioned in an earlier section, $P(detection) = 1$ for $SNRz > TNR$, and zero otherwise, because the steep drop of $P(detection)$ around $z_{max}$, the proportion of fish that can be detected and identified at depth $z$, $p_a(z)$, was modeled by the $P(SNR_z > TNR)$. The probability of detection ($p_a(z)$) was computed by means of the probability density function of fish packing density ($x$) at depth $z$, assuming that $SNR_0$ is proportional to the packing density ($x$), i.e. $SNR_0 = Ax$, where $A$ is the proportionality and is a function of fish size and reflectivity. If reflectivity is the same for all fishes, then $A$ is a function of fish size only, $A \sim 10^4 \times L^2$, where $L$ is the fish length in meters (Churnside et al., 1997). The packing density, $x$, is a lognormal random variable. We could write $SNR_z = SNR_0 \exp(-2z\alpha) = Ax \exp(-2z\alpha)$; thus $SNR_z > TNR$ is equivalent to $x > (TNR/A)\exp(2z\alpha)$, and we approximated the proportion of fish detected at depth $z$ on the basis of the lognormal distribution of packing density ($x$) by

$$\begin{aligned}p_a(z) &= \int_{\exp(2\alpha z)TNR/A} p(x)dx \\ &= p\left(\ln(x) > \left[2\alpha z + \ln(TNR/A)\right]\right) \\ &= 1 - \Phi\left(\frac{2\alpha z + \ln(TNR/A) - \mu}{\sigma}\right),\end{aligned} \tag{16}$$

where $\Phi(u) = P(U<u)$ for the normal random variable, $U$, with mean = 0 and variance = 1; and

$\ln(x)$ has mean $\mu$ and variance $\sigma^2$.

Equation 16 was computed through $SNR_z$, the mean of each individual normalized signal (or pulse). In the appendix of this paper, we computed $P_a(z)$ through individual normalized signals. We also assumed with this computation that the effects of shadowing could be neglected. Although more work on this issue is needed, our results suggest that it is not a serious effect. We observed multiple layers of fish in our

data, suggesting that light was penetrating the first layer. We also observed that the water returned from below and above schools of fish and found that the additional attenuation caused by the fish was small in comparison with the background water attenuation.

### Proportion of fish schools detected ($q$)

The proportion of fish schools detected in the upper $z$ meters ($q_z$) depends on the depth-specific probability of detection ($P_a(z)$; Eq. 16) and the vertical distribution of fish schools (Eq. 13).

The quantity ($q_z$) was computed by numerical integration:

$$q_z = \int_0^x P_a(u) f(u) du \qquad (17)$$
$$= \int_0^z \left[ 1 - \Phi\left( \frac{2\alpha u + \ln(TNR/A) - \mu}{\sigma} \right) \right] \frac{1}{\lambda} e^{-\left(\frac{u}{\lambda}\right)} du,$$

where $p_a(u)$ is derived from Equation 16 and $f(u)$ is the exponential pdf derived from Equation 13:

$$f(u) = \frac{1}{\lambda} e^{-\left(\frac{u}{\lambda}\right)}. \qquad (18)$$

The quantity, $q_z$, increases with depth $z$ and reaches an asymptote at $z_{max}$ ($q$; $q$<=1) and $q$ is defined as the proportion of fish schools detected.

### Criterion for evaluating trade-offs between penetration depth and swath width

If laser power is held constant, an increase in swath width would decrease the maximum depth of penetration of the laser pulse. In this section, we established a criterion for comparing various instruments having different combinations of swath width and laser power (maximum penetration depth). The effectiveness of the width of a swath ($y$) can be measured by the probability that some fish schools will be encountered ($p_y$) in the swath (Eq. 1 from simulation). The effectiveness of a lidar in detecting schools within the swath is measured by the proportion of fish schools detected ($q$) (Eq. 17). The product of $p_y$ $q$ (Eqs. 1 and 17) is then used to evaluate the overall effectiveness of any instruments with a given swath width ($y$).

## Results

### Effects of swath width on encounter probability

We assumed that schools were aggregated into school groups in the survey area (42,204 km$^2$) and that school diameters and densities were equal to, or less than, those reported by Smith (1981). Our simulation results indicated that swath width had little effect on the probability of encountering schools. This was true for all three population sizes: 16,000, 32,000, and 80,000 schools (Fig. 4). Encounter probability was affected by the swath width only when the diameters of the school groups were small and the school density within the school group was so low (both multipliers were 0.5) that their distribution became nearly random rather than aggregated. In these cases, the encounter probability increased sharply when the swath width increased from 1 m to 50 m. Even this very limited effect of swath width diminished as the number of schools in the survey area increased. The encounter probability for swath widths greater than 50 m was almost constant regardless of conditions.

For the multiple swaths, the probability that at least one of them would intercept anchovy schools (Eq. 2) was high in general. The lowest probability was 0.65, for the case where fish were aggregated in few large school groups of low population, i.e. 16,000 (1.5,1.5) for $n$=5 (Eq. 2). For $n$=10, the probability ($p_{y,n}$) was close to one for all cases.

### Depth-specific detection probability

The depth at which a lidar is capable of detecting a school or target will depend in part on the threshold setting of the instrument in relation to the noise (TNR). To illustrate these relationships we fixed a false-alarm rate ($P(false\ alarm)$) for the detection of schools, used an alarm rate to determine the threshold level, and then calculated the detection probability for schools ($P(detection)$). The results of such a calculation are presented in Figure 5, where the detection probability for fish schools was plotted as a function of the probability of a false alarm for signal-to-noise ratios of 1 and 3. Zero, the lower limit of the plot, corresponds to a very high threshold (TNR) setting, where the probability of a false alarm and the probability of detecting a school are both zero. We concluded that fish are never present at a setting of zero. The upper limit of Figure 5 corresponds to a very low threshold setting, where $P(false\ alarm)$ and $P(detection)$ are both unity; at a setting of 1, we concluded that fish are always present.

If one selects a reasonable false-alarm rate and a signal-to-noise ratio at the surface, one can calculate the detection probability as a function of depth. This was done for a false-alarm probability of 1% and a lidar attenuation coefficient of 0.1/m, and the results are plotted in Figure 2 for several values of the surface signal-to-noise ratio. There are several interest-

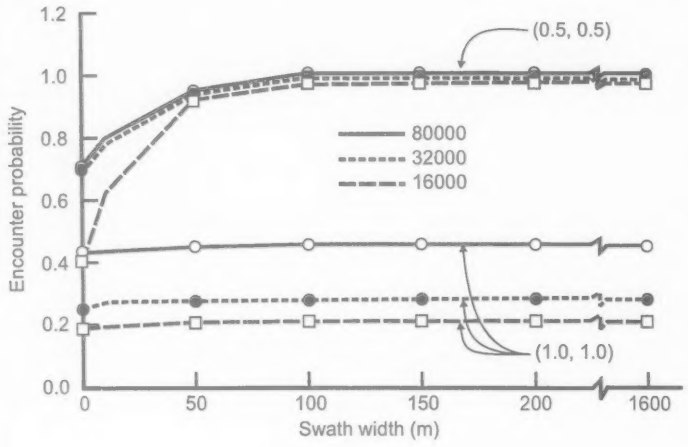


**Figure 4**

Simulated encounter probability of anchovy schools in Los Angeles Bight (Table 2) for 16,000, 32,000, and 80,000 schools. The swath width ranged from 1 m to 1600 m. The multiplier for mean and standard deviation of the log of diameter of school group and the log of school density in a school group are given in parentheses. Values for populations with multiplier (1.5,1.5), similar to populations with multiplier (1.0,1.0), are not shown.

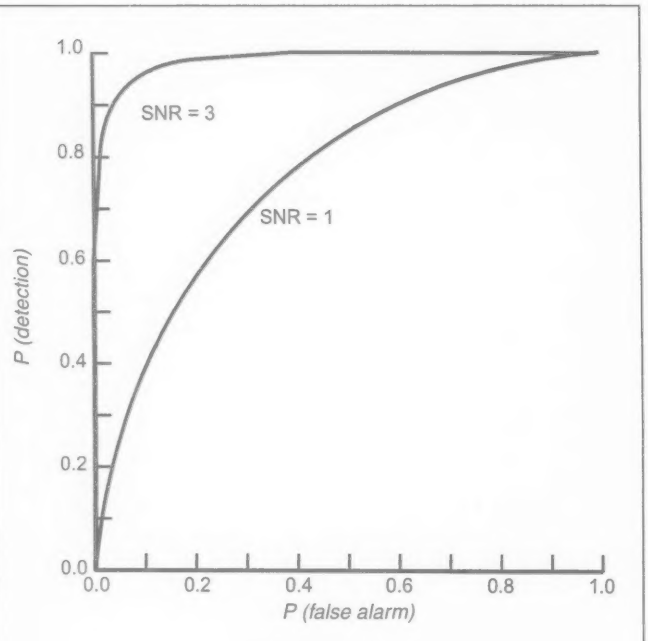


**Figure 5**

Detection probability as a function of the false-alarm probability for lidar systems with signal-to-noise-ratios (SNR) of 1 and 3.

ing features of these results. The first is that when a critical depth is reached, the detection probability drops abruptly from nearly unity to nearly zero over a narrow, 5–10 m span of depth. Because of this sharp transition, we defined a maximum detection depth ($z_{max}$) as the depth at which the detection probability is 0.5. The depth $z_{max}$ depends logarithmically on signal level because of the exponential attenuation of the signal with depth. Thus, each order-of-magnitude increase in signal level (illustrated in Fig. 2) provides an increase in $z_{max}$ of just over 10 m in depth. Ten meters is just about 1 lidar attenuation depth, defined as $1/\alpha$ (Eq. 6). We can rewrite Equation 6 as $z_{max} = \ln(SNR_0/TNR) \times 0.5/\alpha$. Therefore, if the attenuation coefficient (a) is different from 0.1/m, the value used in our study, these $z_{max}$ depth values scale linearly with lidar attenuation depth ($1/\alpha$).

To examine the sensitivity of $z_{max}$ (Eq. 6) to $TNR$ and thus the false alarm probability (Eq. 6), we used the same values of the surface signal-to-noise ratio as those used in Figure 2. This calculation indicated that the maximum detection depth ($z_{max}$) was relatively insensitive to changes in false-alarm probabilities. Decreasing the false alarm rate by a factor 10 from 0.01 to 0.001 would only increase the maximum detection depth by a few meters (Fig. 6). Thus, a fairly low rate of false alarms for a system could be selected without seriously degrading the detection performance. It also implied that we could select a nominal threshold level and obtain a simple expression for the maximum detection depth. A value of $TNR = 3$ results in a false-alarm probability of just above 0.1%. Therefore, according to Equation 6, $z_{max}$ is determined by

$$z_{\max} \approx -\frac{1}{2\alpha}\ln\left(\frac{3}{SNR_0}\right). \qquad (19)$$

We then considered the depth in the water colum at which schools can be detected by

a single lidar pulse and computed, using Equation 16, the proportion of fish schools that could be detected for anchovy (Fig. 3). During the daytime, and at a depth of 30 m, 97% of 10-cm anchovy would be detected ($p_a(z)$, when $\alpha$=0.1/m). Moreover, one can also compute a signal-to-noise ratio from the packing density($x$): $SNR_z = Ax \exp(-2\alpha z)$ for a fish length of 10 cm and compare it to the threshold target-to-noise ratio ($TNR$) of 3. At the surface, $SNR_0$ was 11,480 for 10-cm anchovy and $z_{max}$ = 41.24 m. At a depth of 30 m, $SNR_{30}$ ($\alpha$=0.1) was 28.5, which was above $TNR$ = 3, indicating that most of the schools in the upper 30 m could be detected. The detection probability for anchovy was unity over the upper 30 m (Fig. 3), which was consistent with the results we obtained from Equation 16 (Fig. 3).

For the schools at night, we used a very low packing density (0.53 anchovy/m$^3$). The signal-to-noise ratio at the surface ($SNR_0$) for such diffuse schools was 53, substantially above a $TNR$ of 3, and $z_{max}$ = 14 m. At 20 m, the $SNR_{20}$ for anchovy schools declined to 0.97 with a probability of detection of only 13%. At 30 m, the detectability of anchovy was less than 1%.

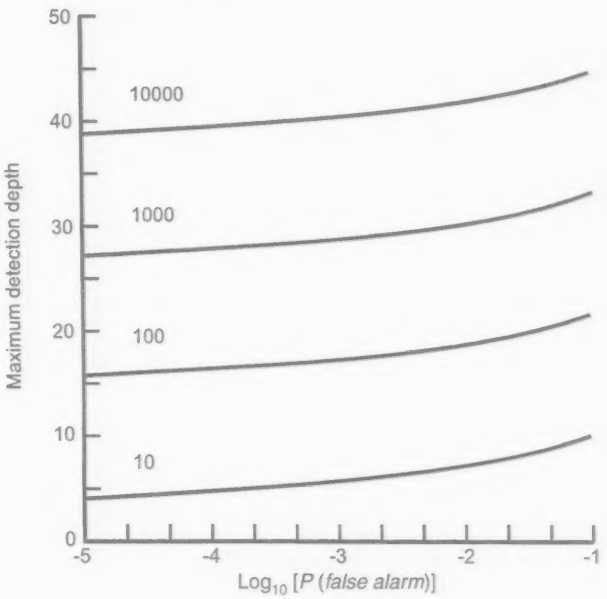


**Figure 6**

Maximum detection depth as a function of the false-alarm probability for a lidar system operating in water with an attenuation coefficient of 0.1/m. Curves are labeled by the value of the signal-to-noise ratio ($SNR_0$) at the surface.

## Overall vulnerability of schools to lidar detection in the vertical plane

We estimated the cumulated proportion of schools of anchovy that might be detected by a lidar assuming constant day and night vertical distributions. As the first step in the discussion that follows, we focused on the two components used to make the estimate: 1) the average vertical distributions of schools of anchovy during the day and the night (Fig. 3; Eq. 13); and 2) the depth-specific probability of detecting a school, which was discussed in the previous section (Eq. 16). These two components were combined to obtain the final estimates .

The probability of detecting a school during the day declined from about 1 at the surface to 0.50 at 40 m and approached zero at 60 m ($\alpha$=0.1, Eq. 16; Fig. 3). Because of the lower packing density of the school, the depth-specific probability of detecting a school was much lower at night (with the detection probability dropping from 1 at the surface to 0.10 at 20 m and zero at 30 m). Thus, even the very diffuse nighttime aggregations of anchovy (0.53 fish/m$^3$) observed by Aoki and Inagaki (1988) could be distinguished from background noise. That shallow nighttime schools can readily be detected by an airborne lidar despite their low packing density means that during the night lidar surveys are feasible.

By combining the detection probabilities with the vertical distributions (Eq. 17), we could calculate the proportion of anchovy schools that could be detected ($q$) by the lidar (Fig. 7). This calculation indicated that a lidar survey at night would be more accurate than one during the day because the cumulated proportion of schools detected during the night was 60% in the upper 20 m, whereas during the day, it was 40% in the upper 20 m. Thus, despite the higher packing density in the day (115 fish/m$^3$) which permitted detection down to about 50 m, schools were detected more often at night. This feature was due to the difference in vertical distributions between night and day.

Up to this point we have discussed only cases in which the lidar attenuation coefficient, $\alpha$, equals 0.1/m, a typical value for the coastal waters of southern California. To illustrate the effect of water clarity, we varied $\alpha$ from 0.05 to 0.6, where the attenuation coefficient for the most turbid coastal water was 0.52. Generally, the proportion of anchovy schools detected ($q$) declines rapidly with increasing $\alpha$, although detection also depends on the design

and settings of the lidar as well. Some generalizations can be made. During the night the lidar field of view can be large because less background light exits to interfere with the signal. Under these conditions, the lidar attenuation coefficient ($\alpha$) will be very nearly equal to the diffuse attenuation coefficient. For the Jerlov open-ocean water types at 532 nmi, $\alpha$ varies from about 0.05/m (type I) to about 0.11/m (type III). The values for the Jerlov coastal water types range from 0.15 (type 1) to about 0.53 (type 9). From our analysis, we expected that most anchovy schools would be detected during the night in the open ocean for $\alpha \leq 0.1$.

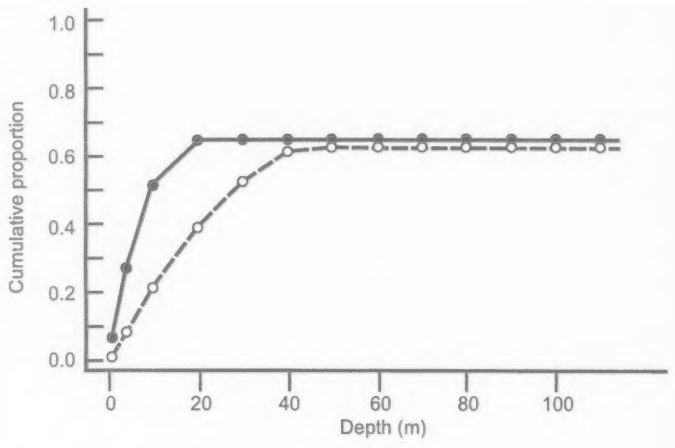


**Figure 7**

Proportion of fish schools detected in the upper meter depth (Eq. 17) for 10-cm anchovy during the day (open circles) and night (solid circles). The attenuation coefficient is 0.1/m.

During the day, the situation is more complicated. A lidar system with a large field of view will have a smaller signal-to-noise ratio because scattered sunlight reaches the receiver. We could have increased the signal to noise by decreasing the field of view, but this would tend to increase $\alpha$. Besides, an increase in the signal-to-noise ratio during the day would have little effect on $q$, because the vertical distribution of schools during the day has a long tail extending down to 155 m (Castillo Valderrama, 1995). At night, an increase in the signal strength that extends the maximum depth of a return by 10 m or so could have an important consequence because of shallow vertical distribution (82% of the school are in the upper 20 m).

### Comparisons with vision-based methods

We compared the ability of a human observer to count fish schools with the capability of a lidar. Hara (1990) reported that an observer flying at 500 m would be able to detect sardine schools along a 1600-m swath and to a depth of about 4 m. We assumed that all schools at 4 m could be detected visually and none was detected below that depth. For the lidar, we used a swath width of 7 m, and we considered the product of encounter probability ($p_y$) (Eq. 1) depicted by swath width and the maximum proportion of schools detected ($q$) depicted by depth (Eq. 17) to be a measure of the overall performance.

A human observer detects somewhat more schools in the horizontal plane than does a lidar system because of the relatively large swath width provided by aerial viewing (Table 5). The encounter probabilities in the horizontal plane (Eq. 1) obtained from simulation for a population of 32,000 schools was 0.51 for visual detection and 0.42 for lidar detection. In the vertical plane, however, our analysis demonstrated that lidar is superior in detecting schools both during the day and night. During the night, the proportion of anchovy schools detected ($q$) by the lidar was 0.65, whereas it was 0.28 for the human observer. The difference between visual detection and lidar detection was much greater during the day ($q$ was 0.63 for the lidar), whereas that for the observer was only 0.095.

The $p_y q$ (an overall measure of detection performance) for a lidar was at least 1.9 times that of an aerial observer. This means on the average that the proportion of anchovy schools detected during a survey would be about twice as great for a lidar as it would be for an aerial observer.

We have considered here, however, only one aspect of the two systems—detection rates. Many other differences also exist in relation to species identifications, biomass, and effects of environmental conditions on the observing system.

### Laser power and penetration depth

A set of parameters used to compute the laser power and penetration depth for schools of anchovy is listed in Table 3. The lidar signal was computed by using Equation 8, and the penetration depth was computed from the attenuation coefficient estimated from Equation 12. The relation of penetration

**Table 5**

Comparison of the effectiveness of lidar and aerial observation with different swath width ($y$) and depth penetration for 10-cm anchovy during the night and day. $p_y$ is the probability of encountering schools for a population of 32,000 schools and swath width $y$. $q$ proportion of fish school detected for $\alpha = 0.1$ and 0.05, where $\alpha$ is the instantaneous attenuation rate per meter. The product, $p_y q_y$ is used to evaluate the efficiency of instruments.

| Lidar aerial ratio | Maximum detection depth (m) | Swath width ($y$) (m) | $p_y$ | Proportion of fish schools detected ($q$) | | Overall efficiency ($p_y q$) | |
|---|---|---|---|---|---|---|---|
| | | | | night | day | night | day |
| $\alpha$=0.1 | | | | | | | |
| Lidar | | 7 | 0.42 | 0.65 | 0.63 | 0.27 | 0.26 |
| Aerial | 4 | 1600 | 0.51 | 0.28 | 0.095 | 0.14 | 0.048 |
| Ratio | | | | | | 1.92 | 5.410 |
| $\alpha$=0.05 | | | | | | | |
| Lidar | | 7 | 0.42 | 0.84 | 0.85 | 0.35 | 0.35 |
| Aerial | 4 | 1600 | 0.51 | 0.28 | 0.095 | 0.14 | 0.048 |
| Ratio | | | | | | 2.44 | 7.50 |

depth and the logarithmic laser energy for both open ocean and coastal waters was obtained (Fig. 8). Calculations of $SNR_0$ were made at two laser power levels, and logarithmic dependence was used to generate the curves.

We calculated the maximum penetration depth for the NOAA lidar with a power of 67 mJ and scaled that depth with laser power (Churnside and Hunter, 1996; Table 3). For this calculation, we assumed the presence of 10-cm anchovy with a packing density of 0.5/m$^3$ (Table 3). Night flights at 100 m altitude were also assumed. Two water types were used, one typical of open ocean water (Jerlov type IB) and one more typical of coastal water (Jerlov type III) (Jerlov, 1968).

The NOAA lidar presently in use is capable of operating from a single-engine plane; it weighs about 100 kg, requires less than 1 kW of power, and the cost of its components is about $50K. The penetration depth for this system under these somewhat optimum conditions is estimated to be about 45 m at 67 mJ (Fig. 8). Some cost can be saved by using a lower-power laser and smaller telescope, but not a great deal. A savings of only about $10K is likely even if one uses an equivalent energy of 1 mJ. This amount of energy still provides close to 32 m of depth penetration for the conditions assumed in our study.

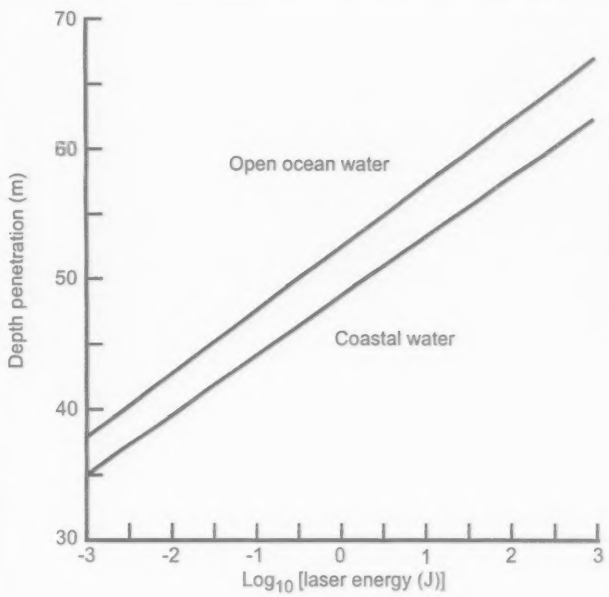


**Figure 8**

Depth penetration (m) for different laser energy levels (J) on a logarithmic scale for open ocean water and coastal water.

On the other end, one can obtain approximately 57 m of penetration by using a system with an equivalent pulse energy of 100 J (Fig. 8), but such a system would be a very large and expensive to set up and operate. Part of the equivalent energy could be obtained by using a larger telescope at a power only a little over an order of magnitude of that currently used—one that would emit a laser energy of 10J. This type of laser would require a custom design, with a cost that we estimated to be in the order of one million dollars. In addition, it would require about 100 kW of power, which cannot be supplied by a small,

single-engine aircraft. An aircraft something like the DeHaviland Twin Otter may be necessary to accommodate the size and power requirements of the NOAA lidar system. The system size and cost would probably increase significantly at an equivalent energy of about 1 J. Thus, a practical range for penetration depths would be between about 35 and 50 m.

## Discussion

### Interpretation of modeling results

Our goal was to model various aspects of a lidar survey system for anchovy with a focus on features that might affect survey accuracy and precision. We learned from our modeling of swath width that this width has little or no effect on the rate at which schools are encountered when they are aggregated into school groups, as is commonly the case with small pelagic fish, like sardines and anchovy, except under very low biomass levels. Under conditions of very low biomass, schools may become scattered rather than aggregated, in which case encounter rates would increase with swath width. Our analyses also showed that the chance that all the transects would not intercept any fish school was extremely small because the number of transect lines is likely to be much greater than 5, owing to the high speed of the survey airplane. Thus, from the standpoint of survey precision, swath width may be given a low priority.

Lack of full vulnerability to the counting technique is one of the most important potential sources of bias for biomass surveys. Fish may not be fully vulnerable because the survey does not extend over the full geographic range of the stock and because there are limitations to the counting system. Nearly all fishery-independent surveys suffer to some extent from these problems. In the case of an airborne lidar survey, the depth limits of the sensing system could produce a large potential bias, particularly if the system is used during the day. Our model indicated that, on average, 36% of schools of anchovy during the day would be expected to be below the maximum detection depth of the lidar ($z_{max}$=41 m) (Figs. 3 and 8). Because the vertical distribution of schools can vary considerably between surveys, the undetected fraction would vary, thus affecting survey accuracy. This computation is driven by our vertical distribution curve for the daytime and the rapid attenuation of light in water; packing density and fish size have negligible effects. Thus, a reliable estimation of the biomass of such small schooling fishes during the day in offshore waters does not seem practical unless a reliable unbiased estimate of vertical distribution of schools is available. On the other hand, in water up to 30 m depth over the shelf, accurate estimates of biomass for the daytime are practical because the vertical movements of the fish would be restricted.

If a lidar survey were restricted to night flights, when schools are closer to the surface, the bias caused by the uncounted fraction of deep schools would be considerably reduced. During the night, however, schools may become very diffuse and consequently have a much lower target strength which reduces their detectability. The good news from our modeling work was that even the very diffuse schools of 10-cm Japanese anchovy (0.53/m$^3$, Aoki and Inagaki, 1988) at night were detectable over the upper 20 m. Our model indicated that 65% of all anchovy schools would be detected during the night.

In our study, we focused only on 10-cm anchovy schools at two known and widely differing packing densities and vertical distributions. We ran our models with other packing densities and fish sizes, using data from herring, sardine, and mackerel but keeping the vertical distributions the same as that for anchovy.[2] These results indicated that packing density is an important factor in the detection of schools at night when the vertical distribution is shallow but is unimportant during the day when fish have a deeper vertical distribution. The effect of packing density at night can be significant. For example, at night at 30 m the *SNR* for schools of 10-cm anchovy (packing density 0.53) was only 0.97, whereas that for 13-cm sardine (4.0 packing density) was 12.38 (their detectability was 13% and 77%, respectively). Schools of small fishes may be inherently more detectable than those of larger fish because the decline in average packing densities of schools with increasing fish size is not completely compensated by the increase in reflective area of the fish (packing density changes in proportion to $1/L^3$ (Misund, 1993), whereas the reflective area changes in proportion to $L^2$). However, this theoretical relationship is eclipsed by the huge variation in packing density due to behavioral factors. The density of anchovy schools at night varies from compact schools suitable for capture by the purse-seine fishery (Squire, 1972) to schools so diffuse that many authors have concluded that schooling ceases (Whitney, 1969; Baxter and Hunter, 1982). The packing density used in our example of an anchovy school at night from Aoki and Inagaki (1988) represents such an extremely dispersed state, but dense concentrations of anchovy do occur at night, only their packing density has not been measured. In fact, 4 fish/m$^3$ used in the sardine night example might be equally appropriate for anchovy. Unfortunately, because field measurements of packing densities at night are so infrequent, it is impossible to tell at this

point where the mean may fall or what differences might exist between species.

Detection of schools during the night would improve if maximum schooling depth and $\alpha$ were correlated as Hunter and Nicholl (1985) speculated. They determined the visual threshold for schooling in northern anchovy ($6\times10^{-11}W/cm^2$) and suggested that maximum nighttime depth was a function of the ability of fish to see one another. They estimated that the visual threshold for schooling would occur at 38 m during a full moon and at 30 m on a starlit night where chlorophyll was 0.2 mg Chla/$m^3$ and at 8 m (starlit) and 20 m (full moon) when chlorophyll was 2.0 mg Chla/$m^3$. If Hunter and Nicholl (1985) are correct, then the maximum lidar detection depth should increase as the schooling depth increases at night, as long as survey flights are made under the same moon phase. This relationship between visual threshold and moon phase also indicates that it may also be important to exclude survey nights during a full moon—a rule long observed by pilots who locate schools for the fishing industry.

It may be possible in practice to detect schools somewhat deeper than those that our model indicates because the model estimates the detection of a single pulse at one range gate or depth. In practice, a lidar will generate a composite image of a school derived from a number of such pulses over a range of gates (depths) analogous to an echogram trace. Such a composite image produced from multiple returns and gates can be more readily separated from background noise than can a single pulse, but such a separation involves a more complex, and at the present time, somewhat more qualitative discrimination process. Signal-processing algorithms can be developed for this application, but their performance would depend on the exact algorithm used. More accurate estimates of detection depth would depend upon the development of such signal-processing algorithms. Development of such algorithms is one of the most promising directions for future research on fisheries lidar. Their development would greatly improve both the accuracy and precision of future lidar surveys for fisheries, as well as reduce the work in processing images. Similarly, a more thorough understanding of the causes of the observed variation in the vertical distribution of fish could improve survey accuracy and precision. The phase of the moon, time of day, mixed layer depth, temperature, location of forage, fish size, season, and spawning habitats, may all influence where in the water column a school may be found.

It seems unlikely that depth of detection will be greatly improved by increasing sensitivity or power of a lidar system over the basic radiometric system used in our model. Our analysis indicated that an order of magnitude increase in equivalent laser power (laser power plus sensor changes) would gain about 10 m in detection depth. Such a change would require a custom, rather than an "off-the-shelf" laser, which would cost around a million dollars, in addition to associated costs, including a larger aircraft to satisfy the new power and weight requirements. In addition, increasing the depth of penetration by 10 or 20 m, on the average, would not increase the numbers of schools detected by more than about 10% during the day because school distributions tend to be skewed with a long tail extending to depths far beyond the practical limits of lidar detection in coastal waters. A 10-m gain would be more significant during the night but may not be worth the additional cost.

We have treated the failure of a lidar to count deep schools as a potential bias, which is true unless an unbiased estimate of the mean vertical distribution of schools exists for the particular survey region and season and an appropriate statistical model is used for the survey. When these conditions are met, the failure of a lidar to count deep schools becomes a matter of precision rather than bias. An unbiased estimate of the mean vertical distribution of schools could be estimated from data generated by lidar and acoustic surveys for the same region because by combining the two surveys, one corrects for the vertical bias in each. The appropriate statistical model for a lidar survey would be one based on line transect theory (Buckland et al., 1993). Line transect theory usually deals with encounter rates on the horizontal plane, and animals are assumed to be uniformly distributed in space. In the case of lidar, we turned the model on its side and used an average vertical distribution of anchovy schools in the survey area. An empirically derived vertical distribution does not seem to be subject to any more bias than a uniform, horizontal distribution, one that is commonly assummed in line transect surveys.

To provide indices of relative abundance based on airborne lidar is an important fishery application that is less demanding than that of estimating biomass. For an index of abundance, the extent to which schools are available for counting is not a major concern. Lidar seems uniquely well-suited for taking an inventory of the juveniles of small pelagic fishes (prerecruits) because they are extremely patchy and tend to inhabit shallow water near the coast in areas difficult to sample with a research vessel. Lidar surveys can provide useful indices of adult biomass as well. Aerial observations (Lo et al., 1992) and passive imaging (Nakashima, 1990; Nakashima and Borstad[7])

[7] Nakashima, B. S., and G. A. Borstad. 1993. Detecting and measuring pelagic fish schools using remote sensing techniques. ICES Report C.M. 1993/B:7, session T, Fish Capture Committee, 18 p.

from aircraft are currently used in several fisheries as indices of the abundance of small pelagic fishes and a lidar-based system would have several advantages over these passive methods. Our computation with a deterministic model showed that a lidar survey may be about twice as efficient in detecting schools as a vision-based system during the night and five times more efficient during the day. At night, a lidar will detect more schools than an observer, but the difference is not huge because the very wide swath width (1600 m) of our hypothetical aerial observer compensated, to some degree, for the observer not seeing farther beneath the surface. During the day, the efficiency of lidar detection, in contrast to visual detection, increases greatly because schools inhabit deeper water. In addition to increased detection efficiency, lidar has several other advantages over aerial observers: lidar images can be better quantified than those based on visual detection or cameras because the school volume rather than school area can be estimated, thereby improving the precision of the index; in addition, detection is less dependent on sea state and is little affected by sun angle or moon phases. On the other hand, skilled fishermen working in aerial surveys can identify species of schooling fish with remarkable accuracy; a remote species identification algorithm for a lidar will be difficult, if not impossible, to develop.

As with hydroacoustic methods, species identification with lidar is a major concern. Even after 50 years of hydroacoustic research, the only method for identifying acoustic targets with certainty is by securing voucher specimens. Radiometric backscatter has no magical properties in relation to those of acoustic back scatter that might allow a rapid solution to the problem of species identificaton. The lesson learned from hydroacoustics is that for species identification to be a reality in lidar surveys, additional sensing systems will be needed. That skillful humans make accurate species identifications visually provides the hope that species recognition algorithms eventually will be practical. We believe it will be possible over the long term to develop species recognition algorithms for lidar in combination with advanced lidar signal processing, digital video cameras, and local knowledge, but at present species identifications must depend upon combining lidar survey data with other information. From the lidar data, we could distinguish reliably between small (about 30 cm length) and large (about 1-m) fish. Identification of intermediate lengths may become possible with more practical experience. One possible approach for obtaining additional information is to use visual identifications of fish schools by aerial observers prorated to lidar targets. Other possible approaches are to combine airborne lidar survey with a research trawler that can provide voucher specimens or to combine airborne lidar with simultaneous sampling of fish eggs from a research vessel (Checkley et al., 1997). The latter approach has been used successfully in a test of the NOAA lidar (Churnside, 1999).

### Future application of airborne lidar

An airborne lidar survey could provide a census of epipelagic fishes an order of magnitude faster than that provided by ships, thus reducing costs in dollars (based on 1999 dollar amounts) from about $100 per ship-survey mile to $3 per aerial-survey mile (research ship cost=$12,000 per day, net ship speed including stopping at stations=5 kn; airplane=$600 per hour at 200 kn).

Faster surveys not only cost less but improve accuracy because steady state assumptions are reduced, vessel avoidance is eliminated, and, most important, high speed makes it practical to survey a much larger area, thereby eliminating the errors associated with partial coverage. No major technical barrier exists in acquiring a suitable instrument; adequate fish detection lidars already exist. Fish-detecting lidars may be purchased from one or more vendors or a radiometric lidar may be assembled from "off the shelf" components as has been done with the NOAA lidar (Churnside and Hunter, 1996). However, to implement routine surveys, signal-processing algorithms for rapid quantification of targets are needed, and if the fish targets are to be converted to biomass, direct calibrations of target strength will be needed.

The depth limitation of lidar is not a major barrier to implementation. Our analysis demonstrates, as does our practical experience, that school detection depths of 30–40 m can be expected for California coastal waters using off-the-shelf instrumentation. In fact, more powerful systems are unlikely to do much better owing to the rapid attenuation of signal with depth. The 30–40 m depth limitation is less important at night because most epipelagic fish schools are found within the volume of water that is to be detected by lidar. Our analysis demonstrated that schools can be detected at night despite a much lower packing density. To deal most effectively with the fraction of undetected schools, survey design should be based on line transect theory and should require an estimate of the average vertical distribution of schools under the specific survey conditions (region, species, season, time of day).

In conclusion, the census of epipelagic fish schools with airborne lidar would be practical and useful today if three conditions could be met: assumptions regarding species identity are acceptable; a line transect survey design is used in conjunction with

the known vertical distribution of schools; and algorithms are developed to process the data.

## Acknowledgments

We thank Edgeworth Wester and Wynn Eberhard of Environmental Technology Laboratory, Boulder, Colorado, for reading an early draft, and two anonymous reviewers for their constructive comments and suggestions that improved the presentation of the manuscript. Partial support for J. Churnside was provided by the Advanced Sensor Applications Program of the U.S. Department of Defense.

## Literature cited

**Aoki, I., and T. Inagaki.**
**1988.** Photographic observations on the behaviour of Japanese anchovy *Engraulis japonica* during the night in the sea. Mar. Ecol. Prog. Ser. 43:213–221.

**Baxter, J. H. S., and J. R. Hunter.**
**1982.** The biology of the clupeoid fishes. *In* Advances in marine biology, p. 1–223. Academic Press, New York, NY.

**Buckland, S. T., D. R. Anderson, K. P. Burnham, and J. L. Laake.**
**1993.** Distance sampling: estimating abundance of biological populations. Chapman and Hall, London, 446 p.

**Castillo Valderrama, P. R.**
**1995.** Disribucion de los principales recursos pelagicos durante los veranos de 1992 a 1994. Instituto Del Mar Del Peru Informe 114:17–18.

**Checkley, D. M., P. B. Ortner, L. R. Settle, and S. R. Cummings.**
**1997.** A continuous, underway fish egg sampler. Fish. Oceanogr. 6(2):58–73.

**Churnside, J. H.**
**1999.** Can we see fish from an airplane? *In* Airborne and in-water underwater imaging (Gary D. Gilbert, ed.), p. 45–48. Proc. SPIE (Society of Photo-Optical Instrumentation Engineers) 3761. SPIE, Bellingham, WA.

**Churnside, J. H., and J. R. Hunter.**
**1996.** Laser remote sensing of epipelagic fishes. *In* Laser remote sensing of natural waters: from theory to practice (V. I. Feigels and Y. I. Kopilevich, eds.), p. 38–53. SPIE, Bellingham, WA.

**Churnside, J. H., J. J. Wilson, and V. V. Tatarskii.**
**1997.** Lidar profiles of fish schools. Appl. Opt. 36:6011–6020.

**Cram, D. L., and I. Hampton.**
**1976.** A proposed aerial/acoustic strategy for pelagic fish stock assessment. J. Const. Int. Explor. Mer 37(1):91–97.

**Feigels, V. I., and Yu. I. Kopilevich.**
**1994.** Applicability of lidar remote sensing methods for vertical structure investigation of ocean optical properties distribution. *In* Ocean optics XII (J. Jaffe. ed.), p. 449–457. Proc. SPIE 2258.

**Fiedler, P. C.**
**1978.** The precision of simulated transect surveys of northern anchovy, *Engraulis mordax*, school groups. Fish. Bull. 76(3):679–685.

**Gordon, H. R.**
**1982.** Interpretation of airborne oceanic lidar: effects of multiple scattering. Appl. Opt. 21:2996–3001.

**Graves, J.**
**1977.** Photographic method for measuring spacing and density within pelagic fish schools at sea. Fish. Bull. 75: 230–234.

**Gunderson, D. R.**
**1993.** Surveys of fisheries resources. John Wiley and Sons, Inc., New York, NY, 248 p.

**Hara, I.**
**1990.** Comparison of ship and aerial surveys of sardine schools. IEEE (Institute of Electrical and Electronic Engineers) Trans. Geosci. Remote Sens. 28(4):693–695.

**Holliday D. V., and H. L. Larsen.**
**1979.** Thickness and depth distributions of some epipelagic fish schools off southern California. Fish. Bull. 77(2):489–494.

**Hunter, J., and R. Nicholl.**
**1985.** Visual threshold for schooling in northern anchovy *Engraulis mordax*. Fish. Bull. 83(3):235—242.

**Jacobson, L. D., N. C. H. Lo, and J. T. Barnes.**
**1994.** A biomass-based assessment model for northern anchovy, *Engraulis mordax*. Fish. Bull. 92:711–724.

**Jerlov, N. G.**
**1968.** Optical oceanography. Elsevier, Amsterdam, 194 p.

**Lo, N. C. H., I. D. Jacobson, and J. L. Squire.**
**1992.** Indices of relative abundance from fish spotter data based on delta-lognormal models. Can. J. Fish. Aquat. Sci. 49:2515–2526.

**Mais, K. F.**
**1974.** Pelagic fish surveys in the California Current. Calif. Dep. Fish Game, Fish. Bull. 162, 79 p.

**Misund, O. A.**
**1993.** Dynamics of moving masses: variability in packing density, shape, and size among herring, sprat, and saithe schools. ICES J. Mar. Sci. 50:145–160.

**Mobley, C. D.**
**1995.** The optical properties of sea water. *In* Handbook of optics, second ed., vol.1, chap. 43 (M. Bass, ed.), p. 36. McGraw-Hill, New York, NY.

**Nakashima, B. S.**
**1990.** Capelin school surface area index for NAFO Div. 3L during the 1989 spawning season. Northwest Atlantic Fisheries Organization (NAFO) SCR Doc. 90/59, serial no. N1780.

**Petzhold, T. J.**
**1972.** Volume scattering functions for selected ocean waters. SIO (Scripps Institution of Oceanography) Ref. Doc. 72-78. Scripps Inst. Oceanogr., La Jolla, CA, 82 p.

**Pommeranz, T., and H. G. Moser.**
**1987.** Data report on the vertical distribution of the eggs and larvae of northern anchovy, *Engraullis mordax*, at two stations in the Southern California Bight March–April 1980. U.S. Dep. Commer., NOAA Tech. Memo. NOAA-TM-NMFS- SWFC-75, 140 p.

**Smith. P. E.**
**1981.** Fisheries on coastal pelagic schooling fish. *In* Marine fish larvae: morphology, ecology and relation to fisheries (R. Lasker, ed.), 1–31 p. Washington Sea Grant Program, Univ. Washington Press, Seattle, WA.

**Squire, J. L., Jr.**
**1972.** Apparent abundance of some pelagic marine fishes off the southern and central California coast as surveyed by an airborne monitoring program. Fish. Bull. 70:1005–1019.

**Whitney, R. R.**
**1969.** Schooling of fishes relative to available light. Tran. Am. Fish. Soc. 98(3):497–504.

## Appendix

The detection probability by depth ($p_a(z)$) was defined as the proportion by which the mean values of $SNR_z$ exceed the threshold, $TNR$ (Eq. 16). Strictly speaking, one should define the detection probability as the expected probability that each signal exceeds the threshold. The expectation would be computed by integrating over the pdf of mean $SNR_z$. For a lognormal distribution of mean $SNR_z$, we would have

$$P_a(z) = \int P(s > TNR \mid SNR_z)\text{lognormal}\,(SNR_z)dSNR_z$$

$$= \int_0^\infty [1 - \Phi(TNR - SNR_z)]\frac{1}{\sqrt{2\pi}\sigma\, SNR_z}$$

$$\exp\left(-0.5\left(\frac{\ln(SNR_z) - \mu_z}{\sigma}\right)^2\right)d(SNR_z), \qquad (20)$$

where $s$ = the signal-noise-ratio which follows normal ($SNRz$, 1); and

$SNR_z$ = a lognormal random variable with mean $\mu_z = \ln(A) + E(\ln(x)) - 2\alpha z$; and

standard deviation $\sigma$ = SD($\ln(x)$) where $x$ is the packing density.

Our exercise indicated that both detection probabilities from Equations 16 and 20 were very similar. Equation 16, although an approximation, was used in our computation because of its simplicity.

# Spawning frequency and batch fecundity of Brazilian menhaden, *Brevoortia aurea*, in the Río de la Plata estuary off Argentina and Uruguay*

**Gustavo J. Macchi**
Consejo Nacional de Investigaciones Científicas y Técnicas (CONICET)
Rivadavia 1917
(1033) Buenos Aires, Argentina
Present address: Instituto Nacional de Investigación y Desarrollo Pesquero (INIDEP)
Paseo Victoria Ocampo No. 1
Mar del Plata (7600), Argentina
E-mail address: gmacchi@inidep.edu.ar

**Eduardo M. Acha**
Dto. Ciencias Marinas
Universidad Nacional de Mar del Plata
Funes 3350
(7600) Mar del Plata, Argentina

**Abstract.**—The reproductive biology of Brazilian menhaden, *Brevoortia aurea*, inhabiting the estuarine waters of the Río de la Plata (Argentina–Uruguay), was studied by using histological analysis of the ovaries. The samples were collected during the peak of the spawning period of this species (November) during 1994, 1995, and 1997. *Brevoortia aurea* is a multiple spawner with indeterminate annual fecundity. Spawning frequency, determined from the percentage of females with postovulatory follicles, was about 12% during November 1995. At this frequency, each female on average spawned a new batch of eggs about every 8 days. Batch fecundity, estimated from counts of hydrated oocytes, was fitted to a power function of length and a linear function of ovary-free female weight. Batch fecundity estimates ranged from 20,000 (27 cm fork length) to 130,000 (34 cm fork length) hydrated oocytes. Annual differences in the size-fecundity relationship were observed. Relative fecundity estimates obtained from the different years sampled ranged from 60 to 212 hydrated oocytes/g of female (ovary-free weight).

Manuscript accepted 20 October 1999.
Fish. Bull. 98:283–289 (2000).

The Brazilian menhaden (*Brevoortia aurea*) is a pelagic coastal species of the southwest Atlantic ranging from Salvador de Bahía, Brazil (13°S), to the south of Buenos Aires province, Argentina (40°S) (Cousseau and Díaz de Astarloa, 1993). It is abundant in the estuarine waters of the Río de la Plata area, where it is caught by the commercial fleets of Argentina and Uruguay, although it is a resource of little economic value (Argentine landings in 1997 were 893 metric tons (t); Anonymous, 1998). Maximum body size is about 41 cm total length (36 cm fork length), which corresponds to an age of 11 years (López Cazorla, 1985). These attributes are similar to those for Atlantic menhaden (*Brevoortia tyrannus*) from the Atlantic coast of the United States, which attains a maximum body size of 36–37 cm fork length and a maximum age of about 10 years (Powell, 1994). Estimation of size at sexual maturity of Brazilian menhaden has not been documented, but the minimum length at maturity for female is 22.5 cm TL (Cassia et al., 1979). Previous reports on life history attributes include descriptions of embryonic and larval development (de Ciechomski, 1968; Weiss and Krug, 1977), growth (López Cazorla, 1985), taxonomy (Cousseau and Díaz de Astarloa, 1993; Díaz de Astarloa and Cousseau, 1993), and feeding (Sánchez, 1989; Giangiobbe and Sánchez, 1993). Comprehensive information on reproduction of Brazilian menhaden does not exist. Recently, we reported that major spawning in the Río de la Plata area occurs from September to December, in estuarine waters across a wide range of salinities (Acha and Macchi, 2000). Cassia et al. (1979) reported total fecundity estimates based on the assumption that the number of eggs spawned by a female is fixed prior to the onset of spawning. Brazilian menhaden may be a multiple spawner, in which case

* Contribution 1128 of the Instituto Nacional de Investigación y Desarrollo Pesquero, Mar del Plata, Argentina.

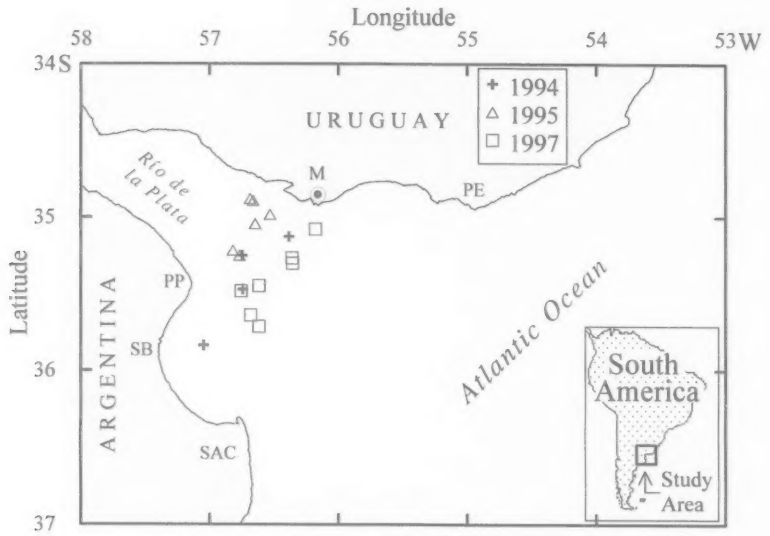


**Figure 1**

Sample locations for female Brazilian menhaden taken in the Río de la Plata estuary, during November 1994, 1995, and 1997. PE = Punta del Este, M = Montevideo, PP = Piedras Point, SB = Samborombón Bay, SAC = San Antonio Cape.

batch fecundity and spawning frequency must be estimated to determine annual fecundity (Hunter and Goldberg, 1980).

Through histological analysis of the ovaries, we investigated the reproductive biology of *B. aurea* from the Río de la Plata estuary to determine the pattern of spawning and estimate spawning frequency and batch fecundity during the main spawning peak.

## Materials and methods

*Brevoortia aurea* females were collected from the Río de la Plata estuary during three fortnightly research cruises in November 1994, 1995, and 1997 (Fig. 1). Fish samples and oceanographic data (temperature and salinity) were taken for each trawl station from 6 to 20 m depths. Fork length (FL, cm) and total weight (TW, g) were recorded for each fish sampled. Length distributions obtained for the three years were compared with a Kolmogorov-Smirnov Test (KS) (Sokal and Rohlf, 1969). During 1994, only gravid females with hydrated oocytes ($n$=54) for fecundity estimation were sampled. Females collected in 1995 ($n$=169) and 1997 ($n$=92) were randomly selected including different maturity stages. The ovaries were removed and fixed in 10% neutral-buffered formalin for one week. In the laboratory, the gonads were weighed, and a portion of tissue (about 2.0 g) was removed from the center of each ovary, dehydrated in methanol, cleared in benzol, and embedded in paraffin. Tissues were cut into 4-µm sections, and stained with Harris's hematoxylin followed by eosin counterstain. Classification of ovaries was based on the stage of oocyte development and on the occurrence of postovulatory follicles (POF) according to Hunter and Goldberg (1980). Our description of the stages of POF degeneration was adapted from that given by Fitzhugh and Hettler (1995) for *B. tyrannus* and these stages were classified as day-0 and day-1, according to the elapsed time from spawning. A day-0 POF (elapsed time from spawning <24 h) has an irregular, convoluted shape; the granulosa cells are aligned, and many folds and the lumen are clearly visible (Fig. 2, A and B). A Day-1 POF (elapsed time from spawning >24 h) shows degenerative process, the linear appearance of the granulosa cells is not distinct and the lumen becomes reduced (Fig. 2, C and D).

Oocyte diameters for five gravid ovaries were measured after fixation ( 40 ±µm) with an ocular micrometer ($n$=749). Spawning frequency was estimated from samples ($n$=169) collected during November 1995. Daily fraction of spawning females was estimated by the incidence of fish with day-0 and day-1 POFs (Hunter and Goldberg, 1980) and spawning frequency was determined from the average of the percentages of day-0 and day-1 spawning females (Fitzhugh et al., 1993; Macchi, 1998).

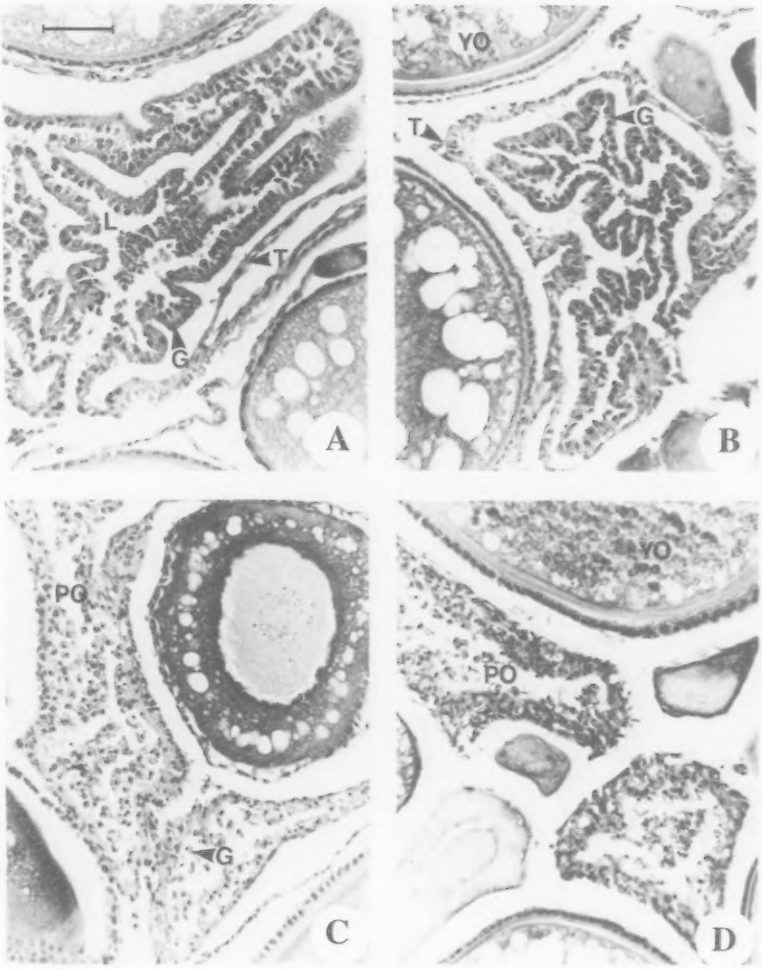


**Figure 2**

Postovulatoty follicles from female Brazilian menhaden at different stages: (**A** and **B**) day-0, cordlike appearance of the granulosa layer can be observed; (**C** and **D**) day-1, reduction in size and degeneration of follicles are evident. T = thecal layer; G = granulosa layer; L = lumen; YO = yolked oocytes; PO = postovulatory follicles. Bar = 50 µm.

Batch fecundity (BF; number of oocytes released per spawning) was estimated gravimetrically by the hydrated oocyte method (Hunter et al., 1985) for 112 females (44 from 1994, 38 from 1995, and 30 from 1997). The hydrated ovaries showed no evidence of recent spawning (no POFs). Three pieces of ovary, approximately 0.1–0.2 g each, were removed from the anterior, middle, and posterior parts of one gonad, weighed (±0.1 mg), and the number of hydrated oocytes were counted. Batch fecundity for each female was the product of the mean number of hydrated oocytes per unit of weight and the total weight of the ovaries. Relative fecundity (RF; hydrated oocytes per gram of body weight) was determined as the batch fecundity divided by female weight (without ovary). The relationships of batch fecundity to fork length and to total weight (ovary free) were described by regression analysis (Draper and Smith, 1981), and the significance evaluated by testing whether the slope of the regression was significantly different from zero. Interannual comparisons were based on coincident length ranges in the

three years, and an analysis of covariance to log-transformed data was applied (Draper and Smith, 1981).

## Results

Length distributions for Brazilian menhaden ranged from 26 to 36 cm FL and did not differ among the years sampled ($P>20$). All individuals collected were adult mature females with yolked or hydrated oocytes; no immature ovaries were observed.

The oocyte diameter distribution of gravid *B. aurea* females (with hydrated oocytes) showed four groups of oocytes (Fig. 3). The smallest group was composed mainly of primary growth oocytes (smaller than 120 µm). The next larger group was composed of cortical alveolus stage and partially yolked oocytes (primary yolk stage) ranging from 120 to 500 µm. A third group included advanced yolked oocytes (secondary yolk stage) ranging from 500 to 700 µm. The fourth group was the largest and corresponded to the hydrated oocytes measuring 1100 to 1500 µm. The continuous distribution from primary growth oocytes to advanced yolked oocytes is a characteristic pattern in multiple spawning fishes.

Spawning frequency was estimated by examining ovarian tissue from 169 mature females sampled between 21 and 23 of November 1995 during the main spawning peak. Of all specimens examined, about 14% had new postovulatory follicles (day-0) and 10% had day-1 postovulatory follicles (Table 1), the average was 11.98% (SD=7.53%).

Batch fecundity estimates ranged from 20,000 hydrated oocytes for a 27-cm-FL female to 130,000 hydrated oocytes for a 34-cm-FL female. A power model and a linear model were fitted to the relationships BF versus FL and BF versus TW, respectively (Fig. 4). Analysis of covariance indicated that the slope of the regression of fecundity on length did not differ between years, but the intercepts were significantly different (1994–95, $F_{(1, 74)}=6.68$, $P<0.05$; 1994–97, $F_{(1, 68)}=26.02$, $P<0.01$; 1995–97, $F_{(1, 61)}=4.53$, $P<0.05$). Relative fecundity ranged from 60 to 212 hydrated oocytes per gram of female (ovary free). These values were different ($P<0.05$) between the years 1994 (107 ±29 hydrated oocytes) and 1995 (135 ±34 hydrated oocytes), and 1994 versus 1997 (149 ±30 hydrated oocytes), but not between 1995 and 1997.

## Discussion

*Brevoortia aurea* is a multiple spawner with indeterminate annual fecundity, according to our observations of maturing ovaries with postovulatory follicles and yolked oocytes (partially spent stage). These observations suggest that after one batch of eggs is spawned, a new batch develops and is released (Hunter et al., 1992). Further, the oocyte size-frequency distribution of gravid females shows different batches of growing oocytes, including hydrated eggs. Fractional spawning has been suggested for other congeners, such as Atlantic menhaden and gulf menhaden (*Brevoortia patronus*), on the basis of oocyte diameter distributions (Lewis and Roithmayr, 1980; Lewis et al., 1987). These species have a long reproductive season, 6–8 mo. (Powell, 1994), similar to that of *B. aurea*. Atlantic and gulf menhaden spawn during the fall and winter (Powell, 1994), whereas Brazilian menhaden spawn in spring–summer, as do most of the fishes inhabiting the Río de la Plata estuary (Macchi and Acha, 1998).

During November the temperature ranges from 19° to 21°C in the spawning area of Brazilian menhaden. Because duration of the POF stage varies at different temperatures, disappearance of the lumen

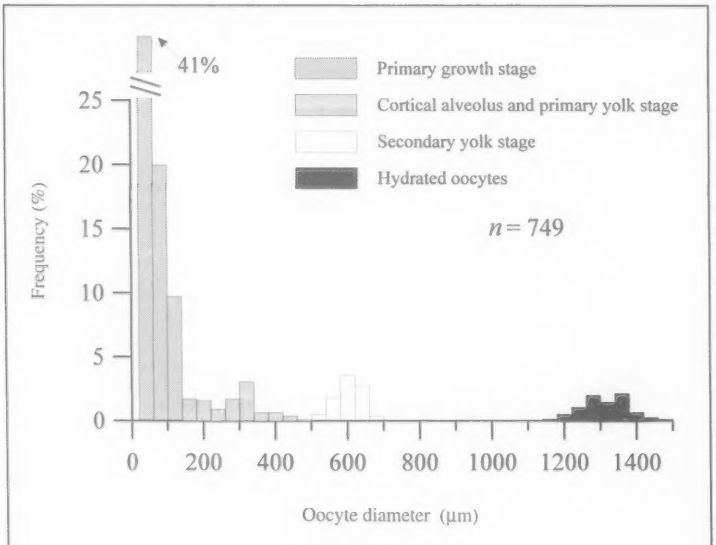


**Figure 3**

Oocyte diameter distribution for an ovary of Brazilian menhaden containing hydrated oocytes. The different shadings represent the four groups of oocytes identified.

**Table 1**

Number of Brazilian menhaden females in reproductive activity from the Río de la Plata estuary that were histologically staged for estimation of spawning frequency. POF = postovulatory follicles; CI = confidence interval.

| Day of month (November 1995) | Yolked oocytes and no POF | Hydrated oocytes | Day-0 POF | Day-1 POF | Total mature females |
|---|---|---|---|---|---|
| 21 | 2 | 13 | 3 | 2 | 20 |
| 21 | 1 | 11 | 1 | 2 | 15 |
| 22 | 0 | 19 | 1 | 0 | 20 |
| 22 | 4 | 13 | 0 | 3 | 20 |
| 22 | 4 | 0 | 9 | 7 | 20 |
| 22 | 8 | 9 | 3 | 0 | 20 |
| 23 | 1 | 18 | 1 | 0 | 20 |
| 23 | 5 | 12 | 1 | 2 | 20 |
| 23 | 9 | 0 | 4 | 1 | 14 |
| Total | 34 | 95 | 23 | 17 | 169 |
| % (average) | | | 13.7 | 10.1 | |
| 95% CI | | | ±9.43 | ±7.19 | |

after the loss of the alignment of the granulosa layer was used as the main characteristic to distinguish day-0 from day-1 postspawning ovaries, according to Fitzhugh and Hettler (1995). They concluded that this is the most important feature for classification of POFs in Atlantic menhaden spawning at about 20°C. Spawning frequency estimated from the average between day-0 and day-1 POF percentages (11.98%, SD=7.53%) indicated that *B. aurea* spawn once every eight days during the peak of the reproductive season (November). This value should be considered a preliminary estimate because we did not have samples during other months in the spawning period. Daily spawning fraction of Brazilian menhaden was similar to that of other clupeoids inhabiting temperate waters, such as *Engraulis mordax* (Hunter and Goldberg, 1980), *E. ringens* (Alheith et al., 1984), *Sardinops sagax* (Herrera and Claramunt, 1990), *Sardina pilchardus* (Pérez et al., 1992), *E. capensis* (Melo, 1994), and *E. anchoita* (Pájaro et al., 1997).

Cassia et al. (1979) reported Brazilian menhaden fecundity by counts of yolked oocytes (diameter >540 µm) from ovaries in an advanced maturity stage. They estimated a potential fecundity of 120,000 oocytes for one 30-cm-FL female but did not consider a multiple spawning pattern. Our estimated batch fecundity for females of this length was about 60,000 hydrated oocytes. During the main reproductive period (September–December), a female Brazilian menhaden with a spawning frequency of 8 days would spawn 15 times. Although total fecundity has been calculated for Atlantic menhaden (Higham and Nicholson, 1964; Dietrich, 1979; Lewis et al., 1987) and gulf menhaden (Lewis and Roithmayr, 1980), batch fecundity estimates have not been reported, and gravid females in wild population have rarely been observed (Ahrenholz, 1991).

Batch fecundity was fitted to a power function of fork length and a linear function of ovary-free body weight. Analysis of covariance showed significant differences ($P<0.05$) in regression coefficients among the three years considered (1994, 1995, and 1997). The low coefficients of determination in regressions were similar to those obtained for Atlantic menhaden (Lewis et al., 1987), possibly as a consequence of different ages occurring within length classes after sexual maturity (Lopez Cazorla, 1985). Mean relative fecundities for *B. aurea* (107 [in 1994], 135 [in 1995], and 149 [in 1997] oocytes/g ovary-free body weight) were much lower than those for *Engraulis anchoita* (about 600 oocytes/g ovary-free body weight), the most abundant clupeoid of the Argentine Sea (Pájaro et al., 1997). The difference may reflect the larger egg size of *B. aurea* (1500–1600 µm), compared with *E. anchoita* (about 900 µm; de Ciechomski and Weiss, 1973). The reproductive strategy of some species indicates that egg size takes priority over fecundity (Kjesbu et al., 1996). The larger eggs may be advantageous during the first days of life because hatchlings have larger yolk reserves, contributing to higher growth rates, and may avoid predation more effectively (Hinckley, 1990; Wootton, 1994). Our paper provides the first estimation of spawning frequency and batch fecundity of Brazilian menhaden during the spawning peak. These parameters should also be estimated at the end of the reproductive season to evaluate possible variations and their effect over the annual egg production. Future stud-

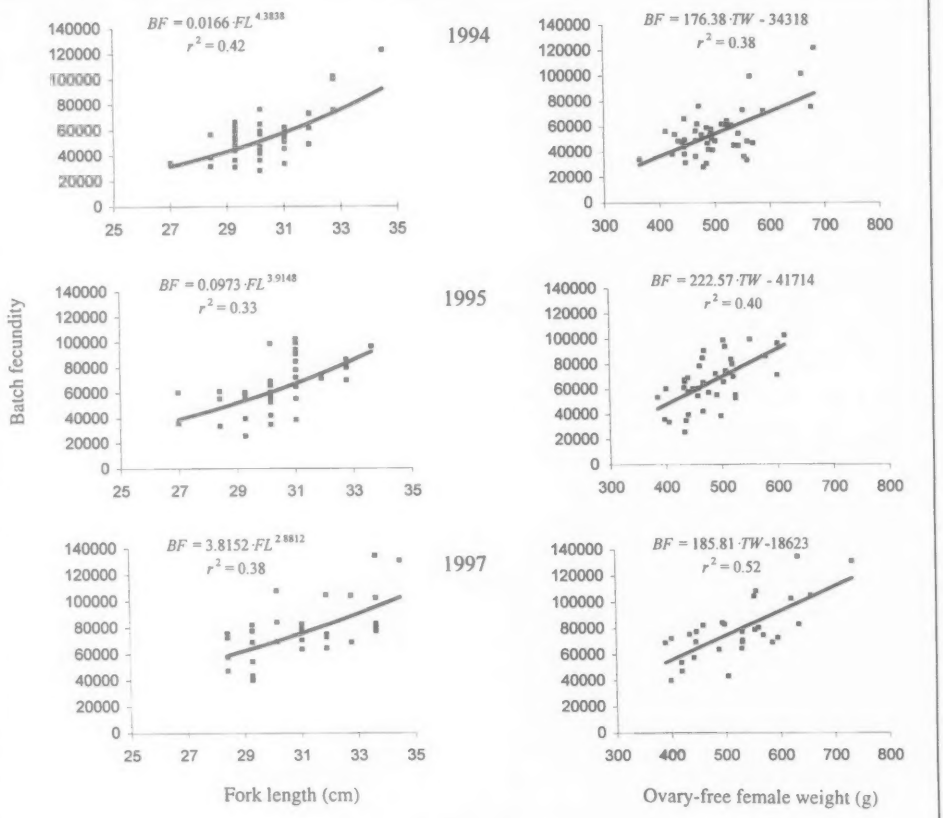


**Figure 4**

Batch fecundity as a function of fork length and total weight (without ovary) obtained from the different sampled years.

ies about egg quality of *B. aurea* compared with that of *E. anchoita* should include determination of oocyte dry weight, ash dry weight, and total lipid and fatty acid composition.

## Acknowledgments

This research was conducted within the INIDEP's Coastal Project. We thank Teresa Carlé and Haraldo E. Christiansen for the preparation of histological sections and Marcela Tobio who was responsible for the photographic procedures. We would also like to thank Norberto Scarlato and two anonymous reviewers for a critical review of our manuscript.

## Literature cited

**Acha, E. M., and G. J. Macchi.**
**2000.** Spawning of Brazilian menhaden, *Brevoortia aurea*, in the Río de la Plata estuary off Argentina and Uruguay. Fish. Bull. 98:227–235.

**Ahrenholz, D. W.**
**1991.** Population biology and life history of the North American menhadens, *Brevoortia* spp. Mar. Fish. Rev. 53(4): 3–19.

**Alheith, J., V. H. Alarcón, and B. J. Macewicz.**
**1984.** Spawning frequency and sex ratio in the Peruvian anchovy *Engraulis ringens*. CalCOFI Rep. 25:43–52.

**Anonymous.**
**1998.** Capturas marítimas totales 1997. Ministerio de Economía y Obras y Servicios Públicos. Secretaría de Agricultura, Ganadería, Pesca y Alimentación. Subsecretaría de

Pesca, Dirección Nacional de Pesca y Acuicultura, Buenos Aires, 45 p.

**Cassia, M. C., J. D. de Ciechomski, and H. E. Christiansen.**
**1979.** Estudios sobre la reproducción y fecundidad de la saraca, *Brevoortia aurea* (Agassiz, 1829) Hildebrand, 1948 (Pisces. Clupeidae) y la comparación de dos métodos utilizados. Physis 94:39–46.

**Cousseau, M. B., and J. M. Díaz de Astarloa.**
**1993.** El género Brevoortia en la costa atlántica sudamericana. Frente Marítimo 14:49–58.

**de Ciechomski, J. D.**
**1968.** Huevos y larvas de tres peces marinos: anchoa marini, *Brevoortia aurea* y *Prionotus nudigula* de la zona de Mar del Plata. Boletin Instituto Biología Marina 17:1–27.

**de Ciechomski, J. D., and G. Weiss.**
**1973.** Desove y fecundidad de la anchoíta argentina, *Engraulis anchoita*, Hubbs & Marini. Physis 32 (84):137–153.

**Díaz de Astarloa, J. M., and M. B. Cousseau.**
**1993.** Características regionales de la saraca (*Brevoortia aurea*) dentro del área costera bonaerense. Frente Marítimo 14:59–62.

**Dietrich, Ch. S., Jr.**
**1979.** Fecundity of the Atlantic menhaden, *Brevoortia tyrannus*. Fish. Bull. 77(1):308–311.

**Draper, N., and H. Smith.**
**1981.** Applied regression analysis, second edition. J. Wiley and Sons, New York, NY, 709 p.

**Fitzhugh, G. R., and W. F. Hettler.**
**1995.** Temperature influence on postovulatory follicle degeneration in Atlantic menhaden, *Brevoortia tyrannus*. Fish. Bull. 93:568–572.

**Fitzhugh, G. R., B. A. Thompson, and T. G. Snider III.**
**1993.** Ovarian development, fecundity, and spawning frequency of black drum *Pogonia cromis* in Louisiana. Fish. Bull. 91:244–253.

**Giangiobbe, A., and F. Sánchez.**
**1993.** Alimentación de la saraca (*Brevoortia aurea*). Frente Marítimo 14:71–80.

**Herrera, G., and G. Claramunt.**
**1990.** Estimaciones de la fecundidad parcial y frecuencia de desove de *Sardinops sagax* durante 1987 y 1988, en el norte de Chile. Invest. Cient. y Tec., Serie: Ciencias de Mar 1:55–68.

**Higham, J., and W. R. Nicholson.**
**1964.** Sexual maturation and spawning of Atlantic menhaden. Fish. Bull. 63(2):255–271.

**Hinckley, S.**
**1990.** Variation of egg size of walleye pollack *Theragra chalcogramma* with a preliminary examination of the effect of egg size on larval size. Fish. Bull. 88:471–483.

**Hunter, J. R., and S. R. Goldberg.**
**1980.** Spawning incidence and batch fecundity in northern anchovy, *Engraulis mordax*. Fish. Bull. 77(3):641–652.

**Hunter, J. R., N. C. H. Lo, and R. J. H. Leong.**
**1985.** Batch fecundity in multiple spawning fishes. *In* An egg production method for estimating spawning biomass of pelagics fish: application to the northern anchovy, *Engraulis mordax* (R. M. Lasker, ed.), p. 67–77. U.S. Dep. Commer., NOAA Tech. Rep. NMFS 36.

**Hunter, J. R., B. J. Macewicz, N. C. H. Lo, and C. A. Kimbrell.**
**1992.** Fecundity, spawning, and maturity of female Dover sole *Microstomus pacificus*, with an evaluation of assumptions and precision. Fish. Bull. 90:101–128.

**Kjesbu, O. S., P. Solemdal, P. Bratland, and M. Fonn.**
**1996.** Variation in annual egg production in individual captive atlantic cod (*Gadus morhua*). Can. J. Fish. Aquat. Sci. 53:610–620.

**Lewis, R. M., D. W. Ahrenholz, and S. P. Epperly.**
**1987.** Fecundity of Atlantic menhaden, *Brevoortia tyrannus*. Estuaries 10(4):347–350.

**Lewis, R. M., and Ch. M. Roithmayr.**
**1980.** Spawning and sexual maturity of Gulf menhaden, *Brevoortia patronus*. Fish. Bull. 78(4):947–951.

**López Cazorla, A.**
**1985.** Edad, crecimiento y comportamiento migratorio de *Brevoortia aurea* (Agassiz, 1829) (Osteichthyes, Clupeidae) de Bahía Blanca (Argentina). Inv. Pesq. 49(2):297–313.

**Macchi, G. J.**
**1998.** Preliminary estimate of spawning frequency and batch fecundity of striped weakfish, *Cynoscion striatus*, in coastal waters off Buenos Aires province. Fish. Bull. 96:375–381.

**Macchi, G. J., and E. M. Acha.**
**1998.** Aspectos reproductivos de las principales especies de peces muestreadas durante la campaña costera H-13/94. INIDEP Inf. Téc. 21:67–89

**Melo, Y. C.**
**1994.** Spawning frequency of the anchovy *Engraulis capensis*. S. Afr. J. Mar. Sci. 14: 321–331.

**Pájaro, M., G. J. Macchi, and R. P. Sánchez.**
**1997.** Fecundidad y frecuencia reproductiva de las poblaciones bonaerense y patagónica de anchoita argentina (*Engraulis anchoita*). Rev. Invest. Des. Pesq. 11:19–38.

**Pérez, N., I. Figueiredo, and B. J. Macewicz.**
**1992.** The spawning frequency of sardine, *Sardina pilchardus* (Walb.), off the Atlantic Iberian coast. Bol. Inst. Esp. Oceanogr. 8 (1):175–189.

**Powell, A. B.**
**1994.** Life history traits of two allopatric clupeids, Atlantic menhaden and Gulf menhaden, and the effects of harvesting on these traits. N. Am. J. Fish. Manage. 14:53–64.

**Sánchez, M. F.**
**1989.** Características morfológicas del aparato digestivo y espectro trófico de la saraca (*Brevoortia aurea*, Clupeiformes, Pisces). Physis 47(112):21–33.

**Sokal, R. R., and F. J. Rohlf.**
**1969.** Biometry: the principles and practice of statistic in biological research. W. H. Freeman, San Francisco, CA, 776 p.

**Weiss, G., and L. C. Krug.**
**1977.** Caracteristicas do desenvolvimento e metamorfose de *Lycengraulis olidus* (Engraulidae) e *Brevoortia pectinata* (Clupeidae) no estuário da Lagoa dos Patos, Brasil. Atlántica 2(1):83–117.

**Wootton, R. J.**
**1994.** Life histories as sampling devices: optimum egg size in pelagic fishes. J. Fish Biol. 45:1067–1077.

# Age and growth of the yellowedge grouper, *Epinephelus flavolimbatus*, and the yellowmouth grouper, *Mycteroperca interstitialis*, off Trinidad and Tobago

**Sherry C. Manickchand-Heileman**
Institute of Marine Affairs
P.O. Box 3160
Carenage, Trinidad, West Indies
Present address: c/o L. Heileman
United Nations Environment Programme
P.O. Box 47074
Nairobi, Kenya
E-mail address: sh_heileman@yahoo.com

**Dawn A. T. Phillip**
Institute of Marine Affairs
P.O. Box 3160
Carenage
Trinidad, West Indies

**Abstract.**—Age and growth were determined for the yellowedge grouper, *Epinephelus flavolimbatus*, and the yellowmouth grouper, *Mycteroperca interstitialis*, off Trinidad and Tobago. Age was determined from cross sections of sagittae and opaque rings were counted as annuli. From the monthly variation in marginal increment ratio (marginal increment divided by the distance between the penultimate and outermost annulus), rings were found to be deposited annually from October to February in the yellowedge grouper. Monthly variation in the frequency of otoliths with an opaque margin showed that opaque rings were deposited from September to January in the yellowmouth grouper. Both species were found to grow slowly, to have long lifespans, and to achieve high asymptotic lengths. Ages between 3 and 35 years (282–985 mm TL) were found for the yellowedge grouper, for which the von Bertalanffy growth equation was $L_t = 963\ (1-e^{-0.099(t+0.08)})$, where $L_t$ is length (mm) at time $t$ (yr). Yellowmouth groupers between ages 5 and 41 years (335–827 mm FL) were found and the von Bertalanffy growth equation was $L_t = 854\ (1-e^{-0.057(t+4.6)})$. The length-weight relationship for the yellowedge grouper was $Wt = 5 \times 10^{-5}TL^{2.80}$, where $Wt$ is body weight (g) and $TL$ is total length (mm). For the yellowmouth grouper this relationship was $Wt = 1.88 \times 10^{-5}FL^{2.94}$, where $FL$ is fork length (mm). Both species appear to grow more slowly and to achieve a greater asymptotic size and age than populations in higher latitudes, in contrast to what was expected based on differences in environmental temperature. This may be attributed to differences in fishing pressure because the populations in this study might have been subjected to a lower level of exploitation over a shorter period of time.

Manuscript accepted 26 November 1999.
Fish. Bull. 98:290–298 (2000).

The yellowedge grouper (*Epinephelus flavolimbatus*) and the yellowmouth grouper (*Mycteroperca interstitialis*) are two large serranids commonly caught in the trap fishery off Trinidad and Tobago. The yellowedge grouper has been recorded from North and South Carolina (Huntsman, 1976), the Gulf of Mexico, the West Indies, and the north coast of South America to Brazil at depths of 35–370 m (Smith, 1978). The yellowmouth grouper is found in rocky areas from the shoreline to depths of at least 55 m and is distributed from Bermuda, the South Atlantic Bight, the Gulf of Mexico, throughout the West Indies, Venezuela and Brazil (Smith, 1978), replacing the northern species *M. phenax* in some areas.

Both species are of significant commercial value in Venezuela (Smith, 1971; Gonzalez and Celaya[1]). The yellowmouth grouper is also commercially exploited in Bermuda (Smith, 1971) and the eastern Gulf of Mexico (Bullock and Murphy, 1994). Groupers are also of commercial importance in Trinidad and Tobago where they form part of a lucrative export trade in chilled fish. Yellowedge and yellowmouth groupers are the most commonly caught groupers in traps and are also caught by handlines (Manickchand-Heileman and Phillip, 1993). Historically, these species have been fished on the continental shelf and shelf edge northwest of Tobago and along the north and northeastern coasts of Trinidad by artisanal vessels from Trinidad and Tobago, as well as from Venezuela (Mendoza and Larez, 1996). Due to the decline in catch rates in these areas (Manickchand-Heileman and Phillip, 1993; Mendoza and Larez, 1996), the fishery has expanded to

[1] Gonzalez, L.W., and J. Celaya. 1986. Diagnostico socio-economico de la pesqueria de media altura pargo-mero del estado Nueva Esparta. Contrib. 8, Centro de Investigaciones Cientificas, Univ. Oriente, Venezuela. 31 p. Univ. del Oriente, Apdo. Postal 245, Cumana, Sucre, Venezuela.

the offshore continental shelf and shelf edge to the east of Trinidad. At present, this fishery is not managed and the decline in catches in the traditional fishing areas emphasizes the need for proper management. However, lack of data is an impediment to the development of appropriate management strategies for this important fishery.

Groupers are relatively long-lived and slow-growing and are protogynous hermaphrodites, making them especially susceptible to overexploitation (Bannerot et al., 1987; Shapiro, 1987; Bohnsack[2]). In reviewing the status of grouper stocks in the western central Atlantic, Sadovy (1990) found that these stocks are heavily fished throughout the region and that many are growth or recruitment overfished, or both. Sadovy also emphasized the need for management to ensure their continued commercial and recreational viability.

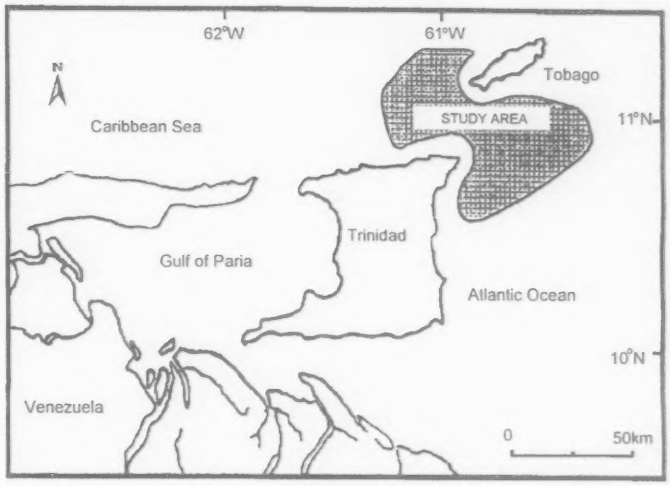


**Figure 1**
Location of study area.

Published information on the yellowedge and yellowmouth grouper is scarce. Age, growth and reproduction of the yellowedge grouper in South Carolina have been investigated by Keener (1984) and in the eastern Gulf of Mexico by Bullock and Godcharles.[3] Randall (1967) documented the food habits of yellowmouth grouper from the Bahamas and Thompson and Munro (1978) recorded the occurrence of spawning individuals in Jamaica. Aspects of the life history, including age and growth, of yellowmouth grouper in the eastern Gulf of Mexico have been reported by Bullock and Smith (1991) and Bullock and Murphy (1994).

In Trinidad and Tobago, information on reproduction, age, and growth of the yellowedge and yellowmouth groupers have been presented by Manickchand-Heileman and Phillip.[4] However, age was not validated and results were only preliminary. Our study reports on the age and growth of these two species off Trinidad and Tobago. It was carried out as part of a national fish stock assessment project, in collaboration with the Fisheries Division, Ministry of Agriculture, Lands and Marine Resources (Trinidad and Tobago), the United Nations Development Program (UNDP), and the Food and Agriculture Organization (FAO).

## Materials and methods

### Study area

Trinidad and Tobago, a twin-island Republic, are the southernmost of the Caribbean chain of islands (Fig. 1). Both islands are situated on the South American continental shelf; Tobago is about 32 km to the northeast of Trinidad. Topographically, the shelf in this area is relatively featureless; a substratum of fine mud is interspersed with occasional patches of shell debris and fine sand (Kenny and Bacon, 1981). The shelf edge lies along the 90–100 m contour (Gade[5]) which ranges from a distance of approximately 12 km from the northwest coast of Tobago to approximately 50 km from the north coast of Trinidad.

This area experiences a dry season from December to May and a wet season from June to November. Bottom temperatures at depths of about 100 m vary from a maximum of 25°C in the dry season to a minimum of 22°C in the wet season (Gade[5]). During the wet season the large input of fresh water from

[2] Bohnsack, J. A. 1989. Protection of grouper spawning aggregations. Coastal Resour. Div. Contrib. Rep. CRD 88-89-06, NMFS Southeast Fish. Sci. Cent., Miami, FL, 8 p.

[3] Bullock, L. H., and M. F. Godcharles. 1984. Life history aspects of the yellowedge grouper, *Epinephelus flavolimbatus* (Pisces: Serranidae) from the eastern Gulf of Mexico. Annual Report, Fla. Dep. Nat. Resour., Mar. Res. Lab., St. Petersburg, FL, 28 p. Unpubl. data.

[4] Manickhand-Heileman, S., and D. A. T. Phillip. 1992. Preliminary stock assessment of the fishpot fishery of Tobago. Technical report of the Project for the Establishment of Data Collection Systems and Assessment of the Fisheries Resources. Report FAO/UNDP:TRI/91/001/TR12, 38 p.

[5] Gade, H. 1989. The environmental-ecological regimes. *In* Report on surveys of the fish resources in the shelf areas between Suriname and Colombia with the R/V *Dr. Fridtjof Nansen*, p. 8–41. Institute of Marine Research, Bergen.

local precipitation and runoff from South American rivers, particularly the Orinoco River, affect surface salinity which ranges from 35.5‰ in the dry season to less than 27‰ in the wet season. However, the salinity of deeper waters is not greatly affected and ranges from about 36.8‰ in the wet season to 36.5‰ in the dry season (Gade[5]).

## Methods

Monthly samples of yellowedge and yellowmouth grouper were obtained from commercial fish landings at a fish processing plant on the island of Tobago. Fish were caught by Antillean fish traps (Munro et al., 1971) on the continental shelf and slope to the northeast of Trinidad and northwest of Tobago in depths of 37–128 m (Fig. 1). A total of 729 yellowedge and 116 yellowmouth groupers were obtained during the study period.

Total length (mm) was recorded for the yellowedge grouper, whereas fork length (FL) was recorded for the yellowmouth grouper because, in most cases, the filamentous rays of the caudal fin of this species were damaged. Total body weight (g) was recorded for both species. For most fish the left sagittal otolith was removed unless broken or lost, in which case the right was obtained. Otoliths were stored dry in labelled envelopes.

For sectioning, otoliths were embedded in Spurr resin (Spurr, 1969) and allowed to harden overnight. One or two 0.5-mm transverse sections of each otolith were taken through the focus along a dorsoventral plane with a high-speed circular saw. Sections were ground and polished with several grades of silicon carbide paper. They were placed in glycerol and viewed against a black background with reflected light under a dissecting microscope at a magnification of 20×. Alternating opaque and translucent bands were visible and the former were counted as annuli.

For each species, otolith radius (distance from the core to the otolith edge) and the distance from the core to the distal edge of each opaque ring were measured under a binocular microscope with an ocular micrometer (1 micrometer unit=0.125 mm). All measurements were taken along the ventral surface of the sulcus acousticus. In order to validate that rings were formed annually in the yellowedge grouper, the monthly mean marginal increment ratio, that is, the marginal increment (distance between the distal edge of the outermost annulus and the otolith margin) divided by the distance between the distal edge of the penultimate annulus and proximal edge of the outermost annulus (Bullock et al., 1992), was calculated. Because of difficulty in measuring annulus radius in the yellowmouth grouper, it was not possible to carry out this analysis in sufficiently large monthly samples. Instead, for this species the monthly frequency of occurrence of otoliths with an opaque edge was determined. Mean monthly marginal increment ratios in the yellowedge grouper and frequency of occurrence of opaque edges in the yellowmouth grouper were compared by using the chi-square goodness-of-fit test for circular data (Zar, 1974). Least squares linear regression of otolith radius on fish length was carried out and the relationship used to backcalculate lengths of fish at earlier ages.

The von Bertalanffy growth function was used to describe growth (Ricker, 1975):

$$L_t = L_\infty\left(1-e^{-K(t-t_0)}\right),$$

where $L_t$ = total or fork length (mm) at time $t$ (years);
$L_\infty$ = the asymptotic length;
$K$ = the growth coefficient; and
$t_0$ = theoretical age at zero length.

This function was fitted to observed lengths at age by using the FISHPARM program (Prager et al., 1987). The length-weight relationship was determined by least squares linear regression with logarithmically transformed data:

$$W = aL^b,$$

where $W$ = body weight (g);
$L$ = fish length (mm); and
$a$ and $b$ are constants.

## Results

### Validation

Satisfactory annuli counts were made on 326 of the 367 yellowedge grouper otoliths examined. A randomly chosen subsample of 63 otoliths was read by an independent reader and a 95% agreement was found. This species showed a significant difference among monthly mean marginal increment ratios ($P<0.001$), with elevated values (greater than 50%) occurring from March to September (Fig. 2). This finding suggests that there is one main period of annulus formation during the year from October to February, even though otoliths with opaque edges were observed throughout the year.

Growth of the otolith was proportional to growth in length of the fish and the relationship between total length (TL) and otolith radius (OR) was

$$TL = 111.4OR - 105.2 \qquad (n=330,\ r^2=0.93).$$

Number of rings increased with fish length; 3–35 rings were found in yellowedge grouper between 282 and 985 mm TL.

Of the 90 otoliths read for the yellowmouth grouper, satisfactory annuli counts were made on 80. A random subsample of 33 otoliths was read by an independent reader and a 98% agreement was found. For this species frequency of otoliths with an opaque edge showed significant monthly variation ($P<0.001$), with elevated values occurring from September to January (Fig. 3). Growth of the otolith was proportional to growth in length and the relationship between fork length (FL) and otolith radius was

$$FL = 162.97 + 90.86OR \qquad (n=57,\ r^2=0.81).$$

The number of rings increased with fish length; 5–41 rings were found in yellowmouth grouper between 335 and 827 mm FL.

The monthly sample sizes shown in Figures 2 and 3 indicate the seasonal pattern of catches for both species in this study area. At the extremities of the year, catches were low because fishing is restricted to shallow waters owing to rough seas that prevail at this time.

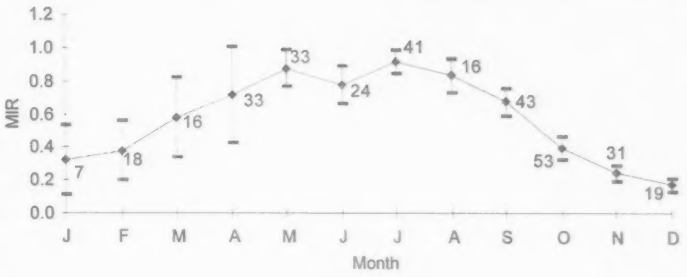


**Figure 2**

Monthly variation in mean marginal increment ratio (MIR) for yellowedge grouper, *E. flavolimbatus*. Sample sizes are given next to means and standard deviation is represented by the horizontal bars .

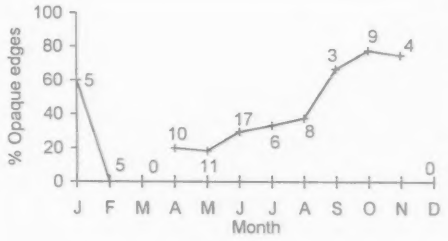


**Figure 3**

Monthly variation in the frequency of occurrence of otoliths with opaque margin for yellowmouth grouper, *M. interstitialis*. Sample sizes are given next to data points.

## Age and growth

For both species, the growth parameters are presented for combined sexes because in some instances otoliths were obtained from fish that were gutted at sea and thus of unknown sex. The relationship between fish length and otolith radius was used to backcalculate lengths of fish at earlier ages. Owing to the narrowing of the space between successive annuli in older individuals and the resulting difficulty in making accurate measurements, radii were measured in 231 yellowedge grouper with 3 to 15 rings. Mean backcalculated lengths for yellowedge grouper are given in Table 1. Close agreement was found between the observed, backcalculated, and theoretical growth curves for this species, although for some age groups the backcalculated lengths were greater than observed lengths (Fig. 4). The von Bertalanffy growth parameters (asymptotic standard error) for observed length and age data for the yellowedge grouper were $L_\infty = 963$ mm TL (18.8 mm), $K = 0.099$/yr (0.01 yr), $t_0 = -0.08$ years (0.28 yr).

Owing to narrowing of the space between annuli in older individuals and difficulty in making accurate measurements, it was possible to measure radii in only 20 yellowmouth grouper, with 5 to 19 rings. Mean backcalculated lengths for yellowmouth grouper are given in Table 2. Close agreement was also found between the observed, backcalculated and theoretical growth curves for this species, although some backcalculated lengths were greater than observed lengths, particularly for the younger age groups (Fig. 5). For the yellowmouth grouper, the von Bertalanffy growth parameters (asymptotic standard error) for observed length at age data were $L_\infty = 854$ mm FL (59.9 mm), $K = 0.057$/yr (0.01/yr), $t_0 = -4.6$ years (2.29 yr).

## Length-weight relationship

For the yellowedge grouper, the relationship between total body weight (Wt) and length (TL) was

**Table 1**

Observed and backcalculated mean total lengths (TL mm) at age (yr) for the yellowedge grouper, *E. flavolimbatus*. Roman numerals represent annulus number, beginning at the focus of the otolith.

| Age (yr) | *n* | Mean TL (mm) | SD (mm) | I | II | III | IV | V | VI | VII | VIII | IX | X | XI | XII | XIII | XIV | XV |
|---|---|---|---|---|---|---|---|---|---|---|---|---|---|---|---|---|---|---|
| 3 | 3 | 317 | 14 | 185 | 251 | 313 | | | | | | | | | | | | |
| 4 | 2 | 299 | 23 | 123 | 198 | 241 | 294 | | | | | | | | | | | |
| 5 | 15 | 389 | 24 | 136 | 203 | 269 | 331 | 381 | | | | | | | | | | |
| 6 | 29 | 438 | 35 | 128 | 206 | 277 | 340 | 395 | 431 | | | | | | | | | |
| 7 | 41 | 469 | 47 | 120 | 194 | 265 | 334 | 389 | 434 | 465 | | | | | | | | |
| 8 | 33 | 534 | 50 | 126 | 209 | 281 | 350 | 412 | 461 | 502 | 530 | | | | | | | |
| 9 | 26 | 586 | 61 | 135 | 221 | 300 | 363 | 426 | 478 | 519 | 552 | 579 | | | | | | |
| 10 | 22 | 618 | 44 | 135 | 220 | 292 | 360 | 420 | 469 | 513 | 552 | 578 | 605 | | | | | |
| 11 | 32 | 638 | 36 | 124 | 202 | 281 | 353 | 411 | 466 | 511 | 550 | 583 | 612 | 629 | | | | |
| 12 | 13 | 666 | 74 | 129 | 197 | 259 | 333 | 400 | 451 | 497 | 537 | 577 | 610 | 638 | 659 | | | |
| 13 | 6 | 696 | 61 | 162 | 215 | 290 | 354 | 408 | 452 | 492 | 534 | 573 | 610 | 644 | 669 | 690 | | |
| 14 | 5 | 725 | 72 | 129 | 197 | 250 | 317 | 369 | 423 | 474 | 517 | 545 | 586 | 623 | 661 | 694 | 718 | |
| 15 | 4 | 769 | 57 | 121 | 201 | 264 | 327 | 382 | 442 | 482 | 519 | 562 | 603 | 640 | 677 | 709 | 743 | 766 |
| Total | 231 | | | | | | | | | | | | | | | | | |
| Weighted backcalculated mean TL (mm) | | | | 129 | 207 | 278 | 345 | 403 | 453 | 497 | 542 | 577 | 607 | 633 | 664 | 696 | 728 | 766 |
| Growth increment (mm) | | | | | 78 | 71 | 67 | 58 | 50 | 44 | 45 | 35 | 30 | 26 | 31 | 32 | 32 | 38 |

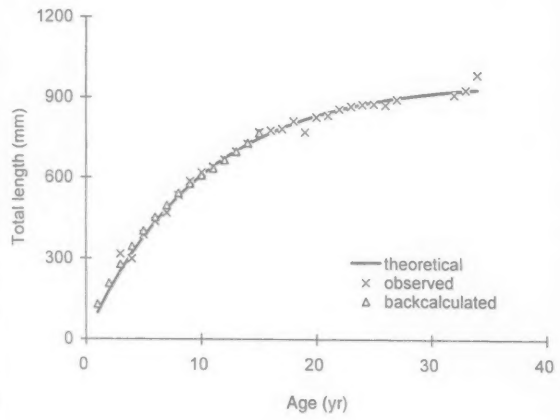


**Figure 4**

Observed, backcalculated, and theoretical lengths at age for yellowedge grouper, *E. flavolimbatus*.

$$Wt = 5.0 \times 10^{-5}\mathrm{TL}^{2.80} \qquad (n=335,\ r^2=0.88).$$

The exponent $b$ was significantly different from 3 ($t$-test, $t$=17.98, $P$<0.001). For the yellowmouth grouper this relationship was

$$Wt = 1.88 \times 10^{-5}FL^{2.94} \qquad (n=50,\ r^2=0.94),$$

with $b$ being significantly different from 3 ($t$-test, $t$=5.19, $P$<0.001).

## Discussion

The annual formation of opaque rings was demonstrated in both yellowedge and yellowmouth groupers in the study area. Deposition of annuli occurs over a protracted period of about five months, beginning in the wet season and continuing into the early part of the dry season. A protracted period of annulus deposition has been observed in other grouper populations, e.g. *Mycteroperca phenax* (Matheson et al., 1986), *Epinephelus itajara* (Bullock et al., 1992), and *M. microlepis* (Hood and Schlieder, 1992). Factors affecting annulus formation in groupers have been discussed by Moe (1969), who attributed annulus formation in red grouper to spawning and related physiological processes. In contrast, in our study area, annulus formation in the yellowmouth and yellowedge groupers occurred after the period of peak spawning from about April to July for both species (Manickchand-Heileman and Phillip[4]). Formation of annuli after spawning was also reported for the Nassau grouper, *E. striatus*, in the Cayman Islands (Bush et al., 1996). Annulus formation has also been found to occur out of phase with spawning in other grou-

**Table 2**

Observed and backcalculated mean fork lengths (FL mm) at age (yr) for the yellowmouth grouper, *M. interstitialis*. Roman numerals represent annulus number.

| Age (yr) | *n* | Mean TL (mm) | SD (mm) | I | II | III | IV | V | VI | VII | VIII | IX | X | XI | XII | XIII | XIV | XV | XVI | XVII | XVIII | XIX |
|---|---|---|---|---|---|---|---|---|---|---|---|---|---|---|---|---|---|---|---|---|---|---|
| 5 | 3 | 335 | 3 | 234 | 273 | 298 | 320 | 332 | | | | | | | | | | | | | | |
| 6 | 1 | 355 | — | 236 | 262 | 302 | 322 | 335 | 349 | | | | | | | | | | | | | |
| 8 | 2 | 482 | 23 | 269 | 315 | 355 | 380 | 411 | 436 | 456 | 474 | | | | | | | | | | | |
| 9 | 1 | 516 | — | 271 | 310 | 349 | 379 | 398 | 428 | 457 | 487 | 506 | | | | | | | | | | |
| 10 | 1 | 557 | — | 290 | 337 | 372 | 406 | 430 | 453 | 476 | 511 | 534 | 557 | | | | | | | | | |
| 12 | 3 | 566 | 48 | 279 | 321 | 360 | 394 | 418 | 445 | 469 | 492 | 511 | 525 | 544 | 558 | | | | | | | |
| 13 | 1 | 603 | — | 273 | 346 | 395 | 432 | 456 | 481 | 505 | 530 | 554 | 566 | 579 | 591 | 603 | | | | | | |
| 14 | 5 | 605 | 38 | 277 | 324 | 359 | 382 | 404 | 427 | 449 | 469 | 489 | 508 | 528 | 544 | 555 | 564 | | | | | |
| 15 | 1 | 559 | — | 331 | 321 | 341 | 371 | 391 | 410 | 430 | 450 | 480 | 499 | 519 | 529 | 539 | 549 | 559 | | | | |
| 17 | 1 | 634 | — | 289 | 335 | 381 | 404 | 427 | 450 | 473 | 496 | 508 | 531 | 554 | 565 | 577 | 588 | 600 | 611 | 623 | | |
| 19 | 1 | 700 | — | 336 | 380 | 405 | 431 | 457 | 475 | 492 | 509 | 527 | 544 | 553 | 579 | 605 | 622 | 626 | 631 | 635 | 639 | 644 |
| Total | 20 | | | | | | | | | | | | | | | | | | | | | |
| Weighted backcalculated mean TL (mm) | | | | 274 | 316 | 351 | 378 | 399 | 434 | 462 | 484 | 506 | 524 | 540 | 555 | 566 | 572 | 595 | 621 | 629 | 639 | 644 |
| Growth increment (mm) | | | | | 42 | 35 | 27 | 22 | 35 | 28 | 22 | 22 | 18 | 16 | 15 | 11 | 6 | 23 | 26 | 8 | 11 | 4 |

pers in higher latitudes, e.g. *M. phenax* in the South Atlantic Bight (Matheson et al., 1986), *E. itajara* (Bullock et al., 1992) and *M. microlepis* (Hood and Schlieder, 1992) in the eastern Gulf of Mexico, and *M. bonaci* in south Florida (Crabtree and Bullock, 1998). For the two species in our study, annulus formation may be associated with changes in environmental factors, notably reduced bottom temperature during the wet season. On the continental shelf, where our study was conducted, bottom temperature has been found to decrease to a minimum of about 22°C in the wet season (Gade[5]).

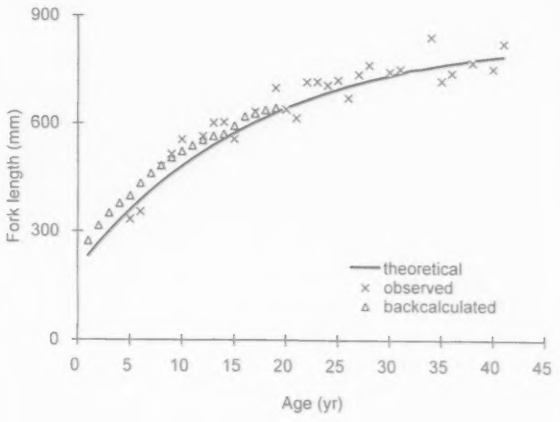


**Figure 5**

Observed, backcalculated, and theoretical lengths at age for yellowmouth grouper, *M. interstitialis*.

Annual rings were found in otoliths of yellowedge and yellowmouth groupers in other geographical areas, although time of annulus formation differed, which may be attributed to differences in annulus measurement techniques. For yellowedge grouper in the South Atlantic Bight, annulus formation occurred in March–September and coincided with time of peak spawning (Keener, 1984), whereas in the eastern Gulf of Mexico it occurred from May to November (Bullock and Godcharles[3]). The yellowmouth grouper formed annuli in August–October in the eastern Gulf of Mexico (Bullock and Murphy, 1994).

Some backcalculated lengths were larger than observed lengths, especially for the younger age groups. This reverse "Rosa Lee" phenomenon may have resulted from increased survival of fast-growing fish (Ricker, 1975). For the yellowmouth grouper, the small number of fish available for ring measurements may have also contributed to discrepancies in the backcalculated lengths.

The growth pattern of these two species is similar to that reported for other groupers, in that they are long-lived and have low growth rates and high asymptotic lengths (e.g. *M. phenax*, Matheson et al., 1986; *M. bonaci*, Manooch and Mason, 1987, Crabtree and Bullock, 1998; *E. itajara*, Bullock et al., 1992; *M. micro-*

*lepis*, Hood and Schlieder, 1992; *E. guttatus*, Sadovy et al., 1992). In the southern United States, the yellowedge grouper has a lower asymptotic length and higher growth rate ($L_\infty$=891mm TL, $K$=0.163, Keener, 1984; $L_\infty$=831 mm TL, $K$=0.191, Bullock and Godcharles[3]) than those found in our study. Our maximum observed age (35 years) was greater than those (15 and 27 years) reported by Keener (1984) and Bullock and Godcharles,[3] respectively.

Comparison of growth curves using $\Phi'$, where $\Phi' = \log K + 2\log L_\infty$ (Munro and Pauly, 1983; Pauly and Munro, 1984) showed close agreement with those in other areas ($\Phi'$=2.96, our study, $\Phi'$=3.11 and 3.12, southern United States with growth parameters of Keener, 1984, and Bullock and Godcharles[3], respectively). This comparison suggests that the general growth pattern of yellowedge grouper observed in our study is similar to that for the southern United States and further validates the results obtained in our study.

The yellowmouth grouper also showed a higher $L_\infty$ (854 mm FL or 934 mm TL) and lower $K$ than reported for the eastern Gulf of Mexico where $L_\infty$ was 828 mm TL and $K$ was 0.076 (Bullock and Murphy, 1994). The maximum observed age (41 years) was higher than that (28 years) reported by Bullock and Murphy (1994). Comparison of growth curves using $\Phi'$ showed close agreement between the growth curve obtained in our study ($\Phi'$=2.70) and that obtained by Bullock and Murphy (1994) whose growth parameters resulted in $\Phi'$ of 2.72.

Results suggest that the growth curve of each species belongs to the same family of curves as their counterparts in other geographical areas, i.e. the relationship between $L_\infty$ and $K$ is similar (Pauly, 1991). However, comparison of actual growth rates and asymptotic lengths indicates that each species grows slower and achieves a greater size and age than those reported for populations in the southern United States. This finding is in contrast to what is expected in the growth patterns of tropical versus subtropical and temperate populations. Tropical fish generally grow faster and reach smaller sizes than populations in higher latitudes, mainly because of differences in environmental temperature (Longhurst and Pauly, 1987). It appears that factors other than those related to the environment may be responsible for the differences observed, or may mask the real growth pattern. Such factors may include intrinsic differences between populations, or differences in fishing patterns between the two areas. The latter may contribute significantly to differences in growth because grouper populations in the southern United States have been fished since the late 1970s (Bullock and Murphy, 1994; Bullock et al., 1996) for a longer period of time than the populations in our study. Populations subjected to high exploitation rates for long time periods generally exhibit changes in growth and reproductive patterns, such as faster growth and smaller sizes (Gulland, 1983), as well as smaller size at maturity (McGovern et al., 1998) than populations that have not been as heavily fished.

The slow growth, long life spans, and presumed low natural mortality rates of yellowedge and yellowmouth grouper reported for our study, imply that they are highly susceptible to overfishing (Bullock et al., 1992). These characteristics suggest that maximum yield would be obtained at either low exploitation rates or with capture of only large individuals (Bullock et al., 1992). In addition, the protogynous hermaphroditic strategy of some groupers may also make them more susceptible to overfishing than gonochoristic species (Bannerot et al., 1987). Evidence of hermaphroditism has been reported for the yellowedge grouper (Keener, 1984; Bullock et al., 1996) and other species of *Mycteroperca* (Matheson et al., 1986; Collins et al., 1987; Hood and Schlieder, 1992; Crabtree and Bullock, 1998). We did not consider differences in growth patterns and population dynamics specific to an alternative reproductive strategy in our study. For protogynous hermaphrodites, the pooling of data for combined sexes may mask certain growth patterns such as enhanced growth rates following sexual transition and could lead to errors in the predictions obtained from standard yield models (Bannerot et al., 1987). Thus, subsequent studies should consider the effects of an alternative reproductive strategy on population parameters and the predictions for management of these species in Trinidad and Tobago.

## Acknowledgments

This project was accomplished with financial and technical assistance from the United Nations Development Programme and the Food and Agricultural Organization. The authors wish to thank the following: Edward Brothers for assistance with otolith reading; Daniel Pauly for technical advice; Maxwell Sturm for reviewing earlier drafts of the manuscript; and the Yeates brothers for allowing access to fish catches and for facilitating field sampling. Two anonymous reviewers contributed comments that significantly improved the manuscript.

## Literature cited

**Bannerot, S. P., W. W. Fox Jr., and J. E. Powers.**
**1987.** Reproductive strategies and the management of snappers and groupers in the Gulf of Mexico and Caribbean. *In* Tropical snappers and groupers: biology and fisheries man-

agement (J. J. Polovina and S. Ralston, eds.), p. 561–603. Westview Press, Boulder.

**Bullock, L. H., M. F. Godcharles, and R. E. Crabtree.**
**1996.** Reproduction of yellowedge grouper *Epinephelus flavolimbatus*, from the eastern Gulf of Mexico. Bull. Mar. Sci. 59(1):216–224.

**Bullock, L. H., and M. D. Murphy.**
**1994.** Aspects of the life history of the yellowmouth grouper, *Mycteroperca interstitialis*, in the eastern Gulf of Mexico. Bull. Mar. Sci. 55(1):30–45.

**Bullock, L. H., M. D. Murphy, M. F. Godcharles, and M. E. Mitchell.**
**1992.** Age, growth, and reproduction of jewfish *Epinephelus itajara* in the eastern Gulf of Mexico. Fish. Bull. 90: 243–249.

**Bullock, L. H., and G. B. Smith.**
**1991.** Seabasses (Pisces: Serranidae). Mem. Hourglass Cruises 8(2):1–243.

**Bush, P. G., G. C. Ebanks, and E. D. Lane.**
**1996.** Validation of ageing technique for Nassau grouper (*Epinephelus striatus*) in the Cayman Islands. *In* Biology, fisheries and culture of tropical snappers and groupers (F. Arreguin-Sanchez, J. L. Munro, M. C. Balgos and D. Pauly, eds.), p.150–157. ICLARM Conf. Proc. 48.

**Collins, M. R., C. W. Waltz, W. A. Roumillat, and D. L. Stubbs.**
**1987.** Contribution to the life history and reproductive biology of gag, *Mycteroperca microlepis* (Serranidae), in the South Atlantic Bight. Fish. Bull. 85:648–653.

**Crabtree, R. E., and L. H. Bullock.**
**1998.** Age, growth and reproduction of black grouper, *Mycteroperca bonaci*, in Florida waters. Fish. Bull. 95:735–753.

**Gulland, J.A.**
**1983.** Fish stock assessment. A manual of basic methods, vol.1. FAO/Wiley series on Food and Agriculture, 223 p.

**Hood, P. B., and R. C. Schlieder.**
**1992.** Age, growth and reproduction of gag, *Mycteroperca microlepis*, in the eastern Gulf of Mexico. Bull. Mar. Sci. 51(3):337–352.

**Huntsman, G. R.**
**1976.** Offshore bottom-fisheries of the United States south Atlantic coast. *In* Proc. Coll. on snapper-grouper fishery resources of the western central Atlantic Ocean (H. R. Bullis and A. C. Jones, eds.), p. 192–221. Florida. Sea Grant Rep. 17, Gainesville, FL.

**Keener, P.**
**1984.** Age, growth, and reproductive biology of the yellowedge grouper, *Epinephelus flavolimbatus*, off the coast of South Carolina. M.S. thesis, College of Charleston, Charleston, SC, 65 p.

**Kenny, J. S., and P. R. Bacon.**
**1981.** Aquatic resources. *In* The natural resources of Trinidad and Tobago (St. G. C. Cooper and P. R. Bacon, eds.), p. 112–144. Edward Arnold Ltd., London.

**Longhurst, A. R. , and D. Pauly.**
**1987.** Ecology of tropical oceans. Academic Press Inc. Ltd., London, 407 p.

**Manickchand-Heileman, S., and D. A.T . Phillip.**
**1993.** Description and status of the snapper grouper fishery of Trinidad and Tobago. Gulf and Caribb. Fish. Inst. 45th Annual Meeting, 11 p. Harbour Branch Oceanographic Institute, Fort Pierce, FL.

**Manooch, C. S. III, and D. L. Mason.**
**1987.** Age and growth of the Warsaw grouper and black grouper form the southeast region of the United States. Northeast Gulf Science 9(2):65–75.

**Matheson, R. H. III, G. R. Huntsman, and C. S. Manooch III.**
**1986.** Age, growth, mortality, food and reproduction of the scamp, *Mycteroperca phenax*, collected off North Carolina and South Carolina. Bull. Mar. Sci. 38(2):300–312.

**McGovern, J. C., D. M. Wyanski, O. Pashuk, C. S. Manooch, and G. R. Sedberry.**
**1998.** Changes in sex ratio and size at maturity of gag, *Mycteroperca microlepis*, from the Atlantic coast of the southeastern United States during 1976–1995. Fish. Bull. 96:797–807.

**Mendoza, J. J., and A. Larez.**
**1996.** Abundance and distribution of snappers and groupers targeted by the artisanal medium range fishery off northeastern Venezuela (1981–1992). *In* Biology, fisheries and culture of tropical snappers and groupers (F. Arreguin-Sanchez, J. L. Munro, M. C. Balgos, and D. Pauly, eds.), p. 266–275. ICLARM Conf. Proc. 48.

**Moe, M. A.**
**1969.** Biology of the red grouper *Epinephelus morio* (Valenciennes) from the eastern Gulf of Mexico. Fla. Dep. Nat. Resour. Mar. Res. Lab. Prof. Pap. Ser. 10, 95 p.

**Munro, J. L., and D. Pauly.**
**1983.** A simple method for comparing growth of fishes and invertebrates. ICLARM Fishbyte 1(1):5–6.

**Munro, J. L., P. H. Reeson, and V. C. Gaut.**
**1971.** Dynamic factors affecting the performance of the Antillean fish trap. Proc. Gulf and Caribb. Fish. Inst. 23: 184–194.

**Pauly, D.**
**1991.** Growth performance in fishes: rigorous description of patterns as a basis for understanding causal mechanisms. Aquabyte 4(3):3–6.

**Pauly, D., and J. L. Munro.**
**1984.** Once more on the comparison of growth in fish and invertebrates. ICLARM Fishbyte 2(1):21.

**Prager, M. H., S. B. Sailer, and C. W. Recksiek.**
**1987.** FISHPARM: a microcomputer program for parameter estimation of nonlinear models in Fishery Science. Oceanography Technical Report. 87–10, 18 p. Old Dominion University, Norfolk, VA.

**Randall, J. E.**
**1967.** Food habits of reef fishes of the West Indies. Stud. Trop. Oceanogr. Inst. Mar. Sci. Univ. Miami, 5:665–847.

**Ricker, W. E.**
**1975.** Computation and interpretation of biological statistics of fish populations. Fish. Res. Board Can. Bull. 191, 382 p.

**Sadovy, Y.**
**1990.** Grouper stocks of the western central Atlantic: the need for management and management needs. Gulf and Caribb. Fish.Inst. 43rd Annual Meeting, 17 p. Harbour Branch Oceanographic Institute, Fort Pierce, FL.

**Sadovy, Y., M. Figuerola, and A. Roman.**
**1992.** Age and growth of the red hind *Epinephelus guttatus* in Puerto Rico and St. Thomas. Fish. Bull. 90:516–528.

**Shapiro, D. Y.**
**1987.** Reproduction in groupers. *In* Tropical snappers and groupers: biology and fisheries management (J. J. Polovina and S. Ralston, eds.), p. 295–327. Westview Press, Boulder, CO.

**Smith, C. L.**
**1971.** A revision of the American groupers: *Epinephelus* and allied genera. Bull. Am. Mus. Nat. Hist. 146(2):69–241.
**1978.** Serranidae. *In* FAO species identification sheets for fisheries purposes (W. Fischer, ed.), vol. IV, Western Central Atlantic (fishing area 31). FAO, Rome.

**Spurr, A. R.**
**1969.** A low-viscosity epoxy resin embedding medium for electron microscopy. J. Ultrastructure Res. 26:31–43.
**Thompson, R., and J. Munro.**
**1978.** Aspects of the biology and ecology of Caribbean reef fishes: Serranidae (hinds and groupers). J. Fish. Biol. 12: 115–146.
**Zar, J. H.**
**1974.** Biostatistical analysis. Prentice Hall Inc., Englewood Cliffs, NJ, 620 p.

# Reproductive biology of the female shortfin mako, *Isurus oxyrinchus* Rafinesque, 1810, with comments on the embryonic development of lamnoids

**Henry F. Mollet**
Monterey Bay Aquarium
886 Cannery Row
Monterey, California 93940
E-mail address: mollet@mbay.net

**Geremy Cliff**
Natal Sharks Board
Private Bag 2
Umhlanga Rocks 4320, South Africa

**Harold L. Pratt Jr.**
Narragansett Laboratory
28 Tarzwell Drive
Narragansett, Rhode Island 02882

**John D. Stevens**
CSIRO Marine Research
P. O. Box 1538
Hobart, Tasmania 7001, Australia

**Abstract.**—Reproductive data from 95 mature female shortfin mako sharks, *Isurus oxyrinchus* Rafinesque, 1810, including 35 pregnant females, together with data on 450 postnatal fish were collected from around the world. Size at birth was approximately 70 cm total length (TL) and litter size varied from 4 to 25, increasing with maternal size. Embryo length-at-capture data predicted a gestation period of 15–18 months and late winter to midspring parturition in both hemispheres. A temporal analysis of uterus width index and gonadosomatic index of pregnant and postpartum females indicated that the reproductive cycle is three years. The median TL-at-maturity of females from the western North Atlantic (2.98 m) was greater than that of females from the Southern Hemisphere (2.73 m) and they were 16–19% heavier in the TL range of 2.5–3.5 m.

Recently ovulated females and a litter with 2.6–3.3 cm TL embryos having external gills, a large yolk sac, and still inside their egg cases, are described. We describe a litter of embryos (52.0 cm TL) with huge yolk-filled stomachs. Litters of 59.9- and 68.8-cm-TL embryos showed a decline in the mass of the yolk-filled stomach from 29.1% to 10.9% of total mass and an increase in hepatosomatic indices from 3.7% to 7.0% as gestation advances. When the mass of the yolk-filled stomach was excluded, the mass-length relationship of shortfin mako embryos could be fitted with a power regression similar to that for postnatal fish. The condition factor of lamnid embryos (including yolk-stomach mass) reaches a maximum between 20 and 35 kg/m$^3$ when the embryos are midterm and have the largest yolk stomachs. The condition factor of alopiid embryos remains constant, indicating that no large yolk-filled stomach develops.

Manuscript accepted 23 November 1999.
Fish. Bull. 98:299–318 (2000).

The shortfin mako, *Isurus oxyrinchus* Rafinesque, 1810, is a pelagic species with a circumglobal distribution in tropical and temperate seas (Garrick, 1967). It is frequently taken by commercial fisheries, mainly as bycatch of tuna and swordfish longlining, and is an important recreational species (e.g. Casey and Kohler, 1992; Pepperell, 1992). It is one of five species in the family Lamnidae comprising the genera *Isurus*, *Carcharodon*, and *Lamna* (Compagno, 1984). All lamnids are large, active pelagic sharks that regulate their body temperature (Carey et al., 1985; Goldman, 1997). Reproduction in lamnids is oophagous (Swenander, 1907; Lohberger, 1910; Bass et al., 1975; Gilmore, 1993; Francis, 1996).

Our knowledge of shortfin mako biology and reproductive parameters has increased considerably in the last 30 years. Garrick (1967) showed that the 12 nominal species of *Isurus* represent a single worldwide species, *I. oxyrinchus*; these findings were confirmed by Heist et al. (1996). Both males and females were thought to mature at around 1.8 m TL (Bigelow and Schroeder, 1948; Gubanov, 1978; Cailliet et al., 1983). With the collection of more extensive data it has become apparent that females mature at a much larger size than males (2.7–2.8 m; Pratt and Casey, 1983; Stevens, 1983; Cliff et al., 1990).

Our review of available reproductive data showed that female shortfin makos have similar reproductive characteristics in all regions. Based on a small number of mostly near-term litters, litter size is 4–16 in Australia (Stevens, 1983) and 9–14 in South Africa (Cliff et al., 1990). Litter sizes from other parts of the world are reported to be between 6 and 18, with the exception of a

litter of 25–30 from the Mediterranean Sea (Sanzo, 1912; Mollet et al.[1]). Pratt and Casey (1983) reported April parturition at a size of 65–75 cm TL in the western North Atlantic. Stevens (1983) and Cliff et al. (1990) suggested November parturition at about 70 cm TL in New South Wales and KwaZulu-Natal, respectively. The data presented by Gilmore (1993) showed no clear time of parturition, but investigation during the course of our study revealed several data errors (see Table 1). Cliff et al. (1990) proposed a 6- or 18-month gestation but indicated that 18 months appeared more feasible, based on a gestation of a little over 1 year postulated by Pratt and Casey (1983). Pratt and Casey (1983) reported first year growth rates of about 50 cm per year in the western North Atlantic, whereas Cailliet et al. (1983) suggested growth rates half as fast off California. Recent tagging results from California[2] and New Zealand (Saul and Holdsworth, 1992; Saul[3]) have shown that growth rates in the Pacific are similar to those reported for the Atlantic.[4] The size-frequency modes reported by Hanan et al. (1993) and O'Brian and Sunada (1994) confirmed high juvenile growth rates for California sharks.[4]

Currently there is growing concern over the extent of pelagic shark catches worldwide, both as targeted fishing and, particularly, as bycatch of high-seas longlining. Further attempts to manage resources of shortfin makos will require, among other demographic data,[4] information on reproductive parameters. Although this species is commonly caught in a variety of fisheries (Bonfil, 1994), few pregnant females have been documented and extensive biological data from a single location do not exist. Given all these factors and assuming reproductive synchronism of mating and gestation, spring parturition, and consistency in growth and size at birth of sharks from several widely spaced regions, we decided to combine all available information, adjusting for seasonal shifts between hemispheres. Our study documents the reproductive biology of female shortfin mako sharks from around the world.

[1] Mollet, H. F., A. D. Testi, L. J. V. Compagno, and M. P. Francis. 1999. Re-identification of a lamnid shark embryo. In review.

[2] Laughlin, L. 1997. California Department of Fish and Game, 330 Golden Shore, Long Beach, CA 90802. Personal commun.

[3] Saul, P. 1997. Blue Water Marine Research, RD 3, Whangarei New Zealand. Personal commun.

[4] Mollet, H. F., and G. M. Cailliet. 1997. Preliminary demographic analysis of the shortfin mako shark, *Isurus oxyrinchus*. Program and Abstract of the American Society of Ichthyologists and Herpetologists (ASIH) and American Elasmobranch Society (AES) Annual Meeting, University of Washington, Seattle WA, June 26–July 1, 1997, 336 p.

## Materials and methods

### Materials examined

Reproductive and morphometric data from 95 mature females, including 35 pregnant individuals (Table 1), together with data on 450 postnatal fish, including almost 200 age-0+ fish, were collected from around the world. Much of the data came from the western North Atlantic (largely unpublished, with the exception of data on three pregnant females), from eastern Australia (all unpublished, except four pregnant females reported by Stevens [1983]), and from KwaZulu-Natal, South Africa (either unpublished or providing substantially more detailed information than that reported by Cliff et al. [1990]). For methods of collection, measurement, and assessment of maturity see Pratt and Casey (1983); Stevens (1983); Cliff et al. (1990); and Stevens and McLoughlin (1991).

### Morphometrics

We used total length (TL, expressed in meters or cm) for our length measurement following Stevens (1983) and calculated TL of western North Atlantic and some South African sharks from the relationship with fork length (FL) (Casey and Kohler, 1992) or precaudal length (PCL) (Cliff et al., 1990), respectively. Total length of embryos, if not measured, was estimated from TL-FL ratios (1.156 at TL 60 cm; 1.203 at TL 35 cm) and the TL-PCL ratio (1.294 at TL 60 cm) of similar-size specimens.

We defined power regression as a linear $y$-on-$x$ regression of log-transformed data. We used Student residuals and leverage, an index of the leverage of each observation on the size of the mean square error, to carry out linear regression residual analyses (Wilkinson, 1986). We fitted power regressions to our mass-length data of females weighing more than 55 kg (TL=~2 m) from the western North Atlantic and the Southern Hemisphere (no maternal data were available from Brazilian litters) and reported back-transformed equations in the form $M$ (kg)=$a$ $TL^b$ (m). The prepower coefficient "$a$" predicts the mass of a 1-m-TL shortfin mako because we used meters as the unit of length in all such calculations (Mollet and Cailliet, 1996). We were interested only in possible mass differences of adolescent and mature females from different regions and chose 55 kg as the suitable minimum. A geometrical mean (GM) regression gives the correct functional relationship (Mollet and Cailliet, 1996), but we wanted to compare our results with previously reported back-transformed $y$-on-$x$ power regressions. An $F$-test and the linear interaction model were used to check for statisti-

**Table 1**

Summary of *Isurus oxyrinchus* litter data. SST = sea surface temperature. ECS = eggcases with single egg; NIA = not included in analysis; WY = without yolk (yolk-stomach punctured).

| No. | TL embryo[1] (cm) | Mass embryo[1] (kg) | Litter size | TL female (m) | Mass female (kg) | Capture date | Capture location | SST (°C) | References and comments |
|---|---|---|---|---|---|---|---|---|---|
| 1 | 0 (ECS) | | 11 | 2.92 | 236 | 19 Mar 87 | KwaZulu-Natal | 23.0 | This study; Cliff et al. (1990) |
| 2 | 0 (ECS) | | 14 | 2.88 | 217 | 10 Jun 86 | KwaZulu-Natal | 21.1 | This study; Cliff et al. (1990) |
| 3 | 2.6–3.3 (5) | | 9 | 3.09[2] | 270[3] | 9 Jan 93 | W. North Atlantic | | This study |
| 4 | 25–31 | | 18 | ~3.05 | 334 | 22 Aug 78 | DeSoto Canyon, FL | | Branstetter (1981); Gilmore (1993) |
| 5 | 29.5–39.5 | | 15 | 3.37[3] | 363 | 5 Dec 92 | Daytona Beach, FL | | Putz[6]; Colket[7]; this study |
| 6 | 36.1(1) | 0.80(1) | 25–30 | 3.85[3] | ~500 | ~Aug 1903 | Strait of Messina, Italy | | Sanzo (1912); Gilmore (1993); Mollet et al.[8]; this study |
| 7 | 34.8 mean | | 13 | 2.88[2] | 217[3] | late Jun 93 | Gulf of Guinea (1.5N, 1W) | 28.5 | Castro and Mejuto (1995) |
| 8 | 39.4 mean | 1.456 mean | 16(11F) | 3.37 | 380 | 15 Nov 84 | Okinawa Japan | | Uchida et al. (1987); Gilmore (1993, embryo TL range reported were means of L and R uterus) |
| 9 | | | 6 | 3.15[3] | ~270 | ~Apr 79 | New South Wales, Au | 18–21 | Stevens (1983) |
| 10 | ~41 NIA | | 18 | ~3.66(12') | 547 | 2 Mar 90 | Kona, HI | 27.8 | This study; Rizzuto[9]; Hodson[10] |
| 11 | 42.3–49.2 | | 12(6F) | | | 1 Apr 85 | Florida Straits | | Gilmore (1993), Putz[6] |
| 12 | 45.0–48.5 | 0.60–0.90(WY) | 12(8F) | 2.97[2] | 224[3] | 18 Sep 92 | S. Pacific (24S, 155E) | ~20 | This study |
| 13 | | | 9 | 2.84[4] | 195[3] | 10 Aug 81 | Port Edward, SA | 19.5 | Cliff et al. (1990) |
| 14 | ~50(1) | ~3.25(1) | | | | pre-1832 | Marseille, Med. Sea | | Vaillant (1889) |
| 15 | 49.5–53.0(2) | 1.63–2.30(2) | 12(6F) | 3.04[2] | 271 | 17 Aug 92 | S. Pacific (30S, 156E) | ~20 | This study |
| 16 | 50.4–54.0 | 1.435–2.370 | 15(5F,9M) | 3.25 | 313 | 15 Jan 92 | Puerto Rico | 26.3 | This study; Gilmore (1993, incorrect TL for mother and embryos) |
| 17 | 53.0–60.8 | | 14 | 2.77[4] | 180[3] | 10 Jul 84 | KwaZulu-Natal | 21.0 | Cliff et al. (1990) |
| 18 | 53.0–59.0 | | 12 | 3.31 | 337[3] | 13 Feb 94 | WNA, 20.4N, 73.5 W | | This study; Castro[11] |
| 19 | 59.0(1) | 3.53(1) | 5 | 2.69[2] | 165[3] | 24 Aug 92 | S. Pacific (30S, 160E) | ~20 | This study |
| 20 | 56.8–62.0 | 2.100–2.800 | 9(5F) | 3.34 | 284 | 27 Aug 97 | KwaZulu-Natal | 19.3 | This study |
| 21 | ~60 | | 4 | 3.11[3] | 259 | Sep 79 | New South Wales, Au | 18–21 | Stevens (1983); Gilmore (1993) |
| 22 | ~60 | | 14 | 3.39[3] | 340 | 4 Oct 80 | New South Wales, Au | 18–21 | Stevens (1983); Gilmore (1993) |
| 23 | 60 | fully developed | 6 | 2.63 | 153[3] | | Red Sea | | Gohar and Mazhar (1964) |

*Continued*

**Table 1 (continued)**

| No. | TL embryo[1] (cm) | Mass embryo[1] (kg) | Litter size | TL female (m) | Mass female (kg) | Capture date | Capture location | SST (°C) | References and comments |
|---|---|---|---|---|---|---|---|---|---|
| 24 | 60.5(1) | ~1.134(10) | 10 | 2.93[3] | 229 | 20 Feb 52 | Cat Cay, Bahamas | | Depperman[12]; Garrick (1967); Gilmore (1993, incorrect embryo TL); this study |
| 25 | 60.5(1) | | | | | 26 Mar 09 | Nagasaki, Japan | | Garrick (1967) |
| 26 | 58.2–64.0(5) | 1.42–1.72(5) | 16 | 2.80[3] | 186 | 28 Sep 80 | New South Wales, Au | 18–21 | Stevens (1983); Gilmore (1993) |
| 27 | 65.0(1) | | | | | 1971–73 | Atlantic (off NW Cuba) | | Guitart-Manday (1975) |
| 28 | 63.5–69.8 | | 10(5F) | | | | | | IGFA[13]; this study |
| NIA | | | 10 | | | | | | Gubanov (1978) |
| 29 | 64.5–70.4 | 1.84–2.49(13[5]) | 10(6F) | | | Oct 92 | S/SW Brazil | | Costa et al.[14]; this study |
| 30 | 64.6–70.7 | 2.300–3.125 | 13(6F) | 3.14[2] | 266[3] | 15 Aug 97 | S. Pacific 24.5S, 156.5E | 21.2 | This study |
| 31 | 66–70 | | 10 | | | | S. W. Indian Ocean | | Bass et al. (1975) |
| 32 | 65.5–73.8(15) | 2.30–2.84(15) | 16(9F, 6M) | | | Sep 94 | S/SW Brazil | | Costa et al.[15]; this study |
| 33 | 66.1–69.3(2) | | 14 | | | Oct 92 | S/SW Brazil | | Costa et al.[14]; this study |
| 34 | 71.2(1) | | | | | Oct 92 | S/SW Brazil | | Costa et al.[14]; this study |
| 35 | ~75 NIA | fully developed | 11 | | | late Jan 83? | Green Canyon, LA | | Branstetter[16]; this study |

[1] Number in parentheses gives number of embryos of litter investigated if not all were available;

[2] Estimated from $FL = 0.9286\ TL - 0.0171$ (Casey and Kohler, 1992);

[3] Estimated from $M = 7.658\ TL^{3.1}$ (Stevens, 1983), Southern Hemisphere, $M = 9.933\ FL^{3.1546}$ (Casey and Kohler, 1992), northern hemisphere;

[4] Used data given in Cliff et al. (1990) to calculate TL from PCL;

[5] Mass range of 3 litters with 10, 2, and 1 embryo (stored in same bag and weighed later).

[6] Putz, O. 1995. Grolmanstrasse 48, 10623 Berlin, Germany. Personal commun.

[7] Colket, T. 1996. 2020 Cordova Ave., Vero Beach, FL 32960. Personal commun.

[8] Mollet, H. F., A. D. Testi., L. J. V. Compagno, and M. P. Francis. 1999. Re-identification of a lamnid shark embryo. In review.

[9] Rizzuto, J. 1996. Kona mako the world's biggest? New Zealand Fishing News 19(7):22, 102.

[10] Hodson, G. 1996. Hustler Sportfishing, P.O. Box 4976, Kailua-Kona, HI 96755.

[11] Castro, J. 1998. NOAA/NMFS, SEFC, 75 Virginia Beach Dr., Miami, FL 33149. Personal commun.

[12] Depperman, B. 1953. Maternity mako model. Sports Afield, March 1953:86-7.

[13] International Game Fish Association (IGFA). 1979. Game Fish Yearbook, p. 138. 300 Gulf Stream Way, Dania Beach, FL 33004..

[14] Costa, F. E. S., F. M. S. Braga, A. F. Amorim, C. A. Arfelli. 1994. Analysis of mako sharks, *Isurus oxyrinchus*, from Santos longliners off South and Southeast Brazil. Program and Abstracts ASIH and AES Annual Meeting. USC Los Angeles, California, June 1994, 217 p. Dates from A. F. Amorim 1995. CPPM Santos, São Paulo-Brazil. Personal commun.

[15] Costa, F. E. S., F. M. S. Braga, A. F. Amorim, C. A. Arfelli. 1995. Reproductive biology of shortfin mako, *Isurus oxyrinchus*, Rafinesque 1809. Resumos VII Reunião do Grupo de Trabalho sobre Pesca e Pesquisa de Tubarões e Raias do Brasil, Rio Grande, November 20–24, 1995.

[16] Branstetter, S. 1996. NMFS Southeast Regional Office, 9721 Executive Center Dr. N., St. Petersburg, FL 33702. Personal commun.

cally significant differences between hemispheres (Neter and Wassermann, 1974). The condition factor ($CF$=*total mass*/$TL^3$, in units of kg/m$^3$) was used as a qualitative estimate of the size of the yolk-filled stomach in lamnid and alopiid embryos.

The calculation of gonadosomatic index (GSI) (ovary mass as percentage of total mass) and hematosomatic index (HSI) (liver mass as percentage of total mass) required a mass estimate if the shark was not weighed. For a few sharks only the mass was available and a TL estimate was required. We estimated mass or TL (from FL) of western North Atlantic and Southern Hemisphere sharks from the equations of Casey and Kohler (1992) and Stevens (1983), respectively. Only two dimensions (length and width) were available for the ovaries of western North Atlantic sharks and the mass had to be estimated. The estimates were calibrated with an ovary of dimensions 19.6×8.7 cm and mass of 0.630 kg (Fig. 2C in Stevens, 1983). The resulting GSI values proved to be comparable with those obtained from weighed ovaries of mature Southern Hemisphere sharks.

### Size at maturity

In the absence of embryos or egg cases, the maturity of nonpregnant females was determined from GSI, maximum ova diameter (MOD), oviducal gland diameter (measured in western North Atlantic specimens only), uterus width, and absence of a hymen. We fitted a logistical model $Y=[1+e^{-(a+bX)}]^{-1}$ to our binomial maturity data (immature=0, mature=1) of female specimens with TL > 2.0 m (Wilkinson, 1986; Welch and Foucher, 1988). Two meaningful parameters to characterize maturation, namely median TL-at-maturity ($MTL=-a/b$) and slope at MTL ($S=b/4$), can be expressed in terms of $a$ and $b$ as given. An $F$-test was used to check for statistically significant differences between hemispheres (Neter and Wassermann, 1974).

### Litters, gestation, and parturition

Data collected on litters included number of embryos , length and mass of embryos, maternal length and mass, capture date and location, and sea surface temperature (Table 1). Data for 21 litters, either not previously published or published with errors, are presented. We fitted a power regression to the litter size and maternal length data. For two recently fertilized South African fish, the number of uterine egg cases containing a single blastodisc ovum was assumed to be the litter size. The gestation period was estimated from seven litters from the western North Atlantic, one from the Gulf of Guinea, one from the Mediterranean Sea, two from Japan, seven from Australia, four from South Africa, and four from Brazil ($n$=26). The litters from Hawaii (no. 10 in Table 1) and the Gulf of Mexico (no. 35) were not included because of uncertain length data. We defined early-, mid-, and near-term litters as having embryo size between 0 to 20, 20 to 45, and 45 to 70 cm TL, respectively. Embryos of a term litter had TLs between 65–75 cm. Capture dates and TL estimates of 188 age-0+ fish from the western North Atlantic (extrapolations based on Fig. 3 in Pratt and Casey [1983] [$n$=45]), from California (Cailliet et al., 1983; Cailliet[5]) ($n$=16), and from New South Wales, Australia (Pepperell, 1992; Pepperell[6]) ($n$=119), and South Africa ($n$=8), were also considered in the estimation of size at birth and time of parturition.

Capture dates from Northern and Southern Hemisphere fish were combined on a single time scale based on seasons. For example, spring was defined as 21 March to 21 June in the north and from 23 September to 23 December in the south. Seasons were further divided into three periods of equal length to define the terms early, mid, and late (e.g. early spring in the north lasts from 21 March to 20 April).

To support the combination of Northern and Southern Hemisphere data for the shortfin mako, we examined sandtiger shark (*Carcharias taurus*) data from South Africa (Bass et al., 1975) and the eastern United States (Gilmore et al., 1983). These data were also used to support our use of a linear regression to estimate gestation and parturition from the slope of the embryo TL versus seasonal time regression, as well as size at birth. Bass et al. (1975) reported that 100-cm neonate sandtiger sharks were born from June through August after a gestation of 8–9 months. Gilmore et al. (1983) reported that 100-cm neonates were born from December through March after 9–12 months of gestation. We analyzed reported length-at-capture data by using a linear regression which yielded similar estimates for time of parturition and gestation period from intercept and slope:

South Africa: Jul.–Aug. parturition, 10 months gestation, $n$=27, $r^2$=0.93;
Eastern United States: Jan.–Feb. parturition, 8 months gestation, $n$=14, $r^2$=0.83;
Combined data: midwinter parturition, 9 months parturition, $n$=41, $r^2$=0.93.

[5] Cailliet, G. M. 1997. Moss Landing Marine Laboratory, PO Box 530, Moss Landing, CA 95039. Personal commun.

[6] Pepperell, J. G. 1997. Pepperell Research and Consulting Pty, PO Box 818, Caringbah, NSW 2229, Australia. Personal commun.

These results justified combining shortfin mako data from different regions and the use of a linear regression. Embryonic development may, however, deviate from a straight line and be more S-shaped; therefore a straight line may underestimate time of fertilization and overestimate parturition. These deviations cancel each other and a straight line still provides a good estimate of gestation.

### Reproductive cycle

We lacked sufficient numbers of females in all reproductive stages to determine the reproductive cycle from a stage-frequency distribution. For many litters, little or no maternal data were available, which precluded the use of a more rigorous multivariate statistical analysis in determining the reproductive cycle. We used temporal uterus width index data (UWI, uterus width as % of TL) of pregnant and postpartum females with a graphical comparison of 2- and 3-year reproductive cycles. The uterus of postpartum shortfin mako sharks shrinks after parturition. We chose the reproductive cycle compatible with this, given that our results suggested an extended gestation period of 15–18 months. For easier graphic interpretation, we plotted the 19 March (1988) Southern Hemisphere specimen a few days later. This procedure assured that the specimen appeared at the beginning of the gestation period (fall) on the far left-hand side of the temporal graphs. The use of polar coordinates did not provide a better presentation.

## Results

### Pregnant females and details of selected litters

There were 35 pregnant females on record (Table 1), with mean length of 3.1 m (range 2.63–3.85 m, $n$=24) and mass range of 153–547 kg. Capture dates ranged from pre-1832 (Vaillant, 1889; no. 14, Table 1) to 27 August 1997 (no. 20, Table 1). Capture locations were distributed worldwide and corresponding sea surface temperatures, where available, ranged from 18° to 28.5°C. Detailed information was available for six females, three in very early pregnancy and three with well-developed embryos (Table 2).

Two recently fertilized South African sharks of 2.92 and 2.88 m were caught in late summer and late fall of 1987 and 1986 (nos. 1 and 2 in Tables 1 and 2, respectively). A 3.09-m female was caught near Puerto Rico in January (early winter) with a litter of nine early-term embryos (no. 3 in Tables 1 and 2). The 2.6–3.3 cm embryos, each still inside an egg case, had external gills and a large yolk sac (Fig. 1A). The size of the yolk sac was estimated from Fig. 1A to be 0.9 × 0.6 cm, assuming the embryo in the center of the figure was 3.0 cm. There were over 40 nutritive egg cases in each uterus (Fig. 1B).

A 3.25-m female with a near-term litter was caught in the same month and location (January and Puerto Rico, respectively) by a commercial swordfish longliner (no. 16 in Table 1, no. 4 in Table 2). This female carried 15 embryos of around 52 cm, each with a similarly large yolk-filled stomach (Fig. 1C). No uterine compartments were observed and no egg cases remained in the uterus. A 3.34-m female shark stranded on the beach at Umhlanga, South Africa, in late winter (no. 20 in Table 1; no. 5 in Table 2). This female carried a litter comprising nine embryos of about 60 cm. Emerging adultlike teeth were present in both jaws of the embryo examined. The stomachs of four embryos that were cut open had no shed teeth but had large amounts of yolk (Fig. 1D). No uterine compartments were observed and no egg cases remained in the uterus. About one liter of clear, viscous fluid (not seawater) was found in each uterus but was not analyzed. A Japanese longliner caught a 3.14-m female in the southern Pacific in midwinter (no. 30 in Table 1, no. 6 in Table 2). The 13 full-term embryos had a length of about 69 cm and a total mass of 36.8 kg, 14% of the estimated maternal mass of 266 kg. The embryo stomachs were slightly distended and contained small but variable amounts of yolk.

### Litter size

The majority of the litters examined for this study were near-term. The mean number of embryos per litter (litter size) was 12.5 (range: 4 to 27.5, $n$=30). The largest litter comprised 25–30 embryos (we used 27.5 in our calculations) in a female caught in the Mediterranean Sea in about August of 1903 (Sanzo, 1912). The capture date was inferred from the observation that it occurred during a long holiday period (summer) at the University of Messina.[7] A summer date agrees with the dates of the traditional swordfish fishery, in which this shark was probably caught.[8] One of these embryos was described by Sanzo (1912) as being a great white shark, *Carcharodon carcharias*, but a recent re-examination has shown it to be a shortfin mako shark.[1] The male to female ratio of 10 litters was 57:68 and is not significantly different from 1:1 (pooled $\chi^2$=0.80, Yates corrected, $P$=0.37).

[7] Notarbartolo di Sciara, G. 1997. Instituto Centrale per la Ricerca Applicata al Mare (ICRAM), via di Casalotti 300, 00166 Rome, Italy. Personal commun.

[8] Fergusson, I. 1998. The Shark Trust, 36 Kingfisher Court, Hambridge Road, Newbury, UK RG14 5SJ. Personal commun.

**Table 2**

Details for pregnant *Isurus oxyrinchus*. (1–3) Females in very early pregnancy with blastodisc and nutritive egg cases. Observations appear in proposed chronological order. (4–6) Females with well-developed embryos. (L=left; R=right.) GSI = gonadosomatic index; HSI = hematosomatic index.

| No. | TL (m) | Date | Location | Observations |
|---|---|---|---|---|
| 1 | 2.92 | 19 Mar. 1987 | KwaZulu-Natal | 6(L)+5(R) egg cases with single egg; no blastodisc observed; 4(L)+8(R) nutritive egg cases with numerous burst eggs; capsule being formed in left oviducal gland; GSI = 1.13%, HSI = 10.6%; mating bites. |
| 2 | 2.88 | 10 June 1986 | KwaZulu-Natal | 7(L)+7(R) egg cases with single egg (some blastodisc); 12(L+R) nutritive egg cases with up to 14 eggs of 4 mm diameter; several ova being encapsulated in right oviducal gland; GSI = 1.21%, HSI = 10.3%; mating bites. |
| 3 | 3.09 | 9 Jan. 1993 | Puerto Rico | 7(L) empty egg cases; 4(L) blastodisc egg cases at least, with one embryo each (~3.0 cm TL, badly disintegrated when measured); 5(R) blastodisc egg cases (3×10 cm) with one embryo each (2.6, 2.9, 3.0, 3.0, & 3.3 cm TL); 43(L) + 42(R) nutritive egg cases (3×5 cm) with 16–20 eggs per capsule, 7–9 g each capsule, 334 g total (R); 2(L) egg cases in lower oviduct; GSI ~5% (estimate from ovary dimensions 44×27 cm). |
| 4 | 3.25 | 15 Jan. 1992 | Puerto Rico | 7(L) embryos (1 female, 5 males, and 1 lost), 51.0–54.0 cm, 1.660–2.300 kg; 8(R) embryos (4 females), 50.5–53.8 cm, 1.435–2.370 kg; mean length and mass of 14 embryos 52.0 cm (SE 0.4) and 2.000 kg (SE 0.071); uteri dimensions 103×22 cm (L), 111×22 cm (R); GSI ~0.3% (estimate from ovary dimensions 27×9 cm), spent ovary. |
| 5 | 3.34 | 27 Aug. 1997 | KwaZulu-Natal | 9(L+R) embryos (5 females), 56.8–62.0 cm (mean 59.9 cm, SE 0.6), 2.100–2.800 kg (mean 2.416 kg, SE 0.094); embryo stomachs with 551–846 g yolk, 26.2–32.0% of total embryo mass ($n$=4); embryo livers 75-110 g, HSI range 3.4–4.1% ($n$=4); GSI = 0.185% (spent ovary), HSI = 2.465%. |
| 6 | 3.14 | 15 Aug. 1997 | South Pacific | 13 (L+R) embryos (6 females), 64.6–70.7 cm (mean 68.8 cm, SE 0.5); 2.300–3.125 kg (mean 2.830 kg, SD 0.062); embryo stomachs with 73–478 g yolk, 2.6–15.3% of embryo mass; embryo spiral valve with 68–88 g yolk, 2.4–3.3% of embryo mass (mean 2.9%); embryo livers 146–234 g, HSI range 5.2–8.0% (mean 7.0%, SE 0.2); GSI and HSI of female not available. |

Litter size (LS) increased with maternal TL according to

$$LS=0.810\ TL^{2.346} \qquad (n=24,\ P=0.013,\ r^2=0.25)$$

and fell within the band of a model calculation ($LS$=(0.26 to 0.46) $TL^{3.10}$). The model was derived from the maternal mass-length relationship ($M$= 7.658 $TL^{3.10}$; Stevens, 1983) by postulating that the litter mass is a constant fraction of the pregnant female mass (10–15%, based on available data) and by using an estimate of the embryo mass at birth (2.5–3.0 kg, based on available data). The power regression was still significant ($P$=0.029) if the smallest litter of four (an outlier) and the largest litter of 27.5 were excluded.

There were no significant differences between the mean litter size of Northern (14.0, $n$=13) and Southern Hemisphere females (11.1, $n$=17, ANOVA, $P$=0.09) or between western North Atlantic (12.8, $n$=8) and Southern Hemisphere females (ANOVA, $P$=0.28).

## Indicators of sexual maturity

The size of reproductive organs increased as the shortfin mako approached maturity (Fig. 2). A logarithmic scale was necessary to present the large GSI range between 0.00044% and ~5.0% (Fig. 2A), reflecting ovaries weighing less than 10 g in immature sharks smaller than 2.4 m, up to an estimated 11.3–13.5 kg in a female in early pregnancy (no. 3 in Table 2). There was considerable overlap in the GSI of adolescent females (range: 0.005–0.28%, $n$=28) and that of mature, nonpregnant females with inactive ovaries (range: 0.08–0.81%, $n$=38) or pregnant females with near-term embryos and spent ovaries (GSI=0.185% and ~0.3%, $n$=2). The GSI (1.1%) of recently fertilized females with egg cases and the GSI (~5%) of the female with the 3-cm embryos were the largest observed (Fig. 2A).

Oocytes of noticeable size (1 mm) appeared in maturing females larger than 2.4 m (Fig. 2B). The MOD of immature fish ranged from 1.0 to 4.0 mm

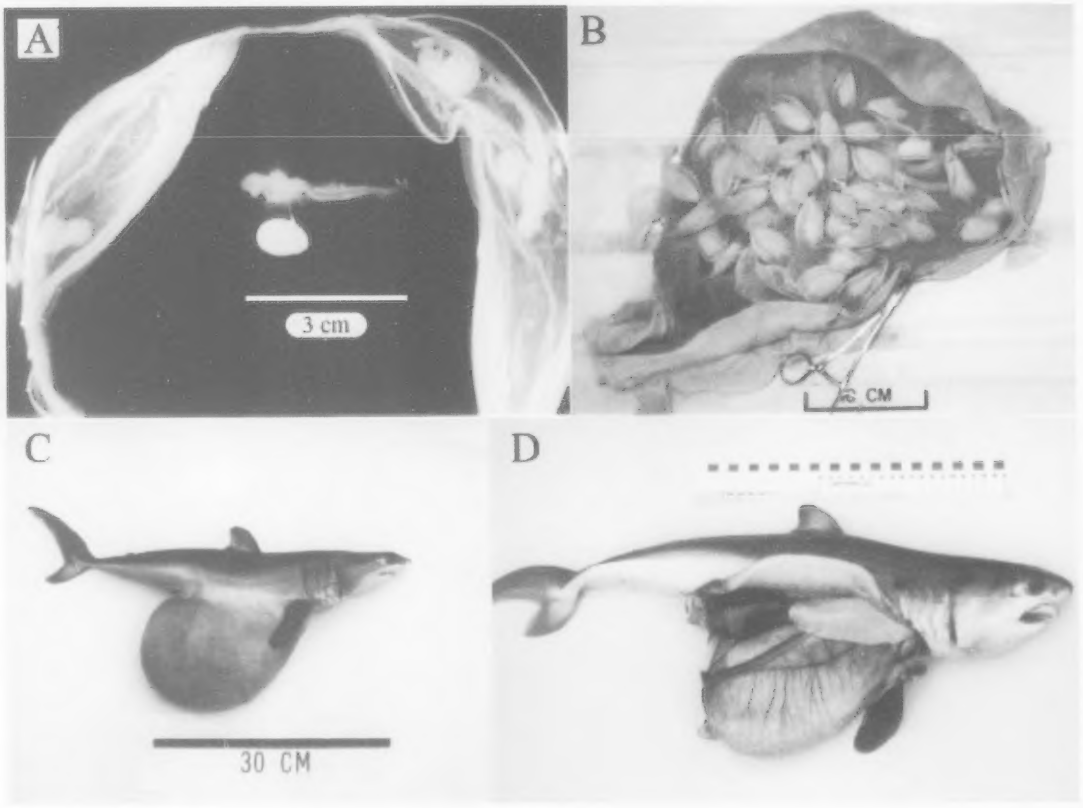


**Figure 1**

*Isurus oxyrinchus* embryos and egg cases. (**A**) 3-cm-TL embryos with external gills, large yolk sac, and still within the egg cases from right uterus of pregnant female (no. 3 in Tables 1 and 2). Embryo in the center was removed from egg case. (**B**) Right uterus containing 42 nutritive egg cases from female with embryos shown in A. Scale bar, 10 cm (**C**) Embryo from a litter of 15 with mean TL=52.0 cm and mean mass=2.000 kg with large yolk stomach of estimated dimensions 19 × 12 cm (no. 16 in Table 1). (**D**) Embryo from a litter of 9 (mean TL=59.9 cm, mean mass=2.426 kg, mean yolk mass=29.1%, mean HSI=3.7%) dissected to show yolk stomach, spiral valve, and right liver lobe. Upper jaw cartilage is visible and emerging adultlike teeth are present in both jaws (no. 20 in Table 1). Scale bar, 30 cm.

($n$=17) and overlapped considerably with that in mature sharks which had a range of 1–8 mm ($n$=26). The blastodisc ova appeared to be 6–8 mm in diameter, given the MOD of 8 mm and the estimated spherical diameter of 7 mm of the yolk sac of a 3-cm embryo (Fig. 2B). Nutritive eggs appeared to have a slightly smaller diameter at 4–6 mm. This diameter was based on a MOD of 6 mm for the female in early pregnancy (Fig. 2B) and on the 4-mm ova found in the uteri of two fertilized South African females (Table 2). A spent ovary in a female with large embryos also contained 6-mm ova (Fig. 2B).

The oviducal gland remained undeveloped until the onset of maturity and then increased rapidly in diameter in females of 2.7–3.0 m, as they matured (Fig. 2C, western North Atlantic specimens only). The range in immature fish was from 0.1 to 1.1 cm ($n$=32). There was considerable overlap in the diameter of the adolescent oviducal gland, ranging from 2.5 to 4.7 cm ($n$=11) and in the diameter of mature females, ranging from 2.3 to 5.1 cm ($n$=19). The oviducal gland diameter of two pregnant females, one with early-term, the other with near-term embryos, were similar (4.9 and 4.2 mm, respectively) to that of nonpregnant mature females.

Uterus width provided the best indication of maturity. There was little overlap between immature females in the range of 0.3–6.5 cm (mean 1.6, SE=0.2,

$n$=58) and mature females in the range of 5.0–22.7 cm (mean 10.7, SE 0.7, $n$=44) (Fig. 2D). The uterus widths of pregnant (with egg cases or embryos) and nonpregnant females overlapped.

The HSI of immature and mature females in the TL range of 0.73–3.66 m varied from 1.2 to 17.9% and the overall mean HSI of 6.7% (SE=0.25%, $n$=161) was a little lower than the HSI of near-term embryos (see below). The large HSI range of immature females (1.2–17.6%, $n$=125) was almost the same as that of mature females (2.5–17.9%, $n$=36).

### Gestation and parturition

The capture of two females with litters containing 3.0- and 52-cm embryos (Table 2, nos. 3 and 4) in the same month (January) and location (Puerto Rico) suggested that gestation is longer than one year. Assuming a gestation in excess of 12 months, the mean embryo length for 26 litters and the length for 188 age-0+ fish from both the Northern and Southern Hemisphere were graphed against season of capture (Fig. 3A). Based on the three females caught in early pregnancy (Table 2), ovulation takes place in fall. Parturition occurs in late winter to mid-spring at ca. 70 cm. The length-at-capture data of the age-0+ fish indicated a smooth continuation of the growth rate evident *in utero*.

The relationship between embryo length and time of capture of all western North Atlantic litters ($n$=7, slope=3.7 cm/month, SE=0.6 cm/mo., $P$=0.002, $r^2$=0.87) predicted a gestation of 19 months. The combined Northern Hemisphere data, which include five mid-term litters, yielded a gestation of 20 months ($n$=11, slope=3.4 cm/month, SE=0.05 cm/mo., $P$<0.001, $r^2$=0.84).

There were no mid-term litters from the Southern Hemisphere. If the two females with recently fer-

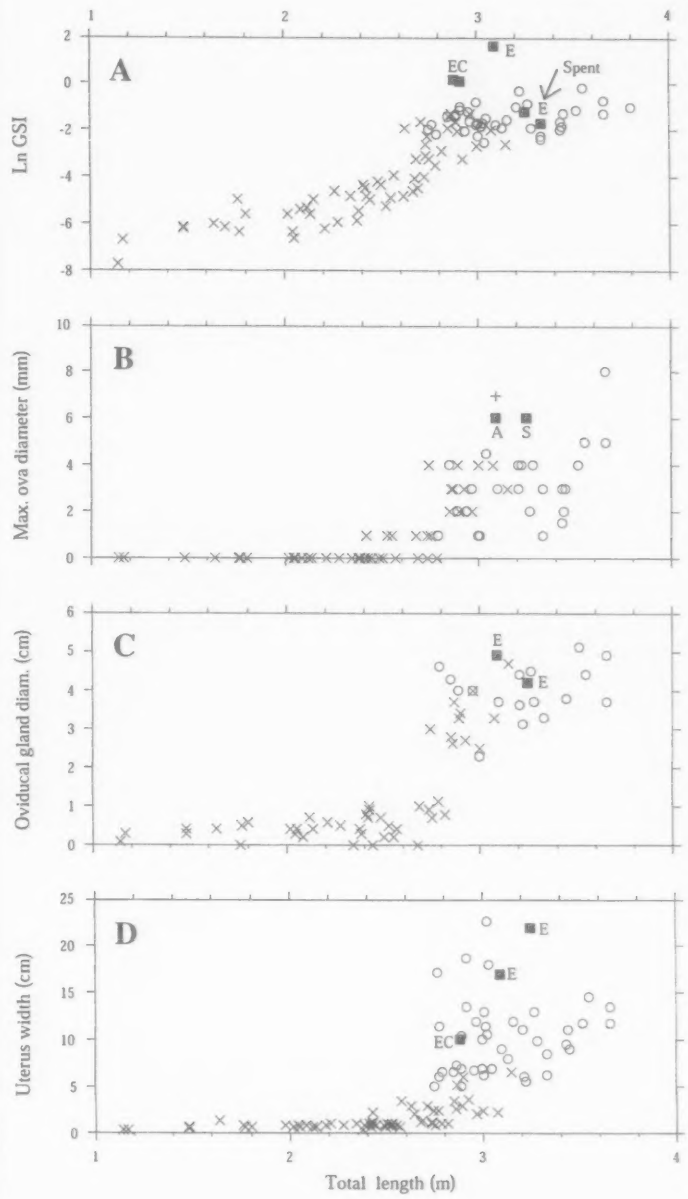


**Figure 2**

The relationships between four reproductive parameters and length of female *Isurus oxyrinchus*. (**A**) Natural logarithm (Ln) of gonadosomatic index (GSI) was used. (**B**) Maximum ova diameter. Lack of, or very small oocytes, are indicated by 0 diameter. A = female with active ovary and 3-cm-TL embryos; + = diameter of yolk sac of 3-cm-TL embryo; S = female with spent ovary and 52-cm-TL embryos. (**C**) Oviducal gland diameter of western North Atlantic specimens. (**D**) Uterus width. (■ = pregnant; ○ = mature, not pregnant; × = immature and adolescent; E=embryos present; EC=egg cases with single ovum present.)

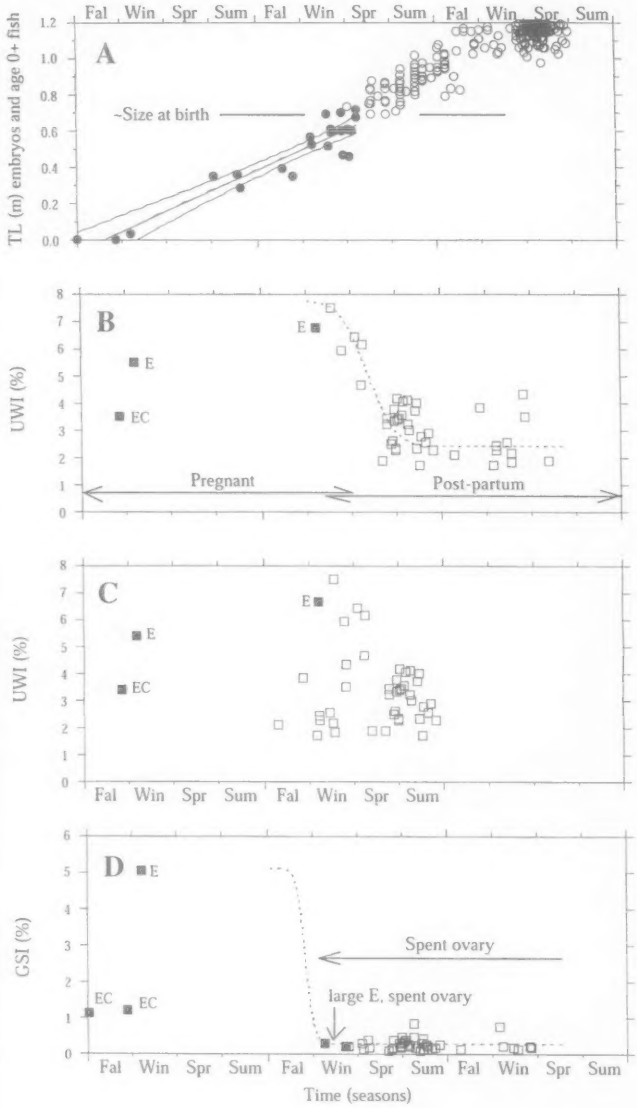


**Figure 3**

Gestation, parturition, and reproductive cycle of *Isurus oxyrinchus*. (**A**) The relationships between length of embryos and age-0+ fish, and time of capture. Regression with 95% confidence band for the line of combined embryo data from Northern and Southern Hemispheres is shown. ●=embryos; ○=age-0+ fish. (**B**) Temporal uterus width index (UWI) of mature females based on a 3-year reproductive cycle. The dotted line was fitted to the data by eye. (**C**) Temporal UWI of mature females based on a 2-year reproductive cycle. (**D**) Temporal gonadosomatic index (GSI) based on a 3-year reproductive cycle. The dotted line shows suggested decrease of GSI during last third of gestation. (■=pregnant; □=mature, not pregnant; E=embryos present; EC=egg cases with single ovum present).

ova (Table 2, nos. 1 and 2) are more than one year apart from the near-term litters (on the basis of the Northern Hemisphere data), the regression predicted a 19-mo. gestation period ($n$=15, slope=3.7 cm/mo., SE=0.3 cm/mo., $P$<0.001, $r^2$=0.92). It is also possible to fit these data with a regression that predicts a 6.7-mo. gestation period ($n$=15, slope=10.4 cm/mo., SE=1.8 cm/mo., $P$<0.001, $n$=15, $r^2$=0.73).

The intercept and slope of Northern and Southern Hemisphere regressions, assuming a gestation longer than 12 months, were not significantly different ($P$=0.8 and 0.7, respectively) and the combined regression was

$$\textit{Embryo TL}\ (\text{cm}) = 3.71\ (\text{SE}=0.27)T,\quad (P<0.001,\ r^2=0.89\ n=26)$$

where $T$ = the number of months since midfall.

It predicted a gestation period of 15–24 months (19 for the line) with 70 cm for the size-at-birth (Fig. 3A). However, we suggest the shorter estimate is more realistic because parturition appears to be a little earlier than what was indicated by the regression. The GM regression line (not shown) was slightly steeper than the $y$-on-$x$ regression and predicted a gestation of 17.8 months. The GM regression reflects the functional relationship better because of the uncertainties of several dates. Therefore, we concluded that the best estimate for the gestation is 15–18 months. When the three early-term litters with fairly high leverage (L=0.2–0.35) were excluded, the gestation was still around 18 months based on a significant regression ($P$=0.001) with a slope of 3.8 cm/month (SE= 0.6, $n$=23).

## Reproductive cycle

A three-year reproductive cycle provided the best fit to the temporal UWI data. UWI increased in early-term females and reached a maximum of 7–8% at parturition (Fig. 3B). The pregnant female with the 52-cm embryos and UWI of 6.8% would be expected to give birth

about 3–4 months later and have a UWI around 7% at that time. The UWI decreased in postpartum females over a 6 month period to values around 2–4% (Fig. 3B, curve fitted by eye). With a 2-year cycle, UWI showed no decreasing pattern for postpartum females and low UWI values between 2% and 4% extended over almost the entire second year of the reproductive cycle (Fig. 3C). This result would suggest aseasonal parturition; however, this conclusion is in conflict with the observed seasonal parturition indicated by Figure 3A.

The GSI was not as useful in determining the length of the reproductive cycle because it decreased during pregnancy. Recently ovulated females had a GSI of 1.1% and an early-term female had an estimated GSI of about 5% (Fig. 3D). We suggest that the GSI remains high until the embryos are about 40–50 cm long, and then decreases (Fig. 3D, curve fitted by eye). Two females with large embryos (mean: 52.0 and 59.9 cm) had low GSIs of ~0.3% and 0.185%, respectively, indicating that ovulation had ceased (spent ovary). The GSI during at least the last quarter of gestation (i.e. ≥4 months) was similar to that of postpartum females (mean: 0.26%, SE=0.03%, $n$=38). When we tried to fit the GSI data with a 2-year cycle, we found that data for six postpartum females caught in winter (five from South Africa) overlapped with those for the two pregnant females with large embryos. This would extend parturition into fall and would conflict with convincing seasonal parturition data (Fig. 3A).

The remaining reproductive parameters were not helpful in determining the reproductive cycle. No temporal pattern was evident for MOD. Oviducal gland diameters were available mostly for summer captures only and possible temporal changes could not be investigated. There was no clear temporal pattern in the HSI because we had few data for preovulating and early-term pregnant females.

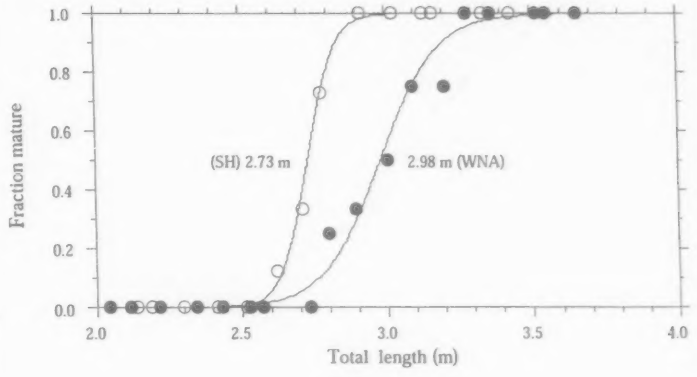


**Figure 4**

The relationships between maturity and length of female *Isurus oxyrinchus* from the western North Atlantic and the Southern Hemisphere. A logistical model was fitted to the binomial maturity data (0=immature, 1=mature). Mean TL and mean fraction mature of 10-cm-TL ranges (instead of individual data points) were plotted for clarity. Estimated TLs when 50% are mature (MTL) are included. ● = western North Atlantic ($n$=61); ○ = Southern Hemisphere ($n$=82).

## Regional differences

The scarcity of data precluded a meaningful statistical comparison of many reproductive parameters for female shortfin makos from different regions. However, we were able to substantiate differences for mass and length-at-maturity for females from the western North Atlantic and the Southern Hemisphere (South Africa and Australia; no data were available from Brazil).

Western North Atlantic females were significantly heavier by 19–66 kg or 16–19% than Southern Hemisphere females ($P$<0.001 in TL range 2.5–3.5 m). The latter data were combined because the power regressions for South African ($n$=47) and Australian females ($n$=22) were not statistically different ($P$=0.164, $F^* < F$ (0.95,2,65)). The back-transformed M-TL relationships were

$M$=7.299 $TL^{3.224}$ ($n$=63, $r^2$=0.94, western North Atlantic females 2.0–3.7 m TL);

$M$=6.824 $TL^{3.137}$ ($n$=69, $r^2$=0.90, Southern Hemisphere females 2.0–3.4 m TL).

The median TL-at-maturity (MTL) of 61 western North Atlantic females (2.98 m, SE=0.045) was significantly larger by 25 cm ($P$<0.001, $F^* >> F$ (0.95,2,147), than that of 82 Southern Hemisphere females (2.73 m, SE=0.02 m) (Fig. 4). The data from South Africa and Australia were combined because MTL in South Africa was only 11 cm smaller than MTL in Australia and the length of these fish was not measured consistently. The maturation size of western North Atlantic sharks extended from 2.76 m, when 10% were mature, to 3.20 m when 90% were mature and was 16–35 cm larger than that in the Southern Hemisphere, where the range was 2.60–2.85 m. The largest immature female from the western

North Atlantic (3.15 m) was a virgin. The smallest mature female from the Southern Hemisphere of 2.63 m was pregnant (no. 23 in Table 1).

### Liver-, yolk-, and total mass of embryos

There was a significant positive relation between the HSI and the length of near-term embryos, rising from 3.8% in a litter with a mean length size of 59.9 cm to 7.0% in a litter with a mean length size of 68.8 cm. The slope was 0.34%/cm (SE=0.04%/cm, $P<0.001$, $r^2=0.83$, $n=17$). The TL range of the embryos in these two litters was small (12.5 cm) but they covered almost 50% of the HSI range. The increasing HSI was accompanied by a corresponding decrease in the amount of yolk in the stomach from 29.1% to 10.9% of total mass. The yolk percentage versus TL regression was significant with slope –1.64%/cm (SE= 0.33%/cm, $P<0.001$, $r^2=0.62$, $n=17$).

The mass-length relationship of embryos is complicated owing to the highly variable mass of the yolk-filled stomach. The scarce data indicated that the yolk mass amounts to 60–70% of total mass for mid-term litters and then decreases to around 10% in a full-term litter (Fig. 5, *y*-axis on left). When the mass of the yolk-filled stomach was subtracted from the total mass, a power regression could be fitted to net embryo mass ($M_{net}$) (Fig. 5, *y*-axis on right). The back-transformed equation was

$$M_{net}=8.198\ TL^{3.117}$$

($n=21$, $r^2=0.98$, TL range= 0.36–0.71 m).

The mass of the smallest free-swimming fish agreed with the predicted mass based on the extrapolated curve beyond the upper limit of the embryo data (Fig. 5). The corresponding condition factors of shortfin mako embryos ($CF_{net}=M_{net}/TL^3$) were between 7.3 and 7.9 kg/m$^3$ and were similar to postnatal values. If the mass of the yolk-filled stomach was included, the condition factor ($CF=M/TL^3$) reached values as large as 26 kg/m$^3$ when the embryos were mid-term and had the largest yolk stomachs (Fig. 6, *I. oxyrinchus* data).

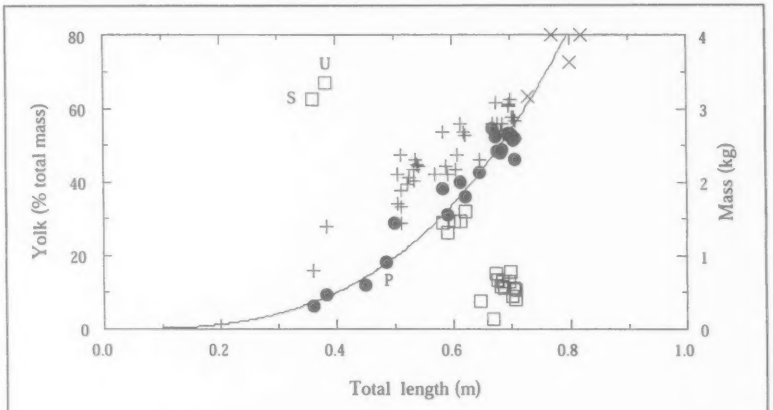


**Figure 5**

The relationships between 1) yolk % (left *y*-axis), 2) embryo mass with and without yolk (right *y*-axis), and length of *Isurus oxyrinchus* embryos. A power regression was fitted to embryo mass without yolk data. □=yolk %; ●=embryo mass without yolk; + = embryo mass with yolk; ×=mass of free swimmers; S = Sanzo (1912); U = Uchida et al. (1987); remaining data from this study including P = upper and lower limit of mass range of litter with punctured yolk-stomachs.

## Discussion

### Embryonic development

Our data documented early and late embryonic development of the shortfin mako. As expected, it was similar to that reported for other lamnids (Swenander, 1907; Lohberger, 1910; Otake, 1990; Gilmore, 1993; Francis and Stevens, 2000) in which the embryos hatch at about 6 cm TL and then feed on nutritive eggs (oophagy) until the beginning of the last third of the gestation period. Embryonic nutrition may also include egg jelly absorbed through the external gill filaments in the prehatching phase and uterine milk in the posthatching phase (Hamlett, et al. 1985; Gilmore, 1993; Koob and Straus, 1998).

After mating, the largest of the relatively small ova are ovulated, fertilized, and packaged into egg cases (one blastodisc ovum per egg case) as evident in three cases in our study (Table 2). The diameter of these blastodisc ova appears to be slightly larger (~7 mm) than the nutritive ova (4–6 mm) and the ova remaining in the ovary (4–6 mm); this larger diameter may also apply to other lamnids and lamnoids. Mating may stimulate the enlargement of the largest ova in the ovary and trigger subsequent ovulation. The capsules with nutritive ova are formed after the blastodisc ova have been encapsulated. Blastodisc egg cases with only one fairly large ovum were observed in the bigeye thresher shark, *Alopias superciliosus* (Moreno and Morón, 1992). In

the sandtiger shark, the blastodisc capsules contain up to 14 blastodisc ova, but only one egg develops and absorbed material and other encapsulated ova contribute more to initial development than does the yolk sac (Gilmore et al., 1983). A possible early-term great white shark had a total of 192 egg cases of three types of different size and mass in the left uterus, but the size and number of the ova were not reported (Uchida et al., 1987).

We observed 3-cm-TL shortfin mako embryos still attached to a relatively large yolk sac and inside egg cases (Fig. 1A). It is not clear at what size the embryos hatch from the egg cases, possibly 5–6 cm, the size at which porbeagle (*Lamna nasus*) and sandtiger sharks hatch (Swenander, 1907; Gilmore et al., 1983). This estimate agrees with an estimate of the embryo TL calculated from the diameter of the blastodisc ovum (Mollet, unpubl. data). Bigeye thresher embryos hatch at a slightly larger size (7–8 cm FL) because their yolk sac diameter (11 mm) is greater than that of porbeage and sandtiger sharks (Chen et al., 1997).

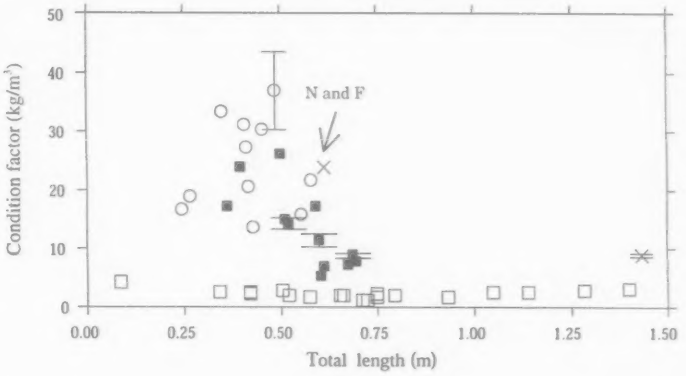


**Figure 6**

The relationship between condition factor ($M/TL^3$) and TL of lamnid and alopiid embryos. Error bars give ±2 SE of mean, if available. ■ = *Isurus oxyrinchus*; ○ = *Lamna spp.*; × =*Carcharodon carcharias*; □ = *Alopias spp.* See Table 1 for sources of *I. oxyrinchus* data. *Lamna* spp. data from Lohberger (1910); Templeman (1963); Otake (1990); Francis;[9] Otake[10]. *Carcharodon carcharias* data from Norman and Fraser (1938, NandF); combined Francis (1996) and Uchida et al. (1996). *Alopias* spp. data from Joseph (1954); Cadenat (1956); Gubanov (1972); Hixon (1979); Gilmore (1983); Moreno and Morón (1992); Otake (1990).

During the oophagous embryonic phase, lamnids develop huge yolk-filled stomachs, sandtiger sharks develop large yolk-filled stomachs, and alopiids develop only slightly extended yolk-filled stomachs according to photographs and our calculated condition factors (Nakamura, 1935; Gilmore et al., 1983; Moreno and Morón, 1992; our Fig. 6 for lamnids and alopiids). The condition factors of the shortfin mako (our data and references in Table 1), the porbeagle (Templeman, 1963; Francis[9]), the salmon shark, *Lamna ditropis* (Lohberger, 1910; Otake, 1990), and the great white shark (Norman and Fraser, 1938) reach a maximum between 20 and 35 $kg/m^3$ when the embryos are midterm. The condition factor decreases in the last third of gestation and approaches values similar to those of postnatal lamnids (our data for the shortfin mako; Francis and Stevens (2000) for the porbeagle; Uchida et al., 1996; Francis, 1996 for the great white shark). The yolk-stomach in the sandtiger shark reaches its largest size between 33.4 and 80 cm TL, but no embryo masses were reported by Gilmore et al. (1983) and therefore the condition factor could not be calculated. The condition factors of thresher shark embryos are much smaller if TL rather than PCL is used as the length parameter. However, if the alopiids were to develop a large yolk-filled stomach, then the condition factor of mid-term embryos would be considerably larger compared with that of early- and near-term embryos, which is not the case (Fig. 6). The embryonic development of alopiids proceeds at a steady rate without development of a large yolk-filled stomach and we expect ovulation of nutritive ova right up to parturition. Francis and Stevens (2000) have suggested that the puzzling gross abdominal distention observed in porbeagle embryos (and other lamnids) is energetically inefficient for the pregnant female.

The HSIs of shortfin mako embryos from a full-term litter were between 5% and 8 % and the yolk-stomach constituted 3–15% of body mass. These combined nutrient reserves may provide neonates with nutrition while they improve their hunting ability. From the metabolic rate of a shortfin mako pup reported by Graham et al. (1990) (1.5% of bodymass/d), we estimated that a 20% reserve would enable pups to survive for about 20–30 days. This

[9] Francis, M. P. 1997. National Institute of Water and Atmospheric Research (NIWA), P.O. Box 14-901, Wellington, New Zealand. Personal commun.

[10] Otake, T. 1998. Mie University, 1515 Kamihama, Tsu, Mie 514, Japan. Personal commun.

estimate agrees with the observation that a sandtiger pup born in captivity at Sea World of Orlando did not eat until 25 d after birth (Gilmore et al., 1983). By comparison, HSI values of 13–19% were recorded in three great white shark full-term embryos with stomach yolk mass between 0% and 4% (Francis, 1996; Uchida et al., 1996). A near-term 97-cm-TL longfin mako, *Isurus paucus*, embryo had a large liver but surprisingly small amounts of yolk in the cardiac stomach (0.54%) (Gilmore, 1983).

There is no convincing evidence[11] to confirm that older shortfin mako embryos eat smaller ones while in the uterus, as claimed by Tricas et al. (1997). They possibly inferred this conclusion from a misleading statement in Compagno (1988, p. 83).[12] Costa et al.[13] suggested that uterine cannibalism occurs on the basis of a piece of lower jaw found in the stomach of a term embryo. This behavior is difficult to explain, and Francis (1996) observed only shed teeth in the stomach of a great white shark full-term embryo. We expected to but did not find any shed teeth in the stomach of near-term embryos. Embryonic cannibalism has only been documented in the sandtiger shark (Gilmore et al., 1983) and seems unlikely in the shortfin mako with a litter size as high as 25–30.

### Litter size

Data on litter size of shortfin makos were scarce and possibly biased by low values due to abortion during capture and the reported large value of 25–30 in Sanzo (1912). The lowest values of 4–6 were for near-term litters (TL~60 cm) reported anecdotally by game fishermen. Although we are sure they are reliable, they should be taken as minimum estimates because such low values suggest abortion during capture, especially for near-term litters. Abortion is unlikely for mid-term embryos with their huge yolk stomachs.[11] A means model test was not conclusive because litter size also depends on maternal size, which was not available for five near-term litters. The number of embryos in the Sanzo (1912) litter was also based on information from a fisherman; however, a study of the original Italian text has suggested that the value of 25–30 is reliable.[7] Although western North Atlantic females are slightly heavier than females of similar size from South Africa and Australia, there were no regional differences in litter size between the two regions.

The mean litter size of 12.5 is larger than that for other lamnids, although data for some species are scarce. The longfin mako has a mean litter size of four (range 2–8, $n$=3, Compagno, 1984; Killam and Parsons, 1986; Casey[14]). The mean litter size of the great white shark is 8.9 (range: 4–14, $n$=11; Francis, 1996; Uchida et al., 1996). A single litter of four was reported for the salmon shark (Otake, 1990). The litter size of the porbeagle is 2–5, mostly 4 (e.g. Swenander, 1907; Templeman, 1963; Francis and Stevens, 2000). A weak relationship between litter size and maternal length in the shortfin mako also exists for the great white shark (based on data in Francis, 1996). A positive relation between litter size and maternal size has been observed for many carcharhinids (Compagno, 1988).

### Indicators of sexual maturity

The GSI was not conclusive in determining sexual maturity in lamnids because near-term and postpartum females both have low values. In oophagous sharks the ovary continues production to nourish the embryos well into gestation, thus producing high GSIs. The large variations in ovary size in mature shortfin makos (0.2–12 kg; GSI ~0.1–5.0%) were as expected. Data from other lamnids are scarce. A longfin mako with near-term embryos had a spent ovary with GSI=0.46% (Gilmore, 1983). Active ovaries in mid-term porbeagles weighed 2.75 kg (GSI 2.35%) and 6.3 kg (GSI 3.6%) (Francis and Stevens, 2000; Swenander, 1907). Arfelli and de Amorim[15] observed a 12-kg ovary (GSI 0.48%) in a nonpregnant 5.3-m-TL great white shark.

We found that MOD was not useful for determining maturity in shortfin makos, whereas it is in sharks without oophagy (e.g. Pratt, 1979; Peres and Vooren, 1991; Parsons, 1993). The values near the upper limit of the observed range (1–8 mm, Fig. 2B) were similar to values (5–11 mm) reported for other lamnids (Swenander, 1907; Gilmore, 1983; Bruce,

[11] Gilmore, R. G. 1999. Dynamic Corp., Kennedy Space Center, FL 32899. Personal commun.

[12] Compagno, L. V. C. 1998 and 1999. Shark Research Centre, P.O. Box 61, 8000 Cape Town, South Africa. Personal commun.

[13] Costa, F. E. S., F. M. S. Braga, A. F. Amorim, and C. A. Arfelli. 1995. Reproductive biology of shortfin mako, *Isurus oxyrinchus*, Rafinesque 1809. Resumos VII Reunião do Grupo de Trabalho sobre Pesca e Pesquisa de Tubarões e Raias do Brasil. Rio Grande, November 20–24, 1995. Fundacao Universidade do Rio Grance, FURG Rio Grande, RS Brasil.

[14] Casey, J. 1986. Distribution of the longfin mako (*Isurus paucus*) in the northwest Atlantic. Program and Abstracts ASIH and AES Annual Meeting, Victoria BC, Canada, 15–21 June 1986, no page numbers.

[15] Arfelli, C. A., and A. F. de Amorim. 1993. Notes on the white shark (*Carcharodon carcharias*) caught off Cananéia, São Paulo-Brazil. Program and Abstracts ASIH and AES Annual Meeting. The University of Texas at Austin, 27 May–2 June 1993, 348 p.

1992; Francis and Stevens, 2000) and lamnoids (Matthews, 1950; Gilmore et al., 1983; Chen et al., 1997; Yano et al., 1999). The report of a 50-mm diameter egg in the ovary of a 3.37-m-TL shortfin mako with an empty uterus (Applegate, 1966) is inexplicable.

Uterus width was the most suitable reproductive parameter for distinguishing between immature and mature female shortfin makos and also between different reproductive stages of mature females. Our data indicated that immature shortfin mako have UWIs between 0.17% and 2.1%, whereas mature shortfin makos have UWIs between 1.7% and 7.5%, with the largest values occurring at parturition and in early postpartum females (Fig. 3B). Little comparative data for other lamnids were available. Two immature great white sharks of 4.8 m and 4.9 m had a UWI of 2.1% and 1.6%, respectively.[12, 16] A 5.2-m-TL great white shark had a UWI of 7.7%; this fish may have recently given birth (Stevens, unpubl. data). However, a 5.2-m, 1520 kg female reported by Bruce (1992) to be mature, and bearing possible mating scars had UWIs of only 0.88–1.0% (left) and 0.44–0.56% (right); these values appear to be far too small for a mature shark of this size.

Our study failed to confirm the potential of HSI as a good indicator of reproductive status. Our sample size was large (immature, $n$=125; mature, $n$=35); however, we had few data for pregnant fish. Cliff et al. (1990) observed the highest HSIs in two recently fertilized females, which also had high GSIs. Their observations suggested that HSI might be useful as an indicator of reproductive status; however, their sample size was small ($n$=12). They also noted that the HSIs of males were just as variable and covered about the same range (2.9–13.7%). For sharks with long gestation period, the HSI may not be tied closely to the reproductive cycle. Because the shortfin mako has a high metabolic rate (Graham et al., 1990), reserves in the liver cannot be expected to last longer than a few weeks.

### Gestation period

A small number of early and mid-term litters from the western North Atlantic and the Northern Hemisphere supported a gestation period in excess of 12 months. By contrast, the absence of measured mid-term litters from the Southern Hemisphere made it possible also to fit the data with a 6–7 month gestation period. It is highly unlikely that a regional difference of this magnitude could exist in a widely distributed species such as the shortfin mako. It is therefore most probable that the duration of gestation is 15–18 months in both hemispheres.

Is a 6–7 month gestation possible for the Northern Hemisphere? Reproductive asynchrony (where individuals in an accessory population are out of phase with the principal population) is a possibility for wide-ranging oceanic sharks, and was suggested for the great white shark (Lineaweaver and Backus, 1970). For our shortfin mako data, we would have to propose that the early-term (no. 3 in Table 1) and all five mid-term litters (nos. 4–8) belong to the accessory population(s). However, the gestation period becomes indeterminate when these litters are excluded from the calculations. It is far more probable that these pregnant females belong to the principal populations, should this theory apply to the shortfin mako, and that the gestation period is 15–18 months. Additional data would be needed to test the hypothesis of reproductive asynchrony for elasmobranchs.

No embryo length data were available for an early fall litter from the Southern Hemisphere (no. 9 in Table 1). If the gestation period were 6–7 months, this litter would have been at the blastodisc stage (as were litters no. 1 and no. 2 in Table 2) and might have been overlooked without detailed examination of the uterus. If the gestation period was 18 months, the embryos of this litter would have been 35–45 cm long and would have been observed (as they were) during gutting of the pregnant fish on the boat.

Body temperature may account for some of the difference in the gestation between the shortfin mako (15–18 months) and the porbeagle (9 months in both hemispheres; Francis and Stevens, 2000). The porbeagle and the salmon shark possess a sizable kidney rete, which is not found in the shortfin mako, and body temperatures are in general higher in *Lamna* than in *Isurus*.[17] Cloacal temperature measurements from 21 salmon sharks had a mean of 23.3°C (SD=1.1°) which is probably most representative of the uterus area.[17] This temperature could be 5°C higher than the temperature of the uterus in the shortfin mako, which prefers water temperatures around 18°C and is known for vertical movements into colder water (Casey and Kohler, 1992; Carey and Scharold 1990; Holts and Bedford, 1993).

Our litter of 3.0-cm-TL embryos confirmed slow shortfin mako embryonic development, at least during the early stage. These very early-term embryos were found next to more than 40 nutritive egg cases in each uterus (Fig. 1B, Table 2). Gilmore (1993) reported that

[16] Bruce, B. 1998. CSIRO Marine Research, P.O. Box 1538, Hobart, Tasmania 7001. Personal commun.

[17] Goldman, K. 1998. Virginia Institute of Marine Science (VIMS), P.O. Box 1346, Gloucester Pt., VA 23062. Personal commun.

production of empty and blastodisc egg cases preceded that of nutritive egg cases in the sandtiger shark and that each oviducal gland produced one egg case per day. We observed that blastodisc egg cases preceded the nutritive egg cases in the shortfin mako (no. 2 in Table 2). Therefore, the 2.7–3.3 cm TL embryos would be about 40–50 days old. They were at a very early stage of development because the yolk sac was almost intact, and oophagy may not begin until the embryos are about 3–4 months old and 5–6 cm long.

The gestation period of the shortfin mako is about twice as long as that of the sandtiger shark (9 months; Cliff, unpubl. data), which has a term litter mass (13 kg), about half that of the shortfin mako (25–40 kg). Scant ovary data for the shortfin mako and extensive ovary data for the sandtiger shark (Gilmore et al., 1983; Cliff, unpubl. data) suggested that the masses of ovulating ovaries are similar in the two species. The shortfin mako would therefore require about twice as long to nourish a litter double the weight of that of the sandtiger shark.

Our interpretation of reported great white shark data suggested that the gestation is longer than one year and probably similar to that of the shortfin mako. Parturition is in late spring (Klimley, 1985; Francis, 1996; Uchida et al., 1996). Uchida et al. (1987; 1996) suggested that a 5.55-m-TL, 1970-kg female captured in mid-February had aborted an entire litter of near-term embryos. However, the presence of almost 200 egg cases in the left uterus (weighing 9 kg) and the robust appearance of the specimen, probably due to a large liver, suggest that this great white shark was at an early stage of gestation. Further support for our gestation estimate of about 18 months was the capture of a great white shark with a midterm litter of nine embryos in the summer of 1934 (Norman and Fraser, 1938). Length and mass of these embryos (61 cm TL, 5.4 kg as suggested by Ellis and McCosker, 1991) were as expected for midterm embryos with a large yolk-filled stomach ($M/TL^3$=23.8 kg/m$^3$, Fig. 6) and birth was expected 9 months later in spring.

Gestation periods longer than 12 months were reported for the whitetip reef shark, *Triaenodon obesus* (13.5 mo.), the tiger shark, *Galeocerdo cuvier* (13–16 and 15–16 mo.), the dusky shark, *Carcharhinus obscurus* (22 mo.), and the spiny dogfish, *Squalus acanthias* (18–24 mo.) (Compagno, 1984; Uchida et al., 1990; Randall, 1992; Musick et al., 1993; Crow[18]). The basking shark, *Cetorhinus maximus,* probably has a gestation period longer than 12 months, but we agree with Pauly[19] that the reported gestation period of 3.5 years by Parker and Stott (1965) was based on fallacious reasoning.

### Parturition in Northern and Southern Hemispheres

Based on a few full-term litters and a large number of neonates, parturition occurred mainly in late winter to midspring in both hemispheres (Fig. 3A). Pratt and Casey (1983) reported "late spring parturition" in the western North Atlantic, but April should be called early spring; and the data in their Figure 3 suggest that parturition begins as early as late February (late winter). Other large pelagic and nearshore sharks have seasonal parturition in late spring to early summer in both hemispheres (e.g. Bass et al., 1973; Pratt, 1979; Klimley, 1985; Randall, 1992; Musick et al., 1993; Francis, 1996; Crow[18]). Parturition of the porbeagle peaks in June–July in both hemispheres which Francis and Stevens (2000) found puzzling.

### Reproductive cycle and resting period

Given a gestation period of about 18 months and a distinct seasonal spring parturition, the reproductive cycle for shortfin makos is either 2 or 3 years. There were insufficient data to determine its duration conclusively, but a 2-year cycle would only allow a recovery period of some 6 months, which would appear to be insufficient. Our temporal UWI data (Fig. 3B) support a 3-year reproductive cycle, which would mean an 18-month resting period.

There is conflicting evidence about the need for a resting period after parturition in elasmobranchs. For many medium to large sharks a resting period has been documented. Peres and Vooren (1991) reported a 3-year reproductive cycle for the soupfin shark, *Galeorhinus galeus,* off southern Brazil with a gestation of 12 months. The gestation for the whitetip reef shark is 13.5 months and the reproductive cycle is 2 or 3 years (Uchida et al., 1990). Musick et al. (1993) suggested that the sandbar shark, *Carcharhinus plumbeus* (with one-year gestation), must have a resting period of at least one year, requiring a 2-year reproductive cycle. The 2-year reproductive cycle for the sandtiger shark with 8–9 mo. gestation period is well documented (Branstetter and Musick, 1994; Cliff, unpubl. data). Tagging and cap-

[18] Crow, G. L. 1995. The reproductive biology of the tiger shark, *Galeocerdo cuvier*, in Hawaii: a compilation of historical and contemporary data. Program and Abstract ASIH and AES Annual Meeting, University of Alberta, Edmonton, Alberta, Canada, June 15–19 1995, 229 p.

[19] Pauly, D. 1978. A critique of some literature data on the growth, reproduction and mortalities of the lamnid shark *Cetorhinus maximus* (Gunnerus). Report to the Pelagic Fisheries Commission, International Council for the Exploration of the Seas, CM 1978/H17, Copenhagen.

tive grow-out studies indicated that the nurse shark *Ginglymostoma cirratum* has a 2-year reproductive cycle with a 3.5–4.5 months gestation and a ~20 months resting period.[20] A 3-yr reproductive cycle was proposed for the dusky shark and the tiger shark with 22-mo. and 15–16 mo. gestation periods, respectively (Musicke et al., 1993; Crow[18]). Francis and Stevens (2000) reported that gestation in the porbeagle lasts 9 months, which would allow for only a very short resting period if they have pups every year. Francis (1996) suggested that the great white shark might have little or no resting period because mating was observed immediately after parturition.

In the 3-year cycle of the shortfin mako, mating could occur either after parturition, which would require sperm storage, or after the resting period and before ovulation. Two recently fertilized shortfin makos from South Africa caught in March and June had fresh mating scars, suggesting mating takes place in late summer–fall before ovulation. It may be selectively advantageous for mating to occur in summer–fall prior to ovulation when the females appear to be in a different geographical area, rather than after parturition in spring of the previous year near the pupping grounds, because both sexes may be feeding actively at that time.

There was an uneven distribution of reproductive stages in our shortfin mako data. Pre-ovulating and early to mid-term pregnant females were poorly represented. Casey and Kohler (1992) suggested that adult females remain far offshore in more tropical waters. We propose that this suggestion applies particularly to pre-ovulating females ready to be mated and early to midterm females. Because the shortfin mako prefers 18°C water (Casey and Kohler, 1992), these females are likely to be found in deeper water and are less likely to be caught.

### Regional differences

The studies of Garrick (1967) and Heist et al. (1996) have suggested that there is only one circumglobal species of shortfin mako, *Isurus oxyrinchus*. Despite this conclusion, we found that there were significant differences in the median TL-at-maturity of females and in their mass-length relationship between the Northern and Southern Hemispheres. Small regional differences in size at maturity have been reported for a number of other elasmobranch species, including widely distributed species such as the sandbar shark (Last and Stevens, 1994), scalloped hammerhead shark, *Sphyrna lewini* (Branstetter, 1987; Chen et al., 1990), soupfin shark (Peres and Vooren, 1991), and dusky shark, *Carcharhinus obscurus* (Natanson and Kohler, 1996). Our estimates of the duration of gestation and reproductive cycle are unlikely to be greatly affected by these differences.

Determining reproductive parameters for the large, wide-ranging and oceanic shortfin mako proved difficult. A dedicated sampling program conducted throughout the year within a particular region may still not provide the necessary data. We believe our approach of combining scarce data from widely spaced localities was justified.

[20] Carrier, J. C., and H. L. Pratt. 1998. Albion College, 4705 Kellogg Ctr., Albion, MI 49224. Unpubl. data.

## Acknowledgments

The data collected by Abner Kingman as an observer on a swordfish longliner proved to be very useful. We are most grateful to Malcolm P. Francis and Ken J. Goldman for many suggestions and for data on porbeagles and salmon sharks. We thank Fabio E. S. Costa and Alberto F. Amorim for litter data from Brazil, David W. Welch for help with the statistical analysis, Nancy E. Kohler for providing HSI data, Dave B. Holts for the California drift gillnet fishery data, and Gregor M. Cailliet for reviewing the manuscript. A large number of people provided data and useful suggestions, and we acknowledge Shelton P. Applegate, Steven Branstetter, Barry D. Bruce, José I. Castro, Tris Colket; Leonard J. V. Compagno; Gerald L. Crow; David A. Ebert, Ian K. Fergusson, R. Grant Gilmore and Oliver Putz, William C. Hamlett, Glen Hodson, Leanne Laughlin, Robert N. Lea, Jean R. C. de Marignac, Sanford A. and Barbara Moss, John A. Musick, Gavin J. P. Naylor, Giuseppe Notarbartolo di Sciara, Tsuguo Otake, Daniel Pauly, Julian G. Pepperell, John E. Randall, Peter Saul, Jeffrey A. Seigel, Colin A. Simpfendorfer, Antonio D. Testi, and Senzo Uchida. GC wishes to thank his colleagues at the Natal Sharks Board for assistance in providing and examining specimens. HFM wishes to thank Cherilyn Chin, Juan E. Ezcurra, Scott R. Greenwald, John B. O'Sullivan, and Gilbert Van Dykhuizen at the Monterey Bay Aquarium for help and support. Anne L. Mollet proofread the manuscript. Comments by four anonymous and two NMFS reviewers helped us to focus and strengthen our findings.

## Literature cited

**Applegate, S. P.**
**1966.** A possible record-sized bonito shark, *Isurus oxyrinchus* Rafinesque, from Southern California. Calif. Fish Game 52:204–207.

**Bass, A. J., J. D. D'Aubrey, and N. Kistnasamy.**
**1973.** Sharks of the east coast of southern Africa. I. The genus *Carcharhinus* (Carcharhinidae). Oceanogr. Res. Inst. Invest. Rep. 33:1–168.
**1975.** Sharks of the east coast of southern Africa. IV. The families Odontaspididae, Scapanorhynchidae, Isuridae, Cetorhinidae, Alopiidae, Orectolobidae and Rhiniodontidae. Oceanogr. Res. Inst. Invest. Rep. 39:1–102.

**Bigelow, H. B., and W. C. Schroeder.**
**1948.** Part 1: sharks. *In* Fishes of the western North Atlantic, p. 59–546. Sears Foundation for Marine Research, Yale Univ.

**Bonfil, R.**
**1994.** Overview of world elasmobranch fisheries. FAO Fisheries Technical Paper 341:1–119.

**Branstetter, S.**
**1981.** Biological notes on the sharks of the north central Gulf of Mexico. Contribb. Mar. Sci. 24:13–34.
**1987.** Age, growth and reproductive biology of the silky shark, *Carcharhinus falciformis*, and the scalloped hammerhead, *Sphyrna lewini*, from the northwestern Gulf of Mexico. Env. Biol. Fish. 19:161–173.

**Branstetter, S., and J. A. Musick.**
**1994.** Age and growth estimates for the sandtiger in the northwestern Atlantic Ocean. Trans. Am. Fish. Soc. 123: 242–254.

**Bruce, B. D.**
**1992.** Preliminary observation on the biology of the white shark, *Carcharodon carcharias*, in South Australian waters. *In* Sharks: biology and fisheries (J. G. Pepperell, ed.), p. 1–11. Aust. J. Mar. Freshwater Res. 43.

**Cadenat, J.**
**1956.** Note d'ichthyologie ouest-africaine. Vol. XV: Sur un requin-renard nouveau pour la faune d'afrique occidentale francaise *Alopius superciliosus* (Lowe) 1840? Bull. Inst. Fr. Afr. Noire 18A:1257–1266.

**Cailliet, G. M., L. K. Martin, J. T. Harvey, D. Kusher, and B. A. Weldon.**
**1983.** Preliminary studies on the age and growth of the blue shark, *Prionace glauca*, common thresher, *Alopias vulpinus*, and shortfin mako, *Isurus oxyrinchus*, from California waters. *In* Proceedings of the international workshop on age determination of oceanic pelagic fishes: tunas, billfishes, and sharks (E. D. Prince and L. M. Pulos, eds.), p. 179–188. U. S. Dep. Commer., NOAA Tech. Rep. NMFS 8.

**Carey, F. G., J. G. Casey, H. L. Pratt, D. Urquhart, and J. E. McCosker.**
**1985.** Temperature, heat production and heat exchange in the lamnid sharks. Memo. S. Cal. Acad. Sci. 9:92–108.

**Carey, F. G., and J. V. Scharold.**
**1990.** Movements of blue sharks (*Prionace glauca*) in depth and course. Mar. Biol. 106:329–342.

**Casey, J. G., and N. E. Kohler.**
**1992.** Tagging studies on the shortfin mako shark (*Isurus oxyrinchus*) in the western North Atlantic. *In* Sharks: biology and fisheries (J. G. Pepperell, ed.), p. 45–60. Aust. J. Mar. Freshwater Res. 43.

**Castro, J. A., and J. Mejuto.**
**1995.** Reproductive parameters of blue shark, *Prionace glauca*, and other sharks in the Gulf of Guinea. Mar. Freshwater Res. 46:967–73.

**Chen, C. T., T. C. Leu, S. J. Joung, and N. C. H. Lo.**
**1990.** Age and growth of the scalloped hammerhead, *Sphyrna lewini*, in northeastern Taiwan waters. Pac. Sci. 44: 156–170.

**Chen C. T., K. M. Liu, and Y. C. Chang.**
**1997.** Reproductive biology of the bigeye thresher shark, *Alopias superciliosus* (Lowe, 1839) (Chondrichthyes: Alopiidae), in the northwestern Pacific. Ichthyological Research 44:227–235.

**Cliff, G., S. F. J. Dudley, and B. Davis.**
**1990.** Sharks caught in the protective gill nets off Natal, South Africa. 3. The shortfin mako, *Isurus oxyrinchus* (Rafinesque). S. Afr. J. Mar. Sci. 9:115–126.

**Compagno, L. J. V.**
**1984.** FAO species catalogue: sharks of the world. An annotated and illustrated catalogue of shark species known to date. FAO Fisheries Synopsis (125), vol. 4, part 1: Hexanchiformes to Lamniformes, 249 p. FAO, Rome.
**1988.** Sharks of the order Carcharhiniformes. Princeton Univ. Press, Princeton, NJ, 467 p.

**Ellis, R., and J. E. McCosker.**
**1991.** Great white shark. Harper Collins Publishers, New York NY, 270 p.

**Francis, M. P.**
**1996.** Observations on a pregnant white shark with a review of reproductive biology. *In* Great white sharks: the biology of *Carcharodon carcharias* (A. P. Klimley and D. G. Ainley, eds.), p. 157–172. Academic Press, San Diego CA.

**Francis, M. P., and J. D. Stevens.**
**2000.** Reproduction, embryonic development, and growth of the porbeagle shark, *Lamna nasus*, in the Southwest Pacific Ocean. Fish. Bull. 98(1):41–63.

**Garrick, J. A. F.**
**1967.** Revision of sharks of genus *Isurus* with description of a new species (Galeoidea, Lamnidae). Proc. U. S. Nat. Mus. 118:663–694.

**Gilmore, R. G.**
**1983.** Observation on the embryos of the longfin mako, *Isurus paucus*, and the bigeye thresher, *Alopias superciliosus*. Copeia 1983:375–382.
**1993.** Reproductive biology of lamnoid sharks. Env. Biol. Fish. 38:95–114.

**Gilmore, R. G., J. W. Dodrill, and P. A. Linley.**
**1983.** Reproduction and embryonic development of the sandtiger shark, *Odontaspis taurus* (Rafinesque). Fish. Bull. 81:201–225.

**Gohar, H. A. F., and F. M. Mazhar.**
**1964.** The elasmobranchs of the north-western Red Sea. Publ. Mar. Biol. Stat. Al-Ghardaqa (Red Sea) No. 13:1–144.

**Goldman, K. J.**
**1997.** Regulation of body temperature in the white shark, *Carcharodon carcharias*. J. Comp. Physiol. B 167:423–429.

**Graham, J. B., H. Dewar, N. C. Lai, W. R. Lowell, and S. M. Arce.**
**1990.** Aspects of shark swimming performance determined using a large water tunnel. J. Exp. Biol. 151:175–192.

**Gubanov, Ye. P.**
**1972.** On the biology of thresher shark (*Alopias vulpinus*) in the North-west Indian Ocean. J. Ichthyol. 12:591–600.
**1978.** The reproduction of some species of pelagic sharks from the equatorial zone of the Indian ocean. J. Ichthyol. 18:781–792.

**Guitart-Manday, D.**
**1975.** Las pesquerías pelágico-oceánicas de corte radio de acción en la región noroccidental de Cuba [Short-range marine pelagic fishing of northeast Cuba]. Seria Oceanologica, Oceanographic Institute Academy of Sciences of

Cuba 31, p. 3–26. [Translated for the National Science Foundation and the US Department of Commerce, NOAA, NMFS by the Agence Tunisiennes de Public-Relations, Tunis.]

**Hamlett, W. C., D. J. Allen, M. D. Stribling, F. J. Schwartz, and L. J. A. DiDio.**
**1985.** Permeability of external gill filaments in the embryonic shark. Electron microscopic observations using horseradish peroxidase as a macromolecular tracer. J. Submicrosc. Cytol. 17:31–40.

**Hanan, D. A., D. B. Holts, and A. L. Coan Jr.**
**1993.** The California drift gill net fishery for shark and swordfish 1981–82 through 1990–91. Fish. Bull. 175: 1–93.

**Heist, E. J., J. A. Musick, and J. E. Graves.**
**1996.** Genetic population structure of the shortfin mako (*Isurus oxyrinchus*) inferred from restriction fragment length polymorphism analysis of mitochondrial DNA. Can. J. Fish. Aquat. Sci. 53:583–538.

**Hixon, M. A.**
**1979.** Term fetuses from a large common thresher shark, *Alopias vulpinus*. Calif. Fish Game 65:191–2.

**Holts, D. B., and D. W. Bedford.**
**1993.** Horizontal and vertical movements of the shortfin mako shark, *Isurus oxyrinchus*, in the Southern California Bight. Aust. J. Mar. Freshwater Res. 44:501–509.

**Joseph, D. C.**
**1954.** A record-size thresher from Southern California. Calif. Fish Game 40:433–435.

**Killam, K., and G. Parsons.**
**1986.** First record off the longfin mako, *Isurus paucus*, in the Gulf of Mexico. Fish. Bull. 84:748–749.

**Klimley, A. P.**
**1985.** The areal distribution and autoecology of the white shark, *Carcharodon carcharias*, off the west coast of North America. Mem. S. Cal. Acad. Sci. 9:15–40.

**Koob, T. J., and J. W. Straus.**
**1998.** On the role of egg jelly in *Raja erinacea* egg capsule. Bull. Mt. Desert Island Biol. Lab. 37:117–119.

**Last, P. R., and J. D. Stevens.**
**1994.** Sharks and rays of Australia. Commonwealth Scientific and Industrial Research Organization (CSIRO), Australia, 513 p. + 84 color plates.

**Lineaweaver, T. H., and R. H. Backus.**
**1970.** The natural history of sharks. 1984 reprint, Nick Lyons Books/Schocken Books, New York, NY, 256 p.

**Lohberger, J.**
**1910.** Über zwei riesige Embryonen von *Lamna*. Abh. K. Bayer. Akad. Wiss. IV. Suppl. Bd. 2:1–45.

**Matthews, L. H.**
**1950.** Reproduction in the basking shark, *Cetorhinus maximus*, (Gunnerus). Phil. Trans. B. Royal Soc. Lond. 234: 247–316.

**Mollet, H. F., and G. M. Cailliet.**
**1996.** Using allometry to predict body mass from linear measurements of the white shark. *In* Great white sharks: the biology of *Carcharodon carcharias* (A. P. Klimley and D. G. Ainley, eds.), p. 81–89. Academic Press, San Diego CA.

**Moreno, J. A., and J. Morón.**
**1992.** Reproductive biology of the bigeye thresher shark, *Alopias superciliosus* (Lowe, 1839). *In* Sharks: biology and fisheries (J. G. Pepperell, ed.), p. 77–86. Aust. J. Mar. Freshwater Res. 43.

**Musick, J. A., S. Branstetter, and J. A. Colvocoresses.**
**1993.** Trends in shark abundance from 1974 to 1991 for the Chesapeake Bight region of the U.S. mid-Atlantic coast. *In* Conservation biology of elasmobranchs (S. Branstetter, ed.), p. 1–19. U.S. Dep. Commer., NOAA Tech. Rep. NMFS 115.

**Nakamura, H.**
**1935.** On the two species of the thresher shark from Formosan waters. Mem. Fac. Sci. Agric. Taihoku Imp. Univ. 14:1–6.

**Natanson, L. J., and N. E. Kohler.**
**1996.** A preliminary estimate of age and growth of the dusky shark *Carcharhinus obscurus* from the south-west Indian Ocean, with comparison to the western North Atlantic population. S. Afr. J. Mar. Sci. 17:217–224.

**Neter, J., and W. Wassermann.**
**1974.** Applied linear statistical models. Richard D. Irwin Inc., Homewood, IL, 842 p.

**Norman, J. R., and F. C. Fraser.**
**1938.** Giant fishes, whales and dolphins. W. W. Norton and Company Inc., New York, NY, 361 p.

**O'Brian, J. W., and J. S. Sunada.**
**1994.** A review of the southern California experimental drift longline fishery for sharks, 1988–1991. CalCOFI Rep. 35: 222–229.

**Otake, T.**
**1990.** Classification of reproductive modes in sharks with comments on female reproductive tissues and structures. *In* Elasmobranchs as living resources: advances in the biology, ecology, systematics and the status of fisheries (H. L. Pratt, S. H. Gruber, T. Taniuchi, eds.), p. 113–130. U.S. Dep. Commer., NOAA Tech. Rep. NMFS 90.

**Parker, H. W., and F. C. Stott.**
**1965.** Age, size, and vertebral calcification in the basking shark *Cetorhinus maximus* (Gunnerus). Zool. Meded. (Leiden) 40:305–319.

**Parsons, G. R.**
**1993.** Geographic variation in the reproduction between two populations of the bonnethead shark, *Sphyrna tiburo*. Env. Biol. Fish. 38:25–35.

**Pepperell, J. G.**
**1992.** Trends in the distribution, species composition and size of sharks caught by gamefish anglers off South-eastern Australia, 1961–90. *In* Sharks: biology and fisheries (J. G. Pepperell, ed.), p. 213–225. Aust. J. Mar. Freshwater Res. 43.

**Peres, M. B., and C. M. Vooren.**
**1991.** Sexual development, reproductive cycle, and fecundity of the school shark *Galeorhinus galeus* off southern Brazil. Fish. Bull. 89:655–667.

**Pratt, H. L., Jr.**
**1979.** Reproduction in the blue shark, *Prionace glauca*. Fish. Bull. 77:445–70.

**Pratt, H. L., Jr., and J. G. Casey.**
**1983.** Age and growth of the shortfin mako, *Isurus oxyrinchus*, using four methods. Can. J. Fish. Aquat. Sci. 40:1944–1957.

**Randall, J. E.**
**1992.** Review of the biology of the tiger shark (*Galeocerdo cuvier*). *In* Sharks: biology and fisheries (J. G. Pepperell, ed.), p. 21–31. Aust. J. Mar. Freshwater Res. 43.

**Sanzo, L.**
**1912.** Embrione di *Carcharodon Rondeletii* M. Hle. (?) con particolare disposizione del sacco vitellino. Regio Comitato Talassografico Italiano, Memoria XI:1–12.

**Saul, P., and J. Holdsworth.**
**1992.** Cooperative gamefish tagging in New Zealand waters 1975–90. New Zealand Fisheries Technical Report No. 33, 24 p.

**Stevens, J. D.**
**1983.** Observations on reproduction in the shortfin mako *Isurus oxyrinchus*. Copeia 1983:126–130.

**Stevens, J. D., and K. J. McLoughlin.**
**1991.** Distribution, size and sex composition, reproductive biology, and diet of sharks from Northern Australia. Aust. J. Mar. Freshwater Res. 42:151–199.

**Swenander, G.**
**1907.** Über die Ernäherung des Embryos der *Lamna cornubica*. Zoologiske Studier Tollagnade Tullberg Uppsala 1907:283–289.

**Templeman, W.**
**1963.** Distribution of sharks in the Canadian Atlantic (with special reference to Newfoundland waters). Bull. Fish. Res. Board Can. 140:1–77.

**Tricas, T. C., K. Deacon, P. Last, J. E. McCosker, T. I. Walker, and L. Taylor.**
**1997**. The Nature Company guides. Sharks and rays (L. Taylor, consultant ed.). Time-Life Books, Time Life Inc. San Francisco, CA, 288 p.

**Uchida S., M. Toda, and Y. Kamei.**
**1990.** Reproduction of elasmobranchs in captivity. *In* Elasmobranchs as living resources: advances in the biology, ecology, systematics, and the status of fisheries (H. L. Pratt, S. H. Gruber, T. Taniuchi, eds.), p. 211–237. U.S. Dep. Commer., NOAA Tech. Rep. NMFS 90.

**Uchida, S., M. Toda, K. Teshima, and K. Yano.**
**1996.** Pregnant white sharks with near-term fetuses from Japan. *In* Great white sharks. The biology of *Carcharodon carcharias* (A. P. Klimley and D. G. Ainley, eds.). Academic Press, San Diego, CA, p. 139–155.

**Uchida, S., F. Yasuzumi, M. Toda, and N. Okura.**
**1987.** On the observation of reproduction in *Carcharodon carcharias* and *Isurus oxyrinchus*. Rep. of Japanese Group for Elasmobranch Studies 24:5–6.

**Vaillant, L.**
**1889.** Note sur un foetus gigantesque d'*Oxyrhina spallanzani* Bonap. Bull. Soc. Philom. Paris 1:38–39.

**Welch, D. W., and R. P. Foucher.**
**1988.** A maximum likelihood methodology for estimating length-at-maturity with application to Pacific cod *(Gadus macrocephalus)* population dynamics. Can. J. Fish. Aquat. Sci. 45:333–343.

**Wilkinson, L.**
**1986.** SYSTAT: The system for statistics. SYSTAT Inc., Evanston IL, 18 chapters and 4 appendices without continuous page numbers.

**Yano K., Y. Yabumoyo, S. Tanaka, O. Tsukada, and M. Furuta.**
**1999**. Capture of a mature female megamouth shark, *Megachasma pelagios*, from Mie, Japan. *In* Proc. 5th Indo-Pac. Fish Conf., Noumea 3–8 November 1997 (B. Seret and J. Y. Sire, eds.), p. 351–365. Société Francaise d'Ichtyologie and Institut de Recherche pour le Développement, Paris.

# The relation between early marine growth of pink salmon, *Oncorhynchus gorbuscha*, and marine water temperature, secondary production, and survival to adulthood

**Donald Mortensen**
**Alex Wertheimer**
**Sidney Taylor**
**Joyce Landingham**
Auke Bay Laboratory
Alaska Fisheries Science Center
National Marine Fisheries Service, NOAA
11305 Glacier Highway
Juneau, Alaska 99801-8626
E-mail address (for D. Mortensen): don.mortensen@noaa.gov

**Abstract.**—Juvenile pink salmon, *Oncorhynchus gorbuscha*, from four consecutive brood years were tagged as they emigrated to the estuarine waters of Auke Bay, and information was obtained on the relationships between early marine growth, environmental conditions, and survival to adulthood. Juveniles that emigrated from Auke Creek later in the spring spent significantly less time in the estuary. Individual growth rates of tagged fish recovered in Auke Bay ranged from 3.1% to 7.1% per day. In all study years, juvenile pink salmon grew more slowly in early April than in late April and early May. Water temperature and growth were significantly correlated in all years, but growth did not consistently correlate with the biomass of epibenthic prey or zooplankton available to the fish. Comparisons of expected and observed growth rates suggested that low prey availability, as well as low temperatures, may have limited growth for early spring emigrants. Although early emigrants encountered poorer growth conditions, survivors were larger at a given date than later emigrants, their larger size possibly protecting them from size-selective predation. Early marine growth was significantly related to intra-annual cohort survival to adults ($r^2$=0.65, $P$<0.05). Larger fish consistently survived better than their smaller cohorts for all years. Although early marine growth was an important determinate of survival within a cohort of pink salmon, other factors, such as predator abundance, contributed to the large interannual variability observed.

Manuscript accepted 29 November 1999.
Fish. Bull. 98:319–335 (2000).

Pink salmon, *Oncorhynchus gorbuscha*, are the most abundant Pacific salmon species native to the west coast of the United States and Canada (Morrow, 1980). In southeastern Alaska pink salmon typically mature after 15 to18 months at sea and return to their native streams to spawn in late summer and early fall. Pink salmon usually spawn in the lower portions of streams just above the intertidal zone and in intertidal areas at stream mouths (Bailey, 1969). Eggs hatch in January or February and the embryos (alevins) continue to develop within the gravel of the stream bed. In late March or early April juvenile pink salmon (fry) emerge from the gravel and emigrate downstream to salt water and begin feeding on epibenthic organisms and small zooplankton. They form schools and reside in the nearshore marine habitat for several weeks (Heard, 1991). This early marine residency is evidently a critical stage in the early life history of salmon and can significantly affect year-class strength (Parker, 1968; Walters et al., 1978; Bax, 1983; Nichelson, 1986). Rapid growth during this early marine period may be a mechanism by which size-selective mortality is reduced (Parker, 1971; Hargreaves and LeBrasseur, 1985).

Growth and mortality of juvenile fish is thought to be coupled with the magnitude and timing of primary and secondary production (Cushing, 1976; Pitcher and Hart, 1982; D'Amours, 1987). Slight variations in migration timing and the developmental rate of juvenile fish in relation to secondary production influence feeding success and may in turn affect growth and survival. Subarctic estuarine ecosystems are characterized by high levels of primary and secondary production in spring (Russell-Hunter, 1970; Larrance, 1971; Goering et al., 1973). Consequently, the timing of emigration of species such as juvenile pink and chum, *O. keta*, salmon may have evolved so that this highly productive period maximizes growth and survival (Murphy et al., 1988; Holtby et al., 1989). This concept is somewhat

intuitive and there is little direct supportive evidence. To test this idea, we designed our study with the following objectives: 1) to examine emigration timing and growth of tagged individual juvenile pink salmon in relation to secondary production and water temperature and 2) to investigate the relation between timing of emigration, early marine growth, and intra- and interannual variability in marine survival.

## Methods

This research focused on the Auke Creek pink salmon population. Auke Creek is a small, lake-fed stream that empties into Auke Bay in southeast Alaska (Fig. 1). The National Marine Fisheries Service maintains a permanent two-way counting weir (where both seaward-migrating and returning salmon are counted) at the confluence of Auke Creek with Auke Bay. The pink salmon run at Auke Creek is bimodal, that is it has a distinct early and late spawning component. Salmon in the early run begin spawning in late July through August and salmon in late run spawn from September through mid-October. The emigration of fry in the spring lasts from late March to mid-May and is relatively unimodal. The peak emigration usually occurs in late April (Taylor, 1980)

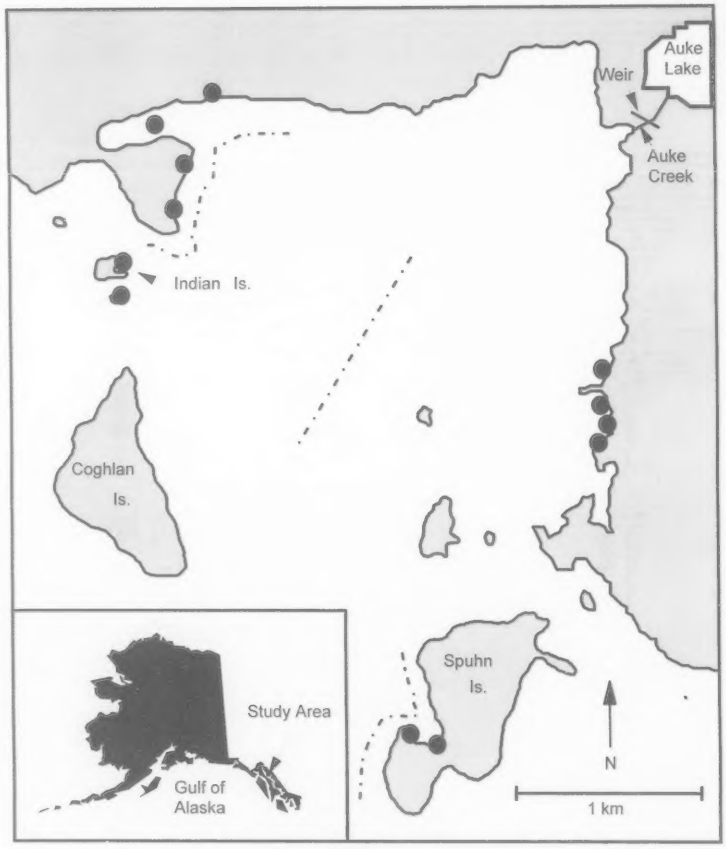


**Figure 1**

Map of Auke Bay, Alaska, showing beach seine sites (circles) and surface trawl transects (dashed lines).

The downstream emigration of wild pink salmon juveniles from Auke Creek into Auke Bay generally begins in early March, peaks between mid-April and early May, and ends by mid-May. From 1986 to 1989, 53,526, 17,249, 38,149, and 42,599 juvenile pink salmon emigrated from Auke Creek respectively. Each day all captured emigrants were counted and samples were measured to the nearest millimeter fork length.

Each year a portion of the emigrants was marked. Marking involved the excision of the entire adipose fin after a 0.5-mm binary coded wire was injected into the snout. Tag codes were assigned in lots of 10,000; therefore to use all the tags in a particular code-lot, tagging was conducted over several days each week. The 1985 brood was tagged in five-day emigration periods when sufficient numbers of fish were captured. The 1986 through 1988 broods were tagged in two to three-day emigration periods. After having been tagged, the fish were held for one day (1985 and 1986 broods) or three days (1987 and 1988 broods) to assess mortality and tag loss. Dead fish and those missing tags were deducted from the total tagged in each group. Release dates were similar each year.

Nearshore areas of Auke Bay were sampled for juvenile pink salmon from late March to early July with a 37-m long × 3-m deep beach seine. All captured juvenile salmon were identified to species, counted, and checked for evidence of tagging at the capture site; recaptured tagged fish were retained for tag recovery and size measurements. Random samples of up to 100 unmarked fish from each beach seine from sites on Spuhn and Indian Islands in Auke Bay were retained for length and weight measurements and stomach analysis. Other species (nonsalmonid) that were captured in the beach seines were enumerated and measured to the nearest millimeter (fork length

[FL] or total length [TL] depending upon the species). These fish have the potential to be either predators on or competitors with pink salmon juveniles.

Beginning in 1987, offshore areas of Auke Bay (>100 m from shore) were sampled weekly, at night, with a 6.1-m wide × 3.0-m deep surface trawl (Bax et al.[1]). All tagged salmon and a sample of up to 100 untagged juvenile pink salmon from each tow were retained for length and weight measurements and stomach analysis. All other fish captured in each tow were identified, enumerated, and measured.

Water temperature at 1-m depth was recorded daily in Auke Bay. Spuhn Island was sampled weekly for littoral epibenthic crustaceans in 1987–1989, with an epibenthic pump (1987) (Simenstad et al.[2]) or an epibenthic sled (1988 and 1989) (Celewycz and Wertheimer, 1996b). Zooplankton data for the upper 5-m and upper 40-m water column in Auke Bay were collected concurrently with our study by University of Alaska researchers (Coyle and Paul, 1990).

Stomachs of a subsample of untagged juvenile pink salmon retained from beach seine and trawl catches were examined to determine feeding habits. Stomach contents were weighed, and prey items were identified, measured, and counted. A mean volume and dry weight were calculated for each prey category, and the index of relative importance (IRI; Pinkas et al., 1971) was then computed by using the formula

$$IRI = (N + V)\,F,$$

where $N$ = the numerical percentage;
$V$ = the volumetric percentage of each prey item in the diet; and
$F$ = the percent frequency of occurrence of the prey item.

The importance of individual prey groups were compared as a percentage of the total *IRI* for all prey.

The maximum residence of tagged fish from each weekly release group in Auke Bay was calculated by subtracting the actual release date for a particular lot of tagged fish from the last recovery date of a tagged juvenile from the same lot of tagged fish, yielding the number of days from release to recapture. The weighted mean residence time for each tag release group ($\overline{D}_{res_i}$) was calculated by subtracting the weighted mean release date for each weekly release group from the weighted mean recovery date for each release group. The weighted mean release date ($\overline{D}_{rel_i}$) for weekly release group $i$ was calculated from the formula

$$\overline{D}_{rel_i} = \frac{\sum_{d=1}^{d=n} d_{rel} N_{d_{rel}}}{\sum_{d=1}^{d=n} N_{d_{rel}}},$$

where $n$ = the number of release days per week;
$d_{rel}$ = the actual release day (Julian date); and
$N_{d_{rel_i}}$ = the number of tagged fish from that day that were released. The weighted mean residence for each weekly group was then calculated by subtracting the weighted mean release date of a juvenile for a given week from the weighted mean recovery date. The weighted mean recovery date ($\overline{D}_{rec_i}$), for a particular release group was calculated as

$$\overline{D}_{rec_i} = \frac{\sum_{d=1}^{d=n} d_{rec} N_{d_{rec}}}{\sum_{d=1}^{d=n} N_{d_{rec}}},$$

where $n$ = the number of recovery days per week;
$d_{rec}$ = the actual recovery day (Julian date) of a tagged juvenile; and
$N_{d_{rec_i}}$ = the number of tagged fish recovered on day $d$.

The weighted mean residence time ($\overline{D}_{res_i}$) was regressed against release date for each year. Analysis of covariance (ANCOVA) was used to determine whether significant differences existed among years, followed by the Newman-Keuls multiple comparison test to determine if significant differences ($\alpha$=0.05) existed within years.

The instantaneous growth rate, $g$, for individual tagged pink salmon juvenile was calculated as

$$W_2 = W_1 \exp^{gt},$$

where $t$ = the period in days from the mean release date, over which the growth rate was calculated; and
$W_1$ and $W_2$ = the fish weight at the beginning and end of the period, respectively.

In addition the natural log of the weight of tagged fish at capture was regressed against days from

[1] Bax, N. J., E. O. Salo, B. P. Snyder, C. A. Simenstad, and W. J. Kinney. 1978. Salmonid outmigration studies in Hood Canal. Final Report FRI-UW-7819, Phase III, January to July 1977. University of Washington, College of Fisheries, Fisheries Research Institute, Seattl, WA.

[2] Simenstad, C. A., C. D. Tanner, and R. M. Thom. 1989. Estuarine wetland restoration and monitoring protocol. Report FRI-UW-8918, University of Washington, College of Fisheries, Fisheries Research Institute, Seattle, WA.

release to recovery to provide the growth rate (the slope of the regression line) for each release group. Using $g$ we then calculated the relative growth, $h$, as the percentage of body weight per day (%bwd) for each fish and for each group was calculated from the formula

$$h = (\exp^g - 1)\ 100.$$

Tagged juveniles that were recaptured within a week of the mean release date from the Auke Creek weir were not used in growth rate calculations. It was assumed that after a week the fish had acclimated to the marine environment and were recovered from prerelease tagging stress. In addition to the above calculations, the weights of tagged and untagged juveniles at successive capture dates were logarithmically transformed and regressed against days from the mean release day to the day of capture.

To determine how water temperature and food abundance relate to growth in the estuary, individual growth rates of tagged fish were correlated with average surface water temperature and prey biomass over the period between release and recapture. The average daily biomass of prey organisms was calculated for three habitats: the upper 5-m of the water column, the upper 40-m of the water column, and the littoral zone (harpacticoid copepods only). Correlation analysis and stepwise regression (Zar, 1974) were employed to determine significant correlations and provide partial correlation coefficients for each of the above parameters.

To test the possibility that estuarine growth of juvenile pink salmon could be limited by prey availability, the residual (difference) between expected and actual growth of individual juvenile pink salmon at given water temperatures was calculated and plotted against average water temperature. Expected maximum growth rates for given temperatures were obtained from (Mortensen and Savikko, 1993).

Growth of the tagged juvenile pink salmon was also computed for two periods or stanzas. Each year, the early period was that before and including 5 May, and the late period was that after 5 May. These dates were chosen because of the distinct change in size of juveniles between the two periods and the distribution of tag recoveries. Each year a dramatic increase in length was noted in the tagged fish at the beginning of May. Growth for each tagged group within a year was calculated for the early period; this rate was then used to estimate the initial weight for each tag group for computation of growth in the late period. Differences in growth between periods and years were tested by using analysis of covariance (ANCOVA) and the Newman-Keuls multiple comparison or Dunnet's tests (Zar, 1974). Significance levels were set at $\alpha = 0.05$.

Survival of fish from each release group for each emigrant year, 1986–1989 (brood years 1985–1988) was determined from the number of adult salmon returning to the Auke Creek weir. Each pink salmon adult passing through the weir was examined for a coded wire tag (cwt) on the adipose fin. Clipped fish were killed and their heads removed. Fish with adipose fins were returned to the creek to spawn. Coded-wire tags were removed from heads of the clipped fish later at the laboratory. Fish that showed a clip mark but were missing cwts were assigned to an emigration group that was based upon the proportion of all tag codes recovered each return week. Therefore, the return of each emigration group was the number of known tagged fish plus an expansion for clipped fish that had lost their tags. The total return of pink salmon adults to Auke Creek was the product of weir recoveries and a fishery correction factor. The fishery correction factor for each brood year was determined as

$$1/(1 - h),$$

where $h$ = harvest rate determined as the proportion of the total return that is caught in the commercial fishery according to estimates by Alaska Department of Fish and Game (ADF&G) commercial fisheries management personnel.

Fishery correction factors obtained from the commercial fisheries branch of ADF&G for the 1985–1988 broods at Auke Creek were 1.45, 1.03, 1.53, and 1.43, respectively.[3] Growth and survival of the individual release groups within each year were standardized as a proportion of the highest rates observed. The proportional growth rate for each release group was regressed against proportional survival to determine the degree to which growth rate was a predictor of intra-annual survival. Survival rates were regressed against growth rates to determine the relation between growth and interannual survival.

## Results

### Catch and residency times

Juvenile pink salmon use Auke Bay as a nursery area throughout the spring and early summer and reside nearshore from late March until mid-June. Pink salmon

[3] Ingledue, D. 1987–90. Alaska Department of Fish and Game, Division of Commercial Fisheries, Southeast Regional Office, 802 Third Street, Douglas, Alaska 99609. Personal commun.

were most abundant in late April and early May; 70–80% of the catch occurred between 5 May and 1 June. Most pink salmon left the nearshore area by late May. Salmon catch offshore tended to increase coincidentally with the decline in catch near shore; offshore catches peaked between May and mid-June, depending on the year (Fig. 2). Most tagged juveniles were recaptured near shore; only 11 and 2 fish were recaptured offshore in 1987 and 1988, respectively (no fish were recaptured in 1989, and no offshore sampling occurred in 1986). By mid-July of each year, juveniles were not present in nearshore or offshore catches.

Estuarine residence time (based on recaptures of tagged fish) generally decreased with progressive release dates. The exception was 1988, when residence time was similar between all release groups. Mean residence time ranged from a high of 30 d for the early release in 1986 and 1987 to about 7 d for the late release in 1989. The mean residence was also significantly longer in the first two weeks of 1986 and 1987 than in 1988 and 1989 (Table 1). Mean residence times did not differ significantly by release week between 1986 and 1987 or between 1988 and 1989, but were significantly different between 1987 and 1988. Based on recaptured tagged fish, maximum residence times in Auke Bay ranged from 19 d for juveniles from the 3 May release in 1988 to 72 d for the juveniles from the 13 April release in 1987 (Table 1).

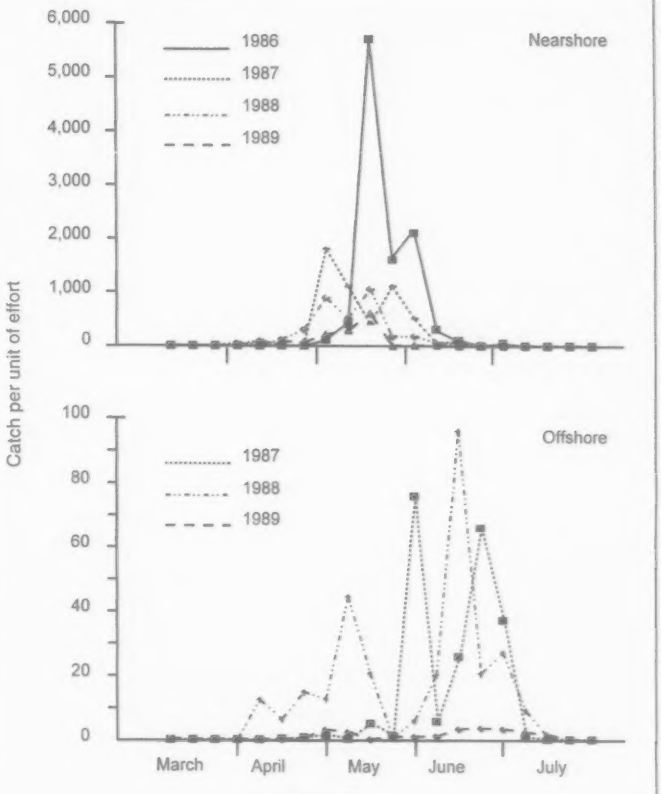


**Figure 2**

Catch per unit of effort (CPUE) of juvenile pink salmon at nearshore and offshore transects in Auke Bay, Alaska.

Nearshore catches consisted primarily of juvenile pink and chum salmon (Fig. 3). In even years, pink salmon juveniles were more abundant than chum salmon juveniles; pink salmon juveniles made up 83% and 65% of the catch in 1986 and 1988, versus 16% and 17% for chum salmon juveniles. In contrast, the ratios of pink and chum salmon in odd years were nearly equal (52–43%, 1987, and 52–44%, 1989). Coho (*O. kisutch*) and sockeye (*O. nerka*) salmon smolts and juvenile and adult Dolly Varden (*Salvelinus malma*) were also captured each year. Other nonsalmonid fishes captured included juvenile Pacific herring (*Clupea pallasi*) sculpins (Cottidae,) juvenile flatfish (Pleuronectidae), and juvenile walleye pollock (*Theragra chalcogramma*). Juvenile Pacific herring made up a significant proportion of the nearshore catch (14%) only in 1988.

Offshore catch composition for 1987 through 1989 consisted primarily of Pacific herring and capelin (*Mallotus villosus*). Pink salmon were the most abundant salmonid captured in offshore sampling. In 1987 and 1988, pink salmon made up 10% and 13% of the offshore catch respectively. Juvenile herring and capelin accounted for 76% and 74% of the offshore catch in 1987 and 1988, respectively. In 1989, pink salmon accounted for only 0.1% of the offshore catches, whereas juvenile Pacific herring were abundant and accounted for 97% of the total fish numbers. Fewer chum salmon juveniles and sockeye, coho, and chinook (*O. tshawytscha*) smolts were caught offshore than inshore. Other fish caught included juvenile and adult walleye pollock, sculpins, Pacific sandfish (*Trichodon trichodon*) and starry flounder (*Platichthys stellatus*).

## Predators

Coho salmon smolts, medium (fork length $15 \geq x \geq 30$ mm) and large (fork length >30 cm) Dolly Varden, and three sculpin species (great sculpin, *Myoxoceph-*

**Table 1**

Release dates, number released, maximum and weighted mean residence (days), growth rate (percent body weight per day), and adult survival of coded-wire-tagged Auke Creek pink salmon for each release year followed by brood year in parentheses. Standard deviations for mean residence and growth are given in parentheses.

| | Release week | | | | | | |
|---|---|---|---|---|---|---|---|
| | 1 April | 7 April | 15 April | 22 April | 29 April | 6 May | 13 May |
| 1986 (1985) | | | | | | | |
| Number released | 4322 | 8697 | 7416 | 10,136 | 11,446 | 10,866 | 643 |
| Number recaptured | 1 | 32 | 11 | 27 | 22 | 9 | 0 |
| Maximum residence | 29 | 47 | 35 | 65 | 31 | | — |
| Mean residence | 29 (0) | 30.5 (10.6) | 17.6 (10.1) | 18.3 (14.7) | 12.8 (9.6) | 10.6 (8.7) | — |
| Growth rate | — | 3.6 (0.01) | 4.0 (0.06) | 4.0 (0.07) | 3.7 (0.06) | 3.4 (0.10) | — |
| Survival rate | 1.14 | 1.44 | 2.62 | 2.17 | 3.14 | 1.18 | 0 |
| 1987 (1986) | | | | | | | |
| Number released | 3442 | 4646 | 7684 | 1477 | — | — | — |
| Number recaptured | 17 | 54 | 53 | 8 | — | — | — |
| Maximum residence | 62 | 71 | 72 | 28 | — | — | — |
| Mean residence | 27.5 (16.3) | 23.2 (8.7) | 20.2 (12.2) | 14.9 (9.3) | — | — | — |
| Growth rate | 3.8 (0.08) | 4.3 (0.07) | 4.6 (0.09) | 4.6 (0.05) | — | — | — |
| Survival rate | 1.97 | 3.10 | 3.41 | 3.76 | — | — | — |
| 1988 (1987) | | | | | | | |
| Number released | 5207 | 6031 | 8548 | 10,513 | 7880 | — | — |
| Number recaptured | 25 | 33 | 27 | 47 | 34 | — | — |
| Maximum residence | 26 | 34 | 33 | 41 | 19 | — | — |
| Mean residence | 15.5 (5.4) | 12.0 (11.3) | 16.8 (10.9) | 15.4 (8.3) | 13.5 (7.6) | — | — |
| Growth rate | 3.5 (0.08) | 4.3 (0.08) | 5.6 (0.14) | 5.8 (0.06) | 6.4 (0.08 | — | — |
| Survival rate | 0.48 | 0.69 | 1.03 | 1.44 | 1.83 | — | — |
| 1989 (1988) | | | | | | | |
| Number released | — | 3670 | 5113 | 8819 | 10,160 | 11,467 | 3370 |
| Number recaptured | — | 5 | 2 | 27 | 56 | 120 | 21 |
| Maximum residenc | — | 33 | 27 | 31 | 34 | 27 | 22 |
| Mean residence | — | 14.0 (15.1) | 21.7 (5.2) | 10.0 (8.7) | 12.5 (10.6) | 9.4 (12.3) | 6.9 (11.1) |
| Growth rate | — | 4.5 (0.05) | 5.6 (0.02) | 5.3 (0.06) | 6.1 (0.07) | 5.9 (0.06) | 4.2 (0.09) |
| Survival rate | — | 2.58 | 4.33 | 5.34 | 5.88 | 4.86 | 3.30 |

*alus polyacanthocephalus*, Pacific staghorn sculpin, *Leptocottus armatus*, and buffalo sculpin, *Enophrys bison*) were captured in beach seines and surface trawls along with juvenile salmon. We also observed these fish striking at schools of juvenile pink salmon in nearshore areas. Examination of the stomachs of a few of these predators showed that pink salmon juveniles were indeed a dietary item. The abundance of potential predators captured in beach seines and tow net trawls was similar for all study years. Temporally, the number of predators initially increased slowly in April, then rose sharply in late April, peaked by late May, and declined sharply in June (Fig. 4). The period of rapid increase and decline each year was due primarily to the pulse of coho salmon smolts entering Auke Bay in May and leaving in June. Dolly Varden and sculpin numbers increased more gradually in the spring and remained steady throughout late spring and early summer.

### Water temperature and prey

Water temperature generally increased rapidly during April, May, and early June (Wing and Pella, 1998). Temperatures ranged from 3° to 5°C in late March to 10–14°C in June (Fig. 5). Temperature in 1986 and 1987 remained below 8%C for at least a week longer in April compared with temperature in 1988 and 1989.

Prey organisms of the juvenile salmon consisted primarily of zooplankton and littoral harpacticoid copepods. The seasonal dynamics of the biomass of zooplankton prey in the upper 40 m and upper 5 m of the Auke Bay water column have been discussed

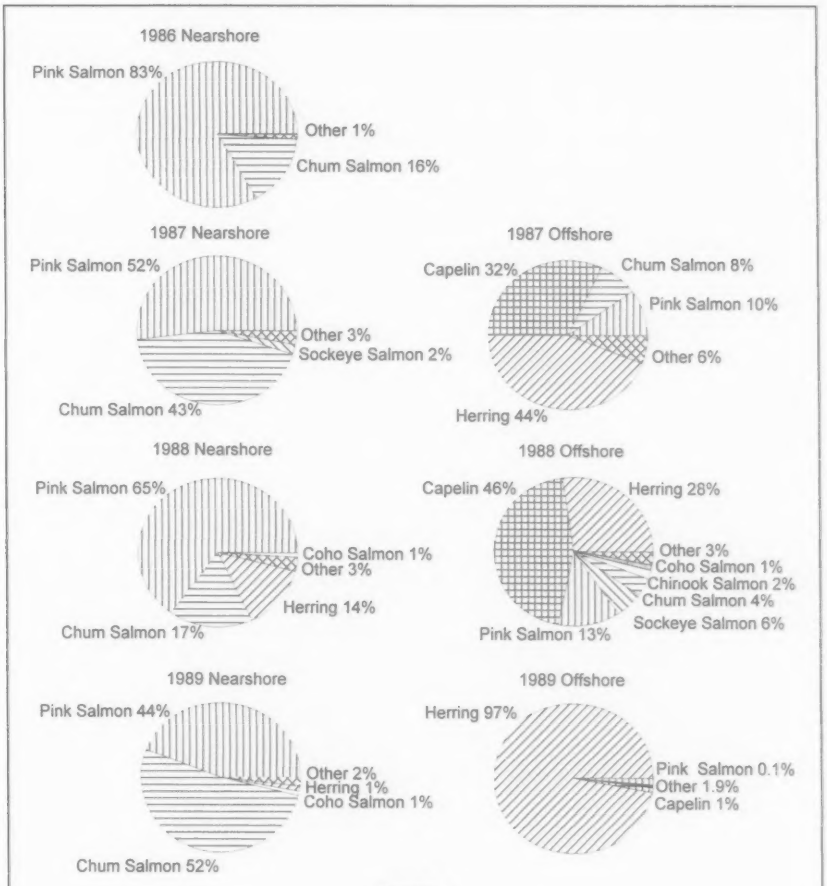


**Figure 3**

Species composition of nearshore and offshore catches from Auke Bay, Alaska, 1986–89.

by Coyle and Paul (1990), and we used their data to develop these profiles. Generally the biomass of zooplankton prey in the upper 40 and the upper 5 m of the water column began rising in mid-April and peaked in mid-June. However, in 1986 the biomass of prey in the upper 5 m remained low throughout the spring (Fig. 5).

Littoral harpacticoids were sampled at Spuhn Island in 1987, 1988, and 1989. Although the sampling method changed between 1987 and 1988, an indication of the dynamics of the harpacticoid population is achieved by presenting indices of biomass as a proportion of the highest value within each year. In 1987, harpacticoid copepod biomass was characterized by rapid fluctuations but remained low, except for a peak in mid-May. The biomass in 1988 again fluctuated rapidly, with peaks in late April and early May. In 1989, the biomass peaked in early April and again in early May.

## Diet

Harpacticoid copepods and zooplankton (principally calanoid copepods, euphausid larvae, *Oikopleura* sp., and fish eggs and larvae) were eaten by the pink salmon juveniles captured near shore (Fig. 6). Between April and May, pink salmon consumed epibenthic prey more than pelagic prey; by mid-May they switched to a predominately pelagic diet.

Pink salmon juveniles captured offshore in Auke Bay exhibited a predominately pelagic diet, but some epibenthic organisms were still present. This finding may indicate that at times epibenthic prey are transported to offshore areas by water currents, or that the juvenile salmon optimize feeding by moving between pelagic and epibenthic areas in Auke Bay.

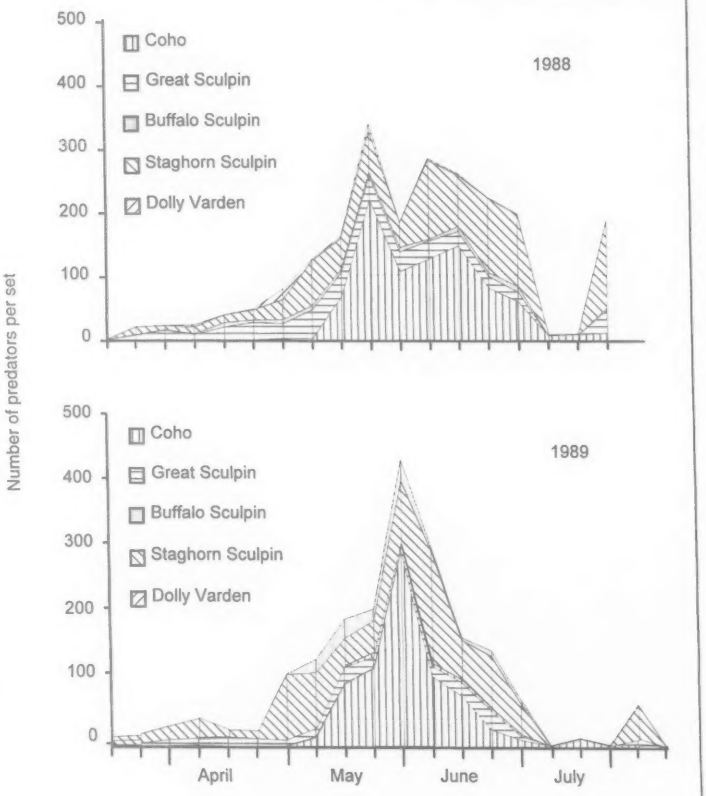


**Figure 4**

Mean catch per set of potential predators of juvenile pink salmon in the nearshore areas of Auke Bay, Alaska, 1988 and 1989.

## Growth rates

Growth (as a percentage [bwd]), of tagged and untagged juvenile pink salmon was examined in two periods, 1 April to 6 May (early) and 7 May to 16 June (late) in all study years (Table 2). Growth of tagged fish in the early period ranged from 2.93% bwd in 1986 to 4.88% in 1989 and of untagged fish from 1.21% bwd in 1987 to 2.10% in 1989. In the late period, growth of tagged fish ranged from 4.82% bwd in 1986 to 6.66% in 1988, and of untagged fish from 2.87% bwd in 1989 to 4.86% in 1988. Tagged and untagged juvenile pink salmon grew significantly slower in the early period than in the late period in all years.

Growth rates calculated for tagged juvenile pink salmon in any given period in a year were consistently higher than the apparent growth rates calculated from the mean weights of samples of untagged pink salmon (Table 2). Continuous recruitment of newly emigrated juveniles (fork length <33 mm) into the untagged population caused this pattern. The number of untagged juvenile pink salmon shorter than 33 mm that were captured by beach seine ranged from highs between 59% and 100% in late March each year to below 10% by 20 May of each year except 1989, when they remained at 11% until 12 June. Such variations in the number of new recruits and the number of larger fish leaving the nearshore juvenile pink salmon population resulted in a bias for growth rate calculations from untagged populations. Tagged fish provided a more realistic assessment of growth in relation to the environment.

## Factors limiting growth

Fish growth can be limited by low water temperatures (Weatherley and Gill, 1995) and low prey abundance (Brant et al., 1992). To determine when growth

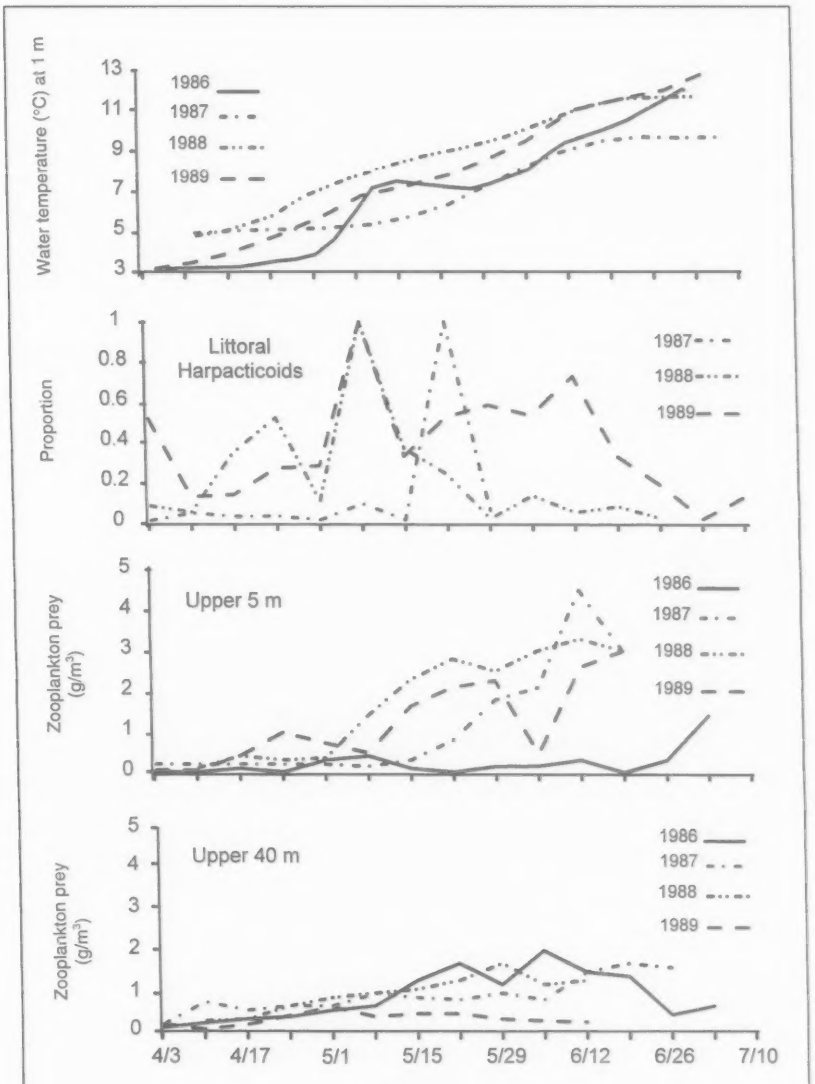


**Figure 5**

Water temperature, biomass of zooplankton and harpacticoid copepod prey of juvenile pink salmon from the epibenthos, upper 5 m, and 40 m of Auke Bay, Alaska. Owing to differences in collection technique between years, the values depicted for littoral harpacticoids are expressed as a proportion of the highest biomass within each year. Littoral harpacticoids were not collected in 1986. Zooplankton data for the upper 5 m and 40 m were taken from Coyle and Paul (1990).

of juvenile pink salmon might be restrained by prey abundance, the observed growth of each tagged fish was compared to maximum expected growth at similar water temperatures. In all years, the residuals between observed and expected growth (observed–expected) had significant positive slopes (Fig. 7), indicating that a higher proportion of early emigrants (rearing in relatively cool water) were below expected growth rates compared with fish at higher water temperatures (later emigrants). If abundance of prey is not growth-limiting, the growth rate of juvenile pink salmon at 5°C water temperature in

**Table 2**

Growth rate (as percent body weight per day [% bwd]), of tagged and untagged juvenile pink salmon caught in Auke Bay in early and late growth periods (1 April–6 May and 7 May–16 June). Growth of tagged juveniles was calculated between release and recapture within the early period and the number of days from the end of the early period to recapture within the late period. To calculate the rate of growth of tagged fish, the average weight of the fish from release to recapture within the early period was used, whereas in the late period the estimated weight of fish at the end of the early period and at the date of recapture within the late period was used. The growth of untagged fish was calculated similarly, except that the number of days from the beginning to the end of a specific growth period was used. The standard deviation (SD), coefficient of determination ($r^2$), and sample size ($n$) are also shown.

| Growth period | Tagged | Growth rate (% bwd) | SD | $r^2$ | $n$ | Growth period | Tagged | Growth rate (% bwd) | SD | $r^2$ | $n$ |
|---|---|---|---|---|---|---|---|---|---|---|---|
| 1986 | | | | | | 1988 | | | | | |
| Early | tagged | 2.93 | 0.237 | 0.84 | 76 | Early | tagged | 2.95 | 0.208 | 0.62 | 134 |
| | untagged | 1.41 | 0.213 | 0.71 | 422 | | untagged | 1.51 | 0.398 | 0.50 | 2019 |
| Late | tagged | 4.82 | 0.221 | 0.83 | 23 | Late | tagged | 6.66 | 0.274 | 0.60 | 32 |
| | untagged | 3.21 | 0.391 | 0.65 | 955 | | untagged | 4.86 | 0.341 | 0.42 | 2535 |
| 1987 | | | | | | 1989 | | | | | |
| Early | tagged | 3.14 | 0.203 | 0.78 | 101 | Early | tagged | 4.88 | 0.287 | 0.44 | 173 |
| | untagged | 1.21 | 0.333 | 0.62 | 569 | | untagged | 2.10 | 0.335 | 0.36 | 462 |
| Late | tagged | 5.40 | 0.173 | 0.94 | 31 | Late | tagged | 5.40 | 0.202 | 0.82 | 58 |
| | untagged | 4.34 | 0.433 | 0.77 | 1658 | | untagged | 2.87 | 0.387 | 0.36 | 1030 |

early April should be about 2.0% or more (Mortensen and Savikko, 1993). Examination of growth residuals from tagged juveniles in relation to those at "maximum" feeding levels, indicates that fish in early April tended to have lower than expected growth rates, up to 2% lower depending upon the year. The slope of the residuals was lowest in 1988, when a higher proportion of the observations fell below the zero line throughout the temperature range observed.

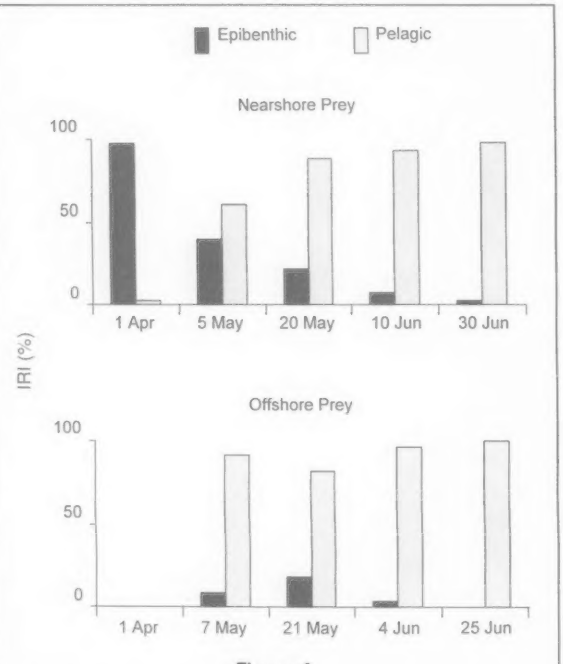


**Figure 6**

Index of relative importance (IRI) of pink salmon prey during residence in the nearshore and offshore areas of Auke Bay, Alaska.

### Intra-annual growth of tagged pink salmon

Growth of tagged juvenile pink salmon generally increased each year with successive release dates, reaching a maximum in late April, and then declining for later emigrants (Table 1). Recovery year is specified in the following sections, and brood year (BY) is given in parentheses. In our study, brood year corresponded to the spawning year of the parental generation and was always the year prior to the year when the sample was taken. Growth of weekly release groups varied from a low of 3.38% bwd in 1986 (1985 BY) to a high of 6.39% in 1988 (1987 BY). The decline in growth of emigrants from late releases was not observed in 1987 (1986 BY) and 1988 (1987 BY), when emigration ended before the end of April. In 1986 (1985 BY), the lowest growth rates were observed for the latest fish emigrating in the first week of May. In 1989 (1988 BY), the lowest growth rates were also observed for the last emigrants. However, these fish emigrated in the second week in May; fish emigrating in the first week in May in 1989 (1988 BY) had growth rates similar to those at the midpoint of the emigration timing.

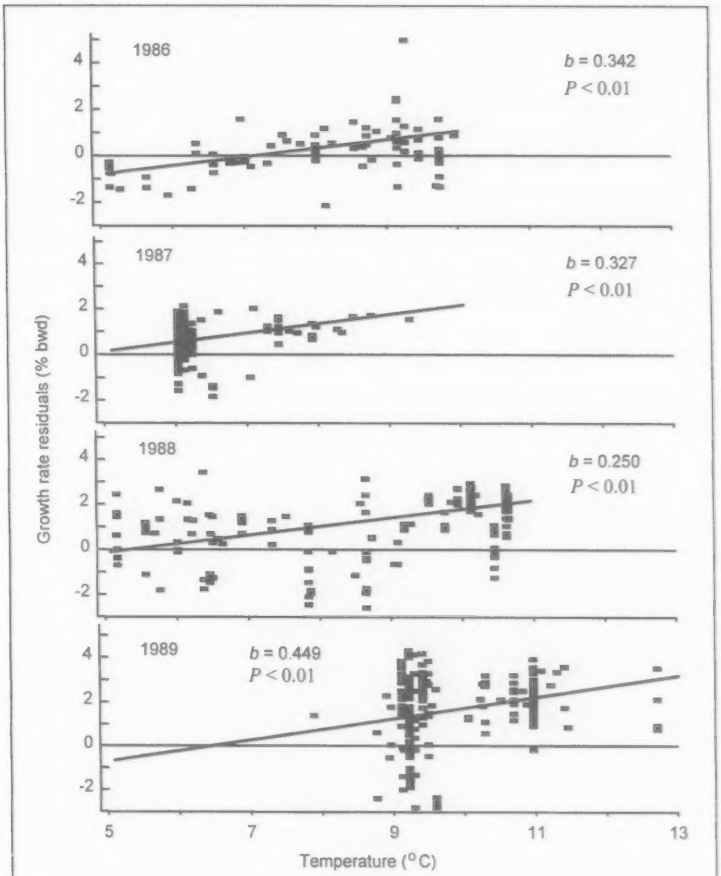


**Figure 7**

Residuals between the observed growth rate of tagged juvenile pink salmon and expected growth rate of juvenile pink salmon fed excess ration. Year shown refers to recovery year.

### Interannual growth of tagged pink salmon

The growth rates of juvenile pink salmon from individual release groups varied substantially between years (Table 1). All release groups of juvenile pink salmon in recovery year 1986 (1985 BY) grew significantly slower than those of juveniles in subsequent years. In 1987 (1986 BY) and 1988 (1987 BY), the only years when tagged juveniles from the 1 April group were recovered, growth was not significantly different. Similarly the growth of juveniles from the 7 April groups were not significantly different between years. Juvenile pink salmon from the 15 April and 22 April releases grew significantly slower in 1987(1986 BY) than in 1988 (1987 BY) or 1989 (1988 BY), by nearly 1%. Growth was significantly slower (about 0.5% bwd) for the 22 April release group in 1989 (1988 BY) than in 1988 (1987 BY). The juveniles from the 29 April release grew significantly faster (0.3% bwd) in 1988 (1987 BY) than in 1989 (1988 BY).

### Growth in relation to water temperature and prey biomass

Water temperature was the only environmental parameter measured that was significantly correlated with growth rate over all years (Table 3). Both simple and partial correlations were significant (<0.05) in each year for water temperature, and in every year except 1988, temperature explained the most variation in the parameters tested.

**Table 3**

Simple and partial (S/P) correlation coefficients between the instantaneous growth rate of juvenile pink salmon and average water temperature; average harpacticoid biomass; average biomass of prey integrated from 40 m to surface; average biomass of prey in the upper 5 m; and average biomass of harpacticoids + prey from the integrated water column. An * indicates a significant ($P<0.05$) correlation. NA = not available.

| Year | Average water temperature | Average harpacticoid biomass | Average integrated column biomass | Average biomass in upper 5 m |
|---|---|---|---|---|
| 1986 | 0.696*/0.696* | NA | 0.630*/0.187* | –0.187/-0.046 |
| 1987 | 0.312*/0.312* | –0.201*/-0.017* | 0.193/0.248 | 0.228/0.046 |
| 1988 | 0.423*/0.047* | 0.337/0.000 | 0.505*/0.505* | 0.472/0.228 |
| 1989 | 0.354*/0.354* | –0.226*/-0.118* | 0.057/0.003 | 0.254/0.128* |

The 5-m depth zooplankton biomass was not significantly related to growth in any year, whereas biomass from the 40-m integrated water column was significantly correlated in two of the four years. In 1988, the biomass from the 40-m integrated water column was the parameter most correlated with growth.

The biomass of littoral harpacticoids was significantly correlated with juvenile pink salmon growth for two of the three years for which data were available. In both cases, the relationship was negative (Table 3). Because feeding habits showed that the pink salmon were switching between epibenthic and zooplankton resources during the nearshore phase, growth rate was also correlated with a combined index of the biomass of littoral harpacticoids and the 40-m depth zooplankton. This combined index did not fit the growth data as well as either water temperature or zooplankton biomass considered independently (Table 3).

### Growth and survival

Mid- to late April emigrants had significantly higher survival than the earliest emigrants within a year (Table 1). Brood year is specified in the following paragraphs unless otherwise noted. When emigration extended into May (1985 and 1988 brood years), survival decreased by as much as 2% from the groups released from mid- to late April. The last emigrants from both the 1985 and 1988 broods, which had the lowest growth rates of those years, also had significantly lower survival than emigrants from mid- to late April.

The intra-annual survival of cwt juvenile pink salmon exhibited a pattern similar to that for growth rates. Regression of growth rate against survival (as proportions within each year) indicated a highly significant relationship ($r^2=0.65$, $P<0.003$; Fig. 8). Within-year survival generally increased with growth rate.

To examine the relation between growth and survival interannually, growth rate (%bwd) was regressed against survival rate of each release group. Although survival appears to increase with increasing growth rate, there was no relationship when all years were considered ($r^2=0.02$, $P>0.397$). Fish from the 1987 brood year (1988 emigrants, 1989 adults) had a distinctly different growth versus survival trajectory than fish for other years (Fig. 9). Data from brood years 1985, 1986, and 1988 fitted well ($r^2=0.88$, slope=1.82, $P=0.001$). Survivals of the 1987 brood were also significantly related to growth when considered separately from the other years ($r^2=0.93$, slope=0.40, $P=0.001$).

## Discussion

Pink salmon juveniles were abundant in the nearshore areas of Auke Bay in April and May; by the end of May or early June, the fish had moved farther offshore. This pattern is typical for juvenile pink salmon, which generally follow shorelines during their first weeks in the marine environment, then migrate offshore as they grow (Heard, 1991; Celewycz and Wertheimer, 1996a).We found water temperature to be the main factor that determined the growth rate of juvenile pink salmon during their early marine existence. The metabolism and growth of fish are influenced extensively by water temperature and prey density (Brett et al., 1969; Weatherley and Gill, 1995). To attain maximum growth at a particular temperature, prey concentrations must be adequate (Bailey et al., 1975; Cooney et al., 1981). In our study there were indications in early spring of each year that the growth of juvenile pink salmon was limited by abundance of prey. These early fish enter the Auke Bay estuary before the spring zooplankton bloom and rely on overwintering epibenthic prey organisms such as harpacticoid copepods.

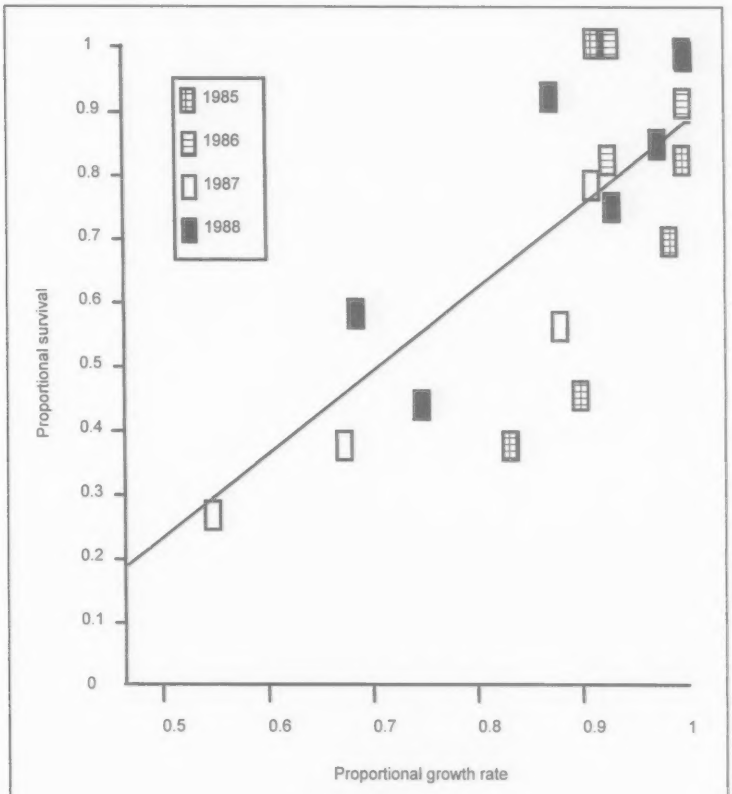


**Figure 8**

Intra-annual survival depicted as a regression of proportional survival on proportional growth rate of tagged Auke Creek pink salmon ($r^2$=0.65, $P$=0.003). Years represent brood year.

The relatively sparse population of potential predators in early spring allow a portion of the juveniles to survive the period of low growth. Growth was strongly related to adult survival within each of the study years; however, this relationship did not hold true between years.

Growth of fish in the tag groups over all recovery years ranged from 3.4% (8 May 1986 release) to 6.4% (29 April 1988 release). These rates are within the 1.5–7.6% range of growth rates previously reported for pink salmon during their initial marine residency (LeBrasseur and Parker, 1964; Healey, 1980). Willette (1996) also observed growth rates of 3.5–5.2% for cwt pink salmon in Prince William Sound.

Variations in the feeding activity of salmonids is characteristic of opportunistic and broad-spectrum predators, which optimize their food consumption in response to prey density (Parker and Vanstone, 1966; Parker, 1969; Ware, 1972; Hunter and Thomas, 1974; Godin, 1981). Both epibenthic crustaceans and zooplankton were important components of the prey of juvenile pink salmon during their nearshore residence in Auke Bay. In previous studies, harpacticoid copepods, among other epibenthic organisms, have been reported as the primary prey of pink salmon juveniles in nearshore marine habitats (Healey, 1980; Godin, 1981; Landingham, 1982; Webb, 1991). In Alaska waters, however, planktonic prey often predominate in the early diet of pink salmon (Bailey et al., 1975; Cooney et al., 1981; Sturdevant et al., 1996; Willette, 1996). Some of these differences are due to the types of beaches where juvenile pink salmon are sampled. In studies where harpacticoid copepods are the primary dietary component, the fish are sampled at low-gradient beaches with substantial epibenthic production (e.g. Kaczynski et al., 1973; Godin, 1981; Webb, 1991). Sturdevant et al. (1996) also found that a higher proportion of epibenthic prey was consumed by juvenile pink salmon captured on lower-gradient than on steep-gradient beaches. In Auke

Bay, pink salmon samples for diet analysis were taken from low-gradient beaches where there is a high production of epibenthic harpacticoid copepods (Landingham, 1982; Cordell, 1986). However, even at this habitat type, pelagic zooplankton was an important dietary component. Similarly, Sturdevant et al. (1996) found zooplankton to be the dominant dietary component of pink salmon juveniles from all nearshore habitat types sampled in Prince William Sound, Alaska.

From a bioenergetics standpoint, prey density and water temperature are critical factors affecting fish growth by influencing consumption rate, metabolic rate, and gastric evacuation rate (Willette, 1996). Temperature was significantly correlated with observed growth of juvenile pink salmon, but indices of prey abundance were not consistently correlated with growth and were even inversely related in the case of harpacticoid copepods. This lack of correlation may be due to the typically high and variable productivity of zooplankton and littoral epibenthos found in subarctic ecosystems such as Auke Bay (Cordell, 1986; Coyle and Paul, 1990). Assuming there is some threshold level of prey density required to sustain maximum growth of juveniles, then the pronounced spikes in biomass of prey populations associated with the spring bloom would mean that much of the variability in prey occurs above the density threshold, thereby masking a relationship between prey biomass and juvenile pink salmon growth. Any such relationship should occur primarily before or after the prey population peaks. Analysis of residuals between expected growth of pink salmon and observed initial growth indicated that food abundance did limit growth at low water temperatures, (i.e. growth rates observed in the early period of nearshore residency were possibly constrained by food availability as well as lower temperatures (Fig. 7).

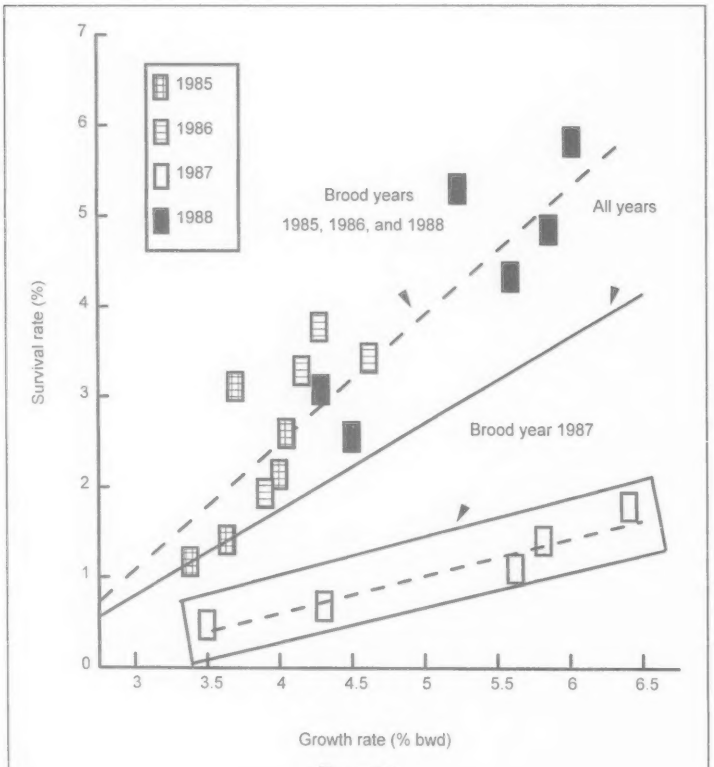


**Figure 9**

Interannual survival depicted as the regression of survival (adjusted for catch rate) versus growth rate of tagged Auke Creek pink salmon. When all four brood years are included in the regression, a poor relationship results ($r^2$=0.02, $P$>0.397). However, when brood year 1987 is excluded from the regression, the relationship between survival and growth rate improves ($r^2$=0.88, $P$=0.001). This relationship is also very good when based on data from just brood year 1987 ($r^2$=0.93, $P$=0.001).

The emigration of Auke Creek pink salmon extended from late March to mid-May; most of the fish emigrated within 2–3 weeks in mid- to late April. Holtby et al. (1989) proposed that the synchronous timing of emigration of chum salmon may be an adaptive feature based upon advantageous growth conditions in the estuarine environments, with synchrony acting as a mechanism to saturate predators and enhance survival. By this premise, it would be beneficial for all Auke Creek juveniles to emigrate together, later in the spring, within a narrow time window, so as to ensure optimum growth conditions. Each year, however, a portion of the Auke Creek pink salmon juveniles emigrate in early spring and they consistently encounter poor growth conditions. Water temperatures are usually 4°C, and zooplankton abundance is very low. These juveniles take longer to reach a particular size than do later emigrants and generally reside longer in estuarine nursery areas than the later, faster-growing emigrants (Table 1). Even though predator populations are relatively low in early spring, the early emigrants are exposed to predation over a longer period than are later

emigrants. Despite spending more time in low-growth conditions, they will have the advantage of being larger at a given date than subsequent, faster-growing emigrants (Fig. 10). Thus, there is an adaptive advantage in lessening size-selective predation by being on the "leading edge" of the synchronous emigration to marine waters. However, this advantage is constrained by poorer growth early in the spring and poorer survival to adulthood.

The abundance of potential predators (coho salmon, Dolly Varden, and sculpins) near shore increases rapidly in May, emphasizing the importance of larger size and larger numbers for pink salmon to avoid predation. Late emigrants, although encountering what appear to be good conditions for growth, may not be able to effectively outgrow increasing predation pressure or may not be abundant enough to saturate the predator population. Other factors may combine to affect the growth and ultimately the survival of the late emigrants. The abundance of competitors such as young-of-the-year and juvenile herring and capelin may affect the availability of prey at critical times and could explain the lower growth rates observed for late-emerging pink salmon.

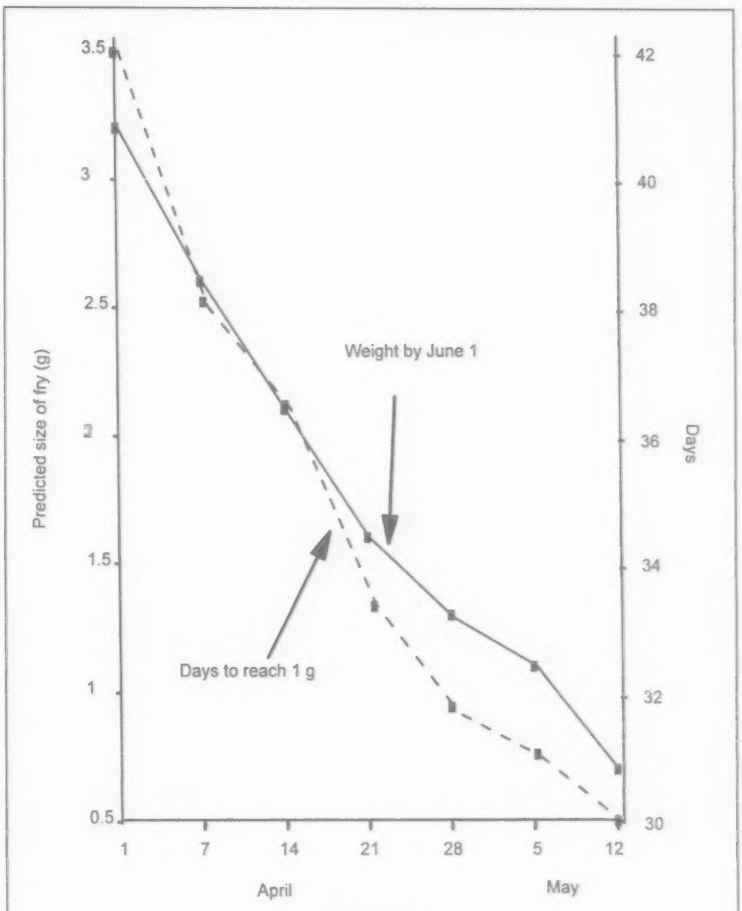


**Figure 10**

The predicted size of pink salmon fry by 1 June and the number of days to reach 1 g for emigration dates between 1 April and 12 May.

Growth rate of pink salmon juveniles in Auke Bay was consistently related to survival within a given year. This finding is consistent with the concept that high growth rates during early marine residency give a survival advantage by minimizing the intensity of predation (Parker, 1971; Heard, 1991). Following the *Exxon Valdez* oil spill in Prince William Sound in 1989, Willette (1996) found a direct relationship between growth and survival of pink salmon juveniles. However, he did not observe this association for juveniles captured in 1990 or 1991 and speculated that changes in the feeding habits of predators due to the absence of alternate prey obscured the relationship between growth and survival. Correlations of parameters for scale growth rates with run size of pink salmon in northern southeastern Alaska indicated that nearshore growth conditions are a significant contributor to the interannual variation in marine survival. Early scale growth (Jaenicke et al., 1994) was positively correlated with survival, indicating that high early marine growth lessens mortality due to predation. In our study, for three of the four years, growth rate was an excellent predictor of survival interannually, explaining 85% of the observed variability. The anomalous year was 1988 (1987 brood), which was also the year of highest overall growth rates. Fish from all release groups of the 1987 brood returned to the weir at consistently lower rates than fish from the other brood years. Fishery exploitation on returning adults may be a factor. We corrected the rate of survival each year for those fish taken in the commercial fishery with the correction factor used by the Alaska Department of Fish and Game; however, the correction factor was relatively crude with no measure of variance. It is conceiv-

able that fishery exploitation could still have affected the growth and survival relationship. Changes in nearshore predation or conditions (both environmental and biological) after the fish had moved offshore could also have been the cause. Although we noted no unusually high concentrations of piscivorous sea birds or marine mammals in the Auke Bay area in the spring of 1987, that observation does not preclude the possibility that larger than normal populations of predators may have caused significant mortality on the juveniles beyond our study area of Auke Bay. Identification of the elements causing such anomalous years would provide insight into how these factors interact with growth conditions to drive interannual variation.

## Acknowledgments

We thank our colleagues at the Auke Bay Laboratory who participated in this project. We are particularly indebted to Joe Orsi, Adrian Celewycz, Molly Sturdevant, Herbert Jaenicke, and Judy Lum. Without their unfailing dedication, expertise, and excellent attitudes this project would not have been as successful or enjoyable. Additionally, we extend our appreciation to Mark Carls, Jon Heifetz, and John Joyce who provided in-house reviews of this manuscript.

## Literature cited

**Bailey J. E.**
**1969.** Alaska's fishery resources—the pink salmon. U. S. Fish and Wildlife Serv., Bur. of Comm. Fish. Leaflet 619.

**Bailey, J. E., B. L. Wing, and C. R. Mattson.**
**1975.** Zooplankton abundance and feeding habits of fry of pink salmon, *Oncorhynchus gorbuscha*, and chum salmon, *Oncorhynchus keta*, in Traitor's Cove, Alaska, with speculations on the carrying capacity of the area. Fish. Bull. 73:846–861.

**Bax, N. J.**
**1983.** Early marine mortality of marked juvenile chum salmon (*Oncorhynchus keta*) released into Hood Canal, Puget Sound, Washington, in 1980. Can. J. Fish. Aquat. Sci. 40:426–435.

**Brant, S. B., D. M. Mason, and E. V. Patrick.**
**1992.** Spatially-explicit models of fish growth rate. Fisheries 17(2):23–33.

**Brett, J. R., J. E. Shelbourn, and C. T. Shoop.**
**1969.** Growth rate and body composition of fingerling sockeye salmon, *Oncorhynchus nerka*, in relation to temperature and ration size. J. Fish. Res. Board Can. 26:2363–2394.

**Celewycz, A. C., and A. C. Wertheimer.**
**1996a.** Abundance and growth of juvenile pink salmon in oiled and non-oiled locations of western Prince William Sound after the *Exxon Valdez* oil spill. Am. Fish. Soc. Symp. 18:518–532.
**1996b.** Prey availability to juvenile salmon after the *Exxon Valdez* oil spill. Am. Fish. Soc. Symp. 18:564–577.

**Cooney, R. T., D. Urquhart, and D. Barnard.**
**1981.** The behavior, feeding biology and growth of hatchery-released pink and chum salmon fry in Prince William Sound, Alaska. Univ. Alaska, Sea Grant Report 81-5, 114 p.

**Cordell, J. R.**
**1986.** Structure and dynamics of an epibenthic harpacticoid assemblage and the role of predation by juvenile salmon. M.S. thesis, Univ. Washington, Seattle, WA, 134 p.

**Coyle, K. O., and A. J. Paul.**
**1990.** Interannual variations in zooplankton population and biomass during the spring bloom in an Alaskan subarctic embayment. *In* APPRISE—Interannual variability and fisheries recruitment (D. A. Ziemann and K. W. Fulton-Bennett, eds.), p. 179–228. The Oceanic Institute, Honolulu, HI, and The School of Fisheries and Ocean Sciences, Fairbanks, AK.

**Cushing, D. H.**
**1976.** Biology of fishes in the pelagic community. *In* The ecology of the seas (D. H. Cushing and J. J. Walsh, eds.), p. 317–340. W. B. Saunders Co., Philadelphia.

**D'Amours, D.**
**1987.** Trophic phasing of juvenile chum salmon (*Oncorhynchus keta* Walbaum) and harpacticoid copepods in the Fraser River estuary, British Columbia. Ph.D. diss., Univ. British Columbia, Canada, 163 p.

**Godin, J.-G. J.**
**1981.** Effects of hunger on the daily pattern of feeding rate in juvenile pink salmon (*Oncorhynchus gorbuscha* Walbaum). J. Fish. Biol. 19:63–71.

**Goering, J. J., W. E. Shiels, and C. J. Patton.**
**1973.** Primary production. *In* Environmental studies of Port Valdez (D. W. Hood, W. E. Shiels, and E. J. Kelley, eds.), p. 253–279. Univ. Alaska, Fairbanks, Inst. Mar. Sci. Occas. Publ. 3.

**Hargreaves, N. B., and R. J. LeBrasseur.**
**1985.** Species selective predation on juvenile pink (*Oncorhynchus gorbuscha*) and chum (*O. keta*) by coho salmon (*O. kisutch*). Can. J. Fish. Aquat. Sci. 42:659–668.

**Healey, M. C.**
**1980.** The ecology of juvenile salmon in Georgia Strait, British Columbia. *In* Salmonid ecosystems of the North Pacific (W. J. McNeil and D. C. Himsworth, eds.), p. 203–229. Oregon State Univ. Press, Corvallis, OR.

**Heard, W. R.**
**1991.** Life history of pink salmon (*Oncorhynchus gorbuscha*). *In* Pacific salmon life histories (C. Groot and L. Margolis, eds.), p. 119–230. Univ. British Columbia Press, Vancouver, Canada.

**Holtby, L. B., T. E. McMahon, and J. C. Scrivener.**
**1989.** Stream temperatures and inter-annual variability in the emigration timing of coho salmon (*Oncorhynchus kisutch*) smolts and fry and chum salmon (*O. keta*) fry from Carnation Creek, British Columbia. Can. J. Fish. Aquat. Sci. 46:1396–1405.

**Hunter, J. R., and G. L. Thomas.**
**1974.** Effect of prey distribution and density on the searching and feeding behaviour of larval anchovy *Engraulis mordax*. *In* The early life history of fish (J. S. H. Blaxter, ed.), p. 559–574. Springer-Verlag, New York, NY.

**Jaenicke, H. W., M. J. Jaenicke, and G. T. Oliver.**
**1994.** Predicting northern southeast Alaska pink salmon returns by early marine scale growth. *In* Proceedings of the 16th Northeast Pacific Pink and Chum Salmon Workshop, p. 97–109. Alaska Sea Grant College Program Report 94-02.

**Kaczynski, V. W., R. J. Feller, and J. Clayton.**
**1973.** Trophic analysis of juvenile pink and chum salmon (*Oncorhynchus gorbuscha* and *O. keta*), in Puget Sound. J. Fish. Res. Board Can. 30:1003–1008.

**Landingham, J. H.**
**1982.** Feeding ecology of pink and chum salmon fry in the nearshore habitat of Auke Bay, Alaska. M.S. thesis, Univ. Alaska, Juneau, AK, 132 p.

**Larrance, J. D.**
**1971.** Primary production in the mid-subarctic Pacific region 1966–68. Fish. Bull. 69:595–613.

**LeBrasseur, R. J., and R. R. Parker.**
**1964.** Growth rate of central British Columbia pink salmon (*Oncorhynchus gorbuscha*). J. Fish. Res. Board Can. 21:1101–1128.

**Morrow, J. E.**
**1980.** The freshwater fishes of Alaska. Alaska Northwest Publishing Company, Anchorage, AK, 248 p.

**Mortensen, D. G., and H. Savikko.**
**1993.** Effects of water temperature on growth of juvenile pink salmon (*Oncorhynchus gorbuscha*). U.S. Dep. Commer., NOAA Tech. Memo. NMFS-AFSC-28, 12 p.

**Murphy, M. L., J. F. Thedinga, and K V. Koski.**
**1988.** Size and diet of juvenile Pacific salmon during seaward migration through a small estuary in southeastern Alaska. Fish. Bull. 86:213–222.

**Nichelson, T. E.**
**1986.** Influences of upwelling, ocean temperature, and smolt abundance on marine survival of coho salmon (*Oncorhynchus kisutch*) in the Oregon production area. Can. J. Fish. Aquat. Sci. 43:527–535.

**Parker, R. R.**
**1968.** Marine mortality schedules of pink salmon of the Bella Coola River, central British Columbia. J. Fish. Res. Board Can. 25:757–794.
**1969.** Foods and feeding of juvenile pink salmon in central British Columbia waters. I. 1966 diel series. Fish. Res. Board Can. Manuscr. Rep. Ser. 1017, no pages given.
**1971.** Size selective predation among juvenile salmonid fishes in a British Columbia inlet. J. Fish. Res. Board Can. 28:1503–1510.

**Parker R. R., and W. E. Vanstone.**
**1966.** Changes in chemical composition of central British Columbia pink salmon during early sea life. J. Fish. Res. Board Can. 23:1353–1384.

**Pinkas, L., M. S. Oliphant, and I. L. K. Iverson.**
**1971.** Food habits of albacore, bluefin tuna, and bonito in California waters. California Dep. Fish and Game, Fish. Bull. 152, 64 p.

**Pitcher, T. J., and P. J. B. Hart.**
**1982.** Fisheries ecology. AVI Publishing Co., Westport, CT, 414 p.

**Russell-Hunter, W. D.**
**1970.** Aquatic productivity. Macmillan Co., New York, NY, 306 p.

**Sturdevant, M. V., A. C. Wertheimer, and J. L. Lum.**
**1996.** Diets of juvenile pink and chum salmon in oiled and non-oiled nearshore habitats in Prince William Sound, 1989 and 1990. Am. Fish. Soc. Symp. 18:578–592.

**Taylor, S. G.**
**1980.** Marine survival of pink salmon fry from early and late spawners. Trans. Am. Fish. Soc. 109:79–82.

**Walters, C. J., R. Hilborn, R. M. Peterman, and M. J. Staley.**
**1978.** Model for examining early ocean limitation of Pacific salmon production. J. Fish. Res. Board Can. 35:1303–1315.

**Ware, D. M.**
**1972.** Predation by rainbow trout (*Salmo gairdneri*): the influence of hunger, prey density, and prey size. J. Fish. Res. Board Can. 29:1193–1201.

**Weatherley, A. H., and H. S. Gill.**
**1995.** Growth. *In* Physiological ecology of Pacific salmon (C. Groot, L. Margolis, and W. C. Clarke, eds.), p. 101–158. Univ. British Columbia Press, Vancouver, Canada.

**Webb, D. G.**
**1991.** Effect of predation by juvenile Pacific salmon on marine harpacticoid copepods. I. Comparisons of patterns of copepod mortality with patterns of salmon consumption. Mar. Ecol. Progr. Ser. 72:25–36.

**Willette, M.**
**1996.** Impacts of the *Exxon Valdez* oil spill on the migration, growth, and survival of juvenile pink salmon in Prince William Sound. Am. Fish. Soc. Symp. 18:533–550.

**Wing, B. L., and J. J. Pella**
**1998.** Time series analysis of climatological records from Auke Bay, Alaska. U.S. Dep. Commer., NOAA Tech. Memo. NMFS-AFSC-91, 90 p.

**Zar, J. H.**
**1974.** Biostatistical analysis. Prentice-Hall, Inc., Englewood Cliffs, NJ, 620 p.

# Genetic structure of tautog (*Tautoga onitis*) populations assayed by RFLP and DGGE analysis of mitochondrial and nuclear genes

**Elizabeth A. Orbacz**
**Patrick M. Gaffney**
College of Marine Studies
University of Delaware
Lewes, Delaware 19958
E-mail address (for P. M. Gaffney, contact author):pgaffney@udel.edu

**Abstract.**—The tautog (*Tautoga onitis*) is one of two temperate labrid species commonly inhabiting the coastal marine and estuarine waters of the mid-Atlantic coast of the United States. To delineate population structure throughout its primary range, we examined samples collected from three sites (Rhode Island, Delaware, Virginia). Five regions of the mitochondrial genome (COI, ATPase 6, cyt *b*, ND2 and control region) and one nuclear intron were amplified by PCR and screened for sequence variation with a battery of restriction enzymes (RFLP analysis), or by denaturing gradient gel electrophoresis (DGGE).

With RFLP analysis an average of 129 restriction sites per individual were revealed and 532 bases per individual were surveyed. Polymorphisms were observed in the ND2 and control region fragments, but not in the COI, ATPase 6, or cyt *b* fragments. Mean within-sample haplotype diversity was 0.6905 (±0.00184), within the range of values reported for other marine species. However, mean nucleotide diversity was 0.000782, one of the lowest values reported for a marine teleost. Corrected nucleotide divergence between samples was essentially zero, suggesting the absence of population structuring along the mid-Atlantic Coast. DGGE analyses of COI, cyt *b*, and a lactate dehydrogenase (LDH) intron revealed little additional variation; each product possessed a single common haplotype and occasional rare variants.

The low level of genetic diversity observed in the tautog may reflect a small effective population size resulting from historical population bottlenecks or large variance in reproductive success. The apparent absence of geographic differentiation suggests that tautog from Rhode Island to Virginia form a single genetic stock; data from additional genetic polymorphisms are needed to confirm or disprove this conclusion.

Manuscript accepted 27 September 1999
Fish. Bull. 98:336–344 (2000).

The tautog (*Tautoga onitis*) is one of two temperate labrid species commonly inhabiting the coastal marine and estuarine waters of the mid-Atlantic coast of the United States. Although the species range extends from the outer coast of Nova Scotia to Georgia, tautog are most abundant from Cape Cod to Chesapeake Bay (Bigelow and Schroeder, 1953). They are generally found in high relief, reeflike habitats such as those associated with jetties, breakwaters, and wrecks (Auster, 1989).

In the northern part of the their range, adult tautog generally overwinter in a state of torpor in sheltered areas in deep water offshore and move inshore during the spring to spawn in estuaries and nearshore waters (Cooper, 1966; Olla et al., 1974). Some tautog remain offshore throughout the year, particularly in the southern part of their range (Olla and Samet, 1977; Eklund and Targett, 1991). Those that migrate offshore do not always return to the same sites to overwinter (Olla et al., 1979). Juveniles and some adults have been found to overwinter at inshore sites off Virginia (Hostetter and Munroe, 1993) and Delaware (Eklund and Targett, 1991). In a tagging study, Cooper (1966) found that adult tautog tagged in Narragansett Bay tended to return to the same spawning site each year, and adult movement into and out of the area was negligible. In general, tautog do not appear to undergo extensive alongcoast migration (Cooper, 1966; Olla et al., 1974; Briggs, 1977).

Tautog spawn between mid-May and mid-August; spawning activity peaks in June (Colton et al., 1979). Eggs are buoyant and generally confined to coastal waters. Hatching occurs in 42–45 hours at 20–22°C, and pelagic larval duration is approximately 20–30 days (Victor, 1986). Although spawning occurs primarily in estuaries, offshore spawning has been reported (Eklund and Targett, 1990; Hostetter and Munroe, 1993).

Tautog support important recreational and small commercial fisheries throughout their range. After peaking in 1986, annual harvests have declined, and the species is believed to be overexploited, particularly in the northern part of its range, between New York and Massachusetts.[1]

Despite the economic importance of tautog, little information is available regarding stock structure of the species. Tagging studies suggest that there is little mixing of adult fish between geographical regions (Cooper, 1966; Briggs, 1977). Hostetter and Monroe (1993) reported latitudinal variation in size-at-age; fish from Virginia were found to grow

[1] Atlantic States Marine Fisheries Commission. 1996. Fishery management plan for tautog, April 1996. Fishery Management Report 25 of the Atlantic States Marine Fisheries Commission. 1444 Eye Street, N.W., 6th Floor, Washington D.C. 20005.

**Table 1**

List of primer sequences used in polymerase chain reaction amplifications for RFLP and DGGE-heteroduplex analyses. All sequences are in 5′→3′ orientation. Approximate size of product includes primers.

| Primer | Sequence | Region | Reference |
|---|---|---|---|
| CO1a-H | AGTATAAGCGTCTGGGTAGTC | cytochrome oxidase subunit I (≈680 bp) | Palumbi et al., 1991 |
| CO1f-L | CCTGCAGGAGGAGGAGAYCC | | |
| CB2-H | CCCTCAGAATGATATTTGTCCTCA | cytochrome *b* (≈380 bp) | Palumbi et al., 1991 |
| CB1-L | CCATCCAACATCTCAGCATGATGAAA | | |
| t-Met | AAGCTATCGGCCCCATACCC | NADH dehydrogenase subunit 2 (≈1270 bp) | Park et al., 1993 |
| c-Trp | CTGAGGGCTTTGAAGGCCC | | |
| 12SAR-H | ATAGTGGGGTATCTAATCCCAGTT | control region (≈1250 bp) | Palumbi et al., 1991 |
| L15995 | AACTCTCACCCCTAGCTCCCAAAG | | Meyer et al., 1994 |
| ATPase6-F | ATAAATAGGCTAATTGTTTCG | ATP synthase 6 (≈680 bp) | Quattro[1] |
| ATPase6-R | AAGCACTACGGTTTTAAGC | | |
| LDHA6F1 | TACACTTCCTGGGCSATYGGBATG | LDH A intron 6 (≈240 bp) | Quattro and Jones, 1999 |
| LDHA6R | CGCTSAGGAASACCTCRTCCTTCAC | | |

[1] Courtesy of J. Quattro, Department of Biological Sciences, University of South Carolina, Columbia, SC 29208.

more than twice as fast as fish from Rhode Island during their first year of life. However, in a common-garden experiment with fish from Rhode Island, Delaware, and Virginia, Martin (1993) found no genetic basis for the difference in growth rates. To date, there have been no published genetic analyses of population structure in this species.

The purpose of this study was to evaluate patterns of genetic variation in tautog across the primary range of the species, by examining DNA sequence variation in several mitochondrial and nuclear genes. We used restriction fragment length polymorphism (RFLP) analysis to examine several regions of the mitochondrial genome amplified by the polymerase chain reaction (PCR). These included portions of four protein-coding genes (cytochrome *b*, cytochrome *c* oxidase subunit I, ATP synthetase subunit 6, and NADH dehydrogenase subunit 2) and a segment including the entire control region, $tRNA^{Phe}$, and part of the 12S rRNA gene. In addition, we used denaturing gradient gel electrophoresis (DGGE) heteroduplex analysis to examine a nuclear gene intron and portions of the mitochondrial cytochrome *b* and cytochrome *c* oxidase subunit I genes.

## Materials and methods

### Sample collection and DNA extraction

Juvenile tautog under age two were collected between 1991–1993 from three sites in the northern, middle, and southern portions of the tautog's primary range: Narragansett Bay, Rhode Island; Delaware Bay, Delaware; and Chesapeake Bay, Virginia (for details regarding collection techniques see Martin, 1993). Fish were stored at –20°C. In addition, fin clips were taken from adult fish collected from Delaware Bay in 1996.

Total DNA extracts were prepared from white muscle tissue and fin clip samples from 24 fish from each of the three sites by using a Puregene DNA isolation kit (Gentra Systems, Inc., Minneapolis, MN) following the protocol specified for animal tissue.

### Polymerase chain reaction amplification of DNA

The polymerase chain reaction (PCR) was used to amplify parts of five regions of the mitochondrial genome: cytochrome *c* oxidase subunit I (COI), ATP synthetase 6 (ATPase 6), cytochrome *b* (cyt *b*), NADH dehydrogenase subunit 2 (ND2), and the control region (D-loop). In addition, intron 6 of the LDH-A gene was amplified. Amplifications were performed in a Perkin-Elmer 480 thermocycler under conditions optimized for each primer pair. Primer sequences are listed in Table 1. To create PCR products suitable for use in DGGE, primers CO1f-L, CB1-L ,and LDH849R were modified through the addition of a 15 base pair (bp) GC clamp (5′-CCCGCCGCCGCCGCC-3′) to the 5′ ends.

An approximately 680-bp portion of the COI gene was amplified with universal primers CO1a-H and CO1f-L (Palumbi et al., 1991) by using an initial

denaturation step of 2 min at 94°C followed by 35 cycles of 1 min at 95°C, 1 min at 50°C, and 1 min at 72°C, with a final step of 5 min at 72°C. Reaction volumes of 100 µL contained 1 µL of DNA extract, 2 mM $MgCl_2$, 200 µM each dNTP, 2.5 units *Taq* polymerase (Promega), and 0.17 µM of each primer. An approximately 380-bp fragment of the cyt *b* gene was amplified with universal primers CB2-H and CB1-L (Palumbi et al., 1991) by using the same protocol, except that the final primer concentrations were 0.2 µM.

An approximately 680-bp fragment of the ATPase 6 gene was amplified with primers ATPase6-F and ATPase6-R by using an initial denaturation step of 2 min at 94°C followed by 30 cycles of 45 sec at 94°C, 1 min at 52°C, and 2 min at 72°C, with a final step of 5 min at 72°C. Reagent and template concentrations were identical to those used to amplify the cyt *b* fragment. This PCR reaction protocol was also used to amplify an approximately 1270-bp fragment of ND2 with universal primers t-Met and c-Trp (Park et al., 1993) and an approximately 1455-bp fragment containing the entire control region, $tRNA^{Phe}$, as well as part of the 12S rRNA gene with universal primers L15995 (L-Pro; Meyer et al., 1994) and 12SAR-H (Palumbi et al., 1991).

An approximately 240-bp fragment of the LDH intron 6 was amplified with primers LDHA6F1 and LDHA6R (Quattro and Jones, 1999) by using an initial denaturation step of 2 min at 94°C followed by 35 cycles of 1 min at 95°C, 1 min at 52°C, and 1 min at 72°C, and a final step of 2 min at 72°C. Reaction volumes of 100 µL contained 3 µL of DNA extract, 2 mM $MgCl_2$, 200 µM each dNTP, 2.5 units *Taq* polymerase, and 0.2 µM of each primer.

### Restriction endonuclease digestion of PCR products

Restriction enzyme digestions were performed as specified by the manufacturer (New England BioLabs, Inc., Beverly, MA) in 20 µl reactions containing 5 units of enzyme per reaction. Digestions were incubated for a minimum of 5 hours before being stopped with loading dye (20% Ficoll 400, 0.1 M $Na_2EDTA$ pH 8, 1% SDS, 0.25% bromophenol blue, 0.25% orange G). The digests were run for electrophoresis on 2% agarose gels for at least 2 hours at 100 volts. Gels were stained with ethidium bromide and photographed under UV light. Fragment sizes were determined from migration distances in relation to known standards [*Bst*N I digest of pBR322 (New England Biolabs) and *Hae* III digest of pUC18 (Sigma, St. Louis, MO)] with the computer package Anagel (Mrázek and Spanova, 1992).

A subset of 24 fish, eight from each geographical region, was screened for polymorphisms in the five amplified mitochondrial DNA segments with the following 16 restriction enzymes: *Alu* I, *Aci* I, *Bsm*A I, *Bst*U I, *Dde* I, *Dpn* II, *Hae* III, *Hha* I, *Hinf* I, *Mnl* I, *Mse* I, *Msp* I, *Nla* III, *Rsa* I, *αTaq* I, and *Tsp*509 I. Restriction enzyme and mtDNA region combinations that revealed variation in the initial screening, ND2-*Hinf I* and control region-*Hae* III, were repeated for the entire sample of 72 fish, 24 from each geographic region.

### Denaturing gradient gel electrophoresis

Perpendicular gradient denaturing gels were run to determine the approximate denaturing points of the COI, cyt *b*, and LDH intron PCR products. For each fragment, PCR product was mixed with an equal volume of neutral loading dye (20% sucrose; 10 mM Tris-HCl, pH 7.8; 1 mM ethylenediaminetetraacidic acid [EDTA]; 0.1% bromophenol blue) and run on 6.5% acrylamide gels (14 cm × 19 cm, 0.75 mm thick) containing a perpendicular gradient of 0 to 80% denaturant [100% denaturant was defined as 7 M urea/ 40% (v/v) formamide]. Gels were electrophoresed at 150 volts for a minimum of 5 hours in a recirculating 1 × TAE buffer bath at 60°C (CBS Scientific, Inc., Del Mar, CA). Gels were visualized with ethidium bromide staining and photographed under UV light.

The entire sample of 72 fish was screened for polymorphisms in COI, cyt *b*, and the LDH intron by means of parallel DGGE. The parallel gradient gels spanned a range of 10% denaturant on either side of the experimentally determined melting point of each region: 40% to 60% gels were used to screen COI and cyt *b*, and 20% to 40% gels to screen the LDH intron. Parallel denaturing gels were run at 150 volts under conditions identical to those used for the initial perpendicular DGGE; the running times were optimized for resolution of each region: 4 hours for the LDH intron, 5 hours for cyt *b*, and 6 hours for COI.

In addition, heteroduplex analysis was performed on each individual from each of the three regions. Heteroduplexes were formed by heating samples containing equal volumes of PCR product from two individuals to 95°C for 5 min and then incubating them at –20°C for at least 30 min. Each heteroduplex sample was allowed to thaw slowly at room temperature and was run on the appropriate gradient. To create a chain of comparison linking each individual to all of the others, the samples were sequentially combined: the first was mixed with the second, the second with the third, etc., including the last sample which was combined with the first. Pairs of samples that exhibited a single homoduplex band and no het-

**Table 2**

Frequencies of composite haplotypes from restriction digestion of the COI, cyt *b*, ATPase 6, ND2, and the control region amplified fragments from *T. onitis*. Restriction enzymes used for each PCR product are listed. RI = Rhode Island, DE = Delaware, VA = Virginia. All individuals had identical haplotypes for COI, cyt b, and ATPase 6 for the enzymes surveyed.

COI: *Hae* III, *Hinf* I, *Nla* III, *Dde* I, *Mnl* I, *Aci* I and *Tsp509* I

cyt *b*: *Hae* III, *Hha* I, *αTaq* I, *Nla* III, *Bst*U I, *Mse* I, *Dde* I, *Mnl* I, *Aci* I, and *Tsp*509 I

ATPase 6: *Alu* I, *Rsa* I, *Hae* III, *Hha* I, *αTaq* I, *Hinf* I, *Nla* III, *Bst*U I, *Mse* I, *Dde* I, *Mnl* I, *Aci* I, and *Tsp*509 I

ND 2:*Alu* I, *Hae* III, *Rsa* I, *Hha* I, *Msp* I, *Hinf* I, *Dpn* II, *Nla* III, *Bst*U I, *Mse* I, *Dde* I, *Mnl* I, *Aci* I and *Tsp*509 I

control region: *Alu* I, *Rsa* I, *Hae* III, *Hha* I, *αTaq* I, *Msp* I, *Hinf* I, *Dpn* II, *Nla* III, *Bst*U I, *Mse* I, *Dde* I, *Mnl* I, *Aci* I and *Tsp*509 I

| Haplotype | | | | |
|---|---|---|---|---|
| ND 2 | Control region | RI | DE | VA |
| AAAAAAAAAAAAAA | AAAAAAAAAAAAAAA | 4 | 5 | 4 |
| AAAAA**B**AAAAAAAA | AAAAAAAAAAAAAAA | 2 | 2 | 2 |
| AAAAAAAAAAAAAA | AA**B**AAAAAAAAAAAA | 2 | 1 | 1 |
| AAAAAAAAAAAAAA | AA**C**AAAAAAAAAAAA | 0 | 0 | 1 |

eroduplex bands were considered to possess identical haplotypes.

### DNA sequencing

Haplotypes identified by DGGE-heteroduplex screening of the cytochrome *b* fragment were sequenced by using an ABI 373 automated DNA sequencer with dye terminator chemistry. Sequencing was done in both directions with the original PCR primers.

### Statistical analysis of RFLP data

Restriction patterns were analyzed with the Restriction Enzyme Analysis Package (REAP, version 4.0) (McElroy et al., 1992). For each of the three geographical samples, haplotype diversities were calculated following Nei (1987), and nucleotide diversities were calculated following Nei and Miller (1990). Haplotype diversity ranges from zero (all individuals share a common haplotype) to one (every individual has a unique haplotype) and estimates the probability that two randomly selected individuals in a sample will have different haplotypes. Nucleotide diversity estimates the average number of nucleotide substitutions for a pair of haplotypes randomly drawn from a sample. Nucleotide divergences among samples were estimated and corrected for within-sample variation according to Nei (1987). Heterogeneity of haplotype frequencies across samples was tested with exact R × C tests of independence using the software program StatXact (Cytel, 1992). Additional analyses of population differentiation were conducted using Arlequin 1.1 (Schneider et al.[2]). Power analysis of R × C tests was performed with Power and Precision 1.0 (Borenstein et al., 1997).

## Results

### Restriction site variation

Digestion with 16 restriction enzymes revealed polymorphisms in the ND2 and control region fragments, but not in the COI, ATPase 6, or cyt *b* fragments. Restriction enzyme digestion revealed an average of 129 restriction sites per individual and surveyed an average of 532 bases in each fish.

ND2 gene sequence variation was revealed by digestion with *Hinf* I, and sequence variation in the control region fragment was revealed by digestion with *Hae* III. The remaining enzymes produced invariant patterns. The 16 enzymes revealed four composite haplotypes attributable to restriction site gains or losses in the 24 individuals surveyed (Table 2). No additional haplotypes were uncovered by increasing the sample size to 24 individuals from each geographic region for the ND2-*Hinf* I and control region-*Hae* III combinations (Table 3). No evidence of mitochondrial genome size variation or heteroplasmy was observed in the regions analyzed.

[2] Schneider, S., J.-M. Kueffer, D. Roessli, and L. Excoffier. 1997. Arlequin: a software for population genetic data analysis, vers. 1.1. Genetics and Biometry Lab., Department of Anthropology, Univ. Geneva, Geneva.

One of the composite haplotypes was found only in a single individual from Virginia, whereas the remaining three were found in all three geographical regions. Mean within-sample haplotype diversity was 0.6905 (±0.00184), and mean nucleotide diversity was 0.000782 (Table 4).

Corrected nucleotide divergence between samples varied between –0.0077 and –0.0081%, suggesting the absence of population structuring along the mid-Atlantic Coast. This inference is further supported by exact log-likelihood analysis of the distribution of the four composite haplotypes across the three sites (likelihood ratio statistic=2.82, 6 df, exact $P$=1.00). A similar analysis of the larger data set ($n$=72, only polymorphic sites examined) indicated no significant heterogeneity (likelihood ratio statistic=6.05, 6 df, exact $P$=0.469). Lack of population differentiation was further supported by a mean $F_{ST}$ value of –0.005 (i.e. zero), and the analysis of molecular variance (AMOVA), which found 100% of total haplotype variation to occur within populations.

**Table 3**

Composite haplotypes from restricted gene and restriction enzyme combinations (ND2-*Hinf* I and control region-*Hae* III) for entire sample ($n$=72).

| Haplotype | Rhode Island | Delaware | Virginia |
|---|---|---|---|
| AA | 13 | 14 | 14 |
| BA | 6 | 9 | 7 |
| AB | 5 | 1 | 2 |
| AC | 0 | 0 | 1 |
| Total | 24 | 24 | 24 |

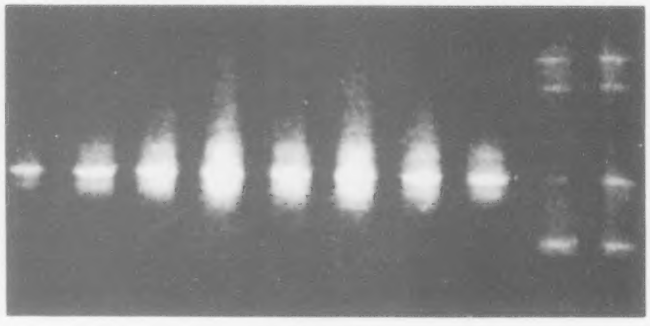

**Figure 1**

Denaturing gradient gel of tautog cyt *b* PCR products. Each lane represents the pooling of PCR products from two individuals, treated to induce heteroduplex formation when two different DNA sequences were present. The single homoduplex bands in lanes 1–8 (from left to right) indicate sequence identity for the nine tautog examined in pairwise combinations. Lanes 9–10 (the two lanes farthest to the right) illustrate the combination of the common haplotype and one rare haplotype. The two lower (faster-migrating) bands represent alternative homoduplex molecules; the upper two bands are the heteroduplex molecules.

### DGGE-heteroduplex analysis

For the entire sample of 72 individuals, analysis of the cyt *b* fragment revealed a total of three haplotypes, two of which were unique and found only in single individuals from Delaware and Virginia (Fig. 1). Sequence analysis of the three cyt *b* haplotypes revealed that the two unique haplotypes differed from the dominant haplotype by synonymous single base substitutions. The unique Virginia haplotype differed from the common haplotype by an A to G transition at base 276, whereas the unique Delaware haplotype resulted from the same substitution at base 291 (Fig. 2).

All 72 tautog appeared to possess a single COI haplotype, a result consistent with the extensive restriction enzyme screening of this region performed on the original subset of 24 individuals. The LDH intron was also relatively invariant. Of the 72 fish screened, DGGE-heteroduplex analysis revealed only a single heterozygous individual, collected in the Delaware region.

## Discussion

RFLP analysis revealed a mean mtDNA haplotype diversity value (0.6905 ±0.00184) for tautog that is intermediate within the range of values reported for other marine fishes. However, the overall nucleotide diversity value (0.078%) for the tautog is one of the lowest reported for a marine fish. It should be noted that values for haplotype diversity are affected by the number of restriction enzymes used and should be compared across studies with caution. In addition, values for haplotype and nucleotide diversity may be biased upwards in analyses that include only polymorphic enzymes.

Low levels of intraspecific sequence diversity in mitochondrial genes are generally attributed to low effective population size ($N_e$) or to reduced rates of mutation (Ovenden, 1990). Effective population sizes inferred from mtDNA data are often orders of magnitude smaller than present-day census estimates; this disparity may reflect the

**Table 4**

Summary statistics from the analysis of variation in the mitochondrial COI, cyt *b*, ATPase 6, ND2, and control region genes. Samples are pooled according to geographic region.

| Population | Sample size | Haplotype diversity | Nucleotide diversity |
|---|---|---|---|
| Rhode Island | 8 | 0.7143 ±0.12275 | 0.000816 |
| Delaware | 8 | 0.6071 ±0.16398 | 0.000648 |
| Virginia | 8 | 0.7500 ±0.13913 | 0.000883 |
| Overall | 24 | 0.6905 ±0.00184 | 0.000782 |

action of historical fluctuations in population size, such as bottlenecks caused by disease epidemics or environmental change, as well as a large variance in reproduction among females (Bowen and Avise, 1990). Low levels of nucleotide sequence diversity observed in some teleost fish have also been attributed to rates of sequence evolution that are lower than those estimated for birds and mammals (Bernatchez and Danzmann, 1993).

The Pleistocene glaciation is believed to have decreased the genetic diversity of many species through bottleneck effects (Bernatchez et al., 1989; Avise, 1992). During the Pleistocene era, ten or more glacial advances and retreats that caused changes in sea level and climate are believed to have had significant impacts on the distributions of coastal and marine fauna (Avise, 1992). Tautog population size may have been reduced through the reduction of suitable habitats for both themselves and their food resources. During the most recent glacial event, ice covered all waters north of Long Island and would have forced temperate populations southward into regions where high relief, hard substrate habitats are patchier and less abundant. Glacial advances also resulted in drops in sea level that would have reduced the availability of estuarine environments. In addition, postglacial dispersal from southern refugia may have created population bottlenecks if current populations were founded by a limited number of propagules. The same considerations may apply to the black sea bass *Centropristis striata*, an estuarine-dependent species with low nucleotide diversity (0.03%), corresponding to an estimate of ≈5,000 for $N_{fle}$, the effective number of females (Bowen and Avise, 1990).

```
TTT GGC TCC CTA CTA GGC CTC TGC TTA GTC GCA CAA ATT CTT ACA  45
 F   G   S   L   L   G   L   C   L   V   A   Q   I   L   T

GGG CTT TTC CTA GCC ATA CAC TAC ACC TCG GAT ATC GCC ACA GCC  90
 G   L   F   L   A   M   H   Y   T   S   D   I   A   T   A

TTT TCA TCA GTC GCC CAC ATC TGC CGC GAC GTT AAT TAC GGC TGA 135
 F   S   S   V   A   H   I   C   R   D   V   N   Y   G   W

CTA ATT CGA AAC ATA CAT GCA AAC GGC GCC TCC TCC TTC TTC ATC 180
 L   I   R   N   M   H   A   N   G   A   S   S   F   F   I

TGC ATC TAC CTA CAC ATT GCA CGG GGC CTT TAC TAC GGC TCA TAC 225
 C   I   Y   L   H   I   A   R   G   L   Y   Y   G   S   Y

CTC CAC AAA GAA ACG TGA AGC ATC GGC GTT GTT CTC CTC CTC CTT 270
 L   H   K   E   T   W   S   I   G   V   V   L   L   L   L

GTT ATa ATA ACT GCC TTC GTa GGC TAT GTC CTC CCC             306
 V   M   M   T   A   F   V   G   Y   V   L   P
```

**Figure 2**

Nucleotide sequence and deduced amino acid sequence of a 306-bp portion of the mitochondrial cyt *b* gene in *T. onitis*. Reading frame was inferred from alignment with published teleost cyt *b* sequences. Two rare haplotypes possessed synonymous A→G transitions at nucleotides 276 and 291 (indicated by lower case letters).

In addition to the low levels of within-population nucleotide diversity observed, this analysis also failed to detect genetic heterogeneity among tautog samples from different geographical regions. The uncorrected mean nucleotide sequence divergences among tautog samples were of the same magnitude as mean nucleotide diversities within samples; the mean difference between haplotypes randomly drawn from a single sample was equivalent to the mean difference between haplotypes drawn from different samples.

Low levels of intraspecific genetic variation do not preclude the detection of genetic differentiation among stocks. Shulman and Bermingham (1995) detected significant population subdivision within the Caribbean reef fish *Stegastes leucostictus*, for which they reported a mean within-sample sequence diversity of 0.07%. Bowen and Avise (1990) reported a mean within-sample sequence diversity of 0.03%

for black sea bass but detected significant divergence between Gulf of Mexico and Atlantic populations.

The results of our study are consistent with the null hypothesis that the tautog form a single genetic stock within the species range. Although tagging studies in Rhode Island have suggested that adult movement into and out of the area is negligible (Cooper, 1966), tautog have a relatively long pelagic larval stage of approximately three weeks which could result in enough gene flow among geographic regions to prevent the genetic differentiation of subpopulations.

The current system off of the mid-Atlantic coast of the United States consists of three major features: the northeastward flow of the Gulf Stream, the southwestward flow of the along-shelf current, and the across-shelf-flowing warm-core ring streamers that split off from the Gulf Stream (Brooks, 1996). The direction of flow is also influenced by local river runoff, seasonal wind patterns and meteorological events, and by the onshore movement of Ekman currents. The flow patterns in the mid-Atlantic region suggest that a high degree of transport of larvae among regions is possible (Hare and Cowen, 1993), especially for species such as the tautog that spawn in nearshore waters and have pelagic eggs. Larval transport has been suspected as the cause of genetic homogeneity over wide geographic ranges for many marine species (Avise, 1994; Hedgecock, 1994).

Other mtDNA analyses of stock structuring of coastal fish species in the mid-Atlantic region have likewise detected no population subdivision, e.g. weakfish (Graves et al., 1992b), bluefish (Graves et al., 1992a), summer flounder (Jones and Quattro, 1999), and Atlantic croaker (Lankford et al., 1999). None of these studies detected significant genetic heterogeneity among samples collected at different sites within the geographical region spanning from Rhode Island to Chesapeake Bay. For many fish species, the extensive mobility of juveniles and adults coupled with larval dispersal is likely to result in substantial gene flow.

We were unable to reject the null hypothesis of genetic homogeneity among three sites in the northern, middle, and southern portions of the tautog's range but we did not not conclusively prove that tautog in the mid-Atlantic region constitute a single genetic stock. Population structure not resolved by our study might be detected by an examination of additional polymorphisms, with rapidly evolving markers better suited for detecting recent subpopulation divergence. Improved resolution would also be gained by increasing sample sizes; the current analysis with a sample size of 24 individuals per population had limited power (40%) to detect significant heterogeneity among populations with the observed haplotype-frequency distributions. However, it is unlikely that by simply increasing sample sizes with the same set of molecular markers the picture of minimal geographic heterogeneity would alter substantially. If we had found the same haplotype proportions in a study with quadrupled sample sizes ($n$=96 individuals per site), estimates of gene flow (Nm) would still be substantial (Nm=8.6 between RI and DE; 28 for VA–RI; 73 for DE–VA). We conclude that the sampled populations are probably genetically homogeneous, as the result of contemporary or recent gene flow.

In many genetic studies of population structure, PCR amplification of DNA is coupled with a restriction fragment length polymorphism (RFLP) analysis or direct sequencing. Although PCR is relatively simple, the subsequent analyses can become expensive and time-consuming when large numbers of individuals must be evaluated. These drawbacks can be alleviated through the use of mutation detection techniques such as DGGE and DNA heteroduplex mobility assays (Lessa 1992; Grompe, 1993; Lessa and Applebaum, 1993). These methods can be used to compare DNA fragments to determine rapidly which individuals have the same haplotype. Only one representative of each haplotype needs to be further characterized, and large numbers of individuals can be rapidly and efficiently screened. High-resolution DNA screening techniques such as DGGE and heteroduplex analysis provide the sensitivity of DNA sequencing and make it possible to screen greater numbers of individuals for less cost and effort than standard sequencing techniques.

Our study employed a DGGE-heteroduplex assay to screen regions of the mitochondrial and nuclear genomes of the tautog for polymorphisms useful for the analysis of population structure. Both the cytochrome *b* and cytochrome *c* oxidase products, as well as the LDH intron, appeared to be invariant in the tautog samples, raising the question of whether the DGGE-heteroduplex technique was providing the high degree of resolution anticipated.

In order to provide an independent assessment of the DGGE-heteroduplex technique, we examined the cytochrome *b* fragment from eight spot (*Leiostomus xanthurus*), a species that has been shown to have a high genetic diversity in a RFLP analysis of the ATPase 6 and control regions (Lankford et al., 1999), with the same protocol used to evaluate tautog samples. Four to six haplotypes were observed in the eight individuals. It is clear that DGGE-heteroduplex analysis is capable of revealing DNA sequence diversity in amplified mtDNA, as has been reported by other investigators (e.g. Campbell et al. 1995; Michikawa et al. 1997; Tek Kay et al. 1997).

Additionally, this study shows that DGGE-heteroduplex analysis is a powerful technique that makes it possible to screen large numbers of samples and to identify haplotypes that differ by as little as a single nucleotide. The unique tautog cytochrome *b* haplotypes identified by DGGE-heteroduplex analysis result from single base substitutions that would not have been revealed by a RFLP analysis because of the lack of restriction enzyme target sequences spanning the mutation sites.

The low level of genetic variation in the tautog mitochondrial genome suggests that further mtDNA analyses would likely prove to be unsuccessful in delineating tautog population structure. It might be more productive to focus instead on highly variable nuclear DNA sequences such as microsatellite loci, major histocompatibility complex genes, and introns. In addition, more thorough tagging studies and observations of tautog egg and larval transport should prove valuable in determining the amount of exchange among regions within the species range. However, until further studies are undertaken, the null hypothesis that tautog populations between Rhode Island and Virginia constitute a single genetic stock cannot be rejected.

## Acknowledgments

This work was performed in partial fulfillment of the requirements for the M.S. degree at the College of Marine Studies, University of Delaware. We thank John Graves and Timothy Targett for their help in project design, execution, and analysis. Laboratory assistance was kindly provided by Ami Wilbur and Thomas Lankford. This research was funded by NOAA Saltonstall-Kennedy Project NA46FD0329 to PMG.

## Literature cited

**Auster, P. J.**
**1989.** Species profiles: life histories and environmental requirements of coastal fishes and invertebrates (North and Mid-Atlantic)—tautog and cunner. U. S. Fish and Wildlife Service Biological Report 82 (11.105), 13 p.

**Avise, J. C.**
**1992.** Molecular population structure and the biogeographic history of a regional fauna: a case history with lessons for conservation biology. Oikos 63:62–76.
**1994.** Molecular markers, natural history and evolution. Chapman Hall, New York, NY, 511 p.

**Bernatchez, L., and R. G. Danzmann.**
**1993.** Congruence in control-region sequence and restriction-site variation in mitochondrial DNA of brook char (*Salvelinus fontinalis* Mitchell). Mol. Biol. Evol. 10:1002–1014.

**Bernatchez, L., J. J. Dodson, and S. Boivin.**
**1989.** Population bottlenecks: influence on mitochondrial DNA diversity and its effect in coregonine stock discrimination. J. Fish. Biol. 35(A):233–244.

**Bigelow, H. B., and W. C. Schroeder.**
**1953.** Fishes of the Gulf of Maine. Fish. Bull. 77:1–576.

**Borenstein, M., H. Rothstein, and J. Cohen.**
**1997.** Power and precision, release 1.0. Dataxiom Software Inc., Los Angeles, CA, 219 p.

**Bowen, B. W., and J. C. Avise.**
**1990.** Genetic structure of Atlantic and Gulf of Mexico populations of sea bass, menhaden, and sturgeon: influence of zoogeographic factors and life-history patterns. Mar. Biol. 107:371–381.

**Briggs, P. T.**
**1977.** Status of tautog populations at artificial reefs in New York waters and effect of fishing. N.Y. Fish Game J. 24:154–167.

**Brooks, D. A.**
**1996.** Physical oceanography of the shelf and slope seas from Cape Hatteras to Georges Bank: a brief overview. *In* The Northeast shelf system: assessment, sustainability, and management (K. Sherman, N. A. Jaworski, and T. J. Smayda, eds.), p. 47–74. Blackwell Science, Inc., Cambridge, MA.

**Campbell, N. J. H., F. C. Harriss, M. S. Elphinstone, and P. R. Baverstock.**
**1995.** Outgroup heteroduplex analysis using temperature gradient gel electrophoresis: high resolution, large scale, screening of DNA variation in the mitochondrial control region. Mol. Ecol. 3:407–418.

**Colton, J. B., Jr., W.G. Smith, A. W. Kendall, Jr., P. L. Berrien, and M. P. Fahay.**
**1979.** Principal spawning areas and times of marine fishes, Cape Sable to Cape Hatteras. Fish. Bull. 76:911–915.

**Cooper, R. A.**
**1966.** Migration and population estimation of the tautog, *Tautoga onitis* (Linnaeus), from Rhode Island. Trans. Am. Fish. Soc. 95:239–247.

**Cytel.**
**1992.** StatXact for SYSTAT, ver. 1.0. Cytel Software Corp., Cambridge, MA, 358 p.

**Eklund, A.M., and T.E. Targett.**
**1990.** Reproductive seasonality of fishes inhabiting hard bottom areas in the Middle Atlantic Bight. Copeia 1990: 1180–1184.
**1991.** Seasonality of fish catch rates and species composition from the hard bottom trap fishery in the Middle Atlantic Bight (US east coast). Fish. Res. 12: 1–22.

**Graves, J. E., J. R. McDowell, A. M. Beardsley, and D. R. Scoles.**
**1992a.** Stock structure of the bluefish *Pomatomus saltatrix* along the mid-Atlantic coast. Fish. Bull. 90:703–710.

**Graves, J. E., J. R. McDowell, and M. L. Jones.**
**1992b.** A genetic analysis of weakfish *Cynoscion regalis* stock structure along the mid-Atlantic Coast. Fish. Bull. 90:469–475.

**Grompe, M.**
**1993.** The rapid detection of unknown mutations in nucleic acids. Nature Genetics 5:111–117.

**Hare, J. A., and R. K.Cowen.**
**1993.** Ecological and evolutionary implications of the larval transport and reproductive strategy of bluefish *Pomatomus saltatrix*. Mar. Ecol. Prog. Ser. 98:1–16.

**Hedgecock, D.**
**1994.** Temporal and spatial genetic structure of marine

animal populations in the California Current. CalCOFI Rep. 35:73–81.

**Hostetter, E. B., and T. A. Munroe.**
**1993.** Age, growth, and reproduction of tautog *Tautoga onitis* (Labridae: Perciformes) from coastal waters of Virginia. Fish. Bull. 91:45–64.

**Jones, W. J., and J. M Quattro.**
**1999.** Genetic structure of summer flounder (*Paralichthys dentatus*) populations north and south of Cape Hatteras. Mar. Biol. 133:129–135.

**Lankford, T. E., Jr., T. E. Targett, and P. M. Gaffney.**
**1999.** Mitochondrial DNA analysis of population structure in the Atlantic croaker, *Micropogonias undulatus* (Perciformes: Sciaenidae). Fish. Bull. 97:884–890.

**Lessa, E. P.**
**1992.** Rapid surveying of DNA sequence variation in natural populations. Mol. Biol. Evol. 9:323–330.

**Lessa, E. P., and G. Applebaum.**
**1993.** Screening techniques for detecting allelic variation in DNA sequences. Mol. Ecol. 2:119–129.

**Martin, D. L.**
**1993.** Latitudinal growth variation in juvenile and larval *Tautoga onitis* (Pisces: Labridae). M.S. thesis, Univ. Delaware, Newark, DE, 62 p.

**McElroy, D., P. Moran, E. Bermingham, and I. Kornfield.**
**1992.** REAP: the restriction enzyme analysis package, version 4.0. Univ. Maine, Orono, ME, 40 p.

**Meyer, A., J. M. Morrissey, and M. Schartl.**
**1994.** Recurrent origin of a sexually selected trait in *Xiphophorus* fishes inferred from a molecular phylogeny. Nature 368:539–542.

**Michikawa, Y., G. Hofhaus, L. S. Lerman, and G. Attardi.**
**1997.** Comprehensive, rapid and sensitive detection of sequence variants of human mitochondrial tRNA genes. Nucleic Acids Research 12:2455–2463.

**Mrázek, J., and A. Spanova.**
**1992.** ANAGEL. Comput. Appli. Biosci. 8:524.

**Nei, M.**
**1987.** Molecular evolutionary genetics. Columbia Univ. Press. New York, NY, 512 p.

**Nei, M., and J. C. Miller.**
**1990.** A simple method for estimating average number of nucleotide substitutions within and between populations from restriction data. Genetics 125:873–879.

**Olla, B. L., A. J. Bejda, and A. D. Martin.**
**1974.** Daily activity, movements, feeding, and seasonal occurrences in the tautog, *Tautoga onitis*. Fish. Bull. 72: 27–35.

**Olla, B. L., and C. Samet.**
**1977.** Courtship and spawning behavior of the tautog, *Tautoga onitis* (Pisces: Labridae), under laboratory conditions. Fish. Bull. 75:585–599.

**Olla, B. L., A. L. Studholme, A. J. Bejda, and C. Samet.**
**1979.** Seasonal dispersal and habitat selection of cunner, *Tautogolabrus adspersus*, and young tautog, *Tautoga onitis*, in Fire Island Inlet, Long Island, New York. Fish. Bull. 77:255–261.

**Ovenden, J. R.**
**1990.** Mitochondrial DNA and marine stock assessment: a review. Aust. J. Mar. Freshwater. Res. 41:835–853.

**Palumbi, S. R., A. Martin, S. Romano, W. O. McMillan, L. Stice and G. Grabowski.**
**1991.** The simple fool's guide to PCR, version 2.0. Univ. Hawaii, Honolulu, HI, 47 p.

**Park, L.K., M. A. Brainard, D.A. Dightman, and G.A. Winans.**
**1993.** Low levels of intraspecific variation in the mitochondrial DNA of chum salmon (*Oncorhynchus keta*). Molec. Mar. Biol. Biotech. 2:362–370.

**Quattro, J. M., and W. J. Jones.**
**1999.** Amplification primers that target locus-specific introns in actinopterygian fishes. Copeia 99:191–196.

**Shulman, M. J., and E. Bermingham.**
**1995.** Early life histories, ocean currents, and the population genetics of Caribbean reef fishes. Evolution 49:897–910.

**Tek Kay, W., J. M. Cook, D. J. Rowe, and R. H. Crozier.**
**1997.** Migration between nests in the Australian arid-zone ant *Rhytidoponera* sp. revealed by DGGE analyses of mitochondrial DNA. Molecular Ecology 6:403–411.

**Victor, B. C.**
**1986.** Duration of the planktonic stage of one hundred species of Pacific and Atlantic wrasses (family Labridae). Mar. Biol. 90:317–326.

# Age and growth of dolphinfish, *Coryphaena hippurus*, off Puerto Rico

**Glauco A. Rivera**

**Richard S. Appeldoorn**

Department of Marine Sciences
University of Puerto Rico
Mayagüez, Puerto Rico 00681-9013

E-mail address (for R. S. Appeldoorn, contact author): R_Appeldoorn@rumac.upr.clu.edu

**Abstract.**—Dolphinfish, *Coryphaena hippurus*, off Puerto Rico were sampled over an 8-month period to study age and growth from daily increments recorded in the sagittae. A total of 121 otoliths were analyzed. Growth was rapid and nonlinear. No significant differences in growth rate were observed based on sex or on location of capture (north or south coast). The von Bertalanffy growth parameters were $L_\infty$ = 1457 mm *FL*, $K$ = 2.19/yr, and $t_0$ = –0.046 yr. With these values, extrapolated growth over the first year averaged 3.6 mm FL/day. An existing hypothesis of two separate stocks (north and south) in the vicinity of Puerto Rico predicts that fish from the north coast caught primarily in the winter would show a much slower growth rate than fish from the south coast caught primarily in the spring. The absence of growth differences between coasts does not match this prediction; however previous growth estimates for the northern stock may have been underestimated. On the basis of these results, the stock structure and migration pattern of dolphinfish are likely to be more complicated than originally postulated.

Manuscript accepted 26 November 1999.
Fish. Bull. 98:345–352 (2000).

The dolphinfish, *Coryphaena hippurus* L., is a pelagic and migratory fish, distributed worldwide throughout tropical and subtropical waters (Gibbs and Collette, 1959; Shcherbachev, 1973). Migrating stocks support important sport and commercial fisheries. In the northwestern Atlantic they are fished off North Carolina (Rose and Hassler, 1968), Florida (Beardsley, 1967), in the Gulf of Mexico (Gibbs and Collette, 1959), off Puerto Rico (Erdman, 1956; Pérez and Sadovy, 1996), off the U.S. Virgin Islands and the Windward Islands (Mahon et al., 1981), and off Barbados (Oxenford and Hunte, 1986).

Age and growth for dolphinfish have been studied in detail by Beardsley (1967), Rose and Hassler (1968), Wang (1979), Oxenford and Hunte (1983), Uchiyama et al. (1986), and Bentivoglio (1988). No such studies have been conducted for fish off Puerto Rico. For the Caribbean region, the most relevant studies are those of Beardsley (1967), off Miami, and Oxenford and Hunte (1983) in Barbados. Beardsley (1967), using annuli on scales, found dolphinfish distributed among five age groups: 379 in group 0, 121 in group I, 9 in group II, 1 in group III, and 1 in group IV. In that study, the mean growth rate in the first year was 1.82 mm SL/day. Oxenford and Hunte (1983) assumed daily increment formation in the otolith and obtained a linear growth rate of 4.71 mm SL/day for all fish. The rate for adult fish (±700 mm SL) was 1.43 mm SL/day. Oxenford and Hunte's assumption of daily increment formation was validated indirectly by comparing their estimated growth rates to modal progression in length frequency distributions; their study was subsequently validated directly by Uchiyama et al. (1986) in a study of Hawaiian dolphinfish. Determination of age from annuli has not been validated and remains subjective.

Dolphinfish have sexually dimorphic growth; older male fish show an enlargement of the forehead (Schuck, 1951; Lozano-Cabo, 1961). Oxenford (1985) and Uchiyama et al. (1986) reported differences in the growth rate in length between sexes, but other studies have reported growth as a combination of both sexes; specifically, Rose and Hassler (1968) found no differences in length at age between males and females.

Oxenford and Hunte (1986) proposed a migration circuit in the western Central Atlantic for two separate northern and southern stocks (Fig. 1). One stock is located southeast, and the other northwest, of Puerto Rico and the Virgin Islands. Abundance of dolphinfish in Puerto Rico peaks from November to January and again (albeit to a lesser degree) from April to June (Pérez and Sadovy, 1996). The U.S. Virgin Islands also has a bimodal distribution in abundance, with a large peak in April–May and small

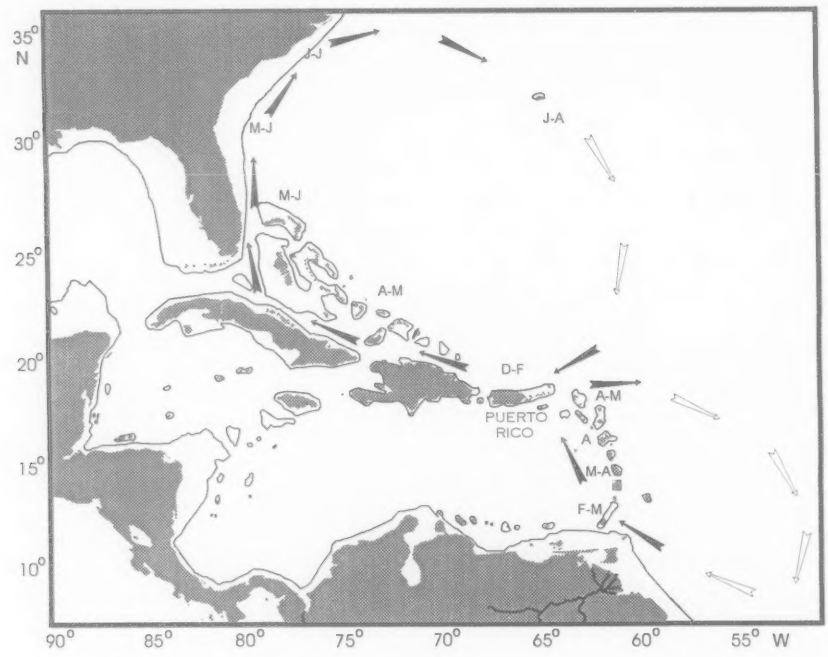


**Figure 1**

Proposed migration circuits for northern and southern stocks of dolphinfish, *Coryphaena hippurus*. Solid arrows indicate proposed migration route, open arrows indicate proposed migration route where catch data are not available. Letter symbols indicate months of peak catch. Redrawn from Oxenford and Hunte (1986).

peak in November. Assuming the migration circuit of the two-stock hypothesis (Oxenford and Hunte, 1986), we interpret the major peak in Puerto Rico as coinciding with the presence of the northern stock, whereas the minor peak coincides with the appearance of the southern stock in the Virgin Islands. The two-stock hypothesis is based on three main observations. First, there are differences in life-history parameters between dolphinfish from the southeast United States (North Carolina and Florida) and those from Barbados. Southern dolphinfish grow faster, attain sexual maturity at a larger size, have lower fecundity for size, and have smaller eggs than northern dolphinfish (Oxenford and Hunte, 1986). Second, the gene flow between both groups is slight. The difference in allele frequencies of the IDH-2 locus in heart extracts and in phenotypic frequencies at the IDH-2,3 loci in liver extracts indicates infrequent breeding between the stocks (Oxenford and Hunte, 1986). Third, the seasonality of catch between regions is different (Oxenford and Hunte, 1986). Because Puerto Rico lies along the boundary for the two proposed stocks, it is an ideal location to test the two-stock hypothesis.

The purpose of our study was to determine age and growth of dolphinfish in Puerto Rico. Comparison of growth rates between Puerto Rico and other areas (Florida, Barbados) was used to test the two-stock hypothesis. Of specific interest was the comparison of growth between fish from the north and fish from the south coasts. All fish from the north coast were caught during the period when abundance first peaked, whereas 92% of the fish from the south coast were caught during the period of the second peak in abundance.

## Materials and methods

Dolphinfish were collected from sportfishing tournaments and commercial fishing villages from September 1991 to April 1992. Twelve dolphin tournaments were held in Puerto Rico, five on the north coast and seven on the south coast. Fifteen billfish tournaments were visited for additional samples. Purchased fish or fish heads supplemented samples when necessary. Fish were caught by trolling lines. Data on date and site of collection, standard, fork, and total lengths,

weight, and sex were recorded. All fish were measured to the nearest millimeter and weighed to the nearest 50 grams. Heads were separated from the body at the site of collection and kept frozen.

The removal and preservation of otoliths followed the methods of Panella (1980) and Brothers (1987). A sagittal (longitudinal) cut through the midline of the frozen head was made with an electric band saw. Under a dissection microscope, sagittae were removed from the sacculi and extraneous tissue was removed. Sagittae were used owing to their relatively larger size in comparison with the lapillus and asteriscus. Each pair of sagittae was stored in glycerin for clearing in labeled vials.

Examination of external otolith microstructure was used to determine age (Panella, 1971). Sagittae were placed on glass slides in glycerin. Otolith structure was examined and the radius measured under a compound light microscope with transmitted light at 200×. Translucent and opaque lines were counted following the procedure of Oxenford and Hunte (1983). Otolith rings were assumed to be daily lines (Uchiyama et al., 1986) and were counted from the focus to the edge of the posterior rostrum.

All otoliths were read twice at random. If there was any difference in reading (10% or more), the otolith was discarded. A subsample of ten otoliths was sent to Hazel Oxenford (Bellairs Research Institute of McGill University, in Barbados) for additional reading and verification of counts. Otoliths were sent in coded vials with no information about length, weight, or sex. Fish length, from which otoliths were sent, ranged from 630 mm FL to 1325 mm FL.

The relation between fish fork length and daily increment of the sagittae was determined with a predictive linear regression of length on number of rings (Ricker, 1975, Francis, 1990). Following Oxenford and Hunte (1983) and Bentivoglio (1988), growth rates were calculated from the linear regressions and reported as mm/day. Analyses were done by coast (north and south) and by sex (male and female). Differences between growth-rate estimates were compared by using a homogeneity of slopes test (ANOVA) (Sokal and Rohlf, 1981).

For a more realistic representation of growth, age-length data were also modeled by using the von Bertalanffy growth function,

$$l_t = L_\infty\left(1-e^{-k(t-t_0)}\right),$$

where $l_t$ = length (mm) at time $t$ (years);
$L_\infty$ = asymptotic length;
$k$ = the growth coefficient; and
$t_0$ = the hypothetical age at which length equals zero.

Parameters were estimated by a nonlinear regression with SYSTAT (Wilkinson, 1987).

## Results

A total of 170 dolphinfish were collected during the eight-month sampling period. From this total, 80 were captured off the north coast and 90 were captured off the south coast. The size range from the south coast was broader than that from the north: north = 475 mm FL (1.25 kg) to 1283 mm FL (18.50 kg); south = 381 mm FL (0.70 kg) to 1479 mm FL (25.00 kg); in addition, the largest fish were found on the south coast. From the total sample, 55 were male and 115 were female. Males were slightly larger than females: males = 630 mm FL (2.50 kg) to 1479 mm FL (25.00 kg); females = 381 mm FL (0.07 kg) to 1283 mm FL (19.75 kg).

The relation between standard length (SL) and fork length (FL) was linear and expressed by the equation

$$SL = -1.37 + 0.92\,FL \qquad (r=0.99).$$

The relation between the logarithms of fish weight ($W$) and fork length was linear and expressed by the equation

$$\log W = -4.42 + 2.78 \log FL \qquad (r=0.98).$$

Otoliths were collected from 22 males and 38 females from the north coast, and from 21 males and 40 females from the south coast. Otoliths were not collected from all fish owing to difficulties in making the longitudinal cut through the head, to breakage during dissection, or to loss during extraction from the cranial tissue. Thus, for the age and growth determinations, fork lengths ranged on the north coast from 746 mm FL to 1283 mm FL for males and from 475 mm FL to 1222 mm FL for females. Males on the south coast ranged from 625 mm FL to 1325 mm FL, and females ranged from 550 mm FL to 1275 mm FL.

Examination of the external structure of the otolith showed clear growth increments. On large otoliths, increments tended to be tightly spaced on the edge of the rostrum. Reading daily increments in this area was difficult owing to poor resolution even after clearing in glycerin; however, independent readings by Oxenford were within 10%. The oldest individual had 336 increments.

Figure 2 shows the length and number of otolith increments for all fish. Linear growth rate was 2.52 mm FL/day for all fish (Table 1, Fig. 2). Differences in linear growth rates by sex or coast (Table 1) were not

significant. For the comparison by sex, however, the test approached significance, with $P$=0.138. Given the variability in data, the power of this test was probably low. Furthermore, growth was clearly nonlinear and decreased over time. To reach a size of 600 mm FL in 100 days, cumulative growth would have to be 6 mm FL/day. The maximum observed cumulative growth rate was 9.5 mm FL/day for a fish of 1303 mm FL and 137 increments. On average, fish of 110–150 days grew 3.3 mm FL/day, those 170–220 days old grew 2.9 mm FL/day and those 230–270 days of age grew 2.1 mm FL/day. Parameter values for the von Bertalanffy model (Fig. 2) are shown in Table 2. It was not possible to fit the model to the data sorted by both coast and sex, owing to reduced sample size in relation to large amount of variance. Differences between sexes were the greatest, and the confidence limits on $k$ indicated statistical significance would occur at a $P$-value of approximately 0.06. Extrapolation of the von Bertalanffy equation for all individuals predicted a cumulative growth rate of 3.59 mm FL/day over the first year.

**Table 1**

Summary of results for linear regressions of sagittal rings on fork length. All = all aged fish, M = male, F = female, N = north coast, S = south coast, $n$ = number of fish. $r$ = coefficient of correlation.

| Group | Slope | (SE) | Intercept | (SE) | $r$ | $n$ |
|---|---|---|---|---|---|---|
| All | 2.52 | (0.26) | 497 | (141) | 0.66 | 121 |
| MN | 2.14 | (0.67) | 535 | (134) | 0.58 | 22 |
| FN | 2.35 | (0.46) | 493 | (130) | 0.65 | 38 |
| MS | 2.23 | (0.72) | 641 | (144) | 0.58 | 21 |
| FS | 2.34 | (0.45) | 535 | (142) | 0.64 | 40 |
| N | 2.28 | (0.37) | 506 | (129) | 0.63 | 60 |
| S | 2.37 | (0.39) | 558 | (146) | 0.62 | 61 |
| M | 2.54 | (0.50) | 518 | (148) | 0.62 | 43 |
| F | 2.46 | (0.31) | 493 | (136) | 0.67 | 78 |

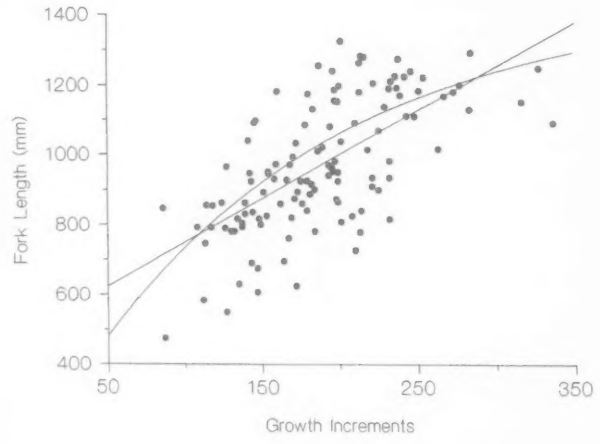


**Figure 2**

Relation between fork length and number of sagittal rings for dolphinfish from Puerto Rico. Straight line indicates linear growth over all fish. Curved line indicates growth according to the von Bertalanffy model (see text).

## Discussion

All linear growth rates for dolphinfish (Table 1) were greater than those reported by Beardsley (1967) and Rose and Hassler (1968) (Table 3). However, use of linear growth estimates is justified largely by the high variability observed in fork lengths for a given age; high variability masks any underlying growth pattern, thus making a linear model the simplest and most parsimonious, but not necessarily the most realistic model. A better approach is to use a biologically realistic model, in this case the von Bertalanffy model. The resulting parameters of the von Bertalanffy model for the Puerto Rico data are consistent with the known biology of dolphinfish. Asymptotic lengths were in accord with known maximum lengths, values of $t_0$ were very close to zero, even though they represented extrapolations of three months (=25% of maximum age observed), and growth coefficients were high. Growth rates predicted for dolphinfish from these equations give a different picture from those provided by the linear model. For all fish, growth averaged over 1 year was 3.59 mm FL/day (3.31 mm SL/day); growth averaged over the first 6 months was 5.57 mm FL/day (5.13 mm SL/day). These rates are comparable to the higher values reported in Table 3.

Growth rates for dolphinfish reported from previous studies (Table 3) are of questionable value when they lack uniformity in length units and in the time over which growth is evaluated, when growth is not portrayed accurately, and when the size for which growth is reported is unclear. The use of the von Bertalanffy growth function allows standardization for comparison of growth. Parameters for the von Bertalanffy model were calculated for four previous studies in which length-at-age data were reported (Table 4). Comparisons using $\Phi'$ (=log$K$ + 2log$L_\infty$), the growth performance index of Pauly and Munro (1984), suggests

**Table 2**

Von Bertalanffy growth parameters ($L_\infty$ = asymptotic length, $K$ = growth coefficient, $t_0$ = length at age = 0) and standard errors (in parentheses) calculated from captured dolphinfish. $n$ = number of fish.

| Group | $n$ | $L_\infty$ (mm FL) | $K$ (per yr) | $t_0$ (yr) |
|---|---|---|---|---|
| All fish | 121 | 1457 (59) | 2.19 (<0.365) | −0.046 (0.037) |
| North coast | 60 | 1289 (66) | 2.19 (<0.365) | −0.090 (0.054) |
| South coast | 61 | 1493 (69) | 2.19 (<0.365) | −0.006 (0.046) |
| Male | 43 | 1380 (92) | 2.55 (0.365) | 0.023 (0.064) |
| Female | 78 | 1506 (79) | 1.82 (<0.365) | −0.087 (0.048) |

**Table 3**

Estimated growth rates (mm/day) for *Coryphaena hippurus* at various locations. $n$ = number of fish, P = period of sampling in months (adapted from Oxenford and Hunte, 1983; and Bentivoglio, 1988).

| Location | $n$ | P | Aging method | Growth rate | Reference |
|---|---|---|---|---|---|
| Gulf of Mexico | 19 | 5 | otolith count | 0.49 SL | Bentivoglio, 1988 for fish >900 mm FL |
| North Carolina | 26 | 3 | days known | 1.07 TL | Hassler and Rainville, 1975 |
| Barbados | 25 | 18 | otolith count | 1.43 SL | Oxenford and Hunte, 1983 for fish 700–1100 mm SL |
| North Carolina | 593 | 3 | scale annuli | 1.64 SL | Rose and Hassler, 1968 |
| Straits of Florida | 121 | 12 | scale annuli | 1.82 SL | Beardsley, 1967 |
| Taiwan | ? | 19 | modal progression | 2.96 SL | Wang 1979 |
| Hawaii | 7 | 6 | days known | 2.82 SL | Uchiyama et al., 1986 |
| | 11 | 14 | otolith count | 3.19 SL | |
| Florida | ? | ? | days known | 3.03 SL | Schekter, personal commun. in Oxenford and Hunte, 1983 |
| Puerto Rico | 121 | 8 | otolith count | 3.31 SL | Our study |
| Hawaii | 94 | 2–3 | days known | 3.56 SL | Hagood et al., 1981 |
| Gulf of Mexico | 81 | 5 | otolith count | 3.88 SL | Bentivoglio, 1988 |
| Barbados | 50 | 18 | otolith count | 4.71 SL | Oxenford and Hunte, 1983 |
| Florida Marineland | 2 | ? | days known | 4.80 SL | Herald, 1961 |
| Miami Seaquarium | 1 | ? | days known | 5.28 SL | Beardsley, 1971 |
| North Carolina | 30 | 1–2 | days known | 5.88 SL | Hassler and Hogarth, 1977 |

**Table 4**

Von Bertalanffy growth parameters calculated for dolphinfish from previous studies. $\Phi' = \text{Log}(K)+2\text{Log}(L_\infty)$.

| Location | $L_\infty$ (mm FL) | $K$ (per yr) | $\Phi'$ | Reference |
|---|---|---|---|---|
| North Carolina | 1733 | 0.31 | 5.59 | Rose and Hassler, 1968 |
| Straits of Florida | 1650 | 0.68 | 6.27 | Beardsley, 1967 |
| Gulf of Mexico | 1427 | 3.13 | 6.80 | Bentivoglio, 1988 |
| Puerto Rico | 1457 | 2.19 | 6.67 | Our study |
| Barbados | 1436 | 2.87 | 6.77 | Oxenford and Hunte, 1983 |

that dolphinfish in North Carolina and Florida grow more slowly than in the Gulf of Mexico, Puerto Rico ($\Phi'$=6.67), and Barbados, or that values of $K$ in the northern areas are underestimated (Table 4). These slower growth rates are derived from unvalidated studies of scales. Furthermore, the age at the time of first annulus formation may be significantly less than one year, depending on the difference between

the period of annulus formation (presumably in winter) and the spawning season. It is distinctly possible that otolith studies in these areas might show significantly faster growth and younger fish. This possibility is also raised by the rapid growth rates of dolphinfish from these areas when maintained in aquaria (Herald, 1961; Beardsley, 1971; Hassler and Hogarth, 1977), which are among the highest reported (Table 3).

The two-stock hypothesis of Oxenford and Hunte (1986) predicts that fish sampled off Puerto Rico from November to March (north coast fish) should show distinctly different growth rates from fish sampled from March to May (south coast fish). However, no such differences were found, and in general growth rates were similar to those reported for the proposed southern stock (Oxenford and Hunte, 1983). Figure 3 shows that most fish sampled may have belonged to a single cohort whose distribution shifted over time. The size differences between fish from the north coast (primarily January–February) and those from the south coast (March–April) can be explained by growth over the 8-month sampling period. There is an influx of small fish in April off the south coast; the growth rates of these fish are equal to those of the rest of the sample. Although these fish may represent the appearance of a different (e.g. southern) stock, an equally likely explanation is that they represent the entry of a new cohort. Dolphinfish are known to spawn several cohorts over the year (Beardsley, 1967; Oxenford, 1985; Pérez and Sadovy, 1996), and a similar appearance of small fish occurs off Barbados in June, where only one stock is hypothesized. Annual length-frequency data from the south coast of Puerto Rico (Fig. 4 in Pérez and Sadovy, 1996) show considerable variation in the most abundant size class landed (from 800–1100 mm FL), which may reflect variations in the relative strengths of the two cohorts.

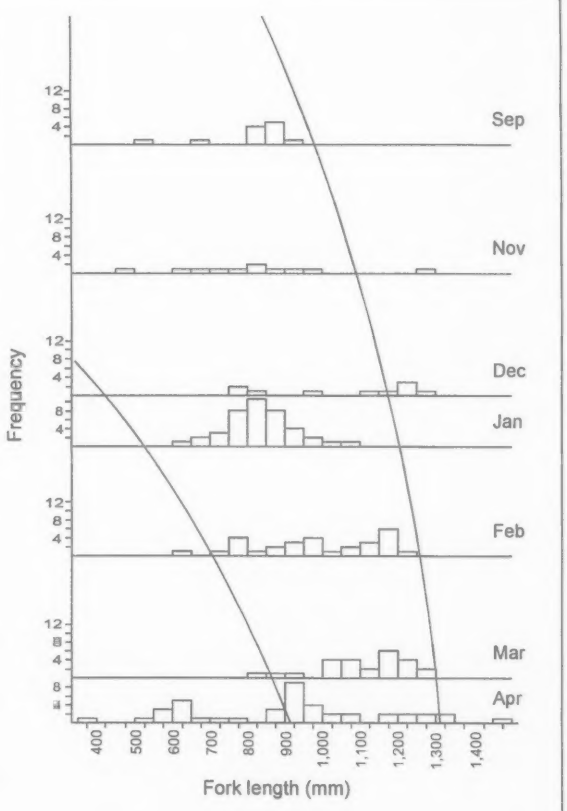


**Figure 3**

Length-frequency distributions of dolphinfish from Puerto Rico by month. Vertical position of the horizontal axes represents the mean sampling date for each month. Curves indicate the von Bertalanffy growth rate estimated from otoliths and are positioned to indicate the main cohort of fish sampled.

These observations do not necessarily negate the two-stock hypothesis if, as postulated above, growth rates for northern dolphinfish are much greater than previously reported. In addition to growth rate, the hypothesis is also based on differences in other life-history parameters, but more recent studies cast doubt on the significance of most of these. Data in Pérez et al.[1] show trends in several parameters related to reproduction. Both the range and mean size of mature oocytes show a gradual increase in fish from Florida, Puerto Rico, and Barbados, although sizes were identical for the north and south coasts of Puerto Rico. A trend of increasing slope among length-fecundity relationships was also evident.[1] Length of minimum maturity in females also increased along the same gradient, from 324 SL mm for Florida (Beardsley, 1967), 400 mm FL (369 mm SL) for Puerto Rico,[1] to 610 mm SL for Barbados (Oxenford and Hunte, 1986). These results, however, could equally be interpreted as representing a cline, as opposed to data for distinct stocks (Mahon and Mahon, 1987). Genetic data showing differences is based on the extremes of the distribution (Florida, Barbados) and thus cannot be used to interpret what occurs at a mid location such as Puerto Rico.

[1] Pérez, R. N., A. Román, and G. A. Rivera. 1992. Investigation of the reproductive dynamics and preliminary evaluation of landings data of the dolphinfish *Coryphaena hippurus*, L. Puerto Rico Department of Natural Resources, Puerto Rico Fisheries Research Laboratory, P.O. Box 3665, Mayaguez, Puerto Rico 00680. Final Report D-J F26-1, 95 p.

Furthermore, the perceived movements of dolphinfish in the vicinity of Puerto Rico is complex. In Puerto Rico, fish generally are caught in abundance first on the north coast and then on the south coast. Fish are caught in the Mona Passage on the west side of Puerto Rico but not off the east coast over the Puerto Rican–Virgin Islands shelf.[1] Off the U.S. Virgin Islands there is a bimodal distribution of catch over time similar to that for Puerto Rico. For recreational boats operating out of St. Croix, increases in catch rates, particularly in the spring are first observed to the southeast, then move progressively closer to St. Croix and then St. Thomas-St. John.[2] The implied direction of movement is from southeast to northwest, opposite to that predicted by the two-stock hypothesis. The temporal distribution of dolphinfish along the southeast coast of the Dominican Republic is similar to that off the south coast of Puerto Rico,[3] but in contrast, off the southwest coast, dolphinfish catch rates show a single sharp peak in the month of November.[4] In agreement with Mahon and Mahon (1987), the real stock structure and migration pattern of dolphinfish are likely to be more complicated than originally proposed, a point well appreciated by Oxenford and Hunte (1986).

## Acknowledgments

Data collection was aided by M. Figuerola, R.N. Pérez, and A.M. Román of the Fisheries Research Laboratory, Puerto Rico Department of Natural and Environmental Resources, and by the Puerto Rico sportfishing community. We thank H. Oxenford for her help and willingness to verify otolith counts. D.A. Hensley and V. Vicente gave valuable criticism.

## Literature cited

**Beardsley, G. L., Jr.**
**1967**. Age, growth and reproduction of the dolphin, *Coryphaena hippurus*, in the Straits of Florida. Copeia 1967: 441–451.
**1971.** Dolphin spectacular. Sea Front. 17:194–201.

**Bentivoglio, A. A.**
**1988**. Investigations into the growth, maturity, mortality rates and occurrence of the dolphin (*Coryphaena hippurus*, Linnaeus) in the Gulf of Mexico. M.S. thesis, Univ. College of North Wales, Bangor, United Kingdom, 37 p.

**Brothers, E. B.**
**1987**. Methodological approaches to the examination of otoliths in aging studies. *In* Age and growth of fish (R. C. Summerfelt and G. E. Hall, eds.), p. 319–330. Iowa State Univ. Press, Ames, IA.

**Erdman, D. S.**
**1956**. Recent fish records from Puerto Rico. Bull. Mar. Sci. Gulf Caribb. 6(4):315–340.

**Francis, R. I. C. C.**
**1990**. Back calculation of fish length: a critical review. J. Fish Biol. 36:883–902.

**Gibbs, R. H., and B.B. Collette.**
**1959**. On the identification, distribution, and biology of the dolphins, *Coryphaena hippurus* and *C. equiselis*. Bull. Mar. Sci. Gulf Caribb. 9(2):117–152.

**Hagood, R. W., G. N. Rothwell, M. Swafford, and M. Tosaki.**
**1981**. Preliminary report on the aquacultural development of the dolphin fish, *Coryphaena hippurus* (Linnaeus). J. World Maricul. Soc. 12(1):135–139.

**Hassler, W. W., and W. T. Hogarth.**
**1977**. The growth and culture of dolphin (*Coryphaena hippurus*) in North Carolina. Aquaculture 12:115–122.

**Hassler, W. W., and R. P. Rainville.**
**1975**. Techniques for hatching and rearing dolphin, *Coryphaena hippurus*, through larvae and juvenile stages. Univ. North Carolina, Sea Grant Program Publ. UNC-SG-75-31, 16 p.

**Herald, E. S.**
**1961**. Living fishes of the world. Doubleday, Garden City, NY, 304 p.

**Lozano-Cabo, F.**
**1961**. Biometría, biología y pesca de la Lampuga (*Coryphaena hippurus* L.) de las islas Baleares. Memorias de la Real Academia de Ciencias Exactas, Físicas y Naturales de Madrid. Serie de Ciencias Naturales, tomo XXI, 93 p.

**Mahon, R., W. Hunte, H. Oxenford, K. Storey, and F. E. Hastings.**
**1981**. Seasonality in the commercial marine fisheries of Barbados. Proc. Gulf Caribb. Fish. Inst. 34:28–37.

**Mahon, R., and S. Mahon.**
**1987**. Seasonality and migration of pelagic fishes in the eastern Caribbean. *In* Report and proceedings of the expert consultation on shared fishery resources of the Lesser Antilles region (R. Mahon, ed.), 192–273 p. Mayagüez, Puerto Rico. 8–12 September 1986. FAO Fish. Rep. 383.

**Oxenford, H. A.**
**1985**. Biology of the dolphin *Corhphaena hippurus* and its implications for the Barbadian fisheries. Ph.D. diss., Univ. West Indies, Cave Hill, Barbados, 366 p.

**Oxenford, H. A., and W. Hunte.**
**1983**. Age and growth of dolphin, *Coryphaena hippurus*, as determined by growth rings in otoliths. Fish. Bull. 81(4): 906–909.
**1986**. A preliminary investigation of the stock structure of the dolphin, *Coryphaena hippurus*, in the western central Atlantic. Fish. Bull. 84(2):451–459.

**Panella, G.**
**1971**. Fish otoliths: daily growth layers and periodical patterns. Science (Wash. D.C.) 173:1124–1127.
**1980**. Methods of preparing fish sagittae for the study of growth patterns. *In* Skeletal growth of aquatic organisms: biological records of environmental change (D. C. Rhoades and R. A. Lutz, eds.), p. 619–624. Plenum Press, New York, NY.

**Pauly, D., and J. L. Munro.**
**1984**. Once more on growth comparisons in fish and invertebrates. Fishbyte 2(1):21.

[2] Adams, A. 1997. Virgin Islands Division of Fish and Wildlife, 101 Estate Nazareth, St. Thomas, USVI 00802. Personal commun.

[3] Felix, E. 1998. Office of the Navy, Santo Domingo, Dominican Republic. Personal commun.

[4] Colom, R. 1995. PROPESCAR-SUR, Apartado 120, Barahona, Dominican Republic. Personal commun.

**Pérez, R. N., and Y. Sadovy.**
**1996**. Preliminary data on the reproductive dynamics and landing records of *Coryphaena hippurus* L., in Puerto Rico. Proc. Gulf Caribb. Fish. Inst. 44:651–670.

**Ricker, W. E.**
**1975**. Computations and interpretations of biological statistics of fish populations. Bull. Fish. Res. Board Can. 191, 382 p.

**Rose, C. D., and W. W. Hassler.**
**1968**. Age and growth of the dolphin, *Coryphaena hippurus* (Linnaeus), in North Carolina waters. Trans. Am. Fish. Soc. 97:271–276.

**Schuck, H. A.**
**1951**. Notes on the dolphin (*Coryphaena hippurus*) in North Carolina waters. Copeia 1951:35–39.

**Shcherbachev, Y. N.**
**1973**. The biology and distribution of the dolphins (Pisces, Coryphaenidae). J. Ichthyol. 13:182–191.

**Sokal, R. R., and F. J. Rohlf.**
**1981**. Biometry, 2nd ed. W. H. Freeman, San Francisco, CA, 859 p.

**Uchiyama, J. H., R. K. Burch, and S. A. Kraul.**
**1986**. Growth of dolphins, *Coryphaena hippurus* and *C. equiselis*, in Hawaiian waters as determined by daily increments in otoliths. Fish. Bull. 84:186–191.

**Wang, C. H.**
**1979**. A study of population dynamics of dolphin fish (*Coryphaena hippurus*) in waters adjacent to eastern Taiwan. Acta Oceanogr. Taiwan 10:233–251.

**Wilkinson, L.**
**1987**. SYSTAT: the system for statistics. SYSTAT Inc., Evanston, IL.

# Molecular identification and description of pelagic young of the rockfishes *Sebastes constellatus* and *Sebastes ensifer*

**Axayácatl Rocha-Olivares**
Scripps Institution of Oceanography
University of California San Diego
9500 Gilman Dr., La Jolla, California 92093-0208
Present address: Louisiana State University
Department of Biological Sciences
508 Life Sciences Building
Baton Rouge, Louisiana 70809-1715
E-mail address: arocha@lsu.edu

**H. Geoffrey Moser**

**Jason Stannard**
La Jolla Laboratory
Southwest Fisheries Science Center
National Marine Fisheries Service, NOAA
P.O. Box 271, La Jolla California 92038

**Abstract.**–Five rockfish juveniles (15.0–30.4 mm SL) collected in midwater trawls from offshore banks off the coast of California were identified by using a combination of morphological and molecular characters. All had pigment patterns consistent with members of the subgenus *Sebastomus*, but each required the use of molecular markers for species identification. Using DNA sequence data from the mitochondrial cytochrome *b*, we identified the juveniles as a transforming larva of *Sebastes constellatus* and a transforming larva and three pelagic juveniles of *S. ensifer*. We provide detailed descriptions of the specimens and compare our results with the developmental stages of other species of *Sebastes* of the subgenus *Sebastomus*. We found some differences in structure and pigmentation that might allow identification of these young stages by traditional means, but more descriptive work is necessary. The use of molecular tools can thus be successfully used to complement traditional identification efforts to solve problems unassailable by morphological and pigment characters alone.

Manuscript accepted 28 September 1999.
Fish. Bull. 98:353–363 (2000).

Live-bearing rockfishes of the genus *Sebastes* constitute the largest genus of scorpaeniform fishes with about 110 species worldwide, 72 of which reside in the Northeast Pacific (Eschmeyer and Herald, 1983; Kendall, 1991; Nelson, 1994). In this geographic region, rockfishes are very important in the bottom trawl fishery as well as in recreational fisheries (Lenarz, 1986; Leet et al., 1992; Low, 1993). Newborn rockfishes are extruded as first-feeding larvae from viviparous females (Yoklavich and Boehlert, 1991), and they rank among the most frequent and abundant of all fish larvae in plankton collections off the coasts of California and Oregon (Moser et al., 1993; Moser, 1996; Doyle[1]). The juvenile stages of *Sebastes* are also important ecologically as prey of larger fishes and birds (Love et al., 1991; Moser and Boehlert, 1991; Ainley et al., 1993). In addition to their biological significance, rockfish larvae and early juveniles have received much attention for their potential use in estimating spawning biomass and recruitment (Moser and Butler, 1987; Hunter and Lo, 1993; Ralston and Howard, 1995).

Species identification has been the most challenging aspect in the study of the early life history stages of *Sebastes*. For instance, of the 59 species distributed in the California Cooperative Oceanic Fisheries Investigations (CalCOFI) region, complete developmental series are available for only thirteen and partial series are available for an additional eight (Moser, 1996). Several factors have influenced this lack of a complete developmental series, including a very large number of sympatric species, the preponderance of small larvae, and the limited number of taxonomic characters identifiable in the early stages (Sakuma and Laidig, 1995; Moser, 1996; Moser et al., 1977). Alternative methods involving the analysis of electrophoretic patterns or DNA

[1] Doyle, M. 1992. Patterns in distribution and abundance of ichthyoplankton off Washington, Oregon, and northern California (1980–1987). U.S. Dep. Commer., NOAA NMFS Alaska Fish. Sci. Center Process Report 92-14, 344 p.

have been proposed to overcome this obstacle (e.g. Seeb and Kendall, 1991; Rocha-Olivares, 1998b). In our paper we describe new developmental stages of two species of *Sebastes* identified using mitochondrial DNA (mtDNA) sequence data.

## Materials and methods

### Sample collection

Specimens were collected in the vicinity of Tanner (32°69'N119°12'W) and Cortes (32°61'N119°33'W) Banks in August 1995 during a rockfish sampling cruise aboard the Scripps Institution of Oceanography RV *Robert Gordon Sproul*. Four specimens were sampled in oblique tows with a 5-$m^2$ Isaacs-Kidd midwater trawl. The fifth specimen was retrieved, intact, from the digestive tract of an adult greenspotted rockfish, *Sebastes chlorostictus*, caught with hook and line. Fish were preserved in 95% ethanol. Except for one specimen that completely dried out upon evaporation of the preserving fluid, the shrinkage effect of ethanol preservation on the length of the specimens has been assumed to be negligible owing to their relatively large size (15.0–30.4 mm SL, Radtke, 1989). The dehydrated specimen was rehydrated in water before description.

### Molecular analyses

Total genomic DNA was extracted and purified from liver or muscle tissue with a GlasPac/GS (U.S. National Scientific Supply CO., San Rafael, CA) DNA purification kit as described in Rocha-Olivares (1998b). Universal primers, and versions customized for *Sebastes*, were used for the polymerase chain reaction (PCR) and automated cycle sequencing (see Rocha-Olivares, 1998a for a complete list of primers). A region spanning 781 base pairs (bp) of the mitochondrial cytochrome *b* (cyt-*b*) was amplified by PCR as described in Rocha-Olivares et al. (1999a). Briefly, 50-mL reactions were performed following Kocher et al. (1989), with 100 ng of genomic DNA and 2 units of Taq DNA polymerase (Perkin Elmer Cetus, Foster City, CA, or Gibco BRL, Rockville, MD). Thermal cycling was performed as follows: hot start at 90°C for 2 min., followed by 36 cycles of 50 s at 94°C; 2 min at 51°C; 1.5 min at 72°C, and a final extension of 3 min at 72°C to ensure complete amplification of products. PCR products were purified with microconcentrators (Microcon® 100, Millipore, Bedford, MA) or purification columns (QIAquick® 250, Qiagen, Valencia, CA) following manufacturers' protocols. Automated DNA sequencing was performed with ABI PRISM (Perkin Elmer Cetus) DyeDeoxy® dRhodamine chemistry on an ABI 377 DNA sequencer in 12 µL reactions (30–100 ng double stranded PCR product, 3 pmol primer, 1.6–2.0 µL terminator ready reaction mix); cycle sequencing annealing was 10 seconds at 55°C; we followed the manufacturer's protocol in respect to all other experimental conditions. Sequence data were obtained by sequencing both DNA strands of the PCR products.

### Molecular identification

The mtDNA data from the unknown pelagic young was aligned with a database of orthologous sequences obtained from adult specimens of congeneric species generated at the genetics and physiology laboratory of the Southwest Fisheries Science Center in La Jolla (Rocha-Olivares, 1998a).[2] Because the morphological and pigmentation patterns of the specimens revealed that they belonged to the subgenus *Sebastomus* (Chen, 1971; 1975), the DNA sequence data were compared to 89 sequences obtained from all 15 species of this subgenus (Rocha-Olivares et al., 1999a; 1999c). Species identification was determined on the basis of the most similar haplotype among the species compared. Sequence comparisons were carried out by using pair-wise measures of sequence divergence calculated as the total number of different nucleotides.

## Results

### Molecular identification

The mtDNA sequence data confirmed morphological observations that the five pelagic young were members of the subgenus *Sebastomus*. The number of conspecific DNA sequences used in the reference database ranged from 1 to 13 (*S. notius*, *S. lentiginosus*, $n$=1; *S. spinorbis*, $n$=3; *S. capensis*, $n$=4; *S. oculatus*, *S. exsul*, *S. helvomaculatus*, $n$=5; *S. rosaceus*, $n$=6; *S. chlorostictus*, *S. ensifer* $n$=7; *S. umbrosus*, *S. constellatus*, *S. simulator*, *S. eos*, $n$=8; *S. rosenblatti*, $n$=13). Two juveniles (CA3 and CA4) had identical mtDNA cyt-*b* sequences. On the basis of the number of nucleotide differences, one specimen (CA1, Fig. 1) was identified as starry rockfish, *S. constellatus*, and the other four as swordspine rockfish, *S. ensifer* (CA2-CA5, Fig. 1). The mitochondrial haplotypes of three specimens (CA1, CA3, and CA4) were identical to adult reference sequences, providing unequivocal

[2] Rocha-Olivares, A., and R. D. Vetter. 1998. Unpubl. data.

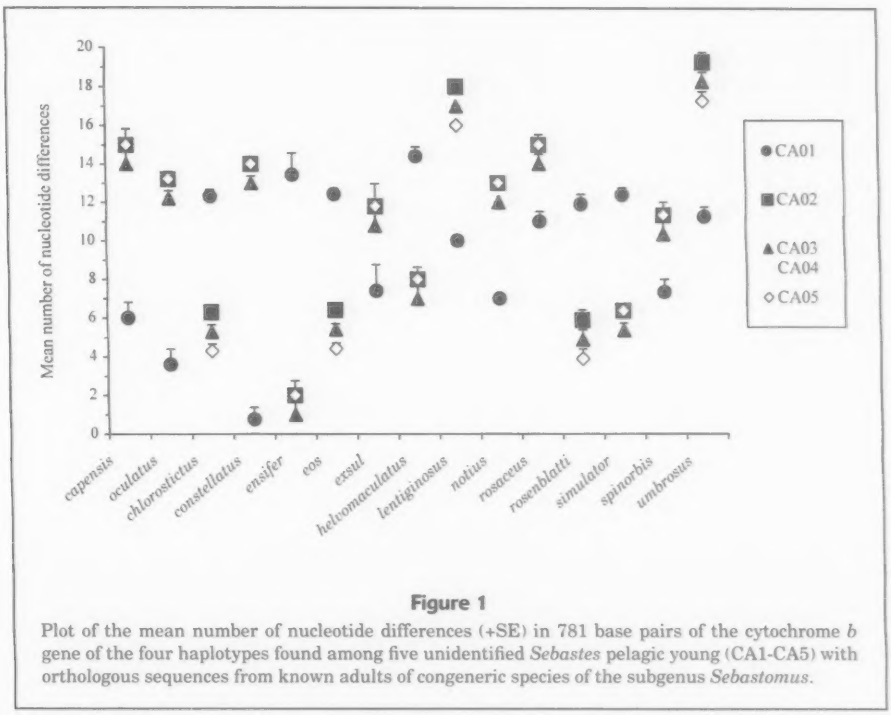


**Figure 1**

Plot of the mean number of nucleotide differences (+SE) in 781 base pairs of the cytochrome *b* gene of the four haplotypes found among five unidentified *Sebastes* pelagic young (CA1-CA5) with orthologous sequences from known adults of congeneric species of the subgenus *Sebastomus*.

evidence of species identity. The others differed from reference data by 1 to 3 nucleotides (Fig. 1).

Cluster analyses (unweighted pair-group method using averages [UPGMA]) performed on the pairwise distance matrices generated from the molecular data clustered CA1 with *S. constellatus* and CA2-CA5 with *S. ensifer* (not shown).

## Description of specimens

### *Sebastes constellatus* (Jordan and Gilbert 1880) Transforming larva: CA1 (15.0 mm SL), Figure 2A

**Literature** Transforming larvae and pelagic juveniles of *S. constellatus* have not been described in the published literature.[3] Larval stages up to notochord flexion (~7.1 mm) show features typical of preflexion larvae of other *Sebastomus* species: robust head and body with strong serrated parietal ridges and spines; strong postocular ridge and spine; heavy pigment on top of head, on jaws, and on paired fins, with heaviest pigment on distal edge of pectoral fin; postanal ventral midline series of 11–17 melanophores (Moser et al., 1977; Moser, 1996).

**General morphology** Body moderately deep and compressed; head, jaws, and eyes large (Table 1).

**Fins and other meristic features** Full complements of spinous and soft rays present; dorsal- and anal-fin rays moderate in length; anteriormost 5 scales of lateral line just beginning to form but visible only after staining with alizarin red-S (Table 2).

**Spination** Supraocular crest and associated spines (preocular, supraocular, postocular) prominent; parietal crests well developed, weakly serrate parietal spine slightly longer than nuchal spine; tympanic spine not yet formed on the upper margin of sensory canal pore but a slight prominence, indicating initial spine development, is noticeable; posterior preopercular series well developed with spine at angle longer than others and finely serrated along the longitudinal flange (dorsal and ventral margins of spine smooth); first and third spines weakly developed in anterior preopercular series; first and second lower infraorbitals present; first and fourth spines in upper series visible only after staining; presence of other spines as listed in Table 3.

[3] A fully pigmented "pelagic juvenile" (length not given) ascribed to *S. constellatus* is illustrated and briefly described *in* Laroche, W. A. 1987. Guide to the larval and juvenile rockfishes (*Sebastes*) of North America. Unpublished manuscript. Stonefish Environm. & Taxon. Serv., Enosburg Falls, VT 05450.

**Table 1**

Morphometric characters of pelagic young of three *Sebastes* (subgenus *Sebastomus*) species. Average values (in percent) are given for each proportion, followed by the standard deviation and the range. Proportions for *S. helvomaculatus* derived from data in Richardson and Laroche (1979). Abbreviations: HL= Head length; SL= standard length.

| | Transforming specimens | | | Pelagic juveniles | |
|---|---|---|---|---|---|
| Proportions | *S. constellatus* $n$ = 1 15.0 mm SL | *S. ensifer* $n$ = 1 19.8 mm SL | *S. helvomaculatus* $n$ = 5 17.8–18.6 mm SL | *S. ensifer* $n$ = 3 27.3–30.4 mm SL | *S. helvomaculatus* $n$ = 8 19.8–41.6 mm SL |
| Body depth at pectoral fin base/SL | 33.3 | 33.3 | 31.6 ±0.50 (31.0–32.1) | 32.9 ±1.23 (31.5–33.9) | 31.2 ±1.57 (28.4–32.9) |
| Body depth at anus/SL | 26.0 | 26.8 | 23.8 ±0.86 (23.1–25.3) | 27.1 ±1.15 (26.0–28.3) | 23.2 ±1.24 (21.2–25.0) |
| Snout to anus length/SL | 64.0 | 63.1 | 61.4 ±2.12 (59.8–64.5) | 63.6 ±2.12 (61.2–65.1) | 62.8 ±2.44 (59.8–66.0) |
| Snout to pelvic fin origin/SL | 41.3 | 39.9 | 41.7 ±4.15 (38.0–47.3) | 40.3 ±1.85 (38.5–42.2) | 42.8 ±3.17 (39.3–48.2) |
| Head length/SL | 37.3 | 39.9 | 40.3 ±2.62 (36.4–43.0) | 32.5 ±0.52 (31.9–32.9) | 40.1 ±1.48 (37.5–41.9) |
| Eye diameter/HL | 39.3 | 38.0 | 34.4 ±2.73 (32.0–37.5) | 36.8 ±0.79 (36.0–37.5) | 33.6 ±1.76 (30.9–36.9) |
| Upper jaw length/HL | 50.0 | 46.8 | 43.4 ±2.80 (39.7–47.2) | 51.8 ±2.29 (49.4–54.0) | 45.2 ±2.63 (40.2–47.6) |
| Snout length/HL | 26.8 | 26.6 | 32.3 ±4.50 (25.0–36.0) | 25.6 ±1.29 (24.7–27.1) | 31.7 ±2.52 (26.7–34.2) |
| Interorbital distance/HL | 30.4 | 24.1 | 24.9 ±2.04 (23.3–28.4) | 26.4 ±1.57 (25.0–28.1) | 21.6 ±3.83 (13.3–25.6) |
| Angle gill raker length/HL | 17.9 | 16.5 | 15.0 ±0.97 (13.8–16.4) | 17.9 ±0.88 (17.0–18.8) | 14.2 ±1.10 (12.7–15.7) |
| Longest dorsal spine length/HL | 28.6 | 36.7 | 33.2 ±3.77 (30.7–37.5) | 40.3 ±1.21 (39.3–41.7) | 30.9 ±2.95 (28.0–35.7) |
| Longest dorsal ray length/HL | ray broken | 39.2 | 36.8 ±4.05 (32.5–41.7) | 44.7 ±3.26 (42.0–48.3) | 35.8 ±2.23 (31.7–38.1) |
| Longest anal spine length/HL | tip broken | 31.7 | 31.3 ±3.34 (28.4–36.1) | 45.5 ±2.64 (42.7–47.9) | 32.4 ±5.69 (23.8–38.8) |
| Pectoral fin length/SL | 22.7 | broken | 26.2 ±1.28 (25.1–28.3) | 26.5 ±1.53 (24.9–28.0) | 25.3 ±3.44 (16.8–26.9) |
| Pectoral fin base depth/SL | 9.3 | 8.6 | 9.6 ±0.33 (9.0–9.8) | 8.5 ±0.42 (8.1–8.9) | 9.0 ±0.34 (8.2–9.3) |
| Pelvic fin length/SL | 17.3 | 20.7 | 19.6 ±1.44 (17.9–21.4) | 19.5 ±1.06 (18.3–20.2) | 19.2 ±1.37 (17.3–21.4) |
| Pelvic spine length/SL | 16.0 | 16.2 | 18.1 ±0.76 (17.3–19.1) | 16.0 ±0.57 (15.4–16.5) | 16.4 ±2.01 (13.5–18.9) |
| Parietal spine length/HL | 8.6 | 5.6 | 11.5 ±2.30 (9.0–14.3) | not present | 5.6 ±3.32 (1.1–9.5) |
| Nuchal spine length/HL | 6.1 | 5.6 | 4.2 ±0.90 (3.0–5.4) | 6.0 ±0.32 (5.6–6.3) | 3.6 ±1.15 (1.7–5.2) |
| Preopercular spine length/HL | 23.2 | 10.6 | 18.3 ±1.94 (16.3–20.9) | 13.3 ±0.38 (13.0–13.5) | 11.7 ±6.25 (2.6–15.9) |

**Table 2**

Meristics from transforming larval specimens and pelagic juveniles of *Sebastes* (subgenus *Sebastomus*) from southern California. CA 1, CA 2, etc. are identification labels for individual fish.

| Features counted | CA 1 *S. constellatus* transforming specimen | CA 2 *S. ensifer* transforming specimen | CA 3 *S. ensifer* pelagic juvenile | CA 4 *S. ensifer* pelagic juvenile | CA 5 *S. ensifer* pelagic juvenile |
|---|---|---|---|---|---|
| Standard length (mm) | 15.0 | 19.8 | 30.4 | 30.1 | 27.3 |
| Dorsal-fin spines and rays | XIII, 13 | XIII, 12 | XIII, 13 | XIII, 12 | XIII, 13 |
| Anal-fin spines and rays | III, 6 | III, 6 | III, 6 | III, 6 | III, 6 |
| Pectoral-fin rays | 17/17 | 17/17 | 17/17 | 17/17 | 17/17 |
| Pelvic-fin spines and rays | I, 5 | I, 5 | I, 5 | I, 5 | I, 5 |
| Gill rakers | 7 + 19 = 26 | 9 + 25 = 34 | 11 + 25 = 36 | 11 + 27 = 38 | 11 + 25 = 36 |
| Lateral line pores | 5 visible | ~10 visible | scales forming; some missing in series | ~40 | 39 |
| Procurrent caudal-fin rays | 9 + 9 | 10 + 11 | 10 + 11 | 11 + 11 | 11 + 11 |

**Pigmentation** Solid sheath over gut; solid patch over brain; shallow, internal, dorsal, and dorsolateral melanophores on snout and some at tip of lower jaw; large postorbital patch continues posteriad to cover opercle; patch of melanophores continuous with dorsal brain sheath, extending back on dorsum to sixth dorsal-fin spine and ventrad to lateral line region to form a saddle; separate patch below the saddle forming at horizontal septum region; melanophore on each side of dorsum at ninth dorsal-fin spine; bar at caudal peduncle complete except at ventral midline; melanistic pigment scattered over pectoral and pelvic fins.

### *Sebastes ensifer* Chen 1971
### Transforming larva: CA2 (19.8 mm SL), Figure 2B
### Pelagic juveniles CA5 (27.3 mm), Figure 2C; CA3 (30.4 mm SL) and CA4 (30.1 mm SL) not illustrated

**Literature** Transforming larvae and pelagic juveniles of *S. ensifer* have not been described in the published literature.[4] A 4.2-mm first-feeding larva has been illustrated (Moser et al., 1977; Moser, 1996), showing features typical of first-feeding *Sebastomus* larvae as summarized above for *S. constellatus*.

**General morphology** Body moderately deep and compressed; head, jaws, and eyes large; relative head length, and eye diameter decrease after transformation to pelagic juveniles; relative interorbital distance dorsal spine and ray length, and anal spine length increase after transformation (Table 1).

**Fins and other meristic features** Full complements of spinous and soft rays present; dorsal and anal-fin rays moderate in length; anterior scales in lateral line series forming, ~10 visible after staining in transforming specimen, full complements of lateral line scales forming in pelagic juveniles (Table 2).

**Spination** Supraocular crest and associated spines well developed; parietal crests well developed, weakly serrate, and parietal and nuchal spines subequal in transforming specimen; in pelagic juveniles the nuchal spine forms the terminus of the parietal ridge and only a remnant of the parietal spine can be seen; tympanic spine present; posterior preopercular series well developed with spine at angle longer than others but not serrated; anterior preopercular spines absent; first and second lower infraorbitals present; upper infraorbitals faintly visible after staining in transforming specimen but not in pelagic juveniles; cleithral spine present in pelagic juveniles but not in transforming specimen; presence of other spines as listed in Table 3.

**Pigmentation** *Transforming specimen*: solid sheath over gut; solid covering over brain; scattered melanophores on snout and some at tip of lower jaw; large postorbital and opercular patches; patch of melanophores continuous with dorsal brain sheath extending back on dorsum to 11th dorsal-fin spine

[4] A 35.5-mm pelagic juvenile ascribed to *Sebastes ensifer* is illustrated and briefly described *in* Laroche, W. A. 1987. Guide to larval and juvenile rockfishes (*Sebastes*) of North America. Unpublished manuscript. Stonefish Environm. & Taxon. Serv., Enosburg Falls, VT 05450.

**Table 3**

Head spines in pelagic young of *Sebastes* (subgenus *Sebastomus*) from southern California. Symbols: + = present; – = absent; ✩ = weakly developed or initial development. CA 1, etc. are identification labels for individual fish.

| | Specimen (standard length) | | | | |
|---|---|---|---|---|---|
| Spine | CA 1 (15.0 mm) | CA 2 (19.8 mm) | CA 3 (30.4 mm) | CA 4 (30.1 mm) | CA 5 (27.3 mm) |
| Parietal | + | + | In these specimens the parietal spines are degenerating and the nuchal spine is becoming the terminus of each parietal ridge. | | |
| Nuchal | + | + | + | + | + |
| Anterior preopercular-1 | ✩ | – | – | – | – |
| Anterior preopercular-2 | – | – | – | – | – |
| Anterior preopercular-3 | ✩ | – | – | – | – |
| Posterior preopercular-1 | + | + | + | + | + |
| Posterior preopercular-2 | + | + | + | + | + |
| Posterior preopercular-3 | + | + | + | + | + |
| Posterior preopercular-4 | + | + | + | + | + |
| Posterior preopercular-5 | + | + | + | + | + |
| Opercular-upper | + | + | + | + | + |
| Opercular-lower | + | + | + | + | + |
| Interopercular | ✩ | ✩ | – | – | – |
| Subopercular | – | – | – | – | – |
| Preocular | + | + | + | + | + |
| Supraocular | + | + | + | + | + |
| Postocular | + | + | + | + | + |
| Lower infraorbital-1 | + | + | + | + | + |
| Lower infraorbital-2 | + | + | + | + | + |
| Lower infraorbital-3 | – | – | – | – | – |
| Upper infraorbital-1 | + | ✩ | – | – | – |
| Upper infraorbital-2 | – | ✩ | – | – | – |
| Upper infraorbital-3 | – | ✩ | – | – | – |
| Upper infraorbital-4 | ✩ | ✩ | – | – | – |
| Nasal | + | + | + | + | + |
| Coronal | – | – | – | – | – |
| Tympanic | ✩ | + | + | + | + |
| Pterotic | ✩ | – | – | – | – |
| Upper posttemporal | + | + | + | + | + |
| Lower posttemporal | + | + | ✩ | ✩ | + |
| Supracleithral | + | + | + | + | + |
| Cleithral | – | – | + | + | + |

and ventrad to lateral line region to form a broad saddle; saddle continues ventrad faintly to horizontal septum; wide bar at caudal peduncle, complete except at ventral midline; scattered melanophores on pelvic fin and at base of pectoral fin. Embedded pigment, barely visible through the musculature of the body, lies on the upper surface of the vertebral column. *Pelagic juveniles*: general melanistic pigment filling in previously unpigmented regions except ventrally on head, chest, and region above anal fin; heavy along dorsum; saddle somewhat variegated, with pale regions that become white patches in adults; caudal peduncle bar enlarged anteriorly, blending with saddle, darkest on peduncle region with several chevrons forming; some pigment on paired fins.

**Table 4**

Geographic ranges and meristic characters for the species of *Sebastes*, subgenus *Sebastomus*, in the eastern North Pacific. All species have three anal spines, one pelvic spine with five rays, and 8+7 principal caudal-fin rays. Data are derived primarily from Miller and Lea (1972), Chen (1971, 1975, 1986), Matarese et al. (1989), Moser (1996). Abbreviations: BCA = Baja California; C = central; CA = California; G of AK = Gulf of Alaska; G of CA = Gulf of California; N = northern; S = southern; WA = Washington. GR = gill rakers.

| | | Fin rays | | | | | | |
|---|---|---|---|---|---|---|---|---|
| | | Dorsal | | | | | | |
| Species | Distribution | Spines | Rays | Anal | Pectoral | Vertebrae | GR (first arch) | Lateral line pores |
| *S. chlorostictus* | WA to C BCA | XIII | 11–15 | 5–7 | 16–18 | 26–27 | 31–36 | 35–43 |
| *S. constellatus* | C CA to S BCA | XIII–XIV | 12–14 | 5–7 | 16–18 | 25–26 | 25–30 | 37–47 |
| *S. ensifer* | C CA to C BCA | XIII | 12–14 | 5–7 | 16–18 | 26 | 34–40 | 34–44 |
| *S. eos* | C CA to C BCA | XIII | 11–13 | 5–7 | 17–18 | 26 | 26–31 | 34–42 |
| *S. exsul* | G of CA | XIII | 12–13 | 5–6 | 16–18 | 26 | 32–37 | 35–43 |
| *S. helvomaculatus* | G of AK to S CA | XII–XIV | 12–14 | 6–7 | 15–18 | 26 | 28–33 | 34–45 |
| *S. lentiginosus* | S CA to N BCA | XIII | 12–13 | 6–7 | 16–18 | 26 | 34–39 | 33–41 |
| *S. notius* | C BCA | XIII | 11–13 | 5–7 | 15–18 | 26 | 33–38 | 34–44 |
| *S. rosaceus* | N WA to C BCA | XIII–XIV | 11–14 | 5–7 | 16–18 | 26–27 | 29–34 | 36–46 |
| *S. rosenblatti* | C CA to C BCA | XIII–XIV | 11–13 | 5–6 | 16–18 | 26 | 28–34 | 34–42 |
| *S. simulator* | S CA to C BCA | XIII | 12–14 | 5–6 | 16–18 | 26 | 28–33 | 33–40 |
| *S. spinorbis* | G of CA | XIII | 13–14 | 6 | 18 | 26 | 30–33 | 33–38 |
| *S. umbrosus* | C CA to S BCA | XII–XIV | 11–13 | 5–7 | 15–18 | 26 | 31–38 | 33–44 |

## Discussion

### Molecular identification

The genetic information encoded in the rockfish mitochondrial cytochrome *b* has been found useful in the study of phylogenetic relationships of the species in the genus *Sebastes* (Rocha-Olivares, 1998a). The degree of genetic variability is large enough to recognize diagnostic mutations characteristic of several species (Rocha-Olivares, 1998a; Rocha-Olivares and Vetter[2]). The use of this information in blind tests of species identification of adult *Sebastes*, independently determined by morphological and genetic techniques, has given satisfactory results (Rocha-Olivares and Lea[5]). Diagnostic mutations have been used to design a method of species identification based on multiplex PCR (Rocha-Olivares, 1998b). In our study we relied on raw DNA sequence data to determine the species identity of five wild-caught pelagic young of *Sebastes*. The very small sequence divergence of their mtDNA with that of known adults (ranging from zero to three bp) provided very strong evidence supporting the identity of the unidentified specimens. Moreover, the small intraspecific genetic variation, indicated by the reduced standard errors in Figure 1, suggests that the possibility of species misidentification with our molecular approach is also very small.

Faster-evolving regions of the mtDNA have been successfully used to study the genetic structure of rockfish populations in both hemispheres (Rocha-Olivares et al., 1999b; Rocha-Olivares and Vetter, 1999); therefore, it is conceivable that molecular tools can also be applied intraspecifically to study, for example, the relative contribution of juvenile recruits from genetically differentiated populations.

### Species comparisons

**Transforming specimens of *S. constellatus* and *S. ensifer*** The specimens of *S. constellatus* and *S. ensifer* are remarkably similar. The meristic similarity reflects the general overlap among species documented for the subgenus (Table 4; Chen, 1971, 1975). The distinctly lower gill raker count for the transforming specimen of *S. constellatus*, compared with that of *S. ensifer* specimens (Table 2), matches the gill raker counts of adults (Table 4; Chen, 1971). Slight differences in spination between the trans-

[5] Rocha-Olivares, A., and Lea, R. N. 1998. Unpubl. data.

forming specimens of the two species (e.g. a longer serrate third preopercular spine in *S. constellatus*, more infraorbitals in *S. ensifer* only visible after staining) may be due to ontogenetic stage or individual variation (Table 3). However, the relatively longer fin rays in *S. ensifer* appear to be a species difference. The relative size and position of the parietal and nuchal spines differs in the two transforming specimens; however, this may be due to difference in stage of development. In the *S. ensifer* series the nuchal spine gradually replaces the parietal spine as the terminus of the parietal ridge and this may also occur in *S. constellatus*. Transforming specimens of the two species differ slightly in pigmentation (e.g. wider dorsal saddle and peduncle patch in *S. ensifer*); however, this difference can not be confirmed without additional specimens.

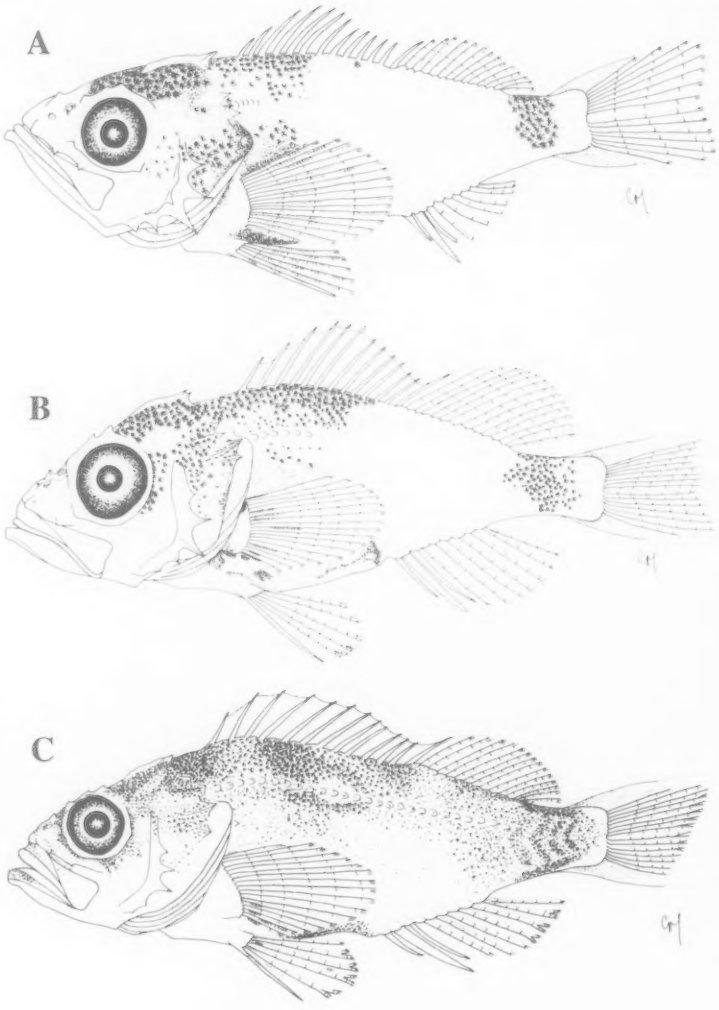


**Figure 2**

Pelagic young of two species of *Sebastes* (*Sebastomus*) from localities off southern California: (**A**) *S. constellatus*, transforming larva, 15.0 mm SL; (**B**) *S. ensifer*, transforming larva, 19.8 mm SL; (**C**) *S. ensifer*, pelagic juvenile, 27.3 mm SL.

**Transforming specimens and pelagic juveniles of *S. ensifer* and *S. helvomaculatus***

The species differ markedly in morphometry (Table 1). *S. ensifer* has a deeper-body than field-caught *S. helvomaculatus* described and illustrated in Richardson and Laroche (1979), as shown by the greater relative body depth measured at the anus (Table 1; Figs. 2 and 3). The two species are different in other morphometric features. Eye diameter, jaw length, and fin ray and spine lengths in the dorsal and anal fins are relatively greater in transforming specimens and pelagic juveniles of *S. ensifer* compared with *S. helvomaculatus*, whereas relative snout length is greater in *S. helvomaculatus*. In pelagic juveniles, relative head length is greater in *S. helvomaculatus* than in *S. ensifer*, whereas relative interorbital length is less compared with that in *S. ensifer*. The two species differ in stage of development at length. The illustrated 18.4-mm transforming specimen of *S. helvomaculatus* lacks a melanistic saddle on the trunk, and the caudal peduncle bar is just beginning to form, whereas these features are well established in the 19.8-mm specimen of *S. ensifer* (Figs. 2 and 3). The pigment saddle is present in the 22.4-mm pelagic juvenile of *S. helvomaculatus* but does not extend ventrad more than about half-way to the lateral line. Moreover, the complex pattern of bars and clear areas present on late-stage pelagic juveniles of *S. ensifer* is not present on *S. helvomaculatus* (Fig. 3). Also, the

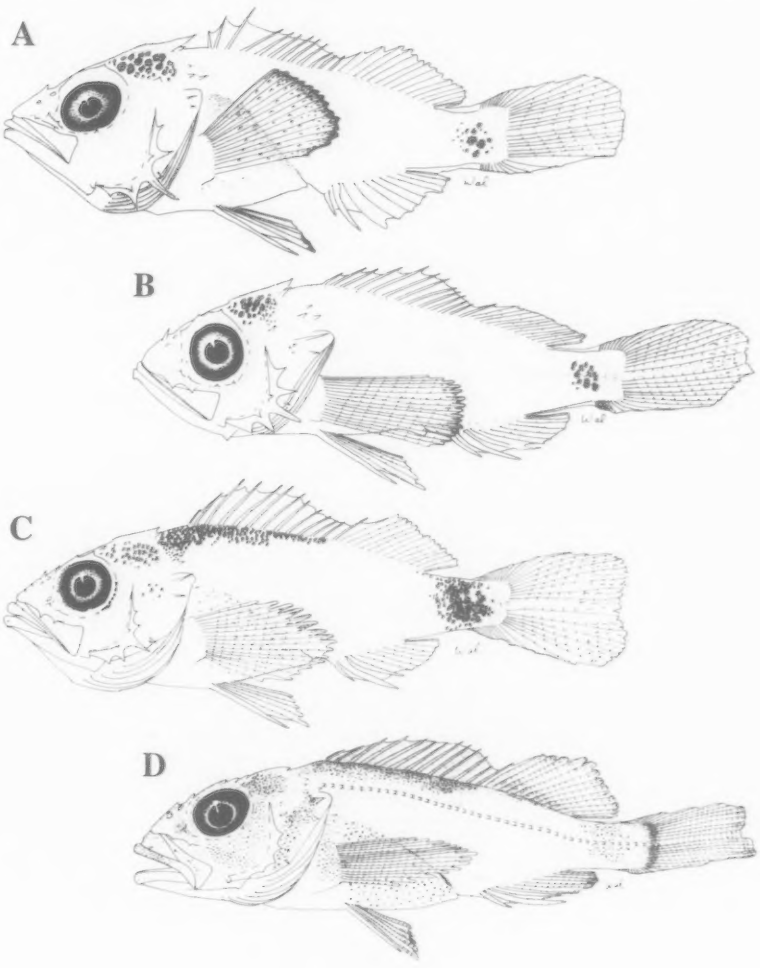


**Figure 3**

Pelagic young of *Sebastes* (*Sebastomus*) *helvomaculatus*: (**A**) transforming larva, 13.4 mm SL; (**B**) transforming larva, 18.4 mm SL; (**C**) pelagic juvenile, 22.4 mm SL; (**D**) pelagic juvenile, 41.6 mm SL. From Richardson and Laroche (1979).

ontogenetic changes in head spines (e.g. loss of infraorbitals and anterior preoperculars; decrease in the relative size of the parietals) occur in *S. helvomaculatus* larger than *S. ensifer* (Figs. 2 and 3).

**Pelagic juveniles of other *Sebastomus* species** A field-caught 21.0-mm pelagic juvenile of *S. chlorostictus* illustrated in Matarese et al. (1989) and Kendall (1991) is generally similar to specimens of *S. constellatus* and *S. ensifer* described in this study. In contrast to these species, the nape area in *S. chlorostictus* appears to lack pigment. In *S. chlorostictus* the dark pigment saddle extends from the first to sixth dorsal-fin spines, becomes wider mid-laterally on the trunk and appears to extend to the abdominal region. The caudal peduncle pigment is equally heavy and forms a complete band around the peduncle in the 21.0-mm specimen. Also, the dorsal and anal fin rays appear to be shorter than those in *S. ensifer*.

**Comments on the identification of pelagic young of *Sebastomus*** The transforming larvae and pelagic

juveniles of *S. constellatus* and *S. ensifer* identified by molecular methods, although conforming to the general facies known for *Sebastomus* pelagic young, show some differences in morphological features and pigmentation that may permit their identification by traditional means. The possibility of identifying the pelagic young of this species-rich subgenus is further suggested by the striking differences between pelagic young of *S. ensifer* and *S. helvomaculatus*. Further advancement will require: 1) the collection of fresh specimens of pelagic young of all species of *Sebastomus* in the waters off California and Baja California; 2) the establishment of ontogenetic series positively identified by molecular methods; and 3) a detailed description and series of illustrations published for each species. Pelagic young of this subgenus are common constituents of the midwater fauna of the continental borderland of the Southern California Bight (Moser and Ahlstrom, 1978; Moser and Boehlert, 1991), and specimens are readily available from midwater trawls.

In conclusion, this paper reports a novel approach to the study of young rockfishes. We have used molecular data in conjunction with morphological descriptions to increase knowledge on the identification of elusive early life history stages of *Sebastes*.

## Acknowledgments

This research was supported by NOAA Fisheries by core funding and a Saltonstall-Kennedy Fisheries Development Grant to R. D. Vetter, H. G. Moser, and W. Watson. Ship time on board the RV *Robert Gordon Sproul* was granted to A. Rocha-Olivares by the Ship Operations Office of the Scripps Institution of Oceanography. Additional support for A. Rocha-Olivares was provided by the Consejo Nacional de Ciencia y Tecnología (México) and the Shirley-Boyd Memorial Fellowship through the Scripps Institution of Oceanography. D. W. Foltz read an earlier version of the manuscript. William Watson and three anonymous reviewers offered helpful suggestions. We are indebted to C. Manning and W. Watson for preparing the illustrations of Figure 2.

## Literature cited

**Ainley, D. G., W. J. Sydeman, R. H. Parrish, and W. H. Lenarz.**
**1993.** Oceanic factors influencing distribution of young rockfish (*Sebastes*) in central California—a predators perspective. Calif. Coop. Oceanic Fish. Invest. Rep. 34:133–139.

**Chen, L.-C.**
**1971.** Systematics, variation, distribution, and biology of the subgenus *Sebastomus* (Pisces, Scorpaenidae, *Sebastes*). Bull. Scripps Inst. Oceanogr. Univ. Calif. 18:1–115.

**1975.** The rockfishes, genus *Sebastes* (Scorpaenidae), of the Gulf of California, including three new species with a discussion of their origin. Proc. Calif. Acad. Sci. Ser.4. 40(6):109–141.

**1986.** Meristic variation in *Sebastes* (Scorpaenidae), with an analysis of character association and bilateral pattern and their significance in species separation. U.S. Dep. Commer., NOAA Tech. Rep. NMFS 45, 25 p.

**Eschmeyer, W. N., and E. S. Herald.**
**1983.** A field guide to Pacific coast fishes North America. Houghton Mifflin Company, Boston, MA, 336 p.

**Hunter, J. R., and N. C. H. Lo.**
**1993.** Ichthyoplankton methods for estimating fish biomass. Introduction and terminology. Bull. Mar. Sci. 53:723–727.

**Kendall, A. W., Jr.**
**1991.** Systematics and identification of larvae and juveniles of the genus *Sebastes*. Environ. Biol. Fishes 30(1-2): 173–190.

**Kocher, T. D., W. K. Thomas, A. Meyer, S. V. Edwards, S. Pääbo, F. X. Villablanca, and A. C. Wilson.**
**1989.** Dynamics of mitochondrial DNA evolution in animals: amplification and sequencing with conserved primers. Proc. Nat. Acad. Sci. U.S.A. 86(16):6196–6200.

**Leet, W. F., C. M. Dewees, and C. W. Haugen (eds.).**
**1992.** California's living marine resources and their utilization. Univ. Calif. Sea Grant Rep. UCSGEP- 92-12, 257 p.

**Lenarz, W. H.**
**1986.** The rockfish fishery, a California perspective. Rockfish: a focus for research? Proceedings of a California Sea Grant Workshop. Report No. T-CSGCP-015, p. 3–9. Univ. Calif., Davis, CA.

**Love, M. S., M. H. Carr, and L. J. Haldorson.**
**1991.** The ecology of substrate-associated juveniles of the genus *Sebastes*. Environ. Biol. Fishes 30(1–2):225–243.

**Low, L., (ed.).**
**1993.** Status of living marine resources off the Pacific coast of the United States for 1993. U.S. Dep. Commer., NOAA Tech. Memo. NMFS-AFSC-26, 90 p.

**Matarese, A. C., A. W. Kendall Jr., D. M. Blood, and B. M. Vinter.**
**1989.** Laboratory guide to early life history stages of northeast Pacific fishes. U.S. Dep. Commer., NOAA Tech. Rep. NMFS 80, 652 p.

**Miller, D. J., and R. N. Lea.**
**1972.** Guide to the coastal marine fishes of California. Calif. Dep. Fish Game Fish Bull. 157, 249 p.

**Moser, H. G.**
**1996.** Scorpaenidae: Scorpionfishes and rockfishes. *In* The early stages of fishes in the California Current Region (H. G. Moser, ed.), p. 733–795. Calif. Coop. Oceanic Fish. Invest. Atlas 33.

**Moser, H. G., and E. H. Ahlstrom.**
**1978.** Larvae and pelagic juveniles of blackgill rockfish, *Sebastes melanostomus*, taken in midwater trawls off southern California and Baja California. J. Fish. Res. Board Can. 35(7):981–996.

**Moser, H. G., E. H. Ahlstrom, and E. M. Sandknop.**
**1977.** Guide to the identification of scorpionfish larvae (family Scorpaenidae) in the eastern Pacific with comparative notes on species of *Sebastes* and *Helicolenus* from other oceans. U.S. Dep. Commer., NOAA Tech. Rep. NMFS Circ. 402, 71 p.

**Moser, H. G., and G. W. Boehlert.**
**1991.** Ecology of pelagic larvae and juveniles of the genus *Sebastes*. Environ. Biol. Fishes 30(1– 2):203–224.

**Moser, H. G., and J. L. Butler.**
**1987.** Descriptions of reared larvae of six species of *Sebastes*. *In* Widow rockfish, Proceedings of a workshop, Tiburon, California, Dec. 11–12, 1980 (W. H. Lenarz and D. R. Gunderson, eds.) p. 19–29. U.S. Dep. Commer., NOAA Tech. Rep. NMFS 48.

**Moser, H. G., R. L. Charter, P. E. Smith, D. A. Ambrose, S. R. Charter, C. A. Meyer, E. M. Sandknop, and W. Watson.**
**1993.** Distributional atlas of fish larvae and eggs in the California current region: taxa with 1000 or more total larvae, 1951 through 1984. Calif. Coop. Oceanic Fish. Invest. Atlas 31, 233 p.

**Nelson, J. S.**
**1994**. Fishes of the world, third ed. John Wiley & Sons, Inc., New York, NY, 600 p.

**Radtke, R. L.**
**1989**. Larval fish age, growth, and body shrinkage: information available from otoliths. Can. J. Fish. Aquat. Sci. 46:1884–1894.

**Ralston, S., and D. F. Howard.**
**1995**. On the development of year-class strength and cohort variability in two northern California rockfishes. Fish. Bull. 93(4):710–720.

**Richardson, S. L., and W. A. Laroche.**
**1979**. Development and occurrence of larvae and juveniles of the rockfishes *Sebastes crameri*, *Sebastes pinniger*, and *Sebastes helvomaculatus* (Family Scorpaenidae) off Oregon. Fish. Bull. 77(1):1–46.

**Rocha-Olivares, A.**
**1998a.** Molecular evolution, systematics, zoogeography and levels of intraspecific genetic differentiation in the species of the antitropical subgenus *Sebastomus*, *Sebastes* (Scorpaeniformes, Teleostei) using mitochondrial DNA sequence data. Ph.D. diss., Scripps Institution of Oceanography, Univ. of California, San Diego, CA, 240 p.

**1998b**. Multiplex haplotype-specific PCR: a new approach for species identification of the early life stages of rockfishes of the species-rich genus *Sebastes* Cuvier. J. Exp. Mar. Biol. Ecol. 231(2):279–290.

**Rocha-Olivares, A., C. A. Kimbrell, B. J. Eitner, and R. D. Vetter.**
**1999a**. Evolution of a mitochondrial cytochrome *b* gene sequence in the species-rich genus *Sebastes* (Teleostei, Scorpaenidae) and its utility in testing the monophyly of the subgenus *Sebastomus*. Mol. Phylogenet. Evol. 11(3):426–440.

**Rocha-Olivares, A., R. H. Rosenblatt, and R. D. Vetter.**
**1999b**. Cryptic species of rockfishes (*Sebastes*: Scorpaenidae) in the Southern Hemisphere inferred from mitochondrial lineages. J. Hered. 90(3):404–411.

**1999c**. Molecular evolution, systematics, and zoogeography of the rockfish subenus *Sebastomus* (*Sebastes*, Scorpaenidae) based on mitochondrial cytochrome *b* and control region sequences. Mol. Phylogenet. Evol. 11(3):441–458.

**Rocha-Olivares, A., and R. D. Vetter.**
**1999**. The effects of oceanographic circulation on the gene flow, genetic structure, and phylogeography of the rosethorn rockfish *Sebastes helvomaculatus*. Can. J. Fish. Aquat. Sci. 56(5):803–813.

**Sakuma, K. M., and T. E. Laidig.**
**1995**. Description of larval and pelagic juvenile chilipepper, *Sebastes goodei* (family Scorpaenidae), with an examination of larval growth. Fish. Bull. 93(4):721–731.

**Seeb, L. W., and A. W. Kendall Jr.**
**1991**. Allozyme polymorphisms permit the identification of larval and juvenile rockfishes of the genus *Sebastes*. Environ. Biol. Fishes 30(1-2):191–201.

**Yoklavich, M. M., and G. W. Boehlert.**
**1991**. Uptake and utilization of 14C-glycine by embryos of *Sebastes melanops*. Environ. Biol. Fishes 30(1–2):147–153.

**Abstract.**—The shapes and volumes of swimbladders of yellowfin tuna, *Thunnus albacares*, were measured from freshly caught fish from the eastern Pacific Ocean. Direct measurements of swimbladder volumes were obtained from a geometric reconstruction with morphometric measurements of intact bladders and by volumetric displacements of the same intact bladders excised from 46 fish (57 to 157 cm in length). The estimates of the swimbladder volumes obtained from geometric reconstruction were not significantly different from those obtained with the corresponding volumetric displacements. There is a nonlinear relationship between yellowfin swimbladder volumes and fish lengths. The mean swimbladder volume was 1.33% of body volume with a minimum of 0.30% and a maximum of 2.84%. A comprehensive model, based on the data from this study and those from a previous investigation, is presented for the relationship of yellowfin swimbladder volumes, estimated from geometric reconstruction and fish lengths for 108 specimens (35 to 157 cm). This predictive model was then used with other formulae to estimate yellowfin tuna swimbladder resonance frequencies for fish lengths and fish depths. Because these resonance frequencies are within the range of frequencies audible to yellowfin tuna, we speculate on the potential distance at which dolphins could be detected by yellowfin tuna.

Manuscript accepted 19 November 1999.
Fish. Bull. 98:364–374 (2000).

# Shape, volume, and resonance frequency of the swimbladder of yellowfin tuna, *Thunnus albacares*

**Kurt M. Schaefer**
Inter-American Tropical Tuna Commission
8604 La Jolla Shores Drive
La Jolla, California 92037-1508
E-mail address: kschaefer@iattc.ucsd.edu

**Charles W. Oliver**
Southwest Fisheries Science Center
National Marine Fisheries Service, NOAA
P.O. Box 271, La Jolla, California 92038

The shape and volume of the swimbladder of yellowfin tuna, *Thunnus albacares*, is obviously important because it functions as a hydrostatic organ, which lowers the energy costs of locomotion (Magnuson, 1973; Alexander, 1993). The yellowfin swimbladder may also function in acoustic detection, providing increased sensitivity in hearing, thus enhancing the ability of fishes to detect other organisms, such as dolphins and prey (Iverson, 1967; Hawkins, 1993). In addition, the swimbladder may also function in acoustical detection of tuna by other species. At low frequencies (< 2 kHz), the maximum acoustic target strength occurs at a resonance frequency determined by the volume of the swimbladder (Love, 1978). At high frequencies (2–200 kHz), the swimbladder has been reported to account for 50% (Harden Jones and Pearce, 1958) to as much as 95% (Foote, 1980) of the acoustic target strength for some fish.

Low-frequency acoustic detection and tracking of yellowfin tuna schools is being investigated by the U.S. National Marine Fisheries Service as an alternative method of locating yellowfin tuna independent of dolphins. Studies suggest that yellowfin tuna schools could be detected at much greater ranges (20 to 40 km) than are currently feasible (Rees, 1998). Development of an acoustic detection system could greatly increase the efficiency of commercial fishing and might also provide a fishery-independent method for assessing yellowfin tuna or other large pelagic fish.

Nero[1] used two acoustic-scattering models to estimate the target strengths of yellowfin tuna schools: a model for very low frequencies (50–1000 Hz) assumed to be near swimbladder resonance (Feuillade et al., 1996; Feuillade and Nero, 1998), and a high-frequency (2–200 kHz) model for frequencies well above swimbladder resonance (Love, 1977; Love, 1981). Yellowfin swimbladders were modeled as gas-filled spheres (Feuillade et al., 1996). Nero's models (1996) included swimbladder volume estimates of approximately 5% of fish volume for yellowfin tuna in excess of 80 cm in length, extrapolated from Magnuson's (1973) relationship of swimbladder volume to fish length for yellowfin tuna 44 to 82 cm in length.

The objectives of our study were 1) to obtain direct measurements

[1] Nero, R. W. 1996. Model estimates of acoustic scattering from schools of large yellowfin tuna. Report NRL/MR/774-95-7708. Naval Research Laboratory, Ocean Acoustics Branch, Acoustics Division, Stennis Space Center, MS 39529-5004, 21 p.

of swimbladder shapes and volumes from freshly caught yellowfin tuna 50 to 150 cm in length, 2) to compare the swimbladder displacement volumes with volumes estimated from geometric reconstruction, 3) to compare the swimbladder volumes estimated from geometric reconstruction for freshly caught and frozen-and-thawed specimens, and 4) to calculate swimbladder resonance frequencies as functions of fish length and depth.

All four objectives are directly related to designing a low-frequency, long-range acoustic detection system to locate large yellowfin tuna. The first objective provides direct measurements of the relation between swimbladder volume and fish length, upon which are based acoustic target strength estimates. The previously modeled relationship was based upon smaller yellowfin tuna (Magnuson, 1973; Nero, 1996). The second and third objectives were to ascertain the practicality of obtaining swimbladder volumes by means other than volumetric displacement of the swimbladder from freshly caught fish, thus providing both a simpler method and wider sampling opportunities. The last objective allows incorporation of fishery information (fish size and swimming depth) to select a particular frequency, or frequency range, in order to optimize an acoustic detection system.

## Materials and methods

Yellowfin tuna specimens were caught by rod and reel. Seventeen specimens, 57 to 70 cm in length, were collected from a skiff during October 1997, in the vicinity of the Frailes Islands (lat. 7°20'N, long. 80°08'W). An additional 29 specimens, 71 to 157 cm in length, were collected aboard the MV *Royal Polaris*, a San Diego-based long-range sportfishing boat, during January and February 1998, primarily in the vicinities of Alijos Bank (lat. 24°49'N, long. 115°56'W) and Hurricane Bank (lat. 16°52'N, long. 117°30'W).

Freshly caught specimens were assigned an identification number. Fish length was measured with a caliper to the nearest millimeter and fish weight was measured with an electronic balance to the nearest pound. Cutting the abdominal cavity open from the anus to the isthmus and removing most of the viscera exposed the swimbladder. A photograph of the intact swimbladder was then taken with a digital camera. Morphometric measurements of length and three widths (rostral, medial, and caudal) were taken for each intact swimbladder, with a dial caliper, to the nearest tenth of a millimeter. The inflated swimbladder and some extraneous tissue were excised from the abdominal cavity, and the volumetric displacement was measured in a graduated cylinder to the nearest 5 mL. The swimbladder was then punctured and the volumetric displacement of the tissue measured. The estimated volume of gas in the swimbladder was calculated as the difference between displacement volumes of the inflated and deflated swimbladder, including the attached extraneous tissues. The volume of the swimbladder wall was not determined and should be considered insignificant, being extremely thin, with respect to volumetric displacement.

Estimates of swimbladder volumes were also computed by a geometric reconstruction from the bladder's length and width measurements. Based on the above four measurements of each bladder, an algorithm was employed to estimate the volumes between several cross sections. Cross sections of the swimbladder were assumed to be elliptical. The rostral and caudal ends of the bladders were assumed to be hemispheres. The total estimate of the volume of gas within the swimbladder was the sum of all the geometrical units. Estimates of swimbladder volumes by a geometric reconstruction for 62 frozen and thawed yellowfin tuna, ranging in length from 35 to 149 cm (Schaefer, 1999), were included in this study for both comparative and comprehensive analyses.

## Results

### Swimbladder shape and volume

Photographic images of the ventral, dorsal, left, and right profiles of an excised intact swimbladder of yellowfin tuna provided definitive views of the overall shape (Fig. 1). The swimbladder is cylindrically shaped and has medial bulging and hemispheric ends. There are paired protuberances on the rostral-dorsal surface. The protuberances are commonly of unequal size (the left is larger than the right) and they fit into sockets located on each side of the vertebral column. As size increased in the yellowfin specimens we examined (Table 1), the ratio of the swimbladder length to the width remained fairly constant, around a mean of 3.1 (range: 2.2–4.8). The swimbladder shape, however, changed noticeably, particularly at the caudal end (Fig. 2).

The swimbladder has thin elastic walls except for the thicker walls of the protuberances. The dorsal surface of the swimbladder is attached to a sheet of thick connective tissue, situated along the dorsal wall of the abdominal cavity adjacent to the vertebral column. In larger specimens, there is a prominent cord of connective tissue originating from the posterior area of this tissue and extending anteriorly to the area of the sockets at the rostral end of the swimbladder. This distinct cord of connective tissue

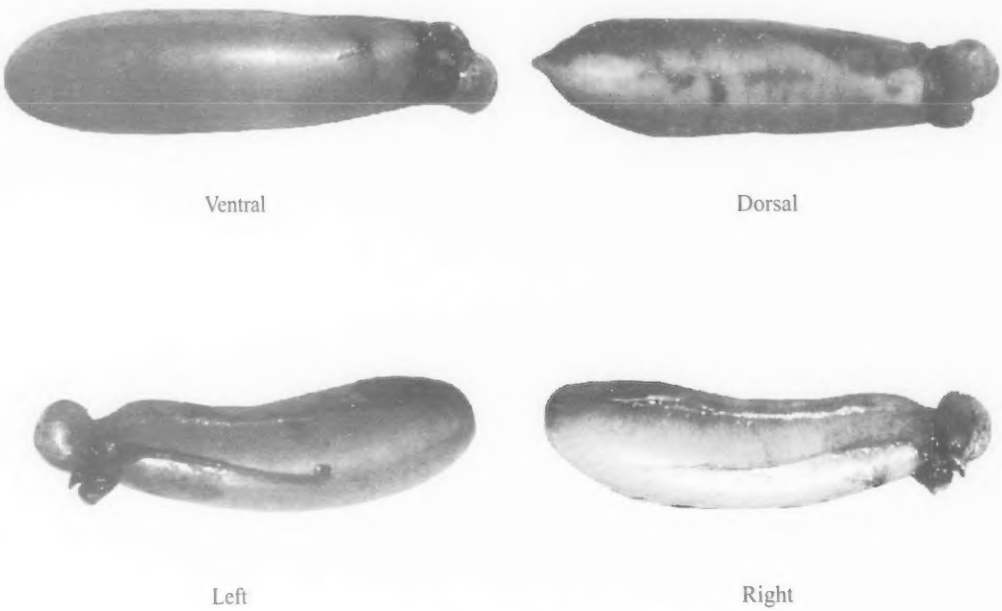


**Figure 1**

Profiles of an excised intact yellowfin tuna swimbladder. The actual length of the swimbladder was 165 mm, the maximum width 69.1 mm, and the displacement volume 245 cc. The fish was 784 mm in length and 8.6 kg in weight.

is situated directly adjacent to the dorsal wall of the swimbladder.

The relationship of swimbladder volume obtained from volumetric displacement, to fish length for the freshly caught yellowfin tuna is shown in Figure 3. The relationship is described by a power function:

$$Y_x = 0.000000005\, x^{3.5715}, \quad (r^2=0.87, n=46) \quad (1)$$

where $Y_x$ = swimbladder volume at fish length $x$.

The relationship of swimbladder volume, obtained from volumetric displacement and expressed as a percentage of the body volume (estimated from body weight) to weight for freshly caught yellowfin tuna is shown in Figure 4. The mean volume was 1.33% (95% CI=0.16%) with minimum and maximum values of 0.30% and 2.84%, respectively. The relation between the swimbladder volume, expressed as the percentage of body volume to body weight is described by the following linear function:

$$Y_x = 1.0822 + 0.0146x, \quad (r^2=0.17, n=46) \quad (2)$$

where $Y_x$ = swimbladder volume, expressed as a percentage of body volume, at weight $x$.

The relationship of swimbladder volume (estimated from geometric reconstruction) to volume obtained from volumetric displacement for freshly caught yellowfin tuna is shown in Figure 5. The relationship was described and analyzed by the following linear function, with the intercept set to zero:

$$Y_x = 1.0735x, \quad r^2=0.96, n=46 \quad (3)$$

where $Y_x$ = swimbladder volume estimated from geometric reconstruction for the corresponding volumetric displacement $x$.

The regression coefficient is significantly different from 1 ($t_{0.05(2),44}$=2.41; $P$<0.05). However, it is apparent from Figure 5 that the two techniques produce similar estimates, providing credence to the estimation of volume from geometric reconstruction.

Analysis of covariance applied to the log-transformed swimbladder volumes by geometric recon-

**Table 1**

Measurements of fresh yellowfin tuna and their swimbladders. The volumes are volumetric displacements in seawater.

| Fish | | Swimbladder | | |
|---|---|---|---|---|
| Length (mm) | Weight (kg) | Length (mm) | Maximum width (mm) | Volume (cc) |
| 572 | 3.7 | 102.0 | 31.3 | 38 |
| 590 | 4.1 | 114.9 | 32.3 | 43 |
| 591 | 4.1 | 109.9 | 36.9 | 53 |
| 591 | 3.7 | 107.0 | 25.9 | 36 |
| 600 | 3.9 | 100.8 | 26.7 | 26 |
| 601 | 3.9 | 103.6 | 36.1 | 41 |
| 608 | 4.2 | 112.6 | 31.0 | 56 |
| 611 | 4.3 | 110.2 | 35.0 | 46 |
| 614 | 4.6 | 119.2 | 34.6 | 71 |
| 624 | 4.6 | 115.6 | 30.2 | 54 |
| 624 | 4.4 | 123.3 | 25.8 | 31 |
| 636 | 4.9 | 101.4 | 34.4 | 35 |
| 650 | 5.2 | 111.3 | 38.3 | 78 |
| 671 | 5.7 | 118.1 | 39.7 | 33 |
| 675 | 6.0 | 136.7 | 42.4 | 111 |
| 681 | 6.5 | 128.7 | 45.0 | 71 |
| 704 | 8.1 | 109.3 | 41.9 | 66 |
| 705 | 7.3 | 132.0 | 54.1 | 91 |
| 736 | 7.3 | 143.0 | 48.2 | 51 |
| 751 | 8.2 | 135.0 | 47.3 | 81 |
| 784 | 8.6 | 165.0 | 69.1 | 245 |
| 789 | 8.6 | 114.0 | 51.3 | 26 |
| 824 | 9.5 | 163.0 | 58.4 | 166 |
| 842 | 11.3 | 164.0 | 50.6 | 161 |
| 861 | 13.2 | 158.0 | 44.9 | 136 |
| 917 | 13.6 | 178.0 | 64.9 | 260 |
| 933 | 15.4 | 168.0 | 64.9 | 106 |
| 940 | 16.8 | 184.0 | 51.6 | 280 |
| 964 | 17.2 | 174.0 | 52.3 | 161 |
| 977 | 19.1 | 205.0 | 61.6 | 410 |
| 1033 | 20.4 | 195.0 | 61.9 | 320 |
| 1039 | 21.8 | 228.0 | 61.7 | 260 |
| 1047 | 21.3 | 196.0 | 48.5 | 147 |
| 1069 | 23.6 | 193.0 | 61.7 | 310 |
| 1087 | 24.9 | 240.0 | 79.1 | 610 |
| 1129 | 27.2 | 205.0 | 66.3 | 495 |
| 1130 | 30.4 | 195.0 | 66.9 | 250 |
| 1179 | 33.6 | 205.0 | 75.9 | 500 |
| 1190 | 33.1 | 235.0 | 69.8 | 540 |
| 1197 | 29.5 | 207.0 | 71.1 | 390 |
| 1218 | 34.0 | 213.0 | 76.8 | 500 |
| 1236 | 35.4 | 215.0 | 75.6 | 540 |
| 1290 | 37.2 | 260.0 | 74.5 | 830 |
| 1346 | 44.5 | 270.0 | 79.5 | 915 |
| 1519 | 62.6 | 230.0 | 104.6 | 800 |
| 1569 | 68.0 | 295.0 | 114.2 | 1530 |

struction and fish-length data truncated to a length range of 60 to 119 cm from the present study ($n$=36) and from Schaefer (1999) ($n$=24) indicated no significant difference in the test for equality of slopes ($F$=2.50, $P$=0.12) or equality of adjusted means ($F$=2.38, $P$=0.13). In addition, an approxi-

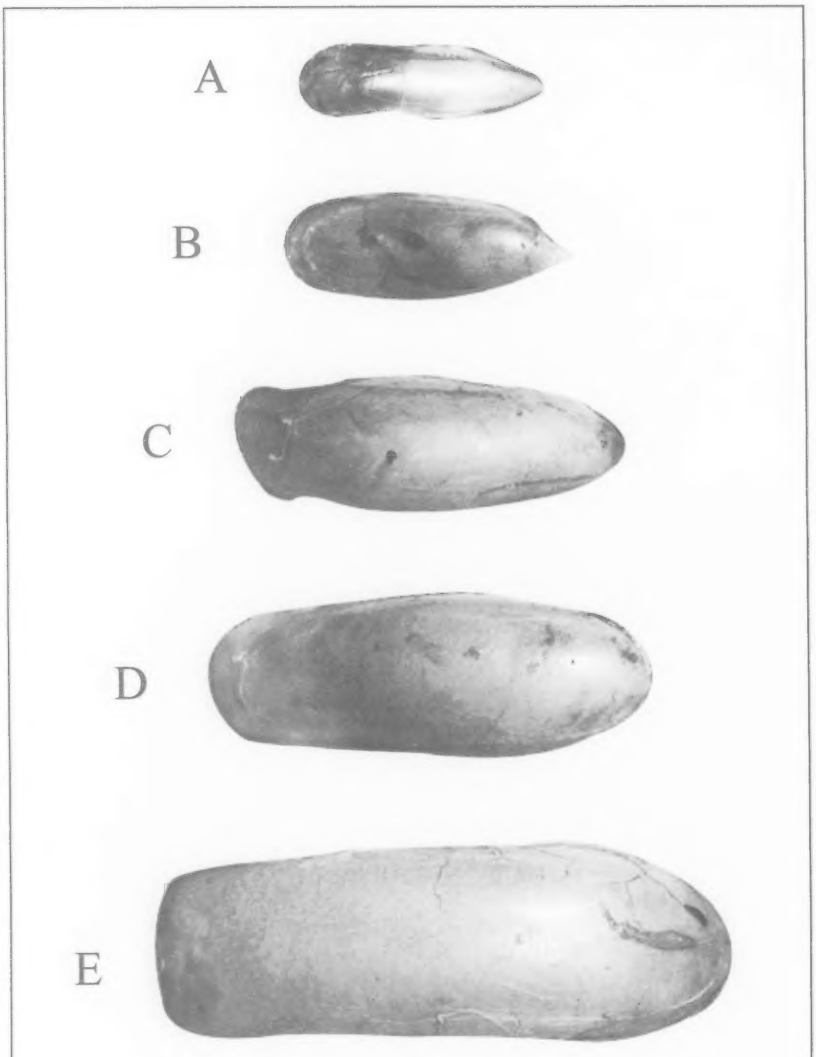


**Figure 2**

Ventral profiles of excised intact yellowfin tuna swimbladders scaled to relative size. Values given for each image are measured lengths and displacement volumes of bladders, fish length, and fish weight. (**A**) 115 mm and 43 cc, 590 mm, 4.1 kg. (**B**) 135 mm and 81 cc, 751 mm, 8.2 kg. (**C**) 184 mm and 280 cc, 940 mm, 16.8 kg. (**D**) 205 mm and 495 cc, 1129 mm, 27.2 kg. (**E**) 270 mm and 915 cc, 1346 mm, 44.5 kg.

mate $F$-ratio statistic (Zar, 1974) indicated that the sample power functions fitted to the data of percentage of swimbladder volume (obtained from geometric reconstruction) to fish length (57 to 157 cm, $n$=46) from our study and (35 to 149 cm, $n$=62) from Schaefer's study (1999) are estimating the same population regression function ($F$=2.65, $P$>0.10). It thus appears appropriate to pool the two sets of data for yellowfin tuna swimbladder volumes obtained from geometric reconstruction, in order to provide the most comprehensive model possible.

The relation of swimbladder volume (estimated by geometric reconstruction) and length of the yellowfin tuna from our study, combined with that from Schae-

fer's (1999) is shown in Figure 6. The relationship is well described by a power function fitted to the nontransformed data by means of a weighted regression procedure:

$$Y_x = 0.00000002\, x^{3.0601}, \quad (r^2=0.83,\ n=108 \text{ [fish length range: 353 to 1569 mm]}) \qquad (4)$$

where $Y_x$ = a swimbladder volume at fish length $x$.

The weighting employed consisted of the reciprocal of the variance about the volumes within each 200-mm length interval.

### Swimbladder resonance frequency

The monopole-dominant resonance frequency of a swimbladder (Andreeva, 1964) is approximated by using a spherical volume of gas (Love, 1978) as follows:

$$\text{Resonance frequency} = \sqrt{\frac{3\Gamma P}{4\pi^2 r^2 D}} \qquad (5)$$

where $\Gamma = 1.4$;
$r$ = radii of equivalent sphere in meters;
$D$ = density of fish flesh (1050 kg/m$^3$); and
$P$ = sound speed parameter at depth $Z$ defined as

$$P = \left[1 + \left[\frac{Z_{\text{meters}}}{10_{\text{meters}}}\right]\right] \times 10100 \text{ Pascals}. \qquad (6)$$

Because yellowfin tuna swimbladders are not spherical, the predicted resonance frequency must be adjusted to account for the approximate prolate spheroid shape of the swimbladder (Figs. 1 and 2). Weston (1967) has provided a formula and figure (Chap. 5, p 59, Fig. 5.2) for this adjustment using the ratio of the swimbladder's maximum (a) and minimum (b) radii (e.g. 1/2 length and 1/2 width). From the figure, we interpolated the magnitude of the upward adjustment at various depths, incorporating Boyle's Law to account for changes in volume with depth. The swimbladder's maximum radius (a) was held constant at all depths because it is firmly attached to the connective tissue sheet adjacent to the dorsal wall of the abdominal cavity. We calculated the expected minimum radii (b) at various depths, using the predictive regression function for swimbladder

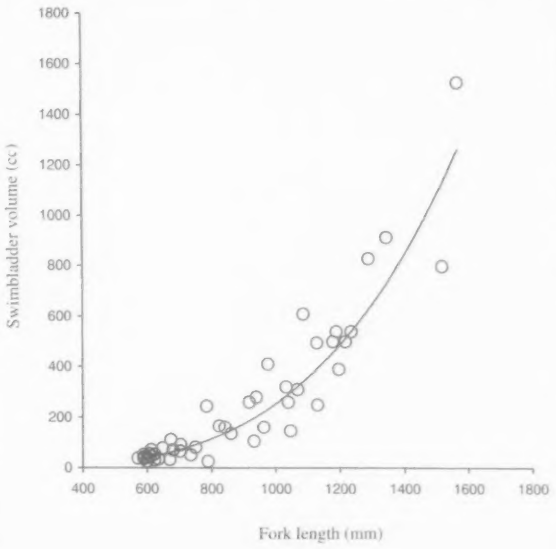


**Figure 3**
Relation between swimbladder displacement volume and length for yellowfin tuna. The fitted line is for a power function given in the text.

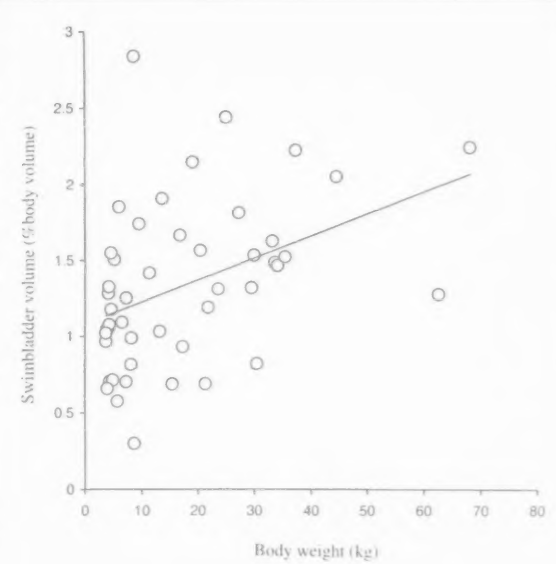


**Figure 4**
Relation between swimbladder displacement volume, as a percentage of estimated body volume, and body weight in air for yellowfin tuna. The fitted line is for a linear function given in the text.

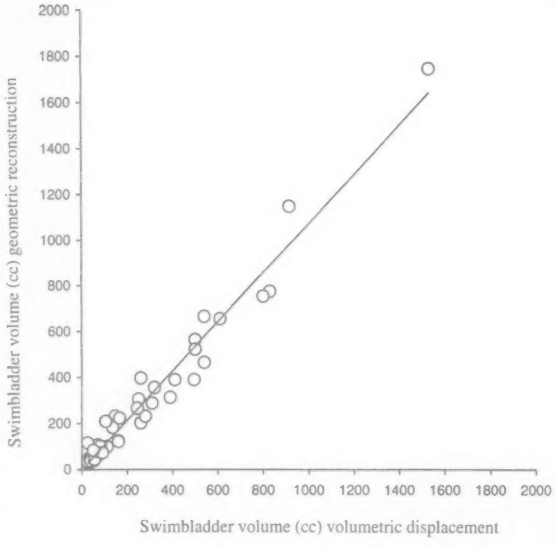


**Figure 5**

Relation between estimated swimbladder volume, from geometric reconstruction, and swimbladder displacement volume for yellowfin tuna. The fitted line is for a linear function given in the text.

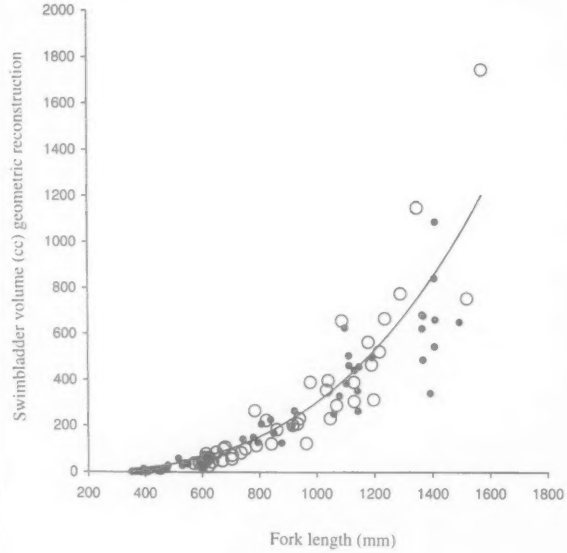


**Figure 6**

Relation between estimated swimbladder volume, from geometric reconstruction, and length for yellowfin tuna. The open circles are for the data from this study and the solid circles are from Schaefer (1999). The fitted line is for a power function given in the text.

volumes at the surface for fish lengths (Fig. 6), and determined the percent increase in the expected resonance frequency. The regression coefficient ($b$=1.053) for the linear relationship of swimbladder volume estimated by geometric reconstruction to the volume estimated from the equation for a prolate spheroid is not significantly different from 1 ($t_{0.05(2),106}$=1.84; $P$>0.05). Solving for $b$ yields:

$$b_{\text{depth}} = \sqrt{\frac{V_{\text{depth}}}{\frac{4}{3}\pi a}} \qquad (7)$$

Resonance frequencies for swimbladders of yellowfin tuna of various lengths and at various depths were estimated (Fig. 7), using the above equations and the predictive regression function for swimbladder volumes for fish lengths (Fig. 6). Applying this correction increased resonance frequencies between 5% and 26% for yellowfin tuna from 40 to 150 cm at depths from 0 to 120 m.

## Discussion

### Swimbladder shape and volume

Godsil and Byers (1944) described the shape of the swimbladder of yellowfin tuna. Additional information regarding yellowfin tuna swimbladder shape is provided through the digital images of the various views of the swimbladder (Figs. 1 and 2) and the morphometric information presented in Table 1.

The swimbladder volume estimates derived by geometric reconstruction in this study and in Schaefer (1999) appear to provide realistic representations for swimbladders of live yellowfin tuna swimming at the surface of the ocean. All of the intact swimbladders within the abdominal cavities for those specimens were sufficiently inflated so that the bladders were taut, rather than flaccid. Many of the yellowfin tuna stomachs were relatively full, and there was a broad range in the stage of gonadal development. There was no extrusion of the bladder or other organs from the initial incision into the abdominal cavity for any specimen. Thus, it does not appear there were any deformations or reduction in swimbladder volumes within the body cavity similar to those described for cod (Ona, 1990). In addition, yellowfin tuna are physoclistous, and the

inflation and deflation of the swimbladder is controlled through special glands that function in the secretion or resorption of gases from, or to, the blood (Alexander, 1993). Virtually nothing is known about inflation and deflation rates in swimbladders of tunas, but it would appear from studies of other fishes (Alexander, 1993) that swimbladder volume adjustments would be extremely slow in relation to the rapid swimming speeds during vertical forays by these species (Holland et al., 1990).

Geometric reconstruction of swimbladders in yellowfin tuna was previously derived from radiographs to estimate volumes, which were validated by volumetric displacement (Chang and Magnuson, 1968). It is apparent from the results of that study and our study that the geometric reconstruction method is sufficiently accurate for deriving estimates of volumes of swimbladders of yellowfin tuna, and possibly other tunas as well. Obtaining swimbladder volumetric data by geometric reconstruction is more practical than by volumetric displacement because of the additional time required and potential of puncturing the swimbladder when excising for determination of volumetric displacement. Furthermore, unless there are instances where it is not feasible to cut open the abdominal cavity of specimens, it does not appear to be necessary to employ an x-ray unit for obtaining these estimates.

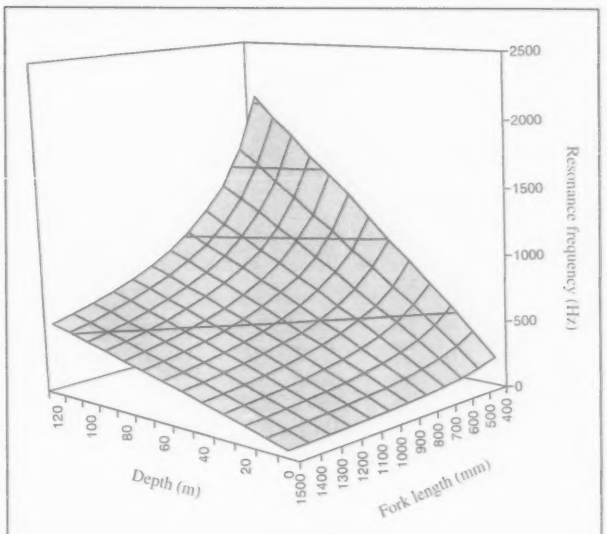


**Figure 7**

Relation between estimated swimbladder resonance frequency, fish length, and fish depth for yellowfin tuna.

Magnuson (1973) reported that swimbladder volumes for 11 yellowfin tuna specimens, 44 to 82 cm in length, ranged from around 0.25% to 4.0% of body volume (estimated from Fig. 4a of Magnuson, 1973). The swimbladder volumes in our study, derived from volumetric displacements, expressed as a percentage of the estimated body volumes (Fig. 4) had a mean of about 1.3%, with a range of about 0.3% to 2.84%, and almost no relation with increasing mass. Swimbladder volumes, from the present study, for yellowfin tuna in the length range presented in Magnuson (1973) appear to be significantly lower (Fig. 4). The data of Magnuson (1973) were based upon measured volumetric displacements of the fish, whereas in the present study body volume was estimated, without adjusting for fish density because those values were not available for these specimens. However, we calculated the body volumes from weights for specimens from the present study, using an adjustment factor for density of 1.05 g/mL (Magnuson, 1973) and found swimbladder volumes, expressed as a percentage of body weight, would be increased by only 0.07% on average. This small increase in volume does not account for the apparent differences in swimbladder volumes between the present study and those in Magnuson (1973). In addition, although Magnuson (1973) reported that specimens of 2 kg or less have no gas in the bladder, Schaefer (1999) reported yellowfin swimbladders are inflated with measurable quantities of gas in specimens as small as 0.85 kg (353 mm) (Fig. 6).

## Swimbladder resonance frequency

Acoustic tracking studies have shown that yellowfin tuna occupy the lower mixed layer during daylight and waters closer to the surface at night (Carey and Olson, 1982; Holland et al., 1990; Block et al., 1997). Although they appear to make frequent short excursions toward the surface, they spend very little time at the surface. In the area of the eastern Pacific surface fishery (Bayliff, 1998), the thermocline depth ranges from about 40 to 120 meters (Fiedler, 1992). Resonance frequency will change with depth because volume is the primary determinant of the resonance frequency of a swimbladder. Thus, the acoustic target strength of a tuna, or school of tunas, will vary as the swimbladder volumes vary at depth for low-frequency acoustic detection systems.

Nero (1996) modeled target strengths for schools of larger yellowfin tuna for both high frequencies (2–200 kHz), and low frequencies (below 2 kHz), using an assumed swimbladder volume equal to 5% of fish volume for calculating resonance frequencies. Nero's (1996) high-frequency model predicted target strengths of 2.5, 1.6, and 0.9 dB re 1μPa for yellowfin

tuna schools of 80, 100, and 130-cm fish respectively. The decreasing trend in school target strength as fish length and bladder volume increases, as shown in Nero (1996), results primarily from the reduced number of fish in a modeled 15-kg school. Some decrease in Nero's reported school target strengths could result from the smaller swimbladder volumes that we measured for fish of similar lengths, depending upon the swimbladder's contribution to target strength at high frequencies (Harden Jones and Pearce, 1958; Foote, 1980).

Nero (1996) estimated low-frequency target strengths for schools of yellowfin tuna at various depths, fish lengths, and packing densities but noted school target strength was complicated because of interference and coupled resonance effects dependent on the fish size, numbers, aspect, and packing density. We expect Nero's reported school target strengths, for low frequencies, to decrease as a result of the smaller swimbladder volumes we report. Because resonance frequency varies inversely with swimbladder volume, overestimating volume results in predicted lower resonance frequencies. Direct measurement of resonance frequency and target strength of *in situ* swimbladders would eliminate the need to model these parameters and provide better information to optimize an acoustic detection system for large yellowfin tuna.

Yellowfin tuna monitor their environment through the use of sensory organs for visual, chemoreceptive, and acoustic information. Although vision (Guthrie and Muntz, 1993) and chemoreception (Hara, 1993) are presumably important to yellowfin tuna in foraging, sex, and social communication, acoustic sensory capacities probably provide greater detection potential because of the light attenuation and chemical dilution effects in the ocean (Hawkins, 1993). Sounds can travel great distances in the sea, depending upon the sound propagation characteristics of the water and the sound frequency and source level. Reception and processing of sounds by fish presents the potential for detection at a greater distance than that by either visual or chemoreceptive senses (Hawkins, 1993). Although the swimbladder of yellowfin tuna may enhance their acoustic detection and their ability to detect sounds, the size and shape of their swimbladder does not appear to provide for any directional information. Directionality in hearing, however, may exist in yellowfin tuna based on the anatomy and organization of the inner ears (Hawkins, 1993).

The physiological behavior of yellowfin tuna and the affect that it potentially has on the acoustic characteristics of the swimbladder should be considered. For instance, the swimming behavior of yellowfin tuna, exemplified by vertical excursions, may enable individuals to actively control the resonance frequencies of their swimbladders (Fig. 7) and to potentially enhance their ability to sense their environment, as previously proposed by Feuillade and Nero (1998) for other fish with swimbladders. By varying the resonance frequency of the swimbladder, yellowfin tuna may be able not only to amplify acoustic signals but also filter auditory signals and thus improve acoustic detection in the presence of high levels of ambient noise (Hawkins, 1993).

Because estimates of yellowfin tuna swimbladder resonance frequencies presented in our study were within the range of frequencies audible to yellowfin tuna (Iverson, 1967) and because swimbladders may enhance yellowfin tuna hearing (Blaxter and Tytler, 1978; Blaxter, 1980), it is tempting to speculate about the potential distance at which yellowfin tuna could become aware of dolphins (*Stenella* spp. and *Delphinus delphis*) or prey, predators, or conspecifics through sound reception. Identification of a mechanism that facilitates the yellowfin tuna and porpoise bond in the eastern Pacific (National Research Council, 1992) may provide a means of breaking the bond prior to setting nets that encircle dolphins, thus enabling the capture of yellowfin tuna without catching dolphins. If the mechanism is an attractant (i.e. yellowfin tuna move towards the sounds of dolphins or other oceanic sounds, or towards the sounds of both), then the possibility exists to attract larger yellowfin tuna artificially with acoustical devices. Active sounds produced by dolphins include clicks, bangs, and whistles (Schevill, 1964; Tavolga, 1965; Norris and Mohl, 1983; Watkins and Wartzok, 1985; Marten et al., 1988) at peak frequencies as high as 160 kHz and peak source levels up to 228 dB re 1μPa (Au, 1993). Passive sounds resulting from tail-slaps, breaches, and other behaviors have also been described as loud (Hult, 1982; Smolker and Richards, 1988). The energy at frequencies between 50 and 1100 Hz is of particular interest because yellowfin tuna have been shown to respond to sounds in this range—the most sensitive responses occurring between 300 and 500 Hz (Iverson, 1967).

Sound intensity decreases with range as a sound propagates through the water, primarily because of transmission loss associated with spherical spreading of the wavefront and absorption (Richardson et al., 1995). At 500 Hz, absorption loss is approximately 0.013 dB/km (Urick, 1983) and total transmission loss can be approximated from spreading loss alone over relatively short distances. We used the best hearing sensitivity at 500 Hz reported by Iversen (1967) for small yellowfin tuna (83 dB re 1μPa) as the minimum received source level (SL) a tuna can hear. In the absence of published data on SL at 500 Hz associated with low-frequency sounds

produced by *Stenella* and *Delphinus*, we use the maximum SL measured for jaw pops of *Tursiops truncatus*, 163 dB re 1µPa (Finneran et al., 2000). Maximum detection range under spherical spreading conditions is calculated as:

$$Range = 10\,(SL_{initial} - SL_{received}) / 20. \quad (8)$$

In the absence of other sounds (e.g. ambient noise), we estimated that yellowfin tuna in the eastern Pacific Ocean may be able to detect a 500-Hz sound of 163 dB re 1µPa out to a distance of approximately 10 km.

Ambient noise in offshore waters results primarily from wind and waves (Richardson et al., 1995) and can mask reception of other sounds. In the region of the eastern Pacific Ocean, where a yellowfin tuna fishery exists, the sea surface is characterized by frequent periods of light winds with wind speed less than 5 m/s (sea state 2) more than 60% of the time (Webb, 1998). At 500 Hz and with sea state 2, broadband ambient noise is approximately 85 dB re 1µPa (Richardson et al., 1995), and would probably mask the ability of tuna to detect our hypothetical 83-dB dolphin sound at the maximum distance we calculated. We are unaware of any data on critical ratios or critical band widths associated with tuna hearing, from which we could estimate the effective received level required for a tuna to detect our sound in the presence of this ambient noise. However, the source level received by a yellowfin tuna would have to be higher than ambient noise level, thus reducing detection distance.

The swimbladder of yellowfin tuna may function as a key mechanism in the formation of the bond between yellowfin tuna and dolphins in the eastern Pacific Ocean. Whether larger yellowfin tuna actively search for dolphins to increase their probability of remaining within food-rich habitat (Fiedler et al., 1998) or whether the dolphin's sonar echolocation ability detects yellowfin tuna (Au, 1993), the swimbladder may play an important role in both sound reception and detectability as an acoustical target. Further research should be conducted on yellowfin tuna bioacoustics, including hearing sensitivity in larger yellowfin tuna, determination of the role of the swimbladder in hearing sensitivity, and measurements of source level sounds produced by dolphins and other marine organisms at frequencies below 1 kHz, referenced to a source.

## Acknowledgments

We thank R. Deriso and E. Edwards for their encouragement and support of this investigation. We are grateful to F. LoPreste and S. Loomis, and also the crew and passengers of the *Royal Polaris*, for their invaluable assistance in obtaining these data. We also gratefully acknowledge R. Allen, W. Bayliff, R. Nero, D. Rees, and three anonymous reviewers for helpful suggestions and comments on the manuscript. This paper is dedicated to the memory of James "Rollo" Heyn (1960–1999) who taught me, K. Schaefer, a great deal over the years aboard the *Royal Polaris* about how to kill large yellowfin tuna with rod and reel, in the name of science.

## Literature cited

**Alexander, R. M.**
**1993.** Buoyancy. *In* The physiology of fishes (D. H. Evans, ed.), p. 75–97. CRC Press, Inc., Boca Raton, FL.

**Andreeva, I. B.,**
**1964.** Scattering of sound by air bladders of fish in deep sound-scattering ocean layers. Sov. Phys. Acoust. 10:17–20.

**Au, W. W. L.**
**1993.** The sonar of dolphins. Springer-Verlag New York, Inc., New York, NY, 277 p.

**Bayliff, W. H. (ed.).**
**1998.** Inter-Amer. Trop. Tuna Comm., Ann. Rep. for 1996, 306 p.

**Blaxter, J. H. S.**
**1980.** The swimbladder and hearing. *In* Hearing and sound communication in fishes (W. N. Tavolga, A. N. Popper, and R. R. Fay. eds.), p. 61–71. Springer-Verlag, New York, NY.

**Blaxter, J. H. S., and P. Tytler.**
**1978.** Physiology and function of the swimbladder. Adv. Comp. Phys. Biochem. 7:311–367.

**Block, B. A., J. E. Keen, B. Castillo, H. Dewar, E. V. Freund, D. J. Marcinek, R. W. Brill, and C. Farwell.**
**1997.** Environmental preferences of yellowfin tuna (*Thunnus albacares*) at the northern extent of its range. Mar. Biol. 130:119–132.

**Carey, F. G., and R. J. Olson.**
**1982.** Sonic tracking experiments with tuna. International Commission for the Conservation of Atlantic Tunas (ICCAT), Collective Volume of Scientific Papers 17:458–468.

**Chang, R. K. C., and J. J. Magnuson.**
**1968.** A radiographic method for determining gas bladder volume of fish. Copeia 1968:187–189.

**Feuillade, C, and R. W. Nero.**
**1998.** A viscous-elastic swimbladder model for describing enhanced-frequency resonance scattering from fish. J. Acoust. Soc. Am. 103:3245–3255.

**Feuillade, C., R. W. Nero, and R. H. Love.**
**1996.** A low frequency acoustic scattering model for small schools of fish. J. Acoust. Soc. Am. 99:196–208.

**Fiedler, P. C.**
**1992.** Seasonal climatologies and variability of eastern tropical Pacific surface waters. U.S. Dep. Commer., NOAA Tech. Rep. NMFS 109:1–65.

**Fiedler, P. C., J. Barlow, and T. Gerrodette.**
**1998.** Dolphin prey abundance determined from acoustic backscatter data in eastern Pacific surveys. Fish. Bull. 96:237–247.

**Finneran, J. J., C. W. Oliver, K. M. Schaefer, and S. H. Ridgway.**
**2000.** Source levels and estimated yellowfin tuna (*Thunnus albacares*) detection ranges for dolphin jaw pops, breaches, and tail slaps. J. Acoust. Soc. Am. 107(1):649–656.

**Foote, K. G.**
**1980.** Importance of the swimbladder in acoustic scattering by fish: a comparison of gadoid and mackerel target strength. J. Acoust. Soc. Am. 67:2084–2089.

**Godsil, H. C., and R. D. Byers.**
**1944.** A systematic study of Pacific tunas. Calif. Div. Fish Game, Fish Bull. 60, 131 p.

**Guthrie, D. M., and W. R. A. Muntz.**
**1993.** Role of vision in fish behaviour. *In* Behaviour of teleost fishes, second ed. (T. J. Pitcher, ed.), p. 89–128. Chapman and Hall, London.

**Hara, T. J.**
**1993.** Role of olfaction in fish behaviour. *In* Behaviour of teleost fishes, second ed. T. J. Pitcher, ed.), p. 171–199. Chapman and Hall, London.

**Harden Jones, F. R., and G. Pearce.**
**1958.** Acoustic reflexion experiments with perch (*Perca flariatilis* Linn.) to determine the proportion of the echo returned by the swimbladder. J. Exp. Biol. 35:437–450.

**Hawkins, A. D.**
**1993.** Underwater sound and fish behaviour. *In* Behaviour of teleost fishes, second ed. (T. J. Pitcher, ed.), p. 129–169. Chapman and Hall, London.

**Holland, K. N., R. W. Brill, and R. K. C. Chang.**
**1990.** Horizontal and vertical movements of yellowfin and bigeye tuna associated with fish aggregating devices. Fish. Bull. 88:493–507.

**Hult, R.**
**1982.** Another function of echolocation for bottlenose dolphins (*Tursiops truncatus*). Cetology 47:1.

**Iverson, R. T. B.**
**1967.** Response of yellowfin tuna (*Thunnus albacares*) to underwater sound. *In* Marine bio-acoustics, vol 2 (W. N. Tavolga,. ed.), p.105–121. Pergamon, New York, NY.

**Love, R. H.**
**1977.** Target strength of an individual fish at any aspect. J. Acoust. Soc. Am. 62:1397–1403.
**1978.** Resonant acoustic scattering by swimbladder-bearing fish. J. Acoust. Soc. Am. 64:571–580.
**1981.** A model for estimating distributions of fish school target strengths. Deep-Sea Res. 28A:705–725.

**Magnuson, J. J.**
**1973.** Comparative study of adaptations for continuous swimming and hydrostatic equilibrium of scombroid and xiphoid fishes. Fish. Bull. 71:337–356.

**Marten, K., K. Norris, P. W. B. Moore, and K. A. Englund.**
**1988.** Loud impulse sounds in odontocete predation and social behavior. *In* Animal sonar: processes and performance (P. E. Nachtigall and P. W. B. Moore, eds.) p. 567–579. Plenum, New York, NY.

**National Research Council.**
**1992.** Committee on reducing porpoise mortality from tuna fishing, dolphins and the tuna industry. National Academy Press, Washington, D.C., 176 p.

**Norris, K. S., and B. Mohl.**
**1983.** Can odontocetes debilitate prey with sound? Am. Nat. 122:85.

**Ona, E.**
**1990.** Physiological factors causing natural variations in acoustic target strength of fish. J. Mar. Biol. Assoc. U.K. 70:107–127.

**Rees, C. D.**
**1998.** Active towed-array acoustic system design study for yellowfin tuna in the eastern tropical Pacific fishery area. U.S Dep. Commer, NOAA Tech. Memo. TM-NMFS-SWFSC-251, 65 p. plus appendices.

**Richardson, J. W., C. R. Greene, C. I. Malme, and D. H. Thomson.**
**1995.** Marine mammals and noise. Academic Press, San Diego, CA, 576 p.

**Schaefer, K. M.**
**1999.** Comparative study of some morphological features of yellowfin (*Thunnus albacares*) and bigeye (*Thunnus obesus*) tunas. Inter-Am. Trop. Tuna Comm., Bull. 21:489–525.

**Schevill, W. E.**
**1964.** Underwater sounds of cetaceans. *In* Marine bio-acoustics, vol. 1 (W. N. Tavolga, ed.), p. 307–316. Pergamon, New York, NY.

**Smolker, R., and A. Richards.**
**1988.** Loud sounds during feeding in Indian Ocean bottlenose dolphins. *In* Animal sonar: processes and performance (P. E. Nachtigall and P. W. B. Moore, eds.), p. 703–706. Plenum, New York, NY.

**Tavolga, W. N.**
**1965.** Review of marine bio-acoustics, state of the art. U.S. Naval Training Device Center Tech. Report 1212-1, 100 p.

**Urick, R. J.**
**1983.** Principles of underwater sound, third ed. McGraw-Hill, New York, NY, 423 p.

**Watkins, W. A., and D. Wartzok.**
**1985.** Sensory biophysics of marine mammals. Mar. Mamm. Sci. 1:219–260.

**Webb, S. C.**
**1998.** Broadband seismology and noise under the ocean. Rev. Geophys. 36:105–142.

**Weston, D. E.**
**1967.** Sound propagation in the presence of bladder fish. *In* Underwater acoustics, vol. 2 (M. Albers, ed.), p. 55–88. Plenum, New York, NY.

**Zar, J. H.**
**1974.** Biostatistical analysis. Prentice-Hall, Englewood Cliffs, NJ, 620 p.

# Identification and distribution of larvae of redfish (*Sebastes fasciatus* and *S. mentella*: Scorpaenidae) in the Gulf of St. Lawrence

**Jean-Marie Sévigny**
Direction des Invertébrés et de la Biologie expérimentale
Institut Maurice-Lamontagne
Ministère des Pêches et des Océans
850 Route de la Mer
Mont-Joli
Québec G5H 3Z4, Canada
E-mail address : Sevignyjm@dfo-mpo.gc.ca

**Patrice Gagné**
Département de Biologie
Faculté des Sciences et de Génie
Université Laval
Québec G1K 7P4, Canada

**Yves de Lafontaine**
Environment Canada
Centre Saint-Laurent, 105 McGill, suite 7400
Montréal, Québec H2Y 2E7, Canada

**Julian Dodson**
Département de Biologie
Faculté des Sciences et de Génie
Université Laval
Québec G1K 7P4, Canada

**Abstract.**—Genetic variation at the liver *MDH** locus was used to describe the species composition and the geographic distribution of the larvae of the two redfish species, (*Sebastes mentella* and *S. fasciatus*) in the Gulf of St. Lawrence in 1991 and 1992. In both years, redfish larvae were more abundant at the junction of the Laurentian and the Esquiman Channels than in other areas surveyed. Electrophoretic analysis of 697 larvae in 1991 and 1041 in 1992 showed that larvae of both species were present in the Gulf during the two years of the study although in very different proportion. Larvae belonging to the genotype *MDH*A1A1* (*S. mentella*) represented at least 61% of the redfish larvae collected in the Gulf in 1991 and 77% in 1992. Strong spatial heterogeneity in the frequency of the two *MDH** alleles was observed; a higher proportion of *S. mentella* occurred in the central and deeper part of the channels and a higher proportion of *S. fasciatus* in shallower zones. Larvae of the genotype *MDH*A1A1* (*S. mentella*) were significantly larger than those of the genotype *MDH*A2A2* (*S. fasciatus*) for both years of the study, suggesting that the extrusion times differ between the two redfish species. The sizes and geographic distributions of the heterozygous larvae (*MDH*A1A2*) did not differ from those of *S. mentella* (*MDH*A1A1*).

The Gulf of St. Lawrence redfish consist of a complex of three putative species, currently identified as deepwater redfish, *Sebastes mentella*, and Acadian redfish, *S. fasciatus*, that dominate the commercial fishery (Atkinson, 1984; 1987; Rubec et al., 1991) and golden redfish, *S. norvegicus*, formerly named *S. marinus* (Fernholm and Wheeler, 1983) which occurs only sporadically and at very low abundance, namely at <1% of the catch (Ni and McKone, 1983; Rubec et al., 1991).

Although *S. fasciatus* differs morphologically from *S. mentella*, the overlap in meristic and morphometric characters is such that the two redfish species are difficult to separate and, frequently, individuals cannot be unequivocally identified (Ni, 1981; 1982; Kenchington, 1986; Rubec et al., 1991). Discrimination among redfish larvae is even more complex because the morphological characters used for adults and juveniles cannot be used for identifying species during the larval stages (Penney, 1987). The taxonomic confusion, as well as the absence of reliable morphological characters to identify the larvae, has limited our understanding of the ecology and population dynamics of redfish in the North Atlantic.

Electrophoretic analysis is an appropriate tool for identifing *Sebastes* species at all stages of their life cycle, including larvae (Payne and Ni, 1982; McGlade et al., 1983; Nedreaas and Naevdal, 1991; Rubec et al., 1991; Seeb and Kendall, 1991;

Manuscript accepted 26 November 1999.
Fish. Bull. 98: 375–388 (2000).

Sévigny and de Lafontaine, 1992; Gagné, 1995; Seeb, 1998). In the Northwest Atlantic, differences in the electrophoretic mobility patterns of the dimeric protein malate dehydrogenase (MDH; EC 1.1.1.37) from liver tissue appear to distinguish *S. fasciatus* from *S. mentella* (Payne and Ni, 1982; McGlade et al., 1983; Rubec et al., 1991). The presence of two alleles (*MDH*A1* and *MDH*A2*) segregating at this locus results in three genotypes that can easily be identified by electrophoresis. A low-mobility banding pattern, corresponding to the genotype *MDH*A2A2* predominates in *S. fasciatus* whereas a high-mobility pattern, corresponding to the genotype *MDH*A1A1*, is more characteristic of *S. mentella*. However, there are two restrictions to using this approach. First and foremost, the heterozygous individuals sharing alleles of both *S. fasciatus* and *S. mentella* cannot be assigned unambiguously to one species. Second, electrophoretic mobility of MDH does not differ between *S. mentella* and *S. norvegicus* (McGlade et al., 1983). Despite these limitations and until a more reliable taxonomic tool becomes available, electrophoretic mobility patterns of liver MDH remain the best approach for identification of redfish species in the Gulf of St. Lawrence, especially at larval stages. However, one should remember that the taxonomic status of redfish is still under debate and although, for convenience, we use and refer to the species names *S. fasciatus* and *S. mentella* throughout the text, these may be putative species.

Redfish of the North Atlantic are ovoviviparous; their eggs are fertilized by sperm stored in the oviducts. Although the reproductive biology of the redfish of the Gulf of St. Lawrence is not well understood, mating (transfer of spermatozoa from male to female) probably takes place during late fall or early winter. Fertilization and embryogenesis take place in winter, and larvae hatch internally and are extruded during late spring and early summer (St-Pierre and de Lafontaine, 1995, and references therein). In consequence, the location of larval extrusion may differ significantly from the location where copulation has taken place. In order to avoid confusion, the term "larval extrusion," rather than "spawning," is used to distinguish between the hatching-extrusion phase and the mating phase of the redfish reproductive cycle. The importance of gene flow within and between species is established during the mating and fertilization phase of the reproductive cycle, whereas the location of larval hatching and extrusion will determine the geographic distribution of the species at the larval stage.

It is commonly assumed that the life cycle of the two species of redfish is completed inside the Gulf and that the redfish larval population represents a mixture of *S. fasciatus* and *S. mentella*. Although the presence of newly hatched redfish larvae in plankton samples from the Gulf did confirm that redfish extrude larvae in this area (de Lafontaine, 1990, and references therein; de Lafontaine et al., 1991), the species composition of these larvae has never been elucidated and their distribution in the Gulf has never been described. The objectives of the present study were 1) to describe the species composition of larval redfish in order to verify that the two species use the Gulf of St. Lawrence as an extrusion site, 2) to determine the spatial co-occurrence of *S. fasciatus* and *S. mentella* within the Gulf, and 3) to describe the larval size distribution of the two species as an indication of the variability in extrusion times.

## Materials and methods

### Sample collection

Sampling was conducted at 32 stations along three transects on the western and eastern side of Anticosti Island in the Gulf of St. Lawrence between 22 June and 4 July 1991 and at 74 stations, located mainly to the east of Anticosti Island, between 10 June and 20 June 1992 (Figs. 1 and 2). Numerous sampling stations were selected in order to obtain the largest spatial coverage for larval redfish distribution in the Gulf of St. Lawrence. Plankton samples were collected with a modified opening-closing 1-$m^2$ rigid "Tucker" trawl equipped with two, 333-m mesh nets and two G.O. model 2030 flowmeters. The gear was hauled in double-oblique tows from the ship's side at a cruising speed of 2.5–3.0 knots. Sampling was restricted to the 0–50 m upper layer where redfish larvae are concentrated (Kenchington, 1991; Runge and de Lafontaine, 1996). Maximum sampling depth was determined by a Vemco acoustic transducer attached to the gear frame and by calculation from the amount of wire length deployed and the wire angle. Tow duration varied between 6 and 10 min. Once back on board, nets were rapidly rinsed and samples were concentrated in codends and transferred to the laboratory on the vessel for larval sorting.

Upon collection, a visual examination of the samples was made. When the estimated number of larvae in one sample was greater than fifty, a subsample was taken for further sorting. All redfish larvae from the subsample were sorted individually and placed gently, while alive, in a drop of water on a plexiglass plate (95 mm diameter and 0.61 mm thickness) next to an inscribed number that served to identify individuals for the videotape recordings (see below)

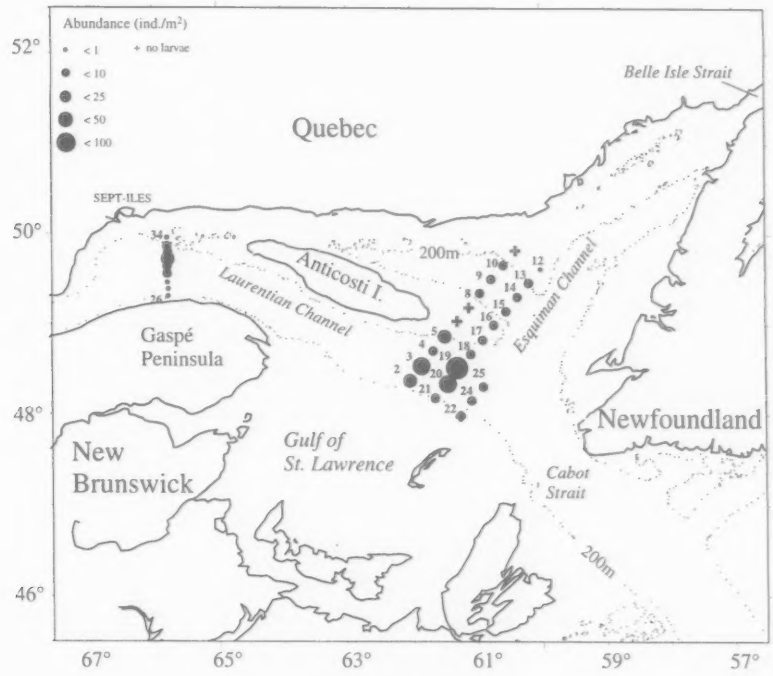


**Figure 1**

Geographic distribution and abundance of redfish larvae at stations sampled in June–July 1991 in the Gulf of St. Lawrence.

and for genotype determination. This procedure was adopted to minimize possible bias towards selection of larger larvae during sorting. A maximum of 10 larvae were placed on each plate. The total number of larvae so treated varied between stations owing to variable larval abundance at each station. The remaining sample with unsorted larvae and plankton was preserved in a 10% formalin seawater solution (4% formaldehyde) for subsequent laboratory sorting. Re-examination of the samples and subsamples in the laboratory showed that the proportion of larvae remaining in the samples was always less than 5% and that in most cases, larvae had been effectively sorted during the initial onboard sorting process.

The larvae placed on plates were individually video-recorded with a Hitachi black and white camera mounted on a stereomicroscope at 6× and 9× magnification and connected to a Sony Beta videotape recording machine. Periodic calibration of the magnification was made by filming a stage micrometer. The overall procedure (from sorting to filming) was completed in less than 5 min. and care was taken to ensure that larvae were alive during the video recording. The fish were sorted and video-taped on board while still alive so that morphometric measurements represented real values; these fish were later used for genetic analyses. This procedure eliminated the necessity of having one subsample for morphometric analyses and another one for biochemical analyses and did not introduce any measurement bias due to postmortem and preservation shrinkage (Magnússon[1]). Afterwards, each plate with larvae was immersed for a few seconds in liquid nitrogen, then placed in a petri dish and stored on board at –40°C. Samples were transferred to a –80°C freezer in the laboratory until electrophoresis analyses were carried out.

### Laboratory analyses

Standard lengths of individual larvae was measured from the video recordings that were digitized with a Bioquant M8 image analyzing system. Repeated measurements of individual larvae indicated a measurement error of less than 3% (de Lafontaine, unpubl. data). Plankton samples were examined completely and the redfish larvae were sorted and enu-

[1] Magnússon, J. V. 1982. Shrinkage of dying redfish larvae. Int. Counc. Explor. Sea (ICES) Council Meeting 1982/G:23.

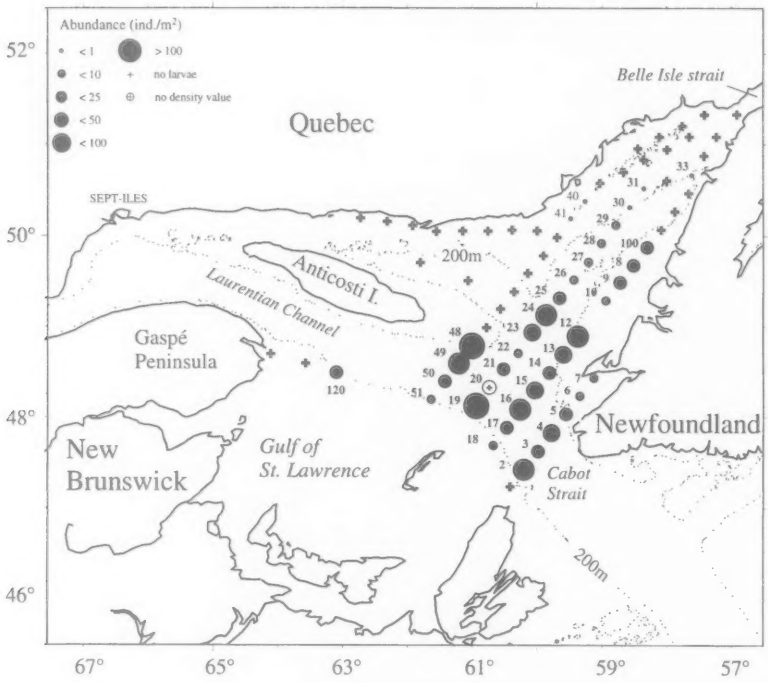


**Figure 2**

Geographic distribution and abundance of redfish larvae at stations sampled in June 1992 in the Gulf of St. Lawrence.

merated. The number of larvae frozen on board and those later sorted from the plankton samples were summed to provide estimates of the total abundance of redfish larvae (individuals/$m^2$) at each station.

### Electrophoretic analyses

All electrophoretic analyses were performed within two to three months after specimen collection. The plexiglass plates supporting the larvae were always kept on ice during laboratory examination and analysis. The tissue in the liver area of individual larva was dissected under a stereomicroscope, placed directly into an individual sample well, and homogenized in an extraction solution containing 10 µL of a 0.01M Tris-HCl (pH 8.0) composed of 30% sucrose, 0.005M dithiothreitol (DTT), 0.5% polyvinylpyrrolidone (PVP) and 0.001M phenylmethylsulfonyl fluoride (PMSF). The tissue was homogenized with a fine glass rod and an aliquot was applied on the cellulose acetate gels. Cellulose acetate gel electrophoresis and gel staining were carried out as described by Hebert and Beaton (1989). A specimen of genotype *MDH*A1A2* was used as a standard on every gel to assess both the quality of the electrophoretic separation and to ensure allele identification. In 1991, a total of 735 larvae was frozen and analyzed for genotypic variation. Interpretable results were obtained for 697 specimens. In 1992, 1041 larvae were analyzed and scored.

Two alleles segregated at the *MDH** locus, resulting in the presence of three phenotypes (Rubec et al. 1991 and references therein). Homozygotes for the slow allele (*MDH*A2*) were assigned to *S. fasciatus*, and the homozygotes for the fast allele (*MDH*A1*) were classified as *S. mentella*. Heterozygotes at the *MDH** locus were left unclassified (see "Results" and "Discussion" sections).

### Statistical analyses

The adequacy of genotypic proportions to Hardy-Weinberg expectations was tested for each sampling station where genotypic variation was observed by using the *G*-test of goodness-of-fit (Tables 1 and 2).

Standard length data were either not homoscedastic or not normally distributed. Therefore, comparisons of larval standard length between 1991 and 1992, between the different sampled areas of the Gulf, were carried out with a Mann Whitney *U*-test. Heterogeneity in the distribution of standard lengths

**Table 1**

Observed (Obs.) and expected (Exp.) number of larvae with each of the three genotypes and allelic frequencies in samples taken during June–July 1991. The mean standard length of the larvae and its coefficient of variation (CV, as a percentage) and the *G*-test values for deviation from Hardy-Weinberg expectations are given. * indicates that results were significant at $P<0.05$; ** indicates that results were significant at $P<0.001$.

| Sampling station | Depth (m) | Larval density (no./m²) | Genotype *A1A1* Obs. | *A1A1* Exp. | *A1A2* Obs. | *A1A2* Exp. | *A2A2* Obs. | *A2A2* Exp. | Allelic frequency *A1 | *A2 | *n* | *G*-test value | Fish length Mean (mm) | Fish length CV (%) |
|---|---|---|---|---|---|---|---|---|---|---|---|---|---|---|
| 2 | 340 | 19.9 | 20 | 20.0 | 9 | 9.0 | 1 | 1.0 | 0.817 | 0.183 | 30 | 0 | 9.63 | 10.12 |
| 3 | 437 | 28.5 | 23 | 22.7 | 12 | 12.5 | 2 | 1.7 | 0.784 | 0.216 | 37 | 0.274 | 9.28 | 8.58 |
| 4 | 380 | 7.2 | 10 | 9.8 | 5 | 5.5 | 1 | 0.8 | 0.781 | 0.219 | 16 | -0.103 | 8.72 | 9.77 |
| 5 | 246 | 20.6 | 33 | 34.1 | 19 | 16.8 | 1 | 2.1 | 0.802 | 0.198 | 53 | 0.514 | 8.60 | 10.18 |
| 8 | 225 | 1.4 | 0 | 0 | 0 | 0 | 10 | 10.0 | 0 | 1 | 10 | — | 7.50 | 8.08 |
| 9 | 290 | 2.1 | 2 | 0.4 | 1 | 4.2 | 13 | 11.4 | 0.156 | 0.844 | 16 | *6.982 | 6.99 | 9.28 |
| 10 | 267 | 1.6 | 0 | 0 | 0 | 0 | 9 | 9.0 | 0 | 1 | 9 | — | 6.98 | 11.78 |
| 13 | 216 | 1.4 | 6 | 3.2 | 1 | 6.5 | 6 | 3.2 | 0.500 | 0.500 | 13 | *11.340 | 7.14 | 7.41 |
| 14 | 276 | 9.7 | 30 | 20.4 | 10 | 29.2 | 20 | 10.4 | 0.583 | 0.417 | 60 | *27.865 | 8.17 | 14.29 |
| 15 | 244 | 4.5 | 1 | 0.2 | 1 | 2.7 | 13 | 12.2 | 0.100 | 0.900 | 15 | 2.884 | 7.29 | 8.55 |
| 16 | 146 | 1.5 | 7 | 6.4 | 2 | 3.2 | 1 | 0.4 | 0.800 | 0.200 | 10 | 1.207 | 8.80 | 15.92 |
| 17 | 174 | 5.5 | 24 | 24.0 | 14 | 14.0 | 2 | 2.0 | 0.775 | 0.225 | 40 | 0 | 9.46 | 11.06 |
| 18 | 375 | 5.9 | 11 | 10.2 | 8 | 9.5 | 3 | 2.2 | 0.682 | 0.318 | 22 | 0.772 | 9.64 | 13.33 |
| 19 | 416 | 62.6 | 30 | 27.8 | 5 | 9.4 | 3 | 0.8 | 0.855 | 0.145 | 38 | *6.187 | 9.25 | 1.074 |
| 20 | 405 | 36.1 | 14 | 14.3 | 9 | 8.4 | 1 | 1.2 | 0.771 | 0.229 | 24 | 0.284 | 10.07 | 6.91 |
| 21 | 405 | 1.1 | 3 | 1.5 | 0 | 3.0 | 3 | 1.5 | 0.500 | 0.500 | 6 | *8.318 | 8.91 | 13.64 |
| 22 | 64 | 1.4 | 6 | 6.0 | 0 | 0 | 0 | 0 | 1 | 0 | 6 | — | 7.16 | 31.04 |
| 24 | 369 | 3.8 | 13 | 12.4 | 7 | 8.2 | 2 | 1.4 | 0.750 | 0.250 | 22 | 0.440 | 9.80 | 16.52 |
| 25 | 475 | 7.0 | 33 | 32.4 | 6 | 7.2 | 1 | 0.4 | 0.900 | 0.100 | 40 | 0.856 | 10.36 | 11.99 |
| 26 | 222 | 0.4 | 0 | 0 | 0 | 0 | 4 | 4.0 | 0 | 1 | 4 | — | 6.47 | 11.89 |
| 27 | 350 | 0.6 | 0 | 0 | 0 | 0 | 7 | 7.0 | 0 | 1 | 7 | — | 6.97 | 8.19 |
| 28 | 346 | 0.5 | 0 | 0 | 0 | 0 | 4 | 4.0 | 0 | 1 | 4 | --- | 6.83 | 4.83 |
| 29 | 330 | 4.0 | 1 | 0.5 | 5 | 6.0 | 19 | 18.4 | 0.140 | 0.860 | 25 | 0.782 | 7.69 | 15.13 |
| 30 | 329 | 7.5 | 38 | 33.6 | 10 | 18.8 | 7 | 2.6 | 0.782 | 0.218 | 55 | *10.593 | 9.25 | 11.24 |
| 31 | 338 | 13.8 | 36 | 31.8 | 10 | 18.5 | 7 | 2.7 | 0.774 | 0.226 | 53 | *9.965 | 8.96 | 14.35 |
| 32 | 335 | 3.6 | 13 | 7.5 | 4 | 15.0 | 13 | 7.5 | 0.5 | 0.5 | 30 | *18.028 | 7.92 | 11.24 |
| 33 | 274 | 3.8 | 1 | 0.1 | 3 | 4.7 | 43 | 42.2 | 0.053 | 0.947 | 47 | 3.526 | 7.15 | 11.15 |
| 34 | 170 | 0.9 | 2 | 1.2 | 1 | 2.5 | 2 | 1.2 | 0.500 | 0.500 | 5 | 2.254 | 8.67 | 12.67 |
| East sites | | | 266 | 219.8 | 109 | 201.2 | 92 | 46.0 | 0.686 | 0.314 | 467 | **95.410 | 8.93 | 15.79 |
| West sites | | | 91 | 50.2 | 33 | 114.5 | 106 | 65.3 | 0.467 | 0.533 | 230 | *128.856 | 8.24 | 16.46 |
| All sites | | | 357 | 262.8 | 142 | 330.4 | 198 | 103.8 | 0.614 | 0.386 | 697 | *234.634 | 8.70 | 16.42 |

among the three genotypes within and between sampled areas and between years was tested with a Kruskal-Wallis test. Nonparametric multiple comparisons (Dunn test) were used *a posteriori* to determine which genotypes had significantly different sizes of larvae. Differences between genotypic pairs were considered significant when $P<0.05$; the statistics $Q$ is thus not provided in our text.

The relative proportion of *S. mentella* and of *S. fasciatus* in the sampled larval population was estimated by using two different approaches depending on the taxonomic status of the heterozygous individuals. With the first approach, the heterozygous individuals were not taken into account and the contribution of *S. mentella* and of *S. fasciatus* was based on the frequencies of the genotypes *MDH*A1A1* and *MDH*A2A2*, respectively. This approach yielded a conservative estimate. With the second approach, the heterozygous individuals were attributed to *S. mentella*. This procedure can be justified by the lack of difference in the size distribution of the *MDH*A1A1* and *MDH*A1A2* individuals and by the similar geographic distribution of these two genotypes (see "Results" and "Discussion" sections).

**Table 2**

Observed (Obs.) and expected (Exp.) number larvae with each of the three genotypes and allelic frequencies in samples taken during June 1992. The mean standard length of the larvae and its coefficient of variation (CV, as a percentage) and the *G*-test values for deviation from Hardy-Weinberg equilibrium are given. * indicates that results were significant at $P<0.05$; ** indicates that results were significant at $P<0.001$; nd = density value was not determined; therefore, this sampling station was not considered in the calculation of the contribution of each genotype to the larval population.

| Sampling station | Depth (m) | Larval density (mo./m²) | Genotype *A1A1* Obs. | *A1A1* Exp. | *A1A2* Obs. | *A1A2* Exp. | *A2A2* Obs. | *A2A2* Exp. | Allelic frequency *A1 | Allelic frequency *A2 | *n* | *G*-test value | Fish length Mean (mm) | Fish length CV (%) |
|---|---|---|---|---|---|---|---|---|---|---|---|---|---|---|
| 2 | 427 | 51.0 | 23 | 21.4 | 8 | 11.1 | 3 | 1.4 | 0.794 | 0.206 | 34 | 2.650 | 8.36 | 5.90 |
| 3 | 531 | 22.1 | 19 | 19.3 | 5 | 4.5 | 0 | 0.3 | 0.896 | 0.104 | 24 | 0.458 | 8.07 | 10.99 |
| 4 | 464 | 33.8 | 25 | 24.0 | 8 | 9.9 | 2 | 1.0 | 0.829 | 0.171 | 35 | 1.404 | 8.74 | 6.62 |
| 5 | 196 | 12.5 | 24 | 23.1 | 8 | 9.9 | 2 | 1.1 | 0.824 | 0.176 | 34 | 0.816 | 8.82 | 5.63 |
| 6 | 126 | 9.2 | 28 | 27.3 | 4 | 5.5 | 1 | 0.3 | 0.909 | 0.091 | 33 | 1.278 | 8.99 | 6.64 |
| 7 | 93 | 1.3 | 18 | 17.9 | 8 | 8.1 | 1 | 0.9 | 0.815 | 0.185 | 27 | 0.212 | 8.77 | 5.42 |
| 8 | 110 | 19.6 | 23 | 20.8 | 8 | 12.3 | 4 | 1.8 | 0.771 | 0.229 | 35 | *4.130 | 9.00 | 4.83 |
| 9 | 128 | 16.0 | 18 | 15.6 | 10 | 14.9 | 6 | 3.6 | 0.676 | 0.324 | 34 | *24.690 | 9.01 | 8.69 |
| 10 | 141 | 3.2 | 15 | 9.5 | 6 | 16.9 | 13 | 7.5 | 0.529 | 0.471 | 34 | *15.577 | 8.30 | 12.01 |
| 12 | 115 | 51.2 | 26 | 25.5 | 6 | 7.0 | 1 | 0.5 | 0.879 | 0.121 | 33 | 0.546 | 8.58 | 8.23 |
| 13 | 158 | 33.4 | 28 | 26.5 | 4 | 7.1 | 2 | 0.5 | 0.882 | 0.118 | 34 | *4.038 | 8.44 | 5.34 |
| 14 | 282 | 13.9 | 26 | 24.0 | 6 | 9.9 | 3 | 1.0 | 0.829 | 0.171 | 35 | *4.745 | 8.35 | 7.18 |
| 15 | 418 | 46.1 | 26 | 26.4 | 7 | 6.3 | 0 | 0.4 | 0.894 | 0.106 | 33 | 0.681 | 8.66 | 5.10 |
| 16 | 490 | 87.6 | 27 | 27.5 | 8 | 7.1 | 0 | 0.5 | 0.886 | 0.114 | 35 | 0.919 | 8.53 | 7.06 |
| 17 | 451 | 14.1 | 24 | 23.4 | 5 | 6.2 | 1 | 0.4 | 0.883 | 0.117 | 30 | 0.897 | 7.11 | 7.91 |
| 18 | 69 | 2.3 | 30 | 29.1 | 1 | 2.9 | 1 | 0.1 | 0.953 | 0.047 | 32 | *4.303 | 8.74 | 8.80 |
| 19 | 401 | 125.4 | 29 | 28.4 | 5 | 6.3 | 1 | 0.4 | 0.900 | 0.100 | 35 | 0.734 | 8.56 | 8.79 |
| 20 | 447 | nd | 30 | 30.2 | 5 | 4.6 | 0 | 0.2 | 0.929 | 0.071 | 35 | 0.435 | 8.70 | 8.24 |
| 21 | 393 | 20.2 | 29 | 28.3 | 4 | 5.5 | 1 | 0.3 | 0.912 | 0.088 | 34 | 1.277 | 7.91 | 7.31 |
| 22 | 317 | 1.8 | 3 | 0.8 | 2 | 6.3 | 14 | 11.8 | 0.211 | 0. 789 | 19 | *8.128 | 6.93 | 14.99 |
| 23 | 321 | 39.9 | 29 | 27.5 | 4 | 7.1 | 2 | 0.5 | 0.886 | 0.114 | 35 | *4.035 | 8.36 | 8.69 |
| 24 | 290 | 74.6 | 29 | 26.6 | 3 | 7.8 | 3 | 0.6 | 0.871 | 0.129 | 35 | *8.934 | 8.21 | 9.42 |
| 25 | 271 | 22.4 | 23 | 21.4 | 8 | 11.1 | 3 | 1.4 | 0.794 | 0.206 | 34 | 2.650 | 8.65 | 8.87 |
| 26 | 246 | 4.6 | 22 | 15.6 | 2 | 14.9 | 10 | 3.6 | 0.676 | 0.324 | 34 | **27.526 | 8.32 | 12.86 |
| 27 | 225 | 1.2 | 8 | 8.0 | 0 | 0 | 0 | 0 | 1 | 0 | 8 | — | 6.40 | 5.22 |
| 28 | 218 | 1.5 | 7 | 4.9 | 0 | 4.2 | 3 | 0.9 | 0.700 | 0.300 | 10 | **12.217 | 7.20 | 12.35 |
| 29 | 263 | 4.1 | 7 | 1.4 | 0 | 11.1 | 27 | 21.4 | 0.206 | 0.794 | 34 | **35.084 | 6.89 | 6.33 |
| 33 | 269 | 0.9 | 0 | 0 | 0 | 0 | 10 | 10.0 | 0 | 1 | 10 | — | 6.70 | 8.65 |
| 48 | 257 | 101.1 | 28 | 27.5 | 6 | 7.1 | 1 | 0.5 | 0.886 | 0.114 | 35 | 0.375 | 8.39 | 8.22 |
| 49 | 413 | 69.5 | 29 | 27.5 | 4 | 7.1 | 2 | 0.5 | 0.886 | 0.114 | 35 | *4.035 | 8.44 | 8.81 |
| 50 | 415 | 14.3 | 26 | 24.9 | 7 | 9.3 | 2 | 0.9 | 0.843 | 0.157 | 35 | 1.464 | 8.53 | 12.35 |
| 51 | 179 | 4.6 | 25 | 24.5 | 6 | 7.0 | 1 | 0.5 | 0.875 | 0.125 | 32 | 0.547 | 8.10 | 10.26 |
| 100 | 123 | 11.9 | 19 | 15.1 | 8 | 15.8 | 8 | 4.1 | 0.657 | 0.343 | 35 | *8.536 | 8.85 | 9.49 |
| 120 | 92 | 14.8 | 21 | 20.2 | 2 | 3.7 | 1 | 0.2 | 0.917 | 0.083 | 24 | 2.389 | 7.74 | 10.65 |
| All sites | | | 744 | 657.9 | 168 | 339.3 | 129 | 43.7 | 0.795 | 0.205 | 1041 | **226.100 | 8.35 | 10.91 |

Larval abundance at each station was taken into account when calculating the contribution of each genotype. The contribution for the entire sampling area was estimated by the sum of the relative contribution of each genotype at each station calculated by the formula:

$$TC = S((N_{MDH^*} / n) \times larval\ abundance),$$

where $TC$ = the total contribution of a genotype to the sampled larval population;

$N_{MDH^*}$ = the number of individuals of a genotype at the *MDH** locus for a given station; and

$n$ = the total number of individuals analyzed for MDH variation for a given station.

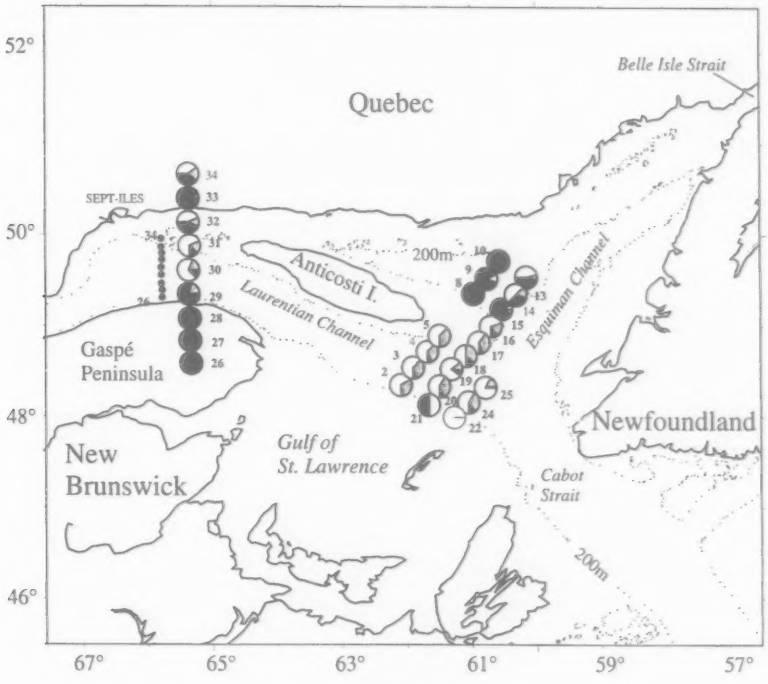


**Figure 3**

Geographic distribution of the larval genotypes *MDH*A1A1* characteristic of *S. mentella* (white), *MDH*A2A2* caracteristic of *S. fasciatus* (black) and *MDH*A1A2* (gray) in June–July 1991.

## Results

### Larval distribution, abundance, and size

In 1991, redfish larvae were caught at all but three sampling stations that were shallower than 200 m (Fig. 1). Larval abundance was highest (max.=62.6 individuals/$m^2$) over the central portion of the Laurentian Channel, on the southeastern side of Anticosti Island, and decreased northward along the Esquiman Channel. Only one larva was captured at the northeasternmost sampling station (12) (Fig. 1; Table 1). On the western side of Anticosti Island, larval abundance was highest (max.=13.8/$m^2$) at the central stations of the transect. Few larvae were caught at coastal stations within the Gaspé current (stations 26–28) or at the northernmost sampling station (<200 m deep) (Fig. 1; Table 1).

In 1992, larvae were collected at 34 of the 74 sampling stations (Fig. 2), and centers of abundance (max =125.4 larvae/$m^2$) were again located in the Laurentian Channel. Abundance gradually declined northwards along the Esquiman Channel. Larval redfish were virtually absent at the mouth of the Belle Isle Strait, along the Quebec north shore, at the shallow (<200 m) sampling stations on the north side of Anticosti Island or at the tip of the Gaspé peninsula (Fig. 2; Table 2).

The size of larvae ranged from 5.0 mm to 12.3 mm in 1991 and from 5.6 mm to 10.9 mm in 1992 (Tables 1 and 2). Larvae collected in 1991 were significantly larger than those collected in 1992 (Mann-Whitney *U*-test, $P<0.0001$; Table 1). Larvae from the eastern sector in 1991 were larger than those collected in the western sector (Mann-Whitney *U*-test, $P<0.0001$), and larvae collected in the eastern sector in 1991 were significantly larger than those collected in approximately the same region in 1992 (Mann-Whitney *U*-test, $P<0.0001$).

### Spatial and temporal genotypic variations

The three genotypes were found in larval redfish and their relative proportion varied between sites and years (Figs. 3 and 4; Tables 1 and 2). In 1991, two groups of stations could be identified on the western side of Anticosti Island (stations 26–34) based on the frequencies of the genotypes observed. The first

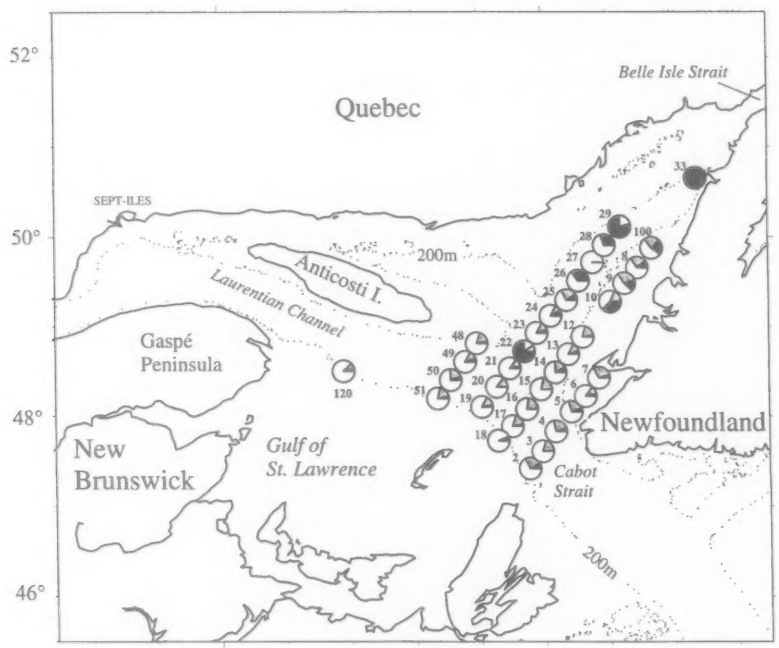


**Figure 4**

Geographic distribution of the larval genotypes *MDH*A1A1* characteristic of *S. mentella* (white), *MDH*A2A2* caracteristic of *S. fasciatus* (black) and *MDH*A1A2* (gray) in 1992. Sampling station numbering does not correspond with that for 1991.

group comprised stations 26–29 and 33–34 where the *MDH*A2A2* genotype is generally the most frequent. The frequency of allele *MDH*A2* at stations 26–29 within the Gaspé current system along the north shore of the Gaspé peninsula was very high, ranging from 0.860 to 1.0. At the northernmost station (33), the allele *MDH*A2* predominated and the frequency of both alleles was equal (0.500) at station 34. There was no significant deviation from Hardy-Weinberg expectations at the stations of this group. The second group comprised the central stations (30 31, 32). At theses stations, the three genotypes were represented but there was an abrupt inversion of the most frequent allele. At these stations, the frequency of allele *MDH*A1* ranged from 0.500 to 0.782. The frequency of this allele never equaled 1.0. Significant departure from Hardy-Weinberg expectations was also observed at these three central stations (Table 1).

On the eastern side of Anticosti Island, the genotype *MDH*A1A1* was most frequent in a group of stations located at the south-east end of the island near the junction of the Laurentian and Esquiman channels. The three genotypes were observed at each site except for station 22, where only *MDH*A1A1* was observed, and at station 21, where the heterozygous genotype was absent (Fig. 3; Table 1). Deviation from Hardy-Weinberg expectation was observed at stations 19 and 21 only (Table 1). The northern stations (8, 9, 10, 13, 14, 15) at the north-eastern end of Anticosti Island formed a distinct group where the genotype *MDH*A2A2* dominated. The frequency of allele *MDH*A2* varied from 0.417 to 1.0 (Table 1). The three genotypes were observed at stations 9, 13, 14, and 15 where significant deviation from Hardy-Weinberg was observed at all but sampling station 15 (Table 1).

In 1992, the genotype *MDH*A1A1* was also the most frequent genotype observed throughout the study area, except for stations 22, 29, and 33, where the genotype *MDH*A2A2* was dominant (Fig. 4). The allele *MDH*A1* was thus the most frequent except at these three sampling stations (Table 2). Stations 29 and 33 were the northernmost stations where larvae were found during our study. The frequency of the genotype *MDH*A2A2* increased towards the north within the sampling area although it was not the most frequent genotype. This trend was also observed in 1991 (Fig. 3). In general, the three genotypes were represented at all stations except at stations 3, 15, 16, 27, and 33, where only one or two genotypes

were observed. As noted in 1991, heterozygous individuals co-occurred with those of the *MDH*A1A1* genotype. The frequency of allele *MDH*A1* varied from 0.794 to 0.953 (Table 2). Allelic frequency of 1.0 was observed at stations 27 (*MDH*A1*) and 33 (*MDH*A2*) only. Deviations from Hardy-Weinberg expectations caused by a deficit in the number of heterozygous individuals were observed at 14 sampling stations (Table 2). When data for the entire study area were pooled, a significant departure from the Hardy-Weinberg equilibrium, also due to a deficit in heterozygotes, was noted for both years and for the eastern and western sectors of the Gulf in 1991 (Tables 1 and 2). Such deviations from Hardy-Weinberg equilibrium at any given station, within the different sectors of the Gulf or over the entire sampling area, indicate that redfish larval populations do not form a panmictic group in the Gulf of St. Lawrence but rather consist of a mixture of at least the two most frequent species, *S. mentella* and *S. fasciatus*.

A strong spatial heterogeneity in the distribution of genotypes was observed. The genotype *MDH*A2A2* dominated or was more frequent at stations located in the northern part of the Gulf whereas *MDH*A1A1* dominated in the southern part of the Gulf. The frequency distribution of the genotypes over the entire area in 1991 differed significantly between the eastern and the western Gulf of St. Lawrence ($\chi^2$=53.0; $P$<0.0001), indicating important spatial variation on a large scale.

### Genotype and larval-size distribution

In 1991, the size of the larvae varied significantly between the three genotypes (Kruskal-Wallis, $P$<0.0001); the *MDH*A2A2* larvae were smaller than those of the other two genotypes (Fig. 5). The size distribution of the larvae was not significantly different between the genotypes *MDH*A1A1* and *MDH*A1A2*. The size distribution of larvae of each genotype did not differ between the eastern and the western sectors of the Gulf. The obvious bimodal distribution of larval size (all genotypes confounded) observed on the west side of Anticosti Island can thus be explained by the difference in size of larvae of the different genotypes.

Similar results were obtained in 1992, where the size of the homozygous larvae *MDH*A2A2* was significantly smaller than those of the genotypes *MDH*A1A1* and *MDH*A1A2*. There was again no significant difference in the standard length between larvae of the *MDH*A1A1* and *MDH*A1A2* genotypes (Fig. 6).

A significant difference in the size of larvae between 1991 and 1992 (Kruskal-Wallis, $P$<0.0001; Fig. 6) was however noted and can be attributed to the smaller size of the *MDH*A1A1* and *MDH*A1A2* larvae in 1992 compared with those in 1991. The size distribution of the homozygous *MDH*A2A2* larvae was similar in both years.

In 1991, the genotype *MDH*A2A2* was more frequently represented in recently extruded larvae (<8.5 mm) and the genotype *MDH*A1A1* was most frequent for larvae >8.5 mm. In 1992, the genotype *MDH*A1A1* was the most frequent genotype in all size classes except for larvae <6.5 mm which were dominated by the genotype *MDH*A2A2*. In both years, the genotypic composition varied between the size classes of larval redfish, indicating that a larval cohort may be dominated by individuals belonging to a single species (Fig. 6). These differences are most likely associated with a difference in the extrusion time between *S. fasciatus* and *S. mentella*.

### Relative proportion of each genotype in the overall larval population

Larvae of the *MDH*A1A1* genotype accounted for 61.8% and 77.6% of all collected larvae in 1991 and 1992 respectively. The contribution of the *MDH*A2A2* genotype was 14.4% in 1991 but dropped to 5.6% in 1992. The heterozygote genotype accounted for 23.8% in 1991 and 16.8% in 1992. The combined contributions of the genotypes *MDH*A1A1* and *MDH*A1A2* thus represented 85.6% and 94.4% of the larval population in 1991 and 1992, respectively.

## Discussion

Our results clearly show that the larval redfish population in the Gulf of St. Lawrence is not genetically homogeneous but rather is multispecific and composed of at least two genetically distinct species currently identified as *S. mentella* and *S. fasciatus*. As previously indicated in the introduction, *S. norvegicus* may also occur in the Gulf but at very low abundance and cannot be distinguished from *S. mentella* at the *MDH** locus. The co-existence and the larval extrusion of the two species of redfish, identified by the number of anal-fin rays, have been inferred for Gulf species in previous studies based on the presence of gravid adults (Ni and Sandeman, 1984) and on the presence of sexually mature females in spawning and postspawning condition for both species (St-Pierre and de Lafontaine, 1995). We report here the first evidence that the two species are clearly identified in the larval population.

The taxonomic status of the heterozygous individuals is however problematic. Rubec et al. (1991) suggested that the presence of heterozygotes was best

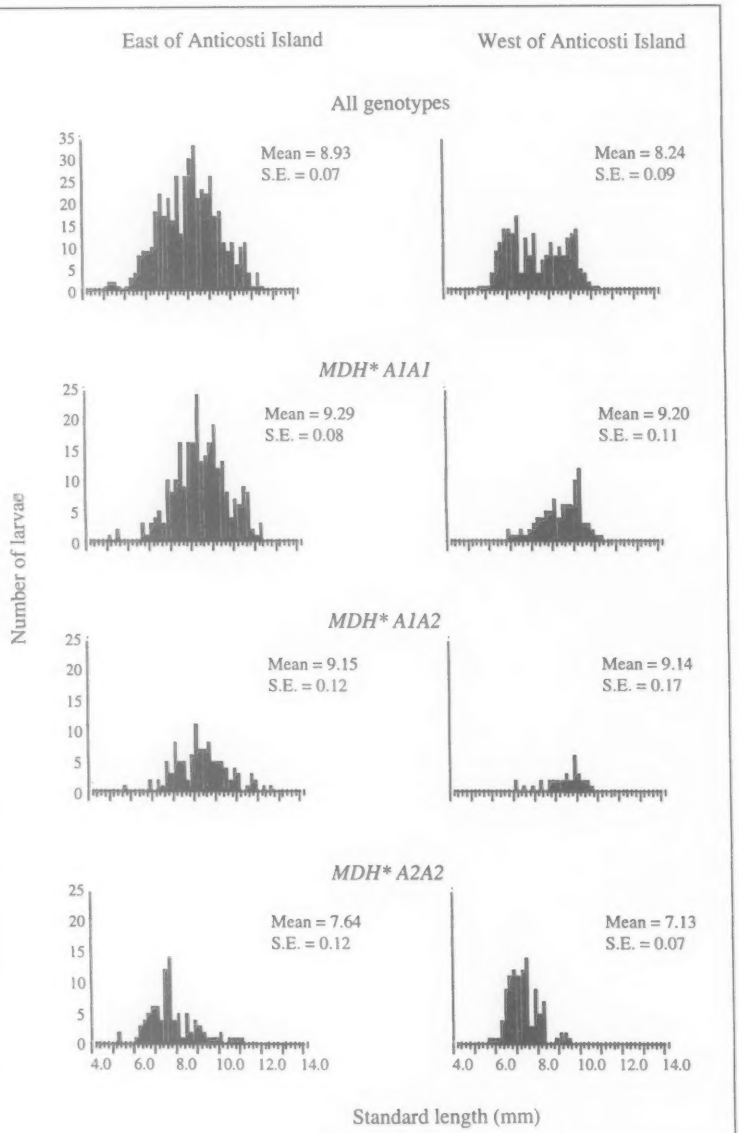


**Figure 5**

Distribution of standard lengths of redfish larvae analyzed for MDH variation in 1991 by eastern and western sectors of the Gulf of St. Lawrence and by genotypes.

explained by introgressive hybridization between *S. fasciatus* and *S. mentella* in the Gulf. Our results do not rule out this possibility. Hybridization between *S. fasciatus* and *S. mentella* was also suggested as one possibility to explain the RFLP patterns of rDNA observed in adult redfish from the Gulf of St. Lawrence (Desrosiers et al., 1999), where individuals with the rDNA hybrid type had more affinities with *S. mentella* than with *S. fasciatus*. In fact, hybridization between *Sebastes* species may not be an uncommon phenomenon because introgression was recently observed between three rockfish species in Puget Sound (Seeb, 1998). In our study, the similar size distribution of larvae of the *MDH*A1A1* and *MDH*A1A2* genotypes suggests that heterozygous individuals have more affinity with the *S. mentella*

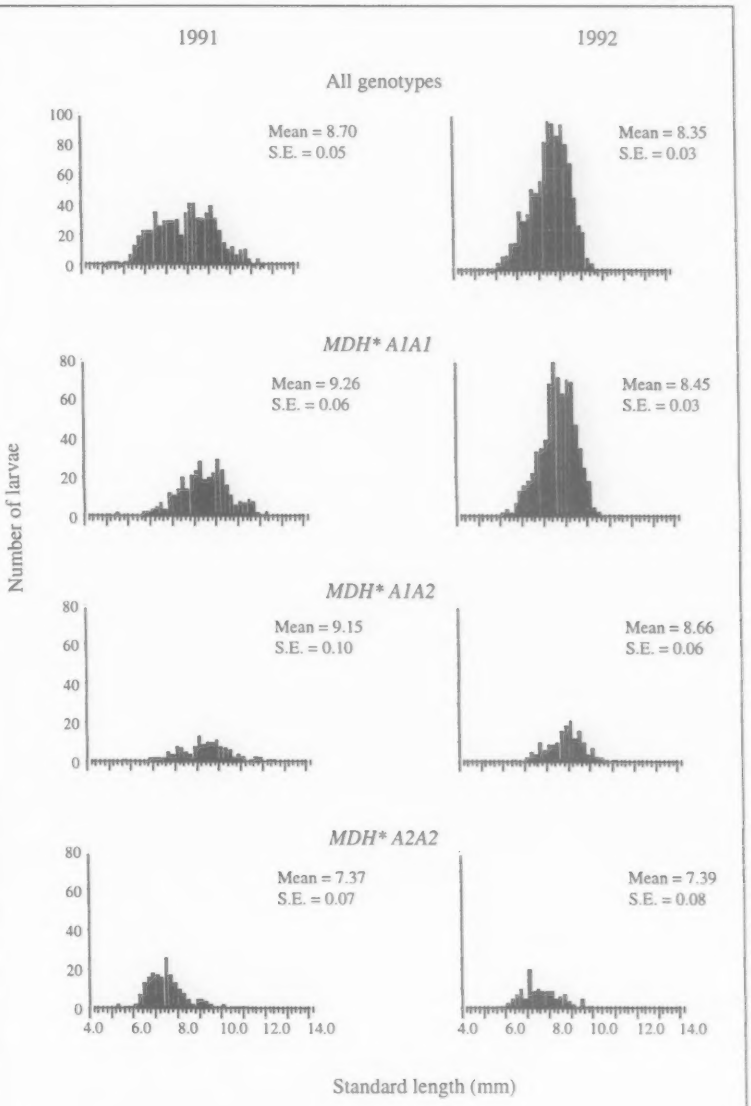


**Figure 6**

Distribution of standard lengths of all redfish larvae analyzed for MDH variation in 1991 and 1992 by year and genotypes.

than with *S. fasciatus*. The geographic distribution of the heterozygote larvae also matched closely that of the genotype *MDH*A1A1*.

Overall, clear geographic patterns in the abundance and the geographic distribution of redfish larval genotypes were observed in the Gulf of St. Lawrence. In both sampling years redfish larvae were mainly concentrated in offshore areas associated with the deep (>200 m) waters of the Laurentian and Esquiman Channels, as previously reported (Kenchington, 1991; de Lafontaine et al., 1991; Runge and de Lafontaine, 1996). The high abundance of redfish larvae on the southeastern side of Anticosti Island is consistent with the observed occurrence of gravid redfish during May and June in the same area (St-Pierre and de Lafontaine, 1995). High abundance of larval redfish east of Anticosti Island has been frequently observed from mid-May to mid-June

and would correspond to the seasonal peak in larval extrusion as indicated by the maturity cycle of adults (Ni and Templeman, 1985; St-Pierre and de Lafontaine, 1995). On the western side of Anticosti Island, the highest larval abundance is associated with a cyclonic residual circulation (El-Sabh, 1976) as found in previous studies (de Lafontaine, 1990; de Lafontaine et al., 1991). Our data suggest however, that in 1991 and 1992 the contribution of the western sector to the entire redfish larval production of the Gulf of St. Lawrence was small and less important than that of the eastern sector. The western sector contributed approximately up to 10.2% of the *S. mentella* (*MDH*A1A1 +MDH*A1A2*) and up to 34.4% of the *S. fasciatus* larvae in the 1991 samples. This observation is in agreement with the estimated lower biomass of adult redfish in the western Gulf of St. Lawrence in relation to the eastern sector (Atkinson, 1984; Morin and Bernier[2]). The proportionally higher contribution of *S. fasciatus* in the western sector would be indicative of slightly higher abundance of *S. fasciatus* periodically observed in that part of the Gulf (Morin[3]).

The different geographic distributions of the various larval genotypes strongly suggest differences in the preferred extrusion sites of *S. fasciatus* and *S. mentella* (Figs. 3 and 4). *Sebastes mentella* seems to prefer zones located in the central and deeper parts of the channels whereas *S. fasciatus* preferably uses shallower zones near the shelf break and along the sides of the channels. This observation is consistent with the reported summer distribution patterns of adult redfish in the Gulf of St. Lawrence (Rubec et al. 1991; St-Pierre and de Lafontaine, 1995). The apparent low proportion of *S. fasciatus* in the southern part of the Gulf may be due to the relative lack of shallower stations. Attempts to infer more precisely the locations of extrusion sites from the observed larval distributions would, however, require that the size frequency of sampled larvae be considered. In this case, size at extrusion would therefore be the best basis from which to infer the vicinity of the extrusion sites. The size at extrusion for redfish larvae in the Gulf of St. Lawrence is unknown. Penney and Evans (1985) indicated that newly extruded redfish (presumably *S. mentella*—see Penney, 1987) larvae from Flemish Cap (east of Newfoundland Grand banks) ranged between 6.2 and 8.9 mm. From the age-length relationships, these authors estimated that the mean size of newly extruded larvae was 7.68 and 8.23 mm in two consecutive years. Magnusson and Magnusson[4] also reported considerable variation in the size at extrusion (5.5–7.2 mm) of redfish larvae from the Northeast Atlantic waters. Penney (1985) indicated that the mean size of pre-extruded larvae in gravid females of *S. fasciatus* and *S. mentella* collected in southern Newfoundland waters was 7.34 and 7.89 mm, respectively. The size range of larvae in our study was 5.0 to 12.3 mm in 1991 and 5.6 to 10.9 mm in 1992. The proportion of larvae <8.5 mm was 46% and 54% in 1991 and 1992, respectively, suggesting that a large number of sampled larvae were recently extruded. Assuming an average size at extrusion of 7.5 mm and given the estimated growth rates (0.1 to 0.15 mm/day) reported in the literature (Penney and Evans, 1985; Herra, 1989), the maximum length of larvae in our samples would correspond to larvae of approximately 22 to 45 days old. The majority of larvae being <10 mm long, the sampled population was certainly less than 1 month old. Although the period of time between larval extrusion and time of collection may allow for some horizontal drift of larvae by the surface currents, the relatively small size and the presumably young age of the larvae would tend to indicate that these larvae did not disperse much (in relation to the large area sampled in our study) and would have been collected close to their extrusion sites. Consequently, the differences in the relative distribution of the genotypes of larvae indicate that the extrusion sites of the two species do not overlap to a large extent within the Gulf of St. Lawrence.

The mean and the range of the size of larvae varied between genotypes where larvae of the *MDH*A2A2* were significantly smaller (by 1.5 to 2.0 mm) than those of the two other genotypes (Fig. 6). This finding is consistent with other observations, suggesting that the length of *S. fasciatus* at extrusion is smaller than that of *S. mentella*, although considerable variability exists (Penney, 1985; 1987; Penney and Evans, 1985). The similar results obtained in the two sampling years of our study would tend to reveal a species-specific characteristic. In addition, the difference between the mean (and modal) size of each homozygote genotype was larger than that for the reported size at extrusion between the two species (0.5–0.6 mm; see Penney, 1985; Penney and Evans,

[2] Morin, B., and B. Bernier. 1997. The status of redfish in Unit 1 (Gulf of St. Lawrence). Can. Stock Assess. Sec. Res. Doc. 97/112, 23 p. Sciences Branch, Department of Fisheries and Oceans, Maurice Lamontagne Institute, 850 Route de la Mer, Mont-Joli, Québec, Canada G5H 3Z4.

[3] Morin, B. 1998. Unpubl. results. Sciences Branch, Department of Fisheries and Oceans, Maurice Lamontagne Institute, 850 Route de la Mer, Mont-Joli, Québec, Canada G5H 3Z4.

[4] Magnússon, J. V., and J. Magnússon. 1977. On the distinction between larvae of *S. marinus* and *S. mentella*: preliminary report. Int. Counc. Explor. Sea (ICES) Council Meeting 1977/F:48.

1985). This finding suggests that the larvae of *S. fasciatus* were extruded slightly later than those of *S. mentella* in the Gulf of St. Lawrence. Once again assuming that larval growth rates can vary between 0.10 mm and 0.15 mm/day, one can conlude that the peak in larval extrusion as determined by the modal size groups of each homozygote genotype (7.5 mm for *MDH*A2A2* and 10.2 mm for *MDH*A1A1* in 1991) would be approximately 15–25 days apart. From age estimates of larvae from otolith microstructure, Penney (1987) concluded that extrusion time of *S. mentella* was earlier than that of *S. fasciatus* in Flemish Cap area. Previous larval collections made over three consecutive summers at a fixed site along the Gaspé coast in the Gulf of St. Lawrence also showed that larvae extruded earlier tend to be larger than those extruded later in the season (Jean, 1955). Such a sampling strategy combined with genetic identification of the larvae (as presented our paper) would permit a more precise description of the seasonal variability in the extrusion of the two redfish species in the Gulf of St. Lawrence. The significantly smaller larvae collected in 1992, compared with 1991, is probably due to the earlier sampling time in 1992.

*Sebastes mentella* dominated the redfish larval population in the Gulf of St. Lawrence, contributing 61.8% and 77.6% of all larvae collected in 1991 and 1992, respectively. If we assume that the heterozygous individuals belong to *S. mentella*, the proportion of *S. mentella* increases to 85.6% and 94.4% for these years, respectively. Furthermore, if the heterozygous individuals belong to *S. mentella*, it might be expected that a small proportion of homozygous *MDH*A2A2* individuals were actually *S. mentella,* although misclassified as *S. fasciatus*. In which case, we would have slightly underestimated the abundance of *S. mentella*. The presence of these individuals in the *MDH*A2A2* group might correspond to the largest individuals of this group (Figs. 5 and 6). In any case, the values we obtained for larval stages are very close to those (90.3%) for adult *S. mentella* from samples in the Gulf of St. Lawrence in 1989 and 1990 (St-Pierre and de Lafontaine, 1995).

These results contrast with those of Sévigny and de Lafontaine (1992) who showed that *S. fasciatus* dominated the population of juveniles sampled in the northeastern sector of the Gulf in summer 1990 and 1991. Those juveniles mostly belonged to the 1988 cohort whose origin is not known, and Sévigny and de Lafontaine (1992) did not rule out the possibility that these fish may have originated from outside the Gulf. This rather distinct variation in the genotypic frequency among the various life stages of redfish in the Gulf of St. Lawrence remains unexplained in the light of present knowledge of the ecology of redfish over the entire distribution area. Change in the relative proportion and the geographic distribution of these two species (both at the larval and juvenile stage) may result from variable annual recruitment or from different larval drift and retention patterns among species. The mechanisms responsible for these recruitment patterns are not known but are consistent with the view that the Gulf of St. Lawrence does not form a homogeneous environmental unit but rather may consist of distinctly different pelagic ecosystems in the eastern and western sectors (de Lafontaine et al., 1991).

## Acknowledgments

This study would not have been made possible without the support, technical skill and expertise of several people to whom we wish to express our sincere gratitude: Pierre Joly, Geneviève Ross, Éric Parent, and Yves Morin for assistance during work at sea and in the laboratory. We also acknowledge the captain and crew of the CSS *Alfred Needler*, for technical help during sampling cruises. A particular and very sincere thank you to M. Jean-François Saint-Pierre who participated in all aspects of this study and who suggested and developed the video camera system for filming larvae at sea. Dominique Gascon and Jean-Denis Dutil made useful comments on an early version of the manuscript. We also want to thank three anonymous reviewers for their useful comments. This study was supported by the Department of Fisheries and Oceans, Canada.

## Literature cited

**Atkinson, D. B.**
**1984**. Distribution and abundance of beaked redfish in the Gulf of St. Lawrence, 1976–81. J. Northwest Atl. Fish. Sci. 5:189–197.
**1987**. The redfish ressources off Canada's east coast. *In* Proceedings of the International Rockfish Symposium, Anchorage, Alaska, October 1986, p. 15–33. Lowell Wakefield Fisheries Symposium Series, Alaska Sea Grant College Program Report 97-2.

**de Lafontaine, Y.**
**1990**. Ichthyoplankton communities in the St. Lawrence Estuary: composition and dynamics. *In* Oceanography of a large scale estuarine system, the St Lawrence (M. I. El-Sabh and N. Silverberg, eds.), p. 321–343. Coastal and Estuarine Studies 39.

**de Lafontaine,Y., S. Demers, and J. A. Runge.**
**1991**. Pelagic food web interactions and productivity in the Gulf of St-Lawrence: a perspective. *In* The Gulf of St-Lawrence: small ocean or big estuary? (J. C. Therriault, ed.), p. 99–123. Can. Spec. Publ. Fish. aquat. Sci. 113.

**Desrosiers, B., J.-M. Sévigny, and J.-P. Chanut.**
**1999**. Restriction fragment length polymorphism of rDNA

in the redfish *Sebastes fasciatus* and *S. mentella* (Scorpaenidae) from the Gulf of St. Lawrence. Can. J. Zool. 77: 267–277.

**El-Sabh, M. I.**
**1976**. Surface circulation pattern in the Gulf of St. Lawrence. J. Fish. Res. Board Can. 33:124–138.

**Fernholm, B., and A. Wheeler.**
**1983**. Linnaean fish specimens in the Swedish Museum of Natural History, Stockholm. Zool. J. Linn. Soc. 78:199–286.

**Gagné, P.**
**1995**. Variation génotypique et distribution spatio-temporelle des larves de sébaste, *Sebastes fasciatus* et *S. mentella* dans le golfe du Saint-Laurent. Mémoire de Maîtrise, Université Laval, Québec, 96 p.

**Hebert, P., and M. Beaton.**
**1989**. Methodologies for allozyme analysis using cellulose acetate. Practical handbook. Educational service of Helena labs, Beaumont, TX, 31 p.

**Herra, T.**
**1989**. Larval redfish drift migration in relation to hydrographic features. Rapp. P-V. Réun. Cons. Int. Explor. Mer 191:92–99.

**Jean, Y.**
**1955**. Présence de larves de *Sebastes marinus* dans la Baie-des-Chaleurs et leurs caractères distinctifs. Nat. Can. 82: 33–43.

**Kenchington, T. J.**
**1986**. Morphological comparison of two northwest Atlantic redfishes, *Sebastes fasciatus* and *S. mentella*, and techniques for their identification. Can. J. Fish. Aquat. Sci. 43:781–787.
**1991**. Vertical distribution and movements of larval redfishes (*Sebastes* spp.) in the southern Gulf of St. Lawrence. J. Northwest Atl. Fish. Sci. 11:43–49.

**McGlade, J. M., C. M.. Annand, and T. J. Kenchington.**
**1983**. Electrophoretic identification of *Sebastes* and *Helicolenus* in the Northwestern Atlantic. Can. J. Fish. Aquat. Sci. 40:1861–1870.

**Nedreaas, K., and G. Naevdal.**
**1991**. Identification of 0-and 1-groups redfish (genus *Sebastes*) using electrophoresis. ICES J. Mar. Sci. 48:91–99.

**Ni, I.-H.**
**1981**. Separation of sharp-beaked redfish, *Sebastes fasciatus* and *S. mentella*, from northeastern Grand Bank by morphology of extrinsic gasbladder musculature. J. Northwest Atl. Fish. Sci. 2:7–12.
**1982**. Meristic variation in beaked redfishes, *Sebastes mentella* and *S. fasciatus*, in the Northwest Atlantic. Can. J. Fish. Aquat. Sci. 39:1664–1685.

**Ni, I.-H., and W. D. McKone.**
**1983**. Distribution and concentration of redfishes in Newfoundland and Labrador waters. North Atlantic Fisheries Organization (NAFO) Sci. Coun. Studies 6:7–14.

**Ni, I.-H., and E. J. Sandeman.**
**1984**. Size at maturity for northwest Atlantic redfishes (*Sebastes*). Can. J. Fish. Aquat. Sci. 41:1753–1762.

**Ni, I.-H., and W. Templeman.**
**1985**. Reproductive cycles of redfishes (*Sebastes*) in southern Newfoundland waters. J. Northwest Atl. Fish. Sci. 6:57–63.

**Payne, R. H., and I.-H. Ni.**
**1982**. Biochemical population genetics of redfishes (*Sebastes*) off Newfoundland. J. Northwest Atl. Fish. Sci. 3:169–172.

**Penney, R. W.**
**1985**. Comparative morphology of preextrusion larvae of the North Atlantic sharp-beaked redfishes, *Sebastes mentella* and *Sebastes fasciatus* (Pisces: Scorpaenidae). Can. J. Zool. 63: 1181–1188.
**1987**. Development of deep-water redfish (*Sebastes mentella*) larvae, with comparative notes on newly extruded Acadian redfish (*Sebastes fasciatus*) from the Flemish Cap. Can. J. Zool. 65:1167–1180.

**Penney, R. W., and G. T. Evans.**
**1985**. Growth histories of larval redfish (*Sebastes* spp.) on an offshore Atlantic fishing bank determined by otolith increment analysis. Can. J. Fish. Aquat. Sci. 42:1452–1464.

**Rubec, P. J., J. M. McGlade, B. L. Trottier, and A. Ferron.**
**1991**. Evaluation of methods for separation of Gulf of St. Lawrence beaked redfishes, *Sebastes fasciatus* and *S. mentella*: malate dehydrogenase mobility patterns compared with extrinsic gasbladder muscle passages and anal fin ray counts. Can. J. Fish. Aquat. Sci. 48:640–660.

**Runge, J. A., and Y. de Lafontaine.**
**1996**. Characterization of the pelagic ecosystem in surface waters of the northern Gulf of St. Lawrence in early summer: the larval redfish-*Calanus*-microplankton interaction. Fish. Oceanogr. 5:21–37

**Seeb, L. W.**
**1998**. Gene flow and introgression within and among three species of rockfishes, *Sebastes auriculatus*, *S. caurinus* and *S. maliger*. J. Heredity 89:393–403.

**Seeb, L. W., and A. W. Kendall Jr.**
**1991**. Allozyme polymorphism permit the identification of larvae and juvenile rockfishes of the genus *Sebastes*. Env. Biol. Fish. 30:191–201.

**Sévigny, J.-M., and Y. de Lafontaine.**
**1992**. Identification of redfish juveniles in the Gulf of St. Lawrence using genotypic specific variations. *In* Juvenile stages: the missing link in fisheries research (Y. de Lafontaine, T. Lambert, G. R. Lilly, W. D McKone, and R. J. Miller, eds.), p. 69–73. Can. Tech. Rep. Fish. Aquat. Sci. 1890.

**St-Pierre, J.-F., and Y. de Lafontaine.**
**1995**. Fecundity and reproduction characteristics of beaked redfish (*Sebastes fasciatus* and *S. mentella*) in the Gulf of St. Lawrence. Can. Tech. Rep. Fish. Aquat. Sci. 2059:32 + vii p.

# Ghost fishing by Tanner crab (*Chionoecetes bairdi*) pots off Kodiak, Alaska: pot density and catch per trap as determined from sidescan sonar and pot recovery data

**Bradley G. Stevens**
Alaska Fisheries Science Center
National Marine Fisheries Service, NOAA
301 Research Ct.
Kodiak, Alaska 99615
e-mail address: bradley.g.stevens@noaa.gov

**Ivan Vining**

**Susie Byersdorfer**
Alaska Department of Fish and Game
211 Mission Road
Kodiak, Alaska 99615

**William Donaldson**
P.O. Box 271
Dublin, New Hampshire 03444

**Abstract.**–Sidescan sonar was used to locate 189 putative lost crab pots in a 4.5 km$^2$ area of Chiniak Bay, near Kodiak, Alaska. Subsequent observations of 15 such objects by submersible and ROV verified that they were indeed crab pots. In 1995 and 1996, 147 pots were recovered from the surveyed and adjacent nonsurveyed areas by grappling, and their condition and contents were examined. Tanner crabs, *Chionoecetes bairdi*, were the most abundant organism, with 227 found in 24 pots (16% frequency of occurrence); sunflower sea stars (*Pycnopodia helianthoides*) were the most frequent (42%) occupant and second most abundant (189 in 62 pots). Octopuses (*Octopus dofleini*) were significantly associated with pots containing Tanner crabs. Occurrence of crabs in pots was primarily a function of background crab density and differed between the surveyed and nonsurveyed areas. Recently lost pots (< 1yr old) had significantly more male crabs, significantly larger male crabs, and contained seven times more total crabs than older pots (those lost two or more years prior to recovery). The proportion of pots with damaged webbing increased with pot age, but holes in pot webbing did not significantly affect catch per pot.

Manuscript accepted 18 November 1999.
Fish. Bull. 98:389–399 (2000).

Lost and derelict fishing gear is a problem because of concerns about aesthetics at sea, entanglement of marine fauna, and ghost fishing by the gear (Sheldon and Dow, 1975; Smolowitz, 1978a; Breen, 1990). Marine mammals, birds and reptiles (Laist, 1996), nontargeted fish and shellfish (Carr et. al., 1990), and even boats (Kirkley and McConnell, 1997) have become entangled in fishing gear. In this paper ghost fishing is "the ability of fishing gear to continue fishing after all control of that gear is lost by the fisherman," as defined by Smolowitz (1978a).

Attempts to quantify the extent and impacts of ghost fishing have met with variable success (Sheldon and Dow, 1975; Smolowitz, 1978b; High and Worlund, 1979; Muir et al., 1984; Breen, 1987; Parish and Kazama, 1992; Guillory, 1993). Parish and Kazama (1992) concluded that ghost fishing of Hawaiian spiny lobsters (*Panulirus marginatus*) was unimportant because the lobsters could escape from pots easily. Conversely, Sheldon and Dow (1975) estimated that approximately one third of all American lobsters (*Homarus americanus*) entering lost pots would perish. Other studies have identified ghost fishing as a concern or possible problem and have identified potential solutions to reduce resource loss (High, 1976; Pecci et al., 1978; Smolowitz, 1978b; High and Worlund, 1979; Carr and Harris, 1997). The impact of ghost fishing by lost crab pots in Alaska waters has been studied by High and Worlund (1979), Kimker (1994), Stevens (1996), Kruse and Kimker,[1] and Ste-

[1] Kruse, G. H. and A. Kimker. 1993. Degradable escape mechanisms for pot gear: a summary report to the Alaska Board of Fisheries. Regional information report 5J93-01. Alaska Department of Fish and Game (ADFG), 211 Mission Rd., Kodiak, AK 99615, 23 p.

vens et al.[2] High and Worlund (1979) placed red king crab in unbaited square pots; after 16 days, 20% of legal-size crabs remained in the pots. Those crabs that escaped after prolonged enclosure were recaptured at lower rates than those that escaped quickly. Crabs that were placed in closed unbaited square pots exhibited mortalities from 4% to 12% after 16 days.

In our report we examined ghost fishing by lost crab pots in specific areas off the northeast shore of Kodiak Island, Alaska. In Chiniak Bay, the locations of 189 putative lost pots were discovered in April 1994 with sidescan sonar. With this sonar survey as a guide, we estimated the extent of ghost fishing by recovering lost pots and examining their contents. Three studies were conducted: 1) a pilot study within Chiniak Bay in 1995 to develop methods for pot recovery; 2) a targeted study in 1996 to recover specifically identified pots from known locations within Chiniak Bay; and 3) a nontargeted study in 1996 within Chiniak, Kalsin, Womans, and Ugak Bays, to recover pots from areas known to have been heavily fished during past crab fisheries, without attempting to target specific pots. These efforts were carried out jointly by the Alaska Department of Fish and Game (ADF&G) and the National Marine Fisheries Service (NMFS), with assistance from the U.S. Army Corps of Engineers (USACE) and the Kodiak Island Borough (KIB).

## Materials and methods

### Sidescan sonar survey and *in-situ* observations

The sonar survey was conducted by scientists at SAIC, Inc., using a dual frequency (100/500 KHz) sidescan sonar system (Klein model 595), with both a paper chart and digital data signal processor. Positions were recorded with a differential GPS receiver. The sonar was operated from the Alaska Department of Fish and Game (ADF&G) RV *Resolution* during 6–8 April 1994, in a portion of Chiniak Bay at depths of 100–150 m. Transects 3 km in length were run at a spacing of 75 m, such that the scanning of each line overlapped those on each side by 50%, providing a total coverage of 150%. A total area of approximately 4.5 $km^2$ was surveyed. From 22 April to 2 May 1995, the two-person submersible *Delta* was used to survey the area for a study of crab behavior (Stevens et al., in press); pots that were encountered accidentally during that study were examined. On 27 April 1995, a remotely operated vehicle (model S2 ROV Phantom, Deep Ocean Engineering, Inc.) equipped with a sector-scanning sonar was also used to locate and examine crab pots.

### 1995 pilot study

Pots identified from the sidescan sonar survey were plotted on a map (Fig. 1), then numbered. A random sample of 23 single pots was chosen for trial recovery in April 1995. A short (7.6-m) grappling chain, designed to hook the pot or its floating line, or both, was towed from the main boom of the RV *Resolution*. The grappling chain was lowered into the water when the ship was approximately 250 m from the estimated position of the targeted pot, then towed past the position at less than 5.6 km/h (3 kn). If the recovery operation was not successful, the vessel would continue to tow the grappling chain in a circle around the same position until the pot was hooked or until we gave up. When a pot was hooked, it was brought onboard with the ship's crane. Information about the pot and its contents was recorded, including pot type, condition, damage to the frame or webbing, and presence of bait jars and biodegradable mesh. In most cases the grapple snagged the steel frame of the pot and it was not possible to determine if snagging action caused additional damage to the webbing.

In our paper, we use the terms "trap" and "pot" interchangeably. The three types of crab traps most commonly used in the Gulf of Alaska are square, pyramidal, and conical (see High and Worlund, 1979, for detailed descriptions). Square pots are the most commonly used type in the Bering Sea and are made with steel frames, usually >2 × 2 m, with two funnel-shaped entrance tunnels on opposite sides. Pyramidal and conical pots are slightly smaller and have a single square or round entrance at the top, which is usually fitted with a plastic collar. All three of these types of pots are covered with nylon twine webbing. Cod pots are square pots that have been modified for cod fishing by the addition of restriction devices to prevent entry of crabs and escapement of cod. Subsistence pots, used to capture crabs for personal consumption, may be any of the above styles of pots or variations thereof. Pot conditions were rated on a subjective five-point scale from "very poor" to "excellent." Criteria used to evaluate condition included the condition of webbing (presence of holes or major gaps), numbers of broken frames and corner joints, and estimated age of the pot. Pots coded as "good" or "excellent" were assumed to have been lost less than one year and were probably placed for subsis-

[2] Stevens, B. G., J. A. Haaga, and W. E. Donaldson. 1993. Underwater observations on behavior of king crabs escaping from crab pots. Alaska Fisheries Science Center processed report 93-06. Alaska Fisheries Science Center, NMFS, 7600 Sand Point Way NE, Seattle, WA 98115, 14 p.

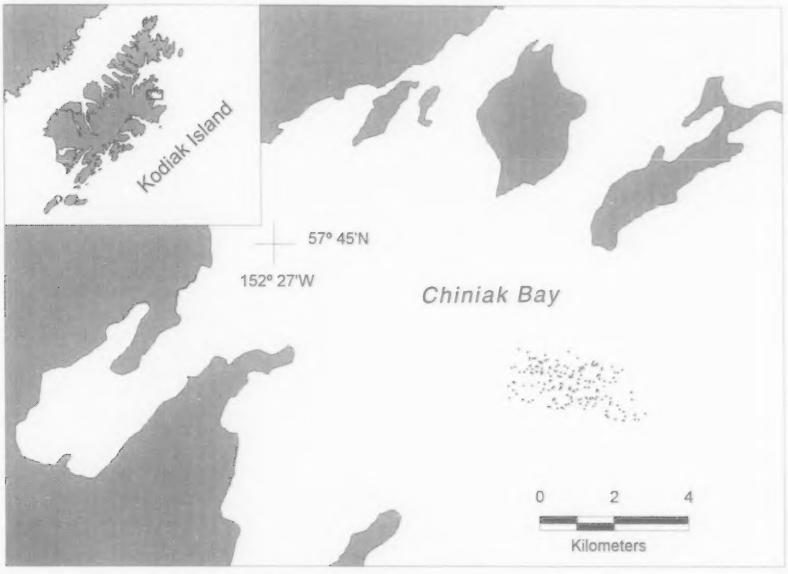


**Figure 1**

Chart of Chiniak Bay, Kodiak Island, Alaska, showing position of pots discovered by sidescan sonar survey. Inset shows location of Chiniak Bay on Kodiak Island.

tence use, whereas pots coded as "fair," "poor," or "very poor" were assumed to have been lost more than one year. Commercial fishing for Tanner crabs around the northeast quadrant of Kodiak Island has been closed since January 1994, and for king crab since 1983[3]; therefore no commercial crab pots have been used in the region since that time, although subsistence pots are still allowed. Therefore, recovered pots would have to have been lost at least 2 years previously (prior to April 1993), unless used for subsistence purposes. Since 1977, the state of Alaska has required that all crab pots contain an 18-inch (45.7-cm) segment of biodegradable twine that degrades within 90 days (Alaska Statutes, 1996). For this reason, all pots were examined for the presence and condition of degradable twine. However, it was not our goal to study the effectiveness of biodegradable twine because suitable control pots were not available. Furthermore, absence of biodegradable twine was inconclusive when holes were present in the webbing, because it could have indicated either that the twine had already degraded or that no twine had been present and holes resulted from some other cause.

[3] ADF&G (Alaska Dept. Fish and Game). 1996. Annual management report for the shellfish fisheries of the Westward Region, 1996. Regional information report 4K97-41. ADF&G, 211 Mission Rd. Kodiak, AK 99615.

For all crabs found in pots, carapace width (CW) was measured to the nearest mm with vernier calipers across the widest part of the carapace, excluding spines. Abundance of all other species inside the pot and size of commercially important species was also recorded. These procedures were repeated for each pot. All retrieved pots had their webbing cut and were disposed of at a location designated by the USACE and the KIB.

### Targeted study

From 17 June to 18 July 1996, the procedures developed during 1995 were again used, with some modifications. The study was conducted by biologists aboard the contracted fishing vessel *Big Valley*. Pots were randomly selected for retrieval from the list of putative pot positions. Gear used for this study was a grappling beam made of 6.4 m long, 5.1 cm diameter steel pipe, and was pulled by a braided steel wire cable with a synthetic bridle. A 183-m tag line and buoy were attached to the beam to retrieve the device if the tow line was broken. Attached to the beam were six grapples, each consisting of a 1.2-m long "V" bar with two 30-cm arms welded so as to project forward and down. After the first week, a second set of arms was welded to the grapples facing upward, and on 8 July 1996, 7.6-cm barbs were welded to the ends of each arm to prevent snagged lines or pot

frames from slipping off during recovery. The grapple beam was lowered into the water with enough cable to maintain a 2:1 scope (ratio of wire out to depth), and towed through the suspected pot position. If no pot was hooked, additional transects were run parallel to the first, or the vessel was set into a sharp turn and the beam was towed in a circle. Hooked pots were retrieved with the ship's crane, while the vessel ran at a slow speed. Recovered pots were designated by the number of the most likely sonar position where they were found, and information was recorded as during the pilot study. The southeast section of the sonar-surveyed area could not be sampled owing to underwater cables and rocks.

### Nontargeted study

The nontargeted study was conducted by the skipper and crew of the FV *Big Valley* without biologists aboard during 19–31 August 1996 and 5–21 October 1996. Previous attempts to snag randomly selected (i.e. targeted) pots were not particularly efficient because only 43 pots were recovered during 32 days of fishing. Therefore, instead of targeting specific pots for recovery, the skipper was instructed to fish haphazardly at his own discretion in areas where commercial crab fishing had previously been conducted, but without knowing specific pot locations. This method was more efficient and productive. The grapple beam was damaged, however; therefore it was replaced with a 30-m long weighted chain, to which were attached six short grapples, each with four barbed tines. The long grapple chain was towed at 2.8 km/h in a constant 10 turn until a pot was hooked. Recovered pots were given sequential numbers, and data were recorded as before.

### Data analysis

Because Tanner crabs were the target species for most pots, associations between the presence of Tanner crabs and other species were tested by contingency table (chi-square) analysis. To reduce empty cells, Tanner crabs were combined into logarithmic categories (0, 1–9, 10–99, >99) before analysis. Association between pot condition and sex of the crabs was also tested by means of chi-square. For this purpose, pots were regrouped into two categories designated "best" (including pots coded as "excellent" or "good") and "worst" (including "fair," "poor," or "very poor" pots). Mean sizes of crabs in various condition categories are given as mean ±SE and were compared by means of the Mann-Whitney *U*-test (MWU) because variances were typically unequal (Zar, 1984). Catch of crabs or other organisms is expressed as catch per pot (CPP, i.e. crab per pot). CPP was not standardized by time because we could not adequately determine how long each pot had been in the water. The effect of holes in pot webbing on crab CPP was tested with the MWU-test; additionally, binomial confidence intervals were calculated for the proportion of pots with crabs and compared for overlap between pots with holes and those without. The null hypothesis was that torn pot webbing had no effect on CPP.

## Results

### Sonar survey and *in-situ* observations

Submersible observations in 1995 and previous years showed that seafloor substrates in the surveyed area were primarily sandy silt with occasional areas of compacted mud, and bottom contour was relatively flat below 100 m depth (senior author, personal obs.). The soft mud bottom absorbed most of the transmitted sonar energy and reflected very little. As a result, crab pots and other anthropogenic objects were easily distinguishable with the sidescan sonar. At least 189 objects were believed to be crab pots; 177 were single and 12 were connected together in groups of 2 to 5. In some cases attached lines could also be distinguished by sonar. Density of crab pots in the 4.5-km$^2$ area examined was 42 pots/km$^2$. At least 15 of these objects were later observed with the submersible *Delta* and the ROV, and all were verified to be crab pots, including a group of five pots connected together by tangled lines. Also noticeable were several large linear features up to 2 km long; one was later observed from the *Delta* to be a drag scar or ditch, approximately 0.5 m deep and 3–5 m wide.

### Condition of pots recovered

A total of 147 pots of varying age, size, and type were retrieved during the three studies (Table 1; Fig. 2). Detailed information on location, condition, and contents of each pot is contained in a separate data report.[4] Seventy-two pots were recovered from inside the sonar-surveyed portion of Chiniak Bay (these are subsequently referred to as "inside" pots), including

[4] Vining, I., S. Byersdorfer, W. E. Donaldson, B. G. Stevens, and G. Edwards. 1997. Lost crab and cod pot recovery and ghost fishing in Chiniak Bay and other areas in the waters around Kodiak Island, Alaska. Regional information report 4K97-42. Alaska Dept. of Fish and Game, 211 Mission Rd., Kodiak, Alaska 99615, 93 p.

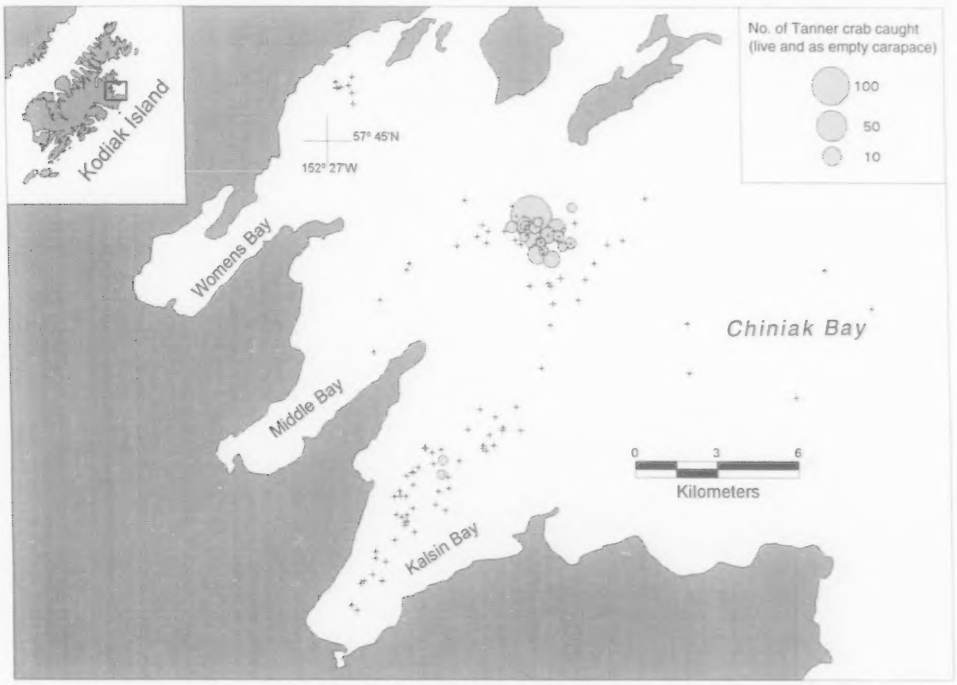


**Figure 2**

Location of pots retrieved from Chiniak Bay and adjacent areas during all studies, and index of Tanner crab catch per pot (crab per pot). Smallest circles represent one crab, and crosses represent pots with no crabs. Location of the three pots retrieved from Ugak Bay is not shown.

7 pots recovered during the pilot study and 43 pots recovered during the targeted study. Three of these were not previously detected by sonar and were presumed to be subsistence pots less than a year old, lost after the sonar survey was conducted, because commercial fishing had been closed in this area for over two years. An additional 22 inside pots were recovered during the nontargeted study. The remaining 75 pots were recovered from outside the surveyed area ("outside" pots) during the nontargeted study. Square pots were the most common (50%, including two cod pots), followed by pyramidal (24%) and conical (16%). Nine round pots (6%) were recovered, all of which were less than 1.07 m in diameter and were covered with a wire mesh that does not degrade easily; these were probably intended to catch Dungeness crabs (*Cancer magister*). Additional pots included two small subsistence type pots, one rectangular shrimp pot, and one made from a 55-gal oil drum.

Intact biodegradable twine was found in only eight commercial pots (3 square, 2 pyramid, 3 conical). Of those eight, four were classified as being in good condition, two as fair, one as poor, and for one pot, data on its condition were not available (Table 2). Three of these had other holes in the webbing. Eighty-eight pots had holes in the webbing; for 85 of these pots, the holes might have been the result of the degradation of biodegradable twine (excluding the three mentioned above with intact twine). However, as stated previously, without evidence of biodegrad-

**Table 1**

Types of pots recovered from Chiniak Bay and other bays during pilot, targeted, and nontargeted studies.

| Pot type | Number of pots | % of total pots |
|---|---|---|
| Square | 73 | 50 |
| Pyramid | 35 | 24 |
| Conical | 24 | 16 |
| Cod | 2 | 1 |
| Round | 9 | 6 |
| Subsistence | 2 | 1 |
| Shrimp | 1 | 1 |
| 55-gal. drum | 1 | 1 |
| Total | 147 | |

**Table 2**

Presence of biodegradable twine and damaged pot webbing, by condition of pot. Only 133 commercial style pots were included.

| Condition | Intact bio-twine | Damaged webbing | Total | % damaged |
|---|---|---|---|---|
| Excellent | 0 | 0 | 2 | 0 |
| Good | 4 | 16 | 33 | 48 |
| Fair | 2 | 33 | 49 | 67 |
| Poor | 1 | 20 | 29 | 69 |
| Very poor | 0 | 15 | 16 | 94 |
| Unknown | 1 | 4 | 4 | 100 |
| Total | 8 | 88 | 133 | |

able twine, we were not able to determine if gaps in the webbing resulted from short-term degradation of biodegradable twine, longer-term degradation of nylon webbing, encounters with other fishing gear, damage during grappling and recovery, or from some other process. Generally, the proportion of pots with damaged webbing increased as the condition of the pot degraded (Table 2). Forty-five (34%) of the commercial pots had no biodegradable twine or gaps in the webbing that would have allowed crabs to escape and therefore were probably illegally set; 19 of these were rated as good or excellent, and 26 as fair to very poor.

## Organisms

Organisms were found within 97 pots, including 40 (56%) of the inside pots and 57 (76%) of the outside pots. Tanner crab was the most abundant species (227 caught, mean 1.54 CPP), and second most frequent occurring in 24 pots (16%) (Table 3). The majority of Tanner crabs occurred in just two inside pots that contained 125 and 22 crabs, respectively; both pots were in good condition and were presumed to have been lost less than a year, so they were probably set for subsistence purposes. Excluding these two pots, Tanner crab CPP was only 0.55. Sunflower stars (*Pycnopodia helianthoides*) occurred most frequently (42%) and were the second most abundant species (189 caught, mean 1.29 CPP). The next most abundant species were hairy tritons (*Fusitriton oregonensis*), 174 were caught (15% occurrence), and white anemones (*Metridium senile*), 64 were caught (3% occurrence), although some of the latter may have been epibionts that were detached from the webbing during pot retrieval. In addition, we found, but did not count, many more individuals and species attached to the exterior of the pot and attached lines, including barnacles, tubiculous polychaetes, anemones, bryozoans, brachiopods, mussels, clams, snails, seastars, and basket stars (*Gorgonocephalus* sp.)

During the pilot study, 3 octopuses (*Octopus dofleini*) were found in 4 pots with Tanner crabs, suggesting that octopuses, which are known predators of Tanner crabs (senior author, personal obs.), entered the pot to prey on the crabs. Of 16 octopuses recovered during the entire study, 6 occurred in pots with Tanner crabs, and all 4 pots with 10 or more Tanner crabs (accounting for 181 of 227 crabs) contained at least one octopus, including the pot with 125 Tanner crabs. Presence and absence of octopuses was significantly associated with Tanner crabs (in logarithmic categories; $\chi^2$=26.3). This association may have been underestimated because octopuses were not always located inside the pot. Using the ROV, we observed one octopus sitting on top of a pyramidal pot; in such a position, it probably would have been lost during grappling and recovery.

## Crabs

The recovered pots contained a total of 195 live Tanner crabs, 2 dead crabs, and 30 empty carapaces. From their size and condition, these empty carapaces were considered to be the result of death or predation, rather than molting, and were not measured. Twenty-three of 32 empty carapaces or dead crabs (72%) were found in pots with octopuses. Of the live crabs, 191 were found in inside pots, and 4 in outside pots. Mean CW of all Tanner crabs was 129.8 ±1.8 mm for males ($n$=160), and 85.1 ±3.0 mm for females ($n$=35).

Pot condition, an indicator of time elapsed since it was lost, was examined for its effect on the size of crabs caught. No excellent pots contained crabs, but 152 crabs were recovered from 4 good pots. A total of 166 Tanner crabs were found in 7 out of 42 best pots (17% frequency of occurrence), whereas 61 Tanner crabs were found in 17 of 105 worst pots (16%) (Table 4); mean CPP was 6.8 times greater in best pots (3.95) than in worst pots (0.58), but this difference was not significant (MWU, $Z$=0.152, $P$>0.5). Mean CW of 141 male Tanner crabs from best pots (135.6 ±1.3 mm) was significantly larger than for 19 males from worst pots (87.1 ±6.0 mm: MWU, $Z$=6.29, $P$<0.001; Table 4). This difference was significant even after excluding pot no. 301, which contained 125 crabs; in this case, mean CW of 26 male crabs in best pots was 130.6 ±5.7 mm (MWU, $Z$=4.194, $P$<0.001). Seventy males larger than legal size (138 mm CW), with a mean CW of 144.9 mm were found in best pots; no legal males were found in worst pots. There was no significant difference in mean CW of

**Table 3**

Abundance of organisms found inside recovered pots. Mean values for all pots, with and without the pot containing the highest number of individuals.

| Common name | Species name | Total | Maximum no. per pot | Average no. per pot | Average without max | Total no. pots with species | % of pots with species |
|---|---|---|---|---|---|---|---|
| Tanner crab | *Chionoecetes bairdi* | 227 | 125 | 1.54 | 0.69 | 24 | 16 |
| sunflower sea star | *Pycnopodia helianthoides* | 189 | 13 | 1.29 | 1.2 | 62 | 42 |
| hairy triton | *Fusitriton oregonensis* | 174 | 50 | 1.18 | 0.84 | 22 | 15 |
| anemone (white) | *Metridium senile* | 64 | 50 | 0.44 | 0.1 | 5 | 3 |
| tube worms | *Crucigera* spp. | 50 | 50 | 0.34 | 0 | 1 | 1 |
| green sea urchin | *Strongylocentrotus droebachiensis* | 38 | 17 | 0.26 | 0.14 | 11 | 7 |
| decorator crab | *Oregonia gracilis* | 17 | 3 | 0.12 | 0.1 | 10 | 7 |
| sun star | *Solaster* spp. | 16 | 12 | 0.11 | 0.03 | 4 | 3 |
| giant Pacific octopus | *Octopus dofleini* | 16 | 3 | 0.11 | 0.09 | 14 | 10 |
| sea cucumber | Holothuroidea | 12 | 3 | 0.08 | 0.06 | 8 | 5 |
| Neptune snail | *Neptunea* spp. | 9 | 3 | 0.06 | 0.04 | 5 | 3 |
| lyre crab | *Hyas lyratus* | 9 | 5 | 0.06 | 0.03 | 4 | 3 |
| kelp crab | *Pugettia gracilis* | 7 | 3 | 0.05 | 0.03 | 4 | 3 |
| candlefish | *Mallosus villosus* | 6 | 6 | 0.04 | 0 | 1 | 1 |
| rough-eye rockfish | *Sebastes aleutianus* | 5 | 2 | 0.03 | 0.02 | 4 | 3 |
| hermit crab | *Pagurus* sp. | 5 | 2 | 0.03 | 0.02 | 4 | 3 |
| sculpin | Cottidae | 5 | 1 | 0.03 | 0.03 | 5 | 3 |
| Hind's scallop | *Chlamys rubida* | 4 | 2 | 0.03 | 0.01 | 3 | 2 |
| yellow Irish lord | *Hemilepidotus jordani* | 4 | 2 | 0.03 | 0.01 | 2 | 1 |
| red king crab | *Paralithodes camtschaticus* | 4 | 3 | 0.03 | 0.01 | 2 | 1 |
| rockfish | *Sebastes* spp. | 3 | 1 | 0.02 | 0.01 | 3 | 2 |
| Pacific cod | *Gadus macrocephalus* | 3 | 1 | 0.02 | 0.01 | 3 | 2 |
| arrowtooth flounder | *Atheresthes stomias* | 1 | 1 | 0.01 | 0 | 1 | 1 |
| basket star | *Gorgonocephalus caryi* | 1 | 1 | 0.01 | 0 | 1 | 1 |
| Beringius snail | *Beringius* sp. | 1 | 1 | 0.01 | 0 | 1 | 1 |
| blue mussel | *Mytilus trossulus* | 1 | 1 | 0.01 | 0 | 1 | 1 |
| dogwinkle | *Nucella lamellosa* | 1 | 1 | 0.01 | 0 | 1 | 1 |
| flathead sole | *Hippoglossoides elassodon* | 1 | 1 | 0.01 | 0 | 1 | 1 |
| red urchin | *Strongylocentrotus franciscanus* | 1 | 1 | 0.01 | 0 | 1 | 1 |
| ribbed Neptune | *Neptunea lyrata* | 1 | 1 | 0.01 | 0 | 1 | 1 |
| mottled sea star | *Evasterias troschelii* | 1 | 1 | 0.01 | 0 | 1 | 1 |

**Table 4**

Comparison of Tanner crab catch, sex, and size, by pot condition. ("Best" pots include those coded as good or excellent; "worst" pots include those coded as fair, poor, very poor, or in unknown condition.)

| Parameter | Best pots | Worst pots | Mann Whitney *U*-test |
|---|---|---|---|
| Number of pots | 42 | 105 | |
| Number with Tanner crabs | 7 (17%) | 17 (16%) | |
| Number of Tanner crabs | 166 | 61 | |
| Crabs per pot | 3.95 | 0.58 | $Z$= 0.152, $P$>0.5 |
| Number of legal males | 70 | 0 | |
| Total males | 141 | 19 | |
| Mean CW (SE), males | 135.6 (1.3) | 87.1 (6.0) | $Z$=6.29, $P$<0.001 |
| Total females | 11 | 24 | |
| Mean CW (SE), females | 81.3 (7.5) | 86.9 (2.7) | $Z$=1.48, $P$>0.1 |

females from best pots (81.3 ±7.5 mm, $n$=11) or worst pots (86.9 ±2.7 mm, $n$=24) (MWU, $Z$=1.48, $P$>0.1). Numbers of male crabs were significantly associated with best pots, whereas female crabs were associated with worst pots $\chi^2$=53.7, $P$<0.001); however, this result was highly dependent on two pots with the highest number of males (117) and females (8) respectively. Exclusion of those two pots reduced the $\chi^2$ value to insignificance (3.4, $P$>0.05). Males composed 93% of crabs in best pots and 44% in worst pots. This result may be due primarily to the fact that pots in good condition retained large males that could have escaped more easily from damaged pots.

Even though we could not determine whether holes in webbing were caused by the degradation of biodegradable twine, recovery, or some other process, we examined their influence on crab CPP. The four highest CPPs for Tanner crabs (10, 17, 22, and 125) occurred in pots without holes, but there was no significant difference in CPP between pots with intact or torn webbing (MWU=1.17, $P$>0.26). Therefore, we could not reject the hypothesis that pot holes have no effect on CPP. The 95% confidence intervals around the proportion of intact pots containing crabs (10 of 41; $P$=0.244, 95% CI range: 0.124–0.403) overlapped those for holed pots with crabs (14 of 106; $P$=0.132, 95% CI range: 0.074–0.211) and included the mean of the latter. Thus the binomial test also failed to reject the null hypothesis. Lack of significance in these tests may be partly due to the high number of pots without crabs in both groups.

In addition to Tanner crabs, four male red king crabs (*Paralithodes camtschaticus*) were found in two outside pots. One pot contained 3 legal-size red king crabs with a mean CW of 161 mm and a recently dead Pacific cod which probably acted as bait; the other pot contained a single red king crab of 54 mm CW.

## Discussion

Sidescan sonar has been used to assess the coverage of fishing grounds by bottom trawlers (Krost et al., 1989) but, to our knowledge, has not previously been used to determine the prevalence of ghost fishing by pots or other lost gear. Sonar is a very effective tool in this regard; lost crab pots could easily be identified by their shape and attached lines were often visible on the sonar plots. Occasionally other unidentified objects were observed; some of these could have been extremely degraded pots and one looked like the chassis of a truck or shipping van. Since this study was conducted, we have also tested a laser line-scanning system; its resolution (±1 cm) is much better than that afforded by sonar and allowed us to identify crabs and other organisms on the bottom as well as inside crab traps (Tracey et al., 1998).

The mean CPP (1.54 crab/pot) for all Tanner crabs does not seem particularly excessive. However, much of these data were obtained from an area where heavy fishing pressure had not occurred for 2.5 years. CPP in the best (i.e. most recently lost) pots was almost seven times that in the worst (i.e. oldest) pots; even though this difference was not statistically significant, it represents an important trend. Thus, examining lost pots soon after an active fishery has closed would probably yield high estimates of trapped crabs, and more males of larger sizes.

In addition to catch rates, it is necessary to know the number of actively fishing ghost pots. One "ballpark" estimate of pot loss rates in the eastern Bering Sea is 20,000 pots per year (Alaska Board of Fisheries, cited in Paul et al., 1994), but this estimate was made at a time when up to 100,000 pots were being used in Bering Sea crab fisheries annually. In 1997, the Alaska Board of Fisheries imposed pot limits in the Bering Sea and required all pots to be registered for each crab fishery, partly to reduce loss of pots when weather or ice prevented their recovery. Since then, fewer pots have been used in the Bering Sea, and pot loss rates are presumably lower. In 1999, 50,720 pots were registered for the Bering Sea snow crab (*C. opilio*) fishery; preliminary information indicates that about 1% of these may be lost and replaced during the fishery, as boats return to port for unloading.[5] However, not all lost pots are replaced during intensive fisheries, and during short (<1 week) king or Tanner crab fishery openings, boats do not return to port (a 2-d round trip) or replace pots until after the fishery closes; such losses are not reported. Pot losses as low as 10% per year would contribute 5000 lost pots each year. Subsistence pots, on the other hand, are not accounted for, are not required to be registered, and have practically no restricted locations.

Stevens (1996) concluded that the number of active ghost pots would reach a maximum over time, due to the arithmetic increase in lost pots and exponential decay processes. If 7000 pots with a half-life of 4 years were lost annually, the number of active ghost pots would stabilize at 44,000 after 40 yr, although most would begin to accumulate by year 25 (Stevens, 1996). This is a reasonable time frame for accumulation, because pot fishing for crabs in the Bering Sea has been conducted since at least 1966. However,

[5] Morrison, R. 1999. ADF&G, P.O. Box 308, Dutch Harbor, AK 99692. Personal commun.

extrapolation of ghost pot densities in Chiniak Bay to a 40,000 km$^2$ area of the Bering Sea (where fishing for king, Tanner, and snow crab is particularly intensive) would yield 1.68 million pots in various stages of degradation. The actual number is probably somewhere between these extremes.

If a reliable estimate of pot loss existed, it would be tempting to speculate on the numbers of crabs killed owing to ghost fishing. However, our estimate of 3.95 Tanner crabs per "best" pot represents only a "snapshot" of the ghost fishing process and does not account for cumulative mortality over time. The difference in CPP between best (3.95) and worst pots (0.58) illustrates that numbers of trapped crabs decline over time, due to escapement, predation, mortality, and reduced capture or retention rates. Starvation may account for a large part of the mortality. Kimker (1994) found 39% mortality among legal-size (>139 mm CW) male Tanner crabs that were kept in closed crab pots for 119 days; some of this mortality was undoubtedly due to cannibalism of weaker crabs (Kimker, 1994). Mortality was low for the first 30 days, then increased linearly through the remainder of the experiment. Starvation may be delayed even longer; Paul et al. (1994) held Tanner crabs in laboratory tanks for fixed periods without food, then gave them unlimited access to food. Only 10% mortality occurred among crabs during 90 d while they were held without food, but 100% mortality occurred during the following 140 days during which time they had access to food. Overall mortality ranged from 40% for those starved 60 days to 100% for those starved 90 days (Paul et al., 1994), which is consistent with the findings of Kimker (1994). Predation by octopus (High, 1976) and sunflower seastars (Breen, 1987) has also been implicated as a cause of mortality of crabs in pots. Octopus were important predators in our study and may cause a significant portion of initial mortality. In a year-long study of blue crab (*Callinectes sapidus*) ghost fishing, Guillory (1993) concluded that, of crabs that were recruited after loss of bait, 51% escaped and 45% died. Although mean CPP was only 1.0 (similar to our study) during weekly pot retrievals, the average total CPP for the entire year was 48 crabs, of which 26 (55%) died (Guillory, 1993).

Escapement probably accounts generally for the decline in numbers of crabs found in lost pots. Escapement of legal-size (>165 mm CW) king crabs from pots tended toward an asymptotic value of 80%, whereas escapement of smaller crabs was 92% after periods of 14 to 16 d (High and Worlund, 1979). Escapement rate probably depends upon behavioral differences between species. Video observations of crabs in square pots showed that both Tanner and king crabs tended to aggregate in the corners of pots, but during random movements some crabs accidentally found the entrance tunnel and escaped through it.[2] Tanner crabs are too small to reach the tunnel unless there are large numbers in the pot, allowing them to climb on top of one another to reach the tunnel opening. In addition, degradable twine in Tanner crab pots should create gaps in the webbing within weeks or months after loss, although 34% of our pots had intact webbing even after 1–2 years in the water. That such a large proportion contained no degradable twine suggests that, at a minimum, one third of the commercial crab pots used in the Kodiak region prior to 1994 were illegally constructed. Apparently, fishermen were taking advantage of the very sparse law enforcement presence in Alaskan ports.

Crabs continue to enter lost pots, even without bait. High and Worlund (1979) showed that king crabs continue to enter unbaited pots for up to 16 days. Breen (1987) showed that unbaited traps caught Dungeness crab (*Cancer magister*) at the same rate one year after becoming lost as they did when first set. He estimated that lost traps caught 17 Dungeness crabs per year, of which almost half (9.3) died, and the remainder escaped. Tanner and king crab traps are quite different from Dungeness crab pots, which are made with stainless steel webbing that degrades very slowly. Nevertheless, Breen's (1987) study clearly demonstrates that entry, escapement, and mortality rates of crabs in lost pots is a dynamic process.

Seasonality is also an important factor in ghost fishing. Breen (1987) found varying crab numbers in pots at different times of the year and concluded that a study must be conducted all year round to obtain the best estimate of crab ingress rates. Guillory (1993) found that recruitment of blue crabs to ghost pots, mortality, and escapement all varied seasonally. High turnover rates can lead to high capture and mortality rates; 2/3 of blue crabs entering traps died or escaped within 2 weeks (Guillory, 1993). Thus it is not possible to estimate mortality from a single observation of recovered traps because the number of crabs in the trap represents a balance of continuous ingress, egress, and mortality rates.

During the 1996 ADF&G annual Gulf of Alaska crab trawl survey,[6] the density of Tanner crabs was approximately 1685 crab/km$^2$ in Chiniak Bay, 97 in Kalsin Bay, and 76 in Middle Bay, for an average

[6] Urban, D. 1997. Bottom trawl survey of crab and groundfish: Kodiak Island, Chignik, and South Peninsula areas, 1996. Regional Information Rep. 4K97-58. Alaska Dept. of Fish and Game, 211 Mission Rd. Kodiak, AK 99615.

density of 943 crab/km$^2$ in the sonar-surveyed and nonsurveyed study areas combined. Relative CPP of pots recovered during our study reflected the trawlable densities in each bay; CPP was 2.70 for pots in Chiniak Bay, 0.04 in Kalsin Bay, and 0 in Middle Bay. For both the 1996 trawl survey and our pot retrieval studies, the Chiniak area had the highest density of Tanner crabs, with Kalsin Bay second, and Middle Bay last. Chiniak Bay is also a site where female Tanner crabs aggregate continuously and form high density spawning aggregations in the spring (Stevens et al., 1994).

Knowledge of the abundance of lost pots and numbers of crabs in these pots is required to estimate the impact of ghost fishing, but are not enough in themselves. A more complete assessment of ghost fishing by crab pots will require estimates for rates of ingress, egress, as well as mortality rates of crabs and studies on the degradation rates of biodegradable twine and other structural components of crab traps. Improved enforcement of existing regulations could help reduce ghost fishing. Current estimates of total pot losses are just guesses but could be substantially improved by surveying fishermen or requiring them to report pot losses.

## Acknowledgments

We are indebted to Capt. Gary Edwards of the FV *Big Valley*, who built and operated the grappling devices during the targeted and nontargeted portions of this study. The pilot study was conducted with the aid of Capt. Ron Kutchick, of the ADF&G RV *Resolution*. We also thank the many "ghost (pot) busters" who assisted us in our effort, including J. Haaga, R. Otto, R. MacIntosh, P. Cummiskey, and K. Phillips. This report benefited from the thoughtful comments of Bob Wilbur and two anonymous reviewers. This study was partially funded by the U.S. Army Corps of Engineers. Funding for use of sidescan sonar was provided by the West Coast and Polar Regions Undersea Research Center, University of Alaska, Fairbanks, AK.

## Literature cited

**Alaska Statutes.**
**1996**. Alaska statutes, vol. 5, Alaska Legislature Council. Michie Law Publishers, Charlottesville, VA.

**Breen, P.A.**
**1987**. Mortality of Dungeness crabs caused by lost traps in the Fraser River Estuary, British Columbia. N. Am. J. Fish. Manage. 7:429–435.
**1990**. A review of ghost fishing by traps and gillnets. *In* Proceedings of the second international conference on marine debris, 2–7 April 1989, Honolulu, Hawaii (R.S. Shomura and M. L. Godfrey, eds.), p. 571–599. U.S. Dep. Commer., NOAA Tech. Memo. NMFS-SWF-SC-154.

**Carr, H. A., and J. Harris.**
**1997**. Ghost-fishing gear: Have fishing practices during the past few years reduced the impact? *In* Marine debris: sources, impacts and solutions (J. M Coe and D. B. Rogers, eds.), p. 171–186. Springer, New York, NY.

**Carr, H. A., E. H. Amaral, A. W. Hulbert, and R. Cooper.**
**1990**. Underwater survey of simulated lost demersal and lost commercial gill nets off New England. *In* Proceedings of the second international conference on marine debris, 2–7 April 1989, Honolulu, Hawaii (R. S. Shomura and M. L. Godfrey, eds.), p. 438–447. U.S. Dep. Commerce, NOAA Tech. Memo. NMFS-SWF-SC-154.

**Guillory, V.**
**1993**. Ghost fishing by blue crab traps. N. Am. J. Fish. Manage. 13:459–466.

**High, W. L.**
**1976**. Escape of Dungeness crabs from pots. Mar. Fish. Rev. 38(4):19–23.

**High, W. L., and D. D. Worlund.**
**1979**. Escape of king crab, *Paralithodes camtschatica*, from derelict pots. U.S. Dep. Commer., NOAA Tech. Rep. NMFS-SSRF-734, 11 p.

**Kirkley, J., and K. E. McConnell.**
**1997**. Marine debris: benefits, costs and choices. *In* Marine debris: sources, impacts and solutions (J. M Coe and D. B. Rogers, eds.), p. 171–186. Springer, New York, NY.

**Kimker, A.**
**1994**. Tanner crab survival in closed pots. Alaska Fish. Res. Bull. 1(2):179–183.

**Krost, P., M. Brenhard, F. Werner, and W. Hukriede.**
**1989**. Otter trawl tracks in Kiel Bay (Western Baltic) mapped by side-scan sonar. Meeresforsch. 32:344–353.

**Laist, D. W.**
**1996**. Marine debris entanglement and ghost fishing: a cryptic and significant type of bycatch. *In* Solving bycatch: considerations for today and tomorrow, p 33–39. Alaska Sea Grant College Program Report 96-03, Univ. Alaska, Fairbanks, AK.

**Muir, W. D., J. T. Durkin, T.C. Coley, and G.T. McCabe Jr.**
**1984**. Escape of captured Dungeness crabs from commercial crab pots in the Columbia River estuary. N. Am. J. Fish. Manage. 4:552–555.

**Parish, F. A., and T. K. Kazama.**
**1992**. Evaluation of ghost fishing in the Hawaiian lobster fishery. Fish. Bull. 90:720–725.

**Paul, J. M., A. J. Paul, and A. Kimker.**
**1994**. Compensatory feeding capacity of 2 brachyuran crabs, Tanner and Dungeness, after starvation periods like those encountered in pots. Alaska Fish. Res. Bull 1(2):184–187.

**Pecci, K. J., R. A. Cooper, C. D. Newell, R. A. Clifford, and R. J. Smolowitz.**
**1978**. Ghost fishing of vented and unvented lobster, *Homarus americanus*, traps. Mar. Fish. Rev. 40(5-6):9–43.

**Sheldon, W. W., and R. L. Dow.**
**1975**. Trap contributions to losses in the American lobster fishery. Fish. Bull. 73:449–451.

**Smolowitz. R. J.**
**1978a**. Trap design and ghost fishing: an overview. Mar. Fish. Rev. 40(5–6):2–8.
**1978b**. Trap design and ghost fishing: discussion. Mar. Fish. Rev. 40(5–6):59–67.

**Stevens, B. G.**
**1996.** Crab bycatch in pot fisheries. *In* Solving bycatch: considerations for today and tomorrow, p.151–158. Alaska Sea Grant Program Report No. 96-03. Univ. Alaska Fairbanks, AK.

**Stevens, B. G., J. A. Haaga, and W. E. Donaldson.**
**1994**. Aggregative mating of Tanner crabs *Chionoecetes bairdi*. Can. J. Fish.Aquat. Sci. 51: 1273–1280.
**In press.** Mound formation by Tanner crabs (*Chionoecetes bairdi*): Tidal phasing of larval launch pads? *In* The biodiversity crisis and crustacea: proceedings of the fourth international crustacean congress, Amsterdam, Netherlands, July 20–24, 1998, vol 2. (F. R. Schram and J. C. von Vaupel Klein, eds). Crustacean Issues 12.

**Tracey, G. A., E. Saade, B. Stevens, P. Selvitelli, and J. Scott.**
**1998**. Laser line scan survey of crab habitats in Alaskan waters. J. Shellfish Res. 17(5):1483–1486.

**Zar, J. H.**
**1984**. Biostatistical analysis, 2nd ed. Prentice Hall, Inc. Englewood Cliffs, NJ, 718 p.

# Spatial distributions of Pacific herring, *Clupea pallasi*, and walleye pollock, *Theragra chalcogramma*, in Prince William Sound, Alaska

**Kevin D. E. Stokesbury**
Institute of Marine Science
University of Alaska-Fairbanks
Fairbanks, Alaska 99775-7220
Present address: Center for Marine Science and Technology
University of Massachusetts Dartmouth
706 South Rodney French Boulevard
New Bedford, Massachusetts 02744-1221
E-mail address: kstokesbury@umassd.edu

**Jay Kirsch**
Prince William Sound Science Center
P.O. Box 705
Cordova, Alaska 99574

**Evelyn D. Brown**
Institute of Marine Science
University of Alaska-Fairbanks
Fairbanks, Alaska 99775-7220

**Gary L. Thomas**
Prince William Sound Science Center
P.O. Box 705
Cordova, Alaska 99574

**Brenda L. Norcross**
Institute of Marine Science
University of Alaska-Fairbanks
Fairbanks, Alaska 99775-7220

**Abstract.**—Nursery areas of Pacific herring, *Clupea pallasi*, and walleye pollock, *Theragra chalcogramma*, were identified by using acoustic surveys in October 1995, and in March and July 1996 in Prince William Sound, Alaska. Pacific herring and walleye pollock were aggregated in the east-northeast and west-southwest areas. Juvenile Pacific herring spent the first two years of their lives isolated within bays. Water temperatures within bays were cooler in the summer and warmer in the winter compared with temperatures measured along coastal passages and the open coast. Although these temperature differences were small and based on point observations their accumulative effect over the season may be considerable. The school structure of juvenile Pacific herring varied seasonally. Newly recruited age-0 Pacific herring were tightly aggregated, forming a few, dense schools within a single-size cohort, in shallow water at the heads of bays in July. Age-0 Pacific herring were still aggregated within bays in shallow water in October, but the school structure was less cohesive and size cohorts began to mix. School structure and distribution completely changed in March as age-0 Pacific herring moved away from the shores into deeper water and spread out forming sparse shoals of mixed-size cohorts. Juvenile Pacific herring joined the adult schools after their second winter, leaving as new recruits entered the bays. Juvenile walleye pollock also aggregated within bays and were spatially segregated from adults. However, there appeared to be little overlap between Pacific herring and walleye pollock juveniles because they occupied different portions of the water column within these bays.

Manuscript accepted 29 November 1999.
Fish. Bull. 98:400–409 (2000).

In Prince William Sound, Alaska, Pacific herring (*Clupea pallasi*) and walleye pollock (*Theragra chalcogramma*) support major commercial fisheries and are primary forage for marine birds, mammals and other fishes (Clausen, 1983; Hatch and Sanger, 1992; Livingston, 1993; Brown et al., 1996). Recently the abundance of both these species in Prince William Sound has fluctuated, particularly that of Pacific herring, which suffered a population crash in 1993 resulting in the closure of the commercial fisheries (bait, sac-roe, and roe on kelp) (Meyers et al., 1994; Paine et al., 1996). Little is known of the spatial distributions and the physical and biological variables influencing Pacific herring and walleye pollock life histories in this biologically rich, high latitude ecosystem (Paine et al., 1996).

We identified Pacific herring and walleye pollock nursery areas by examining their small-scale (km) spatial distributions in Prince William Sound, Alaska. We hypothesized that juvenile Pacific herring and juvenile walleye pollock were contagiously distributed and that

their distributions varied seasonally in relation to the stage of life of fish, school structure, and coastal structure. We then examined the degree of overlap between juvenile Pacific herring and juvenile walleye pollock distributions. Further we determined if cohorts (age and size) of Pacific herring were spatially segregated. Adult Pacific herring and walleye pollock distributions were also observed; however, these fishes appeared to emigrate from Prince William Sound at certain times of the year.

## Materials and methods

Prince William Sound is a large body of water separated from the Gulf of Alaska by a series of mountainous islands and deep passages (Fig. 1). The rocky coastline is highly irregular and has numerous islands, passages, bays, and deep fjords. The Sound had a semidiurnal tide with a maximum range of 4.4 m during the period of our study.

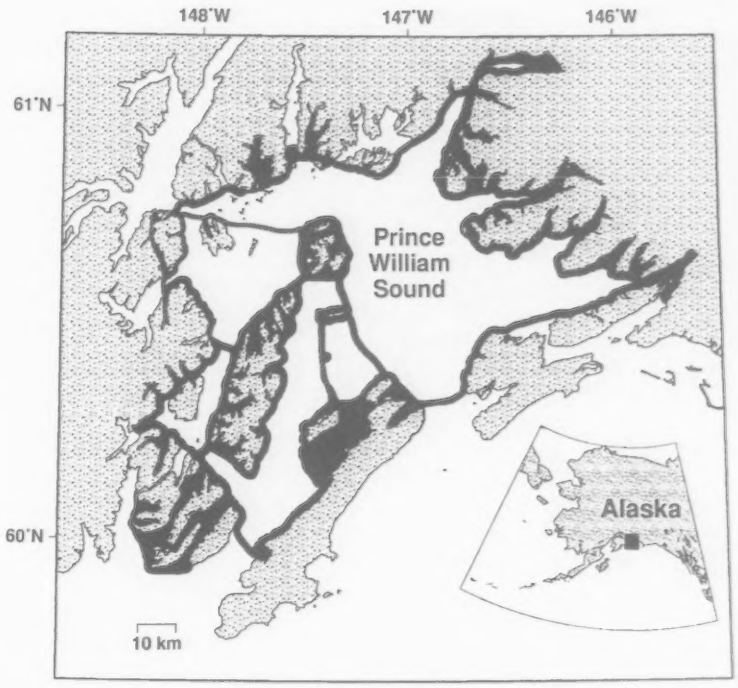


**Figure 1**

Location of the October 1995, March 1996, and July 1996 acoustic survey transects in Prince William Sound, Alaska. The dark areas represent the locations within which we conducted our zigzag transect survey.

Prince William Sound coastal waters were acoustically surveyed in October 1995, and in March and July 1996 (Fig. 1). Five vessels were used during each 10-day survey (12 hours per day): three commercial seiners (≈16.8 m) deployed the acoustic and oceanographic equipment and fished the seines; a trawler (Alaska Department of Fish and Game RV *Pandalus*, ≈20 m) was used for midwater sampling; and a tour vessel (≈25 m) was used for processing samples. Surveys were conducted during the night (2000 to 0800 h) in October 1995 and March 1996, and during the day (0800 to 2000 h) in July 1996. Northern latitude conditions dictated this sampling design because there was little daylight in March and little darkness in July. Further, the summer cruises had to be coordinated with aerial surveys for forage fish that could only be flown during daylight (E. Brown, unpubl. data). We observed and collected both Pacific herring and walleye pollock in surface waters and near the sea floor, a range of area that coincides with the known diel distributions for these two species.

The acoustic vessel followed a zigzag transect pattern along the shore (MacLennan and Simmonds, 1992; Gunderson, 1993) to a distance of ≈1 km at a speed of 14 to 17 km/h. We attempted to survey the same bays, passages, and open coast during all three surveys. The vessel's sonar (50 kHz, 46°) was used to locate fish schools along these transects. When a fish school was encountered, the acoustic vessel slowed to 9 to 11 km/h and completed a series of parallel transects perpendicular to shore by using a 120-kHz BioSonics 101 echosounder with a preamplified dual-beam transducer (6°×15°). The transducer was mounted on a BioSonics 1.2-m BioFin and towed at ≈1 m depth. The acoustic signals were processed in real-time with BioSonics ESP 221 Echo square integration software and ESP 281 Dual beam software, and the raw signal was stored on digital audio tape (Thorne, 1983a; 1983b; MacLennan and Simmonds, 1992). The acoustic system was calibrated before each cruise with a standard target and the source level (SL) was 225.07 dB µPa. Acoustic noise was well below our lowest density of interest.

Fish schools observed with the acoustic equipment were sampled to determine species composition and size structure. Fish were captured with a modified bottom trawl in deep water (1.52 × 2.13 m Nor'Eastern Astoria V trawl doors, 21.3-m head rope, 29.0-m, foot rope, 3 × 20.0-m mouth, 10.2-cm mesh

wings, 8.9-cm middle, and a 32.0-mm codend liner), with one of two anchovy seines in surface water (250.0 × 34.0 m or 20.0 m, 25.0-mm stretch mesh), or with a small salmon fry seine in shallow water (50.0 × 8.0 m, 3.0-mm stretch mesh deployed from a 6-m skiff equipped with a 70-horsepower engine). Fish collections were directed by the acoustic survey and we attempted to sample every observed school. The catchability of the fish species sampled may vary with time of day, season, and between nets. However, we assumed that these collections reflected the actual species and age cohort ratios present within the acoustically observed fish school. A total of 220, 122, and 60 fish collections were made in 15, 29, and 28 locations in October 1995, March 1996, and July 1996, respectively. Each net collection was characterized by species, and 1000 individuals of the dominant fish species, usually Pacific herring, were randomly sampled. Fork lengths (mm) for 550 fish were measured immediately after capture, and 450 fish were frozen and later their fork length and wet weight (g) were measured in the laboratory. After subsampling the remaining fish were released unharmed from the seine.

A length-dependent scaling constant was used to convert estimated target strength ($TS$ $-10 \log_{10} w$) from units of reflected acoustic energy (dB) to units of biomass density (kg/m$^3$):

$$TS - 10 \log_{10} w = -6.0 \log_{10} L - 24.2 \text{ dB m}^2/\text{kg},$$

where $L$ = the mean fork length (cm) of the fish collected in the area (Thorne, 1977; 1983a 1983b; Thorne and Thomas, 1990).

This equation differs from the more standard regression equation (Foote, 1987) because it derives the target strength as a proportion of weight. Thorne's equation was developed for echo integration primarily with Pacific herring surveys from Alaska and Puget Sound (Thorne, 1983a).

For walleye pollock, that have a physoclistic swim bladder, the standard equation:

$$TS = 20 \log_{10} x - 66.0 \text{ dB}$$

was used (Foote and Traynor, 1988).

The acoustic estimates of Pacific herring and walleye pollock school densities were derived from these target strength equations. Many physical and biological variables (including morphologic features [such as physostomic, physoclistic, fat content], the orientation of the fish, water temperature, and depth) affect target strength (Thorne, 1983b; Foote, 1987; Rose and Leggett, 1988; Thorne and Thomas, 1990; MacLennan and Simmonds, 1992; Misund et al., 1995; Huse and Ona, 1996; McClatchie et al., 1996; Ona and Mitson, 1996; Misund, 1997; Misund et al., 1998).

Echo integration measurements were converted into data cells with lengths of 120 m, 40 m, or 20 m and width and depth of 1 m for the October 1995, March 1996, and July 1996 surveys, respectively. Cell length was determined by using the simultaneously recorded latitude and longitude from the GPS navigational system.

Species proportion and size modes per species were determined from the fish collections. The species proportions, based on the number of individuals per fish species in the random subsample, were multiplied by the echo integration densities (kg/m$^3$) and then converted by using length-weight regressions into the number of Pacific herring per size mode, or the number of walleye pollock. Walleye pollock were not divided into size modes because the standard deviations of the mean fork lengths of individual collections indicated that aggregations were unimodal.

A group of data cells was considered to be a fish school if the sum of the absolute differences between latitudes and longitudes of adjacent cells was >0.009°. We concluded that cells containing the equivalent of <0.5 fish/m$^3$ were probably zooplankton on the basis of frequency distributions of the data, and these cells were removed from the data set (MacLennan and Simmonds, 1992; Gunderson, 1993). If fish located near the bottom were difficult to distinguish acoustically, data cells for the bottom 5 m were removed.

Cohorts of Pacific herring and walleye pollock large-scale spatial distributions were examined by using circular statistics (Batschelet, 1981). The angle (0°=true north) for each data cell was determined from an origin in the center of Prince William Sound (60.6000°N, 146.9000°W). These angles represent distributions along the survey transect line and are influenced by inequalities in shoreline distance and sampling bias. Angle frequency distributions were compared with random distributions and with the distributions of other herring size modes along the same transect by using a chi-squared test at the 5% level of significance (Batschelet, 1981). Expected values were grouped according to Cochran's rule, which states that <20% of the expected frequencies should have a value <5 (Sokal and Rohlf, 1981).

Nursery areas were determined by examining the relation between juvenile fish spatial distributions and coastline structure. Bays were defined statistically from passages or open coast by calculating the sum of the three nearest shore distances (Σ3NSD). To determine this value, first the distance between the center of each fish school and the nearest shore was measured. The second distance was determined by

moving 90° on either side of the first line, measuring the distance to shore and selecting the shorter of the two lines. The third distance was determined by moving 90° on either side of the first and second lines, measuring the distance to shore, and selecting the shorter of the two lines. These three distances were summed. This measurement was calculated at specific points inside 26 bays and outside 17 bays to verify that it accurately distinguished between bays, passages, and open coast. The Σ3NSD for each fish school was compared with the same measurements from randomly selected points along the same survey transect by using a chi-squared test grouped according to Cochran's rule (Sokal and Rohlf, 1981). This technique removed sampling and shore structure discrepancies.

Differences in water conditions within bays compared with conditions in passages or along open coastline were examined. Vertical water profiles of temperature and salinity at 1-m intervals, measured with a SeaBird CTD instrument (SEACAT SBE19), were collected inside and outside bays. Differences between means were examined with a Mann-Whitney rank sum test ($U$).

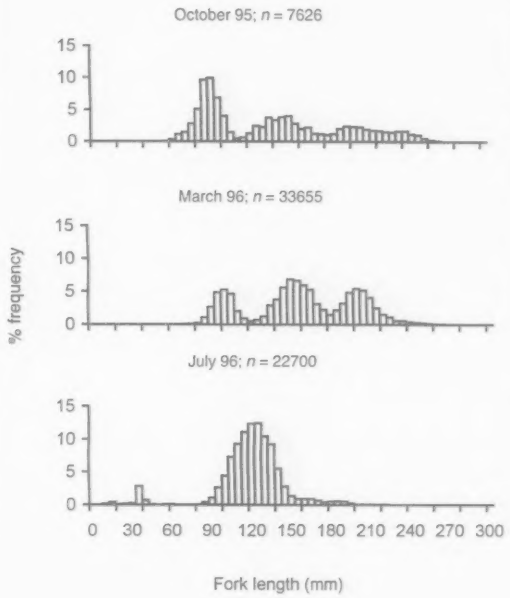


**Figure 2**

Percent size-frequency distributions of Pacific herring, *Clupea pallasi*, (fork length mm) collected during three acoustic surveys of Prince William Sound, Alaska, in 1995 and 1996 ($n$=count).

## Results

Ninety-seven species of fish and macroinvertebrates were collected during the October 1995, and the March and July 1996 surveys. Pacific herring (65.0% of subsample collections) dominated the ichthyofauna followed by walleye pollock (19.2%).

Pacific herring and walleye pollock size frequencies differed. The Pacific herring population consisted of three size modes representing age-0, 1–2 year old, and adult fishes (Stokesbury et al. 1999) (Fig. 2). The walleye pollock population size distribution was bimodal, representing age-0 and adult fishes in October 1995 and March 1996, whereas only age-0 fish were collected during July 1996 (Fig. 3). Age-0 and adult pollock were always collected separately.

The proportion of Pacific herring schools consisting of a single size cohort varied among seasons. In October 1995, 49.0% of the Pacific herring schools sampled consisted of a single size class, mostly age 0. In March 1996, 38.9% of the Pacific herring schools sampled consisted of a single size, primarily 1–2 year olds. In July 1996, 83.3% of the Pacific herring schools sampled consisted of a single size, primarily 1–2 year olds.

Juvenile Pacific herring and walleye pollock were contagiously distributed in the east-northeast and the west-southwest of Prince William Sound (Fig. 4). Adult Pacific herring aggregated in the southwest (210°–240°) in October 1995, in the south (180°) and east (90°) in March 1996, and west (240°–270°) in July 1996 (Fig. 4).

Pacific herring schools had the lowest densities in March 1996 and the highest densities in July 1996 (Table 1). Walleye pollock schools had low densities in October 1995 and March 1996 compared with very high densities in July 1996 (Table 1).

Pacific herring were deeper in the water column in March 1996 (27.0–28.9 m) than in October 1995 (15.0–20.2 m) and July 1996 (14.1–16.7 m) (Fig. 5). Walleye pollock were distributed near the bottom during all three surveys (Fig. 5).

The 26 locations within bays had a mean Σ3NSD value of 3.8 km (SD=2.45), significantly smaller than 9.8 km (SD=6.69) for the 17 locations within passages and along the open coast ($t$=–3.61, df=41, $P$<0.001). The water conditions within these bays generally differed from conditions in passages and open coast (Table 2). The surface water temperatures (0–30 m) were cooler inside than outside the bays by 0.32°C and 0.20°C in October 1995 and July 1996, respectively. The surface water inside the bays was also less saline in October 95 but was similar inside

**Table 1**

Means and standard deviations (SD) of densities (fish/m$^3$) for the three Pacific herring, *Clupea pallasi*, size modes and for walleye pollock, *Theragra chalcogramma*, aggregations observed during three acoustic surveys of Prince William Sound, Alaska, in 1995 and 1996 ($n$=number of schools observed).

| | October 1995 fish/m$^3$ | | | March 1996 fish/m$^3$ | | | July 1996 fish/m$^3$ | | |
|---|---|---|---|---|---|---|---|---|---|
| Herring | $n$ | mean | SD | $n$ | mean | SD | $n$ | mean | SD |
| age-0 | 137 | 2.52 | 8.36 | 179 | 0.91 | 2.84 | 8 | 2.67 | 5.46 |
| age 1–2 | 126 | 0.51 | 1.10 | 223 | 0.81 | 0.95 | 42 | 9.15 | 15.75 |
| adult | 54 | 1.35 | 3.21 | 147 | 0.51 | 0.95 | 32 | 3.62 | 0.86 |
| Pollock | 119 | 3.14 | 8.68 | 148 | 4.20 | 14.59 | 31 | 267.87 | 72.05 |

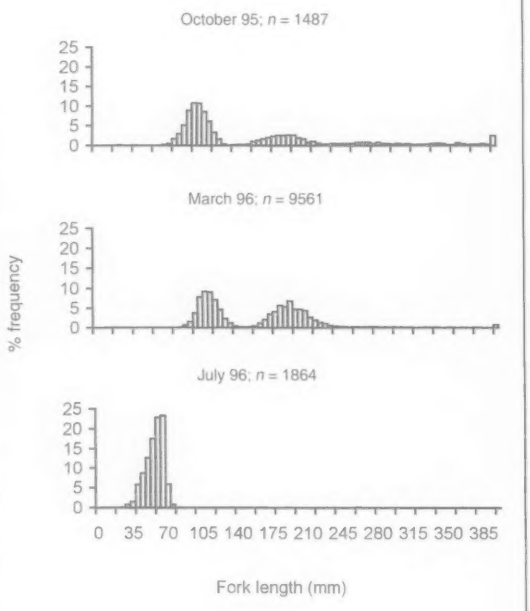


**Figure 3**

Percent size-frequency distributions of walleye pollock, *Theragra chalcogramma* (fork length mm), collected during three acoustic surveys of Prince William Sound, Alaska, in 1995 and 1996 ($n$=count).

and outside the bays in deeper water (31–60 m) and throughout the water columns in July 1996 (Table 2). Deeper waters, where Pacific herring were aggregated, inside the bays were warmer than outside the bays, 0.28°C (31–60 m) in March 1996.

Pacific herring and walleye pollock Σ3NSD distributions differed from randomly calculated Σ3NSD distributions during all three surveys (Table 3; Fig. 6). In October 1995, age-0 and 1–2 year old Pacific herring aggregated at the heads of bays with Σ3NSD values <3 km (Fig. 6). Adult Pacific herring were aggregated in passages or along the open coast (Fig. 6). Walleye pollock distribution was also significantly aggregated within bays but not as tightly as age-0 and 1–2 year old Pacific herring (Table 3; Fig. 6). In March 1996, all size modes of Pacific herring and walleye pollock had greater than expected Σ3NSD values, ranging between 4 and 10 km (Table 3; Fig. 6). In July 1996, age-0 Pacific herring were highly aggregated at the heads of bays (57.1% of Σ3NSD <1 km; Fig. 6). Age 1–2 year old Pacific herring were also aggregated at the head of bays (<2 km). Adult Pacific herring were aggregated within bays (<2 km), but more than expected had Σ3NSD values of 6 to 7 km (Fig. 6). In July 1996, walleye pollock were aggregated within bays and the majority of Σ3NSD values were <3 km (Table 3; Fig. 6).

## Discussion

Pacific herring was the most abundant fish aggregating in the east-northeast and west southwest areas of Prince William Sound. Bays appeared to be nursery areas for age-0 and 1–2 year old Pacific herring. Water conditions within bays fluctuated less than conditions within passages and along the open coast. In October 1995 and July 1996 water temperatures in the upper 30 m were cooler inside these bays than within passages or along the open coast. In March this pattern was reversed and deeper waters, where the Pacific herring were aggregated, were warmer within the bays than within passages or along the open coast. Although, these fluctuations were small, they may have affected juvenile Pacific herring metabolic rates. Temperature and length of winter are critical factors in determining juvenile Pacific herring growth and over-winter survival (Paul and Paul, 1998; Paul et al., 1998; Foy and Paul, 1999).

When larval Pacific herring metamorphose into juveniles, they develop the ability to form and maintain schools (Blaxter, 1985; Gallego and Heath, 1994). Schooling behavior is the juvenile herring's primary defense against predation (Blaxter and Hunter, 1982). School structure results from the dynamic interaction of several variables causing opposing behaviors, primarily the availability of food, the physical size and condition of the fish, and the threat of predation (for a review see Pitcher, 1986). Newly recruited age-0 Pacific herring were tightly aggregated in shallow water at the heads of bays in July. These herring formed a few dense schools of a single-size cohort near the surface. This distribution possibly resulted from a high threat of predation (Stokesbury et al.[1]), coupled with an abundance of food as indicated by the fullness of herring stomachs (Foy and Norcross, 1999) and from zooplankton samples (Foy[2]).

Age-0 Pacific herring were aggregated within bays near the surface, in October. However, the number of schools increased, schools became less cohesive, and size cohorts began to mix in contrast to the highly aggregated unimodal schools observed in July. The distribution observed in October may have resulted from a decrease in food abundance, a decrease in the threat of predation, or both (Foy and Norcross, 1999, Stokesbury et al.[1]).

Age-0 Pacific herring school structure and distribution completely changed in March. These herring had just survived the winter when prey abundance is minimal and the risk of starvation is great (Paul and Paul, 1998; Paul et al., 1998; Foy and Paul, 1999). Herring moved away from the shores into deeper water and spread out forming sparse (<1 fish/m$^3$) shoals of mixed-size cohorts. Distance between fish within schools increases with hunger, reducing cohesion, and causing lower mean densities (Pitcher and Partridge, 1979; Robinson, 1995). This independent segregating behavior reduces competition for food and increases the chance of encountering food by

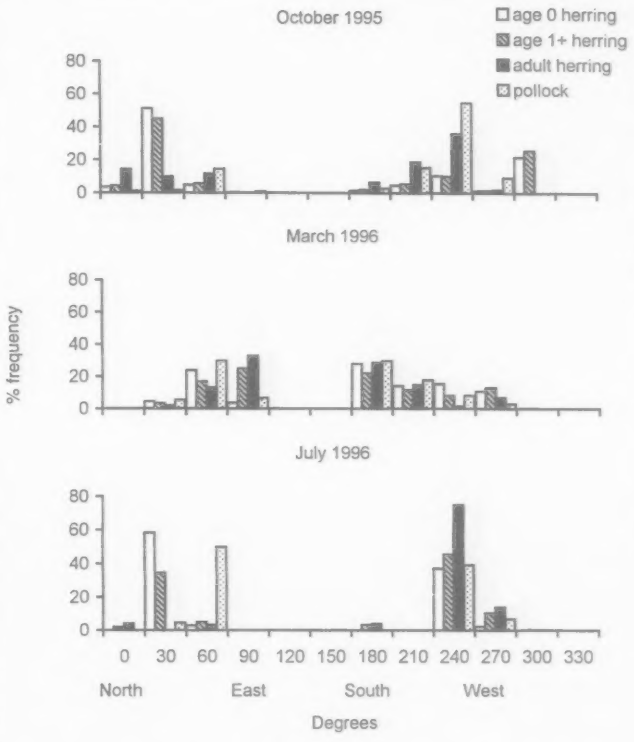


**Figure 4**

Angle percent-frequency distributions of Pacific herring, *Clupea pallasi*, and walleye pollock, *Theragra chalcogramma*, observed during three acoustic surveys of Prince William Sound, Alaska, in 1995 and 1996.

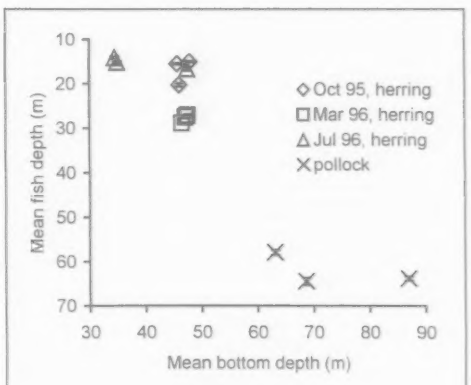


**Figure 5**

Mean depths (m) and standard error bars for Pacific herring, *Clupea pallasi*, and walleye pollock, *Theragra chalcogramma*, compared with mean bottom depths (m) during three acoustic surveys of Prince William Sound, Alaska, in 1995 and 1996.

[1] Stokesbury, K. D. E., J. Kirsch, and B. L. Norcross. 1999. Mortality estimates of juvenile Pacific herring (*Clupea pallasi*) in Prince William Sound, Alaska. Unpubl. manuscript.

[2] Foy, W. 1996–1998. Unpubl. data. Institute of Marine Science, Industrial Technology Center, University of Alaska, Fairbanks, 118 Trident Way, Kodiak, AK 99614-7401.

**Table 2**

Means and standard deviations (SD) of water conditions inside bays and outside bays in passages and along open coast during three surveys of Prince William Sound, Alaska, in 1995 and 1996 ($n$=count; Mann-Whitney rank sum test=$U$).

| | | | Temperature (°C) | | | Salinity (‰) | | |
|---|---|---|---|---|---|---|---|---|
| Water depth (m) | | $n$ | mean | SD | | mean | SD | |
| October 1995 | | | | | | | | |
| 0–30 | inside | 146 | 9.34 | 0.626 | $U$=16135 | 28.77 | 1.111 | $U$=18583 |
| 0–30 | outside | 180 | 9.66 | 0.821 | $P$<0.001 | 29.29 | 1.063 | $P$<0.001 |
| 31–60 | inside | 71 | 7.95 | 2.06 | $U$=4212 | 30.62 | 0.749 | $U$=8610 |
| 31–60 | outside | 186 | 9.87 | 0.393 | $P$<0.001 | 30.36 | 0.21 | $P$=0.303 |
| March 1996 | | | | | | | | |
| 0–30 | inside | 667 | 4.14 | 0.437 | $U$=281130 | 31.65 | 0.225 | $U$=305280 |
| 0–30 | outside | 509 | 4.06 | 0.357 | $P$<0.001 | 31.66 | 0.219 | $P$=0.320 |
| 31–60 | inside | 416 | 4.53 | 0.521 | $U$=228192 | 31.83 | 0.106 | $U$=209925 |
| 31–60 | outside | 512 | 4.25 | 0.344 | $P$<0.001 | 31.80 | 0.106 | $P$<0.001 |
| July 1996 | | | | | | | | |
| 0–30 | inside | 688 | 10.93 | 1.984 | $U$=291730 | 28.98 | 1.772 | $U$=287935 |
| 0–30 | outside | 480 | 11.10 | 1.569 | $P$=0.049 | 29.09 | 1.642 | $P$=0.194 |
| 31–60 | inside | 453 | 6.45 | 1.084 | $U$=192162 | 31.02 | 0.479 | $U$=213780 |
| 31–60 | outside | 492 | 6.94 | 1.238 | $P$<0.001 | 31.08 | 0.265 | $P$=0.911 |

**Table 3**

Chi-squared analysis in which the percent frequency distributions of the sum of the three near shore distances (Σ3NSD) for Pacific herring, *Clupea pallasi*, and walleye pollock, *Theragra chalcogramma*, aggregations were compared with values generated from a random distribution during three acoustic surveys in Prince William Sound, Alaska (Fig. 6 in main text); * = $P$<0.05, ** = $P$<0.01, df = degrees of freedom.

| | October 1995 | | March 1996 | | July 1996 | |
|---|---|---|---|---|---|---|
| | df | $\chi^2$ | df | $\chi^2$ | df | $\chi^2$ |
| Herring | | | | | | |
| age-0 | 12 | 55.30** | 9 | 53.68** | 8 | 182.17** |
| age 1–2 | 12 | 51.41** | 9 | 58.40** | 8 | 59.29** |
| adult | 12 | 123.26** | 9 | 84.55** | 8 | 52.18** |
| Pollock | 12 | 25.16* | 9 | 63.60** | 8 | 64.46** |

increasing the foraging area (Robinson and Pitcher, 1989; Robinson, 1995).

Age-1 Pacific herring repeated this contraction-expansion pattern of school structure and distribution during the year. After their second winter, herring appeared to join the adult schools, leaving as new recruits entered the bays.

Pacific herring and walleye pollock geographic distributions were roughly similar within Prince William Sound. Walleye pollock distribution was bimodal with aggregations in the east-northeast and the west-southwest areas. However, there appeared to be little spatial overlap between these species because they occupied different portions of the water column. Juvenile walleye pollock were highly aggregated, forming a few, very dense schools in July within bays. Juvenile walleye pollock distribution may be influenced by the cannibalistic behavior of adult walleye pollock (Livingston, 1993). Adult walleye pollock were primarily aggregated in the southern portion of Prince William Sound, although a smaller school was evident in the east-northeast.

Bays within Prince William Sound appear to be nursery areas for both Pacific herring and walleye pollock juveniles. Data presented here and growth studies suggest that these nursery areas are isolated (Stokesbury et al., 1999). This finding differs from that for other herring species distributions where juveniles from different populations appear to share a common nursery and feeding areas, separating only when adults begin to spawn (Blaxter and Hunter, 1982; Iles and Sinclair, 1982; Sinclair et

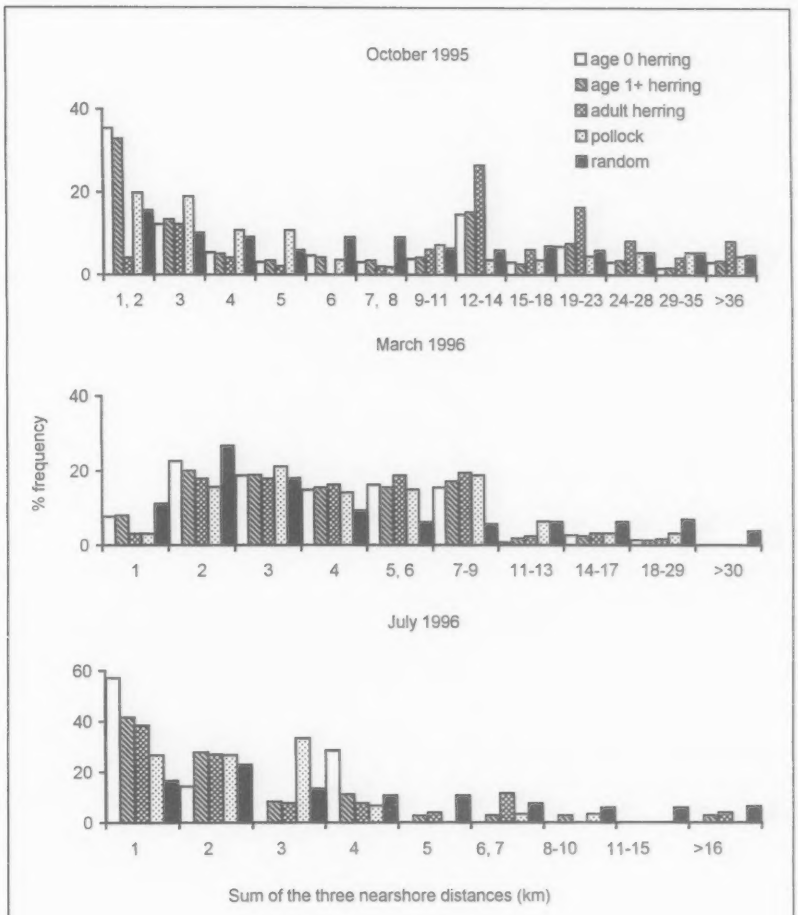


**Figure 6**

Percent frequency distributions of the sum of the three near shore distances (Σ3NSD) for Pacific herring, *Clupea pallasi*, age cohorts and walleye pollock, *Theragra chalcogramma*, aggregations and values generated from a random distribution, during three acoustic surveys in Prince William Sound, Alaska. Fish schools with sum of the three near shore distances <7 were usually within bays.

al., 1985; Sinclair, 1988). Future work should focus on determining the physical and biological variables influencing juvenile Pacific herring and walleye pollock within these bays to estimate population fluctuations that are critical for ecosystem models and effective fisheries management.

## Acknowledgments

We thank R. Foy, M. McEwen, S. Gay, and L. Tuttle for assistance with field collections. N. Peters and G. B. Steinhart assisted in collecting and processing the acoustic data. S. Moreland and M. Vallerino assisted with data analyses. R. Foy, G. B. Steinhart, and S. Moreland provided helpful comments on the manuscript. The comments of three anonymous reviewers further improved this manuscript. We also thank the captains and crews of the FV *Temptation*, FV *Miss Kayley*, FV *Kyle David*, MV *Pacific Star*, FV *Pagan*, FV *Cape Elrington*, RV *Pandalus*, and the Alaska Department of Fish and Game, Cordova, for their help. The Exxon Valdez Oil Spill Trustee Council through the Sound Ecosystem Assessment (SEA) project at the University of Alaska, Fairbanks, and the Prince William Sound Science Center funded this project.

## Literature cited


**Batschelet, E.**
**1981.** Circular statistics in biology. Academic Press, London, 371 p.

**Blaxter, J. H. S.**
**1985.** The herring: a successful species? Can. J. Fish. Aquat. Sci. 42 (suppl. 1):21–30.

**Blaxter, J. H. S., and J. R. Hunter.**
**1982.** The biology of clupeoid fishes. Adv. Mar. Biol. 20:1–223.

**Brown, E. D., T. T. Baker, J. E. Hose, R. M. Kocan, G. D. Marty, M. D. McGurk, B. L. Norcross, and J. Short.**
**1996.** Injury to the early life history stages of Pacific herring in Prince William Sound after the *Exxon Valdez* oil spill. *In* Proceedings of the *Exxon Valdez* oil spill symposium (S. D. Rice, R. B. Spies, D. A. Wolfe, and B. A. Wright, eds.), p. 448–462. Am. Fish. Soc. Symp. 18, Bethesda, MD, 931 p.

**Clausen, D. M**
**1983.** Food of walleye pollock, *Theragra chalcogramma*, in an embayment of southeastern Alaska. Fish. Bull. 81:637–642.

**Foote, K. G.**
**1987.** Fish target strengths for use in echo integrator surveys. J. Acoust. Soc. Am. 82:981–987.

**Foote, K. G., and J. J. Traynor.**
**1988.** Comparison of walleye pollock target strength estimates determined from *in situ* measurements and calculations based in swimbladder form. J. Acoust. Soc. Am. 83:9–17.

**Foy, R. J., and B. L. Norcross.**
**1999.** Spatial and temporal variability in the diet of juvenile Pacific herring (*Clupea pallasi*) in Prince William Sound, Alaska. Can. J. Zool. 77:1–10

**Foy, R. J., and A. J. Paul.**
**1999.** Winter feeding and changes in somatic energy content for age-0 Pacific herring in Prince William Sound, Alaska. Trans. Am. Fish. Soc. 128:1193–1200.

**Gallego, A., and M. R. Heath.**
**1994.** The development of schooling behavior in Atlantic herring *Clupea harengus*. J. Fish. Biol. 45:569–588.

**Gunderson, R. D.**
**1993.** Surveys of fisheries resources. John Wiley and Sons, Inc., New York, NY, 248 p.

**Hatch, S. A., and G. A. Sanger.**
**1992.** Puffins as samplers of juvenile pollock and other forage fish in the Gulf of Alaska. Mar. Ecol. Prog. Ser. 80:1–14.

**Huse, I., and E. Ona.**
**1996.** Tilt angle distribution and swimming speed of overwintering Norwegian spring spawning herring. ICES J. Mar. Sci. 53:863–873.

**Iles T.D., and M. Sinclair.**
**1982.** Atlantic herring: stock discreteness and abundance. Science (Wash. D.C.) 215:627–633.

**Livingston, P. A.**
**1993.** Importance of predation by groundfish, marine mammals and birds on walleye pollock *Theragra chalcogramma* and Pacific herring *Clupea pallasi* in the eastern Bering Sea. Mar. Ecol. Prog. Ser. 102:205–215.

**MacLennan, D. N., and E. J. Simmonds.**
**1992.** Fisheries acoustics. Chapman and Hall, London, 325 p.

**McClatchie, S., J. Alsop, and R. F. Coombs.**
**1996.** A re-evaluation of relationships between fish size, acoustic frequency, and target strength. ICES J. Mar. Sci. 53:780–791.

**Meyers, T. R., S. Short, K. Lipson, W. N. Batts, J. R. Winton, J. Wilcock, and E. Brown.**
**1994.** Association of viral hermorrhagic septicemia virus with epizootic hemorrhages of the skin in Pacific herring *Clupea harengus pallasi* from Prince William Sound and Kodiak Island, Alaska, USA. Dis. Aquat. Org. 19:27–37.

**Misund, O. A.**
**1997.** Underwater acoustics in marine fisheries and fisheries research. Rev. Fish. Biol. Fish. 7:1–34.

**Misund, O. A., A. Aglen, and E. Fronaes.**
**1995.** Mapping the shape, size, and density of fish schools by echo integration and a high-resolution sonar. ICES J. Mar. Sci. 52:11–20.

**Misund, O. A., A. Ferno, T. Pitcher, and B. Totland.**
**1998.** Tracking herring schools with a high resolution sonar. Variations in horizontal area and relative echo intensity. ICES J. Mar. Sci. 55:58–66.

**Ona, E., and R. B. Mitson.**
**1996.** Acoustic sampling and signal processing near the seabed: the deadzone revisited. ICES J. Mar. Sci. 53:677–690.

**Paine R.T., J. L. Ruesink, A. Sun, E. L. Soulanille, M. J. Wonham, C. D. G. Harley, D. R. Brumbaugh, and D. L. Secord.**
**1996.** Trouble on oiled waters: lessons from the *Exxon Valdez* oil spill. Annu. Rev. Ecol. Syst. 27:197–235.

**Paul, A. J., and J. M. Paul.**
**1998.** Comparisons of whole body energy content of captive fasting age zero Alaskan Pacific herring (*Clupea pallasi* Valenciennes 1847) and cohorts over-wintering in nature. J. Exp. Mar. Biol. Ecol. 226:75–86.

**Paul, A. J., J. M. Paul, and E. D. Brown.**
**1998.** Fall and spring somatic energy content for Alaskan Pacific herring (*Clupea pallasi* Valenciennes 1847) relative to age, size and sex. J. Exp. Mar. Biol. Ecol. 223:133–142.

**Pitcher, T. J.**
**1986.** Functions of shoaling behavior in teleosts. *In* The behavior of teleost fishes (T. J. Pitcher, ed.) p. 294–338. Johns hopkins Univ. Press, Baltimore, MD, 553 p.

**Pitcher, T. J., and B. L. Partridge.**
**1979.** Fish school density and volume. Mar. Biol. 54:383–394.

**Robinson, C. J.**
**1995.** Food competition in a shoal of herring: the role of hunger. Mar. Behav. Physiol. 24:237–242.

**Robinson., C. J., and T. J. Pitcher.**
**1989.** Hunger motivation as a promoter of different behaviors within a shoal of herring: selection for homogeneity in fish shoal? J. Fish. Biol. 35:459–460.

**Rose, G. A., and W. C. Leggett.**
**1988.** Hydroacoustic signal classification of fish schools by species. Can. J. Fish. Aquat. Sci. 45:597–604.

**Sinclair, M.**
**1988.** Marine populations: an essay on population regulation and speciation. Washington Sea Grant Program, Univ. Washington Press, Seattle, WA, 252 p.

**Sinclair, M., V. C. Anthony, T. D. Iles, and R. N. O'Boyle.**
**1985.** Stock assessment problems in Atlantic herring (*Clupea harengus*) in the Northwest Atlantic. Can. J. Fish. Aquat. Sci. 42:888–898.

**Sokal, R. R., and F. J. Rohlf.**
**1981.** Biometry, 2nd ed. H. Freeman, San Francisco, CA, 859 p.

**Stokesbury, K. D. E., R. J. Foy, and B. L. Norcross.**
**1999.** Spatial and temporal variability in juvenile Pacific herring, *Clupea pallasi*, growth in Prince William Sound, Alaska. Environ. Biol. Fish. 56:409–418.

**Thorne, R. E.**
**1977.** A new digital hydroacoustic data processor and some observations on herring in Alaska. J. Fish. Res. Board Can. 34:2288–2294.
**1983a.** Assessment of population abundance by hydroacoustics. Biol. Oceanog. 2:253–262.
**1983b.** Hydroacoustics. *In* Fisheries techniques (L. A. Nielsen and D. L. Johnson, eds.), p. 239–259. Am. Fish. Soc., Bethesda, MD, 468 p.

**Thorne, R. E., and G. L. Thomas.**
**1990.** Acoustic observations of gas bubble release by Pacific herring (*Clupea harengus pallasi*). Can. J. Fish. Aquat. Sci. 47:1920–1928.

# A method for estimating dredge catching efficiency for blue crabs, *Callinectes sapidus*, in Chesapeake Bay

**Jon H. Vølstad**
Versar, Inc.
9200 Rumsey Road
Columbia, Maryland 21045
E-mail address: Volstadjon@versar.com

**Alexei F. Sharov**
Maryland Department of Natural Resources
Tawes State Office Building B-2
580 Taylor Avenue
Annapolis, Maryland 21401

**Glenn Davis**

**Brenda Davis**
Maryland Department of Natural Resources
301 Marine Academy Drive
Stevensville, Maryland 21666

**Abstract.**—A winter dredge survey of blue crab (*Callinectes sapidus* Rathbun) is conducted annually in Chesapeake Bay as a key element of a long-term, bay-wide population dynamics study. Removal experiments are performed routinely as part of this stratified random survey of the blue crab population. We present a method for estimating the catching efficiency of the standard Virginia crab dredge used in the winter survey. Data from 88 experiments conducted between November 1992 and March 1995 were analyzed; up to 10 removals were completed in each experiment. Two models were used to estimate catching efficiency for each experiment: 1) the Leslie model, and 2) a log-linear model in which it is assumed that a fixed proportion of crabs is removed in each sweep of the experimental area, allowing for an error term $\varepsilon$. We estimated the catchability coefficient ($\bar{q}$) as a weighted mean of the point estimates from each experiment; its standard error was estimated with the jackknife method. The average catchability coefficients across years were 0.16 (SE=0.01) for model 1, and 0.15 (SE=0.02) for model 2. There were no significant differences in yearly estimates of dredge efficiency for the period investigated in our study. We show how the estimated catching efficiency can be used to calibrate catch per unit of effort in a dredge survey. The precision of estimates of absolute abundance could be improved significantly by increasing the precision of the estimates of catchability. Similar improvements of estimates of absolute abundance are expected for analogous dredging surveys of slow-moving or sedentary benthic species buried in the sediment, such as scallops and clams.

Manuscript accepted 29 November 1999.
Fish. Bull. 98:410–420 (2000).

Stratified random dredge surveys have been conducted in Chesapeake Bay yearly since 1989 during the coldest winter months to estimate abundance and other key statistics for the blue crab (*Callinectes sapidus* Rathbun). The survey design implemented during the winter of 1992–1993 became the standard. Three geographic strata were sampled every year thereafter: upper bay and rivers (61% of the total area), middle bay (27% of the total area), and lower bay (12% of the total area). The number of randomly selected stations in each stratum was proportional to the area of the stratum. The strata were designed to encompass major areas of habitat and to account for differences in spatial distribution of crabs by size and sex. Details of the design of the Chesapeake Bay blue crab winter survey, its characteristics, and history can be found in Vølstad et al.[1] and Rothschild and Sharov.[2] Survey results indicated that the distribution of blue crabs is highly patchy, and the coefficient of variation (CV) of average crab density is usually large. Nevertheless, catch per unit of effort (CPUE) from the annual dredge surveys generally provides accurate estimates of relative abundance because of efficient stratification and large sample sizes.

[1] Vølstad, J. H., B. J. Rothschild, and T. Maurer. 1994. Abundance estimation and population dynamics of the blue crab in the Chesapeake Bay. Ref. No. UMCEES [CBL] 94-014. Final report to the Maryland Department of Natural Resources, the Chesapeake Bay Stock Assessment Committee, and the National Oceanic and Atmospheric Administration (NOAA). Chesapeake Biological Laboratory, P.O. Box 38, Solomons, MD 21236.

[2] Rothschild, B. J., and A. F. Sharov. 1997. Abundance estimation and population dynamics of the blue crab in the Chesapeake Bay. Final report to the Maryland Department of Natural Resources and Chesapeake Bay Stock Assessment Committee. Center for Marine Science and Technology, University of Massachusetts, North Dartmouth, MA 02747-2300.

Accurate estimates of absolute abundance and population characteristics over time provide a means of ensuring a sustainable harvest of the Chesapeake Bay blue crab stock. CPUE must be adjusted for the dredge catching efficiency to estimate absolute abundance from the survey data. Catching efficiency (i.e. the fraction of crabs present in the path of the dredge that is captured) can be estimated from removal experiments (e.g. Seber, 1973; Ricker, 1975; Hilborn and Walters, 1992). In such experiments, a closed population is sampled repeatedly over a relatively short time. An estimate of the catching efficiency is typically based on the slope of a linear regression of CPUE on cumulative catch (Leslie and Davis 1939), or on log-transformed CPUE and cumulative effort (Delury, 1947). It is assumed that no emigration, immigration, or natural mortality occurs during the experiment and that all animals caught are not returned to the population (Otis et al., 1978; Schnute, 1983).

During the summer months, blue crabs are active swimmers; therefore, an otter trawl is more effective for sampling. Estimates of absolute abundance, however, are difficult to obtain during the summer. First, trawling at random locations may be difficult because of the presence of crab pots and trotlines throughout Chesapeake Bay. Second, the catching efficiency of trawls is difficult to estimate because it is affected by the swimming behavior of blue crabs. The key assumption for estimating catching efficiency of a closed population is likely to be violated in depletion experiments conducted with an otter trawl in small geographic areas because of migration.

Blue crabs in Chesapeake Bay are largely inactive and bury themselves in the bottom sediment from November through March (Van Engel, 1958); thus, they are less likely to escape the dredge by swimming. Orth and van Montfrans (1987) reported negligible catches in bottom trawls during winter, further supporting the premise that crabs are buried in the substrate. Blue crabs captured in removal experiments showed little signs of mobility when brought aboard the vessel. We, therefore, believe that the assumption of a closed population is fairly well met during the short time span of each experiment in winter. Also, fishing activity is at a minimum during winter; only crabs in the Virginia mainstem of the bay are harvested.

We report on the catching efficiency of the sampling dredge estimated from multiple removal experiments in the blue crab survey. We demonstrate that catchability estimates from a single or a few removal experiments will not be reliable for the entire bay. We show how the estimated catchability can be used to calibrate the relative estimate of abundance from the survey.

## Material and methods

### Removal experiments

Maryland Department of Natural Resources (MDNR), Chesapeake Biological Laboratory (CBL), and Virginia Institute of Marine Science (VIMS) conducted 88 removal experiments between November 1992 and March 1995 using the standard 1.83-m wide Virginia sampling dredge. The dredge was lined with either 12.7-mm hexagonal chicken wire or nylon mesh and is assumed to have "knife edged" selectivity for crabs with a carapace width (CW) of at least 15 mm (Sulkin and Miller, 1975).

Depletion experiments generally were conducted at locations that represent the variations in depth and sediment type typical of Chesapeake Bay (Fig. 1), taking into account up-to-date survey data. It is impractical to select sites for depletion experiments randomly because blue crabs have a patchy distribution, and the annual baywide dredge survey generally has a large number of zero catches. Because of cost considerations, removal experiments were conducted each year at a random subset of survey stations with positive catches.

Removal experiments were conducted within an area of approximately 100 m by 5.5 m in Maryland waters and 100 m by 9 m in Virginia waters. In both cases experimental areas were marked with buoys. Each removal from the experimental area (coverage) consisted of three (CBL and MDNR) or five (VIMS) parallel, nonoverlapping dredge tows conducted back and forth (Fig. 2) at a standard towing speed of 3 knots. A maximum of 10 removals was completed for each depletion experiment. The unit of effort was one coverage (i.e. the combined 3 or 5 hauls required to sweep the experimental area), and catch was recorded as the total number of crabs caught per coverage.

### Estimating catchability

Hirst (1994) formulated the following standard assumptions for the removal method: 1) there is no immigration to or emigration from the enclosed area during the removal experiments; 2) each animal has an equal probability of being caught; 3) each removal is equally efficient (i.e. the probability of capture for each animal is constant from one removal to the next). The first of these assumptions is reasonable because crabs are largely inactive during winter, and each depletion experiment is conducted over a short time (2 to 4 hours). The latter two assumptions may be less likely to be true because crabs generally are clustered in distribution. In marine surveys the sampling unit is typically a fixed volume, or a unit

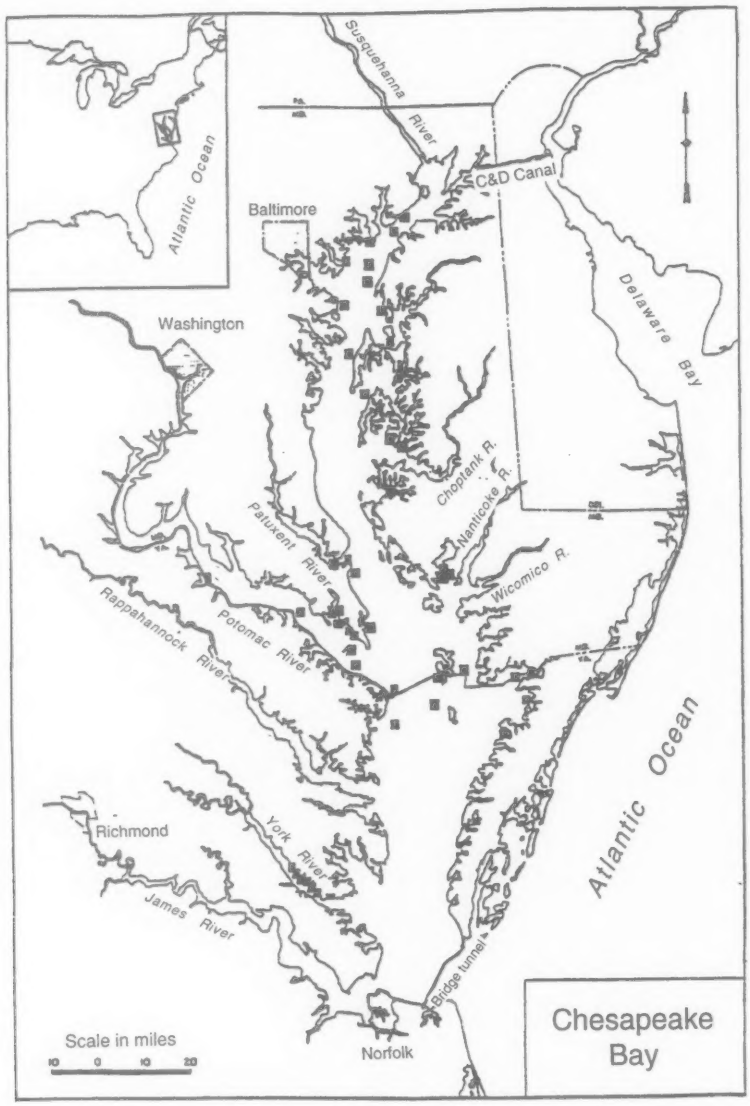


**Figure 1**

Map of Chesapeake Bay with positions of the dredge efficiency experiments conducted between November 1992 and March 1995.

of area swept by a standard tow (see Pennington and Vølstad, 1994). As a result, sampling individuals randomly from the target population generally is not feasible. The possible dependence of animal capture probability on environmental conditions, or on the characteristics of individual animals, such as body size, is another important practical problem.

In our study we assumed that each crab has an equal probability of being caught by the dredge within each experimental area. The catching efficiency of the dredge, however, may vary significantly between experimental sites because of different bottom topography and sediment types. The possible effect of body size on catching efficiency was evaluated by comparing mean carapace width and size-frequency distributions between removals. Assume, for example, that large crabs have a higher probability of capture than small crabs. In this case the mean cara-

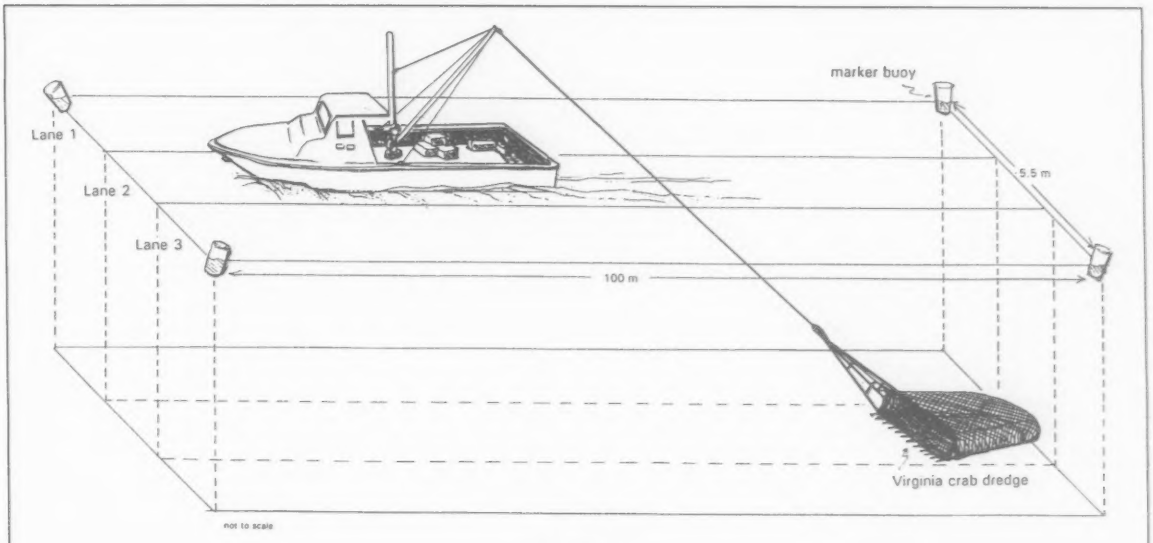


**Figure 2**

Schematic diagram of a standard removal experiment conducted in Maryland waters. Each removal from the area (coverage) consisted of three parallel tows conducted back and forth at a speed of 3 knots. A maximum of ten removals was completed for each experiment.

pace width of crabs in the first removals would, on average, be larger than in the final removals.

We used two models to estimate the dredge efficiency for each experiment. Model 1 is a standard Leslie model (Leslie and Davis, 1939)

$$y_i = q[P_0 - K_{i-1}] = qP_0 - qK_{i-1}, \quad (1)$$

where $y_i$ = the catch from the $i$th removal; and
$K_{i-1}$ = cumulative catch taken before each removal;
$P_0$ = the initial population in the area before the depletion experiment.

The catchability coefficient $q$ = the slope of the linear regression estimated from Equation 1. The basic assumption of this model is that the number of crabs in each removal and the unit of effort is measured without error. An implication of using model 1 is that if the $i$th removal in a particular depletion experiment is zero, then the cumulative catch provides an absolute measure of the initial population $P_0$. Some crabs, however, may remain in the experimental area, even though no crabs are caught in an individual removal. This results in an underestimate of $P_0$ and an overestimate of $q$ for this site.

A different technique may be used to estimate dredge efficiency. For each coverage ($i$) of the experimental area, we can assume that a fixed proportion ($q$) of the true population in the area is removed; therefore, the catch ($y_1$) in the first coverage is $q$ multiplied by $P_0$, the initial population. For the $i$th coverage, we have

$$y_i = q(1-q)^{i-1}P_0\varepsilon$$

and

$$\ln(y_i) = \ln(q) + \ln(P_0) + [\ln(1-q)](i-1) + \ln(\varepsilon). \quad (2)$$

In this model, it is assumed (perhaps more realistically) that the fraction of the population removed for each unit of effort is estimated with an error $\varepsilon$. A simple regression of $\ln y_i$ against $(i-1)$ provides an estimate of the slope, $\ln(1-q)$. An estimate of the expected value of the catchability coefficient ($q$) is obtained after a retransformation, following the method of Finney (1941; see also Johnson et al., 1994, p. 221). The variance of the slope estimate in model 2 is taken into account in the estimation of $(1-q)$, and hence $q$. An approximation for estimating $q$ for a single experiment is

$$\hat{q} = 1 - \exp\left(\hat{\beta} + s^2_{\hat{\beta}}/2\right)$$

where $\hat{\beta}$ = an estimate of the slope in Equation 2, with variance $S^2_{\hat{\beta}}$ (Gilbert 1987).

Characteristically, blue crabs have a patchy distribution, and the estimated CPUE from the dredge survey is driven by relatively few large catches. To estimate a mean catchability coefficient that is applicable to the entire survey area, estimates of catchability from each removal experiment were weighted by the abundance in the experimental area. An estimator for the overall catchability coefficient to use for calibrating CPUE in the dredge survey is

$$\bar{q} = \sum \frac{c_i q_i}{C},$$

where $c_i$ = the total number of crabs caught in the $i$th experiment;
$q_i$ = the corresponding estimated gear efficiency; and
$C$ = total number of crabs caught in the $n$ experiments.

Because $n$ is small within each year, the jackknife estimate of average gear efficiency and its standard error were used (Cochran, 1977; Efron and Gong, 1983). The jackknife estimator of standard error is

$$\hat{\sigma} = \left\{ [(n-1)/n] \sum (\theta_{(i)} - \theta_{(.)})^2 \right\}^{\frac{1}{2}},$$

where

$$\theta_{(i)} = \sum_{i \neq j} \frac{c_i q_i}{(C - c_j)}$$

is the weighted mean catchability deleting the $n$th experiment and

$$\theta_{(\bullet)} = \sum \frac{\theta_{(i)}}{n}$$

is the jackknife estimate of $\bar{q}$ for the $n$ experiments.

For model 2 we also estimated the weighted mean and variance of the slopes from all $n$ experiments. An estimate of $q$ was obtained after retransformation with the method of Finney (1941); the standard error was estimated by jackknifing (Tukey, 1958; Manly, 1997).

In the annual winter dredge survey, a one-minute tow is standard. For soft sediments, the dredge may be saturated before the tow is completed. A randomized block experiment was conducted during the winter of 1992–1993 to investigate such gear-saturation effects on CPUE. Double tows were made at 77 randomly selected stations in the Maryland part of the bay. One tow of one-minute duration and one tow of 30-seconds duration were taken in random order at each station.

During the winter of 1994–1995, the chicken wire liner of the dredge was replaced with nylon mesh because the latter proved to be easier to operate and repair. To investigate any effect of the new liner on the catchability coefficient estimate, we conducted 9 removal experiments using a dredge with a chicken wire liner and 10 experiments using a dredge with a nylon liner.

### Using the estimated catchability to calibrate CPUE

If $r$ is the true blue crab density (number of crabs per $m^2$) in Chesapeake Bay at the time of the winter survey, and if we have an approximately unbiased estimate of the overall catching efficiency $q$ that is uncorrelated with CPUE, an estimator for blue crab density is then

$$\hat{r} = CPUE / \hat{q},$$

where CPUE = the estimated mean number of crabs caught per $m^2$ swept.

A baywide estimate of the population total $\tau$ is

$$\hat{\tau} = A\hat{r},$$

where $A$ = the area of blue crab habitat in Chesapeake Bay, which we estimated using geographic information system (GIS) to be approximately 11,000 $km^2$.

Using Taylor series approximations, we estimated the variance of $\hat{\tau}$ (Thompson, 1992, p 168) as

$$\mathrm{var}(\hat{\tau}) = \frac{A^2}{\hat{q}^2}\left[ \hat{\mathrm{var}}(\bar{y}) + \frac{(1-\hat{q})}{\hat{q}} \bar{y} + \frac{\bar{y}^2}{\hat{q}^2} \hat{\mathrm{var}}(\hat{q}) \right],$$

where $\bar{y}$ = the estimated CPUE.

The relative precision of $\hat{\tau}$ is $k = \sqrt{\mathrm{var}}(\hat{\tau}) / \hat{\tau}$. The variance of estimated catching efficiency thus adds to the variance of absolute abundance estimates.

If sampling fractions differ between strata, the absolute abundance can be estimated separately for each stratum. Here, $\hat{q}$, CPUE, and hence $\hat{\tau}$ can be estimated by stratum, by using the same approach as above. The size of each stratum must also be known. If the sampling in each stratum is independent, the variance in the combined estimate of absolute abundance is additive. This approach would also be appro-

priate if the density of depletion experiments was higher for some strata than for others.

## Results

### Catching efficiency

Estimates of catching efficiency for the standard Virginia crab dredge from individual depletion experiments conducted during the winters between November 1992 and March 1995 are presented in Tables 1 through 3. There was large variation in catchability estimates among individual experiments (from –0.13 to 0.45); however, the difference among average annual catchability coefficients for the entire survey area was small; $\bar{q}$ varied from 0.13 to 0.18 for model 1 and model 2 (Fig. 3). For both depletion models, an analysis of variance revealed that yearly differences in $q$ are not significant (ANOVA, $P>0.3$; we used a significance level of 5% for all tests in our study). Experiments from all years, therefore, were pooled to estimate an overall catchability coefficient for the dredge survey. The weighted mean catchability coefficients were 0.16 (SE=0.01) for model 1 (Eq. 1), and 0.15 (SE=0.02) for model 2 (Eq. 2). The means and standard errors were estimated by using the jackknife method; catchability coefficients from individual experiments were assumed to be independent. The two methods for estimating a mean catchability coefficient for model 2 produced identical estimates. The difference in estimates from the two models was not significant.

Mean carapace width of crabs in each removal for all years combined, which is plotted in Figure 4, did not show any significant trend (nonparametric Mann-Kendall test (Gilbert, 1987), $n=10$, $P=0.19$). Further, the size-frequency distributions of crabs for individual removals were similar (Fig. 5). These results support our assumption that probability of capture is independent of carapace width.

Our test for gear saturation effects resulted in an average catch per minute of 3.7 (SE=0.8) for the half-minute tows, and of 2.3 (SE=0.7) for the 1-minute tows. The higher CPUE for half-minute tows, although not significant, suggests saturation effects and might be explained by the period of time that the dredge continues to be towed along the bottom after it has begun to be hauled back. Such a delay would affect shorter tows more than longer tows.

For the experiments on the effect of the dredge liner, estimates of mean $q$ for the dredge lined with chicken wire were 0.17 (SE=0.02) based on model 1, and 0.15 (SE=0.03) for model 2. For the nylon liner the estimates were 0.22 (SE=0.03) based on model 1, and 0.21 (SE=0.03) for model 2. Means and standard errors were estimated by using the jackknife method. The results indicated that nylon has a higher catching efficiency, but the difference in catchability between the two liners was not significant (ANOVA, $P>0.54$). Results from all 88 experiments combined showed no significant difference in catching efficiency between liners. The jackknife estimates of mean catchability across years for the

**Table 1**

Estimates of dredge efficiency ($\hat{q}$) from depletion experiments carried out during the winter of 1992–1993, with coefficients of determination ($r^2$) and degrees of freedom (df) for the regressions. The jackknife estimates of average $\hat{q}$ for the entire survey area were 0.13 (SE=0.02) for model 1, and 0.13 (SE=0.03) for model 2. CBL = Chesapeake Bay Laboratory; MDNR = Maryland Department of Natural Resources; and VIMS = Virginia Institute of Marine Science.

| | | Model 1 | | Model 2 | | |
|---|---|---|---|---|---|---|
| Institution | Number of crabs | $\hat{q}$ | $r^2$ | $\hat{q}$ | $r^2$ | df |
| CBL[1] | 88 | 0.13 | 0.58 | 0.10 | 0.38 | 9 |
| | 327 | 0.06 | 0.30 | 0.06 | 0.31 | 9 |
| | 67 | 0.07 | 0.18 | 0.08 | 0.22 | 9 |
| | 23 | 0.13 | 0.39 | 0.06 | 0.39 | 8 |
| | 121 | 0.14 | 0.51 | 0.18 | 0.56 | 9 |
| | 89 | 0.01 | 0.02 | 0.01 | 0.04 | 9 |
| | 180 | 0.10 | 0.42 | 0.09 | 0.37 | 9 |
| | 223 | 0.22 | 0.66 | 0.32 | 0.73 | 9 |
| | 59 | 0.30 | 0.65 | 0.38 | 0.36 | 9 |
| | 102 | 0.30 | 0.91 | 0.27 | 0.77 | 9 |
| | 267 | –0.01 | 0.00 | 0.03 | 0.03 | 9 |
| | 615 | 0.01 | 0.12 | –0.03 | 0.17 | 9 |
| | 106 | 0.12 | 0.55 | 0.17 | 0.62 | 9 |
| MDNR[1] | 368 | 0.20 | 0.60 | 0.20 | 0.61 | 5 |
| | 137 | –0.10 | 0.15 | –0.11 | 0.14 | 5 |
| | 190 | 0.14 | 0.61 | 0.16 | 0.66 | 5 |
| | 203 | 0.23 | 0.83 | 0.31 | 0.85 | 5 |
| | 60 | 0.08 | 0.13 | 0.07 | 0.09 | 5 |
| | 109 | 0.17 | 0.24 | 0.11 | 0.11 | 5 |
| | 154 | 0.13 | 0.47 | 0.13 | 0.30 | 5 |
| | 96 | 0.11 | 0.29 | 0.11 | 0.29 | 5 |
| | 311 | 0.14 | 0.85 | 0.16 | 0.85 | 9 |
| | 312 | 0.22 | 0.41 | 0.24 | 0.48 | 4 |
| VIMS[2] | 139 | 0.24 | 0.88 | 0.22 | 0.85 | 4 |
| | 74 | 0.17 | 0.32 | 0.20 | 0.19 | 4 |
| | 129 | 0.17 | 0.71 | 0.16 | 0.55 | 4 |
| | 193 | 0.18 | 0.63 | 0.17 | 0.44 | 9 |
| | 132 | 0.20 | 0.31 | 0.20 | 0.34 | 4 |
| | 161 | 0.09 | 0.18 | 0.09 | 0.52 | 4 |

[1] Chicken wire liner used.
[2] Nylon mesh liner used.

**Table 2**

Estimates of dredge efficiency ($\hat{q}$) from depletion experiments carried out during the winter of 1993–1994, with coefficients of determination ($r^2$) and degrees of freedom (df) for the regressions. The jackknife estimates of average $\hat{q}$ for the entire survey area were 0.18 (SE=0.02) for model 1 and 0.18 (SE=0.02) for model 2. CBL = Chesapeake Bay Laboratory; MDNR = Maryland Department of Natural Resources; and VIMS = Virginia Institute of Marine Studies.

| | | Model 1 | | Model 2 | | |
|---|---|---|---|---|---|---|
| Institution | Number of crabs | $\hat{q}$ | $r^2$ | $\hat{q}$ | $r^2$ | df |
| CBL[1] | 100 | 0.37 | 0.84 | 0.24 | 0.48 | 5 |
| | 118 | 0.05 | 0.11 | 0.05 | 0.12 | 5 |
| | 78 | 0.27 | 0.76 | 0.30 | 0.72 | 5 |
| | 55 | 0.09 | 0.55 | 0.10 | 0.59 | 5 |
| | 83 | 0.41 | 0.88 | 0.35 | 0.59 | 4 |
| | 11 | 0.40 | 0.89 | 0.23 | 0.60 | 3 |
| | 52 | 0.35 | 0.79 | 0.34 | 0.78 | 5 |
| | 34 | 0.39 | 0.85 | 0.43 | 0.86 | 5 |
| | 20 | 0.32 | 0.37 | 0.36 | 0.39 | 3 |
| | 92 | 0.13 | 0.64 | 0.13 | 0.68 | 5 |
| | 321 | 0.25 | 0.57 | 0.38 | 0.73 | 5 |
| MDNR[1] | 35 | 0.23 | 0.60 | 0.17 | 0.48 | 9 |
| | 89 | 0.27 | 0.65 | 0.18 | 0.31 | 9 |
| | 219 | 0.13 | 0.38 | 0.11 | 0.12 | 9 |
| | 145 | 0.12 | 0.64 | 0.14 | 0.59 | 9 |
| | 96 | 0.17 | 0.44 | 0.16 | 0.30 | 9 |
| | 48 | 0.30 | 0.81 | 0.28 | 0.59 | 7 |
| VIMS[2] | 376 | 0.22 | 0.71 | 0.19 | 0.73 | 8 |
| | 232 | 0.34 | 0.89 | 0.35 | 0.77 | 7 |
| | 110 | 0.13 | 0.62 | 0.17 | 0.41 | 8 |
| | 133 | 0.02 | 0.02 | –0.04 | 0.08 | 8 |
| | 188 | 0.03 | 0.02 | 0.04 | 0.02 | 8 |
| | 244 | 0.13 | 0.79 | 0.14 | 0.64 | 8 |
| | 174 | 0.12 | 0.64 | 0.14 | 0.71 | 8 |
| | 346 | 0.10 | 0.31 | 0.14 | 0.43 | 8 |

[1] Chicken wire liner used.
[2] Nylon mesh liner used.

**Table 3**

Estimates of dredge efficiency ($\hat{q}$) from depletion experiments carried out during the winter 1994–1995, with coefficients of determination ($r^2$) and degrees of freedom (df) for the regressions. The jackknife estimates of average $\hat{q}$ for the entire survey area were 0.18 (SE=0.02) for model 1 and 0.14 (SE=-0.03) for model 2. CBL = Chesapeake Bay Laboratory; MDNR = Maryland Department of Natural Resources; and VIMS = Virginia Institute of Marine Studies.

| | | Model 1 | | Model 2 | | |
|---|---|---|---|---|---|---|
| Institution | Number of crabs | $\hat{q}$ | $r^2$ | $\hat{q}$ | $r^2$ | df |
| CBL[1] | 72 | 0.12 | 0.49 | 0.16 | 0.48 | 9 |
| | 29 | 0.21 | 0.34 | 0.28 | 0.48 | 5 |
| | 48 | 0.26 | 0.55 | 0.06 | 0.06 | 9 |
| | 99 | 0.12 | 0.42 | 0.06 | 0.13 | 9 |
| | 67 | 0.19 | 0.57 | 0.18 | 0.44 | 9 |
| | 63 | 0.28 | 0.84 | 0.22 | 0.77 | 9 |
| | 66 | 0.12 | 0.48 | 0.18 | 0.61 | 9 |
| | 40 | 0.13 | 0.39 | 0.13 | 0.41 | 9 |
| | 9 | 0.30 | 0.70 | 0.27 | 0.74 | 4 |
| CBL[2] | 83 | 0.31 | 0.96 | 0.35 | 0.94 | 7 |
| | 55 | 0.20 | 0.69 | 0.24 | 0.73 | 9 |
| | 28 | 0.16 | 0.26 | 0.24 | 0.41 | 5 |
| | 54 | 0.22 | 0.77 | 0.15 | 0.40 | 9 |
| | 12 | 0.22 | 0.60 | 0.08 | 0.30 | 9 |
| | 67 | 0.16 | 0.46 | 0.12 | 0.23 | 9 |
| | 66 | 0.30 | 0.84 | 0.26 | 0.74 | 9 |
| | 92 | 0.11 | 0.64 | 0.17 | 0.51 | 9 |
| | 58 | 0.23 | 0.68 | 0.13 | 0.29 | 9 |
| | 11 | 0.32 | 0.60 | 0.32 | 0.76 | 9 |
| MDNR[2] | 207 | 0.16 | 0.31 | 0.11 | 0.16 | 5 |
| | 151 | 0.22 | 0.42 | 0.19 | 0.48 | 5 |
| | 127 | 0.26 | 0.68 | 0.22 | 0.50 | 5 |
| | 145 | 0.22 | 0.83 | 0.21 | 0.69 | 5 |
| | 61 | 0.38 | 0.86 | 0.55 | 0.86 | 4 |
| | 64 | 0.45 | 0.93 | 0.33 | 0.64 | 5 |
| | 23 | 0.36 | 0.96 | 0.38 | 0.94 | 5 |
| VIMS[2] | 113 | 0.04 | 0.07 | 0.07 | 0.12 | 5 |
| | 114 | 0.11 | 0.79 | 0.11 | 0.81 | 5 |
| | 139 | 0.23 | 0.89 | 0.18 | 0.80 | 5 |
| | 121 | 0.15 | 0.24 | 0.13 | 0.12 | 5 |
| | 185 | 0.24 | 0.16 | –0.13 | 0.11 | 5 |
| | 107 | 0.07 | 0.35 | 0.05 | 0.20 | 5 |
| | 167 | 0.03 | 0.03 | 0.02 | 0.01 | 5 |
| | 103 | 0.04 | 0.05 | –0.10 | 0.19 | 5 |

[1] Chicken wire liner used.
[2] Nylon mesh liner used.

dredge lined with chicken wire were 0.16 (SE=0.02) for model 1, and 0.16 (SE=0.03) for model 2. For the nylon liner, estimates are 0.16 (SE=0.02) for model 1, and 0.13 (SE=0.02) for model 2.

### An estimate of absolute abundance

A stratified random sample of 1412 stations was taken in the Chesapeake Bay during the winter of 1994–1995 (Rothschild and Sharov[2]). At each station, the standard Virginia crab dredge was towed for 1 minute at 3 knots. The sampling intensity was equal in all three geographic strata. The estimated baywide mean number of crabs (CW ≥15 mm) caught per 1000 $m^2$ swept was $\bar{y}$ = 8.53 ($k$=0.07). For age group 1+ (CW ≥60 mm) the estimate was $\bar{y}$ = 3.75 ($k$=0.08). With the catchability coefficient $\bar{q}$ = 0.16 and standard error 0.01 (from model 1), the absolute abundance estimate

for blue crab with CW ≥15 mm was $\hat{\tau}_1$= $5.86\times10^8$ ($k$=0.09), and $2.58\times10^8$ ($k$=0.10) for crabs with CW≥60 mm. Using $\bar{q}$=0.15 with standard error 0.02 (from model 2), we estimated absolute abundance for crabs with CW ≥15 mm to be $\hat{\tau}_2$=$6.26\times10^8$ ($k$=0.15), and $2.75\times10^8$ ($k$=0.16) for crabs with CW ≥60 mm. To check plausibility of these estimates, we compared the absolute abundance estimates of the 1+ age group (CW 60 mm) with estimated total landings for 1995. Blue crabs of age 1+ reach harvestable size (127 mm) the following fishing season. The reported total landings in the commercial fishery were 17,820 metric tons (t). Using an average weight per crab of 150 g (Knotts[3]), we estimated the total number of crabs caught to be $1.19\times10^8$ and the exploitation coefficient (as a ratio of catch in numbers and number of age 1+ crabs) to be about 45%.

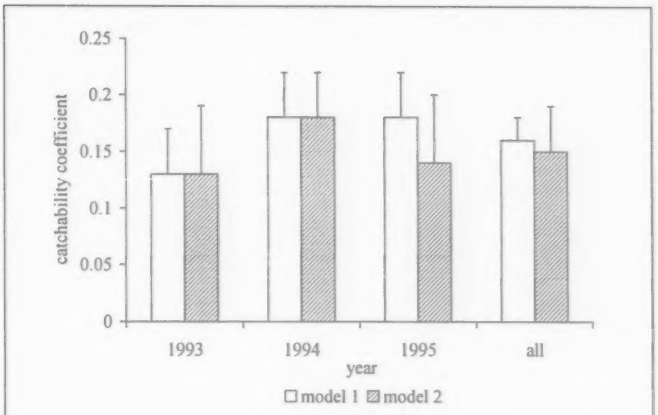


**Figure 3**

Jackknife estimates of average catchability ($\bar{q}$) by year for model 1 and model 2. The error-bars represent the half width of the confidence intervals.

Exploitation rates can be calculated for males and females separately in similar fashion by using mean CPUE and landings by sex. These rates may be very valuable information because there is an evident disproportion in crab landings by sex; on average more males are landed per year (at least by weight) than females (Rugolo et al., 1998a). For example, 9320 t of males and 7230 t of females were landed in Maryland in 1995. If the average weights of males and females in the catch were similar, the exploitation rate for males would be higher than that for females. However, uncorrected for catchability, the density of age 1+ males (2.31 per 1000 $m^2$) observed in 1995 was higher than that of age 1+ females (1.44 per 1000 $m^2$), suggesting that females are being exploited at a higher rate. To obtain precise estimates of sex-specific exploitation rates, data on mean weight of crabs by sex in the harvest are required but are not available.

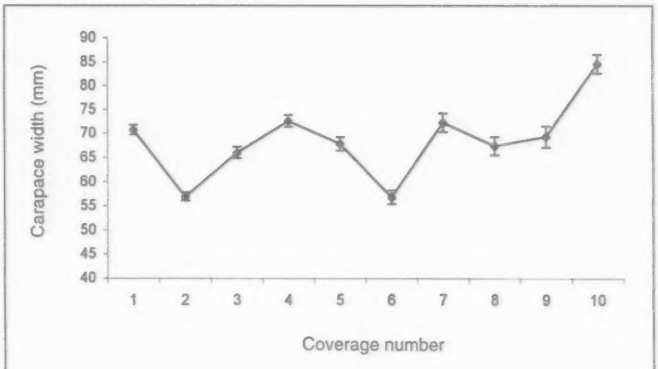


**Figure 4**

Mean carapace width for blue crabs by coverage in the Maryland depletion experiments. Data from all years are combined.

## Discussion

Our method for estimating overall dredge catching efficiency provides consistent estimates over time (Fig. 3). The Leslie model produces the most precise estimate for catching efficiency, but the estimate could be slightly biased upwards if measurement error in effort occurs. In practice, given that the standard unit of effort in the depletion experiments is one complete coverage of the closed area, the three to five tows forming a coverage may partially overlap or extend outside the area because of navigational errors or effects of bottom currents. This measurement error in catch or effort inflates the average catchability coefficient estimates from the Leslie model (Gould et al., 1997). For model 2, the estimate of $q$ for individual experiments depends on the regression slope and its variance and will decrease with increasing variance. The method for estimating $q$ for individual experiments assumes that the distribution of the estimated slope tends toward normality; therefore estimates of based $q$ on model 2 could be biased at low sample sizes, but

[3] Knotts, K. S. 1989. Preliminary stock assessment of the Chesapeake Bay blue crab population. M.S. thesis, Univ. Maryland, College Park, MD, 206 p.

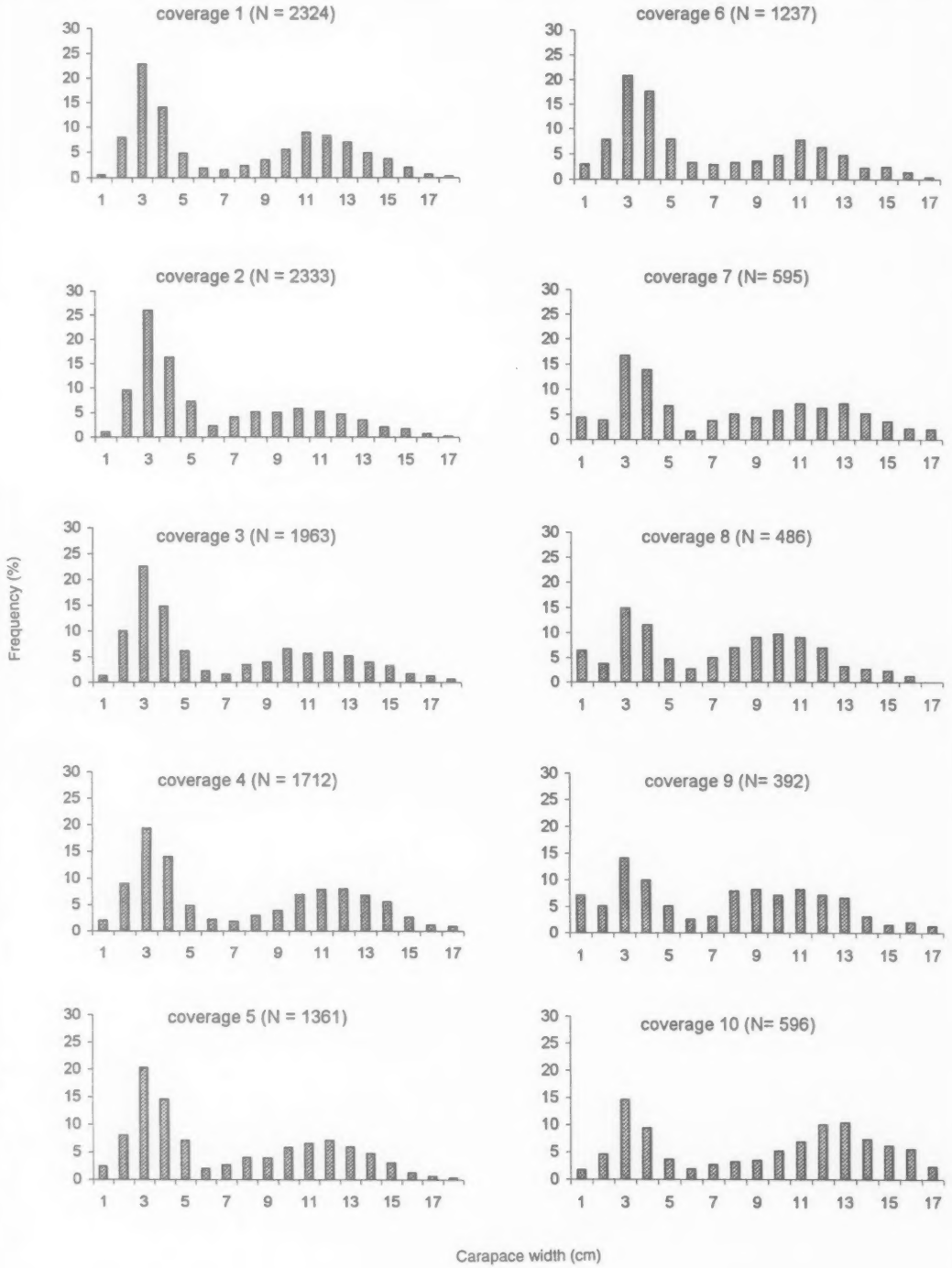
coverage 1 (N = 2324)
coverage 6 (N = 1237)
coverage 2 (N = 2333)
coverage 7 (N= 595)
coverage 3 (N = 1963)
coverage 8 (N = 486)
coverage 4 (N = 1712)
coverage 9 (N= 392)
coverage 5 (N = 1361)
coverage 10 (N= 596)
Frequency (%)
Carapace width (cm)

**Figure 5**

Carapace-width frequency distribution of blue crabs by coverage in Maryland depletion experiments. Data from all years are combined.

the identical estimates of $\bar{q}$ from the two alternative methods indicate that such bias is small.

Obtaining reasonable estimates of catching efficiency from catch-effort techniques requires depleting a substantial proportion (usually more than 30%) of the population (see Gould and Pollock, 1997). Also, estimates of the regression slopes, and hence $q$, are likely to be more accurate for both models if the independent variables (i.e. cumulative catch, $K_i$, or coverage, $i$) have a wider range. For the depletion experiments with ten removals conducted in Maryland waters, estimates of $q$ based on the first five removals were generally higher than estimates of $q$ based on all ten removals. Thus, fewer removals per experiment can bias the estimates of gear efficiency just as vessel effects can. In experiments conducted from two similar vessels in Maryland waters, we did not detect significant differences in catchability between vessels. Environmental factors probably were the principal cause of variability in catchability estimates from different experiments because sediment type, bottom topography, intensity and direction of the current, towing speed, and crab distribution influence dredge performance.

When our overall estimates of catching efficiency are used to adjust CPUE from the baywide winter survey, plausible estimates of absolute abundance of blue crab in the Chesapeake Bay are obtained, resulting in an estimated exploitation rate of about 45% in 1995. The catchability coefficient estimate ($q$=0.26) presented in Zhang et al. (1993), in contrast, would result in an estimated exploitation rate of 75%. Their method eliminated removal experiments with low coefficients of determination ($r^2$) for the regressions, or with negative catchability estimates, which could result in a positive bias in the estimated overall catchability.

We have not accounted for landings from the recreational fishery or for natural mortality in our example; therefore the above exploitation rates were probably underestimates. Recreational harvest data are very scarce, but limited surveys conducted by the Maryland Department of Natural Resources in 1983, 1988, and 1990 have indicated that recreational harvest represented approximately 79%, 50%, and 26% of the reported commercial harvest (Rugolo et al. 1998b). The 1990 survey is considered the most reliable of the three. Assuming that the recreational harvest in 1995 represented 26% of the commercial harvest, then the corrected estimate of total blue crab exploitation rate is 56.7%. A bias in the opposite direction would result if the exploitable part of the stock were underestimated because of recruitment during the fishing season.

The results of this study demonstrate that improved estimates of catching efficiency can substantially increase the accuracy of estimates of absolute abundance. In our example based on survey data from the winter 1994–1995, the variance in the absolute abundance estimate for the 1+ age group is driven by the variance in $\hat{q}$. Size of sampling locations in the Chesapeake Bay winter dredge survey for blue crabs have ranged between 877 and 1412 stations per year, and relative precision ($k$) of the estimated CPUE (i.e. its standard error divided by the mean) has been around 10% for most years. Because of the asymptotic properties of $k$, it would be prohibitively expensive to significantly increase the precision of absolute abundance estimates by increasing the sample size in the survey. We believe a more cost-effective way to increase the precision of estimates of absolute abundance would be to improve the estimate of catchability by increasing the number of depletion experiments. Our results show that an estimate of catching efficiency based on a single experiment or on a few removal experiments would not represent the entire bay accurately because catchability is highly variable among sites owing to differences in bottom conditions and other factors. We included all the depletion estimates of catchability in our study, including those less than zero. We assumed that point estimates of catchability are estimated with a random error that is normally distributed around a mean: estimates in the tails of the distribution could be substantially higher or lower than the true mean catchability. An accurate estimate of catching efficiency, applicable to the entire Chesapeake Bay, requires conducting a large number of depletion experiments at representative locations. Although no statistical differences were found among the annual catchability coefficient estimates for the years analyzed in our study, we caution that interannual variation in $q$ is likely. For example, an increase in water temperature during mild winters may affect crab behavior (they would cease hibernation) and hence probability of capture. We recommend, therefore, that depletion experiments be conducted yearly as part of an annual winter survey of blue crab population.

The conclusions of our study can be generalized and extended to similar resource assessment surveys of other slowly moving or sedentary bottom dwelling species with patchy distribution, such as scallops or clams. In surveys of target species, such as these, attention must be paid to variability in capture efficiency of the gear with respect to sediment type, depth, towing speed, and other factors (such as animal interactions) that affect the gear. Sediment or bottom type are often selected as stratification criteria in bottom surveys of benthic organisms. Properly designed removal experiments can provide reliable estimates of catchability coefficients for each sampling stratum, allowing adjustment of

strata CPUE used in the estimator of absolute abundance. Sediment distribution, however, is often very patchy, and the exact area on the bottom of any type of sediment is typically not known. Accurate mapping of bottom sediment is expensive and thus it makes sediment-based stratification impractical. An alternative approach for taking sediment into account is to conduct a series of depletion experiments at locations that are representative of the entire survey area. If a sufficient number of experiments are conducted, the effects of sediment on catching efficiency will be accounted for. Although we agree that efficient stratification is an important aspect of designing cost-effective marine resource surveys, we stress that careful estimation of sampling gear efficiency through a series of depletion experiments could significantly improve the accuracy of absolute abundance estimates. Both elements are essential in designing effective sample survey programs for estimating vital characteristics of a population.

## Acknowledgments

This project was funded by the National Oceanic and Atmospheric Administration (NOAA) and Maryland Department of Natural Resources. J. H. Vølstad and A. Sharov are grateful to B. Rothschild for providing us the opportunity to work on this project. We thank T. Maurer, E. Connor, and captains A. Moore and D. Pierce for assisting with the field work in Maryland waters. We thank R. Lipcius and M. Montain for their research cooperation and for providing the data from depletion experiments conducted in Virginia. We greatly appreciate suggestions from two anonymous referees that helped improve the manuscript.

## Literature cited

**Cochran W. G.**
**1977.** Sampling techniques. John Wiley and Sons, New York, NY, 428 p.

**DeLury, D. B.**
**1947.** On the estimation of biological populations. Biometrics 3:145–167.

**Efron, B., and G. Gong.**
**1983.** A leisurely look at the bootstrap, the jackknife and cross-validation. Am. Stat. 37:36–48.

**Finney, D. J.**
**1941.** On the distribution of a variate whose logarithm is normally distributed. J. Roy. Statist. Soc. (series B) 7:155–161.

**Gilbert, R. O.**
**1987.** Statistical methods for environmental pollution monitoring. Van Nostrand Reinhold, New York, NY, 320 p.

**Gould, W. R., and K. H. Pollock.**
**1997.** Catch-effort maximum likelihood estimation of important population parameters. Can. J. Fish. Aquat. Sci. 54: 890–897.

**Gould, W. R., L. A. Stefanski, and K. H. Pollock.**
**1997.** Effects of measurement error on catch-effort estimation. Can. J. Fish. Aquat. Sci. 54:898–906.

**Hilborn, R., and C. J. Walters.**
**1992.** Quantitative fisheries stock assessment. Chapman and Hall, New York, NY, 570 p.

**Hirst, D.**
**1994.** An improved removal method for estimating animal abundance. Biometrics 50:501–505.

**Johnson, N. L., S. Kotz, and N. Balakrishnan.**
**1994.** Continuous univariate distributions, vol. 1. John Wiley and Sons, New York, NY, 756 p.

**Leslie, P. H., and D. H. S. Davis.**
**1939.** An attempt to determine the absolute number of rats on a given area. J. Anim. Ecol. 8:94–113.

**Manly, B. F. J.**
**1997.** Randomization, bootstrap and Monte Carlo methods in biology. Chapman and Hall, New York, NY, 399 p.

**Orth, R. J., and J. van Montfrans.**
**1987.** Utilization of a seagrass meadow and tidal marsh creek by blue crabs, *Callinectes sapidus*. I. Seasonal and annual variation in abundance with emphasis on post-settlement juveniles. Mar. Ecol. Prog. Ser. 41:283–294.

**Otis, D. L, K.P Burnham, G. C. White, and D. R. Anderson.**
**1978.** Statistical inference from capture data on closed animal populations. Wildl. Monogr. 62. The Wildlife Society, Inc., Washington, D.C.

**Pennington, M., and J. H.Vølstad.**
**1994.** Assessing the effect of intra-haul correlation and variable density on estimates of population characteristics from trawl surveys. Biometrics. 50:725–732.

**Ricker, W. E.**
**1975.** Computation and interpretation of biological statistics of fish populations. Bull. Fish. Res. Board Can. 191.

**Rugolo, L. J., K. S. Knotts, A. M. Lange, and V. A.Crecco.**
**1998a.** Historical profile of the Chesapeake Bay blue crab (*Callinectes sapidus Rathbun*) fishery. J. Shellfish Res. 17(N2): 383–394.

**1998b.** Stock assessment of Chesapeake Bay blue crab (*Callinectes sapidus* Rathbun). J. Shellfish Res. 17 (N2): 493–518.

**Schnute, J.**
**1983.** A new approach to estimating populations by the removal method. Can. J. Fish. Aquat. Sci. 40:2153–2169.

**Seber G.A.**
**1973.** The estimation of animal abundance and related parameters. Griffin, London, 506 p.

**Sulkin, S. D., and R. E. Miller.**
**1975.** Modified commercial crab and oyster dredges as sampling devices for blue crab, *Callinectes sapidus* Rathbun. Ches. Sci. 16:137–139.

**Thompson, S. K.**
**1992.** Sampling. John Wiley & Sons, New York, NY, 342 p.

**Tukey, J. W.**
**1958.** Bias and confidence in not quite large samples. Ann. Math Statist. 29:614.

**Van Engel, W. A.**
**1958.** The blue crab and its fishery in Chesapeake Bay. Part I: Reproduction, early development, growth and migration. Commer. Fish. Rev. 20:6–17.

**Zhang, C. I., J. S. Ault, and S. Endo.**
**1993.** Estimation of dredge sampling efficiency for blue crabs in Chesapeake Bay. Bull. Korean Fish. Soc. 26:369–379.

# Periodicity of increment formation in otoliths of overwintering postlarval and prejuvenile Atlantic menhaden, *Brevoortia tyrannus*

**Dean W. Ahrenholz**
Beaufort Laboratory, Southeast Fisheries Science Center
National Marine Fisheries Service, NOAA
101 Pivers Island Road
Beaufort, North Carolina 28516-9722
e-mail address: dean.ahrenholz@noaa.gov

**Deborah D. Squires**

**James A. Rice**

**Stephen W. Nixon**
Department of Zoology, North Carolina State University
P.O. Box 7617
Raleigh, North Carolina 27695-7617

**Gary R. Fitzhugh**
Panama City Facility, Southeast Fisheries Science Center
National Marine Fisheries Service, NOAA
3500 Delwood Beach Road
Panama City, Florida 32408-7403

Hypotheses of fishery recruitment processes often have as their foundation studies of incremental otolith growth (e.g. Methot, 1983; Rice et al., 1987). Conclusions from these studies, however, are only as robust as their baseline otolith validation work. This is especially true for investigations on Atlantic menhaden (*Brevoortia tyrannus*), an estuarine-dependent, marine-migratory clupeid ranging from southeastern Florida to Nova Scotia (Reintjes, 1969; Ahrenholz, 1991). The spawning season for Atlantic menhaden is protracted, occurring wherever fish of spawning age are found (Judy and Lewis, 1983). Spawning is probably greatest from October to March (Higham and Nicholson, 1964). The spawning activity that occurs in south coastal U.S. waters normally occurs within this time period, usually peaking during mid- to late winter (Wilkens and Lewis, 1971; Nicholson, 1972). Owing to the extended spawn and seasonal movement of spawning adults, progeny from different temporal spawning periods experience different environmental conditions during similar early life history stages.

Daily age validation studies have been conducted on late larvae and juvenile Atlantic menhaden (Ahrenholz et al., 1995), but none of the specimens were reared in a water temperature regime that typified conditions experienced by fall-spawned larvae. Fall-spawned larvae enter inshore nurseries when estuarine waters are cooling, yet still warm enough for moderate somatic growth and development. These young fish then endure the coldest winter temperatures in a partially transformed condition, i.e. in a postlarval-prejuvenile stage. In contrast, larvae of winter and early spring spawnings ingress into relatively cold, but progressively warming waters, from late winter to midspring; although they probably do not enter during extreme winter cold spells (Reintjes and Pacheco, 1966). Differences in growth patterns in the otolith microstructure of larvae and juveniles from these different spawning periods are detectable (Fitzhugh et al., 1997).

Validation of the otolith daily aging technique should take into account the environmental conditions experienced by field-sampled specimens (Jones, 1986), especially when some field conditions affect the daily periodicity of otolith growth increments. The sagittal growth increments for the fall-spawned Atlantic menhaden are disproportionately narrower (±1 µm) during the coldest overwintering months. Moreover, increments <1 µm potentially indicate less than daily increment formation (Campana et al., 1987). Less than daily increment deposition associated with cold water and slow growth rates has been observed for juvenile summer flounder (*Paralichthys dentatus*), another estuarine-dependent, marine-migratory species (Szedlmayer and Able, 1992).

Previous otolith microstructure validation studies for larval Atlantic menhaden have used larvae collected in the field during April or laboratory-reared specimens spawned in February (Ahrenholz et al., 1995). Test conditions were set at higher salinities than are normally associated with larval to juvenile transformation. Hence, we designed a study to specifically address the periodicity of otolith increment formation in over-wintering, fall-spawned Atlantic menhaden postlarvae and prejuveniles under the thermal and salinity conditions they experience in North Carolinian estuaries.

Manuscript accepted 26 November 1999.
Fish. Bull. 98:421–426 (2000).

## Materials and methods

Atlantic menhaden larvae were collected while ingressing into the Newport River estuary during the week of 7 December 1994. In the laboratory, these larvae were immersed on 8 December, in 100 mg/L solution of alizarin-complexone (ALC) solution for 16 h (overnight) at 18°C. Nearly equal numbers of marked larvae were reared in two concrete ponds (6600 L). Pond one, the high-salinity pond, received flow-through seawater at ambient water temperatures. Pond two, the low-salinity pond, received flow-through seawater and freshwater from a well. Pond two was generally a few degrees warmer and about one-half the salinity of pond one. Menhaden larvae were fed powdered salmon starter, supplemented with brine shrimp larvae, for the first few weeks, followed by salmon starter only.

Two to six specimens were sacrificed periodically, and measured for fork length (FL) to the nearest mm. Sagittal otoliths were removed, mounted in droplets of epoxy resin, and sectioned obliquely with a slow-speed saw with dual diamond wafering blades (Ahrenholz et al., 1995). Polished otolith sections (10–15 µm thick) were viewed through a compound microscope (1000×) and on an image analysis video monitor (3800×). When the otolith sample was examined under blue light epifluoresence, the ALC-marked increment was seen as red-orange. The number of increments from the ALC mark to the otolith margin was estimated as the arithmetic mean of a series of independent counts tallied blindly with a hand-held counter. A section was counted twice when the two counts differed by 0 to 2 increments. A section was counted three to five times when the difference between the initial two counts was greater than two increments. Otoliths from one specimen from the high-salinity pond were deemed unreadable.

An image analysis system was used to measure increment widths in groups of 10, starting from the innermost increment, for a select number of otoliths from each test group. However, the increments measured just prior to the alizarin mark may have numbered from 5 to 10. This procedure was undertaken to separate pre- and postmark increments from width estimates. Measurements were taken from oblique-transverse sections (Ahrenholz et al., 1995) as opposed to similar measurements taken on transverse sections, as done by Fitzhugh et al. (1997). Owing to nearly concentric otolith growth for the life history stage sampled, the measurements taken in our study should be similar to, or slightly greater than, transverse-oriented measurements.

Estimates of the dates when eggs were spawned for the test groups were obtained by sacrificing eight larvae on the day of ALC-marking. Their otoliths were removed, mounted on microscope slides, and read whole. Three independent counts were made from the first increment following the first feeding mark to the margin. Five days were added to the mean counts to account for time from spawning to first increment formation (Warlen, 1992).

Statistical analyses of the results generally followed those of Ahrenholz et al. (1995). The null hypothesis tested was that the growth increments in the otoliths were formed daily during the rearing period. The hypothesis was not rejected if the slope of a regression of increment count on number of days since marking was not significantly different from one and the intercept was not significantly different from zero. The statistical power to test for differences in the slope was also calculated (Rice, 1987). Student's-$t$ test was used to test for statistical significance of the regression parameters. Analysis of covariance (ANCOVA) and regression computations were performed with SAS statistical programs (SAS Institute, 1985). Ninety-five percent confidence intervals (CI) for individual age estimations (see discussion in Rice [1987]) were calculated for an inverse prediction condition (Sokal and Rohlf, 1981; note also discussions of inverse regression in Draper and Smith [1980]).

## Results

Fish were sampled from pond two (the low-salinity regime) on postmarking days 35, 56, 74 (and 75), 98, 119, and 140 (total $n$=22). Fish from pond one (the high-salinity regime) were sampled similarly through day 75 (total $n$=13). Prior to day 75 (for about two weeks), many of the menhaden in pond one died. The remaining fish from the high-salinity regime were sampled on day 75.

Spawned-date estimates determined from larvae sacrificed before being reared ranged from 17 October to 20 October 1994, thus, verifying that the experimental tests were performed on larvae derived from fall-spawning activity.

Temperature and salinity regimes during the rearing period (Fig. 1) were adequate to attain the study's objectives. The cooling and warming pattern, as well as the actual water temperatures were well within the range observed for winters in North Carolina estuaries over a 15-year period (Hettler and Chester, 1982). Salinity levels in both rearing regimes were within ranges observed for larval or juvenile menhaden in the field (Wilkenson and Lewis, 1971; Turner and Johnson, 1973), although the larval forms are more highly associated with lower salinities. Water temperatures were relatively warm in the early por-

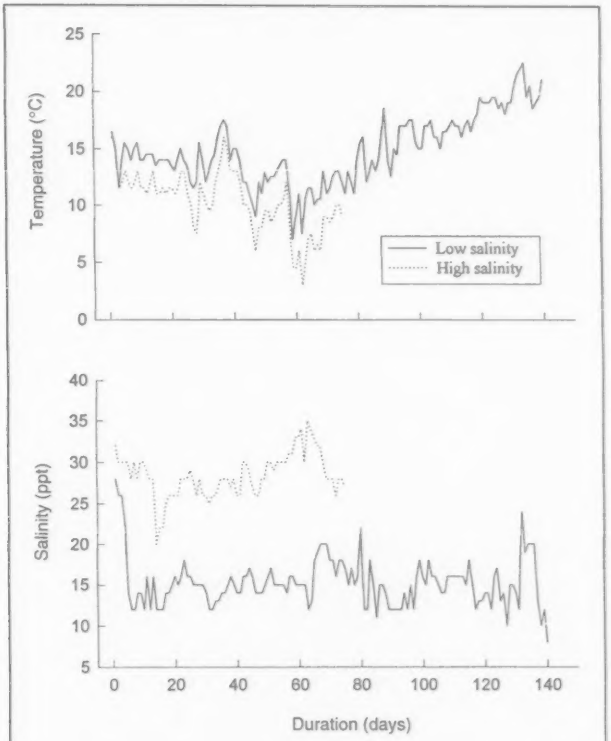


**Figure 1**

Environmental conditions experienced by two groups of ALC-marked larval-juvenile Atlantic menhaden (*Brevoortia tyrannus*) during the otolith validation study. The upper panel depicts temperature histories and the lower panel, the salinity histories. The high-salinity (low-temperature) rearing experiment ended after 75 days owing to high mortality rates.

tion of the study; larval menhaden advanced well into their transformation into juveniles. Through day 60 of rearing, water temperatures steadily declined to low winter minima. During the lower temperature period, the growth rates of fishes were reduced (Fig. 2). The mean width of the otolith growth increments for fish from the high-salinity group gradually dropped below 1 mm following the severe drop in temperature. During the same period, the increments for the low-salinity group reflected the higher growth rates for this group and were wider, with all mean widths above 1 µm (Fig. 3).

Similarity between regression parameters of increment counts versus days since marking between the high- and low-salinity regimes was tested over the shared range of duration (75 days). Tests for homogeneity of slopes showed no differences ($P$=0.679). A subsequent ANCOVA analysis revealed no differences between intercepts ($P$=0.712). Thus, the increment counts for the two rearing regimes were pooled and validation hypotheses were tested with a regression analysis. Results of this analysis revealed that the intercept was not significantly different from zero, and the slope was not significantly different from one (Fig. 4, Table 1). The confidence interval (95%) for estimates of daily age obtained from otoliths of fish which encountered conditions similar to those tested here, would be ±9 to 10 days over a range of 140 days (approximately 50 to 190 days of age).

## Discussion

Growth increments on sagittal otoliths of fall-spawned Atlantic menhaden formed daily, even when experimental water temperatures declined to 3°C

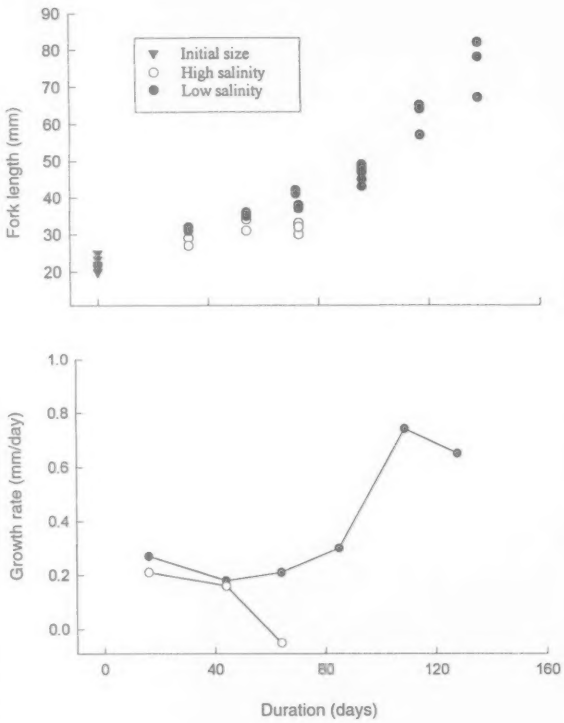


**Figure 2**

The body size (fork length) of ALC-marked juvenile Atlantic menhaden (*Brevoortia tyrannus*) sampled during the validation rearing study (upper panel) and rate of growth estimated from mean size of sampled fish (lower panel). The rates of growth are plotted at midpoints between sampling periods.

**Table 1**

Results of least squares linear regression analysis for marked Atlantic menhaden, *Brevoortia tyrannus*, otolith increment counts ($n$=34, $r^2$=0.984, and SE=standard error).

| Parameter | Estimate | SE | $P$ |
|---|---|---|---|
| Slope | 1.0048 | 0.0224 | 0.168 |
| Power[1] | 99.1% | — | — |
| Intercept | 0.3771 | 1.8257 | 0.162 |

[1] Statistical power to detect a deviation of 0.1 in the estimate of the slope at the $P$=0.05 level.

(Fig. 1). Even though growth rate declined to low levels during initial study weeks, especially for the high-salinity group (Fig. 2), an otolith increment continued to be formed daily even when increment widths fell below 1 µm for a number of days (Fig. 3). If a difference in increment formation rate had occurred between groups, we would not have been able to determine the cause because both temperature and salinity varied between groups. It seems likely that the faster growing fish responded to the higher temperatures. Regardless, both test groups experienced conditions that could be expected in the field during winter. The October-spawned larval menhaden used in our study displayed a growth increment mean width that ranged from values that were greater than those previously measured at sea to those that were less than previously measured in estuaries in a relatively short period of days (compare with Fitzhugh, et al. 1997).

The rearing conditions for specimens maintained during our study and earlier studies (Ahrenholz et al., 1995) should provide otolith increment validations for most, if not all, Atlantic menhaden that recruit

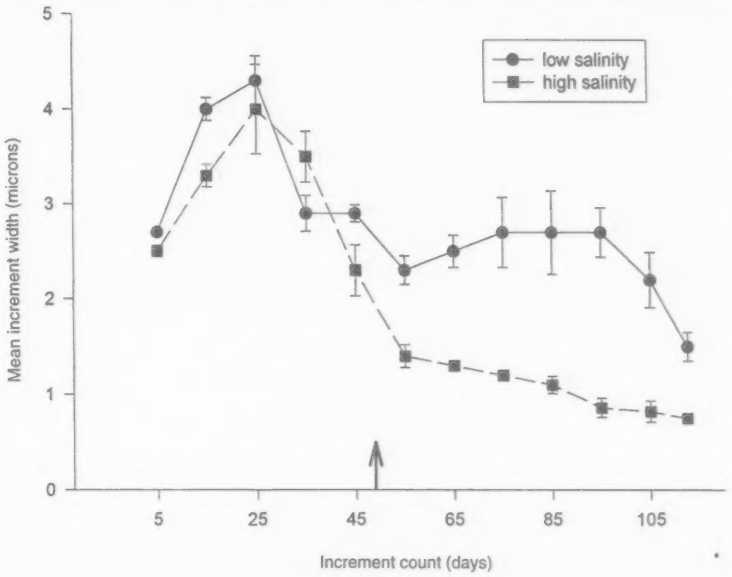


**Figure 3**

Estimates of mean width for otolith growth increments from larval-juvenile Atlantic menhaden (*Brevoortia tyrannus*) from each test-rearing group. The error bars represent ±1 SE, with $n$=3 for each data point (the error bars may be hidden by the symbol for some entries). The arrow denotes when the alizarin marking occurred. At-sea values are thus to the left of the arrow. (Note: after ALC marking, the low-salinity group was reared at a higher temperature than the high-salinity group.)

into estuarine systems from North Carolina to northern Florida. Additional studies may be necessary for more northern systems, such as Chesapeake and Delaware bays, especially for fall-spawned postlarval menhaden that may overwinter in even colder waters and for more extended periods of time.

## Acknowledgments

Critical reviews of the manuscript were provided by A. B. Powell, J. W. Smith, and D. S. Vaughan. Support for the study was provided in part by the SABRE program of the National Oceanic and Atmospheric Administration's Coastal Ocean Program / Coastal Fisheries Ecosystems Studies.

## Literature cited

**Ahrenholz, D. W.**
**1991.** Population biology and life history of the North American menhadens (Genus *Brevoortia*). Mar. Fish. Rev. 53(4):3–19.

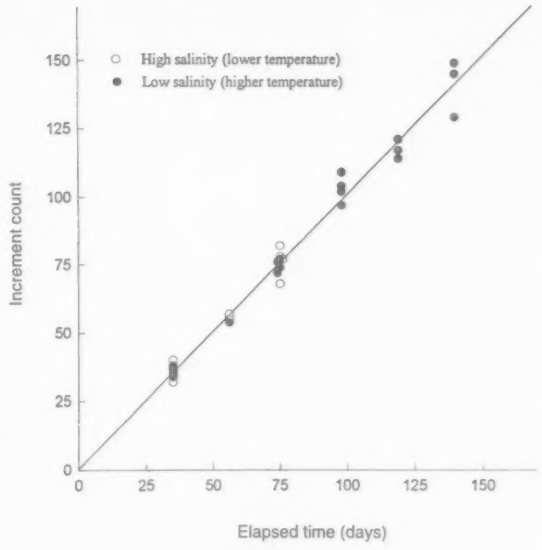


**Figure 4**

Scatterplot of growth increment count on elapsed time since ALC-marking for juvenile Atlantic menhaden (*Brevoortia tyrannus*). The fitted least squares regression line is shown.

**Ahrenholz, D. W., G. R. Fitzhugh, J.A. Rice, S. W. Nixon, and W. C. Pritchard.**
**1995.** Confidence of otolith ageing through the juvenile stage for Atlantic menhaden, *Brevoortia tyrannus.* Fish. Bull. 93:209–216.

**Campana, S. E., J. A. Gagné, and J. Munro.**
**1987.** Otolith microstructure of larval herring (*Clupea harengus*): image or reality? Can. J. Fish. Aquat. Sci. 44:1922–1929.

**Draper, N. R., and H. Smith.**
**1980.** Applied regression analysis, 2nd ed. John Wiley & Sons, Inc., New York, NY, 709 p.

**Fitzhugh, G. R., S. W. Nixon, D. W. Ahrenholz, and J. A. Rice.**
**1997.** Temperature effects on otolith microstructure and birth month estimation from otolith increment patterns in Atlantic menhaden. Trans. Am. Fish. Soc. 126:579–593.

**Hettler, W. F., and A. J. Chester.**
**1982.** The relationship of winter temperature and spring landings of pink shrimp, *Penaeus duorarum*, in North Carolina. Fish. Bull. 80:761–768.

**Higham, J. R., and W. R. Nicholson.**
**1964.** Sexual maturation and spawning of Atlantic menhaden. Fish. Bull. 63:255–271.

**Jones, C.**
**1986.** Determining age of larval fish with the otolith increment technique. Fish. Bull. 84:91–103.

**Judy, M. H., and R. M. Lewis.**
**1983.** Distribution of eggs and larvae of Atlantic menhaden, *Brevoortia tyrannus,* along the Atlantic coast of the United States. U.S. Dep. Commer., NOAA Tech. Rep. NMFS SSRF 774, 23 p.

**Methot, R. D., Jr.**
**1983.** Season variation in survival of larval northern anchovy, *Engraulis mordax*, estimated from the age distribution of juveniles. Fish. Bull. 81:741–750.

**Nicholson, W. R.**
**1972.** Population structure and movements of Atlantic menhaden, *Brevoortia tyrannus*, as inferred from back-calculated length frequencies. Chesapeake Sci. 13:161–174.

**Reintjes, J. W.**
**1969.** Synopsis of biological data on Atlantic menhaden, *Brevoortia tyrannus.* U.S. Dep. Interior, Fish Wildl. Serv., Circ. 320, 30 p.

**Reintjes, J. W., and A. L. Pacheco.**
**1966.** The relation of menhaden to estuaries. Am. Fish. Soc. Spec. Publ. 3:50–58.

**Rice, J. A.**
**1987.** Reliability of age and growth rate estimates from otolith analysis. *In* Age and growth of fish (R. C. Summerfelt and G. E. Hall, eds.), p. 167–176. Iowa State Univ. Press, Ames, IA.

**Rice, J. A., L. B. Crowder, and M. E. Holey.**
**1987.** Exploration of mechanisms regulating larval survival in Lake Michigan bloater: a recruitment analysis based on characteristics of individual larvae. Trans. Am. Fish. Soc. 116:703–718.

**SAS Institute, Inc.**
**1985.** SAS/STAT guide for personal computers, version 6 ed. SAS Inst., Cary, NC, 378 p.

**Sokal, R. R., and F. J. Rohlf.**
**1981.** Biometry, 2nd ed. W.H. Freeman and Co., New York, NY, 859 p.

**Szedlmayer, S. T., and K. W. Able.**
**1992.** Validation studies of daily increment formation for larval and juvenile summer flounder, *Paralichthys dentatus.* Can. J. Fish. Aquat. Sci. 49:1856–1862.

**Turner, W. R., and G. N. Johnson.**
**1973.** Distribution and relative abundance of fishes in Newport River, North Carolina. U.S. Dep. Commer., NOAA Tech. Rep. NMFS SSRF 666, 23 p.

**Warlen, S. M.**
**1992.** Age, growth, and size distribution of larval Atlantic menhaden off North Carolina. Trans. Am. Fish. Soc. 121: 588–598.

**Wilkens, E. P. H., and R. M. Lewis.**
**1971.** Abundance and distribution of young Atlantic menhaden, *Brevoortia tyrannus*, in the White Oak River estuary, North Carolina. Fish. Bull. 69:783–789.

# Larval and pelagic juvenile fishes collected with three types of gear in Gulf Stream and shelf waters in Onslow Bay, North Carolina, and comments on ichthyoplankton distribution and hydrography*

**Allyn B. Powell**
Center for Coastal Fisheries and Habitat Research
Beaufort Laboratory
National Ocean Service, NOAA
101 Pivers Island Road
Beaufort, North Carolina 28516-9722
E-mail address: allyn.powell@noaa.gov

**David G. Lindquist**
University of North Carolina at Wilmington
Department of Biological Sciences and
Center for Marine Science Research
601 South College Road
Wilmington, North Carolina 28403-3297

**Jonathan A. Hare**
Center for Coastal Fisheries and Habitat Research
Beaufort Laboratory
National Ocean Service, NOAA
101 Pivers Island Road
Beaufort, North Carolina 28516-9722

The fish fauna in waters off North Carolina is diverse, receiving contributions from the Virginian, Carolinian, and Caribbean faunal provinces (Gray et al., 1968; Schwartz, 1989). South of Cape Hatteras exist live-bottom habitats, small areas of rock outcroppings containing rich sessile invertebrate communities and many species of commercially and recreationally important subtropical and tropical fishes (Huntsman, 1976; Miller and Richards, 1979). Little is known about the patterns and source of recruitment of many of these and other fishes. Fahay (1975) sampled a transect off New River Inlet, North Carolina, and Cape Fear, North Carlina, at quarterly intervals with a surface-towed meter net. Eldridge et al. (1978) examined the performance of a 2 m × 1 m neuston net in waters off South Carolina. Powles and Stender (1976) surveyed ichthyoplankton from Cape Fear, North Carlina, to Cape Canaveral, Florida, with a standard ichthyoplankton bongo sampler. Ichthyoplankton research targeting live-bottom habitats in Onslow Bay, North Carlina, was recently conducted by Powell and Robbins (1998), who provided information on spatial and temporal spawning. The use of standard ichthyoplankton samplers, however, may introduce bias against the capture of late-larvae and early-juveniles owing to net avoidance (Shima and Bailey, 1994); therefore little information would be gained about recruitment sources and patterns.

The use of complementary gear that could collect a series of pelagic larval stages would be useful in understanding the source of recruits to live-bottom and other habitats off North Carolina. The spatial distributions of larval stages could indicate if recruitment is from local populations, or other sources, (Leis, 1994; Booth and Brosnan, 1995). However, the spatial distribution of larval stages needs to be coupled with oceanographic observations to interpret the source of recruits.

The major goal of our study was 1) to examine the effectiveness of three gear types in collecting a complete series of the pelagic larval phase of reef fishes and associated taxa, and 2) to examine the influence of short-term hydrographic conditions on fish distributions.

## Materials and methods

Sampling was generally conducted in darkness aboard the RV *Cape Hatteras*, 14–16 September 1994, along an onshore-offshore transect in Onslow Bay (Table 1, Fig. 1). With some modifications, we followed Struhsaker (1969) in classifying habitat types: coastal (<18 m); middle-shelf (18–55 m); outer-shelf (55–185 m); and oceanic (>185 m). Station 1 (76°15.0'W, 33°54.0'N) was located in oceanic waters (water depth=341 m); station 2 (76°21.3'W, 33°58.5'N) was located in outer-shelf waters where smooth to highly broken bottom exists (water depth= 75–110 m); station 3 (76°27.8'W, 34°04.0'N) was located in middle-shelf waters (water depth=40 m); and stations 4 (76°34.2'W, 34°08.7'N) and 5 (76°35.5'W, 34°14.3'N) were located on the middle shelf adjacent to live-bottom habitat (water depth=33–35 m and 28–31 m, re-

* Contribution 186 of the Center for Marine Science Research, University of North Carolina, Wilmington, NC 28403-3297.

Manuscript accepted 8 November 1999.
Fish. Bull. 98:427–438 (2000).

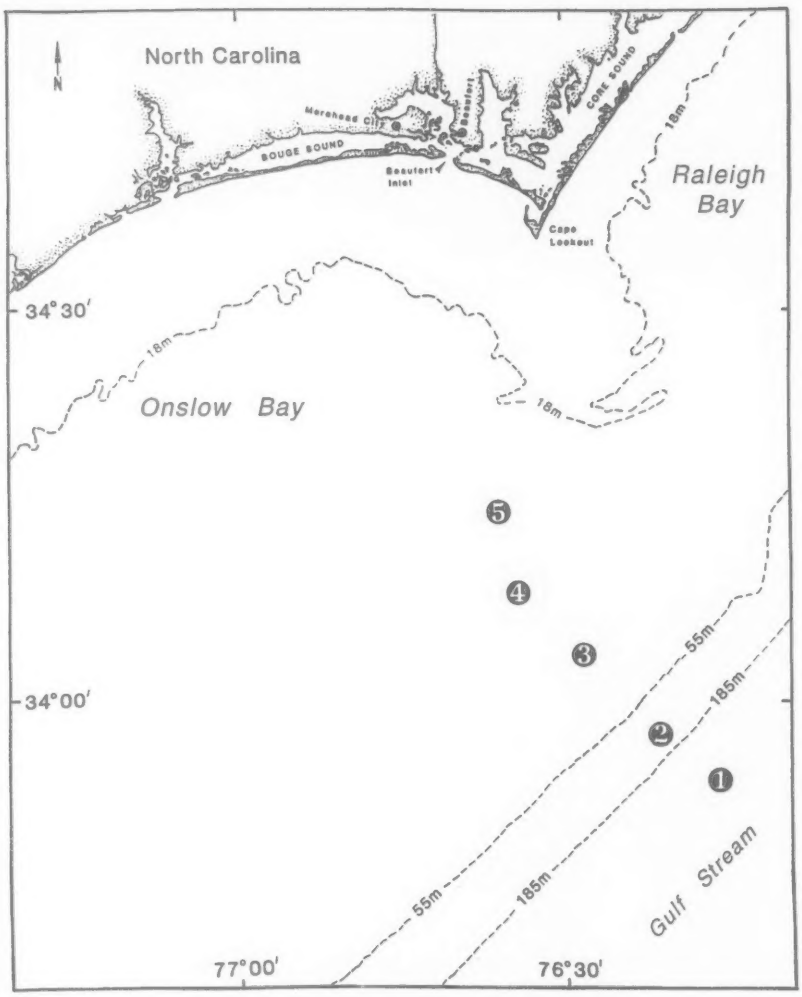


**Figure 1**
Location of sampling stations.

spectively). Stations 1 and 2 were influenced by the Gulf Stream.

Three samplers were used: a 60-cm diameter bongo sampler with 0.333-mm mesh nets, a 5-$m^2$ Methot frame trawl with 2×3 mm oval mesh (Methot, 1986), and a 1×2 m neuston net with 0.947-mm mesh. The bongo sampler was towed obliquely at 1.5 knots for a minimum of 5 min to insure 150 $m^3$ of water was sampled. The Methot frame trawl was towed obliquely at 4 knots for a minimum of 20 min to insure that >10,000 $m^3$ of water had been sampled, except for one tow of 10 min on 14 September 1994 at station 2 at 2111 hours. Both the bongo sampler and frame trawl were retrieved in a modified step oblique tow after deployment to a depth approximately 10 m from the bottom, except at station 1 where nets were deployed to a maximum depth of 170 m. The neuston net was towed for 10 min at 1.5 knots with approximately one-half of the net under water. Volume estimates for bongo nets and Methot frame trawl were based on General Oceanics flowmeter readings. No volume readings were taken for neuston tows. A summary of sample data is presented in Table 1. Samples were preserved in 95% ethyl alcohol. Body length measurements are notochord lengths (preflexion and flexion stages) or standard lengths (postflexion and juvenile stages).

At each station a conductivity-temperature-depth (CTD) probe (Sea-Bird model 911plus) was cast to within 1–3 m of the bottom. Temperature and salin-

**Table 1**

Summary of sample data taken in waters off North Carolina. For gear type: frame = 5 $m^2$-Methot frame trawl with 3×4 mm oval mesh (Methot, 1986); bongo = 60-cm bongo nets with 0.333-mm mesh; neuston = 1×2 m neuston net with 0.947-mm mesh. Density of larvae indicates numbers/100 $m^3$ for bongo nets; numbers/10,000 $m^3$ for frame trawl; and numbers/10-min tow for neuston net.

| Date | Station | Time | Gear | Density of larvae |
|---|---|---|---|---|
| 14 Sep 1994 | 2 | 2111 | frame | 27 |
| | | 2149 | frame | 29 |
| | | 2244 | bongo | 112 |
| | | 2307 | neuston | 32 |
| 15 Sep 1994 | 3 | 0122 | frame | 15 |
| | | 0204 | bongo | 79 |
| | | 0224 | neuston | 33 |
| | 4 | 0401 | frame | 25 |
| | | 0445 | neuston | 29 |
| | | 0458 | bongo | 72 |
| | 5 | 0620 | frame | 3 |
| | 1 | 2108 | frame | 9 |
| | | 2148 | bongo | 26 |
| | | 2207 | neuston | 23 |
| 16 Sep 1994 | 2 | 2341 | frame | 16 |
| | | 0024 | neuston | 26 |
| | | 0040 | bongo | 82 |
| | 3 | 0201 | frame | 8 |
| | | 0235 | bongo | 161 |
| | | 0244 | neuston | 20 |
| | 4 | 0355 | frame | 23 |
| | | 0427 | neuston | 58 |
| | | 0443 | bongo | 156 |
| | 5 | 0541 | frame | 19 |
| | | 0616 | bongo | 118 |
| | | 0625 | neuston | 29 |

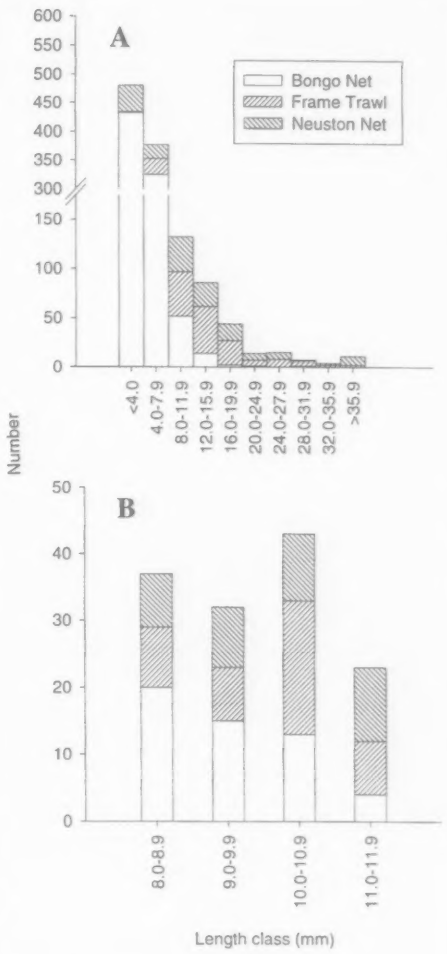


**Figure 2**

Length-frequency distributions by gear of (**A**) all ichthyoplankton (excluding leptocephali); and (**B**) ichthyoplankton between 8.0 and 12.0 mm in length.

ity measurements were reviewed for aberrant data points. Satellite-derived advanced very high resolution radiometer (AVHRR) data (NOAA/NESDIS CoastWatch node, NMFS Beaufort Laboratory) were used to examine sea surface temperature (SST) during the study period (1–20 September 1994). A nonparametric Kruskal-Wallis test (SAS Institute, Inc., 1987) was used to evaluate differences in fish lengths between gear types, and between days at specific stations.

## Results

### Larval length distributions by gear

There was a significant difference in length of larvae among gears (Kruskal-Wallace Test, $P < 0.01$). The neuston net and frame trawl collected larger larvae, whereas the bongo net collected smaller larvae (Fig. 2A). The bongo net was more effective in collecting larvae <10.0 mm, and the frame trawl and neuston net were more effective in collecting larvae 10.0 mm (Fig. 2B). A wide range of size classes was obtained with the neuston net and frame trawl, but catches typically were low (Table 1, Fig. 2).

Some 40 reef fish taxa were collected (Table 2); approximately 25 with the bongo sampler, 24 with the frame trawl, and 14 with the neuston net. Five families were commonly collected (Table 3), but a size series of only two taxa (*Acanthurus* sp(p). and

**Table 2**

The frequency of occurrence from *n* samples and, in parenthesis, the density (bongo net=numbers/100 $m^3$, frame trawl= numbers/10,000 $m^3$, neuston net=numbers/10-min tow: summed over all stations) of reef-associated taxa collected with three different samplers in September, 1995, in waters off North Carolina.

| Family | Taxa | Bongo net (*n*=10) | Frame trawl (*n*=8) | Neuston net (*n*=8) |
|---|---|---|---|---|
| Acanthuridae | *Acanthurus bahianus* | | 2(4.0) | |
| | *A. bahianus/chirurgus* | | 1(0.8) | |
| | *A. chirurgus* | | 1(1.1) | |
| | *A. coeruleus* | 1 (0.8) | 1(1.1) | |
| | *Acanthurus* sp(p). | 1 (0.8) | 2(1.4) | 2(2.0) |
| Balistidae | *Balistes capriscus* | | 1(0.6) | 2(2.0) |
| | unidentified | 3 (2.0) | 1(0.6) | 1(1.0) |
| Carangidae | *Alectis ciliaris* | | 1(0.8) | |
| | *Seriola* sp(p). | 1 (1.3) | 1(0.6) | 1(2.0) |
| Chaetodontidae | *Chaetodon ocellatus* | | 1(0.6) | |
| Diodontidae | unidentified | | 1(0.8) | |
| Fistularidae | *Fistularia* sp(p). | 1 (1.5) | 1(0.8) | |
| Gobiidae | *Ioglossus calliurus* | 3 (2.8) | | |
| Holocentridae | unidentified | 2 (1.0) | 2(1.3) | 3(3.0) |
| Labridae | *Bodianus* sp. | 1 (0.6) | | |
| | *Halichoeres* sp(p). | 2 (5.5) | | |
| Lutjanidae | *Etelis oculatus* | 1 (0.5) | | |
| | *Lutjanus campechanus* | 1 (0.7) | | |
| | *Pristipomoides aquilonaris* | 1 (0.7) | | |
| | *Rhomboplites aurorubens* | 5(11.7) | | 1(1.0) |
| | unidentified | 4(15.2) | | |
| Monacanthidae | *Aluterus scriptus* | | 1(0.8) | |
| | *Aluterus* sp. | | 1(0.8) | |
| | *Cantherines* sp. | | 1(0.6) | |
| | *Monacanthus ciliatus* | | 3(2.2) | |
| | *M. hispidus* | 1 (1.3) | 4(4.4) | 2(6.0) |
| Muraenidae | *Gymnothorax moringa* | | 1(0.6) | |
| | *G. ocellatus* complex | | 3(5.5) | |
| | *Gymnothorax* sp(p). | 1 (1.3) | 1(1.5) | |
| | unidentified | 1 (1.3) | | 1(1.0) |
| Ogcocephalidae | unidentified | 1 (0.7) | 2(2.2) | |
| Pomacanthidae | *Holacanthus* sp(p). | 2 (4.0) | | |
| | unidentified | 1 (1.3) | | |
| Pomacentridae | *Pomacentrus* sp(p). | 3 (2.6) | | |
| | unidentified | 1 (0.7) | | 2(2.0) |
| Priacanthidae | *Pristigenys alta* | | 1(0.9) | |
| | unidentified | 5 (8.4) | 1(0.6) | |
| Scaridae | type A | 6(15.6) | | 2(7.0) |
| | type B | 5 (9.8) | | 1(1.0) |
| | unidentified | 1 (1.5) | | |
| Scorpaenidae | *Scorpaena* sp. | | 1(0.6) | |
| | unidentified | 7 (9.0) | | 1(2.0) |

*continued*

**Table 2 (continued)**

| Family | Taxa | Bongo net ($n$=10) | Frame trawl ($n$=8) | Neuston net ($n$=8) |
|---|---|---|---|---|
| Serranidae | *Diplectrum formosum* | 2 (1.3) | | |
| | *Epinephelus cruenatus* | | 1(1.7) | |
| | *E. niveatus/flavolimbatus* | 1 (0.8) | | |
| | *Hemanthias vivanus* | | | 1(1.0) |
| | *Liopropoma* sp(p). | | | 2(2.0) |
| | *Rypticus* sp(p). | 2 (1.3) | | |
| | Serraninae type A | 2 (2.7) | | |
| | *Serranus* sp. | | 1(0.6) | |
| | subfamily Serraninae | 3(11.8) | | |
| | tribe Epinephelini | | | 1(1.0) |
| Syngnathidae | *Hippocampus erectus* | | 2(1.4) | 3(3.0) |

**Table 3**

The range of body lengths, by gear, for the most commonly collected taxa, identified below the family level. Values in parentheses indicate the number of fish measured. Bongo = 60-cm bongo nets with 0.333-mm mesh; Frame = 5-m$^2$ Methot frame trawl with 3×4 mm oval mesh; and Neuston = 1×2 m neuston net with 0.947-mm mesh.

| Taxa | Bongo net | Frame trawl | Neuston net |
|---|---|---|---|
| Reef fish taxa | | | |
| Acanthuridae | | | |
| *Acanthurus* sp(p). | 2.5–8.6 (11) | 4.7–10.2 (10) | 3.0–3.3 (2) |
| Labridae | | | |
| *Halichoeres* sp(p). | 2.1–5.4 (8) | — | — |
| Lutjanidae | | | |
| *Rhomboplites aurorubens* | 2.9–5.6 (18) | — — | 4.2 (1) |
| unidentified | 1.9–3.4 (30) | — — | — — |
| Priacanthidae | | | |
| *Pristigenys alta* | — | 10.3 (1) | |
| unidentified | 1.8–4.4 (19) | — — | 3.1–4.1 (4) |
| Scaridae | | | |
| type A | 2.9–7.7 (18) | — — | 8.4–9.8 (7) |
| type B | 2.7–7.7 (11) | — — | 7.6 (1) |
| Pelagic taxa | | | |
| Carangidae | | | |
| *Decapterus punctatus* | 2.1–14.7 (30) | 18.7 (1) | 2.9–11.0 (10) |
| *Selar crumenophthalmus* | 3.7–6.7 (5) | 7.3–16.2 (16) | 4.1–5.0 (2) |

*continued*

**Table 3 (continued)**

| Taxa | Bongo net | Frame trawl | Neuston net |
|---|---|---|---|
| Coryphaenidae | | | |
| *Coryphaena equisetus* | 4.4–4.6 | — | *10.0–19.2* |
| | (2) | — | (12) |
| *C. hippurus* | — | — | 12.3–43.0 |
| | — | — | (15) |
| Scombridae | | | |
| *Auxis* sp(p). | 2.6–7.1 | 10.7 | 4.0–18.3 |
| | (20) | (1) | (6) |
| *Scomberomorus cavalla* | 2.8–6.2 | 13.5 | 4.2–7.9 |
| | (38) | (1) | (4) |
| *Thunnus* sp(p). | 2.6–6.2 | 4.6–5.7 | 4.7–5.7 |
| | (12) | (2) | (14) |
| Demersal taxa | | | |
| Bothidae | | | |
| *Bothus* sp(p). | 2.0–15.0 | 6.5–19.5 | 3.4–6.0 |
| | (104) | (30) | (18) |
| *Trichopsetta ventralis* | 30.0 | 13.5–29.8 | — |
| | (1) | (20) | — |
| Callionymidae | | | |
| *Diplogrammus pauciradiatus* | 1.2–3.4 | — | — |
| | (66) | — | — |
| *Paradiplogrammus bairdi* | 1.7–6.2 | — | 3.5–6.0 |
| | (9) | — | (6) |
| Caproidae | | | |
| *Antigonia* sp(p). | 2.8–6.3 | 3.4–8.3 | 2.7–4.0 |
| | (16) | (6) | (2) |
| Labridae | | | |
| *Xyrichtys novacula* | 2.4–9.9 | 6.2 | 6.8–13.5 |
| | (46) | (1) | (2) |
| Ophididae | | | |
| *Ophidion selenops* | 1.9–16.0 | — | — |
| | (8) | — | — |
| *Otophidion omostigmum* | 3.1–8.3 | — | — |
| | (14) | — | — |
| Paralichthyidae | | | |
| *Syacium papillosum* | 1.3–12.7 | 4.2–9.3 | 3.2–4.3 |
| | (92) | (3) | (25) |

Scaridae type A) were collected with complementary gear. The bongo sampler and frame trawl were effective in collecting a series of *Acanthurus* sp(p)., the bongo and neuston net in collecting Scaridae type A. Larvae of the economically important *Rhomboplites aurorubens* were collected almost exclusively with bongo nets and ranged from 2.9 to 5.6 mm (Tables 2 and 3). The unidentified lutjanid larvae were probably *R. aurorubens* because few *Lutjanus campechanus* were collected ($n$=3).

Of the seven commonly collected pelagic taxa, size series of four taxa (*Selar crumenophthalmus*, *Coryphaena equisetus*, *Auxis* sp(p)., and *Scomberomorus cavalla*) were collected with complementary gear (Table 3). Except *S. crumenophthalmus*, which was effectively collected with the bongo sampler and frame trawl, all others were collected with the bongo sampler and neuston net. *Coryphaena hippurus* specimens were large and collected solely with the neuston net.

The frame trawl effectively sampled large anguilliform leptocephali, and the bongo sampler was a good complementary gear for collecting smaller specimens (Fig. 3). Only one leptocephalus was captured with the neuston net. Taxa representing three families were collected: Congridae (*Ariosoma balearicum*, *Bathycongrus* sp(p)., *Heteroconger luteolus*, *Para-*

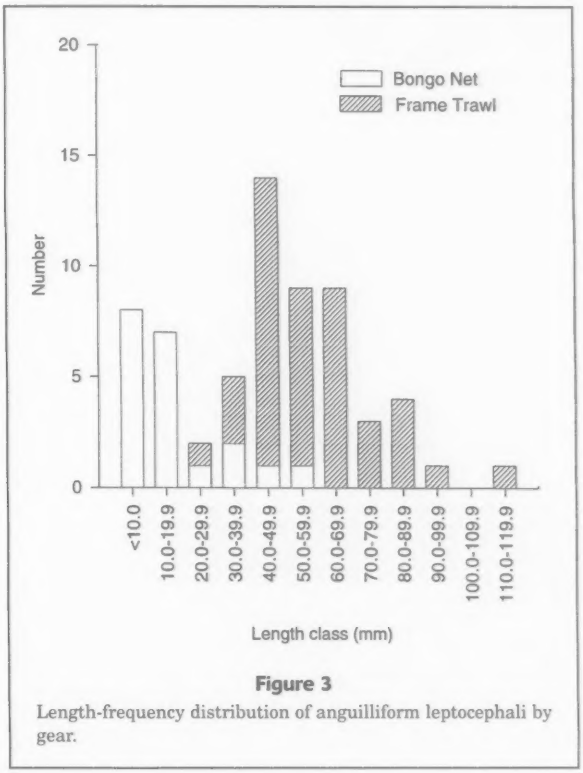


**Figure 3**
Length-frequency distribution of anguilliform leptocephali by gear.

*conger caudilimbatus*); Muraenidae (*Gymnothorax moringa*, *G. ocellatus* complex); and Ophichthidae (*Callechelys muraena*, *Gordiichthys ergodes*, *Letharchus aliculatus*, *Ophichthus gomesii*, *O. melanoporus*, *O. puncticeps*).

A size series of two demersal species (*Bothus* sp(p). and *Antigonia* sp(p).) was collected with the bongo net and frame trawl (Table 3). Because size of *Bothus* at metamorphosis is approximately 16–21 mm (Fahay, 1983), our collections represent a complete size series. Species most likely include *B. ocellatus* and *B. robinsi* (Robins and Ray, 1986), both of which inhabit middle-shelf waters as adults (Schwartz, 1989). The series of antigonids did not include the large pelagic stage (ca. 13–14 mm).[1] All the specimens that had developed meristic characters (ca. 5.0 mm) were *Antigonia capros*. On this basis, the smaller specimens might be *A. capros*, but *A. capros* and *A. combatia* exist sympatrically in the western North Atlantic (Berry, 1959).

[1] Richards, W. J. 1991. National Marine Fisheries Service, Southeast Fisheries Science Center, 75 Virginia drive, Miami, FL 33149. Unpubl. data.

## Hydrography and ichthyoplankton distribution

A major hydrographic feature observed in SST imagery was a large frontal eddy that was propagating northeastward and associated with a Gulf Stream meander crest (Fig. 4). A warm filament of Gulf Stream derived water lay over the shelf and resulted from the cyclonic circulation of the frontal eddy. This filament was bounded inshore by cooler shelf water and separated from the Gulf Stream by cooler water of the frontal eddy.

Temperature and salinity were in concordance with the SST imagery (Fig. 5). On 15 September 1994 (day 1), domed-shaped isotherms and lower salinities were observed at station 2 indicating recent upwelling from the passage of the frontal eddy (Fig. 4). The warmer and more saline water on the shelf on day-1 (Fig. 5) was consistent with the presence of stranded Gulf Stream water resulting from the frontal eddy filament observed on the SST imagery (Fig. 4). Associated with this stranded Gulf Stream water on the middle-shelf was a diverse group of larvae that are not known to occur as adults or spawn in middle-shelf waters (Table 4). The frequency occur-

THE PAPER AND INK USED IN THE ORIGINAL PUBLICATION MAY AFFECT THE QUALITY OF THE MICROFORM EDITION.

**Figure 4**

Sea-surface-temperature satellite imagery during (**A**) 12 and, (**B**) 15 and, (**C**) 16 September 1994 off North Carolina. Station locations are referenced. See Figure 1 for station numbers.

rence of these larvae appeared to be similar on both days as was the presence of Gulf Stream water.

On 16 September 1994 (day 2), hydrographic conditions had changed markedly offshore (Fig. 5). At the surface of station 2, warm, low-salinity water was present, indicating water of coastal origin. But the temperature was higher than observed over the Carolina shelf in the SST imagery (Fig. 4), indicating a more southern coastal origin for this water. Accompanying these changes in outer-shelf waters, the length-frequency distributions of the two most abundant taxa, *Bothus* sp(p). and *S. papillosum*, differed significantly between day 1 and day 2 (Kruskal-Wallace Test; $P<0.01$ for both taxa). Very small larvae of both middle-shelf taxa were abundant in outer-shelf waters on day 2 but absent on day 1 (Fig. 6).

## Discussion

### Gear comparison

A series of pelagic larvae and juveniles was collected with complementary gear for *Acanthurus* sp(p)., *Antigonia* sp(p)., *Bothus* sp(p)., Scaridae type A, and *Selar crumenophthalmus*. The Methot frame trawl was not successful in collecting large larvae or early juveniles of economically important reef fish species (snappers and groupers), probably due to the low abundance of adult populations. In other studies, the frame trawl has successfully collected large larvae and juveniles of those species whose adults are extremely abundant (i.e. *Theragra chalcogramma* [Shima and Bailey, 1994; Brodeur et al., 1995]) and *Engraulis mordax*, [Methot, 1986]). Economically important reef fish species are relatively rare and larger size pelagic larvae and juveniles are rarer than young larvae. Longer frame-trawl tow times (one hour) will be required, but this would limit the extent of the area to be sampled and decrease the quality of the specimens. The bongo sampler is generally limited in its ability to collect late-stage larvae or early pelagic juveniles owing to net avoidance (Shima and Bailey, 1994); however, it is a more effective sampler than either the neuston net or frame trawl in collecting early stage larvae, and it is needed to obtain information on spatial and temporal spawning.

The frame trawl is effective in capturing leptocephali, and because the leptocephalus is a true oceanic form regardless of habitat as an adult (Smith, 1989), it is a valuable indicator species in studies dealing with cross-shelf transport. Similarly, the frame trawl is effective in capturing *Trichopsetta ventralis*, a resident of the Gulf of Mexico (Robins

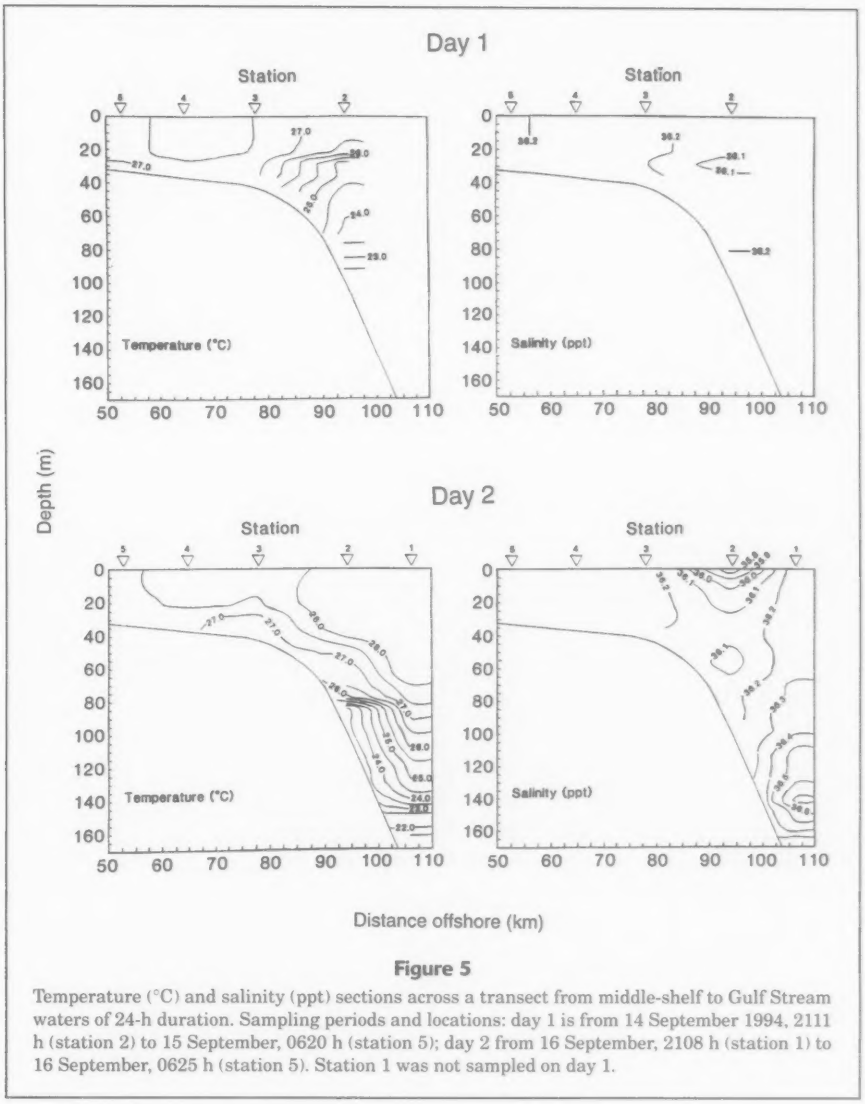


**Figure 5**

Temperature (°C) and salinity (ppt) sections across a transect from middle-shelf to Gulf Stream waters of 24-h duration. Sampling periods and locations: day 1 is from 14 September 1994, 2111 h (station 2) to 15 September, 0620 h (station 5); day 2 from 16 September, 2108 h (station 1) to 16 September, 0625 h (station 5). Station 1 was not sampled on day 1.

and Ray, 1986) and an indicator that certain larvae spawned in the Gulf of Mexico as well as other organisms (Pietrafesa, 1989) can be transported to shelf waters off North Carolina.

Our study and previous studies (Eldridge et al., 1978) indicate that the 1 m × 2 m neuston net is as effective in sampling large larvae and juveniles as is the frame trawl, although a comparison has not been made by using both nets as neuston nets. Eldridge et al. made a large number of neuston tows (24 day, 24 night) and, in some cases, collected larger fishes (e.g. *Decapterus* sp, *Selar crumenopthalmus* and Priacanthidae). However, they did not collect any Acanthuridae, *Trichopsetta*, and *Antigonia* sp(p)., taxa that were relatively common in frame trawl collections. A comparison between the two gear types for neuston tows could be informative.

### Ichthyoplankton distribution in relation to hydrography

Factors influencing the hydrography of the waters off North Carolina are complex and dynamic (Pietrafesa, 1989; Pomeroy et al., 1993; Verity et al., 1993) and

**Table 4**

The occurrence of larvae (denoted by a "+" sign) from taxa that occur or spawn as adults in oceanic (>185 m) and outer-shelf waters (55–185 m) or that occur south of the study area (denoted by an asterisk) collected in middle-shelf waters (stations 3 and 4) during two sampling periods of 24-h duration (denoted by day 1 and day 2).

| Family | Species | Day 1 | Day 2 | Family | Species | Day 1 | Day 2 |
|---|---|---|---|---|---|---|---|
| Acropomatidae | *Synagrops* sp. | | + | Lutjanidae | *Etelis oculatus** | | + |
| Balistidae | *Canthidermis maculatus* | + | | Muraenidae | *Gymnothorax ocellatus* complex | + | |
| Bathypteroidae | unidentified | | + | | | + | |
| Bothidae | *Trichopsetta ventralis** | + | + | | unidentified | | + |
| Caproidae | *Antigonia capros* (?) | + | + | Myctophidae | *Benthosema suborbitale* | + | |
| Carapidae | *Carapus bermudensis** | | + | | *Ceratoscopelus* sp(p). | + | + |
| Chiasmodontidae | unidentified | | + | | *Notolychnus valdiviae* | | + |
| Congridae | *Ariosoma balearicum* | + | + | | unidentified | + | + |
| | Bathycongrus sp(p). | + | + | Nomeidae | *Cubiceps pauciradiatus* | + | |
| | *Heteroconger luteolis* | + | | Notosudidae | *Scopelosaurus smithii* | | + |
| | *Paraconger caudilimbatus* | + | | Ophichthidae | *Gordiichthys ergodes* | | + |
| Gempylidae | *Gempylus serpens* | + | | Paralepididae | *Lestidium atlanticum* | + | |
| | *Nesiarchus nasutus* | | + | | unidentified | + | |
| Gonostomatidae | *Cyclothone* sp(p). | + | + | Paralichthyidae | *Citharichthys gymnorhinus** | + | + |
| Lobotidae | *Lobotes surinamensis** | | + | Phosichthyidae | | + | |

certainly influence the composition of ichthyoplankton on the continental shelf. A major feature is the intrusion of Gulf Stream waters onto the continental shelf. Additionally, during summer, southwest winds result in the advection of shelf waters south of North Carolina onto the North Carolina shelf (Pietrafesa, 1989). Intrusions of the Gulf Stream, along with the advection of Georgian shelf water, appeared to be evident in our study and could have influenced the composition of ichthyoplankton on the shelf—particularly evident at the outer-shelf station (station 2) where hydrographic conditions and size composition of the two most abundant taxa changed within a 24-h period.

We identified 21 species of larvae on the middle shelf from oceanic and outer-shelf waters and five species which, as adults, occur in shelf waters south of the study area (Table 4). The intrusion of these larvae is a common event that occurs throughout all seasons (Powell and Robbins, 1994; 1998; our study) and appears to be related to water expelled from frontal eddies created by Gulf Stream meanders that have stranded on the continental shelf. Nevertheless, we were unable to determine the role of cross shelf transport in the recruitment of subtropical and tropical reef fishes and other taxa to waters off North Carolina.

Our observations on larval fish distribution patterns in relation to hydrography are derived from five stations over a 48-h period. Longer-term studies, with extensive sampling, will be necessary to test assumptions made in our study, especially the transport of larvae from the middle shelf to the outer shelf. *Syacium papillosum* a middle-shelf species that is abundant from spring to early fall (Powell and Robbins 1994; 1998; our study) could serve as an indicator of transport in long-term studies. Such studies could test the hypothesis that circulation patterns during late spring, summer, and early fall in shelf waters off North Carolina retain larvae within the bays. The major goal of future research should be to develop a comprehensive model or scenario of larval transport based on circulation patterns (e.g. Hare and Cowen, 1996). Such a model could provide a lucid framework for testing larval transport hypotheses and be of heuristic value as new problems are discovered.

## Acknowledgments

We wish to express our appreciation to the crew of the RV *Cape Hatteras* and those individuals who participated in the cruise, especially Mike Greene. We especially thank David Smith and Mark Leiby for leptocephali identification, Curtis Lewis for figure preparation, and Dave Colby and Jim Waters for computer assistance. Comments by Bill Hettler, Patti Marraro, and Dave Peters along with those of two anonymous reviewers greatly improved the manuscript.

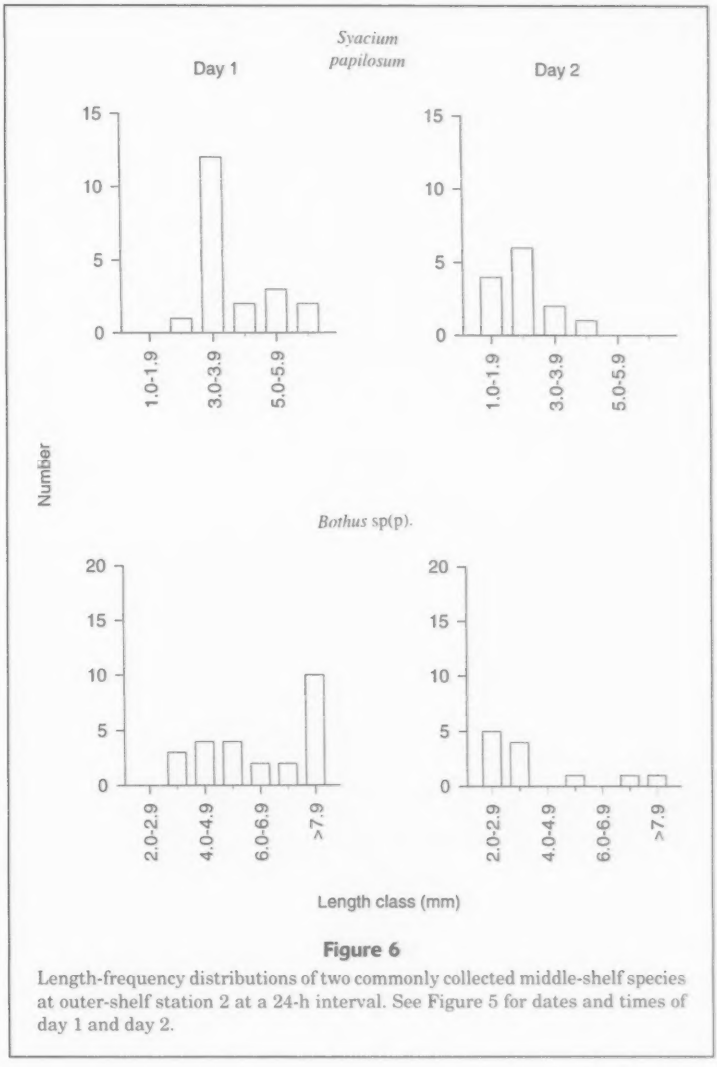


**Figure 6**

Length-frequency distributions of two commonly collected middle-shelf species at outer-shelf station 2 at a 24-h interval. See Figure 5 for dates and times of day 1 and day 2.

## Literature cited

**Berry, F. H.**
**1959.** Boarfishes of the genus *Antigonia* of the western Atlantic. Bull. Fla. State Mus. 4:205–250.

**Booth, D. J., and D. M. Brosnan.**
**1995.** The role of recruitment dynamics in rocky shore and coral reef fish communities. Adv. Ecol. Res. 26:309–385.

**Brodeur, R. D., M. S. Busby, and M. T. Wilson.**
**1995.** Summer distribution of early life stages of walleye pollock, *Theragra chalcogramma*, and associated species in the western Gulf of Alaska. Fish. Bull. 93:603–618.

**Eldridge, P. J., F. H. Berry, and M. C. Miller III.**
**1978.** Diurnal variations in catches of selected species of ichthyoneuston by the Boothbay neuston net off Charleston, South Carolina. Fish. Bull. 76:295–297.

**Fahay, M. P.**
**1975.** An annotated list of larval and juvenile fishes captured with surface-towed meter net in the South Atlantic Bight during four RV *Dolphin* cruises between May1967 and February 1968. U.S. Dep. Commer., NOAA Tech. Rep. NMFS SSRF-685, 39 p.
**1983.** Guide to the early stages of marine fishes occurring in the western north Atlantic Ocean, Cape Hatteras to the southern Scotian Shelf. J. Northwest Atl. Fish. Sci. 4:1–423.

**Gray, I. E., M. E. Downey, and M. J. Cerame-Vivas.**
**1968.** Sea-stars of North Carolina. Fish. Bull. 67:127–164.

**Hare, J. A., and R. K. Cowen.**
**1996.** Transport mechanisms of larval and pelagic juvenile bluefish (*Pomatomus saltatrix*) from South Atlantic Bight spawning grounds to Middle Atlantic Bight nursery habitats. Limnol. Oceanogr. 41:1264–1280.

**Huntsman, G. R.**
**1976.** Offshore headboat fishing in North Carolina and South Carolina. Mar. Fish. Rev. 38:13–23.

**Leis, J. M.**
**1994.** Coral Sea atoll lagoons: closed nurseries for the larvae of a few coral reef fishes. Bull. Mar. Sci. 54:206–227.

**Methot, R. D.**
**1986.** Frame trawl for sampling pelagic juvenile fish. CALCOFI Rep. 27:267–278.

**Miller, G. C., and W. J. Richards.**
**1979.** Reef fish habitat, faunal assemblages, and factors determining distributions in the South Atlantic Bight. Proc. Gulf Caribb. Fish. Inst. 32:114–130.

**Pietrafesa, L. J.**
**1989.** The Gulf Stream and wind events on the Carolina Capes shelf. *In* North Carolina coastal oceanography symposium (R. Y. George and A. Hulbert, eds.), p. 89–129. U.S. Dep. Commer., NOAA-NURP Rep. 89-2.

**Pomeroy, L. R., J. O. Blanton, G.-A. Paffenhöfer, K. L. Von Damn, P. G. Verity, H. L. Windom, and T. N. Lee.**
**1993.** Inner shelf processes. *In* Ocean processes: U. S. southeast continental shelf: a summary of research conducted in the South Atlantic Bight under the auspices of the U. S. Department of Energy from 1977 to 1991 (D. W. Menzel, ed.), p. 9–43. Office of Scientific and Technical Information, Rep. DOE/OSTI-11674.

**Powell, A. B., and R. E. Robbins.**
**1994.** Abundance and distribution of ichthyoplankton along an inshore-offshore transect in Onslow Bay, North Carolina. U.S. Dep. Commer. NOAA Tech. Rep. NMFS 120, 28 p.
**1998.** Ichthyoplankton adjacent to live-bottom habitats in Onslow Bay, North Carolina. U.S. Dep. Commer., NOAA Tech. Rep. NMFS 133, 32 p .

**Powles, H., and B. W. Stender.**
**1976.** Observations on composition, seasonality and distribution of ichthyoplankton from MARMAP cruises in the South Atlantic Bight in 1973. S.C. Mar. Res. Cent., Tech. Rep. Ser. 11.

**Robins, C. R., and G. C. Ray.**
**1986.** A field guide to Atlantic coast fishes of North America. Houghton Mifflin, Boston, MA, 354 p.

**SAS Institute, Inc.**
**1987.** SAS/STAT™ guide for personal computers, version 6 edition. SAS Institute Inc., Cary, NC, 1028 p.

**Schwartz, F. J.**
**1989.** Zoogeography and ecology of fishes inhabiting North Carolina's marine waters to depths of 600 meters. *In* North Carolina coastal oceanography symposium (R. Y. George and A. W. Hulbert, eds), p. 335–374. U.S. Dep. Commer., NOAA-NURP Rep. 89-2.

**Shima, M., and K. M. Bailey.**
**1994.** Comparative analysis of ichthyoplankton sampling gear for early life stages of walleye pollack (*Theragra chalcogramma*). Fish. Oceanogr. 3:50–59.

**Smith, D. G.**
**1989.** Introduction to leptocephali. *In* Fishes of the western north Atlantic, memoir 1, part 9, vol. 2, Leptocephali (E. A. Böhlke, ed.), p. 657–658. Sears Found. Mar. Res., Yale Univ.

**Struhsaker, P.**
**1969.** Demersal fish resources: composition, distribution, and commercial potential of the continental shelf stocks off the southeastern United States. Fish. Indust. Res. 4:261–300.

**Verity, P. G., T. N. Lee, J. A. Yoder, G.-A. Poffenhöfer, J. O. Blanton, and C. R. Alexander.**
**1993.** Outer shelf processes. *In* Ocean processes: U. S. southeast continental shelf: a summary of research conducted in the South Atlantic Bight under the auspices of the U.S. Department of Energy from 1977 to 1991 (D. W. Menzel, ed.), p. 45–74. Office of Scientific and Technical Information, Rep. DOE/OSTI-11674.

Superintendent of Documents **Publications** Order Form

*5178

☐ YES, please send me the following publications:

____ Subscriptions to *Fishery Bulletin*
for $50.00 per year ($62.50 foreign)

The total cost of my order is $ _____ . Prices include regular domestic postage and handling and are subject to change.

_____
(Company or Personal Name) (Please type or print)

_____
(Additional address/attention line)

_____
(Street address)

_____
(City, State, ZIP Code)

_____
(Daytime phone including area code)

_____
(Purchase Order No.)

**Charge your order. IT'S EASY!**

VISA

MasterCard

**Please Choose Method of Payment:**

☐ Check Payable to the Superintendent of Documents
☐ GPO Deposit Account ☐☐☐☐☐☐–☐
☐ VISA or MasterCard Account
☐☐☐☐☐☐☐☐☐☐☐☐☐☐☐☐
☐☐☐☐ (Credit card expiration date)

**To fax your orders (202) 512-2250**

_____
(Authorizing Signature)

Mail To: Superintendent of Documents
P.O. Box 371954, Pittsburgh, PA 15250-7954

***Thank you for your order!***

UMI

PAGES 440-450 MISSING IN NUMBER ONLY.

# Fishery Bulletin

## Guide for Contributors

### Content

**Articles** published in *Fishery Bulletin* describe original research in fishery marine science, engineering and economics, and the environmental and ecological sciences, including modeling. Articles may range from relatively short to extensive.

**Notes** are reports of 5 to 10 pages without an abstract and describing methods or results not supported by a large body of data.

Although all contributions are subject to peer review, responsibility for the contents of papers rests upon the authors and not upon the editor or the publisher. It is therefore important that the contents of the manuscript are carefully considered by the authors.

Submission of an article is understood to imply that the article is original and is not being considered for publication elsewhere. Manuscripts should be written in English. Authors whose native language is not English are strongly advised to have their manuscripts checked by English-speaking colleagues prior to submission.

### Preparation

**Title page** should include authors' full names and mailing addresses, the corresponding author's telephone, FAX number, and e-mail address, and a list of key words to describe the contents of the manuscript.

**Abstract** should not exceed one double-spaced typed page. It should state the main scope of the research but emphasize its conclusions and relevant findings. Because abstracts are circulated by abstracting agencies, it is important that they represent the research clearly and concisely.

**Text** must be typed double-spaced throughout. A brief introduction should portray the broad significance of the paper; the remainder of the paper should be divided into the following sections: Materials and methods, Results, Discussion (or Conclusions), and Acknowledgments. Headings within each section must be short, reflect a logical sequence, and follow the rules of multiple subdivision (i.e. there can be no subdivision without at least two items). The entire text should be intelligible to interdisciplinary readers; therefore, all acronyms, abbreviations, and technical terms should be spelled out the first time they are mentioned. The scientific names of species must be written out the first time they are mentioned; subsequent mention of scientific names may be abbreviated. Follow Scientific Style and Format: the CBE Manual for Authors, Editors, and Publishers (6th ed.), for editorial style, and the most current issue of the American Fisheries Society's Common and Scientific Names of Fishes from the United States and Canada, for fish nomenclature. Dates should be written as follows: 11 November 1991. Measurements should be expressed in metric units, e.g. metric tons as t; if other units of measurement are used, please make this fact explicit to the reader. The numeral one (1) should be typed as a one, not as a lower-case el (l). Use of appendices is discouraged.

**Text footnotes** should be numbered with Arabic numerals and inserted at the bottom of text. Footnote all personal communications, unpublished data, and unpublished manuscripts with full address of the communicator or author, or, as in the case of unpublished data, where the data are on file. Authors are advised to avoid references to nonstandard (gray) literature, such as internal, project, processed, or administrative reports. Where these references are used, please include whether they are available from NTIS (National Technical Information Service) or from some other public depository.

**Literature cited** comprises published works and those accepted for publication in peer reviewed literature (in press). Follow the name and year system for citation format. In the text, cite as follows: Smith and Jones (1977) or (Smith and Jones, 1977). If there is a sequence of citations, list alphabetically by author(s): Smith, 1987; Smith and Jones, 1985; Smith and Peterson, 1986. Abbreviations of serials should conform to abbreviations given in Serial Sources for the BIOSIS Previews Database. Authors are responsible for the accuracy and completeness of all citations.

**Tables** should not be excessive in size and must be cited in numerical order in the text. Headings within tables should be short but ample enough to allow the table to be intelligible on its own. All unusual symbols must be explained in the table legend. Other incidental comments may be footnoted with italic numerals. Use the asterisk only to indicate probability in statistical data. Zeros should precede all decimal points for values less than one.

**Figures** must be cited in numerical order in the text. The senior author's last name and the figure number should be written on the back of each one. Hand-drawn illustrations should be submitted as originals and not as photocopies. Submit photographs as glossy prints or slides with good contrast, otherwise we cannot guarantee a good final printed copy. Graphs should be submitted as laser-printed copies, not as photocopies. Label all figures with Helvetica typeface and capitalize the first letter of the first word in axis labels. Italicize species name and variables in equations. Use zeros before all decimal points. Use uppercase Times Roman bold typeface to label the parts of a figure, e.g. A, B, C, etc. Each figure legend should explain all symbols and abbreviations in the figure and should be double-spaced and placed at the end of the manuscript.

**Copyright law** Government publications are not copyrighted; they fall within the public domain. If an author reproduces any part of a government publication in his work, reference to source is appreciated.

### Submission

Send printed copies (original and three copies without staples) to the Scientific Editor:

Dr. John V. Merriner
Southeast Fisheries Science Center
National Marine Fisheries Service
101 Pivers Island Road
Beaufort, NC 28516

Once the manuscript has been accepted for publication, you will be asked to submit an electronic copy of your manuscript to the Managing Editor. The electronic copy should be submitted in WordPerfect or Microsoft Word text format and placed on a 3.5-inch disk that is double-sided, double or high density, and that is compatible with either DOS or Macintosh systems.

A copy of page proofs will be sent to the author for final approval prior to publication.
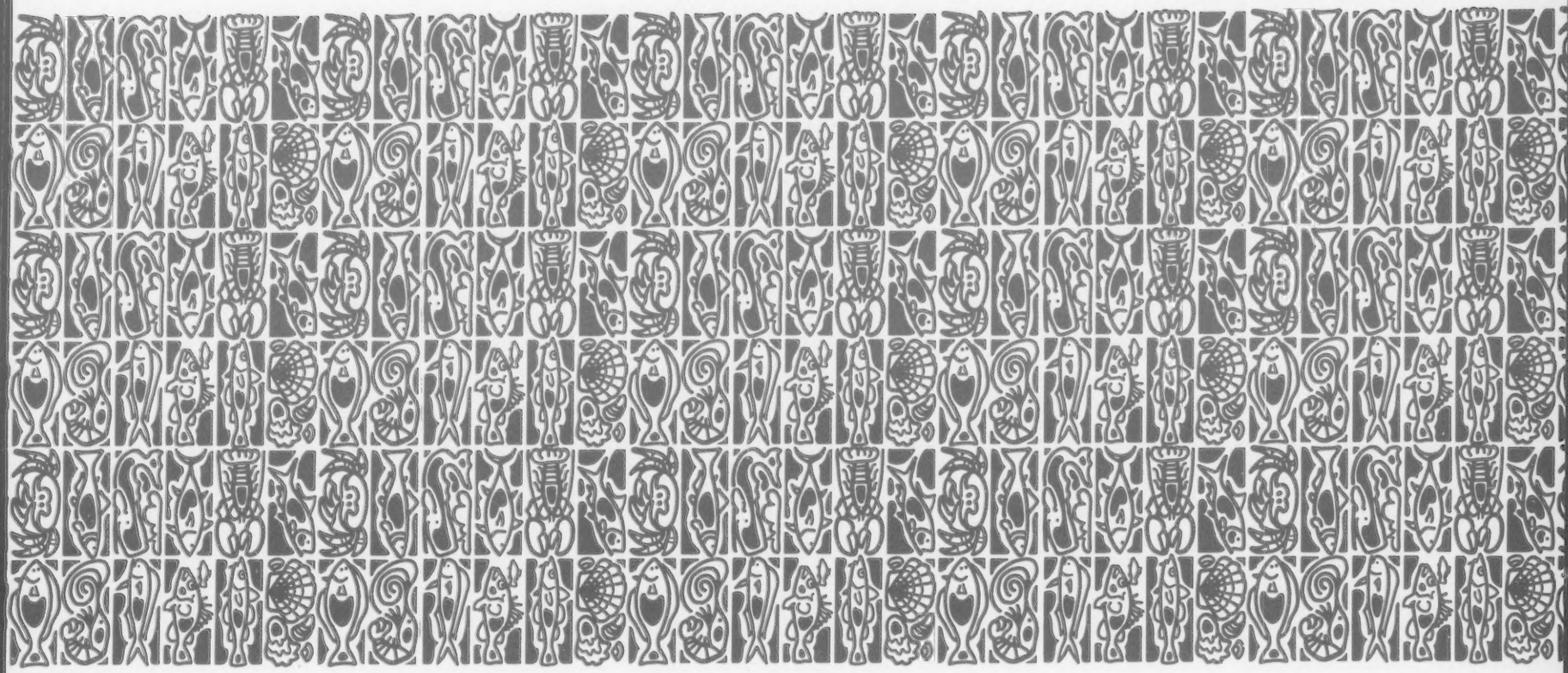
**Reprints (copies of published articles and notes)** are available free of charge to the senior author (50 copies) and to his or her laboratory (50 copies). Additional copies may be purchased in lots of 100 when the author receives page proofs.